SOLID-STATE SCIENCES

J. Zabloudil
R. Hammerling
L. Szunyogh
P. Weinberger

Electron Scattering in Solid Matter

A Theoretical and Computational Treatise

Springer

Springer Series in
SOLID-STATE SCIENCES 147

Springer Series in

SOLID-STATE SCIENCES

The Springer Series in Solid-State Sciences consists of fundamental scientific books prepared by leading researchers in the field. They strive to communicate, in a systematic and comprehensive way, the basic principles as well as new developments in theoretical and experimental solid-state physics.

136 **Nanoscale Phase Separation and Colossal Magnetoresistance**
The Physics of Manganites and Related Compounds
By E. Dagotto

137 **Quantum Transport in Submicron Devices**
A Theoretical Introduction
By W. Magnus and W. Schoenmaker

138 **Phase Separation in Soft Matter Physics**
Micellar Solutions, Microemulsions, Critical Phenomena
By P.K. Khabibullaev and A.A. Saidov

139 **Optical Response of Nanostructures**
Microscopic Nonlocal Theory
By K. Cho

140 **Fractal Concepts in Condensed Matter Physics**
By T. Nakayama and K. Yakubo

141 **Excitons in Low-Dimensional Semiconductors**
Theory, Numerical Methods, Applications By S. Glutsch

142 **Two-Dimensional Coulomb Liquids and Solids**
By Y. Monarkha and K. Kono

143 **X-Ray Multiple-Wave Diffraction**
Theory and Application
By S.-L. Chang

144 **Physics of Transition Metal Oxides**
By S. Maekawa, T. Tohyama, S.E. Barnes, S. Ishihara, W. Koshibae, and G. Khaliullin

145 **Point-Contact Spectroscopy**
By Yu.G. Naidyuk and I.K. Yanson

146 **Optics of Semiconductors and Their Nanostructures**
Editors: H. Kalt and M. Hetterich

147 **Electron Scattering in Solid Matter**
A Theoretical and Computational Treatise
By J. Zabloudil, R. Hammerling, L. Szunyogh, and P. Weinberger

148 **Physical Acoustics in the Solid State**
By B. Lüthi

Volumes 90–135 are listed at the end of the book.

J. Zabloudil R. Hammerling
L. Szunyogh P. Weinberger (Eds.)

Electron Scattering in Solid Matter

A Theoretical and Computational Treatise

With 89 Figures

Springer

Dr. Jan Zabloudil
Dr. Robert Hammerling
Prof. Peter Weinberger
Technical University of Vienna
Center for Computational Materials Science
Getreidemarkt 9/134
1060 Vienna, Austria

Prof. Laszlo Szunyogh
Department of Theoretical Physics
Budapest University of Technology and Economics
Budafoki u. 8
1111 Budapest, Hungary

ISSN 0171-1873

ISBN 3-540-22524-2 Springer Berlin Heidelberg New York

Library of Congress Control Number: 2004109370

Springer is a part of Springer Science+Business Media
springeronline.com

Typesetting by the editors
Cover concept: eStudio Calamar Steinen
Cover production: *design & production* GmbH, Heidelberg

Printed on acid-free paper SPIN: 10991718 57/3141/YL - 5 4 3 2 1 0

Foreword

The use of scattering methods for theoretical and computational studies of the electronic structure of condensed matter now has a history exceeding 50 years. Beginning with the work of Korringa, followed by the alternative formulation of Kohn and Rostoker there have been many important extensions and improvements, and thousands of applications of scientific and/or practical importance. The starting point is an approximate multiple scattering model of particles governed by a single particle Hamiltonian with an effective potential of the following form:

$$v(r) = v_{\text{ext}} + \sum_i v_i(r) \quad ,$$

where the $v_i(r)$ are non-overlapping potentials associated with the constituent atoms i and v_{ext} is a constant potential in the space exterior to the atoms, which may be set equal to zero. In my opinion this model was *a priori* not very plausible. The electron-electron interaction which does not explicitly occur in the model Hamiltonian is known to be strong and the assumed non-overlap of the "atomic potentials" is questionable in view of the long range of the underlying physical Coulomb interactions. However, since the work of Korringa, Kohn and Rostoker, the use of effective single particle Hamiltonians has to a large degree been justified in the Kohn-Sham version of Density Functional Theory; and the multiple scattering model, in its original form or with various improvements has, at least *a posteriori*, been found to be generally very serviceable.

The table of contents of this "*Theoretical and Computational Treatise*" with its 26 chapters and more than 100 sections shows the need for an up-to-date critical effort to bring some order into an enormous and often seemingly chaotic literature. The authors, whose own work exemplifies the wide reach of this subject, deserve our thanks for undertaking this task.

I believe that this work will be of considerable help to many practitioners of electron scattering methods and will also point the way to further methodological progress.

University of California, Santa Barbara,
May 2004

Walter Kohn
Research Professor of Physics

Contents

1 Introduction 1
References 3

2 Preliminary definitions 5
2.1 Real space vectors 5
2.2 Operators and representations 5
2.3 Simple lattices 5
2.4 "Parent" lattices 6
2.5 Reciprocal lattices 6
2.6 Brillouin zones 6
2.7 Translational groups 7
2.8 Complex lattices 8
2.9 Kohn-Sham Hamiltonians 8
2.9.1 Local spin-density functional 9
References 9

3 Multiple scattering 11
3.1 Resolvents & Green's functions 11
3.1.1 Basic definitions 11
3.1.2 The Dyson equation 12
3.1.3 The Lippmann-Schwinger equation 13
3.1.4 "Scaling transformations" 13
3.1.5 Integrated density of states: the Lloyd formula 14
3.2 Superposition of individual potentials 15
3.3 The multiple scattering expansion and the scattering path operator 16
3.3.1 The single-site T-operator 16
3.3.2 The multi-site T-operator 16
3.3.3 The scattering path operator 16
3.3.4 "Structural resolvents" 17
3.4 Non-relativistic angular momentum and partial wave representations 17
3.4.1 Spherical harmonics 18
3.4.2 Partial waves 18
3.4.3 Representations of $\mathcal{G}_0(z)$ 19

3.4.4 Representations of the single-site $\mathcal{T}$-operator 22
3.4.5 Representations of $\mathcal{G}(\varepsilon)$ 24
3.4.6 Representation of $\mathcal{G}(\varepsilon)$ in the basis of scattering solutions 26
3.5 Relativistic formalism 29
3.5.1 The $\kappa\mu$-representation 29
3.5.2 The free-particle solutions 31
3.5.3 The free-particle Green's function 32
3.5.4 Relativistic single-site and multi-site scattering 38
3.6 "Scalar relativistic" formulations 41
3.7 Summary 43
References 43

4 Shape functions 45
4.1 The construction of shape functions 45
4.1.1 Interception of a boundary plane of the polyhedron with a sphere 46
4.1.2 Semi-analytical evaluation 48
4.1.3 Shape functions for the fcc cell 49
4.2 Shape truncated potentials 52
4.2.1 Spherical symmetric potential 53
4.3 Radial mesh and integrations 54
References 56

5 Non-relativistic single-site scattering for spherically symmetric potentials 57
5.1 Direct numerical solution of the coupled radial differential equations 57
5.1.1 Starting values 58
5.1.2 Runge–Kutta extrapolation 59
5.1.3 Predictor-corrector algorithm 60
5.2 Single site Green's function 61
5.2.1 Normalization of regular scattering solutions and the single site t matrix 62
5.2.2 Normalization of irregular scattering solutions 64
References 64

6 Non-relativistic full potential single-site scattering 65
6.1 Schrödinger equation for a single scattering potential of arbitrary shape 65
6.2 Single site Green's function for a single scattering potential of arbitrary shape 65
6.2.1 Single spherically symmetric potential 65
6.2.2 Single potential of general shape 66

6.3 Iterative perturbational approach for the coupled radial differential equations ... 66
6.3.1 Regular solutions ... 67
6.3.2 Irregular solutions ... 67
6.3.3 Numerical integration scheme ... 68
6.3.4 Iterative procedure ... 69
6.4 Direct numerical solution of the coupled radial differential equations ... 72
6.4.1 Starting values ... 73
6.4.2 Runge–Kutta extrapolation ... 74
6.4.3 Predictor-corrector algorithm ... 74
6.5 Single-site t matrix ... 75
6.5.1 Normalization of the regular solutions ... 75
6.5.2 Normalization of the irregular solutions ... 78
References ... 79

7 Spin-polarized non-relativistic single-site scattering ... 81
References ... 82

8 Relativistic single-site scattering for spherically symmetric potentials ... 83
8.1 Direct numerical solution of the coupled differential equations ... 85
8.1.1 Starting values ... 85
8.1.2 Runge–Kutta extrapolation ... 87
8.1.3 Predictor-corrector algorithm ... 87
8.2 Single site Green's function ... 88
8.2.1 Normalization of regular scattering solutions and the single site t matrix ... 89
References ... 90

9 Relativistic full potential single-site scattering ... 91
9.1 Direct numerical solution of the coupled differential equations ... 91
9.1.1 Starting values ... 92
9.1.2 Runge–Kutta extrapolation ... 93
9.1.3 Predictor-corrector algorithm ... 94
9.1.4 Normalization of regular and irregular scattering solutions and the single-site t matrix ... 94
References ... 94

10 Spin-polarized relativistic single-site scattering for spherically symmetric potentials ... 95
10.1 Direct numerical solution of the coupled radial differential equations ... 95

10.1.1 Evaluation of the coefficients 97
10.1.2 Coupled differential equations 98
10.1.3 Start values 99
10.1.4 Runge–Kutta extrapolation 102
10.1.5 Predictor-corrector algorithm 103
10.1.6 Normalization of the regular scattering solutions and the single site t-matrix 105
10.1.7 Normalization of the irregular scattering solutions . . 107
References 107

11 Spin-polarized relativistic full potential single-site scattering 109
11.1 Iterative perturbational (Lippmann-Schwinger-type) approach for relativistic spin-polarized full potential single-site scattering 109
11.1.1 Redefinition of the irregular scattering solutions 110
11.1.2 Regular solutions 111
11.1.3 Irregular solution 113
11.1.4 Angular momentum representations of $\Delta\mathcal{H}$ 114
11.1.5 Representations of angular momenta 115
11.1.6 Calogero's coefficients 117
11.1.7 Single-site Green's function 119
11.2 Direct numerical solution of the coupled radial differential equations 120
11.2.1 Starting values 123
11.2.2 Runge–Kutta extrapolation 124
11.2.3 Predictor-corrector algorithm 124
11.2.4 Normalization of regular solutions 125
11.2.5 Reactance and single-site t matrix 126
11.2.6 Normalization of the irregular solution 127
References 128

12 Scalar-relativistic single-site scattering for spherically symmetric potentials 129
12.1 Derivation of the scalar-relativistic differential equation 129
12.1.1 Transformation to first order coupled differential equations 131
12.2 Numerical solution of the coupled radial differential equations 132
12.2.1 Starting values 132
Reference 133

13 Scalar-relativistic full potential single-site scattering 135
13.1 Derivation of the scalar-relativistic differential equation 135
13.1.1 Transformation to first order coupled differential equations 137
13.2 Numerical solution of the coupled radial differential equations 138

14 Phase shifts and resonance energies 139
14.1 Non-spin-polarized approaches 139
14.2 Spin-polarized approaches 143
References 144

15 Structure constants 145
15.1 Real space structure constants 145
15.2 Two-dimensional translational invariance 146
15.2.1 Complex "square" lattices 146
15.2.2 Multilayer systems 147
15.2.3 Real and reciprocal two-dimensional lattices 147
15.2.4 The "Kambe" structure constants 148
15.2.5 The layer- and sublattice off-diagonal case ($s \neq s'$) .. 149
15.2.6 The layer- and sublattice diagonal case ($s = s'$) 152
15.2.7 Simple two-dimensional lattices 153
15.2.8 Note on the "Kambe structure constants" 154
15.3 Three-dimensional translational invariance 155
15.3.1 Three-dimensional structure constants for simple lattices 155
15.3.2 Three-dimensional structure constants for complex lattices 157
15.3.3 Note on the structure constants for three-dimensional lattices 159
15.4 Relativistic structure constants 159
15.5 Structure constants and Green's function matrix elements .. 159
References 160

16 Green's functions: an in-between summary 161

17 The Screened KKR method for two-dimensional translationally invariant systems 163
17.1 "Screening transformations" 163
17.2 Two-dimensional translational symmetry 165
17.3 Partitioning of configuration space 166
17.4 Numerical procedures 168
17.4.1 Inversion of block tridiagonal matrices 168
17.4.2 Evaluation of the surface scattering path operators . 169
17.4.3 Practical evaluation of screened structure constants . 170

17.4.4 Relativistic screened structure constants 172
17.4.5 Decaying properties of screened structure constants . 173
References 176

18 Charge and magnetization densities 177
18.1 Calculation of physical observables 177
18.2 Non-relativistic formulation 180
18.2.1 Charge density 180
18.2.2 Charges 181
18.2.3 Partial local density of states 182
18.2.4 The spin-polarized non-relativistic case 183
18.3 Relativistic formulation 183
18.3.1 Charge density 185
18.3.2 Spin and orbital magnetization densities 186
18.3.3 Density of States 187
18.3.4 Angular momentum operators and matrix elements . 189
18.4 2D Brillouin zone integrations 190
18.5 Primitive vectors in two-dimensional lattices 191
18.6 Oblique lattice 192
18.7 Centered rectangular lattice 194
18.8 Primitive rectangular lattice 195
18.9 Square lattice 197

18.10 Hexagonal lattice 199
References 201

19 The Poisson equation and the generalized Madelung problem for two- and three-dimensional translationally invariant systems 203
19.1 The Poisson equation: basic definitions 203
19.2 Intracell contribution 204
19.3 Multipole expansion in real-space 205
19.3.1 Charge density 205
19.3.2 Green's functions and Madelung constants 206
19.3.3 Green's functions and reduced Madelung constants . 207
19.4 Three-dimensional complex lattices 208
19.4.1 Evaluation of the Green's function for three-dimensional lattices 209
19.4.2 Derivation of Madelung constants for three-dimensional lattices 213
19.4.3 Reduced Madelung constants for three-dimensional lattices 215
19.5 Complex two-dimensional lattices 216
19.5.1 Evaluation of the Green's function for two-dimensional lattices 216

19.5.2 Derivation of the Madelung constants for two-dimensional lattices . . . 220
19.5.3 The intercell potential . . . 225
19.5.4 Determination of the constants $\mathcal{A}$ and $\mathcal{B}$ . . . 225
19.6 A remark: density functional requirements . . . 230
19.7 Summary . . . 231
References . . . 233

20 "Near field" corrections . . . 235
20.1 Method 1: shifting bounding spheres . . . 235
20.2 Method 2: direct evaluation of the near field corrections . . . 239
20.3 Corrections to the intercell potential . . . 244
References . . . 244

21 Practical aspects of full-potential calculations . . . 247
21.1 Influence of a constant potential shift . . . 247
21.2 ℓ-convergence . . . 251
References . . . 252

22 Total energies . . . 253
22.1 Calculation of the total energy . . . 253
22.2 Kinetic energy . . . 253
22.3 Core energy . . . 254
22.3.1 Radial Dirac equations . . . 254
22.3.2 Numerical solution . . . 255
22.3.3 Core charge density . . . 256
22.3.4 Core potential . . . 258
22.4 Band energy . . . 259
22.4.1 Contour integration . . . 259
22.5 Potential energy . . . 261
22.6 Exchange and correlation energy . . . 262
22.6.1 Numerical angular integration – Gauss quadrature . . . 263
22.7 The Coulomb energy . . . 265
22.8 A computationally efficient expression for the total energy . . . 267
22.9 Illustration of total energy calculations . . . 267
22.9.1 Computational details . . . 269
22.9.2 Results . . . 270
References . . . 273

23 The Coherent Potential Approximation . . . 275
23.1 Configurational averages . . . 275
23.2 Restricted ensemble averages – component projected densities of states . . . 276
23.3 The electron self-energy operator . . . 278
23.4 The coherent potential approximation . . . 279

23.5 Isolated impurities 280
23.5.1 Single impurities 280
23.5.2 Double impurities 281
23.6 The single-site coherent potential approximation 282
23.6.1 Single-site CPA and restricted averages 283
23.7 The single-site CPA equations for three-dimensional translational invariant systems 284
23.7.1 Simple lattices 284
23.7.2 Complex lattices 285
23.8 The single-site CPA equations for two-dimensional translational invariant systems 287
23.8.1 Simple parent lattices 287
23.8.2 Complex lattices 289
23.9 Numerical solution of the CPA equations 290
References 291

24 The embedded cluster method 293
24.1 The Dyson equation of embedding 293
24.2 An embedding procedure for the Poisson equation 294
24.3 Convergence with respect to the size of the embedded cluster 298
References 298

25 Magnetic configurations – rotations of frame 299
25.1 Rotational properties of the Kohn-Sham-Dirac Hamiltonian . 299
25.2 Translational properties of the Kohn-Sham Hamiltonian 301
25.3 Magnetic ordering and symmetry 302
25.3.1 Translational restrictions 302
25.3.2 Rotational restrictions 302
25.4 Magnetic configurations 303
25.4.1 Two-dimensional translational invariance 303
25.4.2 Complex lattices 303
25.4.3 Absence of translational invariance 304
25.5 Rotation of frames 304
25.5.1 Rotational properties of two-dimensional structure constants 305
25.6 Rotational properties and Brillouin zone integrations 307
References 309

26 Related physical properties 311
26.1 Surface properties 311
26.1.1 Potentials at surfaces 312
26.1.2 Work function 316
26.2 Applications of the fully relativistic spin-polarized Screened KKR-ASA scheme 317

26.3 Interlayer exchange coupling, magnetic anisotropies, perpendicular magnetism and reorientation transitions in magnetic multilayer systems . . . 317
26.3.1 Energy difference between different magnetic configurations . . . 317
26.3.2 Interlayer exchange coupling (IEC) . . . 319
26.3.3 An example: the Fe/Cr/Fe system . . . 319
26.3.4 Magnetic anisotropy energy (E_a) . . . 320
26.3.5 Disordered systems . . . 323
26.3.6 An example: Ni_n/Cu(100) and Co_m/Ni_n/Cu(100) . . 324
26.4 Magnetic nanostructures . . . 326
26.4.1 Exchange energies, anisotropy energies . . . 326
26.4.2 An example Co clusters on Pt(100) . . . 330
26.5 Electric transport in semi-inifinite systems . . . 337
26.5.1 Bulk systems . . . 337
26.5.2 An example: the anisotropic magnetoresistance (AMR) in permalloy ($Ni_{1-c}Fe_c$) . . . 339
26.5.3 Spin valves: the giant magneto-resistance . . . 340
26.5.4 An example: the giant magneto-resistance in Fe/Au/Fe multilayers . . . 342
26.6 Magneto-optical transport in semi-infinite systems . . . 347
26.6.1 The (magneto-) optical tensor . . . 347
26.6.2 An example: the magneto-optical conductivity tensor for Co on Pt(111) . . . 348
26.6.3 Kerr angles and ellipticities . . . 349
26.6.4 An example: the optical constants in the "bulk" systems Pt(100), Pt(110), Pt(111) . . . 354
26.7 Mesoscopic systems: magnetic domain walls . . . 354
26.7.1 Phenomenological description of domain walls . . . 354
26.7.2 Ab initio domain wall formation energies . . . 357
26.7.3 An example: domain walls in bcc Fe and hcp Co . . . 358
26.7.4 Another example: domain wall formation in permalloy . . . 359
26.7.5 Domain wall resistivities . . . 361
26.7.6 An example: the CIP-AMR in permalloy domain walls . . . 365
26.8 Spin waves in magnetic multilayer systems . . . 365
26.8.1 An example: magnon spectra for magnetic monolayers on noble metal substrates . . . 370
References . . . 372

A Appendix: Useful relations, expansions, functions and integrals . . . 375
References . . . 379

1 Introduction

When in 1947 the now historic paper by Korringa [1] appeared and seven years later that by Kohn and Rostoker [2], the suggested method to evaluate the electronic structure of periodic solids drew little attention. Korringa's approach was considered to be too "classically minded" (incident and scattered waves, conditions for standing waves), while the treatment by Kohn and Rostoker used at that time perhaps less "familiar mathematical tools" such as Green's functions. In the meantime a more "popular" method for dealing with the electronic structure of solids was already around that used a conceptually easier approach in terms of wave functions, namely the so-called Augmented Plane Wave method, originally suggested by Slater. Even so, the methodological progress within the Korringa-Kohn-Rostoker (KKR) method as it then was called continued – mostly on the basis of analytical developments [3], [4] – and a very first fully relativistic treatment was published [5].

Almost unnoticed remained for quite some time the theoretical approaches devoted to the increasing importance of Low Energy Electron Diffraction (LEED) that seemed to revolutionize surface physics. These approaches [6], [7] – electron scattering theory – seemed at that time to be of little use in dealing with three-dimensionally periodic solids although the quantities appearing there, single-site t matrices and structure constants, are exactly those on which the KKR method is based.

Concomitantly and probably inspired by ideas of linearizing the Augmented Plane Wave method Andersen [8] came up with an ingenious new approach by introducing – mostly in the language of Korringa – the idea of energy linearization. This new approach, the Linearized Muffin Tin Orbital method, or LMTO, quickly became very popular, partly also because a more "traditional" wave function concept was applied. Since then the LMTO has acted as a kind of first cousin of the KKR method, although quite a few practitioners of the LMTO would not like to see this stated explicitly.

There is no question that the final boost for all kinds of so-called band-structure methods was and is based on ever faster increasing computing facilities. However, there is also no question that the enormous success of density functional theory [9], [10] contributed equally to this development.

In the meantime (the seventies) KKR theory was cast into the more general concept of multiple scattering by Lloyd and Smith [11] and arrived at a

– by now – generally accepted formulation in terms of Gyorffy's reformulation of the multiple scattering expansion by introducing a so-called scattering path operator [12]. The main advantage of the KKR, however, namely being a Green's function method, was yet to be discovered: by applying the Coherent Potential Approximation [13] in order to deal with disordered systems and in using the fact that the KKR is probably the only approach whose formal structure is not changed when going from a non-relativistic to a truly relativistic description. In the following years therefore the KKR was mostly used in the context of alloy theory, but increasingly also because of its relativistic formulation.

Since, in the last twenty or so years, the main emphasis in solid state physics changed from bulk systems (infinite systems; three-dimensional translational invariance) to systems with surfaces or interfaces, i.e., to systems exhibiting at best two-dimensional translational invariance, the KKR method had to adjust to these new developments. The main disadvantage of KKR, namely being non-linear in energy and having to deal with full matrices, was finally overcome by introducing a screening transformation [14] and by making use of the analytical properties of Green's functions in the complex plane. Together with the possibility of using a fully relativistic spin-polarized description the now so-called Screened KKR (SKKR) method became the main approach in dealing not only with the problem of perpendicular magnetism, but also – in the context of the Kubo-Greenwood equation – in evaluating electric and magneto-optical transport properties on a truly ab-initio relativistic level as such not accessible in terms of other approaches.

It has to be mentioned that from the eighties on the KKR as well as its cousin the LMTO were subject of review articles [15] and text books [16], [17], [18], [19], and also the exact relationship between these two methods was discussed thoroughly [20].

The present book contains a very detailed theoretical and computational description of multiple scattering in solid matter with particular emphasis on solids with reduced dimensions, on full potential approaches and on relativistic treatments. The first two chapters are meant to give very briefly preliminary definitions (Chap. 2) and an introduction to multiple scattering (Chap. 3), including a relativistic formulation thereof.

As just mentioned, particular emphasis is placed on computational schemes by giving well-tested numerical recipes for the various conceptual steps necessary. Therefore the problem of single-site scattering is discussed at quite some length by considering all possible levels of sophistication, namely from non-relativistic single-site scattering from spherical symmetric potentials to spin-polarized relativistic single-site scattering from potentials of arbitrary shape (Chaps. 5–11). On purpose each of these chapters is more or less selfcontained. Only then are the theoretical and numerical aspects of the so-called structure constants (Chap. 15) and the third "ingredient" of the Screened KKR, the screening procedure (Chap. 17), introduced.

As density functional theory demands (charge-) selfconsistency it was felt necessary to give a detailed account of evaluating charge and magnetization densities (Chap. 18) before discussing the problem of solving the Poisson equation in the most general manner (Chaps. 19–20). It should be noted that the approach chosen here in dealing with the Poisson equation appears for the first time in the literature. Clearly enough the calculation of total energies also had to be described in detail and illustrated (Chap. 22).

After having presented at full length all aspects of the "plain" Screened KKR method, additional theoretical concepts such as the Coherent Potential Approximation (Chap. 23), the Embedded Cluster Method (Chap. 24) are introduced, and the concept of magnetic configurations (Chap. 25), necessary, e.g., in dealing with non-collinear magnetism. Finally, various applications of the Screened KKR with respect to particularly interesting physical properties such as magnetic nanostructures, electric and magneto-optical transport, or spin waves in multilayers are given (Chap. 26).

It is a pleasure to cite all our former and present KKR-collaborators explicitly: B. Újfalussy, C. Uiberacker, L. Udvardi, C. Blaas, H. Herper, A. Vernes, B. Lazarovits, K. Palotas, I. Reichl; contributors and aids: B. L. Gyorffy, P. M. Levy, C. Sommers; and of course to mention the financial support the "Screened KKR-project" obtained from the Austrian Science Ministry, the Austrian Science Foundation, various Hungarian fonds, EU-networks and, last, but not least, from the Vienna University of Technology (TU Vienna) for housing the Center for Computational Materials Science.

References

1. J. Korringa, Physica **XIII**, 392 (1947)
2. W. Kohn and N. Rostoker, Phys. Rev. **94**, 1111 (1954)
3. B. Segall, Phys. Rev. **105**, 108 (1957)
4. F.C. Ham and B. Segall, Phys. Rev. B **124**, 1786 (1961)
5. C. Sommers, Phys. Rev. **188**, 3 (1969)
6. K. Kambe, Zeitschrift für Naturforschung **22a**, 322, 422 (1967), **23a**, 1280 (1968)
7. A.P. Shen, Phys. Rev. **B2**, 382 (1971), **B9**, 1328 (1974)
8. O.K. Andersen and R. V. Kasowski, Phys. Rev. **B4**, 1064 (1971); O.K. Andersen, Phys. Rev. **B12**, 3060 (1975)
9. P. Hohenberg and W. Kohn, Phys. Rev. **136**, B864 (1964)
10. W. Kohn and L.J. Sham, Phys. Rev. **140**, A1133 (1965)
11. P. Lloyd and P.V. Smith, Advances in Physics **21**, 69 (1972)
12. B.L. Gyorffy, Phys. Review **B5**, 2382 (1972)
13. P. Soven, Phys. Rev. **156**, 809 (1967); D. W. Taylor, Phys. Rev. **156**, 1017 (1967); B. Velicky, S. Kirkpatrik and H. Ehrenreich, Phys. Rev. **175**, 747 (1968)
14. L. Szunyogh, B. Újfalussy, P. Weinberger and J. Kollar, Phys. Rev. **B49**, 2721 (1994); R. Zeller, P.H. Dederichs, B. Újfalussy, L. Szunyogh and P. Weinberger, Phys. Rev. **B52**, 8807 (1995)

15. J.S. Faulkner, Progress in Materials Science **27**, 1 (1982)
16. H.L. Skriver, *The LMTO Method* (Springer-Verlag 1984)
17. P. Weinberger, *Electron Scattering Theory of Ordered and Disordered Matter* (Clarendon Press 1990)
18. A. Gonis, *Green Functions for Ordered and Disordered Systems* (Elsevier 1992); A. Gonis and W. H. Butler, *Multiple Scattering in Solids* (Springer 2000)
19. I. Turek, V. Drchal, J. Kudrnovský, M. Šob, and P. Weinberger, *Electronic structure of disordered alloys, surfaces and interfaces* (Kluwer Academic Publishers 1997)
20. P. Weinberger, I. Turek and L. Szunyogh, Int. J. Quant. Chem. **63**, 165 (1997)

2 Preliminary definitions

2.1 Real space vectors

Real space ($\mathbb{R}^3$) vectors shall be denoted by

$$\mathbf{r} = \mathbf{r}_i + \mathbf{R}_i \quad , \tag{2.1}$$

$$\mathbf{r}_i = (r_{i,x}, r_{i,y}, r_{i,z}) \quad , \quad \mathbf{R}_i = (R_{i,x}, R_{i,y}, R_{i,z}) \tag{2.2}$$

where the $\mathbf{R}_i$ refer to positions of Coulomb singularities or origins of other regular potentials.

2.2 Operators and representations

A clear distinction between operators and their representations will be made: if $\mathcal{O}$ denotes an *operator* then, e.g., a diagonal representation of $\mathcal{O}$ in configuration space (real space, $\mathbb{R}^3$), $\langle \mathbf{r}|\mathcal{O}|\mathbf{r}\rangle$ is denoted by $O(\mathbf{r})$; an off-diagonal representation, $\langle \mathbf{r}|\mathcal{O}|\mathbf{r}'\rangle$, by $O(\mathbf{r}, \mathbf{r}')$.

2.3 Simple lattices

A simple lattice is defined by the following invariance condition for the $\mathbb{R}^3$ representation of the (single-particle) Hamilton operator (in here of the Kohn-Sham operator),

$$\mathcal{L}^{(n)} = \left\{ \mathbf{t}_i^{(n)} \mid H(\mathbf{r} + \mathbf{t}_i^{(n)}) = H(\mathbf{r}) \right\} \quad , \tag{2.3}$$

$$\mathbf{t}_i^{(n)} = \sum_{j=1}^{n} i_j \mathbf{a}_j^{(n)} \quad ; \quad i_j \in \mathbb{Z} \quad , \quad \mathbf{a}_j^{(n)} \in \mathbb{R}^n \quad , \tag{2.4}$$

with n specifying the dimensionality of the lattice, $\mathbb{Z}$ being the field of integer numbers and $\mathbb{R}^n$ being a n-dimensional inner product vector space:

$$\mathbf{R}_i = \begin{cases} \mathbf{t}_i^{(3)} & ; \text{ three-dimensional lattice} \\ \\ \mathbf{t}_i^{(2)} + \mathbf{R}_{i,z} & ; \text{ two-dimensional lattice} \end{cases} \quad . \tag{2.5}$$

The set of indices i in (2.3) corresponding to a particular lattice is usually denoted by $I(\mathcal{L}^{(n)})$.

2.4 "Parent" lattices

Very often the term "parent lattice" will occur, which means that although only two-dimensional invariance applies, the $\mathbf{R}_{i,z}$ in (2.5) are assumed to be elements of a specified $\mathcal{L}^{(3)} \supset \mathcal{L}^{(2)}$.

2.5 Reciprocal lattices

Reciprocal lattices are defined in terms of the following sets of vectors $\mathbf{K}_j \in \mathbb{R}^n$

$$\mathcal{L}^{(nd)} = \left\{ \mathbf{K}_j^{(n)} \mid \left(\mathbf{K}_j^{(n)} \cdot \mathbf{t}_i^{(n)} \right) \in 2\pi\mathbb{Z} \quad ; \quad \forall \mathbf{t}_i^{(n)} \in \mathcal{L}^{(n)} \right\} \quad , \tag{2.6}$$

i.e., simply are the so-called dual sets to the corresponding $\mathcal{L}^{(n)}$:

$$\mathcal{L}^{(nd)} = \left\{ \mathbf{K}_i^{(n)} \mid \mathbf{K}_i^{(n)} = \sum_{j=1}^{n} i_j^d \mathbf{b}_j^{(n)} \quad ; \quad i_j^d \in \mathbb{Z} \right\} \quad ,$$
$$\mathcal{L}^{(nd)} \subset \mathbb{R}^n \quad , \quad \mathbf{b}_j^{(n)} \in \mathbb{R}^n \quad , \tag{2.7}$$

$$\left(\mathbf{K}_i^{(n)} \cdot \mathbf{t}_j^{(n)} \right) = 2\pi \sum_{k=1}^{n} i_k^d j_k \in 2\pi\mathbb{Z} \quad . \tag{2.8}$$

2.6 Brillouin zones

Defining the following vectors $\mathbf{k}_j$,

$$\mathbf{k}_j = \mathbf{k}_{j,0} + \mathbf{u} \quad , \tag{2.9}$$

such that

$$|\mathbf{k}_{j,0}| \leq \frac{1}{2} |\mathbf{b}| \quad , \quad |\mathbf{u}| = \frac{1}{2} |\mathbf{b}| \left(\sqrt{I^d} - 1 \right) \quad , \tag{2.10}$$

$$|\mathbf{b}| = \min_{i=1,n} |\mathbf{K}_{i,0}| \quad ; \quad \mathbf{K}_{j,0} = \sum_{j=1}^{n} i_{j,0}^{d} \mathbf{b}_j \quad ; \quad 0 \leq i_{j,0}^{d} \leq 1 \quad , \quad \forall j \quad , \tag{2.11}$$

$$I^d = \max_{j=1,n} \left(I_j^d \right) \quad , \quad I_j^d = \sum_{j=1}^{n} i_{j,0}^{d} \quad , \tag{2.12}$$

then the set of all such $\mathbf{k}_j$ is nothing but the first Brillouin zone:

$$\mathrm{BZ}^{(n)} = \{ \mathbf{k}_j \ | \forall j \} \quad . \tag{2.13}$$

2.7 Translational groups

The set $\mathcal{T}$ of elements $[E|t_i]$, $t_i = \mathbf{t}_i \in \mathcal{L}^{(n)}$, where E denotes an identity rotation, and group closure is ensured such that

$$[E|t_i]\,[E|t_j] = [E|t_i + t_j] \in \mathcal{T} \quad , \tag{2.14}$$

$$[E|t_i]\,([E|t_j]\,[E|t_k]) = ([E|t_i]\,[E|t_j])\,[E|t_k] \quad , \tag{2.15}$$

$$[E|t_i]\,[E|-t_i] = [E|-t_i]\,[E|t_i] = [E|0] \quad , \tag{2.16}$$

$$[E|t_i]^{|\mathcal{T}|} = [E|0] \in \mathcal{T} \quad , \tag{2.17}$$

with $[E|0]$ being the identity element, is usually referred to as the to $\mathcal{L}^{(n)}$ corresponding translational group of order $|\mathcal{T}|$:

$$[E|t_i]\,H(\mathbf{r}) = H([E|t_i]^{-1}\,\mathbf{r}) = H(\mathbf{r} - \mathbf{t}_i) = H(\mathbf{r}) \quad , \quad \mathbf{t}_i \in \mathcal{L}^{(n)} \quad . \tag{2.18}$$

As is well-known only application of this translational group leads then to cyclic boundary conditions for the eigenfunctions of $H(\mathbf{r})$. It should be noted that $|\mathcal{T}|$ has to be always finite. Because of (2.17) the irreducible representations of the translational group are all one-dimensional, the k-th projection operator is therefore given by

$$P_k = \frac{1}{|\mathcal{T}|} \sum_{[E|t_i] \in \mathcal{T}} \exp\left(-\mathrm{i}\mathbf{k} \cdot \mathbf{t}_i\right) [E|t_i] \quad , \quad P_k P_{k'} = P_k \delta_{kk'} \quad , \quad \sum_k P_k = 1 \ . \tag{2.19}$$

A projected solution of $H(\mathbf{r})$ is usually called a Bloch function

$$P_k \psi\left(\mathbf{r}\right) \equiv \psi_k\left(\mathbf{r}\right) \quad , \tag{2.20}$$

$$\sum_k P_k \psi\left(\mathbf{r}\right) = \sum_k \psi_k\left(\mathbf{r}\right) = \psi\left(\mathbf{r}\right) \quad . \tag{2.21}$$

Since for $\mathbf{K}_j \in \mathcal{L}^{(nd)}$ and $\mathbf{t}_i \in \mathcal{L}^{(n)}$,

$$\begin{aligned} \exp\left(-\mathrm{i}(\mathbf{k} + \mathbf{K}_j) \cdot \mathbf{t}_i\right) &= \exp\left(-\mathrm{i}\mathbf{k} \cdot \mathbf{t}_i\right) \exp\left(-\mathrm{i}\mathbf{K}_j \cdot \mathbf{t}_i\right) \\ &= \exp\left(-\mathrm{i}\mathbf{k} \cdot \mathbf{t}_i\right) \quad , \end{aligned} \tag{2.22}$$

in (2.19) $\mathbf{k}$ can be restricted to the first Brillouin zone.

2.8 Complex lattices

For complex lattices non-primitive translations $\mathbf{a}_m \in \mathbb{R}^n, m = 1, \ldots, M$, have to be taken into account for the translational invariance condition of the Hamilton operator,

$$\mathcal{L}_m^{(n)} = \left\{ \mathbf{t}_i^{(n)} \mid H(\mathbf{r} + \mathbf{a}_m + \mathbf{t}_i^{(n)}) = H(\mathbf{r} + \mathbf{a}_m) \right\} \quad , \tag{2.23}$$

where m numbers the occurring sublattices. It should be noted that translational symmetry has to be viewed in general as a (periodic) repetition of unit cells containing M inequivalent atoms.

2.9 Kohn-Sham Hamiltonians

In principle within the (non-relativistic) *Density Functional Theory* (DFT) a Kohn-Sham Hamiltonian is given by

$$\mathcal{H} = \left(\frac{p^2}{2m} + V^{\text{eff}}\left[n, \mathbf{m}\right] \right) \mathsf{I}_2 + \Sigma_z \, B_z^{\text{eff}}\left[n, \mathbf{m}\right] \quad , \tag{2.24}$$

and a Kohn-Sham-Dirac Hamiltonian by

$$\mathcal{H} = c\,\boldsymbol{\alpha} \cdot \mathbf{p} + \beta mc^2 + V^{\text{eff}}\left[n, \mathbf{m}\right] + \beta \boldsymbol{\Sigma} \cdot \mathbf{B}^{\text{eff}}\left[n, \mathbf{m}\right] \quad , \tag{2.25}$$

$$V^{\text{eff}}\left[n, \mathbf{m}\right] = V^{\text{ext}} + V^{\text{Hartree}} + \frac{\delta E_{\text{xc}}[n, \mathbf{m}]}{\delta n} \quad , \tag{2.26}$$

$$\mathbf{B}^{\text{eff}}\left[n, \mathbf{m}\right] = \mathbf{B}^{\text{ext}} + \frac{e\hbar}{2mc} \frac{\delta E_{\text{xc}}[n, \mathbf{m}]}{\delta \mathbf{m}} \quad , \tag{2.27}$$

where m is the electron mass, n the particle density, $\mathbf{m}$ the magnetization density, $V^{\text{eff}}\left[n, \mathbf{m}\right]$ the effective potential, $\mathbf{B}^{\text{eff}}\left[n, \mathbf{m}\right]$ the effective (exchange) magnetic field, V^{ext} and $\mathbf{B}^{\text{ext}}$ the corresponding external fields, and the α_i are Dirac- and the Σ_i Pauli (spin) matrices,

$$\alpha_i = \begin{pmatrix} 0 & \sigma_i \\ \sigma_i & 0 \end{pmatrix} \quad , \quad \beta = \begin{pmatrix} \mathsf{I}_2 & 0 \\ 0 & -\mathsf{I}_2 \end{pmatrix} \quad , \tag{2.28}$$

$$\Sigma_i = \begin{pmatrix} \sigma_i & 0 \\ 0 & \sigma_i \end{pmatrix} \quad , \quad \mathsf{I}_2 = \begin{pmatrix} 1 & 0 \\ 0 & 1 \end{pmatrix} \quad , \tag{2.29}$$

$$\sigma_x = \begin{pmatrix} 0 & 1 \\ 1 & 0 \end{pmatrix} \quad , \quad \sigma_y = \begin{pmatrix} 0 & -\mathrm{i} \\ \mathrm{i} & 0 \end{pmatrix} \quad , \quad \sigma_z = \begin{pmatrix} 1 & 0 \\ 0 & -1 \end{pmatrix} \quad , \tag{2.30}$$

$$\boldsymbol{\alpha} = (\alpha_x, \alpha_y, \alpha_z) \quad , \quad \boldsymbol{\Sigma} = (\Sigma_x, \Sigma_y, \Sigma_z) \quad . \tag{2.31}$$

2.9.1 Local spin-density functional

In the various local approximations to the (spin) density functional (LSDF) the occurring functional derivatives are replaced (approximated) by

$$\frac{\delta E_{\rm xc}[n,\mathbf{m}]}{\delta n(\mathbf{r})} = V_{\rm xc}([n,m],\mathbf{r}) \sim f(r_s) \quad , \tag{2.32}$$

$$\frac{\delta E_{\rm xc}[n,\mathbf{m}]}{\delta \mathbf{m}} = W_{\rm xc}([n,m],\mathbf{r}) \sim g(r_s,\xi) \quad , \tag{2.33}$$

$$r_s = \left(\frac{3}{4\pi}\right) n^{-1}(r) \quad , \quad \xi = \frac{|m(r)|}{n(r)} \quad , \tag{2.34}$$

namely by functions of r_s and ξ, with $n(r)$ and $m(r)$ being usually the spherical averages of the (single) particle and the magnetization density. For further details concerning density functional theory the reader is referred to the various monographs in the field, some of which are listed explicitly below.

References

1. R.G. Parr, Y. Weitao, *Density-Functional Theory of Atoms and Molecules* (Oxford University Press 1994)
2. R.M. Dreizler and E.K.U. Gross, *Density Functional Theory. An Approach to the Quantum Many-Body Problem* (Springer 1996)
3. H. Eschrig, *The Fundamental of Density Functional Theory* (Teubner Verlag 1997)

3 Multiple scattering

3.1 Resolvents & Green's functions

3.1.1 Basic definitions

The resolvent of a Hermitean operator (Hamilton operator) is defined as follows

$$\mathcal{G}(z) = (z\mathcal{I} - \mathcal{H})^{-1} \quad , \quad z = \epsilon + \mathrm{i}\delta \quad , \quad \mathcal{G}\left(z^*\right) = \mathcal{G}\left(z\right)^\dagger \quad , \tag{3.1}$$

where $\mathcal{I}$ is the unity operator. Any representation of such a resolvent is called a Green's functions, e.g., also the following configuration space representation of $\mathcal{G}(z)$,

$$\langle \mathbf{r} \left| \mathcal{G}(z) \right| \mathbf{r}' \rangle \ = G(\mathbf{r}, \mathbf{r}'; z) \quad . \tag{3.2}$$

The so-called side-limits of $\mathcal{G}(z)$ are then defined by

$$\lim_{|\delta| \to 0} \mathcal{G}(z) = \begin{cases} \mathcal{G}^+(\epsilon) \ ; \delta > 0 \\ \\ \mathcal{G}^-(\epsilon) \ ; \delta < 0 \end{cases} \quad , \tag{3.3}$$

$$\mathcal{G}^+(\epsilon) = \mathcal{G}^-(\epsilon)^\dagger \quad , \tag{3.4}$$

and therefore lead to the property,

$$\mathrm{Im}\, \mathcal{G}^+(\epsilon) = \frac{1}{2\mathrm{i}} \left(\mathcal{G}^+(\epsilon) - \mathcal{G}^-(\epsilon) \right) \quad , \tag{3.5}$$

or, e.g., by making use of the properties of Dirac delta functions,

$$\mathrm{ImTr}\, \mathcal{G}^\pm(\epsilon) = \mp \pi^{-1} \sum_k \delta(\epsilon - \epsilon_k) \quad , \tag{3.6}$$

$$n(\epsilon) = \mp \mathrm{ImTr}\, \mathcal{G}^\pm(\epsilon) \quad , \tag{3.7}$$

where Tr denotes the trace of an operator and $n(\epsilon)$ is the density of states (of a Hamiltonian with discrete eigenvalue spectrum, $\{\epsilon_k\}$). A Dirac delta function can therefore be simply viewed as the Cauchy part of a first order pole in the resolvent $\mathcal{G}(z)$.

3.1.2 The Dyson equation

Suppose $\mathcal{H}$ is given in terms of an unperturbed Hamiltonian $\mathcal{H}_0$ and a (Hermitean) perturbation $\mathcal{V}$,

$$\mathcal{H} = \mathcal{H}_0 + \mathcal{V} \quad . \tag{3.8}$$

The resolvents of $\mathcal{H}$ and $\mathcal{H}_0$

$$\mathcal{G}(z) = (z\mathcal{I} - \mathcal{H})^{-1} \quad , \quad \mathcal{G}_0(z) = (z\mathcal{I} - \mathcal{H}_0)^{-1} \quad , \tag{3.9}$$

are then coupled in terms of a Dyson equation,

$$\mathcal{G}(z) = \mathcal{G}_0(z) + \mathcal{G}(z)\mathcal{V}\mathcal{G}_0(z) = \mathcal{G}_0(z) + \mathcal{G}_0(z)\mathcal{V}\mathcal{G}(z) \quad , \tag{3.10}$$

which in turn can be solved iteratively (Born series),

$$\mathcal{G}(z) = \mathcal{G}_0(z) + \mathcal{G}_0(z)\mathcal{V}\mathcal{G}_0(z) + \mathcal{G}_0(z)\mathcal{V}\mathcal{G}_0(z)\mathcal{V}\mathcal{G}_0(z) + \ldots \quad . \tag{3.11}$$

By reformulating (3.11) as

$$\mathcal{G}(z) = \mathcal{G}_0(z) + \mathcal{G}_0(z)(\mathcal{V} + \mathcal{V}\mathcal{G}_0(z)\mathcal{V} + \ldots)\mathcal{G}_0(z) \quad , \tag{3.12}$$

so-called T*-operator* can be defined,

$$\mathcal{T}(z) = \mathcal{V} + \mathcal{V}\mathcal{G}_0(z)\mathcal{V} + \mathcal{V}\mathcal{G}_0(z)\mathcal{V}\mathcal{G}_0(z)\mathcal{V} + \ldots \quad , \tag{3.13}$$

such that

$$\mathcal{G}(z) = \mathcal{G}_0(z) + \mathcal{G}_0(z)\mathcal{T}(z)\mathcal{G}_0(z) \quad . \tag{3.14}$$

or, alternatively,

$$\mathcal{T}(z) = \mathcal{V} + \mathcal{V}\mathcal{G}(z)\mathcal{V}\,, \tag{3.15}$$

$$\mathcal{T}(z) = \mathcal{V} + \mathcal{V}\mathcal{G}_0(z)\mathcal{T}(z) = \mathcal{V} + \mathcal{T}(z)\mathcal{G}_0(z)\mathcal{V} \quad , \tag{3.16}$$

$$\mathcal{G}_0(z)\mathcal{T}(z) = \mathcal{G}(z)\mathcal{V} \quad , \tag{3.17}$$

$$\mathcal{T}(z)\mathcal{G}_0(z) = \mathcal{V}\mathcal{G}(z) \quad . \tag{3.18}$$

Since $\mathcal{V}$ is assumed to be Hermitean, similar to the resolvents, $\mathcal{G}_0(z)$ and $\mathcal{G}(z)$, the T-operator satisfies the relation,

$$\mathcal{T}(z^*) = \mathcal{T}(z)^\dagger \quad , \tag{3.19}$$

and, in particular, for the side-limits the property

$$\mathcal{T}^+(\varepsilon)^\dagger = \mathcal{T}^-(\varepsilon) \tag{3.20}$$

applies.

3.1.3 The Lippmann-Schwinger equation

Suppose $\varphi_\alpha(\varepsilon)$ and $\psi_\alpha(\varepsilon)$ are generalized eigenfunctions of $\mathcal{H}_0$ and $\mathcal{H} = \mathcal{H}_0 + \mathcal{V}$, respectively,

$$(\varepsilon\mathcal{I} - \mathcal{H}_0)\,\varphi_\alpha(\varepsilon) = 0 \quad , \tag{3.21}$$

$$(\varepsilon\mathcal{I} - \mathcal{H}_0)\,\psi_\alpha(\varepsilon) = \mathcal{V}\psi_\alpha(\varepsilon) \quad . \tag{3.22}$$

In using the following Ansatz for $\psi_\alpha(\varepsilon)$,

$$\psi_\alpha(\varepsilon) = \varphi_\alpha(\varepsilon) + \delta\psi_\alpha(\varepsilon) \quad , \tag{3.23}$$

(3.22) can be rewritten as

$$\begin{aligned}(\varepsilon\mathcal{I} - \mathcal{H}_0)\,(\varphi_\alpha(\varepsilon) + \delta\psi_\alpha(\varepsilon)) &= (\varepsilon\mathcal{I} - \mathcal{H}_0)\,\delta\psi_\alpha(\varepsilon) \\ &= \mathcal{V}\varphi_\alpha(\varepsilon) + \mathcal{V}\delta\psi_\alpha(\varepsilon) \quad ,\end{aligned} \tag{3.24}$$

where use was made of (3.21). This then immediately yields

$$(\varepsilon\mathcal{I} - \mathcal{H})\,\delta\psi_\alpha(\varepsilon) = \mathcal{V}\varphi_\alpha(\varepsilon) \quad . \tag{3.25}$$

Since the inverse of $\varepsilon\mathcal{I} - \mathcal{H}$ is defined by two side-limits, two different solutions for $\psi_\alpha(\varepsilon)$ exist, namely

$$\psi_\alpha^{\pm}(\varepsilon) = \varphi_\alpha(\varepsilon) + \mathcal{G}^{\pm}(\varepsilon)\,\mathcal{V}\varphi_\alpha(\varepsilon) \quad , \tag{3.26}$$

or, by using the side-limits of the $\mathcal{T}$- operator,

$$\psi_\alpha^{\pm}(\varepsilon) = \varphi_\alpha(\varepsilon) + \mathcal{G}_0^{\pm}(\varepsilon)\,\mathcal{T}^{\pm}(\varepsilon)\,\varphi_\alpha(\varepsilon) \quad , \tag{3.27}$$

or, in using the relation

$$\mathcal{V}\psi_\alpha^{\pm}(\varepsilon) = \left(\mathcal{V} + \mathcal{V}\mathcal{G}_0^{\pm}(\varepsilon)\,\mathcal{T}^{\pm}(\varepsilon)\right)\varphi_\alpha(\varepsilon) = \mathcal{T}^{\pm}(\varepsilon)\,\varphi_\alpha(\varepsilon) \quad , \tag{3.28}$$

$$\psi_\alpha^{\pm}(\varepsilon) = \varphi_\alpha(\varepsilon) + \mathcal{G}_0^{\pm}(\varepsilon)\,\mathcal{V}\psi_\alpha^{\pm}(\varepsilon) \quad . \tag{3.29}$$

Either of the equations (3.26), (3.27) or (3.29) is called the *Lippmann-Schwinger equation*, which relates the generalized eigenfunctions (scattering solutions) of the perturbed system to those of the unperturbed system.

3.1.4 "Scaling transformations"

Clearly enough, by introducing a "scaling potential" $\mathcal{W}$, the Hamilton operator $\mathcal{H}$ in (3.8) can be rewritten as

$$\mathcal{H} = \mathcal{H}_0 + \mathcal{V} \equiv \mathcal{H}_0 + \mathcal{V} + \mathcal{W} - \mathcal{W} \equiv \mathcal{H}_0' + \mathcal{V}' \quad , \tag{3.30}$$

where

$$\mathcal{H}_0' = \mathcal{H}_0 - \mathcal{W} \quad , \quad \mathcal{V}' = \mathcal{V} + \mathcal{W} \quad . \tag{3.31}$$

From the resolvent of $\mathcal{H}_0'$,

$$\mathcal{G}_0'(z) = (z - \mathcal{H}_0')^{-1} = (z - \mathcal{H}_0 + \mathcal{W})^{-1} \quad , \tag{3.32}$$

written below in terms of a Dyson equation,

$$\mathcal{G}_0'(z) = \mathcal{G}_0(z)[1 - \mathcal{W}\mathcal{G}_0'(z)] \quad , \tag{3.33}$$

then follows directly that the Dyson equation for $\mathcal{G}(z)$ can be expressed either in terms of $\mathcal{G}_0(z)$ or $\mathcal{G}_0'(z)$,

$$\mathcal{G}(z) = \mathcal{G}_0(z)[1 + \mathcal{V}\mathcal{G}(z)] = \mathcal{G}_0'(z)[1 + \mathcal{V}'\mathcal{G}(z)] \quad . \tag{3.34}$$

(3.34) has to be regarded as the key-equation for the *"screening procedure"* to be described later on, see Chap. 17.

3.1.5 Integrated density of states: the Lloyd formula

Substituting (3.14) into (3.7) yields

$$n(\varepsilon) = -\frac{1}{\pi}\mathrm{ImTr}\left(\mathcal{G}_0^+(\varepsilon) + \mathcal{G}_0^+(\varepsilon)\mathcal{T}^+(\varepsilon)\mathcal{G}_0^+(\varepsilon)\right) \tag{3.35}$$

$$= n_0(\varepsilon) + \delta n(\varepsilon) \quad , \tag{3.36}$$

where

$$n_0(\varepsilon) = -\frac{1}{\pi}\mathrm{ImTr}\left(\mathcal{G}_0^+(\varepsilon)\right) \quad , \tag{3.37}$$

$$\delta n(\varepsilon) = -\frac{1}{\pi}\mathrm{ImTr}\left(\mathcal{G}_0^+(\varepsilon)\mathcal{T}^+(\varepsilon)\mathcal{G}_0^+(\varepsilon)\right) \tag{3.38}$$

$$= -\frac{1}{\pi}\mathrm{ImTr}\left(\mathcal{G}_0^+(\varepsilon)^2\mathcal{T}^+(\varepsilon)\right) \tag{3.39}$$

$$= \frac{1}{\pi}\mathrm{ImTr}\left(\frac{\mathrm{d}\mathcal{G}_0^+(\varepsilon)}{\mathrm{d}\varepsilon}\mathcal{T}^+(\varepsilon)\right) \quad , \tag{3.40}$$

and use was made of the following identity

$$\frac{\mathrm{d}\mathcal{G}(z)}{\mathrm{d}z} = -\mathcal{G}(z)^2 \quad . \tag{3.41}$$

Based on (3.15), (3.17) and (3.18) one further can derive that

$$\frac{\mathrm{d}\mathcal{T}(z)}{\mathrm{d}z} = \mathcal{V}\frac{\mathrm{d}\mathcal{G}(z)}{\mathrm{d}z}\mathcal{V} \tag{3.42}$$

$$= -\mathcal{V}\mathcal{G}(z)^2\mathcal{V} \tag{3.43}$$

$$= -\mathcal{T}(z)\mathcal{G}_0(z)^2\mathcal{T}(z) \tag{3.44}$$

$$= \mathcal{T}(z)\frac{\mathrm{d}\mathcal{G}_0(z)}{\mathrm{d}z}\mathcal{T}(z) \quad , \tag{3.45}$$

and therefore

$$\mathcal{T}(z)^{-1}\frac{\mathrm{d}\mathcal{T}(z)}{\mathrm{d}z}=\frac{\mathrm{d}\mathcal{G}_0(z)}{\mathrm{d}z}\mathcal{T}(z) \quad , \tag{3.46}$$

which substituted into (3.40) yields

$$\delta n(\varepsilon)=\frac{1}{\pi}\mathrm{ImTr}\left(\mathcal{T}^{+}(\varepsilon)^{-1}\frac{\mathrm{d}\mathcal{T}^{+}(\varepsilon)}{\mathrm{d}\varepsilon}\right) \tag{3.47}$$

$$=\frac{\mathrm{d}}{\mathrm{d}\varepsilon}\left(\frac{1}{\pi}\mathrm{ImTr}\,\ln\mathcal{T}^{+}(\varepsilon)\right) \quad . \tag{3.48}$$

The integrated DOS,

$$N(\varepsilon)=\int_{-\infty}^{\varepsilon}\mathrm{d}\varepsilon'\,n(\varepsilon') \quad , \tag{3.49}$$

can then be directly expressed as

$$N(\varepsilon)=N_0(\varepsilon)+\delta N(\varepsilon) \quad , \tag{3.50}$$

where

$$N_0(\varepsilon)=\int_{-\infty}^{\varepsilon}\mathrm{d}\varepsilon'\,n_0(\varepsilon') \tag{3.51}$$

and

$$\delta N(\varepsilon)=\frac{1}{\pi}\mathrm{ImTr}\,\ln\mathcal{T}^{+}(\varepsilon) \quad , \tag{3.52}$$

or, in terms of (3.13) as

$$\delta N(\varepsilon)=-\frac{1}{\pi}\mathrm{ImTr}\,\ln\left(I-\mathcal{G}_0^{+}(\varepsilon)\,\mathcal{V}\right) \quad . \tag{3.53}$$

The above expression is usually referred to as the *Lloyd formula*.

3.2 Superposition of individual potentials

In general for an ensemble of N "scatterers", not necessarily confined to atoms, the Kohn-Sham Hamiltonian is given by an appropriate expression K for the kinetic energy operator $\mathcal{K}$, which can be either non-relativistic or relativistic, and the effective single particle potential $V(\mathbf{r})$,

$$H(\mathbf{r})=K+V(\mathbf{r}) \quad , \quad V(\mathbf{r})=\langle\mathbf{r}|\,\mathcal{V}\,|\mathbf{r}\rangle \quad . \tag{3.54}$$

which can be viewed as a sum of individual (effective) potentials measured from particular positions $\mathbf{R}_i$,

$$V(\mathbf{r})=\sum_{i=1}^{N}V_i(\mathbf{r}_i) \quad , \quad \mathbf{r}_i=\mathbf{r}-\mathbf{R}_i \quad , \tag{3.55}$$

such that the domains D_{V_i} of these potentials are disjoint in $\mathbb{R}^3$,

$$D_{V_i} \cap D_{V_j} = \delta_{ij} D_{V_i} \quad . \tag{3.56}$$

3.3 The multiple scattering expansion and the scattering path operator

3.3.1 The single-site T-operator

If only a single potential, $\mathcal{V}_n$, is present the corresponding T-operator is termed *single-site T-operator*, and, in dropping for a moment the complex energy argument z, is usually denoted by t^n,

$$t^n = \mathcal{V}_n + \mathcal{V}_n \mathcal{G}_0 t^n = \left(\mathcal{I} - \mathcal{V}_n \mathcal{G}_0\right)^{-1} \mathcal{V}_n \quad . \tag{3.57}$$

3.3.2 The multi-site T-operator

For an ensemble of N "scatterers" the T-operator,

$$\mathcal{T} = \sum_n \mathcal{V}_n + \sum_{n,m} \mathcal{V}_n \mathcal{G}_0 \mathcal{V}_m + \sum_{n,m,k} \mathcal{V}_n \mathcal{G}_0 \mathcal{V}_m \mathcal{G}_0 \mathcal{V}_k + \ldots \quad ; \quad n,m,k,.. \leq N \quad , \tag{3.58}$$

can be rewritten in terms of single-site T-operators, see (3.57),

$$\begin{aligned} \mathcal{T} = & \sum_n t^n + \sum_{n,m} t^n \mathcal{G}_0 \left(1 - \delta_{nm}\right) t^m + \sum_{n,m,k} t^n \mathcal{G}_0 \left(1 - \delta_{nm}\right) t^m \mathcal{G}_0 \left(1 - \delta_{mk}\right) t^k \\ & + \sum_{n,m,k,j} t^n \mathcal{G}_0 \left(1 - \delta_{nm}\right) t^m \mathcal{G}_0 \left(1 - \delta_{mk}\right) t^k \mathcal{G}_0 \left(1 - \delta_{kj}\right) t^j + \ldots \quad . \end{aligned} \tag{3.59}$$

3.3.3 The scattering path operator

A different kind of summation over sites for $\mathcal{T}$, namely in terms of the so-called *scattering path operators* (SPO),

$$\mathcal{T} = \sum_{nm} \tau^{nm} \quad , \tag{3.60}$$

$$\begin{aligned} \tau^{nm} = & t^n \delta_{nm} + t^n \mathcal{G}_0 \left(1 - \delta_{nm}\right) t^m + \sum_k t^n \mathcal{G}_0 \left(1 - \delta_{nk}\right) t^k \mathcal{G}_0 \left(1 - \delta_{km}\right) t^k \\ & + \sum_{k,j} t^n \mathcal{G}_0 \left(1 - \delta_{nk}\right) t^k \mathcal{G}_0 \left(1 - \delta_{kj}\right) t^j \mathcal{G}_0 \left(1 - \delta_{jm}\right) t^m + \ldots \quad . \end{aligned} \tag{3.61}$$

or, equivalently for $\mathcal{G}$,

$$\mathcal{G} = \mathcal{G}_0 + \sum_{n,m} \mathcal{G}_0 \tau^{nm} \mathcal{G}_0 \quad , \tag{3.62}$$

is in particular useful, since the following Dyson equation applies

$$\tau^{nm} = t^n \delta_{nm} + \sum_k t^n \mathcal{G}_0 \left(1 - \delta_{nk}\right) \tau^{km} \tag{3.63}$$

$$= t^n \delta_{nm} + \sum_k \tau^{nk} \mathcal{G}_0 \left(1 - \delta_{km}\right) t^m \quad . \tag{3.64}$$

3.3.4 "Structural resolvents"

Occasionally also the concept of a *"structural resolvent"* , $\mathcal{G}^{nm}$, is used:

$$\mathcal{G}^{nm} = \mathcal{G}_0 \left(1 - \delta_{nm}\right) + \sum_{k,j} \mathcal{G}_0 \left(1 - \delta_{nk}\right) \tau^{kj} \mathcal{G}_0 \left(1 - \delta_{jm}\right) \quad , \tag{3.65}$$

which is related to τ^{nm} by

$$\tau^{nm} = t^n \delta_{nm} + t^n \mathcal{G}^{nm} t^m \quad , \tag{3.66}$$

or,

$$\sum_k \mathcal{G}_0 \left(1 - \delta_{nk}\right) \tau^{km} = \mathcal{G}^{nm} t^m \quad , \tag{3.67}$$

or,

$$\sum_k \tau^{nk} \mathcal{G}_0 \left(1 - \delta_{km}\right) = t^n \mathcal{G}^{nm} \quad . \tag{3.68}$$

3.4 Non-relativistic angular momentum and partial wave representations

In order to use the above discussed operator relations in practical terms angular momentum and partial wave representations need to be formed. In the following for matters of simplicity only non-relativistic representations of $\mathcal{G}_0(z), \mathcal{T}, \tau$ and $\mathcal{G}(z)$ will be discussed, i.e., it will be assumed that $\mathcal{H}$ and $\mathcal{H}_0$ are non-relativistic, their relativistic counterparts will be discussed later on in this chapter. Non-relativistic and relativistic in this context means that $\mathcal{H}$ and $\mathcal{H}_0$ are either *Schrödinger*- or *Dirac*-type Kohn-Sham-Hamiltonians. Furthermore, it will be assumed that non-magnetic systems have to be described, a discussion of magnetic systems will be given in due course. The following few paragraphs are meant to illustrate in sufficient details the formal concept of operator representations; a generalization to other cases such relativistic descriptions, etc., is then easy to follow.

3.4.1 Spherical harmonics

For the eigenfunctions of the angular momentum operators $\mathcal{L}^2$ and $\mathcal{L}_z$, i.e., the spherical harmonics, $Y_L(\hat{\mathbf{r}}) \equiv Y_L(\theta,\varphi), \hat{\mathbf{r}} = \mathbf{r}/r, r = |\mathbf{r}|$, where L refers to a composite index (ℓ, m) with $\ell = 0, 1, 2, \ldots$ and $m = 0, \pm 1, \pm 2, \ldots$,

$$L = \ell(\ell+1) + m + 1 \quad , \tag{3.69}$$

the following well-known orthogonality and completeness relations apply

$$\int \mathrm{d}\hat{\mathbf{r}}\, Y_L(\hat{\mathbf{r}})^* Y_{L'}(\hat{\mathbf{r}}) = \delta_{LL'} \quad , \tag{3.70}$$

$$\sum_L Y_L(\hat{\mathbf{r}}) Y_{L'}^*(\hat{\mathbf{r}}') = \delta(\hat{\mathbf{r}} - \hat{\mathbf{r}}') \equiv \frac{1}{\sin\vartheta} \delta(\theta - \theta') \delta(\varphi - \varphi') \quad , \tag{3.71}$$

whereby most frequently the Condon-Shortley phase convention is used

$$Y_{\ell,-m}(\hat{\mathbf{r}}) = (-1)^m Y_{\ell,m}(\hat{\mathbf{r}})^* \quad . \tag{3.72}$$

3.4.2 Partial waves

Partial waves usually refer to the following well-known solutions of the *Schrödinger equation* for free particles,

$$\begin{aligned} j_L(\varepsilon;\mathbf{r}) &= j_\ell(pr) Y_L(\hat{\mathbf{r}}) \quad , \quad n_L(\varepsilon;\mathbf{r}) = n_\ell(pr) Y_L(\hat{\mathbf{r}}) \quad , \\ h_L^\pm(\varepsilon;\mathbf{r}) &= h_\ell^\pm(pr) Y_L(\hat{\mathbf{r}}) \quad , \end{aligned} \tag{3.73}$$

where $j_\ell(x)$, $n_\ell(x)$ and $h_\ell^\pm(x) = j_\ell(x) \pm i\, n_\ell(x)$ are spherical Bessel, Neumann and Hankel-functions, respectively, and $p = \sqrt{\varepsilon}$. In particular an orthonormal set of basis functions is given by

$$\varphi_L(\varepsilon;\mathbf{r}) = \frac{\varepsilon^{1/4}}{\pi^{1/2}} j_L(\varepsilon;\mathbf{r}) \quad (\varepsilon > 0) \quad , \tag{3.74}$$

since,

$$\int \mathrm{d}\mathbf{r}\, \varphi_L(\varepsilon;\mathbf{r})^* \varphi_{L'}(\varepsilon';\mathbf{r}) = \delta_{LL'} \delta(\varepsilon - \varepsilon') \tag{3.75}$$

and

$$\int_0^\infty \mathrm{d}\varepsilon \sum_L \varphi_L(\varepsilon;\mathbf{r}) \varphi_L(\varepsilon;\mathbf{r}')^* = \delta(\mathbf{r} - \mathbf{r}') \quad . \tag{3.76}$$

3.4.3 Representations of $\mathcal{G}_0(z)$

Using the spectral resolution of $\mathcal{G}_0(z)$ the respective configuration space representation can be written in terms of (3.74) as

$$G_0(z;\mathbf{r},\mathbf{r}') = \int_0^\infty \mathrm{d}\varepsilon \sum_L \frac{\sqrt{\varepsilon}}{\pi} \frac{j_L(\varepsilon;\mathbf{r})\; j_L(\varepsilon;\mathbf{r}')^*}{z-\varepsilon} \quad , \tag{3.77}$$

which in turn can be reformulated as an angular momentum representation

$$G_0(z;\mathbf{r},\mathbf{r}') = \sum_L G_\ell(z;r,r')\, Y_L(\hat{\mathbf{r}}) Y_L(\hat{\mathbf{r}}')^* \quad , \tag{3.78}$$

where

$$\begin{aligned} G_\ell(z;r,r') &= \frac{2}{\pi}\int_0^\infty k^2 \mathrm{d}k\, \frac{j_\ell(kr)\; j_\ell(kr')}{z-k^2} \\ &= \frac{1}{\pi}\int_{-\infty}^\infty k^2 \mathrm{d}k\, \frac{j_\ell(kr)\; j_\ell(kr')}{z-k^2} \quad , \end{aligned} \tag{3.79}$$

with $\varepsilon = k^2$. Since $j_\ell(x) = \frac{1}{2}\left(h_\ell^+(x) + h_\ell^-(x)\right)$, $G_\ell(z;r,r')$ can be decomposed as

$$\begin{aligned} G_\ell(z;r,r') = {} & G_\ell^{++}(z;r,r') + G_\ell^{+-}(z;r,r') \\ & + G_\ell^{-+}(z;r,r') + G_\ell^{--}(z;r,r') \quad , \end{aligned} \tag{3.80}$$

with

$$G_\ell^{ss'}(z;r,r') = \frac{1}{4\pi}\int_{-\infty}^\infty \mathrm{d}k\, \frac{k^2}{(p+k)(p-k)}\, h_\ell^s(kr)\; h_\ell^{s'}(kr') \quad , \tag{3.81}$$

$$\left(s,s' = + \text{ or } - \quad , \quad p^2 = z,\ \mathrm{Im}p > 0\right) \quad .$$

Single-center expansion of $\mathcal{G}_0(z)$

Inspecting the asymptotic behavior of the Hankel functions, the integrals in (3.81) can be performed by closing the contour of integration in either the upper or the lower complex semiplane. Adding up all the contributions and using the notation $r_< = \min(r,r')$ and $r_> = \max(r,r')$, $G_0(z;\mathbf{r},\mathbf{r}')$ can compactly be written as,

$$G_0(z;\mathbf{r},\mathbf{r}') = -\mathrm{i}p \sum_L j_\ell(pr_<)\; h_\ell^+(pr_>)\, Y_L(\hat{\mathbf{r}}) Y_L(\hat{\mathbf{r}}')^* \,. \tag{3.82}$$

Introducing *complex energy* arguments,

$$f_L(z;\mathbf{r}) \equiv f_\ell(pr)\, Y_L(\hat{\mathbf{r}})$$
$$f_\ell = j_\ell,\, n_\ell \text{ or } h_\ell^\pm \quad , \quad p^2 = z,\ \mathrm{Im}p > 0 \quad , \tag{3.83}$$

(3.82) can simply be written as

$$G_0(z;\mathbf{r},\mathbf{r}') = -\mathrm{i}p \sum_L j_L(z;\mathbf{r}_<)\ h_L^+(z;\mathbf{r}_>)^\times$$
$$= -\mathrm{i}p \sum_L h_L^+(z;\mathbf{r}_>)\ j_L(z;\mathbf{r}_<)^\times \quad , \tag{3.84}$$

where

$$f_L(z;\mathbf{r})^\times \equiv f_\ell(pr)\, Y_L(\hat{\mathbf{r}})^* \quad . \tag{3.85}$$

Since obviously

$$G_0(z^*;\mathbf{r},\mathbf{r}') = G_0(z;\mathbf{r}',\mathbf{r})^* \quad , \tag{3.86}$$

this implies for the side limits

$$G_0^\pm(\varepsilon;\mathbf{r},\mathbf{r}') = \mp\mathrm{i}p \sum_L j_\ell(pr_<)\ h_\ell^\pm(pr_>)\, Y_L(\hat{\mathbf{r}}) Y_L(\hat{\mathbf{r}}')^* \quad , \tag{3.87}$$
$$\varepsilon > 0 \quad , \quad p = \sqrt{\varepsilon} \quad ,$$

$$G_0^\pm(\varepsilon;\mathbf{r},\mathbf{r}') = p \sum_L j_\ell(\mathrm{i}pr_<)\ h_\ell^+(\mathrm{i}pr_>)\, Y_L(\hat{\mathbf{r}}) Y_L(\hat{\mathbf{r}}')^* \quad , \tag{3.88}$$
$$\varepsilon < 0 \quad , \quad p = \sqrt{-\varepsilon} \quad .$$

It is therefore sufficient to consider only the *positive side-limit* (upper complex semi-plane), since the corresponding quantity for the negative side-limit (lower complex semi-plane) can simply be obtained by replacing p by $-p^*$. In the following therefore the superscript $\pm$ will be dropped, $G_0(\varepsilon;\mathbf{r},\mathbf{r}') \equiv G_0^+(\varepsilon;\mathbf{r},\mathbf{r}')$, and all quantities obtained can be continued analytically into the upper complex semi-plane.

For later purposes it is useful to introduce the following *vector notation*

$$\mathsf{f}(\varepsilon;\mathbf{r}) \equiv \left[f_1(\varepsilon;\mathbf{r}),\, f_2(\varepsilon;\mathbf{r}),\, f_3(\varepsilon;\mathbf{r}),\, \cdots \right] \quad , \tag{3.89}$$

$$\mathsf{f}(\varepsilon;\mathbf{r})^\times \equiv \begin{bmatrix} f_1(\varepsilon;\mathbf{r})^\times \\ f_2(\varepsilon;\mathbf{r})^\times \\ f_3(\varepsilon;\mathbf{r})^\times \\ \vdots \end{bmatrix} \quad . \tag{3.90}$$

Using this type of notation $G_0(\varepsilon;\mathbf{r},\mathbf{r}')$ can be compactly written as

$$G_0(\varepsilon;\mathbf{r},\mathbf{r}') = -\mathrm{i}p\,\mathsf{j}(\varepsilon;\mathbf{r}_<)\,\mathsf{h}^+(\varepsilon;\mathbf{r}_>)^\times = -\mathrm{i}p\,\mathsf{h}^+(\varepsilon;\mathbf{r}_>)\,\mathsf{j}(\varepsilon;\mathbf{r}_<)^\times \quad , \tag{3.91}$$

or,

$$G_0\left(z;\mathbf{r},\mathbf{r}'\right) = -\mathrm{i}p\left\{\mathsf{j}\left(z;\mathbf{r}\right)\,\mathsf{h}^{+}\left(z;\mathbf{r}'\right)^{\times}\,\Theta\left(r'-r\right)\right.$$
$$\left.+\mathsf{h}^{+}\left(z;\mathbf{r}\right)\,\mathsf{j}\left(z;\mathbf{r}'\right)^{\times}\,\Theta\left(r-r'\right)\right\} \quad , \tag{3.92}$$

where $\Theta\left(x\right)$ denotes the Heavyside step-function.

Two-center expansion of $\mathcal{G}_0\left(z\right)$

If in $G_0\left(\varepsilon;\mathbf{r},\mathbf{r}'\right)$ the arguments $\mathbf{r}$ and $\mathbf{r}'$ refer to different origins,

$$\mathbf{r} = \mathbf{r}_n + \mathbf{R}_n \quad , \quad \mathbf{r}' = \mathbf{r}'_n + \mathbf{R}_n \quad , \tag{3.93}$$

$$n \neq m \quad ; \quad \left|\mathbf{r}_n - \mathbf{r}'_m\right| < \left|\mathbf{R}_{nm}\right| \quad , \quad \mathbf{R}_{nm} = \mathbf{R}_m - \mathbf{R}_n \quad , \tag{3.94}$$

an expansion of the free-particle Green function, $G_0\left(\varepsilon;\mathbf{r},\mathbf{r}'\right)$ in terms of spherical Bessel functions centered around two different sites is needed,

$$G_0\left(\varepsilon;\mathbf{r}_n+\mathbf{R}_n,\mathbf{r}'_m+\mathbf{R}_m\right) = \sum_{LL'} j_L\left(\varepsilon;\mathbf{r}_n\right) G^{nm}_{0,LL'}\left(\varepsilon\right)\; j_{L'}\left(\varepsilon;\mathbf{r}'_m\right)^{\times} \quad , \tag{3.95}$$

or, using the notation introduced in (3.89),

$$G_0\left(\varepsilon;\mathbf{r}_n+\mathbf{R}_n,\mathbf{r}'_m+\mathbf{R}_m\right) = \mathsf{j}\left(\varepsilon;\mathbf{r}_n\right) \underline{G}^{nm}_0\left(\varepsilon\right)\, \mathsf{j}\left(\varepsilon;\mathbf{r}'_m\right)^{\times} \quad , \tag{3.96}$$

where the expansion coefficients

$$\underline{G}^{nm}_0\left(\varepsilon\right) = \left\{G^{nm}_{0,LL'}\left(\varepsilon\right)\right\} \tag{3.97}$$

usually are referred to as the *"real-space, free (or bare) structure constants"* .

Since the free-particle Green's function only depends on the difference $\mathbf{r}-\mathbf{r}'$, i.e.,

$$G_0\left(\varepsilon;\mathbf{r}_n+\mathbf{R}_n,\mathbf{r}'_m+\mathbf{R}_m\right) \equiv G_0\left(\varepsilon;\mathbf{r}_n-\mathbf{r}'_m,\mathbf{R}_{nm}\right) \quad , \tag{3.98}$$

the following one-center expansion has to apply

$$G_0\left(\varepsilon;\mathbf{r}_n+\mathbf{R}_n,\mathbf{r}'_m+\mathbf{R}_m\right) = -\mathrm{i}p\sum_L h^{+}_L(\varepsilon;\mathbf{R}_{nm})\, j_L(\varepsilon;\mathbf{r}_n-\mathbf{r}'_m)^{\times} \quad . \tag{3.99}$$

In using the well-known expansion of plane waves into spherical Bessel functions and spherical harmonics (Bauer's identity), $k^2=\varepsilon$, $k=|\mathbf{k}|, \hat{\mathbf{k}}=\mathbf{k}/k$,

$$\begin{aligned} e^{i\mathbf{k}\cdot\left(\mathbf{r}_n-\mathbf{r}'_m\right)} &= 4\pi\sum_L \mathrm{i}^{\ell}\, j_L\left(\varepsilon;\mathbf{r}_n-\mathbf{r}'_m\right)^{\times} Y_L(\hat{\mathbf{k}}) \\ &= (4\pi)^2 \sum_{L,L'}\left\{\mathrm{i}^{\ell-\ell'}\, j_L\left(\varepsilon;\mathbf{r}_n\right)\, j_{L'}\left(\varepsilon;\mathbf{r}'_m\right)^{\times}\right. \\ &\quad \left.\times\, Y_L(\hat{\mathbf{k}})^{*} Y_{L'}(\hat{\mathbf{k}})\right\} \quad , \end{aligned} \tag{3.100}$$

an expansion for $j_L(\varepsilon;\mathbf{r}_n-\mathbf{r}'_m)^\times$ can be found:

$$\begin{aligned} j_L\left(\varepsilon;\mathbf{r}_n-\mathbf{r}'_m\right)^\times &= \frac{\mathrm{i}^{-\ell}}{4\pi}\int \mathrm{d}\hat{\mathbf{k}}\, e^{i\mathbf{k}\cdot\left(\mathbf{r}-\mathbf{r}'_m\right)} Y_L(\hat{\mathbf{k}})^* \\ &= 4\pi \sum_{L',L''} \mathrm{i}^{\ell'-\ell''-\ell}\, j_{L'}\left(\varepsilon;\mathbf{r}_n\right)\, j_{L''}\left(\varepsilon;\mathbf{r}'_m\right)^\times\, C_{LL'}^{L''} \quad , \end{aligned} \tag{3.101}$$

where the $C_{LL'}^{L''}$ refer to the so-called Gaunt coefficients,

$$C_{LL'}^{L''} = \int \mathrm{d}\hat{\mathbf{k}}\, Y_L(\hat{\mathbf{k}})^* Y_{L'}(\hat{\mathbf{k}})^* Y_{L''}(\hat{\mathbf{k}}) = \int \mathrm{d}\hat{\mathbf{k}}\, Y_L(\hat{\mathbf{k}}) Y_{L'}(\hat{\mathbf{k}}) Y_{L''}(\hat{\mathbf{k}})^* \,. \tag{3.102}$$

Inserting (3.101) into (3.99) then yields

$$\begin{aligned} &G_0\left(\varepsilon;\mathbf{r}_n+\mathbf{R}_n,\mathbf{r}'_m+\mathbf{R}_m\right) = \\ &= -4\pi p\mathrm{i} \sum_{L,L',L''} h_L^+(\varepsilon;\mathbf{R}_{nm})\mathrm{i}^{\ell'-\ell''-\ell}\, j_{L'}\left(\varepsilon;\mathbf{r}_n\right)\, j_{L''}\left(\varepsilon;\mathbf{r}'_m\right)^\times\, C_{LL'}^{L''} \quad , \end{aligned} \tag{3.103}$$

which, by interchanging the indices, $(L,L',L'') \rightarrow (L'',L,L')$, immediately yields the real-space structure constants in (3.97),

$$G_{0,LL'}^{nm}\left(\varepsilon\right) = -4\pi p\mathrm{i} \sum_{L''} \mathrm{i}^{\ell-\ell'-\ell''}\, h_{L''}^+(\varepsilon;\mathbf{R}_{nm})\, C_{LL''}^{L'} \quad . \tag{3.104}$$

In summary by combining (3.91), (3.96) and (3.104) the free-particle Green's function is given by

$$\begin{aligned} &G_0\left(\varepsilon;\mathbf{r}_n+\mathbf{R}_n,\mathbf{r}'_m+\mathbf{R}_m\right) = \\ &\quad (1-\delta_{nm})\, \mathsf{j}\left(\varepsilon;\mathbf{r}_n\right)\, \underline{G}_0^{nm}\left(\varepsilon\right)\, \mathsf{j}\left(\varepsilon;\mathbf{r}'_m\right)^\times \\ &\quad - \mathrm{i}p\delta_{nm}\ \Big\{ \mathsf{j}\left(\varepsilon;\mathbf{r}_n\right)\, \mathsf{h}^+\left(\varepsilon;\mathbf{r}'_n\right)^\times\, \Theta\left(r'_n-r_n\right) \\ &\qquad\qquad + \mathsf{h}^+\left(\varepsilon;\mathbf{r}_n\right)\, \mathsf{j}\left(\varepsilon;\mathbf{r}'_n\right)^\times\, \Theta\left(r_n-r'_n\right)\Big\} \quad . \end{aligned} \tag{3.105}$$

3.4.4 Representations of the single-site $\mathcal{T}$-operator

Because of (3.56) the configurational representation of $t^n\left(\varepsilon\right)$ is characterized by the following property

$$t^n\left(\varepsilon;\mathbf{r},\mathbf{r}'\right) = t^n\left(\varepsilon;\mathbf{r}+\mathbf{R}_n,\mathbf{r}'+\mathbf{R}_n\right) = 0 \quad \text{for} \quad \mathbf{r}\notin D_{V_n} \quad \text{or} \quad \mathbf{r}'\notin D_{V_n} \quad , \tag{3.106}$$

where D_{V_n} is the domain of $V(\mathbf{r}+\mathbf{R}_n)$, i.e., of that single scattering potential centred at $\mathbf{R}_n$.

Regular scattering solutions

Since traditionally partial waves of the type $j_L(\varepsilon;\mathbf{r})$ are considered as eigenfunctions of the free-particle Hamiltonian $\mathcal{H}_0$, for $\mathbf{r}_n \in D_{V_n}$ the Lippmann-Schwinger equation, see (3.26), yields

$$R_L^n(\varepsilon;\mathbf{r}_n) = j_L(\varepsilon;\mathbf{r}_n) + \iint\limits_{\{\mathbf{x}_n,\mathbf{y}_n \in D_{V_n}\}} \mathrm{d}\mathbf{x}_n \mathrm{d}\mathbf{y}_n\, G_0(\varepsilon;\mathbf{r}_n,\mathbf{x}_n)\; t^n(\varepsilon;\mathbf{x}_n,\mathbf{y}_n)\; j_L(\varepsilon;\mathbf{y}_n) \quad , \tag{3.107}$$

while for $\mathbf{r}_n \notin D_{V_n}$ the one-center expansion of $G_0(\varepsilon;\mathbf{r},\mathbf{r}')$ in (3.87) can be used

$$R_L^n(\varepsilon;\mathbf{r}_n) = j_L(\varepsilon;\mathbf{r}_n) - \mathrm{i}p \sum_{L'} h_{L'}^+(\varepsilon;\mathbf{r}_n)\; t_{L'L}^n(\varepsilon) \quad , \tag{3.108}$$

where the matrix elements $t_{L'L}^n(\varepsilon)$ (single-site t matrix, partial wave representation of the single-site T-operator) are defined as

$$t_{L'L}^n(\varepsilon) = \iint\limits_{\{\mathbf{x}_n,\mathbf{y}_n \in D_{V_n}\}} \mathrm{d}\mathbf{x}_n \mathrm{d}\mathbf{y}_n\; j_{L'}(\varepsilon;\mathbf{x}_n)^{\times}\; t^n(\varepsilon;\mathbf{x}_n,\mathbf{y}_n)\; j_L(\varepsilon;\mathbf{y}_n) \quad . \tag{3.109}$$

By using the shorthand notation introduced in (3.89) and the following matrix notation

$$\underline{t}^n(\varepsilon) \equiv \{t_{L'L}^n(\varepsilon)\} \quad , \tag{3.110}$$

(3.109) can compactly be written as

$$\underline{t}^n(\varepsilon) = \iint\limits_{\{\mathbf{x}_n,\mathbf{y}_n \in D_{V_n}\}} \mathrm{d}\mathbf{x}_n \mathrm{d}\mathbf{y}_n\; \mathsf{j}(\varepsilon;\mathbf{x}_n)^{\times}\; t^n(\varepsilon;\mathbf{x}_n,\mathbf{y}_n)\; \mathsf{j}(\varepsilon;\mathbf{y}_n) \tag{3.111}$$

and (3.108) as

$$\mathsf{R}^n(\varepsilon;\mathbf{r}_n) = \mathsf{j}(\varepsilon;\mathbf{r}_n) - \mathrm{i}p\,\mathsf{h}^+(\varepsilon;\mathbf{r}_n)\;\underline{t}^n(\varepsilon) \quad , \quad \mathbf{r}_n \notin D_{V_n} \quad . \tag{3.112}$$

Note that because of the properties of the spherical Bessel functions the functions $R_L^n(\varepsilon;\mathbf{r}_n)$ are regular at the origin ($|\mathbf{r}_n| \to 0$).

Frequently a different kind of regular functions, usually termed scattering solutions, is used,

$$\mathsf{Z}^n(\varepsilon;\mathbf{r}_n) = \mathsf{R}^n(\varepsilon;\mathbf{r}_n)\,\underline{t}^n(\varepsilon)^{-1} \quad , \quad \mathbf{r}_n \in D_{V_n} \quad , \tag{3.113}$$

$$\mathsf{Z}^n(\varepsilon;\mathbf{r}_n) = \mathsf{j}(\varepsilon;\mathbf{r}_n)\,\underline{t}^n(\varepsilon)^{-1} - \mathrm{i}p\,\mathsf{h}^+(\varepsilon;\mathbf{r}_n) \tag{3.114}$$

$$= \mathsf{j}(\varepsilon;\mathbf{r}_n)\left(\underline{t}^n(\varepsilon)^{-1} - \mathrm{i}p\underline{I}\right) + p\,\mathsf{n}(\varepsilon;\mathbf{r}_n) \quad , \quad (\mathbf{r}_n \notin D_{V_n}) \quad . \tag{3.115}$$

Irregular scattering solutions

From the expression of the single center expansion of $G_0(z)$ in (3.87) it can be seen, that eventually also scattering solutions that are irregular at the origin will be needed. These irregular scattering solutions are usually normalized for $\mathbf{r}_n \notin D_{V_n}$ either as

$$\mathsf{H}^n(\varepsilon;\mathbf{r}_n) = -\mathrm{i}p\,\mathsf{h}^+(\varepsilon;\mathbf{r}_n) \quad , \tag{3.116}$$

or

$$\mathsf{J}^n(\varepsilon;\mathbf{r}_n) = \mathsf{j}(\varepsilon;\mathbf{r}_n) \quad . \tag{3.117}$$

The above two types of irregular scattering functions are related to each other via

$$\mathsf{J}^n(\varepsilon;\mathbf{r}_n) = \mathsf{R}^n(\varepsilon;\mathbf{r}_n) - \mathsf{H}^n(\varepsilon;\mathbf{r}_n)\,\underline{t}^n(\varepsilon) \quad . \tag{3.118}$$

3.4.5 Representations of $\mathcal{G}(\varepsilon)$

The configurational space representation of the structural resolvent $\mathcal{G}^{nm}(\varepsilon)$ in (3.65) can readily be transformed into a partial wave representation,

$$G^{nm}(\varepsilon;\mathbf{r}_n+\mathbf{R}_n,\mathbf{r}'_m+\mathbf{R}_m) = \mathsf{j}(\varepsilon;\mathbf{r}_n)\,\underline{G}^{nm}(\varepsilon)\,\mathsf{j}(\varepsilon;\mathbf{r}'_m)^{\times} \quad , \tag{3.119}$$

where $\underline{G}^{nm}(\varepsilon)$ usually is referred to as the *structural Green's function matrix*,

$$\underline{G}^{nm}(\varepsilon) = \underline{G}_0^{nm}(\varepsilon)\,(1-\delta_{nm}) + \sum_{k(\neq n)}\sum_{j(\neq m)} \underline{G}_0^{nk}(\varepsilon)\,\underline{\tau}^{kj}(\varepsilon)\,\underline{G}_0^{jm}(\varepsilon) \quad . \tag{3.120}$$

In (3.120) $\underline{G}_0^{nm}(\varepsilon)$ is defined in (3.104) and (3.105), and since

$$\tau^{kj}(z;\mathbf{x}_k+\mathbf{R}_k,\mathbf{y}_j+\mathbf{R}_j) = 0 \quad , \quad \mathbf{x}_k \notin D_{V_k} \text{ or } \mathbf{y}_j \notin D_{V_j} \quad , \tag{3.121}$$

the *matrix of the scattering path operator*, $\underline{\tau}^{kj}(\varepsilon)$, is given by

$$\underline{\tau}^{kj}(\varepsilon) = \int\limits_{\{\mathbf{x}_k\in D_{V_k}\}} \mathrm{d}\mathbf{x}_k \int\limits_{\{\mathbf{y}_j\in D_{V_j}\}} \mathrm{d}\mathbf{y}_j\,\mathsf{j}(\varepsilon;\mathbf{x}_k)^{\times}\,\tau^{kj}(\varepsilon;\mathbf{x}_k,\mathbf{y}_j)\,\mathsf{j}(\varepsilon;\mathbf{y}_j) \quad . \tag{3.122}$$

Equations (3.63), (3.64), and (3.66) imply therefore the following matrix equations,

$$\underline{\tau}^{nm}(\varepsilon) = \delta_{nm}\underline{t}^n(\varepsilon) + \sum_k \underline{t}^n(\varepsilon)\,\underline{G}_0^{nk}(\varepsilon)\,(1-\delta_{nk})\,\underline{\tau}^{km}(\varepsilon) \quad , \tag{3.123}$$

$$\underline{\tau}^{nm}(\varepsilon) = \delta_{nm}\underline{t}^n(\varepsilon) + \sum_k \underline{\tau}^{nk}(\varepsilon)\,\underline{G}_0^{km}(\varepsilon)\,(1-\delta_{km})\,\underline{t}^m(\varepsilon) \quad , \tag{3.124}$$

and

$$\underline{\tau}^{nm}(\varepsilon) = \delta_{nm}\underline{t}^{n}(\varepsilon) + \underline{t}^{n}(\varepsilon)\,\underline{G}^{nm}(\varepsilon)\,\underline{t}^{m}(\varepsilon) \quad , \tag{3.125}$$

respectively. Recalling the notation in (3.89) for the basis $\mathrm{j}(\varepsilon;\mathbf{r}_n)$ it is easy to see that the matrices introduced above all carry angular momentum indices, $L = (\ell, m)$, i.e., can be referred to as *angular momentum representations* of the respective quantity:

$$\begin{aligned} \underline{G}^{nm}(\varepsilon) &= \{G^{nm}_{LL'}(\varepsilon)\} \quad , \quad \underline{t}^{n}(\varepsilon) = \{t^{n}_{LL'}(\varepsilon)\} \quad , \\ \underline{G}^{nm}_{0}(\varepsilon) &= \left\{G^{nm}_{0,LL'}(\varepsilon)\right\} \quad , \quad \underline{\tau}^{nm}(\varepsilon) = \{\tau^{nm}_{LL'}(\varepsilon)\} \ . \end{aligned} \tag{3.126}$$

The notation used up to now can further be reduced by the concept of supermatrices

$$\begin{aligned} \mathbf{G}(\varepsilon) &= \{\underline{G}^{nm}(\varepsilon)\} \quad , \quad \mathbf{t}(\varepsilon) = \{\underline{t}^{n}(\varepsilon)\,\delta_{nm}\} \quad , \\ \mathbf{G}_0(\varepsilon) &= \{\underline{G}^{nm}_{0}(\varepsilon)\,(1-\delta_{nm})\} \quad , \quad \tau(\varepsilon) = \{\underline{\tau}^{nm}(\varepsilon)\} \quad , \end{aligned} \tag{3.127}$$

by which, e.g., (3.120), (3.123), (3.124) and (3.125) can compactly be written as

$$\mathbf{G}(\varepsilon) = \mathbf{G}_0(\varepsilon) + \mathbf{G}_0(\varepsilon)\,\tau(\varepsilon)\,\mathbf{G}_0(\varepsilon) \quad , \tag{3.128}$$

$$\tau(\varepsilon) = \mathbf{t}(\varepsilon) + \mathbf{t}(\varepsilon)\;\mathbf{G}_0(\varepsilon)\;\tau(\varepsilon) \quad , \tag{3.129}$$

$$\tau(\varepsilon) = \mathbf{t}(\varepsilon) + \tau(\varepsilon)\;\mathbf{G}_0(\varepsilon)\;\mathbf{t}(\varepsilon) \quad , \tag{3.130}$$

and

$$\tau(\varepsilon) = \mathbf{t}(\varepsilon) + \mathbf{t}(\varepsilon)\;\mathbf{G}(\varepsilon)\;\mathbf{t}(\varepsilon) \quad , \tag{3.131}$$

respectively. In particular, in an angular momentum representation the Dyson equation for the scattering path operators is then given by

$$\tau(\varepsilon) = \left(\mathbf{t}(\varepsilon)^{-1} - \mathbf{G}_0(\varepsilon)\right)^{-1} \quad , \tag{3.132}$$

i.e., can be solved in terms of a simple matrix inversion. Alternatively, a similar expression can be found for $\mathbf{G}(\varepsilon)$, namely

$$\mathbf{G}(\varepsilon) = \mathbf{G}_0(\varepsilon)\;\left(\mathbf{I} - \mathbf{t}(\varepsilon)\;\mathbf{G}_0(\varepsilon)\right)^{-1} \quad . \tag{3.133}$$

Equations (3.132) or (3.133) are very often called *the fundamental equations of the Multiple Scattering Theory.*

It is worthwhile to note that for practical applications the so-called *Lloyd formula* in (3.52) or (3.53), can be expressed in terms of the above matrix representations as

$$\delta N(\varepsilon) = \frac{1}{\pi}\mathrm{Im}\ln\det\tau(\varepsilon) \quad , \tag{3.134}$$

or,

$$\delta N(\varepsilon) = \frac{1}{\pi}\mathrm{Im}\ln\det\mathbf{t}(\varepsilon) - \frac{1}{\pi}\mathrm{Im}\ln\det\left(I - \mathbf{G}_0(\varepsilon)\,\mathbf{t}(\varepsilon)\right) \quad . \tag{3.135}$$

3.4.6 Representation of $\mathcal{G}(\varepsilon)$ in the basis of scattering solutions

Clearly enough any other complete basis set can be used for a transformation of the configuration space representation of $\mathcal{G}(\varepsilon)$ into another representation: starting from (3.119), e.g., one in principle has to find the transformation of the basis $\mathsf{j}(\varepsilon;\mathbf{r}_n)$ into another complete set of functions regular at the origin **and** has to take care of their respective irregular counterparts needed in the one center expansion of $\mathcal{G}_0(\varepsilon)$, see (3.91). In particular it can be shown that $G(\varepsilon;\mathbf{r},\mathbf{r}')$ can also be formulated in terms of a basis set consisting of the functions $\mathsf{R}^n(\varepsilon;\mathbf{r}_n)$ and $\mathsf{H}^n(\varepsilon;\mathbf{r}_n)$ defined in (3.107) and (3.108) or (3.112) as well as in (3.116), respectively, $\mathsf{H}^n(\varepsilon;\mathbf{r}_n)$, being defined in (3.116).

Below, for matters of completeness the original derivation by Faulkner and Stocks [6] for non-overlapping *muffin tin potentials*,

$$V^n(\mathbf{r}_n) = \begin{cases} V^n(r_n) & \text{if} \quad r_n \le r_n^{\mathrm{MT}} \\ 0 & \text{if} \quad r_n > r_n^{\mathrm{MT}} \end{cases} \quad , \tag{3.136}$$

is reproduced, where r_n^{MT} is the so-called muffin tin radius, which, however, was shown by Gonis [1] applies also for potentials of *arbitrary shape*.

In choosing a particular pair of sites, say n and m, (3.62) can be rewritten as

$$\mathcal{G}(\varepsilon) = \mathcal{G}^{(nm)}(\varepsilon) + \mathcal{G}^{(\bar{n}m)}(\varepsilon) + \mathcal{G}^{(n\bar{m})}(\varepsilon) + \mathcal{G}^{(\bar{n}\bar{m})}(\varepsilon) \quad , \tag{3.137}$$

where

$$\begin{aligned} \mathcal{G}^{(nm)}(\varepsilon) &\equiv \mathcal{G}_0(\varepsilon)\,\tau^{nm}(\varepsilon)\,\mathcal{G}_0(\varepsilon) \\ &= \delta_{nm}\mathcal{G}_0(\varepsilon)\,t^n(\varepsilon)\,\mathcal{G}_0(\varepsilon) + \mathcal{G}_0(\varepsilon)\,t^n(\varepsilon)\,\mathcal{G}^{nm}(\varepsilon)\,t^m(\varepsilon)\,\mathcal{G}_0(\varepsilon) \quad , \end{aligned} \tag{3.138}$$

$$\mathcal{G}^{(\bar{n}m)}(\varepsilon) \equiv \sum_{i(\neq n)} \mathcal{G}_0(\varepsilon)\,\tau^{im}(\varepsilon)\,\mathcal{G}_0(\varepsilon) = \mathcal{G}^{nm}(\varepsilon)\,t^m(\varepsilon)\,\mathcal{G}_0(\varepsilon) \quad , \tag{3.139}$$

$$\mathcal{G}^{(n\bar{m})}(\varepsilon) \equiv \sum_{j(\neq m)} \mathcal{G}_0(\varepsilon)\,\tau^{nj}(\varepsilon)\,\mathcal{G}_0(\varepsilon) = \mathcal{G}_0(\varepsilon)\,t^n(\varepsilon)\,\mathcal{G}^{nm}(\varepsilon) \quad , \tag{3.140}$$

$$\begin{aligned} \mathcal{G}^{(\bar{n}\bar{m})}(\varepsilon) &\equiv \sum_{i(\neq n)} \sum_{j(\neq m)} \mathcal{G}_0(\varepsilon)\,\tau^{ij}(\varepsilon)\,\mathcal{G}_0(\varepsilon) + \mathcal{G}_0(\varepsilon) \\ &= \mathcal{G}^{nm}(\varepsilon) + \delta_{nm}\mathcal{G}_0(\varepsilon) \quad , \end{aligned} \tag{3.141}$$

see also (3.65) and (3.66).

By making use of the expansion of the free-particle Green's function in (3.105) as well as that of the structural resolvent in (3.119), the corresponding integrations for the case of $r_n > r_n^{\mathrm{MT}}$, $r'_m > r_m^{\mathrm{MT}}$ can easily be performed,

$$\begin{aligned} G^{(nm)}(\varepsilon;\mathbf{r}_n + \mathbf{R}_n, \mathbf{r}'_m + \mathbf{R}_m) &= \delta_{nm}\,(-\mathrm{i}p)^2\,\mathsf{h}^+(\varepsilon;\mathbf{r}_n)\,\underline{t}^n(\varepsilon)\,\mathsf{h}^+(\varepsilon;\mathbf{r}'_n)^\times \\ &+ (-\mathrm{i}p)^2\,\mathsf{h}^+(\varepsilon;\mathbf{r}_n)\,\underline{t}^n(\varepsilon)\,\underline{G}^{nm}(\varepsilon)\,\underline{t}^m(\varepsilon)\,\mathsf{h}^+(\varepsilon;\mathbf{r}'_m)^\times \quad , \end{aligned} \tag{3.142}$$

$$G^{(\bar{n}m)}\left(\varepsilon;\mathbf{r}_n+\mathbf{R}_n,\mathbf{r}'_m+\mathbf{R}_m\right)=(-\mathrm{i}p)\;\mathsf{j}\left(\varepsilon;\mathbf{r}_n\right)\underline{G}^{nm}\left(\varepsilon\right)\times\underline{t}^{m}\left(\varepsilon\right)\mathsf{h}^{+}\left(\varepsilon;\mathbf{r}'_m\right)^{\times}\quad,\tag{3.143}$$

$$G^{(n\bar{m})}\left(\varepsilon;\mathbf{r}_n+\mathbf{R}_n,\mathbf{r}'_m+\mathbf{R}_m\right)=(-\mathrm{i}p)\;\mathsf{h}^{+}\left(\varepsilon;\mathbf{r}_n\right)\underline{t}^{n}\left(\varepsilon\right)\times\underline{G}^{nm}\left(\varepsilon\right)\mathsf{j}\left(\varepsilon;\mathbf{r}'_m\right)^{\times}\quad,\tag{3.144}$$

$$\begin{aligned}G^{(\bar{n}\bar{m})}\left(\varepsilon;\mathbf{r}_n+\mathbf{R}_n,\mathbf{r}'_m+\mathbf{R}_m\right)&=\mathsf{j}\left(\varepsilon;\mathbf{r}_n\right)\underline{G}^{nm}\left(\varepsilon\right)\;\mathsf{j}\left(\varepsilon;\mathbf{r}'_m\right)^{\times}\\&-\mathrm{i}p\,\delta_{nm}\;\Big(\mathsf{j}\left(\varepsilon;\mathbf{r}_n\right)\mathsf{h}^{+}\left(\varepsilon;\mathbf{r}'_n\right)^{\times}\;\Theta\left(r'_n-r_n\right)\\&+\mathsf{h}^{+}\left(\varepsilon;\mathbf{r}_n\right)\;\mathsf{j}\left(\varepsilon;\mathbf{r}'_n\right)^{\times}\;\Theta\left(r_n-r'_n\right)\Big)\quad.\end{aligned}\tag{3.145}$$

Collecting all the contributions one therefore gets,

$$\begin{aligned}&G\left(\varepsilon;\mathbf{r}_n+\mathbf{R}_n,\mathbf{r}'_m+\mathbf{R}_m\right)=\\&\left[\mathsf{j}\left(\varepsilon;\mathbf{r}_n\right)-\mathrm{i}p\,\mathsf{h}^{+}\left(\varepsilon;\mathbf{r}_n\right)\underline{t}^{n}\left(\varepsilon\right)\right]\;\underline{G}^{nm}\left(\varepsilon\right)\;\left[\mathsf{j}\left(\varepsilon;\mathbf{r}'_m\right)^{\times}-\mathrm{i}p\,\underline{t}^{m}\left(\varepsilon\right)\mathsf{h}^{+}\left(\varepsilon;\mathbf{r}'_m\right)^{\times}\right]\\&-\mathrm{i}p\,\delta_{nm}\;\Big\{\left[\mathsf{j}\left(\varepsilon;\mathbf{r}_n\right)-\mathrm{i}p\,\mathsf{h}^{+}\left(\varepsilon;\mathbf{r}_n\right)\underline{t}^{n}\left(\varepsilon\right)\right]\;\mathsf{h}^{+}\left(\varepsilon;\mathbf{r}'_n\right)^{\times}\;\Theta\left(r'_n-r_n\right)\\&+\mathsf{h}^{+}\left(\varepsilon;\mathbf{r}_n\right)\left[\mathsf{j}\left(\varepsilon;\mathbf{r}'_n\right)^{\times}-\mathrm{i}p\,\underline{t}^{n}\left(\varepsilon\right)\mathsf{h}^{+}\left(\varepsilon;\mathbf{r}'_n\right)^{\times}\right]\;\Theta\left(r_n-r'_n\right)\Big\}\quad.\end{aligned}\tag{3.146}$$

Since the Green's function has to satisfy the below second order differential equations,

$$\left(-\Delta+V\left(\mathbf{r}\right)-\varepsilon\right)G\left(\varepsilon;\mathbf{r},\mathbf{r}'\right)=\delta\left(\mathbf{r}-\mathbf{r}'\right)\quad,\tag{3.147}$$

$$G\left(\varepsilon;\mathbf{r},\mathbf{r}'\right)\left(-\Delta'+V\left(\mathbf{r}'\right)-\varepsilon\right)=\delta\left(\mathbf{r}-\mathbf{r}'\right)\quad,\tag{3.148}$$

in all space, it can readily be continued inside the muffin tins. By considering the boundary conditions in (3.112) and (3.116) this then yields

$$\begin{aligned}G\left(\varepsilon;\mathbf{r}_n+\mathbf{R}_n,\mathbf{r}'_m+\mathbf{R}_m\right)&=\mathsf{R}^{n}\left(\varepsilon;\mathbf{r}_n\right)\;\underline{G}^{nm}\left(\varepsilon\right)\;\widetilde{\mathsf{R}}^{m}\left(\varepsilon;\mathbf{r}'_m\right)^{*}\\&+\delta_{nm}\;\Big\{\mathsf{R}^{n}\left(\varepsilon;\mathbf{r}_n\right)\;\widetilde{\mathsf{H}}^{n}\left(\varepsilon;\mathbf{r}'_n\right)^{*}\;\Theta\left(r'_n-r_n\right)\\&+\mathsf{H}^{n}\left(\varepsilon;\mathbf{r}_n\right)\;\widetilde{\mathsf{R}}^{n}\left(\varepsilon;\mathbf{r}'_n\right)^{*}\;\Theta\left(r_n-r'_n\right)\Big\}\quad.\end{aligned}\tag{3.149}$$

In (3.149) so-called *left-hand-side solutions* of the Schrödinger equation, $\widetilde{\mathsf{R}}^{n}\left(z;\mathbf{r}_n\right)$ and $\widetilde{\mathsf{H}}^{n}\left(z;\mathbf{r}_n\right)$ were introduced

$$\left(-\Delta+V_n\left(\mathbf{r}_n\right)-z^{*}\right)\left\{\begin{array}{c}\widetilde{\mathsf{R}}^{n}\left(z;\mathbf{r}_n\right)\\\widetilde{\mathsf{H}}^{n}\left(z;\mathbf{r}_n\right)\end{array}\right\}=0\tag{3.150}$$

with the boundary conditions

$$\left.\begin{array}{c}\widetilde{\mathsf{R}}^n\left(z;\mathbf{r}_n\right)\\ \widetilde{\mathsf{H}}^n\left(z;\mathbf{r}_n\right)\end{array}\right\}=\left\{\begin{array}{c}\mathsf{j}\left(z^*;\mathbf{r}_n\right)+ip^*\,\mathsf{h}^-\left(z^*;\mathbf{r}_n\right)\underline{t}^n\left(z^*\right)\\ ip^*\mathsf{h}^-\left(z^*;\mathbf{r}_n\right)\end{array}\right.\quad,\quad\left(\mathbf{r}\notin D_{V_n}\right)\quad, \tag{3.151}$$

or, equivalently,

$$\left.\begin{array}{c}\widetilde{\mathsf{R}}^n\left(z;\mathbf{r}_n\right)^*\\ \widetilde{\mathsf{H}}^n\left(z;\mathbf{r}_n\right)^*\end{array}\right\}=\left\{\begin{array}{c}\mathsf{j}\left(z;\mathbf{r}_n\right)^\times-\mathrm{i}p\,\underline{t}^n\left(z\right)\mathsf{h}^+\left(z;\mathbf{r}_n\right)^\times\\ -\mathrm{i}p\mathsf{h}^+\left(z;\mathbf{r}_n\right)^\times\end{array}\right.\quad,\quad\left(\mathbf{r}\notin D_{V_n}\right)\quad, \tag{3.152}$$

and use was made of the relation

$$\underline{t}^n\left(z^*\right)=\underline{t}^n\left(z\right)^\dagger\quad. \tag{3.153}$$

Considering the radial Schrödinger equation together with the matching condition in (3.108), it turns out that for real potentials, $V_n(\mathbf{r}_n)$, the t-matrix is symmetric. In this case

$$\left.\begin{array}{c}\widetilde{\mathsf{R}}^n\left(z;\mathbf{r}_n\right)^*\\ \widetilde{\mathsf{H}}^n\left(z;\mathbf{r}_n\right)^*\end{array}\right\}=\left\{\begin{array}{c}\mathsf{R}^n\left(z;\mathbf{r}_n\right)^\times\\ \mathsf{H}^n\left(z;\mathbf{r}_n\right)^\times\end{array}\right.\quad, \tag{3.154}$$

and therefore there is no need to solve the Schrödinger equation for the left-hand-side solutions. Consequently the Green's function is of the form

$$\begin{aligned}G\left(\varepsilon;\mathbf{r}_n+\mathbf{R}_n,\mathbf{r}'_m+\mathbf{R}_m\right)&=\mathsf{R}^n\left(\varepsilon;\mathbf{r}_n\right)\,\underline{G}^{nm}\left(\varepsilon\right)\,\mathsf{R}^m\left(\varepsilon;\mathbf{r}'_m\right)^\times\\&+\delta_{nm}\,\Big\{\mathsf{R}^n\left(\varepsilon;\mathbf{r}_n\right)\,\mathsf{H}^n\left(\varepsilon;\mathbf{r}'_n\right)^\times\,\Theta\left(r'_n-r_n\right)\\&+\mathsf{H}^n\left(\varepsilon;\mathbf{r}_n\right)\,\mathsf{R}^n\left(\varepsilon;\mathbf{r}'_n\right)^\times\,\Theta\left(r_n-r'_n\right)\Big\}\quad.\end{aligned} \tag{3.155}$$

It is easy to show that an alternative representation of $G\left(\varepsilon;\mathbf{r},\mathbf{r}'\right)$ can be obtained using the so-called *scattering solutions,* $\mathsf{Z}^n\left(\varepsilon;\mathbf{r}_n\right)$, in (3.113)-(3.115), namely,

$$\begin{aligned}G\left(\varepsilon;\mathbf{r}_n+\mathbf{R}_n,\mathbf{r}'_m+\mathbf{R}_m\right)&=\mathsf{Z}^n\left(\varepsilon;\mathbf{r}_n\right)\underline{\tau}^{nm}\left(\varepsilon\right)\,\mathsf{Z}^m\left(\varepsilon;\mathbf{r}'_m\right)^\times\\&-\delta_{nm}\,\Big\{\mathsf{Z}^n\left(\varepsilon;\mathbf{r}_n\right)\,\mathsf{J}^n\left(\varepsilon;\mathbf{r}'_n\right)^\times\,\Theta\left(r'_n-r_n\right)\\&+\mathsf{J}^n\left(\varepsilon;\mathbf{r}_n\right)\,\mathsf{Z}^n\left(\varepsilon;\mathbf{r}'_n\right)^\times\,\Theta\left(r_n-r'_n\right)\Big\}\quad,\end{aligned} \tag{3.156}$$

with $\mathsf{J}^n\left(\varepsilon;\mathbf{r}_n\right)$ being defined in (3.117) or (3.118).

This then is the *main equation in (non-relativistic) multiple scattering*, since in principle all one-particle properties such as the particle density, the density of states and related quantities can directly be obtained from $G\left(\varepsilon;\mathbf{r},\mathbf{r}'\right)$. Most of the following sections will deal in detail with particular specifications for $\mathcal{H}$ and $\mathcal{H}_0$ (relativistic, magnetic systems) and of course differently shaped potentials $V_n(\mathbf{r})$.

3.5 Relativistic formalism

3.5.1 The $\kappa\mu$-representation

The eigenfunctions of the Kohn-Sham-Dirac Hamiltonian,

$$\mathcal{H}(\mathbf{r})\,\psi(\varepsilon;\mathbf{r}) = W\psi(\varepsilon;\mathbf{r}) \quad , \tag{3.157}$$
$$W^2 = c^2p^2 + m^2c^4 \quad , \quad \varepsilon \equiv W - mc^2 \quad ,$$

$$\mathcal{H}(\mathbf{r}) = c\,\boldsymbol{\alpha}\cdot\mathbf{p} + \beta mc^2 + U(\mathbf{r}) \quad , \tag{3.158}$$

$$U(\mathbf{r}) = V^{\text{eff}}(\mathbf{r})\,\mathsf{I}_4 + \beta\boldsymbol{\Sigma}\cdot\mathbf{B}^{\text{eff}}(\mathbf{r}) \quad , \tag{3.159}$$

$$\boldsymbol{\alpha} = \begin{pmatrix} 0 & \sigma \\ \sigma & 0 \end{pmatrix} \quad , \quad \beta = \begin{pmatrix} \mathsf{I}_2 & 0 \\ 0 & -\mathsf{I}_2 \end{pmatrix} \quad , \quad \boldsymbol{\Sigma} = \begin{pmatrix} \sigma & 0 \\ 0 & \sigma \end{pmatrix} \quad , \tag{3.160}$$

where

$$\sigma = (\sigma_x, \sigma_y, \sigma_z) \quad , \tag{3.161}$$

and

$$\sigma_x = \begin{pmatrix} 0 & 1 \\ 1 & 0 \end{pmatrix} \quad , \quad \sigma_y = \begin{pmatrix} 0 & -\mathrm{i} \\ \mathrm{i} & 0 \end{pmatrix} \quad , \quad \sigma_z = \begin{pmatrix} 1 & 0 \\ 0 & -1 \end{pmatrix} \quad , \tag{3.162}$$

are the Pauli spin matrices and I_n is a n-dimensional unit matrix, can be viewed as a combination of bi-spinors,

$$\psi(\varepsilon;\mathbf{r}) = \sum_{\kappa\mu} \begin{pmatrix} g_{\kappa\mu}(\varepsilon;r)\chi_{\kappa\mu}(\hat{\mathbf{r}}) \\ \mathrm{i}f_{\kappa\mu}(\varepsilon;r)\chi_{-\kappa\mu}(\hat{\mathbf{r}}) \end{pmatrix} \quad . \tag{3.163}$$

Here the relativistic angular momentum quantum number κ is related to ℓ and j as follows

$$\kappa = \begin{cases} \ell \quad , & j = \ell - 1/2 \\ -\ell - 1 \quad , & j = \ell + 1/2 \end{cases} \quad ; \quad j = \ell \pm \frac{1}{2} \quad , \tag{3.164}$$

while

$$\mu \in \{-j, -j+1, \ldots, j-1, j\} \quad . \tag{3.165}$$

Furthermore, the below quantum numbers shall be used

$$\bar{\ell} = \ell - S_\kappa \quad , \quad S_\kappa = \kappa/|\kappa| \quad . \tag{3.166}$$

Throughout this book the composite index $(\kappa\mu)$ will often be abbreviated by Q. The spin spherical harmonics, $\chi_{\kappa\mu}(\hat{\mathbf{r}})$, are defined as

$$\chi_{\kappa\mu}(\hat{\mathbf{r}}) = \sum_{s=\pm 1/2} C(\ell, \kappa, \frac{1}{2}|\ \mu - s, s) Y_{\ell,\mu-s}(\hat{\mathbf{r}}) \Phi_s \quad , \tag{3.167}$$

with the $C(\ell,\kappa,\frac{1}{2}|\ \mu-s,s)$ referring to the Clebsch-Gordan coefficients and the Φ_s denoting the following spinor basis functions

$$\Phi_{1/2}=\begin{pmatrix}1\\0\end{pmatrix}\quad,\quad \Phi_{-1/2}=\begin{pmatrix}0\\1\end{pmatrix}\quad. \tag{3.168}$$

The spin spherical harmonics, very often simply written as,

$$\langle\mathbf{r}\mid Q\rangle=\chi_{\kappa\mu}(\hat{\mathbf{r}})\quad,\quad \langle\mathbf{r}\mid \bar{Q}\rangle=\chi_{-\kappa\mu}(\hat{\mathbf{r}})\quad, \tag{3.169}$$

are eigenfunctions of $\mathcal{J}^2$, $\mathcal{J}_z$ and $\mathcal{K}=\sigma\cdot\mathcal{L}+\mathcal{I}\hbar$, $\mathcal{I}$ being the identity operator,

$$\mathcal{J}^2\mid\kappa\mu\rangle=j(j+1)\hbar^2\mid\kappa\mu\rangle\quad, \tag{3.170}$$
$$\mathcal{J}_z\mid\kappa\mu\rangle=\mu\hbar\mid\kappa\mu\rangle\quad, \tag{3.171}$$
$$\mathcal{K}\mid\kappa\mu\rangle=-\kappa\hbar\mid\kappa\mu\rangle\quad. \tag{3.172}$$

By making use of the orthogonality relations of the Clebsch-Gordan coefficients,

$$\begin{aligned}&\sum_{j=\ell\pm\frac{1}{2}}C(\ell,\kappa,\frac{1}{2}|\ m,s)\sum_{\substack{m's'\\(m+s=m'+s')}}C(\ell,\kappa,\frac{1}{2}|\ m',s')\varphi_{\ell m's'}(\hat{\mathbf{r}})\\ =&\sum_{\substack{m's'\\(m+s=m'+s')}}\underbrace{\sum_{j=\ell\pm\frac{1}{2}}C(\ell,\kappa,\frac{1}{2}|\ m,s)C(\ell,\kappa,\frac{1}{2}|\ m',s')}_{\delta_{mm'}\delta_{ss'}}\varphi_{\ell m's'}(\hat{\mathbf{r}})=\varphi_{\ell ms}(\hat{\mathbf{r}})\end{aligned}$$

it is useful to note the relationship between the (non-relativistic) ℓms- and the $\kappa\mu$-representation

$$\varphi_{\ell ms}(\hat{\mathbf{r}})\equiv Y_{\ell m}(\hat{\mathbf{r}})\Phi_s=\sum_{j=\ell\pm\frac{1}{2}}C(\ell,\kappa,\frac{1}{2}|\ m,s)\chi_{\kappa,m+s}(\hat{\mathbf{r}})\quad. \tag{3.173}$$

Table 3.1. Clebsch-Gordan Coefficients: $\mu=m+s$, where μ is an eigenvalue to $\mathcal{J}_z$, m to $\mathcal{L}_z$, and s to $\mathcal{S}_z$.

$C\,(\ell,j,1/2\,\vert\,(\mu-s)\,s)$	$s=\frac{1}{2}$	$s=-\frac{1}{2}$
$j=\ell+\frac{1}{2}$	$\left(\frac{\ell+m+1}{2\ell+1}\right)^{1/2}$	$\left(\frac{\ell-m+1}{2\ell+1}\right)^{1/2}$
$j=\ell-\frac{1}{2}$	$-\left(\frac{\ell-m}{2\ell+1}\right)^{1/2}$	$\left(\frac{\ell+m}{2\ell+1}\right)^{1/2}$

Inserting (3.163) into (3.157) and eliminating the spin spherical harmonics in terms of angular integrations, leads to the following system of coupled first order differential equations,

$$\sum_{Q'} \begin{bmatrix} W - mc^2 - u^{+}_{QQ'}(r) & -\mathrm{i}\hbar c[\frac{\mathrm{d}}{\mathrm{d}r} + \frac{1}{r} - \frac{\kappa}{r}] \\ -\mathrm{i}\hbar c[\frac{\mathrm{d}}{\mathrm{d}r} + \frac{1}{r} + \frac{\kappa}{r}] & W + mc^2 - u^{-}_{QQ'}(r) \end{bmatrix} \begin{bmatrix} g_{Q'}(\varepsilon; r) \\ \mathrm{i} f_{Q'}(\varepsilon; r) \end{bmatrix} = 0 \quad , \tag{3.174}$$

where

$$u^{\pm}_{\kappa\mu,\kappa'\mu'}(r) = \left\langle \pm\kappa, \mu \left| V^{\mathrm{eff}}(\mathbf{r}) \pm \sigma \cdot \mathbf{B}^{\mathrm{eff}}(\mathbf{r}) \right| \pm\kappa', \mu' \right\rangle \ . \tag{3.175}$$

Methods of how to solve (3.174) will be discussed in detail in the corresponding chapters devoted to single-site scattering.

3.5.2 The free-particle solutions

In the case of $V(\mathbf{r}) = 0$ and $\mathbf{B}(\mathbf{r}) = 0$ the eigenfunction of the Dirac equation,

$$\psi(\varepsilon; \mathbf{r}) = \begin{pmatrix} \psi_{\mathrm{b}}(\varepsilon; \mathbf{r}) \\ \psi_{\mathrm{s}}(\varepsilon; \mathbf{r}) \end{pmatrix} \quad , \tag{3.176}$$

where $\psi_{\mathrm{b}}(\hat{\mathbf{r}})$ and $\psi_{\mathrm{s}}(\hat{\mathbf{r}})$ are usually termed *big* and *small* component, respectively, satisfy the equation

$$\begin{bmatrix} \left(W - mc^2\right) \mathsf{I}_2 & -c\sigma \cdot \mathbf{p} \\ -c\sigma \cdot \mathbf{p} & \left(W + mc^2\right) \mathsf{I}_2 \end{bmatrix} \begin{bmatrix} \psi_{\mathrm{b}}(\varepsilon; \mathbf{r}) \\ \psi_{\mathrm{s}}(\varepsilon; \mathbf{r}) \end{bmatrix} = 0 \quad , \tag{3.177}$$

from which the relationship,

$$\psi_{\mathrm{s}}(\varepsilon; \mathbf{r}) = \frac{c\sigma \cdot \mathbf{p}}{W + mc^2} \psi_{\mathrm{b}}(\varepsilon; \mathbf{r}) \quad , \tag{3.178}$$

immediately follows. The well-known solutions are then given by

$$f_{\kappa\mu}(\varepsilon; \mathbf{r}) = \begin{bmatrix} \mathsf{I}_2 \\ \frac{c\sigma \cdot \mathbf{p}}{W + mc^2} \end{bmatrix} \otimes f_\ell\left(\frac{pr}{\hbar}\right) \chi_{\kappa\mu}(\hat{\mathbf{r}}) \tag{3.179}$$

$$= \begin{bmatrix} f_\ell\left(\frac{pr}{\hbar}\right) \chi_{\kappa\mu}(\hat{\mathbf{r}}) \\ \frac{\mathrm{i}S_\kappa pc}{W + mc^2} f_{\bar{\ell}}\left(\frac{pr}{\hbar}\right) \chi_{-\kappa\mu}(\hat{\mathbf{r}}) \end{bmatrix} \quad , \tag{3.180}$$

where $\otimes$ denotes tensorial product, the functions f_ℓ can be either j_ℓ, n_ℓ,or $h^{\pm}_\ell$, i.e., spherical Bessel-, Neumann- or Hankel-functions and

$$p = \sqrt{W^2 - m^2c^4} \quad .$$

3.5.3 The free-particle Green's function

As in this section, the Green's function of the relativistic free-space Hamilton operator will be related to that of the non-relativistic free-space Hamilton operator, the corresponding quantities will be labelled by subscripts D (Dirac) and S (Schrödinger), respectively. The free-space resolvent, $G_0^D(\varepsilon)$, operator is defined by

$$\left(W\mathsf{I}_4 - \mathcal{H}_0^D\right)\mathcal{G}_0^D(\varepsilon) = \mathcal{I} \quad , \tag{3.181}$$

where

$$\mathcal{H}_0^D = \begin{bmatrix} mc^2\mathsf{I}_2 & c\sigma\cdot\mathbf{p} \\ c\sigma\cdot\mathbf{p} & -mc^2\mathsf{I}_2 \end{bmatrix} \quad . \tag{3.182}$$

Multiplying (3.182) from the left with $\left(W\mathsf{I}_4 - \mathcal{H}_0^D\right)$ one gets

$$\begin{aligned} \left(W\mathsf{I}_4 + \mathcal{H}_0^D\right)\left(WI_4 - \mathcal{H}_0^D\right)\mathcal{G}_0^D(\varepsilon) = \\ \left(W^2\mathsf{I}_4 - \left(\mathcal{H}_0^D\right)^2\right)\mathcal{G}_0^D(\varepsilon) = W\mathsf{I}_4 + \mathcal{H}_0^D \quad . \end{aligned} \tag{3.183}$$

However, in using (3.182) and the identity

$$(\sigma\cdot\mathbf{a})(\sigma\cdot\mathbf{b}) = \mathbf{a}\cdot\mathbf{b} + \mathrm{i}\sigma\cdot\ (\mathbf{a}\times\mathbf{b}) \quad , \tag{3.184}$$

one easily can show that

$$\left(\mathcal{H}_0^D\right)^2 = \left(m^2c^4 + c^2\mathbf{p}^2\right)\mathsf{I}_4 \quad . \tag{3.185}$$

and therefore

$$\begin{aligned} W^2\mathsf{I}_4 - \left(\mathcal{H}_0^D\right)^2 &= \left(W^2 - m^2c^4 - c^2\mathbf{p}^2\right)\mathsf{I}_4 \\ &= c^2\left(p^2 - \mathbf{p}^2\right)\mathsf{I}_4 = 2mc^2\left(\frac{p^2}{2m} - \mathcal{H}_0^S\right)\mathsf{I}_4 \quad , \end{aligned} \tag{3.186}$$

where $\mathcal{H}_0^S = \mathbf{p}^2/2m$. Since $\mathcal{H}_0^S\,\mathsf{I}_4$ commutes with $\mathcal{H}_0^D$, one arrives at

$$\mathcal{G}_0^D(\varepsilon) = \frac{1}{2mc^2}\mathcal{G}_0^S\left(p^2/2m\right)\ \mathsf{I}_4\ \left(WI_4 + \mathcal{H}_0^D\right) \tag{3.187}$$

$$= \frac{1}{2mc^2}\left(W\mathsf{I}_4 + \mathcal{H}_0^D\right)\ \mathcal{G}_0^S\left(p^2/2m\right)\ \mathsf{I}_4 \quad . \tag{3.188}$$

Single-center expansion

Recalling the single-center expansion of $G_0^S(\varepsilon;\mathbf{r},\mathbf{r}')$, see (3.82), and using again the orthogonality of the spin spherical harmonics as well as the property of completeness of the spinor basis functions in (3.168) yields ($\mathrm{Im}p > 0$),

$$G_0^S(\varepsilon;\mathbf{r},\mathbf{r}')\ \mathrm{I}_2 =$$
$$= -\mathrm{i}p\sum_Q j_\ell(pr_<)\ h_\ell^+(pr_>)\,\chi_Q(\hat{\mathbf{r}})\chi_Q(\hat{\mathbf{r}}')^+ \tag{3.189}$$
$$= -\mathrm{i}p\sum_Q j_{\bar{\ell}}(pr_<)\ h_{\bar{\ell}}^+(pr_>)\,\chi_{\bar{Q}}(\hat{\mathbf{r}})\chi_{\bar{Q}}(\hat{\mathbf{r}}')^+ \quad , \tag{3.190}$$

where the last equation has been obtained by changing the variable κ to $-\kappa$ in (3.189). $\mathcal{G}_0^D(\varepsilon;\mathbf{r},\mathbf{r}')$ can then be written as a 2×2 matrix,

$$G_0^D(\varepsilon;\mathbf{r},\mathbf{r}') = \begin{bmatrix} G_{0,11}(\varepsilon;\mathbf{r},\mathbf{r}')\ G_{0,12}(\varepsilon;\mathbf{r},\mathbf{r}') \\ G_{0,21}(\varepsilon;\mathbf{r},\mathbf{r}')\ G_{0,22}(\varepsilon;\mathbf{r},\mathbf{r}') \end{bmatrix} \quad , \tag{3.191}$$

with

$$G_{0,11}(\varepsilon;\mathbf{r},\mathbf{r}') = -\mathrm{i}p\frac{W+mc^2}{2mc^2}\times$$
$$\sum_Q j_\ell(pr_<)\ h_\ell^+(pr_>)\,\chi_Q(\hat{\mathbf{r}})\chi_Q(\hat{\mathbf{r}}')^+ \quad , \tag{3.192}$$

$$G_{0,22}(\varepsilon;\mathbf{r},\mathbf{r}') = \frac{W-mc^2}{W+mc^2}G_{0,11}(z;\mathbf{r},\mathbf{r}')$$
$$= -\mathrm{i}p\frac{W-mc^2}{2mc^2}\sum_Q j_{\bar{\ell}}(pr')\ h_{\bar{\ell}}^+(pr)\,\chi_{\bar{Q}}(\hat{\mathbf{r}})\chi_{\bar{Q}}(\hat{\mathbf{r}}')^+ \quad , \tag{3.193}$$

$$G_{0,12}(\varepsilon;\mathbf{r},\mathbf{r}') = G_{0,21}(\varepsilon;\mathbf{r},\mathbf{r}')$$
$$= -\mathrm{i}p\frac{c\sigma\cdot\mathbf{p}}{2mc^2}\sum_Q j_\ell(pr_<)\ h_\ell^+(pr_>)\,\chi_Q(\hat{\mathbf{r}})\chi_Q(\hat{\mathbf{r}}')^+ \quad . \tag{3.194}$$

Consider now $r > r'$. By using trivial manipulations as well as (3.178)–(3.180), one can reformulate (3.193) and (3.194) as follows

$$G_{0,22}(\varepsilon;\mathbf{r},\mathbf{r}') = -\mathrm{i}p\frac{W+mc^2}{2mc^2}\times$$
$$\sum_Q \frac{-\mathrm{i}S_\kappa cp}{W+mc^2}j_{\bar{\ell}}(pr')\ \frac{\mathrm{i}S_\kappa cp}{W+mc^2}h_{\bar{\ell}}^+(pr)\,\chi_{\bar{Q}}(\hat{\mathbf{r}})\chi_{\bar{Q}}(\hat{\mathbf{r}}')^+ \quad , \tag{3.195}$$

$$G_{0,21}(\varepsilon;\mathbf{r},\mathbf{r}') = -\mathrm{i}p\frac{W+mc^2}{2mc^2}\times$$
$$\sum_Q j_\ell(pr')\ \frac{\mathrm{i}S_\kappa cp}{W+mc^2}h_{\bar{\ell}}^+(pr)\,\chi_{\bar{Q}}(\hat{\mathbf{r}})\chi_Q(\hat{\mathbf{r}}')^+ \quad , \tag{3.196}$$

$$G_{0,12}\left(\varepsilon;\mathbf{r},\mathbf{r}'\right)=-\mathrm{i}p\frac{W+mc^2}{2mc^2}\times \sum_{Q}\frac{-\mathrm{i}S_\kappa cp}{W+mc^2}\,j_{\bar{\ell}}\left(pr'\right)\,h_\ell^+\left(pr\right)\chi_Q(\hat{\mathbf{r}})\chi_{\bar{Q}}(\hat{\mathbf{r}}')^+ \quad . \tag{3.197}$$

Note that (3.197) has been deduced from (3.196) by changing again the variable κ to $-\kappa$ and by using the relation $S_{-\kappa}=-S_\kappa$. Combining the terms in (3.192), (3.195), (3.196) and (3.197), $\mathcal{G}_0^D\left(\varepsilon;\mathbf{r},\mathbf{r}'\right)$ obviously can be written as

$$G_0^D\left(\varepsilon;\mathbf{r},\mathbf{r}'\right)=-\mathrm{i}p\frac{W+mc^2}{2mc^2}\sum_{Q}h_Q^+\left(\varepsilon;\mathbf{r}\right)j_Q\left(\varepsilon;\mathbf{r}'\right)^\times \quad , \tag{3.198}$$

where $h_Q^+\left(\varepsilon;\mathbf{r}\right)$ is defined as in (3.180) in terms of spherical Hankel-functions, h_ℓ^+. As a relativistic counterpart of (3.85) the below definition shall therefore be introduced

$$f_{\kappa\mu}\left(\varepsilon;\mathbf{r}\right)^\times=\left[\,f_\ell\left(\tfrac{pr}{\hbar}\right)\chi_{\kappa\mu}(\hat{\mathbf{r}})^+\;,\;\tfrac{-\mathrm{i}S_\kappa pc}{W+mc^2}f_{\bar{\ell}}\left(\tfrac{pr}{\hbar}\right)\chi_{-\kappa\mu}(\hat{\mathbf{r}})^+\,\right] \quad , \tag{3.199}$$
$$f_\ell=j_\ell,n_\ell \text{ and } h_\ell^\pm \quad .$$

In here, the relation

$$c^2p^2=W^2-m^2c^4=\left(\varepsilon+mc^2\right)^2-m^2c^4 \tag{3.200}$$

has again to be emphasized.

For the case of $r'>r$ (3.195), (3.196) and (3.197) have to be replaced by

$$G_{0,22}\left(\varepsilon;\mathbf{r},\mathbf{r}'\right)=-\mathrm{i}p\frac{W+mc^2}{2mc^2}\times \sum_{Q}\frac{\mathrm{i}S_\kappa cp}{W+mc^2}j_{\bar{\ell}}\left(pr\right)\,\frac{-\mathrm{i}S_\kappa cp}{W+mc^2}h_{\bar{\ell}}^+\left(pr'\right)\chi_{\bar{Q}}(\hat{\mathbf{r}})\chi_{\bar{Q}}(\hat{\mathbf{r}}')^+ \quad , \tag{3.201}$$

$$G_{0,21}\left(\varepsilon;\mathbf{r},\mathbf{r}'\right)=-\mathrm{i}p\frac{W+mc^2}{2mc^2}\times \sum_{Q}\frac{\mathrm{i}S_\kappa cp}{W+mc^2}\,j_{\bar{\ell}}\left(pr\right)\,h_\ell^+\left(pr'\right)\chi_{\bar{Q}}(\hat{\mathbf{r}})\chi_Q(\hat{\mathbf{r}}')^+ \quad , \tag{3.202}$$

$$G_{0,12}\left(\varepsilon;\mathbf{r},\mathbf{r}'\right)=-\mathrm{i}p\frac{W+mc^2}{2mc^2}\times \sum_{Q}j_\ell\left(pr'\right)\frac{-\mathrm{i}S_\kappa cp}{W+mc^2}\,h_{\bar{\ell}}^+\left(pr'\right)\chi_Q(\hat{\mathbf{r}})\chi_{\bar{Q}}(\hat{\mathbf{r}}')^+ \quad . \tag{3.203}$$

Thus one gets

$$G_0^D\left(\varepsilon;\mathbf{r},\mathbf{r}'\right)=-\mathrm{i}p\frac{W+mc^2}{2mc^2}\sum_Q j_Q\left(\varepsilon;\mathbf{r}\right)\,h_Q^+\left(\varepsilon;\mathbf{r}'\right)^\times \quad . \tag{3.204}$$

The single-center expansion of $\mathcal{G}_0^D\left(\varepsilon;\mathbf{r},\mathbf{r}'\right)$ can then be written as

$$\begin{aligned}&G_0^D\left(\varepsilon;\mathbf{r},\mathbf{r}'\right)=-\mathrm{i}p\frac{W+mc^2}{2mc^2}\times\\&\sum_Q\left(h_Q^+\left(\varepsilon;\mathbf{r}\right)j_Q\left(\varepsilon;\mathbf{r}'\right)^\times\,\Theta\left(r-r'\right)+j_Q\left(\varepsilon;\mathbf{r}\right)h_Q^+\left(\varepsilon;\mathbf{r}'\right)^\times\,\Theta\left(r'-r\right)\right) \quad ,\end{aligned} \tag{3.205}$$

and has to be regarded as the relativistic analogon of (3.84). Furthermore, by introducing row- and column- vectors, see (3.89) and (3.90), composed now from four-component wavefunctions of type (3.180) and (3.199), (3.205) can be written compactly as

$$\begin{aligned}G_0^D\left(\varepsilon;\mathbf{r},\mathbf{r}'\right)=&-\mathrm{i}p\frac{W+mc^2}{2mc^2}\times\\&\left(\mathsf{h}^+\left(\varepsilon;\mathbf{r}\right)\mathsf{j}\left(\varepsilon;\mathbf{r}'\right)^\times\,\Theta\left(r-r'\right)+\mathsf{j}\left(\varepsilon;\mathbf{r}\right)\mathsf{h}^+\left(\varepsilon;\mathbf{r}'\right)^\times\,\Theta\left(r'-r\right)\right) \quad .\end{aligned} \tag{3.206}$$

Assuringly enough, the above expression satisfies the analyticity condition for the Green's function, namely, for $\mathrm{Im}p>0$

$$\begin{aligned}G_0^D\left(z;\mathbf{r}',\mathbf{r}\right)^+=&\,\mathrm{i}p^*\frac{W^*+mc^2}{2mc^2}\times\\&\left(\mathsf{h}^-\left(z;\mathbf{r}\right)\mathsf{j}\left(z;\mathbf{r}'\right)^\times\,\Theta\left(r-r'\right)+\mathsf{j}\left(z;\mathbf{r}\right)\mathsf{h}^-\left(z;\mathbf{r}'\right)^\times\,\Theta\left(r'-r\right)\right)\\=&\,G_0^D\left(z^*;\mathbf{r},\mathbf{r}'\right) \quad ,\end{aligned} \tag{3.207}$$

which is indeed consistent with (3.87).

Two-center expansion

In order to obtain a two-center expansion of the relativistic free-particle Green's function a slightly different strategy as compared to the previous section has to be applied. Since as far as the space variables are concerned, $\mathcal{G}_0^S\left(p^2/2m;\mathbf{r},\mathbf{r}'\right)$ depends on $|\mathbf{r}-\mathbf{r}'|$ only, the configuration space representation of (3.188) is given by

$$\begin{aligned}G_0^D\left(\varepsilon;\mathbf{r},\mathbf{r}'\right)=&\frac{1}{2mc^2}\begin{bmatrix}\left(W+mc^2\right)\mathsf{I}_2 & c\sigma\cdot\mathbf{p}\\ c\sigma\cdot\mathbf{p} & \left(W-mc^2\right)\mathsf{I}_2\end{bmatrix}\times\\&\mathcal{G}_0^S\left(p^2/2m;\mathbf{r},\mathbf{r}'\right)\,\mathsf{I}_4 \quad ,\end{aligned} \tag{3.208}$$

which can be rewritten as

$$G_0^D\left(\varepsilon;\mathbf{r},\mathbf{r}'\right)=\frac{W+mc^2}{2mc^2}\begin{bmatrix}\mathsf{I}_2 & \frac{c\sigma\mathbf{p}'}{W+mc^2}\\ \frac{c\sigma\cdot\mathbf{p}}{W+mc^2} & \frac{c\sigma\cdot\mathbf{p}}{W+mc^2}\frac{c\sigma\cdot\mathbf{p}'}{W+mc^2}\end{bmatrix}\times \mathcal{G}_0^S\left(p^2/2m;\mathbf{r},\mathbf{r}'\right)\mathsf{I}_4 \quad . \tag{3.209}$$

Therefore, the components of the Green's function, $G_{0,ij}\left(\varepsilon;\mathbf{r},\mathbf{r}'\right),\ i,j=1,2$, as defined in (3.191), can be expressed as

$$G_{0,11}\left(\varepsilon;\mathbf{r},\mathbf{r}'\right)=\frac{W+mc^2}{2mc^2}\mathcal{G}_0^S\left(p^2/2m;|\mathbf{r}-\mathbf{r}'|\right)\mathsf{I}_2 \quad , \tag{3.210}$$

$$G_{0,22}\left(\varepsilon;\mathbf{r},\mathbf{r}'\right)= \frac{c\sigma\cdot\mathbf{p}}{W+mc^2}\frac{W+mc^2}{2mc^2}\mathcal{G}_0^S\left(p^2/2m;|\mathbf{r}-\mathbf{r}'|\right)\mathsf{I}_2\frac{c\sigma\cdot\mathbf{p}'}{W+mc^2} \quad , \tag{3.211}$$

$$G_{0,12}\left(\varepsilon;\mathbf{r},\mathbf{r}'\right)=\frac{c\sigma\cdot\mathbf{p}}{W+mc^2}\frac{W+mc^2}{2mc^2}\mathcal{G}_0^S\left(p^2/2m;|\mathbf{r}-\mathbf{r}'|\right)\mathsf{I}_2 \quad , \tag{3.212}$$

and

$$G_{0,22}\left(\varepsilon;\mathbf{r},\mathbf{r}'\right)=\frac{W+mc^2}{2mc^2}\mathcal{G}_0^S\left(p^2/2m;|\mathbf{r}-\mathbf{r}'|\right)\mathsf{I}_2\frac{c\sigma\cdot\mathbf{p}'}{W+mc^2} \quad . \tag{3.213}$$

Furthermore, one has to recall the two-center expansion in the non-relativistic case, see (3.95),

$$G_0^S\left(p^2/2m;\mathbf{r}_n+\mathbf{R}_n,\mathbf{r}'_m+\mathbf{R}_m\right)= \sum_{LL'} j_\ell\left(pr_n\right)Y_L\left(\hat{\mathbf{r}}_n\right)G_{0,LL'}^{S,nm}\left(p\right)\ j_{\ell'}\left(pr'_m\right)Y_{L'}\left(\hat{\mathbf{r}}'_m\right)^* \quad , \tag{3.214}$$

where the non-relativistic structure constants $G_{0,LL'}^{S,nm}\left(p\right)$ are given in (3.104). By using the transformation between the ℓms- and the $\kappa\mu$-representation, see (3.173),

$$\begin{aligned}
&\frac{W+mc^2}{2mc^2}G_0^S\left(p^2/2m;\mathbf{r}_n+\mathbf{R}_n,\mathbf{r}'_m+\mathbf{R}_m\right)\mathsf{I}_2 = \\
&=\frac{W+mc^2}{2mc^2}\sum_{LL'}\sum_s j_\ell\left(pr_n\right)G_{0,LL'}^{S,nm}\left(p\right)\ j_{\ell'}\left(pr'_m\right)\varphi_{Ls}\left(\hat{\mathbf{r}}_n\right)\varphi_{L's}\left(\hat{\mathbf{r}}'_m\right)^+ \\
&=\frac{W+mc^2}{2mc^2}\sum_{LL'}\sum_s j_\ell\left(pr_n\right)G_{0,LL'}^{S,nm}\left(p\right)j_{\ell'}\left(pr'_m\right)\times \\
&\qquad\sum_{\kappa=\ell\pm\frac{1}{2}}\sum_{\kappa'=\ell'\pm\frac{1}{2}}C(\ell,\kappa,\frac{1}{2}|\ m,s)C(\ell',\kappa',\frac{1}{2}|\ m',s)\times \\
&\qquad\qquad\chi_{\kappa,m+s}\left(\hat{\mathbf{r}}_n\right)\chi_{\kappa',m'+s}\left(\hat{\mathbf{r}}'_m\right)^+ \\
&=\sum_{QQ'} j_\ell\left(pr_n\right)\chi_Q\left(\hat{\mathbf{r}}_n\right)G_{0,QQ'}^{D,nm}\left(\varepsilon\right)\ j_{\ell'}\left(pr'_m\right)\chi_{Q'}\left(\hat{\mathbf{r}}'_m\right)^+ \quad ,
\end{aligned} \tag{3.215}$$

the *relativistic structure constants* are now given by

$$G^{D,nm}_{0,QQ'}(\varepsilon) \equiv \frac{W+mc^2}{2mc^2}\times$$
$$\sum_s C(\ell,\kappa,\frac{1}{2}|\,\mu-s,s)\,G^{S,nm}_{0,\ell(\mu-s),\ell'(\mu'-s)}(p)\;C(\ell',\kappa',\frac{1}{2}|\,\mu'-s,s) \quad . \tag{3.216}$$

Inserting now (3.215) into (3.210)-(3.213) and applying (3.182), special attention has to be given to the expression

$$j_{\ell'}(pr'_m)\,\chi_{Q'}(\hat{\mathbf{r}}'_m)^+\,\frac{c\sigma\cdot\mathbf{p}'}{W+mc^2} = \frac{-\mathrm{i}S_\kappa pc}{W+mc^2}\,j_{\bar{\ell}}\left(\frac{pr'_m}{\hbar}\right)\chi_{\bar{Q}'}(\hat{\mathbf{r}}'_m)^+ \quad , \tag{3.217}$$

since it is valid only for $p\in\mathbb{R}$. However, in terms of an analytic continuation the following expression for the Green's function applies for any p provided $\mathrm{Im}p>0$,

$$G^D_0(\varepsilon;\mathbf{r}_n+\mathbf{R}_n,\mathbf{r}'_m+\mathbf{R}_m) = \sum_{QQ'} j_Q(\varepsilon;\mathbf{r}_n)\;G^{D,nm}_{0,QQ'}(\varepsilon)\;\;j_{Q'}(\varepsilon;\mathbf{r}'_m)^\times \quad , \tag{3.218}$$

or,

$$G^D_0(\varepsilon;\mathbf{r}_n+\mathbf{R}_n,\mathbf{r}'_m+\mathbf{R}_m) = \mathsf{j}(\varepsilon;\mathbf{r}_n)\;\underline{G}^{D,nm}_0(\varepsilon)\;\mathsf{j}(\varepsilon;\mathbf{r}'_m)^\times \quad , \tag{3.219}$$

where similar to (3.97) a matrix notation for the structure constants is introduced

$$\underline{G}^{D,nm}_0(z) = \left\{G^{D,nm}_{0,QQ'}(z)\right\} \quad . \tag{3.220}$$

In full analogy to (3.105) the relativistic free-particle Green's function (omitting from now on the subscript D) is given therefore by

$$\begin{aligned} G_0(\varepsilon;\mathbf{r}_n+\mathbf{R}_n,\mathbf{r}'_m+\mathbf{R}_m) = {} & \\ & (1-\delta_{nm})\,\mathsf{j}(\varepsilon;\mathbf{r}_n)\,\underline{G}^{nm}_0(\varepsilon)\,\mathsf{j}(\varepsilon;\mathbf{r}'_m)^\times \\ & -\mathrm{i}p\,\delta_{nm}\,\Big\{\mathsf{h}^+(\varepsilon;\mathbf{r}_n)\,\mathsf{j}(\varepsilon;\mathbf{r}'_n)^\times\,\Theta(r_n-r'_n) \\ & \qquad +\mathsf{j}(\varepsilon;\mathbf{r}_n)\,\mathsf{h}^+(\varepsilon;\mathbf{r}'_n)^\times\,\Theta(r'_n-r_n)\Big\} \quad . \end{aligned} \tag{3.221}$$

In the forthcoming discussion of relativistic multiple scattering theory the so-called *weak relativistic limit* ($p\ll mc$) shall be used, namely

$$\begin{aligned} p &= \frac{1}{c}\sqrt{W^2-m^2c^4} = \frac{1}{c}\sqrt{(\varepsilon+mc^2)^2-m^2c^4} \\ &= \frac{\sqrt{\varepsilon}}{c}\sqrt{\varepsilon-2mc^2} = \sqrt{2m\varepsilon}\sqrt{1-\frac{\varepsilon}{2mc^2}} \approx \sqrt{2m\varepsilon} \quad . \end{aligned} \tag{3.222}$$

and

$$W + mc^2 \approx 2mc^2 \quad , \tag{3.223}$$

such that

$$\frac{\mathrm{i}S_\kappa pc}{W + mc^2} \approx \frac{\mathrm{i}S_\kappa p}{2mc} \quad . \tag{3.224}$$

or, in Rydberg units:

$$2m = 1 \; , \; \hbar = 1 \quad , \quad e^2 = 2 \quad , \quad c = \frac{2}{\alpha} \sim 274.072 \quad , \tag{3.225}$$

$$p \approx \sqrt{\varepsilon} \quad , \tag{3.226}$$

$$\frac{\mathrm{i}S_\kappa pc}{W + mc^2} \approx \frac{\mathrm{i}S_\kappa p}{c} \quad . \tag{3.227}$$

3.5.4 Relativistic single-site and multi-site scattering

As was to be seen in the non-relativistic case the operator equations given in Sect. 3.3 and the expansion of the non-relativistic free-particle Green's function in (3.105) led unambiguously to the fundamental equations of multiple scattering, (3.74) and (3.133), as well as to expressions of the Green's function for an ensemble of individual scattering potentials, see (3.136). Based on the analogy between the expansions of the free-particle Green's function in the non-relativistic case, (3.105), and in the relativistic case, (3.221), the derivation of the fundamental equations of multiple scattering and the one-electron Green's function in the relativistic case is indeed straightforward. Therefore, for matters of completeness in the following only a list of the most important expressions is given.

For $\mathbf{r}_n \notin D_{V_n}$ the *right-hand-side* regular scattering solutions of the single-scatterer problem,

$$\left(c\boldsymbol{\alpha} \cdot \mathbf{p} + \beta mc^2 + U_n\left(\mathbf{r}_n\right) - z\right) \left\{ \begin{array}{c} R_Q^n\left(z; \mathbf{r}_n\right) \\ Z_Q^n\left(z; \mathbf{r}_n\right) \end{array} \right\} = 0 \quad , \tag{3.228}$$

join smoothly the functions

$$R_Q^n\left(z; \mathbf{r}_n\right) = j_Q\left(z; \mathbf{r}_n\right) - \mathrm{i}p \sum_{Q'} h_{Q'}^+\left(z; \mathbf{r}_n\right) \, t_{Q'Q}^n\left(z\right) \quad , \tag{3.229}$$

$$Z_Q^n\left(z; \mathbf{r}_n\right) = \sum_{Q'} j_{Q'}\left(z; \mathbf{r}_n\right) P_{Q'Q}^n\left(z\right) + pn_Q\left(z; \mathbf{r}_n\right) \quad , \tag{3.230}$$

where

$$\underline{t}^n\left(z\right) = \left\{t_{QQ'}^n\left(z\right)\right\} \quad , \tag{3.231}$$

is the single-site t-matrix and

$$\underline{P}^n\left(z\right) = \left\{P_{QQ'}^n\left(z\right)\right\} \tag{3.232}$$

refers to the inverse of the reactance matrix, $\underline{K}^n(z)$, defined as

$$\underline{P}^n(z) \equiv \underline{K}^n(z)^{-1} = \underline{t}^n(z)^{-1} - \mathrm{i}p\underline{I} \quad . \tag{3.233}$$

Written in terms of scattering solutions,

$$R^n_Q(z;\mathbf{r}_n) = \sum_{Q'} \begin{pmatrix} g^{R,n}_{Q'Q}(z;r_n)\,\chi_{Q'}(\hat{\mathbf{r}}_n) \\ \mathrm{i}f^{R,n}_{Q'Q}(z;r_n)\,\chi_{\bar{Q}'}(\hat{\mathbf{r}}_n) \end{pmatrix} \quad , \tag{3.234}$$

$$Z^n_Q(z;\mathbf{r}_n) = \sum_{Q'} \begin{pmatrix} g^{Z,n}_{Q'Q}(z;r_n)\,\chi_{Q'}(\hat{\mathbf{r}}_n) \\ \mathrm{i}f^{Z,n}_{Q'Q}(z;r_n)\,\chi_{\bar{Q}'}(\hat{\mathbf{r}}_n) \end{pmatrix} \quad , \tag{3.235}$$

Equations (3.229) and (3.230) imply the following matching conditions for the *big* and *small* radial components of $R^n_Q(z;\mathbf{r}_n)$ and $Z^n_Q(z;\mathbf{r}_n)$:

$$g^{R,n}_{Q'Q}(z;r_n) = j_\ell(pr_n)\,\delta_{QQ'} - \mathrm{i}ph^+_{\ell'}(pr_n)\,t^n_{Q'Q}(z) \quad , \tag{3.236}$$

$$f^{Z,n}_{Q'Q}(z;r_n) = \frac{S_\kappa p}{c}\left(j_{\bar{\ell}}(pr_n)\,\delta_{QQ'} - \mathrm{i}ph^+_{\bar{\ell}'}(pr_n)\,t^n_{Q'Q}(z)\right) \quad , \tag{3.237}$$

$$g^{Z,n}_{Q'Q}(z;r_n) = j_{\ell'}(pr_n)\,P^n_{Q'Q}(z) + pn_\ell(pr_n)\,\delta_{QQ'} \quad , \tag{3.238}$$

and

$$f^{Z,n}_{Q'Q}(z;r_n) = \frac{S_\kappa p}{c}\left(j_{\bar{\ell}'}(pr_n)\,P^n_{Q'Q}(\varepsilon) + pn_{\bar{\ell}}(pr_n)\,\delta_{QQ'}\right) \quad . \tag{3.239}$$

For $\mathbf{r}_n \notin D_{V_n}$ the corresponding irregular scattering solutions, $H^n_Q(\varepsilon;\mathbf{r}_n)$ and $J^n_Q(\varepsilon;\mathbf{r}_n)$, satisfy the conditions

$$H^n_Q(\varepsilon;\mathbf{r}_n) = -\mathrm{i}ph^+_Q(\varepsilon;\mathbf{r}_n) \quad , \tag{3.240}$$

$$J^n_Q(\varepsilon;\mathbf{r}_n) = j_Q(\varepsilon;\mathbf{r}_n) \quad . \tag{3.241}$$

The *left-hand-side* solutions of the Dirac equation,

$$\left(c\boldsymbol{\alpha}\cdot\mathbf{p} + \beta mc^2 + U_n(\mathbf{r}_n) - z^*\right)\left\{\begin{matrix} \widetilde{R}^n_Q(z;\mathbf{r}_n) \\ \widetilde{Z}^n_Q(z;\mathbf{r}_n) \end{matrix}\right\} = 0 \quad , \tag{3.242}$$

are obviously related to the *right-hand-side* solutions by

$$\left.\begin{matrix} \widetilde{R}^n_Q(z;\mathbf{r}_n) \\ \widetilde{Z}^n_Q(z;\mathbf{r}_n) \end{matrix}\right\} = \left\{\begin{matrix} R^n_Q(z^*;\mathbf{r}_n) \\ Z^n_Q(z^*;\mathbf{r}_n) \end{matrix}\right. \quad , \tag{3.243}$$

and are therefore normalized as

$$\widetilde{R}^n_Q(z;\mathbf{r}_n)^\dagger = j_Q(z;\mathbf{r}_n)^\times - \mathrm{i}p\sum_{Q'} t^n_{QQ'}(z)\; h^+_{Q'}(z;\mathbf{r}_n)^\times \quad , \tag{3.244}$$

$$\widetilde{Z}_{Q}^{n}\left(z;\mathbf{r}_{n}\right)^{\dagger}=\sum_{Q'}P_{QQ'}^{n}\left(z\right)\;j_{Q'}\left(z;\mathbf{r}_{n}\right)^{\times}+pn_{Q}\left(z;\mathbf{r}_{n}\right)^{\times}\quad . \tag{3.245}$$

As was pointed out by Tamura [10], only in the case of a collinear (effective) magnetic field in which the z axis of the local coordination system can be chosen parallel to the field and therefore only the diagonal Σ_z matrix enters the Hamiltonian, there is a direct relation between the left-hand-side and the right-hand-side solutions, namely

$$\left.\begin{array}{c}\widetilde{R}_{Q}^{n}\left(z;\mathbf{r}_{n}\right)^{\dagger}\\ \widetilde{Z}_{Q}^{n}\left(z;\mathbf{r}_{n}\right)^{\dagger}\end{array}\right\}=\left\{\begin{array}{l}R_{Q}^{n}\left(z;\mathbf{r}_{n}\right)^{\times}\\ Z_{Q}^{n}\left(z;\mathbf{r}_{n}\right)^{\times}\end{array}\right.\quad , \tag{3.246}$$

or, expressed in terms of radial components,

$$\widetilde{R}_{Q}^{n}\left(z;\mathbf{r}_{n}\right)^{\dagger}=\sum_{Q'}\left(g_{Q'Q}^{R,n}\left(z;r_{n}\right)\chi_{Q'}\left(\hat{\mathbf{r}}_{n}\right)^{\dagger}\;-\mathrm{i}f_{Q'Q}^{R,n}\left(z;r_{n}\right)\chi_{\bar{Q}'}\left(\hat{\mathbf{r}}_{n}\right)^{\dagger}\right)\quad , \tag{3.247}$$

$$\widetilde{Z}_{Q}^{n}\left(z;\mathbf{r}_{n}\right)^{\dagger}=\sum_{Q'}\left(g_{Q'Q}^{Z,n}\left(z;r_{n}\right)\chi_{Q'}\left(\hat{\mathbf{r}}_{n}\right)^{\dagger}\;-\mathrm{i}f_{Q'Q}^{Z,n}\left(z;r_{n}\right)\chi_{\bar{Q}'}\left(\hat{\mathbf{r}}_{n}\right)^{\dagger}\right)\quad . \tag{3.248}$$

For $\mathbf{r}_n \notin D_{V_n}$ the normalization of the corresponding irregular scattering solutions, $\widetilde{H}_{Q}^{n}\left(\varepsilon;\mathbf{r}_{n}\right)$ and $\widetilde{J}_{Q}^{n}\left(\varepsilon;\mathbf{r}_{n}\right)$, reads as follows

$$\widetilde{H}_{Q}^{n}\left(z;\mathbf{r}_{n}\right)^{\dagger}=-\mathrm{i}ph_{Q}^{+}\left(z;\mathbf{r}_{n}\right)^{\times}\quad , \tag{3.249}$$

$$\widetilde{J}_{Q}^{n}\left(z;\mathbf{r}_{n}\right)^{\dagger}=j_{Q}\left(z;\mathbf{r}_{n}\right)^{\times}\quad . \tag{3.250}$$

Formally analogous to the non-relativistic case the (super-) matrix representations of the single-site scattering matrices, the structure constants, the scattering path operator, and the structural resolvent are therefore given by

$$\mathbf{t}\left(z\right)=\{\underline{t}^{n}\left(z\right)\}\quad ,\quad \mathbf{G}_{0}\left(z\right)=\{\underline{G}_{0}^{nm}\left(z\right)\left(1-\delta_{nm}\right)\}\quad , \tag{3.251}$$

$$\tau\left(z\right)=\left(\mathbf{t}\left(z\right)^{-1}-\mathbf{G}_{0}\left(z\right)\right)^{-1}\quad , \tag{3.252}$$

$$\mathbf{G}\left(z\right)=\mathbf{G}_{0}\left(z\right)\left(\mathbf{I}-\mathbf{t}\left(z\right)\mathbf{G}_{0}\left(z\right)\right)^{-1}\quad , \tag{3.253}$$

By using the by now familiar vector notation for the scattering solutions the Green's function is then defined by

$$\begin{aligned}G\left(z;\mathbf{r}_{n}+\mathbf{R}_{n},\mathbf{r}'_{m}+\mathbf{R}_{m}\right)=&\\ &\mathsf{R}^{n}\left(z;\mathbf{r}_{n}\right)\underline{G}^{nm}\left(z\right)\widetilde{\mathsf{R}}^{m}\left(z;\mathbf{r}'_{m}\right)^{\dagger}\\ +\delta_{nm}&\left\{\mathsf{H}^{n}\left(z;\mathbf{r}_{n}\right)\widetilde{\mathsf{R}}^{n}\left(z;\mathbf{r}'_{n}\right)^{\dagger}\Theta\left(r_{n}-r'_{n}\right)\right.\\ &\left.+\mathsf{R}^{n}\left(z;\mathbf{r}_{n}\right)\widetilde{\mathsf{H}}^{n}\left(z;\mathbf{r}'_{n}\right)^{\dagger}\Theta\left(r'_{n}-r_{n}\right)\right\}\quad ,\end{aligned} \tag{3.254}$$

or, alternatively, can be expressed as

$$\begin{aligned} G\left(z;\mathbf{r}_n+\mathbf{R}_n,\mathbf{r}'_m+\mathbf{R}_m\right) = \\ \mathsf{Z}^n\left(z;\mathbf{r}_n\right)\,\underline{\tau}^{nm}\left(z\right)\,\widetilde{\mathsf{Z}}^m\left(z;\mathbf{r}'_m\right)^\dagger \\ -\,\delta_{nm}\,\Big\{\mathsf{J}^n\left(z;\mathbf{r}_n\right)\,\widetilde{\mathsf{Z}}^n\left(z;\mathbf{r}'_n\right)^\dagger\,\Theta\left(r_n-r'_n\right) \\ +\mathsf{Z}^n\left(z;\mathbf{r}_n\right)\,\widetilde{\mathsf{J}}^n\left(z;\mathbf{r}'_n\right)^\dagger\,\Theta\left(r'_n-r_n\right)\Big\} \quad , \end{aligned} \tag{3.255}$$

which *only in the case* that the effective fields point uniformly along the z axis of the local coordinate frame, see (3.246), can be transformed to

$$\begin{aligned} G\left(z;\mathbf{r}_n+\mathbf{R}_n,\mathbf{r}'_m+\mathbf{R}_m\right) = \\ \mathsf{R}^n\left(z;\mathbf{r}_n\right)\,\underline{G}^{nm}\left(z\right)\,\mathsf{R}^m\left(z;\mathbf{r}'_m\right)^\times \\ +\,\delta_{nm}\,\Big\{\mathsf{H}^n\left(z;\mathbf{r}_n\right)\,\mathsf{R}^n\left(z;\mathbf{r}'_n\right)^\times\,\Theta\left(r_n-r'_n\right) \\ +\mathsf{R}^n\left(z;\mathbf{r}_n\right)\,\mathsf{H}^n\left(z;\mathbf{r}'_n\right)^\times\,\Theta\left(r'_n-r_n\right)\Big\} \quad , \end{aligned} \tag{3.256}$$

or, equivalently, to

$$\begin{aligned} G\left(z;\mathbf{r}_n+\mathbf{R}_n,\mathbf{r}'_m+\mathbf{R}_m\right) = \\ \mathsf{Z}^n\left(z;\mathbf{r}_n\right)\,\underline{\tau}^{nm}\left(z\right)\,\mathsf{Z}^m\left(z;\mathbf{r}'_m\right)^\times \\ -\,\delta_{nm}\,\Big\{\mathsf{J}^n\left(z;\mathbf{r}_n\right)\,\mathsf{Z}^n\left(z;\mathbf{r}'_n\right)^\times\,\Theta\left(r_n-r'_n\right) \\ +\mathsf{Z}^n\left(z;\mathbf{r}_n\right)\,\mathsf{J}^n\left(z;\mathbf{r}'_n\right)^\times\,\Theta\left(r'_n-r_n\right)\Big\} \quad . \end{aligned} \tag{3.257}$$

3.6 "Scalar relativistic" formulations

Very often terms like *scalar relativistic* or *pseudo-relativistic* are found in the literature. Since the "various levels of relativistic description" are quite frequently misunderstood, the elimination method is applied in the following to trace these levels. By writing the Dirac-type Hamiltonian for a non-magnetic system, see (3.158), in atomic units ($\hbar = m = 1$)

$$\mathcal{H} = c\boldsymbol{\alpha}\cdot\mathbf{p} + \left(\boldsymbol{\beta}-\mathsf{I}_4\right)c^2 + V\mathsf{I}_4 \quad , \tag{3.258}$$

and making use of the bi-spinors property of the wavefunction $|\psi\rangle = |\phi,\chi\rangle$, the corresponding eigenvalue equation can be split into two equations

$$\begin{aligned} c\boldsymbol{\sigma}\cdot\mathbf{p}\,|\chi\rangle - V\,|\phi\rangle = \epsilon\,|\phi\rangle \quad , \\ c\boldsymbol{\sigma}\cdot\mathbf{p}\,|\phi\rangle + \left(V-2c^2\right)|\chi\rangle = \epsilon\,|\chi\rangle \quad . \end{aligned} \tag{3.259}$$

Clearly, the spinor $|\chi\rangle$ can now be expressed in terms of $|\phi\rangle$:

$$|\chi\rangle = (1/2c)\,\mathcal{B}^{-1}\sigma\cdot\mathbf{p}\,|\phi\rangle \quad , \tag{3.260}$$

$$\mathcal{B} = 1 + \left(1/2c^2\right)(\epsilon - V) \quad , \tag{3.261}$$

yielding only one equation for $|\phi\rangle$:

$$\mathcal{D}\,|\phi\rangle = \varepsilon\,|\phi\rangle \quad , \tag{3.262}$$

$$\mathcal{D} = (1/2)\,\sigma\cdot\mathbf{p}\mathcal{B}^{-1}\sigma\cdot\mathbf{p} + V \quad . \tag{3.263}$$

Similar to (3.262), the normalization of the wavefunction $|\psi\rangle$ can be expressed in terms of the spinor $|\phi\rangle$:

$$\begin{aligned}\langle\psi|\,\psi\rangle = \langle\phi|\,\phi\rangle + \langle\chi|\,\chi\rangle \\ \langle\phi|\,1 + \left(1/4c^2\right)\sigma\cdot\mathbf{p}\mathcal{B}^{-2}\sigma\cdot\mathbf{p}\,|\phi\rangle \quad .\end{aligned} \tag{3.264}$$

Because of the bi-spinor form of the wavefunction, for a central field the operator $\mathcal{D}$ in (3.262) has the same constants of motion as the Dirac Hamiltonian, namely $\mathcal{J}^2$, $\mathcal{J}_z$, and $\mathcal{K}$. Equation (3.262) is therefore separable with respect to the radial and angular variables. The differential equation (Rosicky *et al.* 1976 [8]) for the radial amplitudes of $|\phi\rangle$, $R_\kappa(r)/r$, written below for matters of simplicity for a spherical symmetric potential $V(r)$,

$$\begin{aligned}\left[\frac{1}{2}\left(-\frac{\mathrm{d}^2}{\mathrm{d}r^2} + \frac{\ell(\ell+1)}{r^2}\right) + V(r) - \epsilon\right] R_\kappa(r) = \\ = \left\{\frac{1}{4c^2}B^{-2}(r)\frac{\mathrm{d}V(r)}{\mathrm{d}r}\frac{\kappa}{r} + \frac{1}{4c^2}\left[\left[\epsilon - V(r)\right]B^{-1}(r)\left(-\frac{\mathrm{d}^2}{\mathrm{d}r^2} + \frac{\ell(\ell+1)}{r^2}\right)\right]\right. \\ \left. + \frac{1}{4c^2}B^{-2}(r)\frac{\mathrm{d}V(r)}{\mathrm{d}r}\frac{\mathrm{d}}{\mathrm{d}r}\right\} R_\kappa(r) \quad ,\end{aligned} \tag{3.265}$$

shows a remarkably "physical structure" , namely as follows:

1. For $c = \infty$ this equation is reduced to the radial Schrödinger equation.
2. By approximating the elimination operator $\mathcal{B}$, (3.261), by unity ($\mathcal{B} = 1$) the Pauli-Schrödinger equation is obtained, where the terms on the right-hand side of (3.265) are respectively the *spin-orbit coupling*, the *mass velocity term*, and the *Darwin shift*.
3. For $\mathcal{B} \neq 1$ relativistic corrections in order higher than c^{-4}, enter the description of the electronic structure via the normalization, (3.264).

In the case $\mathcal{B} \neq 1$, all three terms on the right-hand side of (3.265) have prefactors $1/4c^2$. The only term which is explicitly dependent on the (relativistic) quantum number κ is the spin-orbit coupling. Omitting this term for (3.265) yields an equation where only the eigenvalue of $\mathcal{L}^2$ occurs:

$$\left[\frac{1}{2}\left[1-\left(1/2c^2\right)\left(\epsilon-V\left(r\right)\right)\right]\left(-\frac{\mathrm{d}^2}{\mathrm{d}r^2}+\frac{\ell\left(\ell+1\right)}{r^2}\right)\right.$$
$$\left.+V\left(r\right)-\frac{1}{4c^2}\frac{\mathrm{d}V\left(r\right)}{\mathrm{d}r}\frac{\mathrm{d}}{\mathrm{d}r}-\epsilon\right]R_\ell\left(r\right)=0 \quad . \tag{3.266}$$

Equation (3.266) has the same formal structure as the radial Schrödinger equation. It is a *modified Schrödinger equation* and is the basis of the so-called *scalar relativistic* calculations. The obvious advantage of (3.266) is that 'some' of the relativistic effects are included, namely the mass velocity term and the Darwin shift, and the much simpler symmetry of the Schrödinger equation can still be used.

3.7 Summary

From the previous discussion it is now obvious that the scope of multiple scattering can be partitioned into two main aspects, namely into *single-site t-matrices* and *structure constants*. In the single-site t-matrices all atomic-like information is contained such as non-magnetic or magnetic, shape corrections for the individual potentials or not, etc., while the structure constants reflect essentially the "geometrical arrangement" of the ensemble of scatterers under investigation. In the following therefore first descriptions of single-site t-matrices will be presented, predominantly in view of full-potential scattering, including also numerical details and recipies, followed only then by further formal developments concerning the structure constants and their numerical evaluation.

References

1. A. Gonis, *Green Functions for Ordered and Disordered Systems* (Elsevier, Amsterdam 1992)
2. A. Gonis and W.H. Butler, *Multiple Scattering in Solids* (Springer, New York 2000)
3. L.D. Landau and E.M. Lifschitz, *Lehrbuch der theoretischen Physik*, Vols. III and IV (Akademie, Berlin 1980)
4. T.L. Loucks, *Augmented Plane Wave Method* (Benjamin, New York 1967)
5. A. Messiah, *Quantum Mechanics* (North-Holland, Amsterdam 1969)
6. J.S. Faulkner and G.M. Stocks, Phys. Rev. B **21**, 3222 (1980)
7. M.E. Rose, *Relativistic Electron Theory* (Wiley, New York 1961)
8. F. Rosicky, P. Weinberger, and F. Mark, J. Phys.: Molec. Phys. **9**, 2971 (1976).
9. P. Strange, *Relativistic Quantum Mechanics* (Cambridge University Press, Cambridge 1998)
10. E. Tamura, Phys. Rev. B **45**, 3271 (1992).
11. X. Wang, X.-G. Zhang, W.H. Butler, G.M. Stocks, and B.N. Harmon, Phys. Rev. B **46**, 9352 (1992).

12. P. Weinberger, *Electron Scattering Theory of Ordered and Disordered Matter* (Clarendon Press, Oxford 1992)
13. P. Weinberger, Phil. Mag. B **75**, 509–533 (1997).

4 Shape functions

4.1 The construction of shape functions

If we consider for matters of simplicity a 2D (simple) square lattice for the moment, see Fig. 4.1, where a denotes the length of the unit square (repeated unit) then two critical radii can be defined, namely that of the inscribed circle,

$$r_{\mathrm{C}_1} = r_{\mathrm{MT}} = a/2 \quad , \tag{4.1}$$

usually referred to as "muffin-tin radius" and that of the circumscribed (bounding) circle

$$r_{\mathrm{C}_2} = r_{\mathrm{BS}} = a\sqrt{2} \quad . \tag{4.2}$$

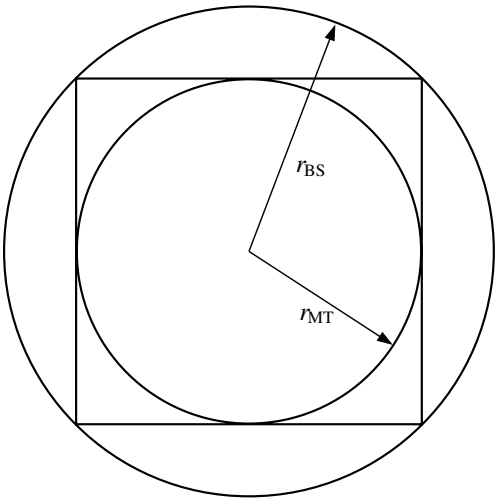

Fig. 4.1. Characteristic radii for a square lattice.

A general convex polyhedron will have a finite number of critical radii at which the sphere intercepts either planes, edges or corners of the polyhedron. The smallest radius is called "muffin-tin radius"and the largest one "circumscribed (bounding) sphere radius"

$$0 < (r_{\mathrm{C}_1} = r_{\mathrm{MT}}) < r_{\mathrm{C}_2} < \ldots < r_{\mathrm{BS}} \quad . \tag{4.3}$$

Let Ω be the region of a convex polyhedron. The shape function of that region is then defined as

$$\sigma(\mathbf{r}) = \begin{cases} 1 & \mathbf{r} \in \Omega \\ 0 & \mathbf{r} \notin \Omega \end{cases} \quad . \tag{4.4}$$

Furthermore, let $Y_L(\hat{\mathbf{r}})$ be the usual complex spherical harmonics,

$$Y_L(\hat{\mathbf{r}}) = Y_{\ell m}(\hat{\mathbf{r}}) = C_{\ell m} P_m^{\ell}(\cos\theta) e^{im\varphi} \quad , \tag{4.5}$$

see also Sect. 3.4.1. Clearly enough for an arbitrary r the function $\sigma(\mathbf{r})$ can be expanded into complex spherical harmonics,

$$\sigma(\mathbf{r}) = \sum_L \sigma_L(r)\, Y_L(\hat{\mathbf{r}}) = \sum_{l=0}^{\infty} \sum_{m=-\ell}^{\ell} \sigma_{\ell m}(r)\, Y_{\ell m}(\hat{\mathbf{r}}) \quad , \tag{4.6}$$

with the *shape functions* appearing as expansion coefficients:

$$\sigma_L(r) = \int_{\Omega} \mathrm{d}\hat{\mathbf{r}}\, \sigma(\mathbf{r})\, Y_L^*(\hat{\mathbf{r}}) \quad . \tag{4.7}$$

Geometrically the so-called *Voronoy polyhedron* (nearest neighbor cell) can precisely be characterized by a set of boundary planes, all given by their normal vector $\mathbf{R}_i$ of magnitude R_i:

$$\mathbf{r} \in \Omega \Leftrightarrow \forall i \ \left(\mathbf{r} \cdot \mathbf{R}_i \leq R_i^2\right) \quad . \tag{4.8}$$

4.1.1 Interception of a boundary plane of the polyhedron with a sphere

Consider now one boundary plane $\mathbf{R}_i = \mathbf{R}_{i,\parallel} + Z_i \mathbf{e}_z, \mathbf{R}_{i,\parallel} = X_i \mathbf{e}_x + Y_i \mathbf{e}_y$, and a sphere of given radius r. If $\mathbf{R}_{i,\parallel} = \mathbf{0}$, i.e., $\mathbf{R}_i$ points in z direction, a special case arrises that will be considered separately. One can always rotate the coordinate system by an angle $\phi_0 = \arccos\left(X_i / \sqrt{X_i^2 + Y_i^2}\right)$ around the z axis such that $\mathbf{R}_{i,\parallel} = X_i \mathbf{e}_x$ (see right part of Fig. 4.2). A typical situation after such a rotation is shown in the lower left part of Fig. 4.2. One now easily can see that all points

$$\mathbf{r} = (x, y, z) = (r\sin\theta\cos\varphi, r\sin\theta\sin\varphi, r\cos\theta)$$

on the intersection circle (shown as an ellipse in the left part of Fig. 4.2) of the sphere and the plane correspond to a value θ that fulfills the condition

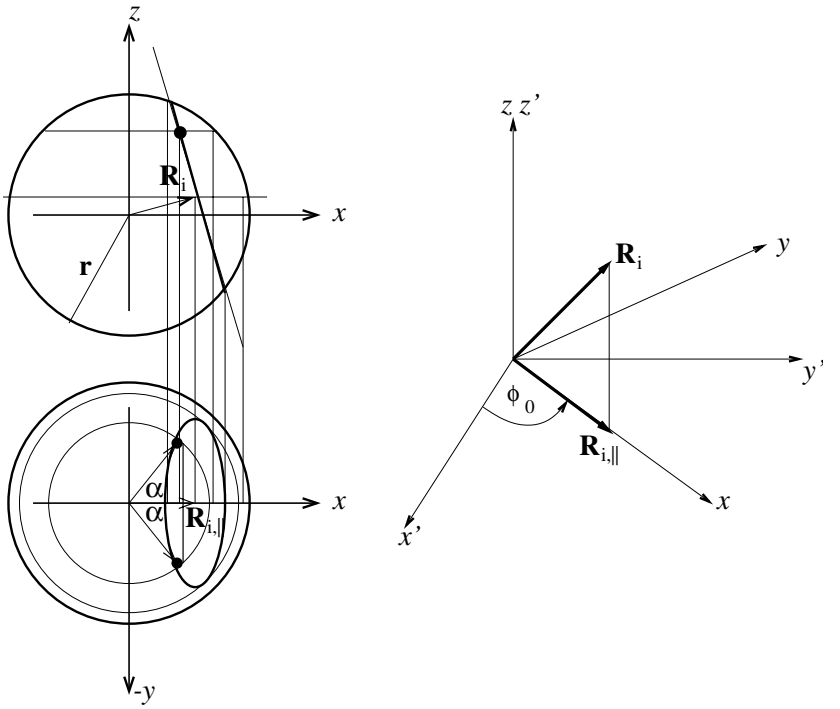

Fig. 4.2. Right part: The coordinate system is rotated around the z axis such that $\mathbf{R}_{i,\parallel}$ points in x direction.
Left part: view from the top (below) and the side (above) of the plane intersecting the sphere.

$$\left| \frac{R_i^2 - Z_i r \cos\theta}{\sqrt{X_i^2 + Y_i^2} r \sin\theta} \right| \leq 1 \quad . \tag{4.9}$$

If θ does not fulfill (4.9) there are no intersection points. For a given θ that does fulfill (4.9) the plane intercepts the sphere whenever φ is given by

$$\text{new coord. system} : \varphi_i^{(\pm)} = \pm\alpha, \alpha = \arccos\left(\frac{R_i^2 - Z_i r \cos\theta}{\sqrt{X_i^2 + Y_i^2} r \sin\theta} \right) \quad ,$$

$$\text{old coord. system} : \varphi_i^{(\pm)} = \arccos\left(\frac{X_i}{\sqrt{X_i^2 + Y_i^2}} \right) \pm \alpha \quad .$$

If a chosen pair (r, θ) does not fulfill (4.9) then the plane $\mathbf{R}_i$ does not belong to the polyhedron, i.e., is not one of its faces.

4.1.2 Semi-analytical evaluation

If one repeats this procedure for all possible boundary planes $\mathbf{R}_i$ one obtains for each pair (r, θ) a set of angles $\varphi, \left\{\varphi_i^{(\pm)}, i = 1, \ldots, N\right\}$, which can be ordered such that $0 \leq \varphi_1 \leq \ldots \leq \varphi_{2N} \leq 2\pi \leq \varphi_{2N+1} = \varphi_1 + 2\pi$. This set can then be used to solve the integral in (4.7) with respect to φ

$$\sigma_L(r) = \int_\Omega \mathrm{d}\hat{\mathbf{r}}\, \sigma(\mathbf{r})\, Y_L^*(\hat{\mathbf{r}}) \tag{4.10}$$

$$= C_{\ell m} \int_0^\pi \mathrm{d}\theta \left[\sin\theta P_m^\ell(\cos\theta)\ f_m(r, \cos\theta)\right] \quad . \tag{4.11}$$

The function $f_m(r, \cos\theta)$ is given by

$$f_m(r, \cos\theta) = \int_0^{2\pi} \mathrm{d}\varphi\, \sigma(r, \theta; \varphi)\, e^{-\mathrm{i}m\varphi}$$

$$= \begin{cases} \sum_{j=1}^{2N} (\varphi_{j+1} - \varphi_j)\, \sigma\left(r, \theta, \varphi_j^M\right) & m = 0 \\ \frac{\mathrm{i}}{m} \sum_{j=1}^{2N} \left(e^{-\mathrm{i}m\varphi_{j+1}} - e^{-\mathrm{i}m\varphi_j}\right) \sigma\left(r, \theta, \varphi_j^M\right) & m \neq 0 \end{cases} , \tag{4.12}$$

where $\sigma\left(r, \theta, \varphi_j^M\right) = 1$, if for $\varphi_j^M = (\varphi_{j+1} - \varphi_j)/2$ the corresponding point

$$\mathbf{r}^M = \left(r\sin\theta\cos\varphi_j^M, r\sin\theta\sin\varphi_j^M, r\cos\theta\right) \tag{4.13}$$

is inside the polyhedron and 0 otherwise. The remaining integral over θ has to be evaluated numerically

$$\sigma_L(r) = C_{\ell m} \int_0^\pi \mathrm{d}\theta\ \sin\theta P_m^\ell(\cos\theta) f_m(r; \cos\theta) = C_{\ell m} \int_{-1}^1 \mathrm{d}u\, P_m^\ell(u) f_m(r; u) \quad . \tag{4.14}$$

It should be noted that the $f_m(r; \cos\theta)$ are not smooth functions of $\cos\theta$: they are only smooth inbetween two of a total of K irregular points θ_k,

$$\{\theta_k = \theta_k(r), k = 1, \ldots, K\} \quad . \tag{4.15}$$

It is therefore advisable to split the integration over θ into several intervals:

$$\sigma_L(r) = C_{\ell m} \sum_{k=1}^{K-1} \left(\int_{\theta_k}^{\theta_{k+1}} \mathrm{d}\theta\ \sin\theta P_m^\ell(\cos\theta) f_m(r; \cos\theta) \right) \quad . \tag{4.16}$$

Table 4.1. Angular momentum quantum numbers of the non-vanishing expansion coefficients of the shape functions for common cubic lattice types.

lattice type	(ℓ, m)
fcc(100), bcc(100)	$(0,0)$, $(4,-4)$, $(4,0)$, $(4,4)$, $(6,-4)$, $(6,0)$, $(6,4)$, ...
fcc(110), bcc(110)	$(0,0)$, $(4,-4)$, $(4,-2)$, $(4,0)$, $(4,2)$, $(4,4)$, $(6,-6)$, $(6,-4)$, $(6,-2)$, $(6,0)$, $(6,2)$, $(6,4)$, $(6,6)$, ...
fcc(111), bcc(111)	$(0,0)$, $(4,-3)$, $(4,0)$, $(4,3)$, $(6,-6)$, $(6,-3)$, $(6,0)$, $(6,3)$, $(6,6)$, ...

4.1.3 Shape functions for the fcc cell

As an example in the following the construction of the shape functions for a simple fcc cell with cubic lattice constant a shall be discussed. In the fcc lattice there are 12 nearest neighbors, each one gives rise to one boundary plane of the Wigner-Seitz cell at a normal distance of $\sqrt{2}a/4$. These planes intercept with each other in a total of 24 edges, each one is equivalent and at a normal distance of $a/\sqrt{6}$. The edges intercept in total at 14 corners, whereof 8 are *near corners* at a distance of $\sqrt{3}a/4$, and 6 are *far corners* at a distance of $2a/4$, namely at the radius of the so-called bounding sphere, r_{BS}. One therefore has to deal with the following critical radii:

$$0 < \left(r_{\mathrm{C}_1} = r_{\mathrm{MT}} = \frac{\sqrt{2}a}{4} \right) < \left(r_{\mathrm{C}_2} = \frac{a}{\sqrt{6}} \right) < \left(r_{\mathrm{C}_3} = \frac{\sqrt{3}a}{4} \right) < \left(r_{\mathrm{C}_4} = r_{\mathrm{BS}} = \frac{2a}{4} \right) \quad . \tag{4.17}$$

Only at the critical radii the number of irregular θ-values, K, can change, whereas at a given r the number of interception points φ, namely N,

$$\left\{ \varphi_i^{(\pm)}, i = 1, \ldots, N \right\}$$

changes exclusively at an irregular θ_k.

While all the above features are independent of the orientation of the coordinate system, quite a few aspects do depend on the choice of the coordinate system. As an example for such a dependency on the coordinate system the neighborhood of $\theta = 0$ shall be compared for $\mathbf{e}_z \parallel [100]$, $\mathbf{e}_z \parallel [110]$ and $\mathbf{e}_z \parallel [111]$ by choosing a radius in the vicinity of the corresponding critical radius. The respective z axis intersects the polyhedron at the following points:

[100] H at $r_{\mathrm{BS}} = \frac{1}{2}a$ *far corner*
[110] N at $r_{\mathrm{MT}} = \frac{\sqrt{2}}{4}a$ *plane center*
[111] P at $r_{\mathrm{C}_3} = \frac{\sqrt{3}}{4}a$ *near corner*

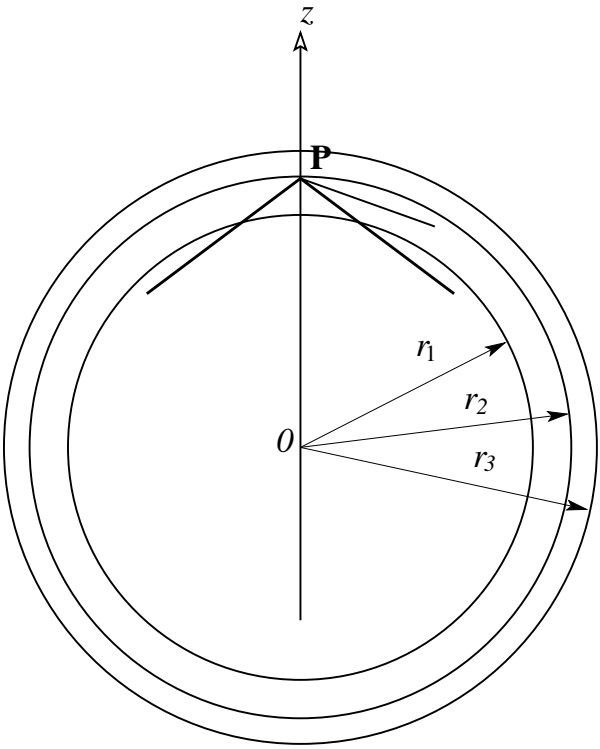

Fig. 4.3. The *near corner* P where 3 edges come together. Shown are spheres with radii smaller, equal to or bigger than the critical radius, $r_1 < r_2 = r_{C3} < r_3$.

The [100] case

Consider a radius r_2 marginally smaller than r_{BS} (the situation for $r \geq r_{\mathrm{BS}}$ is trivial). At this radius all points with a constant angle θ define a circle. The appearance of irregular values of θ when increasing r_2 can be best seen considering occurring intersections in the plane of the circle, $z = r_2 \cos\theta$, see the right column of Fig. 4.4. For $\theta = 0$ the circle is reduced to a point and the plane cuts the polyhedron (4 edges meet at the corner H) in the shape of a square. With θ increasing the circle gets bigger until it touches the (also increasing) square from the inside at an irregular θ-value θ_2. Then the circle intercepts with the square until the square touches the circle at an irregular θ-value θ_3. Beyond θ_3 the circle is outside the polyhedron. For $r_2 \to r_{\mathrm{BS}}^{(-)}$ the irregular θ-points $0 = \theta_1 \leq \theta_2 \leq \theta_3$ all approach 0.

The [110] case

The situation is different in the case of the z axis pointing along [110]. In selecting a radius r_1 marginally larger than r_{MT} (the situation for $r \leq r_{\mathrm{MT}}$

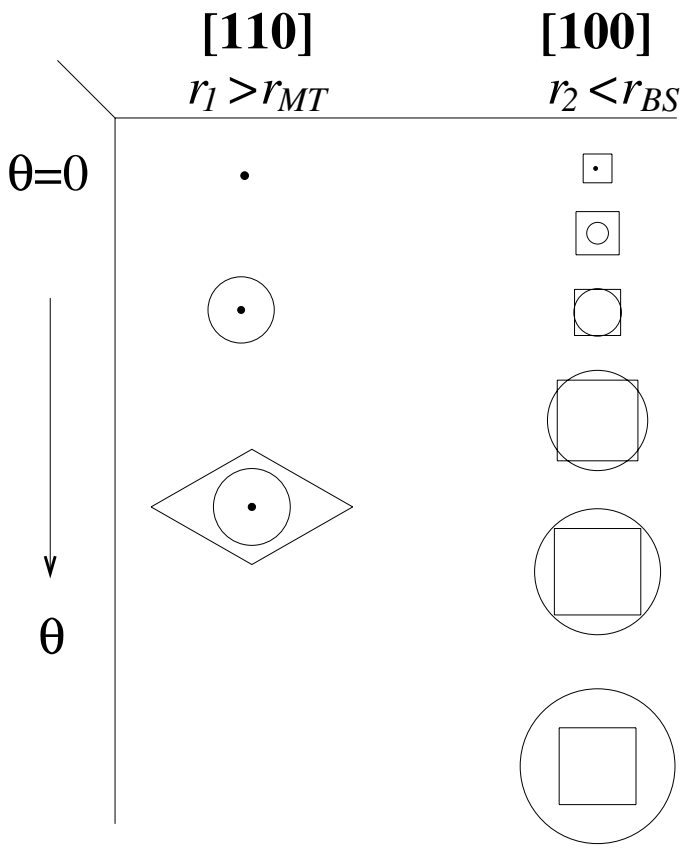

Fig. 4.4. Right column: the z axis points along (110), left column: the z axis points along (100). For further explanations, see text.

is again trivial) all points with a constant θ-value define a again circle in the plane $z = r_1 \cos\theta$, see the left column of Fig. 4.4. For $\theta = 0$ the circle is reduced to a point and the plane does not intersect with the polyhedron. With increasing θ the circle gets bigger until at an irregular θ-value θ_2 the circle is in the plane of the bounding plane. Beyond θ_2 the bounding plane of the polyhedron no longer needs to be considered. For $r_1 \to r_{\mathrm{MT}}^{(+)}$ the irregular θ-points $0 = \theta_1 \leq \theta_2$ all approach 0.

The [111] case

For [111] the situation is more complicated since the z axis intercepts the polyhedron at a *near corner* P, where 3 edges meet, see Fig. (4.3). Therefore one has to examine the situation for different radii r, namely $r_1 < r_2 = r_{C3} < r_3$, r_{C3} being the critical radius.

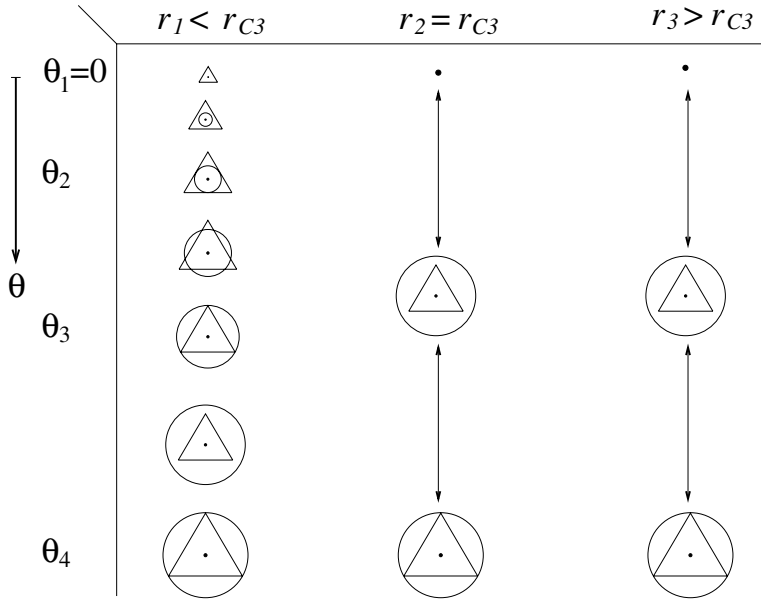

Fig. 4.5. The z axis points along (111). Left column: $r_1 < r_{C3}$, middle column: $r_2 = r_{C3}$ and Right column: $r_3 > r_{C3}$. For further explanations, see text.

Consider first a radius r_1 marginally smaller then r_{C_3} (left column of Fig. 4.5). For $\theta = 0$ the circle is reduced to a point and the plane cuts the polyhedrons (3 edges meet at the *near corner* P) in the shape of a triangle. With increasing θ the circle gets bigger until it touches the (also increasing) triangle from the inside at an irregular θ-value θ_2 beyond which the circle intercepts with the triangle. For $r_1 \to r_{\mathrm{C}_3}^{(-)}$ the irregular points θ, $0 = \theta_1 \leq \theta_2$, all approach 0. Next, consider a radius $r_2 = r_{\mathrm{C}_3}$ (middle column of Fig. 4.5). For $\theta = 0$ the circle and the triangle are reduced to a point. With increasing θ the circle and the triangle get bigger and intercept with each other: there is no other irregular θ-value except $\theta_1 = 0$. Finally, consider a radius r_3 marginally bigger then r_{C_3} (right column of Fig. 4.5). For $\theta = 0$ the circle is reduced to a point outside the polyhedron. With increasing θ the triangle inside the circle gets bigger until it touches the (also increasing) circle from the inside at an irregular θ-value θ_2, beyond which the circle intercepts with the triangle. For $r_3 \to r_{\mathrm{C}_3}^{(+)}$ the irregular points θ, $0 = \theta_1 \leq \theta_2$, all approach 0.

4.2 Shape truncated potentials

In order to cut off the potential $V(\mathbf{r})$ at the boundaries of a given polyhedron it has to be multiplied with the characteristic (shape) function of this specific

cell:

$$\upsilon(\mathbf{r}) = V(\mathbf{r})\,\sigma(\mathbf{r}) \quad . \tag{4.18}$$

By expanding $V(\mathbf{r})$, the shape function $\sigma(\mathbf{r})$, and $\upsilon(\mathbf{r})$, the so-called *truncated potential*, in spherical harmonics

$$V(\mathbf{r}) = \sum_L V_L(r)\,Y_L(\hat{\mathbf{r}}) \quad , \tag{4.19}$$

$$\sigma(\mathbf{r}) = \sum_L \sigma_L(r)\,Y_L(\hat{\mathbf{r}}) \quad , \tag{4.20}$$

$$\upsilon(\mathbf{r}) = \sum_L \upsilon_L(r)\,Y_L(\hat{\mathbf{r}}) \quad . \tag{4.21}$$

one obtains

$$\sum_L \upsilon_L(r)\,Y_L(\hat{\mathbf{r}}) = \sum_{L'L''} V_{L'}(r)\,\sigma_{L''}(r)\,Y_{L'}(\hat{\mathbf{r}})\,Y_{L''}(\hat{\mathbf{r}}) \quad , \tag{4.22}$$

which multiplied by $Y_L^*(\hat{\mathbf{r}})$ and integrated over the angular coordinates leads to the below expression for the components of the truncated potential $\upsilon(\mathbf{r})$

$$\upsilon_L(r) = \sum_{L'L''} C^L_{L'L''}\,V_{L'}(r)\,\sigma_{L''}(r) \quad , \tag{4.23}$$

where the $C^L_{L'L''}$ are Gaunt numbers, see e.g., the Appendix A. For an illustration the expansion coefficients of the shape function for a fcc Wigner-Seitz cell (unit lattice constant) are displayed in Fig. 4.6. In Figs. 4.7 and 4.8 the expansion coefficients of the shape truncated and untruncated potentials are shown.

4.2.1 Spherical symmetric potential

In the case of a spherical symmetric potential there is only one expansion coefficient $V_L(r)$, namely

$$V_{00}(r) = \sqrt{4\pi}\,V(r) \quad , \tag{4.24}$$

which implies for the coefficients of the truncated potential $\upsilon(\mathbf{r})$:

$$\begin{aligned}
\upsilon_{\ell m}(r) &= \sum_{\ell,m} C^{\ell m}_{00,\ell'' m''}\,V_{00}(r)\,\sigma_{\ell'' m''}(r) \\
&= \frac{1}{\sqrt{4\pi}} \sum_{\ell'',m''} \delta_{\ell\ell''}\,\delta_{mm''}\,V_{00}(r)\,\sigma_{\ell'' m''} \\
&= \frac{1}{\sqrt{4\pi}}\,V_{00}(r)\,\sigma_{\ell m}(r) \\
&= V(r)\,\sigma_{\ell m}(r) \quad .
\end{aligned} \tag{4.25}$$

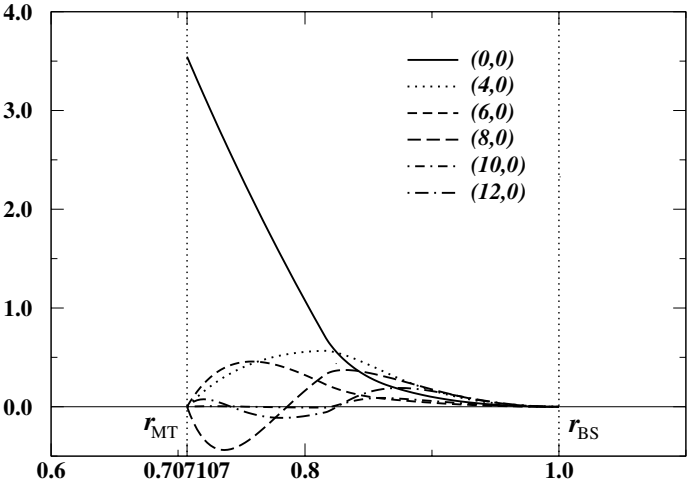

Fig. 4.6. Non-vanishing expansion coefficients of the shape functions for a fcc(001) Wigner-Seitz cell (unit lattice constant). Shown are only the $m = 0$ terms.

Furthermore, since for $r \leq r_{\rm MT}$

$$\sigma_{\ell m} = \delta_{\ell 0}\, \delta_{m0}\, \sqrt{4\pi} \quad , \tag{4.26}$$

one gets

$$\upsilon_{\ell m}(r) = \begin{cases} \delta_{\ell 0}\, \delta_{m0}\, \sqrt{4\pi}\, V(r) & , \quad r \leq r_{\rm MT} \\ V(r)\, \sigma_{\ell m}(r) & , \quad r_{\rm MT} \leq r \leq r_{\rm BS} \end{cases} \quad . \tag{4.27}$$

4.3 Radial mesh and integrations

All quantities that depend on the distance from the origin like the potential, the charge densities, etc., have to be set up on a radial mesh suitable for numerical computations. As will be discussed in the following chapters on single-site scattering (Chaps. 5–13) in most cases these radial points are given in terms of an exponential grid as

$$r_i = e^{x_i} \quad , \tag{4.28}$$

where the x_i are equidistant points corresponding to an increment $dx_i = x_{i+1} - x_i$. However, because of the discontinuous character of the shape functions at certain critical points $r_{{\rm C}_i}$ all radial integrations have to be terminated and restarted at these points. All radial integrals therefore which involve shape-functions have to be calculated in the following manner:

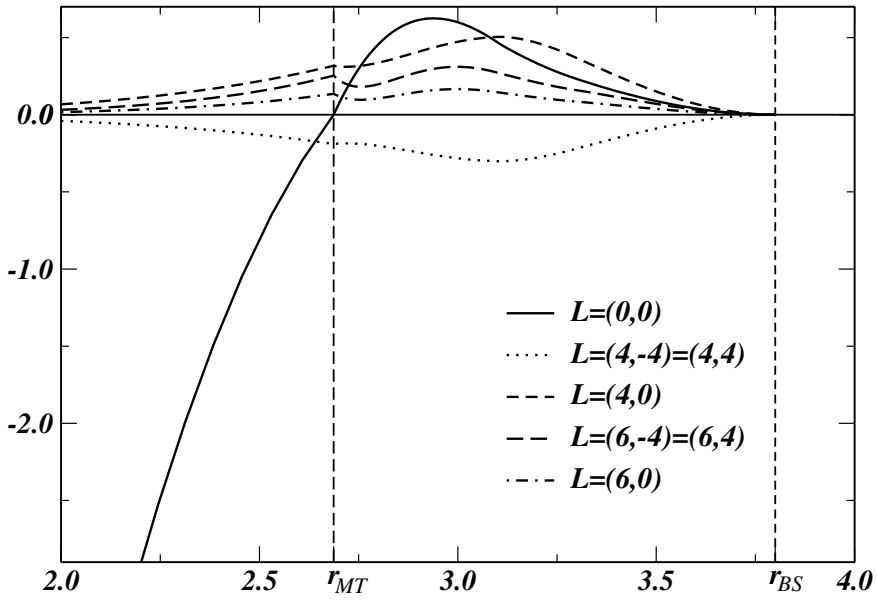

Fig. 4.7. Expansion coefficient of the shape truncated potential $v_L(r)$ for an fcc(001) Wigner-Seitz cell of Pd. The potentials shown resulted from a bulk calculation using $\ell_{\max} = 3$.

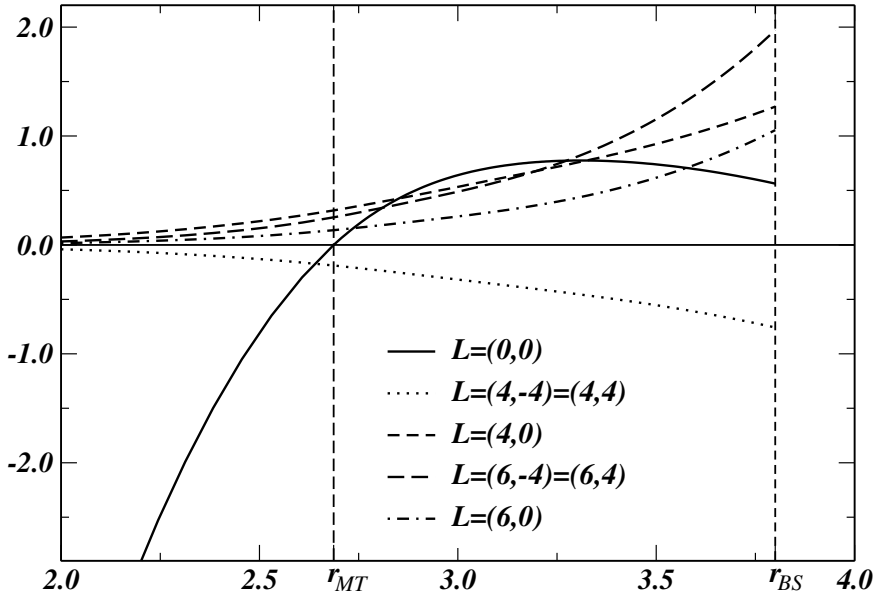

Fig. 4.8. Expansion coefficient of the untruncated potential $V_L(r)$ for an fcc(001) Wigner-Seitz cell of Pd. The potentials shown resulted from a bulk calculation using $\ell_{\max} = 3$.

$$\int_0^{r_{\mathrm{BS}}} \mathrm{d}r\, f(r) = \int_0^{r_{\mathrm{C}_1}} \mathrm{d}r\, f(r) + \int_{r_{\mathrm{C}_1}}^{r_{\mathrm{C}_2}} \mathrm{d}r\, f(r) + \cdots + \int_{r_{\mathrm{C}_{n-1}}}^{r_{\mathrm{C}_n}=r_{\mathrm{BS}}} \mathrm{d}r\, f(r) \quad . \tag{4.29}$$

The regions between adjacent critical points contain a constant number n of points inbetween. Hence the step-size dx_i has to be readjusted in each region:

$$\mathrm{d}x_i = \frac{\ln r_{\mathrm{C}_{i+1}} - \ln r_{\mathrm{C}_i}}{n-1} \quad . \tag{4.30}$$

Furthermore, the first critical point is defined by the radius of the inscribed sphere (muffin-tin radius). The very first mesh point, r_1, is then obtained from the condition:

$$x_1 = \ln r_{\mathrm{C}_1} - \mathrm{d}x_1\,(m-1) \tag{4.31}$$

$$r_1 = e^{x_1} \;=\; r_{\mathrm{C}_1}\, e^{-\mathrm{d}x_1\,(m-1)} \quad , \tag{4.32}$$

where m is the number of points inside the muffin-tin sphere and dx_1 an appropriately chosen step size such that the origin is approached sufficiently close. Usually one uses values for r_1 of the order of $\sim 10^{-4}$ a.u. .

References

1. J. Zabloudil: The full-potential screened KKR method, PHD Thesis, Technical University, Vienna (2000). http://www.cms.tuwien.ac.at/PHD_Theses
2. R. Hammerling: Aspects of dispersion interactions and of the full-potential Korringa–Kohn–Rostoker (KKR) method for semi-infinite systems. PHD Thesis, Technical University, Vienna (2003). http://www.cms.tuwien.ac.at/PhD_Theses
3. Yang Wang, G.M. Stocks, and J.S. Faulkner, Phys. Rev. B **49**, 5028 (1994)
4. N. Stefanou, H. Akai, and R. Zeller, Comp. Phys. Commun. **60**, 231 (1990)
5. N. Stefanou and R. Zeller, J. Phys. Cond. Mat. **3**, 7599 (1991)

5 Non-relativistic single-site scattering for spherically symmetric potentials

In this particular case the non-relativistic Kohn-Sham Hamiltonian is defined in atomic Rydberg units ($m = 1/2, \hbar = 1, e^2 = 2$) as

$$\mathcal{H}(\mathbf{r}) = -\nabla^2 + V^{\text{eff}}(\mathbf{r}) \quad , \tag{5.1}$$

where for single-site scattering the effective potential $V^{\text{eff}}(\mathbf{r})$ is given by

$$V^{\text{eff}}(\mathbf{r}) = \begin{cases} V(r) & r \leq r_{\text{MT}} \\ \\ 0 & r > r_{\text{MT}} \end{cases} \quad , \tag{5.2}$$

i.e., is confined by the so-called muffin-tin radius r_{MT} (e.g., radius of a sphere inscribed to a Wigner-Seitz cell for a simple lattice).

As is well-known separation of variables in (5.1) leads to a radial Schrödinger-type differential equation

$$\left(-\frac{\mathrm{d}^2}{\mathrm{d}r^2} + \frac{\ell(\ell+1)}{r^2} + V(r) - \epsilon \right) R_\ell(\epsilon; r) = 0 \quad , \tag{5.3}$$

the regular solutions $R^{\text{r}}_\ell(\epsilon; r)$ of which fulfill the following boundary conditions

$$\lim_{r \to 0} P^{\text{r}}_\ell(\epsilon; r) = 0 \quad , \quad P^{\text{r}}_\ell(\epsilon; r) = r R^{\text{r}}_\ell(\epsilon; r) \quad . \tag{5.4}$$

5.1 Direct numerical solution of the coupled radial differential equations

In writing (5.3) for an in general complex energy, $z = \epsilon + \mathrm{i}\delta$, as

$$P''_\ell(z; r) = U_\ell(z; r) P_\ell(z; r) \quad , \tag{5.5}$$

where

$$P''_\ell(z; r) \equiv \frac{\mathrm{d}^2}{\mathrm{d}r^2} P_\ell(z; r) \quad , \quad U_\ell(z; r) = V(r) - z + \frac{\ell(\ell+1)}{r^2} \quad , \tag{5.6}$$

the following Ansatz [2]

$$\tilde{Q}_\ell(z;r) = P'_\ell(z;r) - \frac{\ell+1}{r}\, P_\ell(z;r) \quad , \tag{5.7}$$

$$\tilde{Q}'_\ell(z;r) = P''_\ell(z;r) - \frac{\ell+1}{r}\, P'_\ell(z;r) + \frac{\ell+1}{r^2} P_\ell(z;r) \quad , \tag{5.8}$$

$$P'_\ell(z;r) = \frac{\mathrm{d}}{\mathrm{d}r} P_\ell(z;r) \quad , \quad \tilde{Q}'_\ell(z;r) = \frac{\mathrm{d}}{\mathrm{d}r} \tilde{Q}_\ell(z;r) \quad , \tag{5.9}$$

reduces the second order differential equation in (5.3) to two coupled first order differential equations,

$$\frac{\mathrm{d}}{\mathrm{d}r} \tilde{Q}_\ell(z;r) = -\frac{\ell+1}{r}\, \tilde{Q}_\ell(z;r) - [z - V(r)]\, P_\ell(z;r) \quad , \tag{5.10}$$

$$\frac{\mathrm{d}}{\mathrm{d}r} P_\ell(z;r) = \frac{\ell+1}{r} P_\ell(z;r) + \tilde{Q}_\ell(z;r) \quad , \tag{5.11}$$

which in turn can be solved numerically by a predictor–corrector approach very accurately.

Alternatively, one can apply a similar transformation, namely

$$Q_\ell(z;r) = P'_\ell(z;r) - \frac{1}{r}\, P_\ell(z;r) \quad , \tag{5.12}$$

which together with the below equation,

$$Q'_\ell(z;r) = P''_\ell(z;r) - \frac{1}{r}\, P'_\ell(z;r) + \frac{1}{r^2} P_\ell(z;r) \quad , \tag{5.13}$$

leads to a slightly modified set of coupled differential equations (which will be used in what is about to follow), namely:

$$\frac{\mathrm{d}}{\mathrm{d}r} Q_\ell(z;r) = -\frac{1}{r}\, Q_\ell(z;r) + U_\ell(z;r)\, P_\ell(z;r) \quad , \tag{5.14}$$

$$\frac{\mathrm{d}}{\mathrm{d}r} P_\ell(z;r) = \frac{1}{r}\, P_\ell(z;r) + Q_\ell(z;r) \quad . \tag{5.15}$$

Obviously the quantities $Q_\ell(z;r)$ and $\tilde{Q}_\ell(z;r)$ are related via

$$Q_\ell(z;r) = \tilde{Q}_\ell(z;r) + \frac{\ell}{r}\, P_\ell(z;r) \quad . \tag{5.16}$$

5.1.1 Starting values

In suppressing in the following the explicit dependence on the complex energy and by transforming the logarithmic mesh r to an equidistant mesh x with $r = e^x$ and $\mathrm{d}/\mathrm{d}r = e^{-x}\mathrm{d}/\mathrm{d}x$, one gets instead of (5.10) and (5.11),

$$\frac{\mathrm{d}}{\mathrm{d}x} \tilde{Q}_\ell(x) = -(\ell+1)\tilde{Q}_\ell(x) - [z - V(x)]\, e^x\, P_\ell(x) \quad , \tag{5.17}$$

$$\frac{\mathrm{d}}{\mathrm{d}x} P_\ell(x) = (\ell+1) P_\ell(x) + e^x\, \tilde{Q}_\ell(x) \quad . \tag{5.18}$$

For small values of r, or, when x tends to $-\infty$, the last two equations acquire the approximate form:

$$\frac{\mathrm{d}}{\mathrm{d}x}\tilde{Q}_\ell(x) = -(\ell+1)\tilde{Q}_\ell(x) - 2Z\,P_\ell(x) \quad , \tag{5.19}$$

$$\frac{\mathrm{d}}{\mathrm{d}x}P_\ell(x) = (\ell+1)P_\ell(x) \quad , \tag{5.20}$$

as the potential approaches $-2Z/r$ in the vicinity of the origin. One can therefore use the below Ansatz for the solutions of the above equations:

$$\tilde{Q}_\ell(x) = Ae^{ax} \quad , \tag{5.21}$$

$$P_\ell(x) = Be^{ax} \quad , \tag{5.22}$$

which in turn leads to the constant $a = (\ell+1)$ and the relation

$$\tilde{Q}_\ell(x) = \frac{A}{B}\,P_\ell(x) = -\frac{Z}{\ell+1}\,P_\ell(x) \quad . \tag{5.23}$$

Consequently for the first radial value of $P_\ell(x)$ an arbitrary small number can be used, e.g.,

$$P_\ell(x_1) = 10^{-20} \quad , \tag{5.24}$$

while for the function $Q_\ell(x)$ in terms of (5.23) and (5.16) one gets

$$Q_\ell(x_1) = \left(-\frac{Z}{\ell+1} + \frac{\ell}{e^{x_1}}\right) P_\ell(x_1) \quad , \tag{5.25}$$

and for the derivatives of $P_\ell(x)$ and $Q_\ell(x)$ with respect to x,

$$\frac{\mathrm{d}}{\mathrm{d}x}Q_\ell(x_1) = -Q_\ell(x_1) + e^{x_1}U_\ell(x_1)\,P_\ell(x_1) \tag{5.26}$$

$$\frac{\mathrm{d}}{\mathrm{d}x}P_\ell(x_1) = e^{x_1}Q_\ell(x_1) + P_\ell(x_1) \quad . \tag{5.27}$$

The last two expressions can also be obtained by a transformation of variables from r to x in (5.14) and (5.15).

5.1.2 Runge–Kutta extrapolation

The above start values then serve for a five point Runge–Kutta extrapolation to provide the starting values for a predictor–corrector scheme,

$$P_\ell(x_{i+1}) = P_\ell(x_i) + \frac{\Delta x}{6}\,(k_1 + 2k_2 + 2k_3 + k_4) \quad , \tag{5.28}$$

$$Q_\ell(x_{i+1}) = Q_\ell(x_i) + \frac{\Delta x}{6}\,(m_1 + 2m_2 + 2m_3 + m_4) \quad , \tag{5.29}$$

where $\Delta x = |\ln(r_{i+1}) - \ln(r_i)| = |x_{i+1} - x_i|$ and the matrices k_i and m_i are given in Table 5.1. There the functions $\mathbf{P}(x_i)$ and $\mathbf{Q}(x_i)$ have to be identified with $P_\ell(x_i)$ and $Q_\ell(x_i)$, respectively. In the present case the functions $f\,[P_\ell(x_i), Q_\ell(x_i)]$ and $g\,[P_\ell(x_i), Q_\ell(x_i)]$ occurring in Table 5.1 are the derivatives of $P_\ell(x_i)$ and $Q_\ell(x_i)$ as defined in (5.26) and (5.27), namely

$$f\,[P_\ell(x_i), Q_\ell(x_i)] = k_1 = e^{x_i} Q_\ell(x_i) + P_\ell(x_i) \quad , \tag{5.30}$$

$$g\,[P_\ell(x_i), Q_\ell(x_i)] = m_1 = -Q_\ell(x_i) + e^{x_i} U_\ell(x_i)\, P_\ell(x_i) \quad . \tag{5.31}$$

For matters of completeness all other coefficients are denoted explicitly below:

$$k_2 = e^{x_i + \Delta x/2} \left[Q_\ell(x_i) + m_1 \frac{\Delta x}{2} \right] + \left[P_\ell(x_i) + k_1 \frac{\Delta x}{2} \right] \quad , \tag{5.32}$$

$$m_2 = - \left[Q_\ell(x_i) + m_1 \frac{\Delta x}{2} \right] + e^{x_i + \Delta x/2} U_\ell(x_i + \Delta x/2) \left[P_\ell(x_i) + k_1 \frac{\Delta x}{2} \right] \quad , \tag{5.33}$$

$$k_3 = e^{x_i + \Delta x/2} \left[Q_\ell(x_i) + m_2 \frac{\Delta x}{2} \right] + \left[P_\ell(x_i) + k_2 \frac{\Delta x}{2} \right] \quad , \tag{5.34}$$

$$m_3 = - \left[Q_\ell(x_i) + m_2 \frac{\Delta x}{2} \right] + e^{x_i + \Delta x/2} U_\ell(x_i + \Delta x/2) \left[P_\ell(x_i) + k_2 \frac{\Delta x}{2} \right] \quad , \tag{5.35}$$

$$k_4 = e^{x_{i+1}} \left[Q_\ell(x_i) + m_3 \Delta x \right] + \left[P_\ell(x_i) + k_3 \Delta x \right] \quad , \tag{5.36}$$

$$m_4 = - \left[Q_\ell(x_i) + m_3 \Delta x \right] + e^{x_{i+1}} U_\ell(x_{i+1}) \left[P_\ell(x_i) + k_3 \Delta x \right] \quad . \tag{5.37}$$

According to the above expressions one needs the potential at the mesh points x_i, x_{i+1} and at a value inbetween these two. In order to calculate the potential at this position a Lagrange interpolation can be used. This is a standard procedure to be found for example in [3]. In proceeding thus one then can calculate five starting values for a multistep algorithm which – in the present case – is an Adams–Bashforth predictor–corrector scheme [3] [4] [5] [6] that is described in the next section.

5.1.3 Predictor-corrector algorithm

The values of the predictor $f^0(x_i)$ are generally given by

$$\begin{aligned} f^0(x_i) = f(x_{i-1}) + \frac{\Delta x}{720} \left[251 f'(x_{i-5}) - 1274 f'(x_{i-4}) \right. \\ \left. + 2616 f'(x_{i-3}) - 2774 f'(x_{i-2}) + 1901 f'(x_{i-1}) \right] \quad , \end{aligned} \tag{5.38}$$

where in the present case the functions $f(x_i)$ have to be identified with $P_\ell(x_i)$ or $Q_\ell(x_i)$ and

$$f'(x_i) = \frac{\mathrm{d}}{\mathrm{d}x} P_\ell(x_i)\,, \quad \text{or} \qquad \frac{\mathrm{d}}{\mathrm{d}x} Q_\ell(x_i) \quad , \tag{5.39}$$

while the corrector is calculated by means of the following expression

$$f^1(x_i) = f(x_{i-1}) + \frac{\Delta x}{720}\left[251 f^{1\prime}(x_i) + 646 f'(x_{i-1}) - 264 f'(x_{i-2}) + 106 f'(x_{i-3}) - 19 f'(x_{i-4})\right] \quad , \tag{5.40}$$

where $f^{1\prime}(x_i)$ has to be evaluated from either one of the below two equations:

$$\frac{\mathrm{d}}{\mathrm{d}x} P_\ell^1(x_i) = e^{x_i}\, Q_\ell^0(x_i) + P_\ell^0(x_i) \quad , \tag{5.41}$$

$$\frac{\mathrm{d}}{\mathrm{d}x} Q_\ell^1(x_i) = -Q_\ell^0(x_i) + e^{x_i} U_\ell(x_i)\, P_\ell^0(x_i) \quad . \tag{5.42}$$

At a given radial mesh-point x_i the predictors and correctors have to be evaluated iteratively until they assume the same value, then the next mesh point is computed and so forth.

The accuracy of the Runge–Kutta and predictor–corrector algorithms can be greatly improved if the step size Δx is reduced. This obviously implies that the number of mesh points at which the potential and the radial amplitudes and consequently the charge density need to be calculated has to be increased, which, however, also increases the required storage requirement and computing time. In order to avoid these consequences an interpolation scheme can be applied, which is only needed for solving the radial equations. Such a concept, explained in more detail in [7], consists of interpolating the potential inbetween two mesh points at n inbetween values. The radial amplitudes are then calculated for these n points storing, however, only the results at the mesh points. In this manner the step size is reduced and the accuracy of the procedure increased in proportion to the size of n.

What has been said so far about the numerical solution of the radial Schrödinger equation is only valid for the regular solutions. If irregular solutions are to be calculated one can proceed in exactly the same manner, only now an inward integration has to be performed using starting values given by the matching condition at the muffin tin radius discussed below in Sect. 5.2.2.

5.2 Single site Green's function

As discussed in general terms in the chapter on multiple scattering (Chap. 3) the single-site Green's function in the present case is now of the form

$$\begin{aligned} G(z;\mathbf{r},\mathbf{r}') = & \sum_{L,L'} Z_L(z;\mathbf{r})\; t_{LL'}(z)\; \widetilde{Z}_{L'}(z;\mathbf{r}')^\dagger \\ & - \sum_L Z_L(z;\mathbf{r})\; \widetilde{J}_L(z;\mathbf{r}')^\dagger\, \Theta(r'-r) \\ & - \sum_L J_L(z;\mathbf{r})\; \widetilde{Z}_L(z;\mathbf{r}')^\dagger\, \Theta(r-r') \quad , \end{aligned} \tag{5.43}$$

Table 5.1. General definition of coefficients for the Runge–Kutta extrapolation in the case of non-relativistic and relativistic single-site scattering

$$
\begin{aligned}
k_1 &= f\left[\mathbf{P}\left(x_i\right), \mathbf{Q}\left(x_i\right)\right] \\
m_1 &= g\left[\mathbf{P}\left(x_i\right), \mathbf{Q}\left(x_i\right)\right] \\
k_2 &= f\left[\mathbf{P}\left(x_i\right) + k_1 \Delta x/2, \mathbf{Q}\left(x_i\right) + m_1 \Delta x/2\right] \\
m_2 &= g\left[\mathbf{P}\left(x_i\right) + k_1 \Delta x/2, \mathbf{Q}\left(x_i\right) + m_1 \Delta x/2\right] \\
k_3 &= f\left[\mathbf{P}\left(x_i\right) + k_2 \Delta x/2, \mathbf{Q}\left(x_i\right) + m_2 \Delta x/2\right] \\
m_3 &= g\left[\mathbf{P}\left(x_i\right) + k_2 \Delta x/2, \mathbf{Q}\left(x_i\right) + m_2 \Delta x/2\right] \\
k_4 &= f\left[\mathbf{P}\left(x_i\right) + k_3 \Delta x, \mathbf{Q}\left(x_i\right) + m_2 \Delta x\right] \\
m_4 &= g\left[\mathbf{P}\left(x_i\right) + k_3 \Delta x, \mathbf{Q}\left(x_i\right) + m_3 \Delta x\right]
\end{aligned}
$$

where the scattering solutions $Z_L\left(z;\mathbf{r}\right)$ and $J_L\left(z;\mathbf{r}\right)$ are regular for $r \to 0$ and the irregular solutions of (5.1),

$$Z_L\left(z;\mathbf{r}\right) = Z_\ell\left(z;r\right) Y_L\left(\hat{\mathbf{r}}\right) \quad , \tag{5.44}$$

$$J_Q\left(z;\mathbf{r}\right) = J_\ell\left(z;r\right) Y_L\left(\hat{\mathbf{r}}\right) \quad , \tag{5.45}$$

$$\widetilde{Z}_L\left(z;\mathbf{r}\right) = Z_\ell\left(z;r\right)^* Y_L\left(\hat{\mathbf{r}}\right) \quad , \tag{5.46}$$

$$\widetilde{J}_Q\left(z;\mathbf{r}\right) = J_\ell\left(z;r\right)^* Y_L\left(\hat{\mathbf{r}}\right) \quad , \tag{5.47}$$

are defined such that at $r = r_{\mathrm{MT}}$

$$Z_\ell\left(z;\mathbf{r}\right) = j_\ell\left(z;\mathbf{r}\right) K_\ell^{-1}\left(z\right) + pn_\ell\left(z;\mathbf{r}\right) \quad , \tag{5.48}$$

$$J_\ell\left(z;\mathbf{r}\right) = j_\ell\left(z;\mathbf{r}\right) \quad , \tag{5.49}$$

with $K_\ell\left(z\right)$ being the reactance.

5.2.1 Normalization of regular scattering solutions and the single site t matrix

Since the regular solutions $R_\ell^{\mathrm{r}}(z;r) = P_\ell^{\mathrm{r}}(z;r)/r$ found from solving the coupled radial differential equations (5.11)–(5.10), have to be proportional to the

radial amplitudes of the regular scattering solutions, $Z_\ell\,(z;r)$, at $r_{\rm MT}$ one immediately gets two equations for the unknown proportionality constants a_ℓ and the reactance $K_\ell\,(z)$

$$\begin{aligned} a_\ell Z_\ell\,(z;r) &= R^{\rm r}_\ell(z;r) \\ &= j_\ell\,(z;r)\,K_\ell^{-1}\,(z) + pn_\ell\,(z;r) \quad , \end{aligned} \tag{5.50}$$

$$\begin{aligned} a_\ell Z'_\ell\,(z;r) &= R'_\ell(z;r) \\ &= j'_\ell\,(z;r)\,K_\ell^{-1}\,(z) + pn'_\ell\,(z;r) \quad , \end{aligned} \tag{5.51}$$

where as should be recalled

$$R'_\ell(z;r) = \frac{{\rm d}R^{\rm r}_\ell(z;r)}{{\rm d}r} \quad , \tag{5.52}$$

$$j'_\ell\,(z;r) = j'_\ell\,(pr) \quad , \quad n'_\ell\,(z;r) = n'_\ell\,(pr) \quad , \tag{5.53}$$

$$p = \sqrt{z} \quad , \quad {\rm Im}z > 0 \quad .$$

Elimination in (5.50) then immediately yields the following expression for the reactance

$$K_\ell\,(z) = -\frac{1}{p}\frac{L_\ell\,(z;r_{\rm MT})\;j_\ell\,(pr_{\rm MT}) - pj'_\ell\,(pr_{\rm MT})}{L_\ell\,(z;r_{\rm MT})\;n_\ell\,(pr_{\rm MT}) - pn'_\ell\,(pr_{\rm MT})} \quad , \tag{5.54}$$

where the $L_\ell\,(z;r)$ are logarithmic derivatives,

$$L_\ell\,(z;r) = \left.\frac{P'_\ell(z;r)}{P^{\rm r}_\ell(z;r)}\right|_{r=r_{\rm MT}} \quad , \tag{5.55}$$

and the proportionality constants a_ℓ follow *en suite*:

$$a_\ell = \frac{j_\ell\,(pr)\,K_\ell^{-1}\,(z) + pn_\ell\,(pr)}{R^{\rm r}_\ell(z;r)} \quad . \tag{5.56}$$

The single-site t-matrix is then given by

$$t_\ell^{-1}(z) = K_\ell^{-1}\,(z) + {\rm i}p \quad . \tag{5.57}$$

For $z = \epsilon + {\rm i}\delta,\ \varepsilon \geq 0,\ \delta = 0$, for example, one obtains for the single-site t-matrix the well-known expression

$$t_\ell\,(\varepsilon) = -\frac{1}{p}e^{{\rm i}\delta_\ell(\varepsilon)}\sin\delta_\ell\,(\varepsilon) \quad , \tag{5.58}$$

where $\delta_\ell\,(\varepsilon)$ is the ℓ-like phaseshift

$$\delta_\ell\,(\varepsilon) = \arctan\left(\frac{L_\ell\,(\varepsilon;r_{\rm MT})\;j_\ell\,(pr_{\rm MT}) - pj'_\ell\,(pr_{\rm MT})}{L_\ell\,(\varepsilon;r_{\rm MT})\;n_\ell\,(pr_{\rm MT}) - pn'_\ell\,(pr_{\rm MT})}\right) \quad . \tag{5.59}$$

5.2.2 Normalization of irregular scattering solutions

The irregular scattering solutions have to be proportional to the irregular solutions of (8.12)–(8.13), $R_\ell^i(z;r)$, such that at $r = r_{\mathrm{MT}}$

$$b_\ell J_\ell\left(z;r\right) Y_L\left(\hat{\mathbf{r}}\right) = j_\ell\left(pr\right) Y_L\left(\hat{\mathbf{r}}\right) \quad , \tag{5.60}$$

i.e.,

$$b_\ell = \frac{j_\ell\left(pr\right)}{J_\ell\left(z;r\right)} \quad . \tag{5.61}$$

References

1. P. Weinberger, *Electron Scattering Theory of Ordered and Disordered Matter* (Clarendon Press, Oxford 1992)
2. T.L. Loucks, *Augmented Plane Wave Method* (W.A. Benjamin Inc., New York Amsterdam 1967)
3. H.R. Schwarz, *Numerische Mathematik* (B.G. Teubner, Stuttgart 1997)
4. F.Bashforth and J.C. Adams, *Theories of Capillary Action* (Cambridge University Press, London 1883)
5. H. Jeffreys and B.S. Jeffreys, *Methods of Mathematical Physics* (Cambridge University Press, Cambridge, England 1988)
6. W.H. Press, B.P. Flannery, S.A. Teukolsky, and W.T. Vetterling, *Numerical Recipes in FORTRAN: The Art of Scientific Computing, 2nd ed.* (Cambridge University Press, Cambridge, England 1992)
7. J. Zabloudil: The full-potential screened KKR method, PHD Thesis, Technical University, Vienna (2000).http://www.cms.tuwien.ac.at/PHD_Theses

6 Non-relativistic full potential single-site scattering

6.1 Schrödinger equation for a single scattering potential of arbitrary shape

The Schrödinger equation for a single scattering potential $v(\mathbf{r})$ of arbitrary shape,

$$v(\mathbf{r}) = \sum_L v_L(r)\, Y_L(\hat{\mathbf{r}}) \quad ; \quad v(\mathbf{r}) = 0, \quad \mathbf{r} \notin D_v \quad , \tag{6.1}$$

see Chap. 4, leads after separation of the angular parts to the following coupled radial differential equations (in Rydberg units)

$$\left(\frac{\mathrm{d}^2}{\mathrm{d}r^2} + \frac{2}{r}\frac{\mathrm{d}}{\mathrm{d}r} + p^2 - \frac{\ell(\ell+1)}{r^2} \right) \psi_{LL'}(z;r) = \sum_{L''} v_{LL''}(r)\, \psi_{L''L'}(z;r) \quad , \tag{6.2}$$

where $p^2 = z$ and

$$v_{LL'}(r) = \sum_{L''} C^L_{L'L''}\, v_{L''}(r) \quad . \tag{6.3}$$

The regular and irregular scattering solutions of this differential equation are given by $Z_{LL'}(z;r)$ and $J_{LL'}(z;r)$ ($z = \epsilon + \mathrm{i}\delta$, a complex energy), respectively, which match at the boundary r_{BS} to the following functions,

$$Z_{LL'}(z;r_{\mathrm{BS}}) = j_\ell(p\, r_{\mathrm{BS}}) t^{-1}_{LL'}(p) - \mathrm{i} p h_\ell(p\, r_{\mathrm{BS}}) \delta_{LL'} \quad , \tag{6.4}$$

$$J_{LL'}(z;r_{\mathrm{BS}}) = j_\ell(p\, r_{\mathrm{BS}}) \delta_{LL'} \quad , \tag{6.5}$$

where the $j_\ell(pr)$ and $h_\ell(pr)$ are spherical Bessel and Hankel functions, introduced earlier.

6.2 Single site Green's function for a single scattering potential of arbitrary shape

6.2.1 Single spherically symmetric potential

According to Chap. 5 the elements of the angular momentum representation of the single-site Green's function for a spherically symmetric scatterer is given by

$$G_{LL'}(r,r';z) = G_\ell(r,r';z)\delta_{\ell\ell'}\delta_{mm'} \\ = Z_\ell(z;r)\,t_\ell(p)\,Z_\ell(z;r') - Z_\ell(z;r_<)\,J_\ell(z;r_>) \quad , \tag{6.6}$$

which can be rewritten for $r > r'$ in the following compact way,

$$G_\ell(r,r';z) = Z_\ell(z;r)\,I_\ell(z;r') \quad , \tag{6.7}$$

$$I_\ell(p,r) = t_\ell(p)\,Z_\ell(z;r) - J_\ell(z;r) \quad , \tag{6.8}$$

where the function $I_\ell(z;r)$ is again irregular at the origin.

6.2.2 Single potential of general shape

For a single potential of general shape such an element can be written as:

$$G_{LL'}(r,r';z) = \sum_{L''L'''} Z_{LL''}(z;r)\,t_{L''L'''}(p)\,Z_{L'L'''}(z;r') \\ - \sum_{L''} Z_{LL''}(z;r_<)\,J_{L'L''}(z;r_>) \quad , \tag{6.9}$$

where as should be recalled $r_< = \min\{r,r'\}$ and $r_> = \max\{r,r'\}$. Alternatively, in terms of the functions $R_{LL'}(z;r)$ and $H_{LL'}(z;r)$,

$$R_{LL'}(z;r_{\rm BS}) = j_\ell(pr_{\rm BS})\delta_{LL'} - \mathrm{i}\,p\,t_{LL'}(p)\,h_{\ell'}(pr_{\rm BS}) \\ = \sum_{L''} t_{LL''}(p)\,Z_{L''L'}(z;r) \quad , \tag{6.10}$$

$$H_{LL'}(z;r_{\rm BS}) = h_\ell(pr_{\rm BS})\,\delta_{LL'} \quad , \tag{6.11}$$

Equation (6.9) can be written as

$$G_{LL'}(r,r';z) = -\mathrm{i}p \sum_{L''} R_{LL''}(z;r_<)\,H_{L''L'}(z;r_>) \quad . \tag{6.12}$$

6.3 Iterative perturbational approach for the coupled radial differential equations

In order to find the solutions for the differential equation in (6.2) ("coupled channel equation") one can separate [2] the potential into a spherically symmetric and a non-spherical part, since according to (6.3) the functions $v_{LL'}(r)$ can be rewritten as

$$v_{LL'}(r) = \mathring{v}_{00}(r) + \Delta v_{LL'}(r) \quad , \tag{6.13}$$

where

$$\mathring{v}_{00}(r) = \frac{1}{\sqrt{4\pi}}\,v_{00}(r)\delta_{\ell 0}\delta_{\ell' 0}\delta_{m0}\delta_{m'0} \quad , \tag{6.14}$$

$$\Delta v_{LL'}(r) = \sum_{L''>1} C^{L}_{L'L''}\, v_{L''}(r) \quad , \tag{6.15}$$

see also (3.69) in Chap. 3. In using a perturbational approach $\overset{\circ}{v}_{00}(r)$ refers to the unperturbed Hamiltonian and $\Delta v_{LL'}(r)$ is the perturbation. The unperturbed solutions, however, namely $Z_\ell(z;r)$ and $J_\ell(z;r)$, can be assumed to be known and can be used immediately in the corresponding Lippmann-Schwinger equations:

6.3.1 Regular solutions

$$\begin{aligned} Z_{LL'}(z;r) &= Z_\ell(z;r) + \int_0^{r_{\mathrm{BS}}} r'^2 \mathrm{d}r'\, G_\ell(r,r';z) \sum_{L''} \Delta v_{LL''}(r') Z_{L''L'}(z;r') \\ &= Z_\ell(z;r) \\ &\quad + I_\ell(z;r) \left\{ \int_0^{r} r'^2 \mathrm{d}r' Z_\ell(z;r') \sum_{L''} \Delta v_{LL''}(r') Z_{L''L'}(z;r') \right\} \\ &\quad + Z_\ell(z;r) \left\{ \int_r^{r_{\mathrm{BS}}} r'^2 \mathrm{d}r' I_\ell(z;r') \sum_{L''} \Delta v_{LL''}(r') Z_{L''L'}(z;r') \right\} \quad . \end{aligned} \tag{6.16}$$

According to Calogero's approach this equation can be written in the form of

$$Z_{LL'}(z;r) = Z_\ell(z;r) A_{LL'}(z;r) + I_\ell(z;r) B_{LL'}(z;r) \quad , \tag{6.17}$$

where the coefficients $A_{LL'}(z;r)$ and $B_{LL'}(z;r)$ are defined as

$$A_{LL'}(r) = \delta_{LL'} + \int_r^{r_{\mathrm{BS}}} r'^2\, \mathrm{d}r'\, I_\ell(r') \sum_{L''} \Delta v_{LL''}(r')\, Z_{L''L'}(r') \quad , \tag{6.18}$$

$$B_{LL'}(r) = \int_0^{r} r'^2\, \mathrm{d}r'\, Z_\ell(r') \sum_{L''} \Delta v_{LL''}(r')\, Z_{L''L'}(r') \quad . \tag{6.19}$$

6.3.2 Irregular solutions

For the irregular functions the following equations apply:

$$I_{LL'}(z;r) = \varphi_\ell(z;r) + \int_0^{r_{\mathrm{BS}}} r'^2 \mathrm{d}r' G_\ell(r,r';z) \sum_{L''} \Delta v_{LL''}(r') I_{L''L'}(z;r') \quad , \tag{6.20}$$

$$\varphi_\ell(z;r) = I_\ell(z;r)\left\{1 - \int_0^{r_{\rm BS}} r'^2 {\rm d}r' Z_\ell(z;r') \sum_{L''} \Delta\upsilon_{LL''}(r') I_{L''L'}(z;r')\right\} \quad . \tag{6.21}$$

In using again Calogero's formulation the above equation can be rewritten as

$$I_{LL'}(z;r) = I_\ell(z;r) C_{LL'}(z;r) + Z_\ell(z;r) D_{LL'}(z;r) \quad , \tag{6.22}$$

where

$$C_{LL'}(z;r) = \delta_{LL'} - \int_r^{r_{\rm BS}} r'^2 {\rm d}r' Z_\ell(z;r') \sum_{L''} \Delta\upsilon_{LL''}(r') I_{L''L'}(z;r') \quad , \tag{6.23}$$

$$D_{LL'}(z;r) = \int_r^{r_{\rm BS}} r'^2 {\rm d}r' I_\ell(z;r') \sum_{L''} \Delta\upsilon_{LL''}(r') I_{L''L'}(z;r') \quad . \tag{6.24}$$

6.3.3 Numerical integration scheme

As can be seen from the above equations radial integrals of the type

$$f(r) = \int_r^{r_n} {\rm d}r'\, g(r') \quad , \tag{6.25}$$

have to be solved by means of a numerical inward integration. A very reliable approach for this purpose consists of a three point Simpson scheme [1], which implies to evaluate

$$f(r_i) = \int_{r_i}^{r_n} {\rm d}r'\, g(r') = f(r_{i+2}) + \int_{r_i}^{r_{i+2}} {\rm d}r'\, g(r') \quad . \tag{6.26}$$

Within this scheme it is necessary to supply two starting values (for n and $n-1$): the first value of the integral $f(r_n)$ obviously is zero; in order to calculate the second value one can employ a Lagrangian integration,

$$\begin{aligned} f(r_{n-1}) &= \int_{r_{n-1}}^{r_n} {\rm d}r'\, g(r') \\ &= [9\, r_n\, g(r_n) + 19\, r_{n-1}\, g(r_{n-1}) \\ &\quad -5\, r_{n-2}\, g(r_{n-2}) + r_{n-3}\, g(r_{n-3})]\, \frac{{\rm d}x}{24} \quad , \end{aligned} \tag{6.27}$$

where the terms $r_i {\rm d}x$ arise from a change of variables, namely from the condition $dr = r\,{\rm d}x$, see Sect. 4.3.

From there on a three point Simpson rule can be used to compute the respective next integral,

$$\begin{aligned} f(r_{n-2}) &= f(r_n) + \int_{r_{n-2}}^{r_n} \mathrm{d}r'\, g(r') \\ &= f(r_n) + [r_n\, g(r_n) + 4\, r_{n-1}\, g(r_{n-1}) + r_{n-2}\, g(r_{n-2}) \\ &\quad + r_{n-2}\, g(r_{n-2})]\, \frac{r\,\mathrm{d}x}{3} \quad , \end{aligned} \tag{6.28}$$

and so forth.

Integrations of the type:

$$f(r) = \int_0^r \mathrm{d}r'\, g(r') \quad , \tag{6.29}$$

can be performed in exactly the same way, only this time it is an outward integration that starts from zero or at the first value of the radial grid.

6.3.4 Iterative procedure

The above Lippmann-Schwinger equations can now be solved using an iterative procedure. In making the following Ansatz for a zero order approximation,

$$Z^{(0)}_{LL'}(z;r) = Z_\ell(z;r) \tag{6.30}$$

$$I^{(0)}_{LL'}(z;r) = I_\ell(z;r) \tag{6.31}$$

one obtains the first approximation after solving the respective integrals, $Z^{(1)}_{LL'}(z;r)$ and $I^{(1)}_{LL'}(z;r)$, which in turn can be used to get the second approximation by solving again the integral equations, and so on. In Figs. 6.1–6.4 the convergence of this procedure is illustrated for selected angular momentum indices. This iterative procedure is occasionally termed *Born approximation.*

It turns out, however, that the Born approximation does not work sufficiently well for potentials without a Coulomb singularity and in a highly anisotropic surrounding. This is the case for example at surfaces where in the first vacuum layers following the last material layer the potential changes rapidly towards the vacuum level, and clearly enough there are no Coulomb singularities. Therefore the non-spherical corrections are of the same order as the "unperturbed" spherical part of the potential. Hence the Born series converges very slowly: in such a case it is virtually impossible to obtain proper solutions for the coupled channel equations.

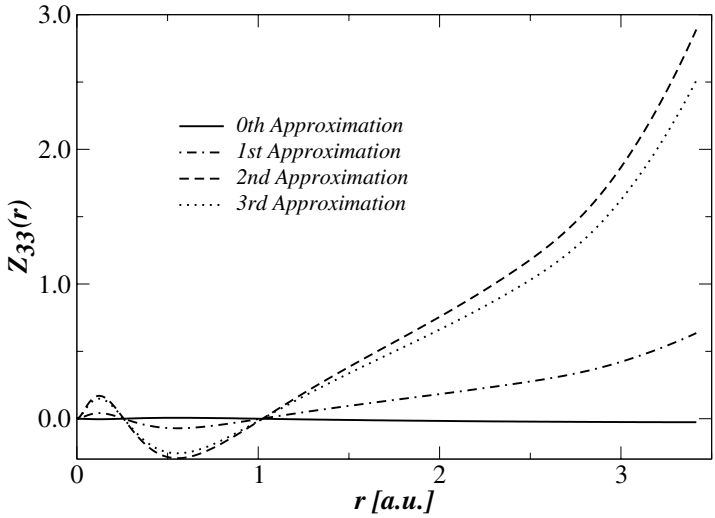

Fig. 6.1. Non-spherical components of regular scattering solutions and their convergence with respect to various Born approximations for (bulk) fcc-Cu(100): $Z_{33}(r)$ at a complex energy below the Fermi energy.

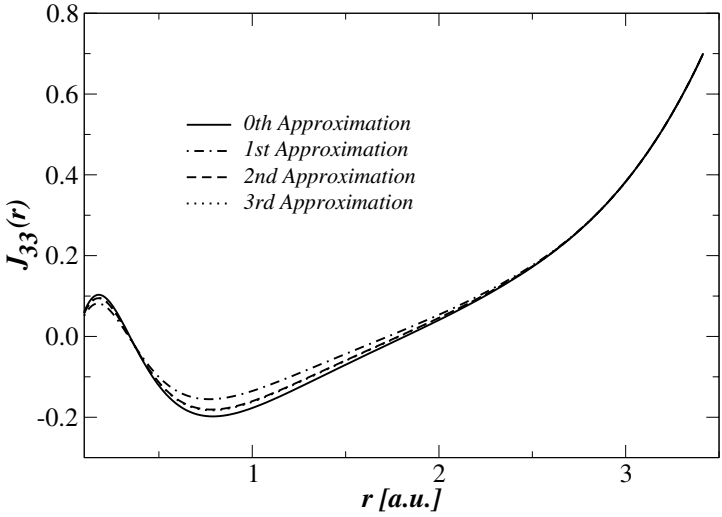

Fig. 6.2. Non-spherical components of irregular scattering solutions and their convergence with respect to various Born approximations for (bulk) fcc-Cu(100): $J_{33}(r)$ at a complex energy below the Fermi energy.

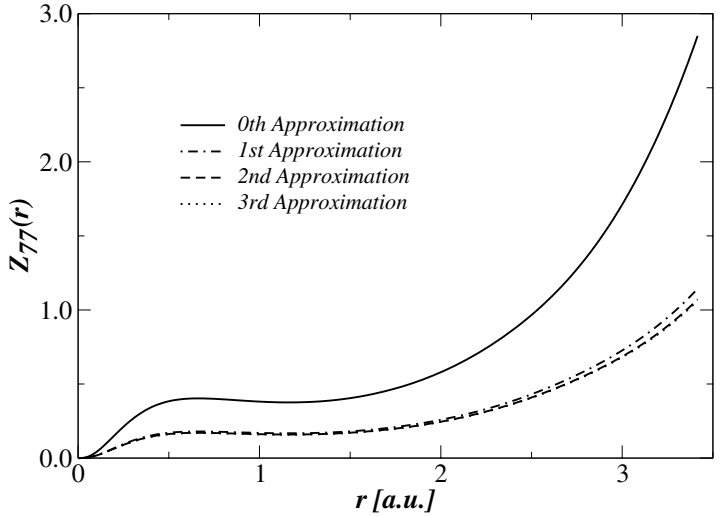

Fig. 6.3. Non-spherical components of regular scattering solutions and their convergence with respect to various Born approximations for (bulk) fcc-Cu(100): $Z_{77}(r)$ at a complex energy below the Fermi energy.

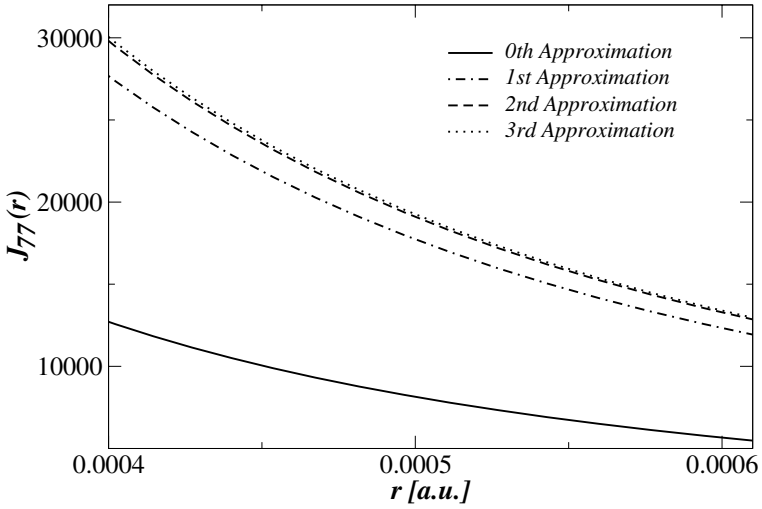

Fig. 6.4. Non-spherical components of irregular scattering solutions and their convergence with respect to various Born approximations for (bulk) fcc-Cu(100): $J_{77}(r)$ at a complex energy below the Fermi energy.

6.4 Direct numerical solution of the coupled radial differential equations

The system of coupled differential equations can also be solved via a predictor-corrector algorithm which makes use of starting values provided by several Runge–Kutta steps, i.e., can be solved exact without any approximation except the numerical limitations of the chosen algorithm, which, however, turn out to be negligible..

Defining a new function $\phi_{LL'}(z;r)$ as

$$\phi_{LL'}(z;r) = r\psi_{LL'}(z;r) \quad , \tag{6.32}$$

one gets

$$\psi_{LL'}(z;r) = \frac{1}{r}\,\phi_{LL'}(z;r) \quad , \tag{6.33}$$

$$\psi'_{LL'}(z;r) = \frac{\mathrm{d}}{\mathrm{d}r}\psi_{LL'}(z;r) = -\frac{1}{r^2}\,\phi_{LL'}(z;r) + \frac{1}{r}\,\phi'_{LL'}(z;r) \quad , \tag{6.34}$$

$$\psi''_{LL'}(z;r) = \frac{2}{r^3}\,\phi_{LL'}(z;r) - \frac{2}{r^2}\,\phi'_{LL'}(z;r) + \frac{1}{r}\,\phi''_{LL'}(z;r) \quad , \tag{6.35}$$

which after inserting into (6.2) yields

$$\phi''_{LL'}(z;r) + \left(z - \frac{\ell(\ell+1)}{r^2}\right)\phi_{LL'}(z;r) - \sum_{L''} \upsilon_{LL''}(r)\,\phi_{L''L'}(z;r) = 0 \quad . \tag{6.36}$$

By defining the following functions

$$P_{LL'}(z;r) = \phi_{LL'}(z;r) \quad , \tag{6.37}$$

$$Q_{LL'}(z;r) = P'_{LL'}(z;r) - \frac{1}{r}\,P_{LL'}(z;r) \quad , \tag{6.38}$$

the above set of second order coupled differential equations can be reduced to a set of first order coupled differential equations

$$P'_{LL'}(z;r) = Q_{LL'}(z;r) + \frac{1}{r}\,P_{LL'}(z;r) \quad , \tag{6.39}$$

$$\begin{aligned} P''_{LL'}(z;r) &= Q'_{LL'}(z;r) - \frac{1}{r^2}\,P_{LL'}(z;r) + \frac{1}{r}\,P'_{LL'}(z;r) \\ &= Q'_{LL'}(z;r) + \frac{1}{r}\,Q_{LL'}(z;r) \quad . \end{aligned} \tag{6.40}$$

$$Q'_{LL'}(z;r) = -\frac{1}{r}\,Q_{LL'}(z;r) - \left(z - \frac{\ell(\ell+1)}{r^2}\right) P_{LL'}(z;r) + \sum_{L''} \upsilon_{LL''}(r)\, P_{L''L'}(z;r) \tag{6.41}$$

$$Q_{LL'}(z;r) = P'_{LL'}(z;r) - \frac{1}{r}\,P_{LL'}(z;r) \quad . \tag{6.42}$$

If $U_{LL'}(z;r)$ denotes the following matrix

$$U_{LL'}(z;r) = \left(-z + \frac{\ell(\ell+1)}{r^2}\right)\delta_{LL'} + \upsilon_{LL'}(r) \quad , \tag{6.43}$$

the last two equations can be rewritten as

$$Q'_{LL'}(z;r) = -\frac{1}{r}\,Q_{LL'}(z;r) + \sum_{L''} U_{LL''}(z;r)\, P_{L''L'}(z;r) \quad , \tag{6.44}$$

$$Q_{LL'}(z;r) = P'_{LL'}(z;r) - \frac{1}{r}\,P_{LL'}(z;r) \quad . \tag{6.45}$$

6.4.1 Starting values

By changing variables, $x = \ln(r)$, and $\mathrm{d}x = (1/r)\,dr$,

$$P'_{LL'}(z;x) = e^{-x}\,\frac{\mathrm{d}}{\mathrm{d}x} P_{LL'}(z;x) \quad , \tag{6.46}$$

the below coupled differential equations

$$\frac{\mathrm{d}}{\mathrm{d}x} Q_{LL'}(z;x) = -Q_{LL'}(z;x) + e^{x} \sum_{L"} U_{LL''}(z;x) P_{L''L'}(z;x) \quad , \tag{6.47}$$

$$\frac{\mathrm{d}}{\mathrm{d}x} P_{LL'}(z;x) = e^{x} Q_{LL'}(z;x) + P_{LL'}(z;x) \quad , \tag{6.48}$$

can be solved by a predictor–corrector algorithm

In order to start a predictor–corrector algorithm one initially has to provide (at least) five starting values for the functions P, Q, P', and Q'. Very close to the origin, i.e., within the radial regime in which $\upsilon(\mathbf{r})$ is spherically symmetric only, one can use exactly the same approximation as in the previous Chap., and the only non-vanishing values of the angular momentum matrices are the diagonal ones. For the first radial mesh-point $r_1 = \exp(x_1)$ it is sufficient to assume an arbitrary small value of $P_{LL}(z;x_1)$. The corresponding derivatives follow then from (6.47)–(6.48).

$$P_{LL}(z;x_1) = 10^{-20} \quad , \tag{6.49}$$

$$Q_{LL}(z;x_1) = \left(\frac{Z}{\ell+1} + \frac{\ell}{e^{x_1}}\right) P_{LL}(z;x_1) \quad , \tag{6.50}$$

$$\frac{\mathrm{d}}{\mathrm{d}x} P_{LL}(z;x_1) = e^{x_1}\, Q_{LL}(z;x_1) + P_{LL}(z;x_1) \quad , \tag{6.51}$$

$$\frac{\mathrm{d}}{\mathrm{d}x} Q_{LL}(z;x_1) = -\, Q_{LL}(z;x_1) + e^{x_1} U_{LL}(z;x_1)\, P_{LL}(z;x_1) \quad . \tag{6.52}$$

6.4.2 Runge–Kutta extrapolation

The above values then serve for a five point Runge–Kutta extrapolation in order to provide the starting values for the predictor–corrector scheme (omitting the dependence on the complex energy z):

$$P_{LL'}(x_{i+1}) = P_{LL'}(x_i) + \frac{\Delta x}{6}\,(k_1 + 2k_2 + 2k_3 + k_4) \tag{6.53}$$

$$Q_{LL'}(x_{i+1}) = Q_{LL'}(x_i) + \frac{\Delta x}{6}\,(m_1 + 2m_2 + 2m_3 + m_4) \tag{6.54}$$

where $\Delta x = |\ln(r_{i+1}) - \ln(r_i)|$. The matrices k_i and m_i, $i = 1, 2, 3, 4$ are given in Table 5.1 and have to be calculated in accordance with (5.30)–(5.37).

6.4.3 Predictor-corrector algorithm

Having provided the first few points a predictor–corrector algorithm [3] [4] [5] [6] can be started. The expressions for the predictors (suffix zero) are identical as in (5.38), only this time the function $f(x_i)$ equals $P_{LL'}(x_i)$ and $Q_{LL'}(x_i)$ respectively. Furthermore the derivative is given by:

$$f'(x_i) = \frac{\mathrm{d}}{\mathrm{d}x} P_{LL'}(x_i)\,, \quad \text{or} \qquad \frac{\mathrm{d}}{\mathrm{d}x} Q_{LL'}(x_i) \quad . \tag{6.55}$$

The correctors are calculated from (5.40) and the function $f^{1\prime}(x_i)$ appearing in that expression is equal to either one of the equations given below:

$$\frac{\mathrm{d}}{\mathrm{d}x} P^1_{LL'}(x_i) = e^{x_i} Q^0_{LL'}(x_i) + P^0_{LL'}(x_i) \quad , \tag{6.56}$$

$$\frac{\mathrm{d}}{\mathrm{d}x} Q^1_{LL'}(x_i) = -Q^0_{LL'}(x_i) + e^{x_i} \sum_{L''} U_{LL''}(x_i) P^0_{L''L'}(x_i) \quad . \tag{6.57}$$

At a given radial mesh-point the predictors and correctors have to be evaluated iteratively until they assume the same value, then the next mesh

point is computed and so forth. In order to evaluate the irregular solutions of (6.47)–(6.48) the same procedure can be utilized, except that now an inward integration has to be performed. The starting values refer in this case to the values at the bounding sphere radius, see (6.5).

6.5 Single-site t matrix

Having solved the coupled radial differential equations the single-site t matrix corresponding to $v(\mathbf{r})$ can be evaluated from the matching condition for the respective regular and irregular solutions at the bounding sphere radius r_{BS}, e.g., in terms of the reactance $K_{LL'}(z)$

$$Z_L(z;\mathbf{r}) = \sum_{L'} j_{L'}(z;\mathbf{r})\, K^{-1}_{L'L}(z) + p\, n_L(z;\mathbf{r}) \quad , \quad |\mathbf{r}| = r_{\mathrm{BS}} \tag{6.58}$$

$$Z_L(z;\mathbf{r}) = \sum_{L'} Z_{LL'}(z;r) Y_L(\hat{\mathbf{r}}) \quad , \tag{6.59}$$

$$j_L(z;\mathbf{r}) = j_\ell(pr)\, Y_L(\hat{\mathbf{r}}) \quad , \tag{6.60}$$

$$n_L(z;\mathbf{r}) = n_\ell(pr)\, Y_L(\hat{\mathbf{r}}) \quad , \quad p = \sqrt{z} \quad , \quad \mathrm{Im} z > 0 \quad . \tag{6.61}$$

As easily can be worked out from (6.9) the reactance $K_{LL'}(z)$ is related to the single-site t matrix $t_{LL'}(z)$ via

$$K^{-1}_{LL'}(z) = t^{-1}_{LL'}(z) - \mathrm{i}p\, \delta_{LL'} \quad . \tag{6.62}$$

The regular and irregular solutions and their respective derivatives can be obtained numerically in a straightforward manner. In the following the normalized regular solutions are referred to as $Z_{LL'}(r)$ and the normalized irregular solutions are called $J_{LL'}(r)$. The $j_\ell(r)$ and $h_\ell(r)$ are spherical Bessel and Hankel functions as defined in [1], while the inverse of the t matrix, $t_{LL'}$, is denoted by $m_{LL'}$, and a total of three coefficients $a_{LL'}$, $b_{LL'}$, and $c_{LL'}$ need to be worked out.

$$Z_{LL'}(r) = \sum_{L''} R_{LL''}(r)\, a_{L''L'} \quad , \tag{6.63}$$

$$J_{LL'}(r) = \sum_{L''} \left[R_{LL''}(r)\, b_{L''L'} + I_{LL''}(r)\, c_{L''L'} \right] \quad . \tag{6.64}$$

6.5.1 Normalization of the regular solutions

The normalization of the regular solutions at the bounding sphere radius $S = r_{\mathrm{BS}}$ is given by

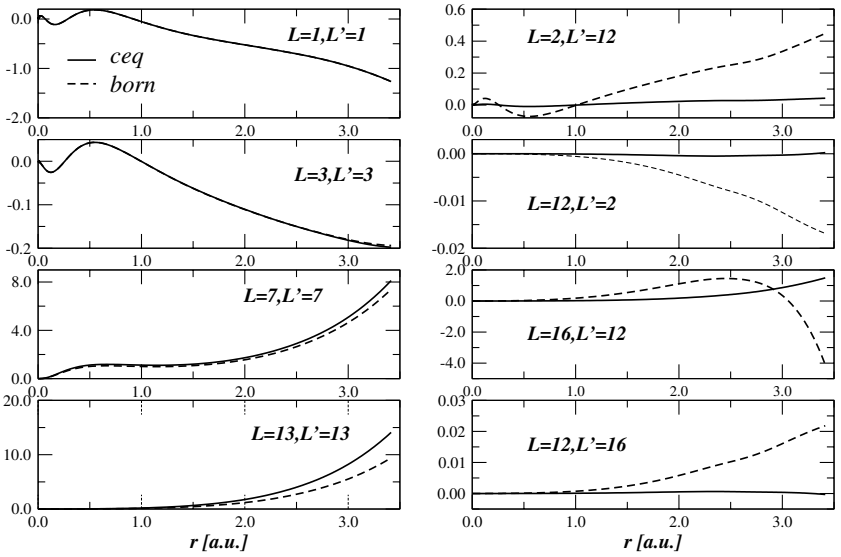

Fig. 6.5. Diagonal (left panel) and off-diagonal (right panel) components of regular scattering solutions for (bulk) fcc-Cu(100) as calculated using the Born approximation (labelled "born") and solving directly the coupled differential equations (6.47)–(6.48) (labelled "ceq").

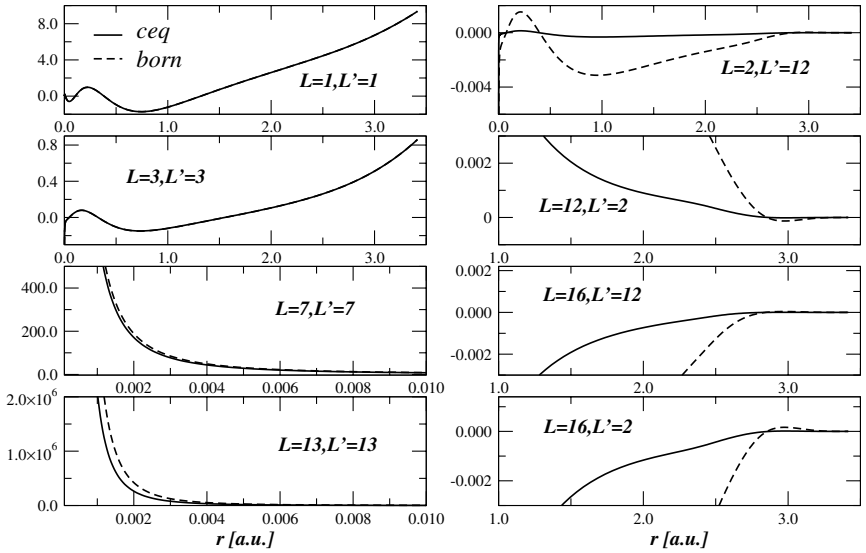

Fig. 6.6. Diagonal (left panel) and off-diagonal (right panel) components of irregular scattering solutions for (bulk) fcc-Cu(100) as calculated using the Born approximation (labelled "born") and solving directly the coupled differential equations (6.47)–(6.48) (labelled "ceq").

$$\sum_{L''} R_{LL''}(S)\, a_{L''L'} = S\left(j_\ell(pS)\, m_{LL'} - \mathrm{i}p\, h_\ell(pS)\, \delta_{LL'}\right) \quad , \tag{6.65}$$

$$\begin{aligned}\sum_{L''} R'_{LL''}(S)\, a_{L''L'} &= j_\ell(pS)\, m_{LL'} - \mathrm{i}p\, h_\ell(pS)\, \delta_{LL'} \\ &\quad + pS\left(j'_\ell(pS)\, m_{LL'} - \mathrm{i}p\, h'_\ell(pS)\, \delta_{LL'}\right) && (6.66)\\ &= \left(j_\ell(pS) + pS\, j'_\ell(pS)\right) m_{LL'} \\ &\quad - \mathrm{i}p\left(h_\ell(pS) + pS\, h'_\ell(pS)\right)\delta_{LL'} && (6.67)\\ &= \left[(\ell+1)\; j_\ell(pS) - pS\, j_{\ell+1}(pS)\right] m_{LL'} && (6.68)\\ &\quad - \mathrm{i}p\left[(\ell+1)\; h_\ell(pS) - pS\, h_{\ell+1}(pS)\right]\delta_{LL'} \quad . && (6.69)\end{aligned}$$

Consider now the following short-hand notations,

$$\mathbf{R} = \{R_{LL'}(S)\} \quad , \tag{6.70}$$

$$\mathbf{R}' = \{R'_{LL'}(S)\} \quad , \tag{6.71}$$

$$\mathbf{a} = \{a_{LL'}\} \quad , \tag{6.72}$$

$$\mathbf{m} = \{m_{LL'}\} \quad , \tag{6.73}$$

$$\mathbf{t} = \{t_{LL'}\} \quad , \tag{6.74}$$

$$\mathbf{j} = \{S\, j_\ell(pS)\, \delta_{LL'}\} \quad , \tag{6.75}$$

$$\mathbf{h} = \{-\mathrm{i}\, pS\, h_\ell(pS)\, \delta_{LL'}\} \quad , \tag{6.76}$$

$$\mathbf{j}' = \{[(\ell+1)\; j_\ell(pS) - pS\, j_{\ell+1}(pS)]\; \delta_{LL'}\} \quad , \tag{6.77}$$

$$\mathbf{h}' = \{-\mathrm{i}\, p\, [(\ell+1)\; h_\ell(pS) - pS\, h_{\ell+1}(pS)]\; \delta_{LL'}\} \quad , \tag{6.78}$$

then obviously the above matrix equation for the normalization can be written in a very compact form as

$$\mathbf{R} \circ \mathbf{a} = \mathbf{j} \circ \mathbf{m} + \mathbf{h} \quad , \tag{6.79}$$

$$\mathbf{R}' \circ \mathbf{a} = \mathbf{j}' \circ \mathbf{m} + \mathbf{h}' \quad , \tag{6.80}$$

where for a better readability matrix multiplications are indicated by the symbol $\circ$. It therefore follows that

$$\mathbf{a} = \mathbf{R}^{-1} \circ \mathbf{j} \circ \mathbf{m} + \mathbf{R}^{-1} \circ \mathbf{h} \;=\; (\mathbf{R}')^{-1} \circ \mathbf{j}' \circ \mathbf{m} + (\mathbf{R}')^{-1} \circ \mathbf{h}' \quad .$$

Defining now the following quantity ρ,

$$\rho = \mathbf{R}' \circ \mathbf{R}^{-1} \quad , \tag{6.81}$$

one obtains

$$\rho \circ \mathbf{j} \circ \mathbf{m} + \rho \circ \mathbf{h} = \mathbf{j}' \circ \mathbf{m} + \mathbf{h}' \quad , \tag{6.82}$$

$$(\rho \circ \mathbf{j} - \mathbf{j}') \circ \mathbf{m} = \mathbf{h}' - \rho \circ \mathbf{h} \quad . \tag{6.83}$$

The t matrix and its inverse are then given by

$$\mathbf{m} = (\rho \circ \mathbf{j} - \mathbf{j}')^{-1} \circ (\mathbf{h}' - \rho \circ \mathbf{h}) \quad , \tag{6.84}$$

$$\mathbf{m}^{-1} = (\mathbf{h}' - \rho \circ \mathbf{h})^{-1} \circ (\rho \circ \mathbf{j} - \mathbf{j}') \quad . \tag{6.85}$$

It should be recalled that

$$\mathbf{t} = \mathbf{m}^{-1} \quad . \tag{6.86}$$

Furthermore, from (6.79) and (6.80) follows that

$$\mathbf{m} = \mathbf{j}^{-1} \circ \mathbf{R} \circ \mathbf{a} - \mathbf{j}^{-1} \circ \mathbf{h} = (\mathbf{j}')^{-1} \circ \mathbf{R}' \circ \mathbf{a} - (\mathbf{j}')^{-1} \circ \mathbf{h}' \quad .$$

Defining now the below quantity

$$\mathbf{r} = \mathbf{j}' \circ \mathbf{j}^{-1} \quad , \tag{6.87}$$

one arrives at

$$\mathbf{r} \circ \mathbf{R} \circ \mathbf{a} - \mathbf{r} \circ \mathbf{h} = \mathbf{R}' \circ \mathbf{a} - \mathbf{h}' \quad , \tag{6.88}$$

$$(\mathbf{r} \circ \mathbf{R} - \mathbf{R}') \circ \mathbf{a} = \mathbf{r} \circ \mathbf{h} - \mathbf{h}' \quad , \tag{6.89}$$

and therefore at an expression for $\mathbf{a}$:

$$\mathbf{a} = (\mathbf{r} \circ \mathbf{R} - \mathbf{R}')^{-1} \circ (\mathbf{r} \circ \mathbf{h} - \mathbf{h}') \quad , \tag{6.90}$$

or, alternatively, in using (6.79):

$$\mathbf{a} = \mathbf{R}^{-1} \circ (\mathbf{j} \circ \mathbf{m} + \mathbf{h}) \quad . \tag{6.91}$$

6.5.2 Normalization of the irregular solutions

The matching condition for the irregular wave-functions is given by:

$$\sum_{L''} (R_{LL''}(S)\, b_{L''L'} + I_{LL''}(S)\, c_{L''L'}) = S\, j_\ell(pS)\, \delta_{LL'} \tag{6.92}$$

$$\begin{aligned} \sum_{L''} (R'_{LL''}(S)\, b_{L''L'} + I'_{LL''}(S)\, c_{L''L'}) &= j_\ell(pS)\, \delta_{LL'} + pS\, j'_\ell(pS)\, \delta_{LL'} \\ &= [(\ell+1)\, j_\ell(pS) \\ &\quad -pS\, j_{\ell+1}(pS)]\, \delta_{LL'} \quad . \end{aligned} \tag{6.93}$$

Defining the following matrices:

$$\mathbf{I} = \{I_{LL'}(S)\} \quad , \tag{6.94}$$

$$\mathbf{b} = \{b_{LL'}\} \quad , \tag{6.95}$$

$$\mathbf{c} = \{c_{LL'}\} \quad , \tag{6.96}$$

the above equations can be rewritten as

$$\mathbf{R} \circ \mathbf{b} + \mathbf{I} \circ \mathbf{c} = \mathbf{j} \quad , \tag{6.97}$$

$$\mathbf{R}' \circ \mathbf{b} + \mathbf{I}' \circ \mathbf{c} = \mathbf{j}' \quad , \tag{6.98}$$

By eliminating the matrix **b**,

$$\mathbf{b} = \mathbf{R}^{-1} \circ \mathbf{j} - \mathbf{R}^{-1} \circ \mathbf{I} \circ \mathbf{c} = (\mathbf{R}')^{-1} \circ \mathbf{j}' - (\mathbf{R}')^{-1} \circ \mathbf{I}' \circ \mathbf{c} \quad ,$$

one then arrives at an expression for the matrix **c:**

$$\rho \circ \mathbf{j} - \rho \circ \mathbf{I} \circ \mathbf{c} = \mathbf{j}' - \mathbf{I}' \circ \mathbf{c} \quad , \tag{6.99}$$

$$\rho \circ \mathbf{j} - \mathbf{j}' = (\rho \circ \mathbf{I} - \mathbf{I}') \circ \mathbf{c} \quad , \tag{6.100}$$

$$\mathbf{c} = (\rho \circ \mathbf{I} - \mathbf{I}')^{-1} \circ (\rho \circ \mathbf{j} - \mathbf{j}') \quad . \tag{6.101}$$

In eliminating in (6.97) and (6.98) the matrix **c** one gets

$$\mathbf{c} = \mathbf{I}^{-1} \circ \mathbf{j} - \mathbf{I}^{-1} \circ \mathbf{R} \circ \mathbf{b} = \mathbf{I}'^{-1} \circ \mathbf{j}' - (\mathbf{I}')^{-1} \circ \mathbf{R}' \circ \mathbf{b} \quad .$$

Defining now a matrix ϱ such that

$$\varrho = \mathbf{I}' \circ \mathbf{I}^{-1} \quad , \tag{6.102}$$

this leads to

$$\varrho \circ \mathbf{j} - \varrho \circ \mathbf{R} \circ \mathbf{b} = \mathbf{j}' - \mathbf{R}' \circ \mathbf{b} \quad , \tag{6.103}$$

$$\varrho \circ \mathbf{j} - \mathbf{j}' = (\varrho \circ \mathbf{R} - \mathbf{R}') \circ \mathbf{b} \quad , \tag{6.104}$$

and therefore finally to an expression for the matrix (of coefficients) **b**:

$$\mathbf{b} = (\varrho \circ \mathbf{R} - \mathbf{R}')^{-1} \circ (\varrho \circ \mathbf{j} - \mathbf{j}') \quad . \tag{6.105}$$

References

1. M. Abramowitz and I. Stegun, *Handbook of mathematical functions* (Dover Publ., New York 1973)
2. B.H. Drittler: KKR-Greensche Funktionsmethode für das volle Zellpotential, PHD Thesis, Aachen (1991)
3. H.R. Schwarz, *Numerische Mathematik* (B.G. Teubner, Stuttgart 1997)
4. F. Bashforth and J.C. Adams, *Theories of Capillary Action* (Cambridge University Press, London 1883)
5. H. Jeffreys and B.S. Jeffreys, *Methods of Mathematical Physics* (Cambridge University Press, Cambridge, England 1988)
6. W.H. Press, B.P. Flannery, S.A. Teukolsky, and W.T. Vetterling, *Numerical Recipes in FORTRAN: The Art of Scientific Computing, 2nd ed.* (Cambridge University Press, Cambridge, England 1992)
7. F. Calogero, Nuovo Cimento XXVII, 1007 (1963); *The Variable Phase Approach to Potential Scattering* (Academic Press, New York 1967)

7 Spin-polarized non-relativistic single-site scattering

Within the *local spin density functional* the non-relativistic Kohn-Sham Hamiltonian is given in Rydberg units by

$$\mathcal{H}(\mathbf{r}) = \left(-\nabla^2 + V^{\text{eff}}(\mathbf{r})\right) \mathsf{I}_2 + \sigma \cdot \mathbf{B}^{\text{eff}}(\mathbf{r}) \quad , \tag{7.1}$$

where as should be recalled $V^{\text{eff}}(\mathbf{r})$ is the effective potential,

$$V^{\text{eff}}(\mathbf{r}) = \begin{cases} V(\mathbf{r}) & \mathbf{r} \in D_V \\ 0 & \mathbf{r} \notin D_V \end{cases} \quad , \tag{7.2}$$

$B^{\text{eff}}(\mathbf{r})$ the effective exchange field,

$$\mathbf{B}^{\text{eff}}(\mathbf{r}) = \begin{cases} \mathbf{B}(\mathbf{r}) & \mathbf{r} \in D_B \\ 0 & \mathbf{r} \notin D_B \end{cases} \quad , \tag{7.3}$$

$D_V \equiv D_B$, and

$$\mathsf{I}_2 = \begin{pmatrix} 1 & 0 \\ 0 & -1 \end{pmatrix} \quad , \quad \sigma_z = \begin{pmatrix} 1 & 0 \\ 0 & -1 \end{pmatrix} \quad . \tag{7.4}$$

It should be noted that in the *local spin-density functional* the effective field $\mathbf{B}(\mathbf{r})$ always points along an assumed z-direction, i.e., $\mathbf{B}(\mathbf{r})$ refers therefore to the following vector,

$$\mathbf{B}(\mathbf{r}) = (0,0,1)B(\mathbf{r}) = B_z(\mathbf{r})\mathbf{e}_z \quad , \tag{7.5}$$

which, however, is of no concern at all in a non-relativistic description, since $\mathcal{H}(\mathbf{r})$ is SU_2 invariant (invariant with respect to rotations in spin space).

Since $\mathcal{H}(\mathbf{r})$ is "diagonal" in spin space, (7.1) can be rewritten in terms of two separate equations

$$\mathcal{H}_s(\mathbf{r}) = -\nabla^2 + V^{\text{eff}}(\mathbf{r}) + sB_z^{\text{eff}}(\mathbf{r}) = -\nabla^2 + W_s^{\text{eff}}(\mathbf{r}) \quad , \quad s = \pm 1 \quad , \tag{7.6}$$

usually termed "spin-up" and "spin-down" channel,

$$\mathcal{H}_\uparrow(\mathbf{r}) = -\nabla^2 + W_\uparrow^{\text{eff}}(\mathbf{r}) \quad , \quad \mathcal{H}_\downarrow(\mathbf{r}) = -\nabla^2 + W_\downarrow^{\text{eff}}(\mathbf{r}) \quad . \tag{7.7}$$

Clearly enough the resolvent of a spin-polarized non-relativistic Kohn-Sham Hamiltonian is also diagonal in spin space and so are corresponding quantities

such as the $\mathcal{T}$ operator and their respective configurational space representations, e.g.,

$$G(z;\mathbf{r},\mathbf{r}') = \begin{pmatrix} G_\uparrow(\mathbf{r},\mathbf{r}',z) & 0 \\ 0 & G_\downarrow(\mathbf{r},\mathbf{r}',z) \end{pmatrix} \equiv \begin{pmatrix} G_{\uparrow\uparrow}(\mathbf{r},\mathbf{r}',z) & 0 \\ 0 & G_{\downarrow\downarrow}(\mathbf{r},\mathbf{r}',z) \end{pmatrix} \quad . \tag{7.8}$$

Independent of whether $V^{\text{eff}}(\mathbf{r})$ and $\mathbf{B}^{\text{eff}}(\mathbf{r})$ correspond to spherical symmetric functions or not, the scattering solutions and the single-site t-matrix can therefore be obtained using exactly the same procedures as discussed in the previous two chapters by considering single-site potentials of the type $W_\uparrow^{\text{eff}}(\mathbf{r})$ and $W_\downarrow^{\text{eff}}(\mathbf{r})$ in turn:

$$Z_{s,L}(z;\mathbf{r}) = \sum_{L'} j_{L'}(z;\mathbf{r}) K^{-1}_{s,L'L}(z) + p n_L(z;\mathbf{r}) \quad , \tag{7.9}$$

$$K^{-1}_{s,L'L}(z) = t^{-1}_{s,L'L}(z) - \mathrm{i}p\delta_{LL'} \quad , \tag{7.10}$$

$$p = \sqrt{z} \quad , \quad \mathrm{Im}z > 0 \quad , \quad s = \uparrow\downarrow \quad . \tag{7.11}$$

Only in the case that $W_\uparrow^{\text{eff}}(\mathbf{r})$ and $W_\downarrow^{\text{eff}}(\mathbf{r})$ are spherical symmetric the reactance and the single-site t-matrix are diagonal angular momentum representations:

$$K_{s,LL'}(z) = K_{s,\ell}(z)\delta_{\ell\ell'}\delta_{mm'} \quad , \quad t_{s,LL'}(z) = t_{s,\ell}(z)\delta_{\ell\ell'}\delta_{mm'} \quad . \tag{7.12}$$

References

1. P. Weinberger, *Electron Scattering Theory of Ordered and Disordered Matter* (Clarendon Press, Oxford 1992)

8 Relativistic single-site scattering for spherically symmetric potentials

The Kohn-Sham-Dirac Hamiltonian for a single spherical symmetric effective potential $V(|\mathbf{r}|)$ of the type

$$V(|\mathbf{r}|) = \begin{cases} V(r) & r \leq r_{\mathrm{MT}} \\ 0 & r > r_{\mathrm{MT}} \end{cases} \quad , \tag{8.1}$$

is a 4×4 matrix operator [1],

$$\mathcal{H}(\mathbf{r}) = c\boldsymbol{\alpha} \cdot \mathbf{p} + \beta mc^2 + V(|\mathbf{r}|)\ \mathsf{I}_4 \quad , \tag{8.2}$$

$$\boldsymbol{\alpha} = \begin{pmatrix} 0 & \sigma \\ \sigma & 0 \end{pmatrix} \quad , \quad \beta = \begin{pmatrix} \mathsf{I}_2 & 0 \\ 0 & -\mathsf{I}_2 \end{pmatrix} \quad , \tag{8.3}$$

$$\sigma = (\sigma_x, \sigma_y, \sigma_z) \quad , \tag{8.4}$$

where the σ_i are the famous Pauli spin matrices

$$\sigma_x = \begin{pmatrix} 0 & 1 \\ 1 & 0 \end{pmatrix} \quad , \quad \sigma_y = \begin{pmatrix} 0 & -\mathrm{i} \\ \mathrm{i} & 0 \end{pmatrix} \quad , \quad \sigma_z = \begin{pmatrix} 1 & 0 \\ 0 & -1 \end{pmatrix} \quad , \tag{8.5}$$

and I_n is a n-dimensional unit matrix. It should be noted that in the case of the atomic sphere approximation (ASA) the so-called muffin-tin radius r_{MT} (inscribed sphere radius in the case of simple lattices) is simply replaced by the Wigner-Seitz radius r_{WS}.

Equation (8.2) leads to the following system of coupled first order differential equations

$$\sum_{\kappa,\mu} \begin{bmatrix} W - mc^2 - V(r) & -\mathrm{i}\hbar c[\frac{\mathrm{d}}{\mathrm{d}r} + \frac{1}{r} - \frac{\kappa}{r}] \\ -\mathrm{i}\hbar c[\frac{\mathrm{d}}{\mathrm{d}r} + \frac{1}{r} + \frac{\kappa}{r}] & W + mc^2 - V(r) \end{bmatrix} \begin{bmatrix} g_\kappa(r)\chi_{\kappa\mu}(\hat{\mathbf{r}}) \\ \mathrm{i}f_\kappa(r)\chi_{-\kappa\mu}(\hat{\mathbf{r}}) \end{bmatrix} = 0 \quad , \tag{8.6}$$

in which the $\chi_{\kappa\mu}(\hat{\mathbf{r}})$ are spin spherical harmonics,

$$\chi_Q(\hat{\mathbf{r}}) \equiv \chi_{\kappa\mu}(\hat{\mathbf{r}}) = \sum_{s=\pm 1/2} C(\ell, j, \frac{1}{2} |\ \mu - s, s) Y_{\ell,\mu-s}(\hat{\mathbf{r}}) \Phi_s \quad , \tag{8.7}$$

with the $C(\ell, j, \frac{1}{2} |\ \mu - s, s)$ referring to Clebsch-Gordan coefficients and the Φ_s denoting the following spinor basis functions,

$$\Phi_{1/2} = \begin{pmatrix} 1 \\ 0 \end{pmatrix} \quad , \quad \Phi_{-1/2} = \begin{pmatrix} 0 \\ 1 \end{pmatrix} \quad , \tag{8.8}$$

see also Table 8.1.

Table 8.1. Indexing of relativistic quantum numbers up to $\kappa = 4$.

Q	ℓ	j	κ	μ
1	0	$\frac{1}{2}$	-1	$-\frac{1}{2}$
2	0	$\frac{1}{2}$	-1	$\frac{1}{2}$
3	1	$\frac{1}{2}$	1	$-\frac{1}{2}$
4	1	$\frac{1}{2}$	1	$\frac{1}{2}$
5	1	$\frac{3}{2}$	-2	$-\frac{3}{2}$
6	1	$\frac{3}{2}$	-2	$-\frac{1}{2}$
7	1	$\frac{3}{2}$	-2	$\frac{1}{2}$
8	1	$\frac{3}{2}$	-2	$\frac{3}{2}$
9	2	$\frac{3}{2}$	2	$-\frac{3}{2}$
10	2	$\frac{3}{2}$	2	$-\frac{1}{2}$
11	2	$\frac{3}{2}$	2	$\frac{1}{2}$
12	2	$\frac{3}{2}$	2	$\frac{3}{2}$
13	2	$\frac{5}{2}$	-3	$-\frac{5}{2}$
14	2	$\frac{5}{2}$	-3	$-\frac{3}{2}$
15	2	$\frac{5}{2}$	-3	$-\frac{1}{2}$
16	2	$\frac{5}{2}$	-3	$\frac{1}{2}$
17	2	$\frac{5}{2}$	-3	$\frac{3}{2}$
18	2	$\frac{5}{2}$	-3	$\frac{5}{2}$
19	3	$\frac{5}{2}$	3	$-\frac{5}{2}$
20	3	$\frac{5}{2}$	3	$-\frac{3}{2}$
21	3	$\frac{5}{2}$	3	$-\frac{1}{2}$
22	3	$\frac{5}{2}$	3	$\frac{1}{2}$
23	3	$\frac{5}{2}$	3	$\frac{3}{2}$
24	3	$\frac{5}{2}$	3	$\frac{5}{2}$
25	3	$\frac{7}{2}$	-4	$-\frac{7}{2}$
26	3	$\frac{7}{2}$	-4	$-\frac{5}{2}$
27	3	$\frac{7}{2}$	-4	$-\frac{3}{2}$
28	3	$\frac{7}{2}$	-4	$-\frac{1}{2}$
29	3	$\frac{7}{2}$	-4	$\frac{1}{2}$
30	3	$\frac{7}{2}$	-4	$\frac{3}{2}$
31	3	$\frac{7}{2}$	-4	$\frac{5}{2}$
32	3	$\frac{7}{2}$	-4	$\frac{7}{2}$
33	4	$\frac{7}{2}$	4	$-\frac{7}{2}$
34	4	$\frac{7}{2}$	4	$-\frac{5}{2}$
35	4	$\frac{7}{2}$	4	$-\frac{3}{2}$
36	4	$\frac{7}{2}$	4	$-\frac{1}{2}$
37	4	$\frac{7}{2}$	4	$\frac{1}{2}$
38	4	$\frac{7}{2}$	4	$\frac{3}{2}$
39	4	$\frac{7}{2}$	4	$\frac{5}{2}$
40	4	$\frac{7}{2}$	4	$\frac{7}{2}$

8.1 Direct numerical solution of the coupled differential equations

Separation of variables in (8.6) leads to the following coupled radial differential equations, occasionally termed "radial Dirac equation",

$$\left[W - mc^2 - V(r)\right] g_\kappa(r) + \hbar c \frac{1}{r}\left[\frac{\mathrm{d}}{\mathrm{d}r} - \frac{\kappa}{r}\right](r f_\kappa(r)) = 0 \quad , \tag{8.9}$$

$$-\hbar c \frac{1}{r}\left[\frac{\mathrm{d}}{\mathrm{d}r} + \frac{\kappa}{r}\right](r g_\kappa(r)) + \left[W + mc^2 - V(r)\right] f_\kappa(r) = 0 \quad . \tag{8.10}$$

Introducing as before the following functions and omitting their explicit dependence on an in general complex energy,

$$P_\kappa(r) \equiv r g_\kappa(r), \qquad Q_\kappa(r) \equiv \hbar c r f_\kappa(r) \quad . \tag{8.11}$$

(in atomic units: $\hbar = 1, m = \frac{1}{2}, c \approx 274$) (8.9) and (8.10) reduce to

$$\frac{\mathrm{d}}{\mathrm{d}r} Q_\kappa(r) = \frac{\kappa}{r} Q_\kappa(r) - \left[\epsilon - V(r)\right] P_\kappa(r) \quad , \tag{8.12}$$

$$\frac{\mathrm{d}}{\mathrm{d}r} P_\kappa(r) = -\frac{\kappa}{r} P_\kappa(r) + \left[\frac{\epsilon - V(r)}{c^2} + 1\right] Q_\kappa(r) \quad , \tag{8.13}$$

with

$$\epsilon = W - mc^2 \quad . \tag{8.14}$$

8.1.1 Starting values

Changing variables, $r = e^x$, these coupled equations transform to

$$\frac{\mathrm{d}}{\mathrm{d}x} Q_\kappa(x) = \kappa Q_\kappa(x) - e^x \left[\epsilon - V(x)\right] P_\kappa(x) \quad , \tag{8.15}$$

$$\frac{\mathrm{d}}{\mathrm{d}x} P_\kappa(x) = -\kappa P_\kappa(x) + e^x \left[\frac{\epsilon - V(x)}{c^2} + 1\right] Q_\kappa(x) \quad . \tag{8.16}$$

In the limit of $x \to -\infty$, or $r \to 0$, one can make the following approximation:

$$r\left(\frac{\epsilon - V(r)}{c^2} + 1\right) \longrightarrow \frac{2Z}{c^2} = \frac{b}{c} \quad . \tag{8.17}$$

By defining

$$b = \frac{2Z}{c} \quad , \tag{8.18}$$

one then obtains the below approximation in the vicinity of the origin

$$\frac{\mathrm{d}}{\mathrm{d}x}P_\kappa(x) = -\kappa\, P_\kappa(x) + \frac{b}{c}\, Q_\kappa(x) \quad , \tag{8.19}$$

$$\frac{\mathrm{d}}{\mathrm{d}x}Q_\kappa(x) = \kappa\, Q_\kappa(x) - bc\, P_\kappa(x) \quad . \tag{8.20}$$

The second derivative of $P_\kappa(r)$ is given by

$$\frac{\mathrm{d}^2}{\mathrm{d}x^2}P_\kappa(x) = -\kappa\,\frac{\mathrm{d}}{\mathrm{d}x}P_\kappa(x) + \frac{b}{c}\,\frac{\mathrm{d}}{\mathrm{d}x}Q_\kappa(x) \tag{8.21}$$

$$= -\kappa\,\frac{\mathrm{d}}{\mathrm{d}x}P_\kappa(x) + \frac{b}{c}\left[\kappa\, Q_\kappa(x) - bc\, P_\kappa(x)\right] \tag{8.22}$$

$$= \kappa^2 P_\kappa(x) - \frac{b\kappa}{c}Q_\kappa(x) + \frac{b}{c}\,\frac{\mathrm{d}}{\mathrm{d}x}Q_\kappa(x) \tag{8.23}$$

$$= \frac{b}{c}\left(\frac{\mathrm{d}}{\mathrm{d}x}Q_\kappa(x) - \kappa Q_\kappa(x)\right) + \kappa^2 P_\kappa(x) \tag{8.24}$$

$$= \left(\kappa^2 - b^2\right) P_\kappa(x) \quad . \tag{8.25}$$

$P_\kappa(x)$ is therefore of the form:

$$P_\kappa(x) = e^{Ax} \quad , \tag{8.26}$$

with

$$A^2 = \kappa^2 - b^2 \quad , \tag{8.27}$$

$$A = \sqrt{\kappa^2 - b^2} \tag{8.28}$$

$$= \sqrt{\kappa^2 - \left(\frac{2Z}{c}\right)^2} \quad . \tag{8.29}$$

Thus one finally arrives at

$$\frac{b}{c}\, Q_\kappa(x_1) = \frac{\mathrm{d}}{\mathrm{d}x}P_\kappa(x_1) + \kappa\, P_\kappa(x_1) \quad , \tag{8.30}$$

$$Q_\kappa(x_1) = \frac{\kappa + \sqrt{\kappa^2 - b^2}}{b/c}\, P_\kappa(x_1) \quad . \tag{8.31}$$

Hence, as start values one can use:

$$P_\kappa(x_1) = 10^{-20} \quad , \tag{8.32}$$

$$Q_\kappa(x_1) = \frac{\kappa + \sqrt{\kappa^2 - b^2}}{b/c}\, P_\kappa(x_1) \quad , \tag{8.33}$$

$$\frac{\mathrm{d}}{\mathrm{d}x}P_\kappa(x_1) = -\kappa\, P_\kappa(x_1) + e^{x_1}\left[\frac{\epsilon - V(x_1)}{c^2} + 1\right] Q_\kappa(x_1) \quad , \tag{8.34}$$

$$\frac{\mathrm{d}}{\mathrm{d}x}Q_\kappa(x_1) = \kappa\, Q_\kappa(x_1) - e^{x_1}\left[\epsilon - V(x_1)\right] P_\kappa(x_1) \quad . \tag{8.35}$$

where clearly enough in principle $P_\kappa(x_1)$ is an arbitrary constant, the value quoted above turned out to be numerically advisable.

8.1.2 Runge–Kutta extrapolation

The first few values (usually 5) are obtained from a Runge–Kutta extrapolation,

$$P_\kappa(x_{i+1}) = P_\kappa(x_i) + \frac{\Delta x}{6}(k_1 + 2k_2 + 2k_3 + k_4) \quad , \tag{8.36}$$

$$Q_\kappa(x_{i+1}) = Q_\kappa(x_i) + \frac{\Delta x}{6}(m_1 + 2m_2 + 2m_3 + m_4) \quad . \tag{8.37}$$

The functions $\mathbf{P}(x_i)$ and $\mathbf{Q}(x_i)$ in Table 5.1 are now given by $P_\kappa(x_i)$ and $Q_\kappa(x_i)$, from which according to this table the constants k_i and m_i follow. The functions $f\,[P_\kappa(x_i), Q_\kappa(x_i)]$ and $g\,[P_\kappa(x_i), Q_\kappa(x_i)]$ have to be evaluated using the below equations,

$$f\,[P_\kappa(x_i), Q_\kappa(x_i)] = k_1 = -\kappa\, P_\kappa(x_i) + e^{x_i}\left[\frac{\epsilon - V(x_i)}{c^2} + 1\right] Q_\kappa(x_i) \quad , \tag{8.38}$$

$$g\,[P_\kappa(x_i), Q_\kappa(x_i)] = m_1 = \kappa\, Q_\kappa(x_i) - e^{x_i}\,[\epsilon - V(x_i)]\, P_\kappa(x_i) \quad . \tag{8.39}$$

The values of the other coefficients are obtained in analogous manner to (5.32)–(5.37) in the non-relativistic case using the scheme in Table 5.1. Finally, at x_{i+1} the derivatives of $P_\kappa(x_{i+1})$ and $Q_\kappa(x_{i+1})$ are easily obtained via (8.34) and (8.35).

8.1.3 Predictor-corrector algorithm

Having provided the first few points a predictor–corrector algorithm [2] [3] [4] [5] can be started. The expressions for the predictors (suffix zero) are obtained in the same manner as in the non-relativistic case in (5.38) with $f(x_i)$ being $P_\kappa(x_i)$ and $Q_\kappa(x_i)$, respectively. Furthermore, their derivatives are given by:

$$f'(x_i) = \frac{\mathrm{d}}{\mathrm{d}x} P_\kappa(x_i) \quad , \quad \text{or} \qquad \frac{\mathrm{d}}{\mathrm{d}x} Q_\kappa(x_i) \quad . \tag{8.40}$$

The correctors are once more calculated from (5.40) and the function $f^{1\prime}(x_i)$ appearing in that expression refers to either one of the equations given below:

$$\frac{\mathrm{d}}{\mathrm{d}x} P^1_\kappa(x_i) = -\kappa\, P^0_\kappa(x_i) + e^{x_i}\left[\frac{\epsilon - V(x_i)}{c^2} + 1\right] Q^0_\kappa(x_i) \quad , \tag{8.41}$$

$$\frac{\mathrm{d}}{\mathrm{d}x} Q^1_\kappa(x_i) = \kappa\, Q^0_\kappa(x_i) - e^{x_i}\,[\epsilon - V(x_i)]\, P^0_\kappa(x_i) \quad . \tag{8.42}$$

At a given radial mesh-point the predictors and correctors have to be evaluated iteratively until they assume the same values, then the next mesh point is computed and so forth. The irregular solutions of (8.12) - (8.13) are obtained in a similar way by an inward integration starting with values provided by the normalization at r_{MT} , see below.

8.2 Single site Green's function

For $|\mathbf{r}| > r_{\mathrm{MT}}$ ($|\mathbf{r}| > r_{\mathrm{WS}}$ in the case of the ASA), i.e., for $V(\mathbf{r}) = 0$, the solutions of (8.2) corresponding to a complex energy $z = \epsilon + \mathrm{i}\delta$ are defined as

$$f_Q(z;\mathbf{r}) = \begin{pmatrix} f_\ell(pr)\,\chi_{\kappa\mu}(\hat{\mathbf{r}}) \\ \\ \frac{\mathrm{i}S_\kappa p}{c}\, f_{\overline{\ell}}(pr)\,\chi_{-\kappa,\mu}(\hat{\mathbf{r}}) \end{pmatrix} \quad , \tag{8.43}$$

$p = \sqrt{z}$, with $f_\ell = j_\ell, n_\ell$ or $h_\ell^\pm$, namely, being spherical Bessel-, Neumann- and Hankel-functions. The single site Green's function is now of the form

$$\begin{aligned} G(z;\mathbf{r},\mathbf{r}') = & \sum_{Q,Q'} Z_Q(z;\mathbf{r})\; t_{QQ'}(z)\; \widetilde{Z}_{Q'}(z;\mathbf{r}')^\dagger \\ & - \sum_Q Z_Q(z;\mathbf{r})\; \widetilde{J}_Q(z;\mathbf{r}')^\dagger\, \Theta(r'-r) \\ & - \sum_Q J_Q(z;\mathbf{r})\; \widetilde{Z}_Q(z;\mathbf{r}')^\dagger\, \Theta(r-r') \quad , \end{aligned} \tag{8.44}$$

see (3.255), where the scattering solutions $Z_Q(z;\mathbf{r})$ and $J_Q(z;\mathbf{r})$ and the irregular solutions of (8.2) are defined by

$$Z_Q(z;\mathbf{r}) = \begin{pmatrix} g_Q^Z(z;r)\,\chi_Q(\hat{\mathbf{r}}) \\ \\ \mathrm{i}f_Q^Z(z;r)\,\chi_{\overline{Q}}(\hat{\mathbf{r}}) \end{pmatrix} \quad , \tag{8.45}$$

$$J_Q(z;\mathbf{r}) = \begin{pmatrix} g_Q^J(z;r)\,\chi_Q(\hat{\mathbf{r}}) \\ \\ \mathrm{i}f_Q^J(z;r)\,\chi_{\overline{Q}}(\hat{\mathbf{r}}) \end{pmatrix} \quad , \tag{8.46}$$

$$\widetilde{Z}_Q(z;\mathbf{r}) = \begin{pmatrix} g_Q^Z(z;r)^*\,\chi_Q(\hat{\mathbf{r}}) \\ \\ \mathrm{i}f_Q^Z(z;r)^*\,\chi_{\overline{Q}}(\hat{\mathbf{r}}) \end{pmatrix} \quad , \tag{8.47}$$

$$\widetilde{J}_Q(z;\mathbf{r}) = \begin{pmatrix} g_Q^J(z;r)^*\,\chi_Q(\hat{\mathbf{r}}) \\ \\ \mathrm{i}f_Q^J(z;r)^*\,\chi_{\overline{Q}}(\hat{\mathbf{r}}) \end{pmatrix} \quad . \tag{8.48}$$

such that at $r = r_{\mathrm{MT}}$

$$Z_Q(z;\mathbf{r}) = j_Q(z;\mathbf{r})\,K_Q^{-1}(z) + pn_Q(z;\mathbf{r}) \quad , \tag{8.49}$$

$$J_Q(z;\mathbf{r}) = j_Q(z;\mathbf{r}) \quad , \tag{8.50}$$

with $K_Q(z)$ being the reactance.

8.2.1 Normalization of regular scattering solutions and the single site t matrix

Since the regular solutions $g^{\mathrm{r}}_{Q}(z;r)$ and $f^{\mathrm{r}}_{Q}(z;r)$ found from solving the coupled radial differential equations (8.12)–(8.13) have to be proportional to the regular scattering solutions,

$$a_Q \begin{pmatrix} g^{\mathrm{r}}_{Q}(z;r)\,\chi_Q(\hat{\mathbf{r}}) \\ \\ \mathrm{i} f^{\mathrm{r}}_{Q}(z;r)\,\chi_{\overline{Q}}(\hat{\mathbf{r}}) \end{pmatrix} = \begin{pmatrix} g^{Z}_{Q}(z;r)\,\chi_Q(\hat{\mathbf{r}}) \\ \\ \mathrm{i} f^{Z}_{Q}(z;r)\,\chi_{\overline{Q}}(\hat{\mathbf{r}}) \end{pmatrix} =$$

$$= \begin{pmatrix} j_\ell(pr)\,\chi_{\kappa\mu}(\hat{\mathbf{r}}) \\ \\ \frac{\mathrm{i}S_\kappa\, p}{c}\, j_{\overline{\ell}}(pr)\,\chi_{-\kappa,\mu}(\hat{\mathbf{r}}) \end{pmatrix} K_Q^{-1}(z) + p \begin{pmatrix} n_\ell(pr)\,\chi_{\kappa\mu}(\hat{\mathbf{r}}) \\ \\ \frac{\mathrm{i}S_\kappa\, p}{c}\, n_{\overline{\ell}}(pr)\,\chi_{-\kappa,\mu}(\hat{\mathbf{r}}) \end{pmatrix} \quad , \tag{8.51}$$

at r_{MT} one immediately gets two equations for the unknown proportionality constants a_Q and the reactance $K_Q(z)$,

$$a_Q g^{\mathrm{r}}_{Q}(z;r) = j_\ell(pr)\,K_Q^{-1}(z) + p n_\ell(pr) \quad , \tag{8.52}$$

$$a_Q f^{\mathrm{r}}_{Q}(z;r) = \frac{S_\kappa\, p}{c} j_{\overline{\ell}}(pr)\,K_Q^{-1}(z) + p\frac{S_\kappa\, p}{c}\, n_{\overline{\ell}}(pr) \quad , \tag{8.53}$$

which yield

$$K_Q(z) = -\frac{1}{p}\frac{\left(f^{\mathrm{r}}_{Q}(z;r)\, j_\ell(pr) - g^{\mathrm{r}}_{Q}(z;r)\,\frac{S_\kappa\, p}{c} j_{\overline{\ell}}(pr)\right)}{\left(f^{\mathrm{r}}_{Q}(z;r)\, n_\ell(pr) - g^{\mathrm{r}}_{Q}(z;r)\,\frac{S_\kappa\, p}{c}\, n_{\overline{\ell}}(pr)\right)} \quad , \tag{8.54}$$

$$a_Q = \frac{\left(j_\ell(pr)\,K_Q^{-1}(z) + p n_\ell(pr)\right)}{g^{\mathrm{r}}_{Q}(z;r)} \quad . \tag{8.55}$$

The single-site t-matrix is then given by the by now familiar expression

$$t_Q^{-1}(z) = K_Q^{-1}(z) + \mathrm{i}p \quad . \tag{8.56}$$

Furthermore, since the radial amplitudes $g_Q(z;r)$ and $f_Q(z;r)$ only depend on the quantum number κ, see (8.12)–(8.13), this expression reduces to

$$t_\kappa^{-1}(z) = K_\kappa^{-1}(z) + \mathrm{i}p \quad , \quad p = \sqrt{z} \quad , \quad \mathrm{Im}z > 0 \quad . \tag{8.57}$$

References

1. P. Weinberger, *Electron Scattering Theory of Ordered and Disordered Matter* (Clarendon Press, Oxford 1992)
2. H.R. Schwarz, *Numerische Mathematik* (B.G. Teubner, Stuttgart 1997)
3. F. Bashforth and J.C. Adams, *Theories of Capillary Action* (Cambridge University Press, London 1883)
4. H. Jeffreys and B.S. Jeffreys, *Methods of Mathematical Physics* (Cambridge University Press, Cambridge, England 1988)
5. W.H. Press, B.P. Flannery, S.A. Teukolsky, and W.T. Vetterling, *Numerical Recipes in FORTRAN: The Art of Scientific Computing, 2nd ed.* (Cambridge University Press, Cambridge, England 1992)

9 Relativistic full potential single-site scattering

The Kohn-Sham-Dirac Hamiltonian is now of the form

$$\mathcal{H}(\mathbf{r}) = c\boldsymbol{\alpha}\cdot\mathbf{p} + \beta mc^2 + \upsilon(\mathbf{r})\ \mathsf{I}_4 \quad , \tag{9.1}$$

where the full potential $\upsilon(\mathbf{r})$, confined to a Wigner-Seitz cell Ω of some arbitrary, polyhedral shape, is defined by

$$\upsilon(\mathbf{r}) = \begin{cases} \upsilon(\mathbf{r}) & r \in \Omega \\ 0 & r \notin \Omega \end{cases} \quad , \tag{9.2}$$

The quantities $\boldsymbol{\alpha}$, $\mathbf{p}$, β, and the Pauli spin matrices σ_i have been defined at the beginning of the previous chapter and need not be repeated here.

9.1 Direct numerical solution of the coupled differential equations

In rewriting the Hamiltonian in spherical coordinates [1] [2] and making the following Ansatz for the solutions

$$\psi_Q(\mathbf{r}) = \sum_{Q'} \begin{pmatrix} g_{Q'Q}(r)\,\chi_{Q'}(\hat{\mathbf{r}}) \\ \mathrm{i} f_{Q'Q}(r)\,\chi_{\bar{Q}'}(\hat{\mathbf{r}}) \end{pmatrix} \quad , \tag{9.3}$$

where $Q = (\kappa, \mu)$ and $\bar{Q} = (-\kappa, \mu)$ refer to the composite indices of the relativistic quantum numbers listed in Table 8.1, one arrives at the below system of coupled radial equations:

$$\begin{bmatrix} W - mc^2 & -\mathrm{i}\hbar c[\frac{\mathrm{d}}{\mathrm{d}r} + \frac{1}{r} - \frac{\kappa}{r}] \\ -\mathrm{i}\hbar c[\frac{\mathrm{d}}{\mathrm{d}r} + \frac{1}{r} + \frac{\kappa}{r}] & W + mc^2 \end{bmatrix} \begin{bmatrix} g_{Q'Q}(r) \\ \mathrm{i} f_{Q'Q}(r) \end{bmatrix} =$$

$$= \sum_{Q''} \begin{bmatrix} \upsilon^{+}_{Q'Q''}(r) g_{Q''Q}(r) \\ \mathrm{i}\upsilon^{-}_{Q'Q''}(r) f_{Q''Q}(r) \end{bmatrix} \quad . \tag{9.4}$$

These equations are obtained after having used the orthonormality of the spin spherical harmonics, $\chi_{Q'}(\hat{\mathbf{r}})$, and having performed an integration over $\hat{\mathbf{r}}$. The "relativistic" full potentials $v^{+}_{QQ'}(r)$ and $v^{-}_{\bar{Q}Q'}(r)$ are now given by

$$v^{+}_{QQ'}(r) = \langle \chi_Q | v(\mathbf{r}) | \chi_{Q'} \rangle \tag{9.5}$$

$$= \sum_{\Lambda} v_{\Lambda}(r) \langle \chi_Q | Y_{\Lambda}(\hat{\mathbf{r}}) | \chi_{Q'} \rangle \tag{9.6}$$

$$= \sum_{s=\pm\frac{1}{2}} C(\ell, j, \frac{1}{2} \,|\, \mu - s, s)\, C(\ell', j', \frac{1}{2} \,|\, \mu' - s, s)\, v_{LL'}(r) \quad , \tag{9.7}$$

$$v^{-}_{\bar{Q}Q'}(r) = \langle \chi_{\bar{Q}} | v(\mathbf{r}) | \chi_{\bar{Q}'} \rangle \tag{9.8}$$

$$= \sum_{s=\pm\frac{1}{2}} C(\bar{\ell}, j, \frac{1}{2} \,|\, \mu - s, s)\, C(\bar{\ell}', j', \frac{1}{2} \,|\, \mu' - s, s)\, v_{\bar{L}\bar{L}'}(r) \quad , \tag{9.9}$$

where

$$v_{LL'}(r) = \sum_{\Lambda} C^{L}_{L'\Lambda} v_{\Lambda}(r) \quad , \tag{9.10}$$

$$v_{\bar{L}\bar{L}'}(r) = \sum_{\Lambda} C^{\bar{L}}_{\bar{L}'\Lambda} v_{\Lambda}(r) \quad . \tag{9.11}$$

Using atomic units ($\hbar = 1$, $m = 1/2$) and the following definitions

$$P_{QQ'}(r) = r g_{QQ'}(r)\,, \quad Q_{QQ'}(r) = c r f_{QQ'}(r) \quad ,$$

the "radial Dirac equations" in (9.4) transform to

$$\frac{\mathrm{d}}{\mathrm{d}r} Q_{Q'Q}(r) = \frac{\kappa}{r} Q_{Q'Q}(r) - \sum_{Q''} \left[\epsilon \delta_{Q'Q''} - v^{+}_{Q'Q''}(r) \right] P_{Q''Q}(r) \tag{9.12}$$

$$\frac{\mathrm{d}}{\mathrm{d}r} P_{Q'Q}(r) = -\frac{\kappa}{r} P_{Q'Q}(r) + \sum_{Q''} \left\{ \frac{1}{c^2} \left[\epsilon \delta_{Q'Q''} - v^{-}_{Q'Q''}(r) \right] + \delta_{Q'Q''} \right\} Q_{Q''Q}(r) \quad . \tag{9.13}$$

where $\epsilon = W - mc^2$ and $\left(W + mc^2\right)/c^2 = \epsilon/c^2 + 1$.

9.1.1 Starting values

In changing variables $x = \ln r$, one obtains

$$\frac{\mathrm{d}}{\mathrm{d}x}Q_{Q'Q}(x) = \kappa\, Q_{Q'Q}(x) - \sum_{Q''} e^x \left[\epsilon\delta_{Q'Q''} - v^+_{Q'Q''}(x)\right] P_{Q''Q}(x) \quad , \tag{9.14}$$

$$\begin{aligned}\frac{\mathrm{d}}{\mathrm{d}x}P_{Q'Q}(x) &= -\kappa\, P_{Q'Q}(x) \\ &\quad + \sum_{Q''} e^x \left\{ \frac{1}{c^2}\left[\epsilon\delta_{Q'Q''} - v^-_{Q'Q''}(x)\right] + \delta_{Q'Q''} \right\} Q_{Q''Q}(x) \quad .\end{aligned} \tag{9.15}$$

As in the vicinity of the origin the potentials have spherical symmetry, for small enough x there are only diagonal terms in the matrices of solutions and consequently the starting values are analogous to those discussed in Sect. 8.1.1, namely

$$P_{QQ}(x_1) = 10^{-20} \quad , \tag{9.16}$$

$$Q_{QQ}(x_1) = \frac{\kappa + \sqrt{\kappa^2 - b^2}}{b/c}\, P_{QQ}(x_1) \quad , \tag{9.17}$$

$$\frac{\mathrm{d}}{\mathrm{d}x}P_{QQ}(x_1) = -\kappa\, P_{QQ}(x_1) + e^{x_1}\left[\frac{\epsilon - v^-_{QQ}(x_1)}{c^2} + 1\right] Q_{QQ}(x_1) \quad , \tag{9.18}$$

$$\frac{\mathrm{d}}{\mathrm{d}x}Q_{QQ}(x_1) = \kappa\, Q_{QQ}(x_1) - e^{x_1}\left[\epsilon - v^+_{QQ}(x_1)\right] P_{QQ}(x_1) \quad . \tag{9.19}$$

9.1.2 Runge–Kutta extrapolation

The extrapolation for the first few mesh points works exactly as discussed in sections 5.1.2 and 8.1.2 except that the functions $\mathbf{P}(x_i)$ and $\mathbf{Q}(x_i)$ are now given by $P_{QQ'}(x_i)$ and $Q_{QQ'}(x_i)$, respectively,

$$P_{QQ'}(x_{i+1}) = P_{QQ'}(x_i) + \frac{\Delta x}{6}\,(k_1 + 2k_2 + 2k_3 + k_4) \quad , \tag{9.20}$$

$$Q_{QQ'}(x_{i+1}) = Q_{QQ'}(x_i) + \frac{\Delta x}{6}\,(m_1 + 2m_2 + 2m_3 + m_4) \quad , \tag{9.21}$$

and that (9.14) and (9.15) have to be used in calculating k_i and m_i:

$$\begin{aligned}k_1 &= -\kappa\, P_{Q'Q}(x) \\ &\quad + \sum_{Q''} e^x \left\{ \frac{1}{c^2}\left[\epsilon\delta_{Q'Q''} - v^-_{Q'Q''}(x)\right] + \delta_{Q'Q''} \right\} Q_{Q''Q}(x) \quad ,\end{aligned} \tag{9.22}$$

$$m_1 = \kappa\, Q_{Q'Q}(x) - \sum_{Q''} e^x \left[\epsilon\delta_{Q'Q''} - v^+_{Q'Q''}(x)\right] P_{Q''Q}(x) \quad . \tag{9.23}$$

All other coefficients k_i and m_i are to be calculated according to Table 5.1.

9.1.3 Predictor-corrector algorithm

Also the predictor–corrector scheme works as in the case of spherical symmetric potentials and is discussed in Sect. 8.1.3. The function $f(x_i)$ is either represented by $P_{QQ'}(x_i)$ or by $Q_{QQ'}(x_i)$, and the predictors are calculated from (5.38). To calculate the correctors (5.40) is used, while in analogy to (8.41) and (8.42) the function $f^{1\prime}(x_i)$ is obtained from (9.14) and (9.15). The function $f^{1\prime}(x_i)$ is given by either

$$\frac{\mathrm{d}}{\mathrm{d}x}P^1_{QQ}(x_i) = -\kappa\, P^0_{Q'Q}(x_i) + \sum_{Q''} e^{x_i}\left\{\frac{1}{c^2}\left[\epsilon\delta_{Q'Q''} - v^-_{Q'Q''}(x_i)\right] + \delta_{Q'Q''}\right\} Q^0_{Q''Q}(x_i) \quad , \tag{9.24}$$

or

$$\frac{\mathrm{d}}{\mathrm{d}x}Q^1_{QQ}(x_i) = \kappa\, Q^0_{Q'Q}(x_i) - \sum_{Q''} e^{x_i}\left[\epsilon\delta_{Q'Q''} - v^+_{Q'Q''}(x_i)\right] P^0_{Q''Q}(x_i) \quad .$$

In order to compute the irregular solutions of the radial Dirac equation the same procedure is used as before, except that now an inward integration has to be performed. In the present case the starting values refer to the values at the bounding sphere radius, see also Sect. 11.2.6.

9.1.4 Normalization of regular and irregular scattering solutions and the single-site t matrix

The normalization of the relativistic scattering solutions and the calculation of the single-site t matrix in the case of full potentials will be discussed in full length in Sects. 11.2.4, 11.2.5, and 11.2.6.

References

1. M.E. Rose, *Relativistic Electron Theory* (Wiley, New York 1961)
2. P. Strange, *Relativistic Quantum Mechanics* (Cambridge University Press, Cambridge 1998)

10 Spin-polarized relativistic single-site scattering for spherically symmetric potentials

The Kohn-Sham-Dirac Hamiltonian corresponding to a spherical symmetric potential $V^{\text{eff}}(|\mathbf{r}|)$,

$$V^{\text{eff}}(|\mathbf{r}|) = \begin{cases} V(r) & r \leq r_{\text{MT}} \\ 0 & r > r_{\text{MT}} \end{cases} \quad , \tag{10.1}$$

and a spherical symmetric effective field $B_z^{\text{eff}}(|\mathbf{r}|)$ along an arbitrary assumed z-direction

$$B_z^{\text{eff}}(|\mathbf{r}|) = \begin{cases} B(r) & r \leq r_{\text{MT}} \\ 0 & r > r_{\text{MT}} \end{cases} \quad , \tag{10.2}$$

is a 4×4 matrix operator [1] [2] [3],

$$\mathcal{H}(\mathbf{r}) = c\,\boldsymbol{\alpha} \cdot \mathbf{p} + \beta mc^2 + V(r)\ \mathsf{I}_4 + \beta\Sigma_z\, B(r) \quad , \tag{10.3}$$

and leads to the following system of coupled first order differential equations

$$\sum_{\kappa,\mu} \begin{bmatrix} W - mc^2 - U^+(r) & -\mathrm{i}\hbar c[\frac{\mathrm{d}}{\mathrm{d}r} + \frac{1}{r} - \frac{\kappa}{r}] \\ -\mathrm{i}\hbar c[\frac{\mathrm{d}}{\mathrm{d}r} + \frac{1}{r} + \frac{\kappa}{r}] & W + mc^2 - U^-(r) \end{bmatrix} \begin{bmatrix} g_{\kappa\mu}(r)\chi_{\kappa\mu}(\hat{\mathbf{r}}) \\ \mathrm{i}f_{\kappa\mu}(r)\chi_{-\kappa\mu}(\hat{\mathbf{r}}) \end{bmatrix} = 0 \tag{10.4}$$

where

$$U^{\pm}(r) = \begin{bmatrix} V(r) \pm B(r) & 0 \\ 0 & V(r) \mp B(r) \end{bmatrix} \quad . \tag{10.5}$$

10.1 Direct numerical solution of the coupled radial differential equations

Integration over the angular parts and making use of the orthonormality of the spin spherical harmonics reduces (10.4) to the following set of coupled first order radial differential equations

$$\begin{bmatrix} W - mc^2 - V(r) & -\mathrm{i}\hbar c[\frac{\mathrm{d}}{\mathrm{d}r} + \frac{1}{r} - \frac{\kappa}{r}] \\ -\mathrm{i}\hbar c[\frac{\mathrm{d}}{\mathrm{d}r} + \frac{1}{r} + \frac{\kappa}{r}] & W + mc^2 - V(r) \end{bmatrix} \begin{bmatrix} g_{\kappa\mu}(r) \\ \mathrm{i}f_{\kappa\mu}(r) \end{bmatrix} =$$

$$\sum_{\kappa'} \begin{bmatrix} \langle\chi_Q|B(r)|\chi_{Q'}\rangle g_{\kappa'\mu}(r) \\ -\mathrm{i}\langle\chi_{\bar{Q}}|B(r)|\chi_{\bar{Q}'}\rangle f_{\kappa'\mu}(r) \end{bmatrix} \quad , \tag{10.6}$$

where

$$\langle\chi_Q|B(r)|\chi_{Q'}\rangle = \delta_{\ell\ell'}\delta_{\mu\mu'}B_{\kappa,\kappa',\mu}(r) = \delta_{\ell\ell'}\delta_{\mu\mu'}\sum_s C(\ell,j,1/2|(\mu-s),s)C(\ell,j',1/2|(\mu-s),s)2sB(r) \tag{10.7}$$

$$\langle\chi_{\bar{Q}}|B(r)|\chi_{\bar{Q}'}\rangle = \delta_{\bar{\ell}\bar{\ell}'}\delta_{\mu\mu'}\bar{B}_{\kappa,\kappa',\mu}(r) = \delta_{\bar{\ell}\bar{\ell}'}\delta_{\mu\mu'}\sum_s C(\bar{\ell},j,1/2|(\mu-s),s)C(\bar{\ell},j',1/2|(\mu-s),s)2sB(r) \tag{10.8}$$

from which in turn the following coupled radial differential equations can be obtained

$$\left[W - mc^2 - V(r)\right] g_{\kappa\mu}(r) + \hbar c\frac{1}{r}\left[\frac{\mathrm{d}}{\mathrm{d}r} - \frac{\kappa}{r}\right] r f_{\kappa\mu}(r) = \sum_{\kappa'} B_{\kappa,\kappa',\mu}(r) g_{\kappa'\mu}(r) \tag{10.9}$$

and

$$-\hbar c\frac{1}{r}\left[\frac{\mathrm{d}}{\mathrm{d}r} - \frac{\kappa}{r}\right] r g_{\kappa\mu}(r) + \left[W + mc^2 - V(r)\right] f_{\kappa\mu}(r) = -\sum_{\kappa'} \bar{B}_{\kappa,\kappa',\mu}(r) f_{\kappa'\mu}(r) \quad . \tag{10.10}$$

Introducing as before the following functions

$$P_{\kappa\mu}(r) \equiv r g_{\kappa\mu}(r), \qquad Q_{\kappa\mu}(r) \equiv \hbar c r f_{\kappa\mu}(r). \tag{10.11}$$

in atomic units ($\hbar = 1, m = \frac{1}{2}, c \approx 274$) (10.9) and (10.10) reduce to

$$\frac{\mathrm{d}}{\mathrm{d}r}Q_{\kappa\mu}(r) = \frac{\kappa}{r}Q_{\kappa\mu}(r) - \left[\epsilon - V(r)\right] P_{\kappa\mu}(r) + \sum_{\kappa'} B_{\kappa\kappa',\mu} P_{\kappa'\mu}(r) \quad , \tag{10.12}$$

$$\frac{\mathrm{d}}{\mathrm{d}r}P_{\kappa\mu}(r) = -\frac{\kappa}{r}P_{\kappa\mu}(r) + \left[\frac{\epsilon - V(r)}{c^2} + 1\right] Q_{\kappa\mu}(r) + \frac{1}{c^2}\sum_{\kappa'} \bar{B}_{\kappa\kappa',\mu} Q_{\kappa'\mu}(r) \quad , \tag{10.13}$$

with

$$\epsilon = W - mc^2 \quad . \tag{10.14}$$

Because of the $\delta_{\ell\ell'}$ in (10.7) and (10.8) the sum over κ' is reduced to κ and $-\kappa - 1$. By using the Foldy-Wouthuysen transformation it can be shown [4] that the coupling between the channels ℓ and $\ell \pm 2$ are of minor importance, therefore, it can be safely neglected. One therefore finally gets the following set of coupled radial equation

$$\begin{aligned}\frac{\mathrm{d}}{\mathrm{d}r}Q_{\kappa\mu}(r) = &\frac{\kappa}{r}Q_{\kappa\mu}(r) - [\epsilon - V(r)]\, P_{\kappa\mu}(r) \\ &+B_{\kappa,\kappa,\mu}(r)P_{\kappa\mu}(r) \\ &+B_{\kappa,-\kappa-1,\mu}(r)P_{-\kappa-1,\mu}(r) \quad ,\end{aligned} \tag{10.15}$$

$$\begin{aligned}\frac{\mathrm{d}}{\mathrm{d}r}P_{\kappa\mu}(r) = &-\frac{\kappa}{r}P_{\kappa\mu}(r) + \left[\frac{\epsilon - V(r)}{c^2} + 1\right] Q_{\kappa\mu}(r) \\ &+\frac{1}{c^2}\bar{B}_{\kappa,\kappa,\mu}(r)Q_{\kappa\mu}(r) \quad ,\end{aligned} \tag{10.16}$$

$$\begin{aligned}\frac{\mathrm{d}}{\mathrm{d}r}Q_{-\kappa-1,\mu}(r) = &\frac{-\kappa-1}{r}Q_{-\kappa-1,\mu}(r) - [\epsilon - V(r)]\, P_{-\kappa-1,\mu}(r) \\ &+B_{-\kappa-1,-\kappa-1,\mu}(r)P_{-\kappa-1,\mu}(r) \\ &+B_{-\kappa-1,\kappa,\mu}(r)P_{\kappa\mu}(r) \quad ,\end{aligned} \tag{10.17}$$

$$\begin{aligned}\frac{\mathrm{d}}{\mathrm{d}r}P_{-\kappa-1,\mu}(r) = &\frac{\kappa+1}{r}P_{-\kappa-1,\mu}(r) + \left[\frac{\epsilon - V(r)}{c^2} + 1\right] Q_{-\kappa-1,\mu}(r) \\ &+\frac{1}{c^2}\bar{B}_{-\kappa-1,-\kappa-1,\mu}(r)Q_{-\kappa-1,\mu}(r) \quad ,\end{aligned} \tag{10.18}$$

which can be solved numerically by the now familiar predictor–corrector method.

10.1.1 Evaluation of the coefficients

$$B_{\kappa,\kappa,\mu}(r) = -\frac{\mu B(r)}{\kappa + 1/2} \quad , \tag{10.19}$$

$$\bar{B}_{\kappa,\kappa,\mu}(r) = \frac{\mu B(r)}{\kappa - 1/2} \quad , \tag{10.20}$$

$$B_{\kappa,-\kappa-1,\mu}(r) = B_{-\kappa-1,\kappa,\mu}(r) = -\sqrt{1 - \left(\frac{\mu}{\kappa + 1/2}\right)^2}\, B(r) \quad , \tag{10.21}$$

$$B_{-\kappa-1,-\kappa-1,\mu}(r) = \frac{\mu B(r)}{\kappa + 1/2} \quad , \tag{10.22}$$

$$\bar{B}_{-\kappa-1,-\kappa-1,\mu}(r) = -\frac{\mu B(r)}{\kappa + 3/2} \quad . \tag{10.23}$$

10.1.2 Coupled differential equations

$$\frac{\mathrm{d}}{\mathrm{d}r}Q_{\kappa\mu}(r) = \frac{\kappa}{r}\,Q_{\kappa\mu}(r) - [\epsilon - V(r)]\,P_{\kappa\mu}(r) - \frac{\mu B(r)}{\kappa+1/2}\,P_{\kappa\mu}(r) - \sqrt{1-\left(\frac{\mu}{\kappa+1/2}\right)^2}\,B(r)\,P_{-\kappa-1,\mu}(r) \quad , \tag{10.24}$$

$$\frac{\mathrm{d}}{\mathrm{d}r}P_{\kappa\mu}(r) = -\frac{\kappa}{r}\,P_{\kappa\mu}(r) + \left[\frac{\epsilon - V(r)}{c^2} + 1\right] Q_{\kappa\mu}(r) + \frac{\mu B(r)}{c^2(\kappa-1/2)}\,Q_{\kappa\mu}(r) \quad , \tag{10.25}$$

$$\frac{\mathrm{d}}{\mathrm{d}r}Q_{-\kappa-1,\mu}(r) = -\frac{\kappa+1}{r}\,Q_{-\kappa-1,\mu}(r) - [\epsilon - V(r)]\,P_{-\kappa-1,\mu}(r) + \frac{\mu B(r)}{\kappa+1/2}\,P_{-\kappa-1,\mu}(r) - \sqrt{1-\left(\frac{\mu}{\kappa+1/2}\right)^2}\,B(r)P_{\kappa\mu}(r) \quad , \tag{10.26}$$

$$\frac{\mathrm{d}}{\mathrm{d}r}P_{-\kappa-1,\mu}(r) = \frac{\kappa+1}{r}\,P_{-\kappa-1,\mu}(r) + \left[\frac{\epsilon - V(r)}{c^2} + 1\right] Q_{-\kappa-1,\mu}(r) - \frac{\mu B(r)}{c^2(\kappa+3/2)}\,Q_{-\kappa-1,\mu}(r) \quad . \tag{10.27}$$

The by now familiar change of variables,

$$x = \ln r \quad ; \quad \frac{\mathrm{d}}{\mathrm{d}r} = \frac{\mathrm{d}}{\mathrm{d}x}e^{-x} \quad , \tag{10.28}$$

leads to:

$$\frac{\mathrm{d}}{\mathrm{d}x}Q_{\kappa\mu}(x) = \kappa\,Q_{\kappa\mu}(x) - e^x\,[\epsilon - V(x)]\,P_{\kappa\mu}(x) - \frac{\mu e^x B(x)}{\kappa+1/2}\,P_{\kappa\mu}(x) - \sqrt{1-\left(\frac{\mu}{\kappa+1/2}\right)^2}\,e^x B(x)\,P_{-\kappa-1,\mu}(x) \quad , \tag{10.29}$$

$$\frac{\mathrm{d}}{\mathrm{d}x}P_{\kappa\mu}(x) = -\kappa\,P_{\kappa\mu}(x) + e^x\left[\frac{\epsilon - V(x)}{c^2} + 1\right] Q_{\kappa\mu}(x) + \frac{\mu e^x B(x)}{c^2(\kappa-1/2)}\,Q_{\kappa\mu}(x) \quad , \tag{10.30}$$

$$\frac{\mathrm{d}}{\mathrm{d}x}Q_{-\kappa-1,\mu}(x) = -(\kappa+1)\,Q_{-\kappa-1,\mu}(x) - e^x\,[\epsilon - V(x)]\,P_{-\kappa-1,\mu}(x) + \frac{\mu e^x B(x)}{\kappa+1/2}\,P_{-\kappa-1,\mu}(x) - \sqrt{1-\left(\frac{\mu}{\kappa+1/2}\right)^2}\,e^x B(x)P_{\kappa\mu}(x) \tag{10.31}$$

$$\frac{\mathrm{d}}{\mathrm{d}x}P_{-\kappa-1,\mu}(x) = (\kappa+1)\,P_{-\kappa-1,\mu}(x) + e^x\left[\frac{\epsilon - V(x)}{c^2} + 1\right]Q_{-\kappa-1,\mu}(x) - \frac{\mu e^x B(x)}{c^2(\kappa+3/2)}\,Q_{-\kappa-1,\mu}(x) \quad . \tag{10.32}$$

10.1.3 Start values

In the limit of $x \to -\infty$, or $r \to 0$:

$$r\left(\frac{\epsilon - V(r)}{c^2} + 1\right) \longrightarrow \frac{2Z}{c^2} = \frac{b}{c} \quad , \tag{10.33}$$

where

$$b = \frac{2Z}{c} \quad . \tag{10.34}$$

Furthermore,

$$\lim_{x\to-\infty} e^x B(x) = 0 \quad . \tag{10.35}$$

Case 1: $\kappa = -\ell - 1$, $\mu = \pm(\ell + 1/2)$

In this case only two equations remain, because for $\kappa = \ell$ the quantum number μ cannot acquire the values $\pm(\ell + 1/2)$. Since

$$\sqrt{1 - \left(\frac{\mu}{\kappa+1/2}\right)^2} = \sqrt{1 - \left(\frac{\ell+1/2}{\ell+1/2}\right)^2} = 0 \quad , \tag{10.36}$$

one gets

$$\begin{aligned}\frac{\mathrm{d}}{\mathrm{d}x}Q_{-\ell-1,\pm(\ell+1/2)}(x) &= -(\ell+1)\,Q_{-\ell-1,\pm(\ell+1/2)}(x) \\ &\quad - e^x\,[\epsilon - V(x)]\,P_{-\ell-1,\pm(\ell+1/2)}(x) \\ &\quad + \frac{\mu e^x B(x)}{\ell+1/2}\,P_{-\ell-1,\pm(\ell+1/2)}(x) \quad , \end{aligned} \tag{10.37}$$

$$\begin{aligned}\frac{\mathrm{d}}{\mathrm{d}x}P_{-\ell-1,\pm(\ell+1/2)}(x) &= (\ell+1)\,P_{-\ell-1,\pm(\ell+1/2)}(x) \\ &\quad + e^x\left[\frac{\epsilon - V(x)}{c^2} + 1\right]Q_{-\ell-1,\pm(\ell+1/2)}(x) \\ &\quad - \frac{\mu e^x B(x)}{c^2(\ell+3/2)}\,Q_{-\ell-1,\pm(\ell+1/2)}(x) \quad . \end{aligned} \tag{10.38}$$

Because there is no μ dependence the start values follow directly from (10.35):

$$\frac{\mathrm{d}}{\mathrm{d}x}Q_{-\ell-1}(x) = -(\ell+1)\,Q_{-\ell-1}(x) - bc\,P_{-\ell-1}(x) \tag{10.39}$$

$$\frac{\mathrm{d}}{\mathrm{d}x}P_{-\ell-1}(x) = (\ell+1)\,P_{-\ell-1}(x) + \frac{b}{c}\,Q_{-\ell-1}(x) \quad . \tag{10.40}$$

The second derivative of $P_{-\ell-1}(z;r)$ is given by

$$\frac{\mathrm{d}^2}{\mathrm{d}x^2}P_{-\ell-1}(x) = (\ell+1)\,\frac{\mathrm{d}}{\mathrm{d}x}P_{-\ell-1}(z;r) + \frac{b}{c}\,\frac{\mathrm{d}}{\mathrm{d}x}Q_{-\ell-1}(x) \tag{10.41}$$

$$= (\ell+1)^2 P_{-\ell-1}(x) + (\ell+1)\frac{b}{c}Q_{-\ell-1}(x) + \frac{b}{c}\,\frac{\mathrm{d}}{\mathrm{d}x}Q_{-\ell-1}(x) \tag{10.42}$$

$$= \left[(\ell+1)^2 - b^2\right] P_{-\ell-1}(x) \quad . \tag{10.43}$$

Therefore the following Ansatz can be made:

$$P_{-\ell-1}(x) = e^{Ax} \quad , \tag{10.44}$$

with

$$A^2 = (\ell+1)^2 - b^2 \quad , \tag{10.45}$$

$$A = \sqrt{(\ell+1)^2 - b^2} \tag{10.46}$$

$$= \sqrt{(\ell+1)^2 - \left(\frac{2Z}{c}\right)^2} \quad . \tag{10.47}$$

and

$$\frac{b}{c}\,Q_{-\ell-1}(x_1) = \frac{\mathrm{d}}{\mathrm{d}x}P_{-\ell-1}(x_1) - (\ell+1)\,P_{-\ell-1}(x_1) \quad , \tag{10.48}$$

$$Q_{-\ell-1}(x_1) = \frac{-\ell-1+\sqrt{(\ell+1)^2-b^2}}{b/c}\,P_{-\ell-1}(x_1) \quad . \tag{10.49}$$

Hence, as start values one can use in this special case:

$$P_{-\ell-1}(x_1) = 10^{-20} \quad , \tag{10.50}$$

$$Q_{-\ell-1}(x_1) = \frac{-\ell-1+\sqrt{(\ell+1)^2-b^2}}{b/c}\,P_{-\ell-1}(x_1) \quad , \tag{10.51}$$

$$\frac{\mathrm{d}}{\mathrm{d}x}P_{-\ell-1}(x_1) = (\ell+1)\,P_{-\ell-1}(x_1) + e^{x_1}\left[\frac{\epsilon - V(x_1)}{c^2} + 1\right] Q_{-\ell-1}(x_1) \quad , \tag{10.52}$$

$$\frac{\mathrm{d}}{\mathrm{d}x}Q_{-\ell-1}(x_1) = -(\ell+1)\,Q_{-\ell-1}(x_1) - e^{x_1}\left[\epsilon - V(x_1)\right] P_{-\ell-1}(x_1) \quad , \tag{10.53}$$

Case 2: $\kappa = \ell, \kappa = -\ell - 1$, $|\mu| < \ell + 1/2$

In this case two sets of linear independent solutions apply, namely

$$\psi_1(r) = \begin{pmatrix} P^1_{\ell\mu}(r) \\ Q^1_{\ell\mu}(r) \\ P^1_{-\ell-1,\mu}(r) \\ Q^1_{-\ell-1,\mu}(r) \end{pmatrix} \quad , \quad \psi_2(r) = \begin{pmatrix} P^2_{\ell\mu}(r) \\ Q^2_{\ell\mu}(r) \\ P^2_{-\ell-1,\mu}(r) \\ Q^2_{-\ell-1,\mu}(r) \end{pmatrix} \quad , \tag{10.54}$$

Analogous to the above derivation for "case 1", by means of the conditions in (10.33) and (10.35) the following start values for these two sets of solutions are found:

$$P^1_{\ell\mu}(x_1) = 10^{-20} \quad , \tag{10.55}$$

$$Q^1_{\ell\mu}(x_1) = \frac{\ell + \sqrt{\ell^2 - b^2}}{b/c} \, P^1_{\ell\mu}(x_1) \quad , \tag{10.56}$$

$$\frac{\mathrm{d}}{\mathrm{d}x} P^1_{\ell\mu}(x_1) = -\ell \, P^1_{\ell\mu}(x_1) + e^{x_1} \left[\frac{\epsilon - V(x_1)}{c^2} + 1 \right] Q^1_{\ell\mu}(x_1) \quad , \tag{10.57}$$

$$\frac{\mathrm{d}}{\mathrm{d}x} Q^1_{\ell\mu}(x_1) = \ell \, Q^1_{\ell\mu}(x_1) - e^{x_1} \left[\epsilon - V(x_1) \right] P^1_{\ell\mu}(x_1) \quad , \tag{10.58}$$

$$P^1_{-\ell-1,\mu}(x_1) = 0 \quad , \tag{10.59}$$

$$Q^1_{-\ell-1,\mu}(x_1) = 0 \quad , \tag{10.60}$$

and

$$P^2_{-\ell-1,\mu}(x_1) = 10^{-20} \quad , \tag{10.61}$$

$$Q^2_{-\ell-1,\mu}(x_1) = \frac{-\ell - 1 + \sqrt{(-\ell-1)^2 - b^2}}{b/c} \, P^2_{-\ell-1,\mu}(x_1) \quad , \tag{10.62}$$

$$\frac{\mathrm{d}}{\mathrm{d}x} Q^2_{-\ell-1,\mu}(x_1) = -(\ell+1) \, Q^2_{-\ell-1,\mu}(x_1) - e^{x_1} \left[\epsilon - V(x_1) \right] P^2_{-\ell-1,\mu}(x_1) \quad , \tag{10.63}$$

$$\frac{\mathrm{d}}{\mathrm{d}x} P^2_{-\ell-1,\mu}(x_1) = (\ell+1) \, P^2_{-\ell-1,\mu}(x_1) + e^{x_1} \left[\frac{\epsilon - V(x_1)}{c^2} + 1 \right] Q^2_{-\ell-1,\mu}(x_1) \tag{10.64}$$

$$P^2_{\ell\mu}(x_1) = 0 \quad , \tag{10.65}$$

$$Q^2_{\ell\mu}(x_1) = 0 \quad . \tag{10.66}$$

In general the $\kappa\mu$-like wave-functions are superpositions of the following kind

$$\psi_{\kappa\mu}(\mathbf{r}) = \sum_{\kappa'\mu'} \begin{pmatrix} p_{\kappa'\mu',\kappa\mu}(r) \, \chi_{\kappa'\mu'}(\hat{\mathbf{r}}) \\ \mathrm{i} q_{\kappa'\mu',\kappa\mu}(r) \, \chi_{-\kappa'\mu'}(\hat{\mathbf{r}}) \end{pmatrix} \quad , \tag{10.67}$$

in which the expansion coefficients $p_{\kappa'\mu',\kappa\mu}(r)$ and $q_{\kappa'\mu',\kappa\mu}(r)$ are related to $P^i_{\kappa\mu}(r)$ and $Q^i_{\kappa\mu}, i = 1, 2$, by

$$\begin{pmatrix} p_{\kappa'\mu',\kappa\mu}(r) \\ \mathrm{i}q_{\kappa'\mu',\kappa\mu}(r) \end{pmatrix} = \sum_i a_i^{\kappa\mu} \begin{pmatrix} P^i_{\kappa'\mu'}(r) \\ \mathrm{i}Q^i_{\kappa'\mu'}(r) \end{pmatrix} \quad . \tag{10.68}$$

For $\kappa = \ell$ it follows therefore that

$$\begin{pmatrix} p_{\ell\mu,\ell\mu}(r) \\ \mathrm{i}q_{\ell\mu,\ell\mu}(r) \\ p_{(-\ell-1,\mu),\ell\mu}(r) \\ \mathrm{i}q_{(-\ell-1,\mu),\ell\mu}(r) \end{pmatrix} = \sum_{i=1,2} a_i^{\ell\mu} \begin{pmatrix} P^i_{\ell\mu}(r) \\ \mathrm{i}Q^i_{\ell\mu}(r) \\ P^i_{-\ell-1,\mu}(r) \\ \mathrm{i}Q^i_{-\ell-1,\mu}(r) \end{pmatrix} \quad , \tag{10.69}$$

and for $\kappa = -\ell - 1$:

$$\begin{pmatrix} p_{\ell\mu,(-\ell-1,\mu)}(r) \\ \mathrm{i}q_{\ell\mu,(-\ell-1,\mu)}(r) \\ p_{(-\ell-1,\mu),(-\ell-1,\mu)}(r) \\ \mathrm{i}q_{(-\ell-1,\mu),(-\ell-1,\mu)}(r) \end{pmatrix} = \sum_{i=1,2} a_i^{-\ell-1,\mu} \begin{pmatrix} P^i_{\ell\mu}(r) \\ \mathrm{i}Q^i_{\ell\mu}(r) \\ P^i_{-\ell-1,\mu}(r) \\ \mathrm{i}Q^i_{-\ell-1,\mu}(r) \end{pmatrix} \quad , \tag{10.70}$$

while in the case of $|\mu| = \ell + 1/2$

$$\begin{pmatrix} p_{(-\ell-1,\mu),(-\ell-1,\mu)}(r) \\ \mathrm{i}q_{(-\ell-1,\mu),(-\ell-1,\mu)}(r) \end{pmatrix} = a^{-\ell-1,\mu} \begin{pmatrix} P_{-\ell-1,\mu}(r) \\ \mathrm{i}Q_{-\ell-1,\mu}(r) \end{pmatrix} \quad . \tag{10.71}$$

10.1.4 Runge–Kutta extrapolation

The Runge–Kutta procedure works again as discussed in the previous chapters dealing with single-site scattering, only this time one needs to distinguish between the two cases specified above.

Case 1: $\kappa = -\ell - 1$, $\mu = \pm(\ell + 1/2)$

In this particular case one needs to evaluate

$$P_{-\ell-1}(x_{i+1}) = P_{-\ell-1}(x_i) + \frac{\Delta x}{6}(k_1 + 2k_2 + 2k_3 + k_4) \quad , \tag{10.72}$$

$$Q_{-\ell-1}(x_{i+1}) = Q_{-\ell-1}(x_i) + \frac{\Delta x}{6}(m_1 + 2m_2 + 2m_3 + m_4) \quad . \tag{10.73}$$

in order to obtain the necessary five start values. The values of k_1 and m_1 follow from (10.37) and (10.38):

$$\begin{aligned} k_1 = {} & (\ell+1)\, P_{-\ell-1,\pm(\ell+1/2)}(x_i) + e^{x_i} \left[\frac{\epsilon - V(x_i)}{c^2} + 1 \right] Q_{-\ell-1,\pm(\ell+1/2)}(x_i) \\ & - \frac{\mu e^{x_i} B(x_i)}{c^2(\ell+3/2)}\, Q_{-\ell-1,\pm(\ell+1/2)}(x_i) \quad , \end{aligned} \tag{10.74}$$

$$\begin{aligned} m_1 = {} & -(\ell+1)\, Q_{-\ell-1,\pm(\ell+1/2)}(x_i) - e^{x_i} \left[\epsilon - V(x_i)\right] P_{-\ell-1,\pm(\ell+1/2)}(x_i) \\ & + \frac{\mu e^{x_i} B(x_i)}{\ell+1/2}\, P_{-\ell-1,\pm(\ell+1/2)}(x_i) \quad . \end{aligned} \tag{10.75}$$

All other coefficients are to be found in Table 5.1.

Case 2: $\kappa = \ell, \kappa = -\ell - 1$, $|\mu| < \ell + 1/2$

In this slightly more complicated but still straightforward case a total of eight functions has to be extrapolated, namely

$$P^1_{\ell\mu}(x_{i+1}) = P^1_{\ell\mu}(x_i) + \frac{\Delta x}{6}\left(k^1_1 + 2k^1_2 + 2k^1_3 + k^1_4\right) \quad , \tag{10.76}$$

$$Q^1_{\ell\mu}(x_{i+1}) = Q^1_{\ell\mu}(x_i) + \frac{\Delta x}{6}\left(m^1_1 + 2m^1_2 + 2m^1_3 + m^1_4\right) \quad , \tag{10.77}$$

$$P^1_{-\ell-1,\mu}(x_{i+1}) = P^1_{-\ell-1,\mu}(x_i) + \frac{\Delta x}{6}\left(k^2_1 + 2k^2_2 + 2k^2_3 + k^2_4\right) \quad , \tag{10.78}$$

$$Q^1_{-\ell-1,\mu}(x_{i+1}) = Q^1_{-\ell-1,\mu}(x_i) + \frac{\Delta x}{6}\left(m^2_1 + 2m^2_2 + 2m^2_3 + m^2_4\right) \quad , \tag{10.79}$$

with k^1_1, k^2_1 and m^1_1, m^2_1 given by (10.29)–(10.32). Clearly once again all other coefficients are obtained from the same equations according to Table 5.1. The remaining functions that have to be calculated are

$$P^2_{\ell\mu}(x_{i+1}) = P^2_{\ell\mu}(x_i) + \frac{\Delta x}{6}\left(k^1_1 + 2k^1_2 + 2k^1_3 + k^1_4\right) \quad , \tag{10.80}$$

$$Q^2_{\ell\mu}(x_{i+1}) = Q^2_{\ell\mu}(x_i) + \frac{\Delta x}{6}\left(m^1_1 + 2m^1_2 + 2m^1_3 + m^1_4\right) \quad , \tag{10.81}$$

$$P^2_{-\ell-1,\mu}(x_{i+1}) = P^2_{-\ell-1,\mu}(x_i) + \frac{\Delta x}{6}\left(k^2_1 + 2k^2_2 + 2k^2_3 + k^2_4\right) \quad , \tag{10.82}$$

$$Q^2_{-\ell-1,\mu}(x_{i+1}) = Q^2_{-\ell-1,\mu}(x_i) + \frac{\Delta x}{6}\left(m^2_1 + 2m^2_2 + 2m^2_3 + m^2_4\right) \quad , \tag{10.83}$$

with the coefficients to be calculated as described above.

Because different start values apply for the functions with superscript 1 and 2 they need to be computed independent of each other – hence the coefficients k_i and m_i are identical in these two cases.

10.1.5 Predictor-corrector algorithm

The general expressions are given in (5.38) and (5.40) and can be found in Sect. 5.1.3.

Case 1: $\kappa = -\ell - 1$, $\mu = \pm(\ell + 1/2)$

In this case the function $f(x_i)$ has to be identified with either $P_{-\ell-1}(x_i)$ or $Q_{-\ell-1}(x_i)$ and $f'(x_i)$ with their respective derivatives. The predictors are then $P^0_{-\ell-1}(x_i)$ and $Q^0_{-\ell-1}(x_i)$, while the correctors are denoted as $P^1_{-\ell-1}(x_i)$ and $Q^1_{-\ell-1}(x_i)$. Furthermore, the functions $f^{1\prime}(x_i)$ are given by $\mathrm{d}P^1_{-\ell-1}(x_i)/\mathrm{d}x$, while the functions $\mathrm{d}Q^1_{-\ell-1}(x_i)/\mathrm{d}x$ can be calculated from the below set of equations

$$\begin{aligned}\frac{\mathrm{d}}{\mathrm{d}x}P^1_{-\ell-1}(x_i) &= (\ell+1)\,P^0_{-\ell-1,\pm(\ell+1/2)}(x_i)\\ &\quad + e^{x_i}\left[\frac{\epsilon - V(x_i)}{c^2}+1\right]Q^0_{-\ell-1,\pm(\ell+1/2)}(x_i)\\ &\quad - \frac{\mu e^{x_i}B(x_i)}{c^2(\ell+3/2)}\,Q^0_{-\ell-1,\pm(\ell+1/2)}(x_i) \quad , \qquad (10.84)\\ \frac{\mathrm{d}}{\mathrm{d}x}Q^1_{-\ell-1}(x_i) &= -(\ell+1)\,Q^0_{-\ell-1,\pm(\ell+1/2)}(x_i)\\ &\quad - e^{x_i}\left[\epsilon - V(x_i)\right]P^0_{-\ell-1,\pm(\ell+1/2)}(x_i)\\ &\quad + \frac{\mu e^{x}B(x)}{\ell+1/2}\,P^0_{-\ell-1,\pm(\ell+1/2)}(x) \quad . \qquad (10.85)\end{aligned}$$

Case 2: $\kappa = \ell, \kappa = -\ell-1$, $|\mu| < \ell + 1/2$

One now has to predict and correct eight functions. Let the predictors be denoted by

$$\begin{pmatrix} P^{1,0}_{\ell\mu}(x_i)\\ Q^{1,0}_{\ell\mu}(x_i)\\ P^{1,0}_{-\ell-1,\mu}(x_i)\\ Q^{1,0}_{-\ell-1,\mu}(x_i)\end{pmatrix} \quad \text{and} \quad \begin{pmatrix} P^{2,0}_{\ell\mu}(x_i)\\ Q^{2,0}_{\ell\mu}(x_i)\\ P^{2,0}_{-\ell-1,\mu}(x_i)\\ Q^{2,0}_{-\ell-1,\mu}(x_i)\end{pmatrix}$$

and the correctors by

$$\begin{pmatrix} P^{1,1}_{\ell\mu}(x_i)\\ Q^{1,1}_{\ell\mu}(x_i)\\ P^{1,1}_{-\ell-1,\mu}(x_i)\\ Q^{1,1}_{-\ell-1,\mu}(x_i)\end{pmatrix} \quad \text{and} \quad \begin{pmatrix} P^{2,1}_{\ell\mu}(x_i)\\ Q^{2,1}_{\ell\mu}(x_i)\\ P^{2,1}_{-\ell-1,\mu}(x_i)\\ Q^{2,1}_{-\ell-1,\mu}(x_i)\end{pmatrix}$$

then the $f^{1\prime}(x_i)$ are obtained from (10.29)–(10.32) as

$$\begin{aligned}\frac{\mathrm{d}}{\mathrm{d}x}Q^{i,1}_{\ell\mu}(x_i) &= \ell\,Q^{i,0}_{\ell\mu}(x_i) - e^{x_i}\left[\epsilon - V(x_i)\right]P^{i,0}_{\ell\mu}(x_i)\\ &\quad - \frac{\mu e^{x_i}B(x_i)}{\ell+1/2}\,P^{i,0}_{\ell\mu}(x_i)\\ &\quad - \sqrt{1-\left(\frac{\mu}{\ell+1/2}\right)^2}\,e^{x_i}B(x_i)\,P^{i,0}_{-\ell-1,\mu}(x_i) \quad , \qquad (10.86)\\ \frac{\mathrm{d}}{\mathrm{d}x}P^{i,1}_{\ell\mu}(x_i) &= -\ell\,P^{i,0}_{\ell\mu}(x_i) + e^{x_i}\left[\frac{\epsilon - V(x_i)}{c^2}+1\right]Q^{i,0}_{\ell\mu}(x_i)\\ &\quad + \frac{\mu e^{x_i}B(x_i)}{c^2(\ell-1/2)}\,Q^{i,0}_{\ell\mu}(x_i) \quad , \qquad (10.87)\end{aligned}$$

$$\frac{\mathrm{d}}{\mathrm{d}x}Q^{i,1}_{-\ell-1,\mu}(x_i) = -(\ell+1)\,Q^{i,0}_{-\ell-1,\mu}(x_i) - e^{x_i}\left[\epsilon - V(x_i)\right]P^{i,0}_{-\ell-1,\mu}(x_i) + \frac{\mu e^{x_i}B(x_i)}{\ell+1/2}\,P^{i,0}_{-\ell-1,\mu}(x_i) - \sqrt{1-\left(\frac{\mu}{\ell+1/2}\right)^2}\,e^{x_i}B(x_i)P^{i,0}_{\ell\mu}(x_i) \quad , \tag{10.88}$$

$$\frac{\mathrm{d}}{\mathrm{d}x}P^{i,1}_{-\ell-1,\mu}(x_i) = (\ell+1)\,P^{i,0}_{-\ell-1,\mu}(x_i) + e^{x_i}\left[\frac{\epsilon - V(x_i)}{c^2}+1\right]Q^{i,0}_{-\ell-1,\mu}(x_i) - \frac{\mu e^{x_i}B(x_i)}{c^2(\ell+3/2)}\,Q^{i,0}_{-\ell-1,\mu}(x_i) \quad . \tag{10.89}$$

with $i = 1, 2$.

10.1.6 Normalization of the regular scattering solutions and the single site *t*-matrix

Case 2: $\kappa = \ell, \kappa = -\ell - 1$, $|\mu| < \ell + 1/2$

The functions to be matched at $s = r_{\mathrm{MT}}$ are spherical Bessel and Neumann functions, $j_\ell(pr)$ and $n_\ell(pr)$, respectively; the reactance is denoted in the following by $K_{\kappa\mu,\kappa\mu}(z)$, $p = \sqrt{z}$, $S_\kappa = \kappa/|\kappa|$, and $\bar{\ell} = \ell - S_\kappa$.

For $\kappa = \ell$ wave-functions matching yields the below equations:

$$p_{\ell\mu,\ell\mu}(s) = j_\ell(ps)K^{-1}_{\ell\mu,\ell\mu}(z) + pn_\ell(ps) \tag{10.90}$$

$$q_{\ell\mu,\ell\mu}(s) = \frac{S_\ell p}{c}\left[j_{\bar{\ell}}(ps)K^{-1}_{\ell\mu,\ell\mu}(z) + pn_{\bar{\ell}}(ps)\right] \tag{10.91}$$

$$= \frac{S_\ell p}{c}\left[j_{\ell-1}(ps)K^{-1}_{\ell\mu,\ell\mu}(z) + pn_{\ell-1}(ps)\right] \tag{10.92}$$

$$p_{(-\ell-1,\mu),\ell\mu}(s) = j_\ell(ps)K^{-1}_{(-\ell-1,\mu),\ell\mu}(z) \tag{10.93}$$

$$q_{(-\ell-1,\mu),\ell\mu}(s) = \frac{S_{-\ell-1}p}{c}j_{\ell+1}(ps)K^{-1}_{(-\ell-1,\mu),\ell\mu}(z) \quad . \tag{10.94}$$

According to (10.69) one therefore gets a set of four equations

$$j_\ell(ps)K^{-1}_{\ell\mu,\ell\mu}(z) + pn_\ell(ps) = a_1^{\ell\mu}P^1_{\ell\mu}(s) + a_2^{\ell\mu}P^2_{\ell\mu}(s) \tag{10.95}$$

$$\frac{S_\ell p}{c}\left[j_{\ell-1}(ps)K^{-1}_{\ell\mu,\ell\mu}(z) + pn_{\ell-1}(ps)\right] = a_1^{\ell\mu}Q^1_{\ell\mu}(s) + a_2^{\ell\mu}Q^2_{\ell\mu}(s) \tag{10.96}$$

$$j_\ell(ps)K^{-1}_{(-\ell-1,\mu),\ell\mu}(z) = a_1^{\ell\mu}P^1_{-\ell-1,\mu}(s) + a_2^{\ell\mu}P^2_{-\ell-1,\mu}(s) \tag{10.97}$$

$$\frac{S_{-\ell-1}p}{c}j_{\ell+1}(ps)K^{-1}_{(-\ell-1,\mu),\ell\mu}(z) = a_1^{\ell\mu}Q^1_{-\ell-1,\mu}(s) + a_2^{\ell\mu}Q^2_{-\ell-1,\mu}(s) \tag{10.98}$$

which have to be solved for the four unknown quantities, namely $K^{-1}_{\ell\mu,\ell\mu}(z)$, $K^{-1}_{(-\ell-1,\mu),\ell\mu}(z)$, $a_1^{\ell\mu}$, and $a_2^{\ell\mu}$.

In a similar manner for $\kappa = -\ell - 1$ one gets as matching conditions:

$$p_{\ell\mu,(-\ell-1,\mu)}(s) = j_\ell(ps) K^{-1}_{\ell\mu,(-\ell-1,\mu)}(z) \tag{10.99}$$

$$q_{\ell\mu,(-\ell-1,\mu)}(s) = \frac{S_\ell p}{c} j_{\ell-1}(ps) K^{-1}_{\ell\mu,(-\ell-1,\mu)}(z) \tag{10.100}$$

$$p_{(-\ell-1,\mu),(-\ell-1,\mu)}(s) = j_\ell(ps) K^{-1}_{(-\ell-1,\mu),(-\ell-1,\mu)}(z) + pn_\ell(ps) \tag{10.101}$$

$$q_{(-\ell-1,\mu),(-\ell-1,\mu)}(s) = \frac{S_{-\ell-1} p}{c} \left[j_{\ell+1}(ps) K^{-1}_{(-\ell-1,\mu),(-\ell-1,\mu)}(z) + pn_{\ell+1}(ps) \right] \tag{10.102}$$

and consequently from (10.70) four equations that have to be solved for $K^{-1}_{\ell\mu,(-\ell-1,\mu)}(z)$, $K^{-1}_{(-\ell-1,\mu),(-\ell-1,\mu)}(z)$, $a_1^{-\ell-1,\mu}$, and $a_2^{-\ell-1,\mu}$:

$$j_\ell K^{-1}_{\ell\mu,(-\ell-1,\mu)} = a_1^{-\ell-1,\mu} P^1_{\ell\mu} + a_2^{-\ell-1,\mu} P^2_{\ell\mu} \quad , \tag{10.103}$$

$$\frac{S_\ell p}{c} j_{\ell-1} K^{-1}_{\ell\mu,(-\ell-1,\mu)} = a_1^{-\ell-1,\mu} Q^1_{\ell\mu} + a_2^{-\ell-1,\mu} Q^2_{\ell\mu} \quad , \tag{10.104}$$

$$j_\ell K^{-1}_{(-\ell-1,\mu),(-\ell-1,\mu)} + pn_\ell = a_1^{-\ell-1,\mu} P^1_{-\ell-1,\mu} + a_2^{-\ell-1,\mu} P^2_{-\ell-1,\mu} \quad , \tag{10.105}$$

$$\frac{S_{-\ell-1} p}{c} \left[j_{\ell+1} K^{-1}_{-\ell-1,\mu,(-\ell-1,\mu)} + pn_{\ell+1} \right] = \left[a_1^{-\ell-1,\mu} Q^1_{-\ell-1,\mu} + a_2^{-\ell-1,\mu} Q^2_{-\ell-1,\mu} \right] \quad . \tag{10.106}$$

It should be noted that matters of simplicity in the above equations all function arguments have been dropped.

Case 1: $\kappa = -\ell - 1$, $\mu = \pm(\ell + 1/2)$

In this case only two matching conditions, namely

$$p_{(-\ell-1,\mu),(-\ell-1,\mu)}(s) = j_\ell(ps) K^{-1}_{(-\ell-1,\mu),(-\ell-1,\mu)}(z) + pn_\ell(ps) \quad , \tag{10.107}$$

$$q_{(-\ell-1,\mu),(-\ell-1,\mu)}(s) = \frac{S_{-\ell-1} p}{c} \left[j_{\ell+1}(ps) K^{-1}_{(-\ell-1,\mu),(-\ell-1,\mu)}(z) + pn_{\ell+1}(ps) \right] \tag{10.108}$$

have to be fulfilled. From (10.71) one obtains therefore the below two equations,

$$j_\ell(ps) K^{-1}_{(-\ell-1,\mu),(-\ell-1,\mu)}(z) + pn_\ell(ps) = a^{-\ell-1,\mu} P_{-\ell-1,\mu}(s) \quad , \tag{10.109}$$

$$\frac{S_{-\ell-1} p}{c} \left[j_{\ell+1}(ps) K^{-1}_{(-\ell-1,\mu),(-\ell-1,\mu)}(z) + pn_{\ell+1}(ps) \right] = a^{-\ell-1,\mu} Q_{-\ell-1,\mu}(s) \tag{10.110}$$

from which the inverse reactance $K^{-1}_{\kappa\mu,\kappa\mu}(z)$ can easily be worked out as

$$K^{-1}_{\kappa\mu,\kappa\mu}(z) = -p\frac{L_{\kappa\mu}(s)n_\ell(ps) - S_\kappa p n_{\ell+1}(ps)}{L_{\kappa\mu}(s)j_\ell(ps) - S_\kappa p j_{\ell+1}(ps)} \quad , \tag{10.111}$$

where $L_{\kappa\mu}(s) = cQ_{\kappa\mu}(s)/P_{\kappa\mu}(s)$, and $\kappa\mu = (-\ell-1,\mu)$ was used for brevity.

Once the reactance is known for both cases the t matrix is given by the now well-known expression

$$t^{-1}_{\kappa'\mu,\kappa\mu}(z) = K^{-1}_{\kappa'\mu,\kappa\mu}(z) + ip\delta_{\kappa'\kappa} \quad . \tag{10.112}$$

10.1.7 Normalization of the irregular scattering solutions

Case 2: $\kappa = \ell, \kappa = -\ell - 1$, $|\mu| < \ell + 1/2$

For $\kappa = \ell$ the irregular wave-functions have to be matched at $s = r_{\rm MT}$ in the following manner

$$p_{\ell\mu,\ell\mu}(s) = j_\ell(ps) \quad , \tag{10.113}$$

$$q_{\ell\mu,\ell\mu}(s) = \frac{S_\ell p}{c}\, j_{\ell-1}(ps) \quad , \tag{10.114}$$

$$p_{(-\ell-1,\mu),\ell\mu}(s) = j_\ell(ps) \quad , \tag{10.115}$$

$$q_{(-\ell-1,\mu),\ell\mu}(s) = \frac{S_{-\ell-1} p}{c}\, j_{\ell+1}(ps) \quad , \tag{10.116}$$

while for $\kappa = -\ell - 1$ one has

$$p_{\ell\mu,(-\ell-1,\mu)}(s) = j_\ell(ps) \quad , \tag{10.117}$$

$$q_{\ell\mu,(-\ell-1,\mu)}(s) = \frac{S_\ell p}{c}\, j_{\ell-1}(ps) \quad , \tag{10.118}$$

$$p_{(-\ell-1,\mu),(-\ell-1,\mu)}(s) = j_\ell(ps) \quad , \tag{10.119}$$

$$q_{(-\ell-1,\mu),(-\ell-1,\mu)}(s) = \frac{S_{-\ell-1} p}{c}\, j_{\ell+1}(ps) \quad . \tag{10.120}$$

Case 1: $\kappa = -\ell - 1$, $\mu = \pm(\ell + 1/2)$

In this particular case again only two matching conditions prevail, namely

$$p_{(-\ell-1,\mu),(-\ell-1,\mu)}(s) = j_\ell(ps) \quad , \tag{10.121}$$

$$q_{(-\ell-1,\mu),(-\ell-1,\mu)}(s) = \frac{S_{-\ell-1} p}{c}\, j_{\ell+1}(ps) \quad . \tag{10.122}$$

References

1. P. Weinberger, *Electron Scattering Theory of Ordered and Disordered Matter* (Clarendon Press, Oxford 1992)
2. M.E. Rose, *Relativistic Electron Theory* (Wiley, New York 1961)
3. P. Strange, *Relativistic Quantum Mechanics* (Cambridge University Press, Cambridge, England 1998)
4. R. Feder, F. Rosicky, and B. Ackermann, Z. Phys. B - Cond. Mat. **52**, 31 (1983).

11 Spin-polarized relativistic full potential single-site scattering

11.1 Iterative perturbational (Lippmann-Schwinger-type) approach for relativistic spin-polarized full potential single-site scattering

As in all cases discussed earlier the Green's function for single-site scattering is formally given by

$$\begin{aligned} G\left(z;\mathbf{r},\mathbf{r}'\right) = & \sum_{Q,Q'} Z_Q\left(z;\mathbf{r}\right)\, t_{QQ'}\left(z\right)\, \widetilde{Z}_{Q'}\left(z;\mathbf{r}'\right)^{\dagger} \\ & - \sum_{Q} Z_Q\left(z;\mathbf{r}\right)\, \widetilde{J}_Q\left(z;\mathbf{r}'\right)^{\dagger} \Theta\left(r'-r\right) \\ & - \sum_{Q} J_Q\left(z;\mathbf{r}\right)\, \widetilde{Z}_Q\left(z;\mathbf{r}'\right)^{\dagger} \Theta\left(r-r'\right) \quad , \end{aligned} \tag{11.1}$$

where relativistically $Q = (\kappa, \mu)$, and the $Z_Q\left(z;\mathbf{r}\right)$ and $J_Q\left(z;\mathbf{r}\right)$ are regular and irregular solutions of the following Dirac-equation,

$$\mathcal{H}\left(\mathbf{r}\right) = c\,\boldsymbol{\alpha}\cdot\mathbf{p} + \beta mc^2 + V^{\mathrm{eff}}\left(\mathbf{r}\right)\, \mathsf{I}_4 + \beta\boldsymbol{\Sigma}\cdot\,\mathbf{B}^{\mathrm{eff}}\left(\mathbf{r}\right) \quad , \tag{11.2}$$

such that

$$Z_Q\left(z;\mathbf{r}\right) = \sum_{Q'} j_{Q'}\left(z;\mathbf{r}\right) K^{-1}_{Q'Q}\left(z\right) + pn_Q\left(z;\mathbf{r}\right) \quad , \quad |\mathbf{r}| = r_{\mathrm{BS}} \quad , \tag{11.3}$$

$$J_Q\left(z;\mathbf{r}\right) = j_Q\left(z;\mathbf{r}\right) \quad , \quad |\mathbf{r}| = r_{\mathrm{BS}} \quad , \tag{11.4}$$

For $|\mathbf{r}| > r_{\mathrm{BS}}$, i.e., for $V\left(\mathbf{r}\right) = 0$, the solutions of (11.2) are defined as in the previous relativistic cases as

$$f_Q\left(z;\mathbf{r}\right) = \begin{pmatrix} f_\ell\left(pr\right)\chi_{\kappa\mu}\left(\hat{\mathbf{r}}\right) \\ \\ \frac{\mathrm{i}S_\kappa\, p}{c}\, f_{\overline{\ell}}\left(pr\right)\chi_{-\kappa,\mu}\left(\hat{\mathbf{r}}\right) \end{pmatrix} \tag{11.5}$$

with $f_\ell = j_\ell, n_\ell$ and $h^{\pm}_\ell$ being spherical Bessel-, Neumann- and Hankel functions, while the $\chi_{\kappa\mu}\left(\hat{\mathbf{r}}\right)$ denote spin spherical harmonics, $p^2 = z$, $S_\kappa = \kappa/\left|\kappa\right|$ and $\overline{\ell} = \ell - S_\kappa$. (Note that atomic Rydberg units: $\hbar = 1$, $2m = 1$, $e^2 = 2$ are

used) The reactance matrix $K_{Q'Q}(z)$ is related to the single-site scattering matrix $t_{Q'Q}(z)$ in the by now familiar way:

$$K^{-1}_{QQ'}(z) = \begin{cases} \left[t(z)^{-1}\right]_{QQ'} - \mathrm{i}p\boldsymbol{\delta}_{QQ'} & \mathrm{Im}z > 0 \\ \left[t(z)^{-1}\right]_{QQ'} + \mathrm{i}p\boldsymbol{\delta}_{QQ'} & \mathrm{Im}z < 0 \end{cases} . \tag{11.6}$$

Note, that the matrices $K_{Q'Q}(z)$ and $t_{Q'Q}(z)$ are symmetric.

The various scattering solutions in (11.1) are of the form of column vectors of functions

$$Z_Q(z;\mathbf{r}) = \sum_{Q'} \begin{pmatrix} g^Z_{Q'Q}(z;r)\,\chi_{Q'}(\hat{\mathbf{r}}) \\ \mathrm{i}f^Z_{Q'Q}(z;r)\,\chi_{\overline{Q}'}(\hat{\mathbf{r}}) \end{pmatrix} , \tag{11.7}$$

$$J_Q(z;\mathbf{r}) = \sum_{Q'} \begin{pmatrix} g^J_{Q'Q}(z;r)\,\chi_{Q'}(\hat{\mathbf{r}}) \\ \mathrm{i}f^J_{Q'Q}(z;r)\,\chi_{\overline{Q}'}(\hat{\mathbf{r}}) \end{pmatrix} , \tag{11.8}$$

$$\widetilde{Z}_Q(z;\mathbf{r}) = \sum_{Q'} \begin{pmatrix} g^Z_{Q'Q}(z^*;r)\,\chi_{Q'}(\hat{\mathbf{r}}) \\ \mathrm{i}f^Z_{Q'Q}(z^*;r)\,\chi_{\overline{Q}'}(\hat{\mathbf{r}}) \end{pmatrix} , \tag{11.9}$$

$$\widetilde{J}_Q(z;\mathbf{r}) = \sum_{Q'} \begin{pmatrix} g^J_{Q'Q}(z^*;r)\,\chi_{Q'}(\hat{\mathbf{r}}) \\ \mathrm{i}f^J_{Q'Q}(z;r)^*\,\chi_{\overline{Q}'}(\hat{\mathbf{r}}) \end{pmatrix} . \tag{11.10}$$

and therefore the needed adjoint scattering solutions are row vectors of functions:

$$\widetilde{Z}_Q(z;\mathbf{r})^\dagger = \sum_{Q'} \left(g^Z_{Q'Q}(z^*;r)^*\,\chi_{Q'}(\hat{\mathbf{r}})^\dagger , -\mathrm{i}f^Z_{Q'Q}(z^*;r)^*\,\chi_{\overline{Q}'}(\hat{\mathbf{r}})^\dagger \right) , \tag{11.11}$$

$$\widetilde{J}_Q(z;\mathbf{r})^\dagger = \sum_{Q'} \left(g^J_{Q'Q}(z^*;r)^*\,\chi_{Q'}(\hat{\mathbf{r}})^\dagger , -\mathrm{i}f^J_{Q'Q}(z^*;r)^*\,\chi_{\overline{Q}'}(\hat{\mathbf{r}})^\dagger \right) . \tag{11.12}$$

11.1.1 Redefinition of the irregular scattering solutions

Redefining in analogy to (6.8) new irregular scattering solutions as

$$\begin{aligned} I_Q(z;\mathbf{r}) &= \sum_{Q'} Z_{Q'}(z;\mathbf{r})\; t_{Q'Q}(z) - J_Q(z;\mathbf{r}) \\ &= \sum_{Q'} \begin{pmatrix} g^I_{Q'Q}(z;r)\,\chi_{Q'}(\hat{\mathbf{r}}) \\ \mathrm{i}f^I_{Q'Q}(z;r)\,\chi_{\overline{Q}'}(\hat{\mathbf{r}}) \end{pmatrix} \quad , \quad r \le r_{\mathrm{BS}} \quad , \\ I_Q(z;\mathbf{r}) &= \mp\mathrm{i}p \sum_{Q'} h^{\pm}_{Q'}(z;\mathbf{r})\; t_{Q'Q}(z) \quad , \quad r > r_{\mathrm{BS}} \quad , \end{aligned} \tag{11.13}$$

where

$$g^I_{Q'Q}(z;r) = \sum_{Q''} g^Z_{Q'Q''}(z;r)\; t_{Q''Q}(z) - g^J_{Q'Q}(z;r) \quad , \tag{11.14}$$

$$f^I_{Q'Q}(z;r) = \sum_{Q''} f^Z_{Q'Q''}(z;r)\; t_{Q''Q}(z) - f^J_{Q'Q}(z;r) \quad , \tag{11.15}$$

and, therefore, since $t_{QQ'}(z^*) = t_{Q'Q}(z)^*$,

$$\begin{aligned}\widetilde{I}_Q(z;\mathbf{r}) &= \sum_{Q'} \begin{pmatrix} g^I_{Q'Q}(z^*;r)\,\chi_{Q'}(\hat{\mathbf{r}}) \\ \mathrm{i} f^I_{Q'Q}(z^*;r)\,\chi_{\overline{Q}'}(\hat{\mathbf{r}}) \end{pmatrix} \\ &= \begin{pmatrix} \sum_{Q'Q''} g^Z_{Q'Q''}(z^*;r)\; t_{Q''Q}(z^*)\,\chi_{Q'}(\hat{\mathbf{r}}) \\ \mathrm{i}\sum_{Q'Q''} f^Z_{Q'Q''}(z^*;r)\; t_{Q''Q}(z^*)\,\chi_{\overline{Q}'}(\hat{\mathbf{r}}) \end{pmatrix} - \widetilde{J}_Q(z;\mathbf{r}) \\ &= \sum_{Q'} t_{QQ'}(z)^*\; \widetilde{Z}_{Q'}(z;\mathbf{r}) - \widetilde{J}_Q(z;\mathbf{r}) \quad , \end{aligned} \tag{11.16}$$

and

$$\widetilde{I}_Q(z;\mathbf{r})^\dagger = \sum_{Q'} t_{QQ'}(z)\; \widetilde{Z}_{Q'}(z;\mathbf{r})^\dagger - \widetilde{J}_Q(z;\mathbf{r})^\dagger \quad , \tag{11.17}$$

one can rewrite (11.1) as

$$\begin{aligned} G(z;\mathbf{r},\mathbf{r}') = \Theta(r'-r) \sum_Q Z_Q(z;\mathbf{r})\; \widetilde{I}_Q(z;\mathbf{r}')^\dagger \\ + \Theta(r-r') \sum_Q I_Q(z;\mathbf{r})\; \widetilde{Z}_Q(z;\mathbf{r}')^\dagger \quad . \end{aligned} \tag{11.18}$$

11.1.2 Regular solutions

Suppose the unperturbed Hamiltonian $\mathcal{H}^0$ in

$$\mathcal{H}(\mathbf{r}) = \mathcal{H}^0(\mathbf{r}) + \Delta\mathcal{H}(\mathbf{r}) \quad , \tag{11.19}$$

refers to that in (10.3), namely to a Kohn-Sham-Dirac Hamiltonian with a spherical symmetric effective potential $V(r)$ and a spherical symmetric effective $\mathbf{B}(r)$ pointing now along an arbitrary direction,

$$\mathcal{H}_0(\mathbf{r}) = c\,\boldsymbol{\alpha}\cdot\mathbf{p} + \beta mc^2 + V(r)\;\mathsf{I}_4 + \beta\boldsymbol{\Sigma}\cdot\mathbf{B}(r) \quad , \tag{11.20}$$

where as should be recalled I_n denotes a n-dimensional unit matrix,

$$\beta = \begin{pmatrix} \mathsf{I}_2 & \\ & -\mathsf{I}_2 \end{pmatrix} \quad , \quad \boldsymbol{\Sigma} = \begin{pmatrix} \sigma & \\ & \sigma \end{pmatrix} \quad . \tag{11.21}$$

Because of the block-diagonal form of β and $\mathbf{\Sigma}$ the perturbation $\Delta\mathcal{H}(\mathbf{r})$ is also block-diagonal,

$$\Delta\mathcal{H}(\mathbf{r}) = \begin{pmatrix} \Delta\mathcal{H}^{+}(\mathbf{r}) & 0 \\ 0 & \Delta\mathcal{H}^{-}(\mathbf{r}) \end{pmatrix} \quad , \tag{11.22}$$

where

$$\Delta\mathcal{H}^{\pm}(\mathbf{r}) \equiv \Delta V(\mathbf{r})\, \mathsf{I}_2 \pm \sigma \cdot \Delta\mathbf{B}(\mathbf{r}) \quad . \tag{11.23}$$

In the Calogero formulation of the Lippmann-Schwinger equation a regular scattering solution $Z_Q(z;\mathbf{r})$ of $\mathcal{H}(\mathbf{r})$, see also section (5.3.1), can be written as

$$Z_Q(z;\mathbf{r}) = \sum_{Q'} Z^0_{Q'}(z;\mathbf{r})\; A_{Q'Q}(z;r) + \sum_{Q'} I^0_{Q'}(z;\mathbf{r})\; B_{Q'Q}(z;r) \quad , \tag{11.24}$$

where in this particular case

$$A_{Q'Q}(z;r) = \delta_{QQ'} + \int\limits_{\mathbf{r}'\in\, D_V} \Big\{ \mathrm{d}\mathbf{r}'\, \Theta(r'-r) \; \widetilde{I}^0_{Q'}(z;\mathbf{r}')^{\dagger}\, \Delta\mathcal{H}(\mathbf{r}')\; Z_Q(z;\mathbf{r}') \Big\} \tag{11.25}$$

$$B_{Q'Q}(z;r) = \int\limits_{\mathbf{r}'\in\, D_V} \mathrm{d}\mathbf{r}'\, \Theta(r-r')\; \widetilde{Z}^0_{Q'}(z;\mathbf{r}')^{\dagger}\, \Delta\mathcal{H}(\mathbf{r}')\; Z_Q(z;\mathbf{r}') \quad . \tag{11.26}$$

and $Z^0_{Q'}(z;\mathbf{r})$ and $I^0_{Q'}(z;\mathbf{r})$ are the regular and the (properly reformulated) irregular scattering solutions of $\mathcal{H}_0(\mathbf{r})$.

Inserting expansions (11.7) and (11.22) into (11.25) and (11.26) one gets for the case that in $\mathcal{H}_0(\mathbf{r})$ the effective field points along the z direction

$$\begin{aligned} A_{Q'Q}(z;r) = \delta_{Q'Q} &+ \sum_{Q''Q'''} \int_r^{r_{\mathrm{BS}}} \Big\{ r'^2 \mathrm{d}r' \\ &\qquad g^{0,I}_{Q'Q''}(z;r')\; \Delta\mathcal{H}^{+}_{Q''Q'''}(r')\; g^{Z}_{Q'''Q}(z;r') \Big\} \\ &+ \sum_{Q''Q'''} \int_r^{r_{\mathrm{BS}}} \Big\{ r'^2 \mathrm{d}r' \\ &\qquad f^{0,I}_{Q'Q''}(z;r')\; \Delta\mathcal{H}^{-}_{Q''Q'''}(r')\; f^{Z}_{Q'''Q}(z;r') \Big\} \end{aligned} \tag{11.27}$$

and

$$B_{Q'Q}(z;r) = \sum_{Q''Q'''} \int_0^r \Big\{ r'^2 \mathrm{d}r' \; g^{0,Z}_{Q'Q''}(z;r') \; \Delta\mathcal{H}^{+}_{Q''Q'''}(r') \; g^{Z}_{Q'''Q}(z;r') \Big\}$$

$$+ \sum_{Q''Q'''} \int_0^r \Big\{ r'^2 \mathrm{d}r' \; f^{0,Z}_{Q'Q''}(z;r') \; \Delta\mathcal{H}^{-}_{Q''Q'''}(r') \; f^{Z}_{Q'''Q}(z;r') \Big\} \quad , \tag{11.28}$$

where

$$\Delta\mathcal{H}^{+}_{QQ'}(r) = \int \mathrm{d}\hat{\mathbf{r}} \, \chi_Q(\hat{\mathbf{r}})^\dagger \; \Delta\mathcal{H}^{+}(\mathbf{r}) \; \chi_{Q'}(\hat{\mathbf{r}}) \quad , \tag{11.29}$$

and

$$\Delta\mathcal{H}^{-}_{QQ'}(r) = \int \mathrm{d}\hat{\mathbf{r}} \, \chi_{\overline{Q}}(\hat{\mathbf{r}})^\dagger \; \Delta\mathcal{H}^{-}(\mathbf{r}) \; \chi_{\overline{Q}'}(\hat{\mathbf{r}}) \quad . \tag{11.30}$$

11.1.3 Irregular solution

For irregular solutions $I_Q(z;\mathbf{r})$ the Lippmann-Schwinger equation is of the form,

$$I_Q(z;\mathbf{r}) = \varphi_Q(z;\mathbf{r}) + \int\limits_{\mathbf{r}' \in D_V} \mathrm{d}\mathbf{r}' \, \mathcal{G}^0(z;\mathbf{r},\mathbf{r}') \, \Delta\mathcal{H}(\mathbf{r}') \, I_Q(z;\mathbf{r}') \quad , \tag{11.31}$$

see also section 5.3.2. Note that D_V and D_B, the domain of $\mathbf{B}(\mathbf{r})$, have to be identical. Since for $|\mathbf{r}| \geq r_{\mathrm{BS}}$

$$I_Q(z;\mathbf{r}) = I^0_Q(z;\mathbf{r}) \quad ,$$

$$\varphi_Q(z;\mathbf{r}) = I^0_Q(z;\mathbf{r}) \left\{ 1 - \int\limits_{\mathbf{r}' \in D_V} \mathrm{d}\mathbf{r}' \, \widetilde{Z}^0_Q(z;\mathbf{r}')^\dagger \, \Delta\mathcal{H}(\mathbf{r}') \, I_Q(z;\mathbf{r}') \right\} \quad . \tag{11.32}$$

Inserting (11.32) into (11.31) yields:

$$I_Q(z;\mathbf{r}) = \sum_{Q'} I^0_{Q'}(z;\mathbf{r}) \, C_{Q'Q}(z;r) + \sum_{Q'} Z^0_{Q'}(z;\mathbf{r}) \, D_{Q'Q}(z;r) \quad , \tag{11.33}$$

with

$$C_{Q'Q}(z;r) = \delta_{QQ'} - \int\limits_{\mathbf{r}' \in D_V} \mathrm{d}\mathbf{r}' \, \theta(r'-r) \; \widetilde{Z}^0_{Q'}(z;\mathbf{r}')^\dagger \, \Delta\mathcal{H}(\mathbf{r}') \, I_Q(z;\mathbf{r}') \quad , \tag{11.34}$$

and

$$D_{Q'Q}(z;r) = \int\limits_{\mathbf{r}' \in\, D_V} \mathrm{d}\mathbf{r}'\, \theta(r'-r)\, \widetilde{I}^{0}_{Q'}(z;\mathbf{r}')^{\dagger}\, \Delta\mathcal{H}(\mathbf{r}')\, I_{Q}(z;\mathbf{r}') \quad . \tag{11.35}$$

Furthermore, by inserting the expansion for the regular scattering solutions (11.7) and making use of (11.29) and (11.30), one gets

$$\begin{aligned} C_{Q'Q}(z;r) = \delta_{QQ'} &- \sum_{Q''Q'''} \int_{r}^{r_{\mathrm{BS}}} \Big\{ r'^{2}\mathrm{d}r' \\ &\qquad g^{0,Z}_{Q'Q''}(z;r')\, \Delta\mathcal{H}^{+}_{Q''Q'''}(r')\, g^{I}_{Q'''Q}(z;r') \Big\} \\ &- \sum_{Q''Q'''} \int_{r}^{r_{\mathrm{BS}}} \Big\{ r'^{2}\mathrm{d}r' \\ &\qquad f^{0,Z}_{Q'Q''}(z;r')\, \Delta\mathcal{H}^{-}_{Q''Q'''}(r')\, f^{I}_{Q'''Q}(z;r') \Big\} \quad , \end{aligned} \tag{11.36}$$

and

$$\begin{aligned} D_{Q'Q}(z;r) = &\sum_{Q''Q'''} \int_{r}^{r_{\mathrm{BS}}} \Big\{ r'^{2}\mathrm{d}r' \\ &\qquad g^{0,I}_{Q'Q''}(z;r')\, \Delta\mathcal{H}^{+}_{Q''Q'''}(r')\, g^{I}_{Q'''Q}(z;r') \Big\} \\ &+ \sum_{Q''Q'''} \int_{r}^{r_{\mathrm{BS}}} \Big\{ r'^{2}\mathrm{d}r' \\ &\qquad f^{0,I}_{Q'Q''}(z;r')\, \Delta\mathcal{H}^{-}_{Q''Q'''}(r')\, f^{I}_{Q'''Q}(z;r') \Big\} \quad . \end{aligned} \tag{11.37}$$

11.1.4 Angular momentum representations of $\Delta\mathcal{H}$

From the expansions in terms of spherical harmonics

$$V(\mathbf{r}) = \sum_{\Lambda} V_{\Lambda}(r)\, Y_{\Lambda}(\hat{\mathbf{r}}) \quad , \tag{11.38}$$

$$B_i(\mathbf{r}) = \sum_{\Lambda} B_{i,\Lambda}(r)\, Y_{\Lambda}(\hat{\mathbf{r}}) \quad , \quad (i = x, y, z) \quad , \tag{11.39}$$

the corresponding shape-truncated functions can be constructed

$$V(\mathbf{r})\,\sigma(\mathbf{r}) = \sum_{\Lambda} v_{\Lambda}(r)\,Y_{\Lambda}(\hat{\mathbf{r}}) \quad , \tag{11.40}$$

$$B_i(\mathbf{r})\,\sigma(\mathbf{r}) = \sum_{\Lambda} b_{i,\Lambda}(r)\,Y_{\Lambda}(\hat{\mathbf{r}}) \quad , \tag{11.41}$$

with

$$v_{\Lambda}(r) = \sum_{\Lambda'\Lambda''} C^{\Lambda}_{\Lambda'\Lambda''} V_{\Lambda'}(r)\,\sigma_{\Lambda''}(r) \quad , \tag{11.42}$$

$$b_{i,\Lambda}(r) = \sum_{\Lambda'\Lambda''} C^{\Lambda}_{\Lambda'\Lambda''} B_{i,\Lambda'}(r)\,\sigma_{\Lambda''}(r) \quad . \tag{11.43}$$

Thus $\Delta\mathcal{H}^{\pm}(\mathbf{r})$ can be written in the form of

$$\begin{aligned}\Delta\mathcal{H}^{\pm}(\mathbf{r}) = \mathsf{I}_2 &\sum_{\Lambda\neq(0,0)} v_{\Lambda}(r)\,Y_{\Lambda}(\hat{\mathbf{r}}) \\ &\pm \sum_{\Lambda\neq(0,0)} \sum_{i=x,y,z} \sigma_i b_{i,\Lambda}(r)\,Y_{\Lambda}(\hat{\mathbf{r}})\end{aligned} \tag{11.44}$$

and therefore the corresponding angular momentum representations as

$$\begin{aligned}\Delta\mathcal{H}^{+}_{QQ'}(r) = &\sum_{\Lambda\neq(0,0)} v_{\Lambda}(r)\,\langle\chi_Q\,|Y_{\Lambda}|\,\chi_{Q'}\rangle \\ &+ \sum_{\Lambda\neq(0,0)} \sum_{i=x,y,z} b_{i,\Lambda}(r)\,\langle\chi_Q\,|\sigma_i Y_{\Lambda}|\,\chi_{Q'}\rangle \quad ,\end{aligned} \tag{11.45}$$

$$\begin{aligned}\Delta\mathcal{H}^{-}_{QQ'}(r) = &\sum_{\Lambda\neq(0,0)} v_{\Lambda}(r)\left\langle\chi_{\overline{Q}}\,|Y_{\Lambda}|\,\chi_{\overline{Q}'}\right\rangle \\ &- \sum_{\Lambda\neq(0,0)} \sum_{i=x,y,z} b_{i,\Lambda}(r)\left\langle\chi_{\overline{Q}}\,|\sigma_i Y_{\Lambda}|\,\chi_{\overline{Q}'}\right\rangle \quad .\end{aligned} \tag{11.46}$$

11.1.5 Representations of angular momenta

The occurring angular momentum matrix elements can easily be evaluated:

$$\begin{aligned}\langle\chi_Q\,|Y_{\Lambda}|\,\chi_{Q'}\rangle = &\sum_{s=\pm 1/2} \{C(\ell, j, 1/2|\,(\mu-s)\;s) \\ &\times\; C(\ell', j', 1/2|\,(\mu'-s)\;s)\;C^{L}_{\Lambda,L'}\} \quad ,\end{aligned} \tag{11.47}$$

$$\begin{aligned}\left\langle\chi_{\overline{Q}}\,|Y_{\Lambda}|\,\chi_{\overline{Q}'}\right\rangle = &\sum_{s=\pm 1/2} \left\{C\left(\overline{\ell}, j, 1/2|\,(\mu-s)\;s\right)\right. \\ &\left.\times\; C\left(\overline{\ell}', j', 1/2|\,(\mu'-s)\;s\right)\;C^{\overline{L}}_{\Lambda,\overline{L}'}\right\} \quad ,\end{aligned} \tag{11.48}$$

with $\overline{L} \equiv \left(\overline{\ell}, m\right)$, while

$$\langle \chi_Q \left|\sigma_i Y_\Lambda\right| \chi_{Q'} \rangle = \sum_{s,s'=\pm 1/2} \Big\{ C\left(\ell, j, 1/2 \right| \left(\mu - s\right)\ s\right) \times\ C\left(\ell', j', 1/2 \right| \left(\mu' - s'\right)\ s'\right)\ C^{L}_{\Lambda,L'} \times\ \langle \phi_s \left|\sigma_i\right| \phi_{s'} \rangle \Big\} \quad , \tag{11.49}$$

$$\left\langle \chi_{\overline{Q}} \left|\sigma_i Y_\Lambda\right| \chi_{\overline{Q}'} \right\rangle = \sum_{s,s'=\pm 1/2} \Big\{ C\left(\overline{\ell}, j, 1/2 \right| \left(\mu - s\right)\ s\right) \times\ C\left(\overline{\ell}', j', 1/2 \right| \left(\mu' - s'\right)\ s'\right)\ C^{\overline{L}}_{\Lambda,\overline{L}'} \times\ \langle \phi_s \left|\sigma_i\right| \phi_{s'} \rangle \Big\} \quad . \tag{11.50}$$

Since $\sigma_z \phi_s = 2s\, \phi_s$,

$$\langle \chi_Q \left|\sigma_z Y_\Lambda\right| \chi_{Q'} \rangle = \sum_{s=\pm 1/2} \Big\{ 2s\, C\left(\ell, j, 1/2 \right| \left(\mu - s\right)\ s\right) \times\ C\left(\ell', j', 1/2 \right| \left(\mu' - s\right)\ s\right)\ C^{L}_{\Lambda,L'} \Big\} \quad , \tag{11.51}$$

and

$$\left\langle \chi_{\overline{Q}} \left|\sigma_z Y_\Lambda\right| \chi_{\overline{Q}'} \right\rangle = \sum_{s=\pm 1/2} \Big\{ 2s\, C\left(\overline{\ell}, j, 1/2 \right| \left(\mu - s\right)\ s\right) \times\ C\left(\overline{\ell}', j', 1/2 \right| \left(\mu' - s\right)\ s\right)\ C^{\overline{L}}_{\Lambda,\overline{L}'} \Big\} \quad . \tag{11.52}$$

Furthermore, in using the following relations,

$$\langle \phi_s \left|\sigma_x\right| \phi_{s'} \rangle = 1 - \delta_{ss'} \quad , \tag{11.53}$$

$$\langle \phi_s \left|\sigma_y\right| \phi_{s'} \rangle = \mathrm{i}\, 2s \left(1 - \delta_{ss'}\right) \quad , \tag{11.54}$$

one gets

$$\langle \chi_Q \left|\sigma_x Y_\Lambda\right| \chi_{Q'} \rangle = \sum_{s=\pm 1/2} \Big\{ C\left(\ell, j, 1/2 \right| \left(\mu - s\right)\ s\right) \times\ C\left(\ell', j', 1/2 \right| \left(\mu' - s^*\right)\ s^*\right)\ C^{L}_{\Lambda,L'} \Big\} \quad , \tag{11.55}$$

$$\langle \chi_Q \left| \sigma_y Y_\Lambda \right| \chi_{Q'} \rangle = \mathrm{i} \sum_{s=\pm 1/2} \Big\{ 2s\, C\left(\ell, j, 1/2 \right| (\mu - s)\ s) \times\ C\left(\ell', j', 1/2 \right| (\mu' - s^*)\ s^*)\ C^L_{\Lambda,L'} \Big\} \quad , \tag{11.56}$$

$$\left\langle \chi_{\overline{Q}} \left| \sigma_x Y_\Lambda \right| \chi_{\overline{Q}'} \right\rangle = \sum_{s=\pm 1/2} \Big\{ C\left(\overline{\ell}, j, 1/2 \right| (\mu - s)\ s) \times\ C\left(\overline{\ell}', j', 1/2 \right| (\mu' - s^*)\ s^*) \Big)\ C^{\overline{L}}_{\Lambda,\overline{L}'} \Big\} \quad , \tag{11.57}$$

$$\left\langle \chi_{\overline{Q}} \left| \sigma_y Y_\Lambda \right| \chi_{\overline{Q}'} \right\rangle = \mathrm{i} \sum_{s=\pm 1/2} 2s \Big\{ C\left(\overline{\ell}, j, 1/2 \right| (\mu - s)\ s) \times\ C\left(\overline{\ell}', j', 1/2 \right| (\mu' - s^*)\ s^*) \Big)\ C^{\overline{L}}_{\Lambda,\overline{L}'} \Big\} \quad , \tag{11.58}$$

where $s^* = -s$.

11.1.6 Calogero's coefficients

Finally, (11.27) and (11.28) can be expressed as

$$\begin{aligned} A_{Q'Q}(z;r) = \delta_{Q'Q} + \sum_{\Lambda\neq(0,0)} \sum_{Q''Q'''} \Big\{ & v^{Q'Q''Q'''Q}_{\Lambda(g,Z)}(r)\ \langle \chi_{Q''} \left| Y_\Lambda \right| \chi_{Q'''} \rangle \\ & + \sum_{i=x,y,z} b^{Q'Q''Q'''Q}_{i,\Lambda(g,Z)}(r)\ \langle \chi_{Q''} \left| \sigma_i Y_\Lambda \right| \chi_{Q'''} \rangle \\ & + v^{Q'Q''Q'''Q}_{\Lambda(f,Z)}(r)\ \left\langle \chi_{\overline{Q}''} \left| Y_\Lambda \right| \chi_{\overline{Q}'''} \right\rangle \\ & - \sum_{i=x,y,z} b^{Q'Q''Q'''Q}_{i,\Lambda(f,Z)}(r)\ \left\langle \chi_{\overline{Q}''} \left| \sigma_i Y_\Lambda \right| \chi_{\overline{Q}'''} \right\rangle \Big\} \quad , \end{aligned} \tag{11.59}$$

and

$$\begin{aligned} B_{Q'Q}(z;r) = \sum_{\Lambda\neq(0,0)} \sum_{Q''Q'''} \Big\{ & \widetilde{v}^{Q'Q''Q'''Q}_{\Lambda(g,Z)}(r)\ \langle \chi_{Q''} \left| Y_\Lambda \right| \chi_{Q'''} \rangle \\ & + \sum_{i=x,y,z} \widetilde{b}^{Q'Q''Q'''Q}_{i,\Lambda(g,Z)}(r)\ \langle \chi_{Q''} \left| \sigma_i Y_\Lambda \right| \chi_{Q'''} \rangle \\ & + \widetilde{v}^{Q'Q''Q'''Q}_{\Lambda(f,Z)}(r)\ \left\langle \chi_{\overline{Q}''} \left| Y_\Lambda \right| \chi_{\overline{Q}'''} \right\rangle \\ & - \sum_{i=x,y,z} \widetilde{b}^{Q'Q''Q'''Q}_{i,\Lambda(f,Z)}(r)\ \left\langle \chi_{\overline{Q}''} \left| \sigma_i Y_\Lambda \right| \chi_{\overline{Q}'''} \right\rangle \Big\} \quad , \end{aligned} \tag{11.60}$$

with the various integrals being defined as

$$v_{\Lambda(g,Z)}^{Q'Q''Q'''Q}(r) = \int_r^{r_{\rm BS}} r'^2 {\rm d}r'\, g_{Q'Q''}^{0,I}(z;r')\; v_\Lambda(r')\; g_{Q'''Q}^{Z}(z;r') \quad , \tag{11.61}$$

$$b_{i,\Lambda(g,Z)}^{Q'Q''Q'''Q}(r) = \int_r^{r_{\rm BS}} r'^2 {\rm d}r'\, g_{Q'Q''}^{0,I}(z;r')\; b_{i,\Lambda}(r')\; g_{Q'''Q}^{Z}(z;r') \quad , \tag{11.62}$$

$$v_{\Lambda(f,Z)}^{Q'Q''Q'''Q}(r) = \int_r^{r_{\rm BS}} r'^2 {\rm d}r'\, f_{Q'Q''}^{0,I}(z;r')\; v_\Lambda(r')\; f_{Q'''Q}^{Z}(z;r') \quad , \tag{11.63}$$

$$b_{i,\Lambda(f,Z)}^{Q'Q''Q'''Q}(r) = \int_r^{r_{\rm BS}} r'^2 {\rm d}r'\, f_{Q'Q''}^{0,I}(z;r')\; b_{i,\Lambda}(r')\; f_{Q'''Q}^{Z}(z;r') \quad , \tag{11.64}$$

$$\widetilde{v}_{\Lambda(g,Z)}^{Q'Q''Q'''Q}(r) = \int_0^{r} r'^2 {\rm d}r'\, g_{Q'Q''}^{0,Z}(z;r')\; v_\Lambda(r')\; g_{Q'''Q}^{Z}(z;r') \quad , \tag{11.65}$$

$$\widetilde{b}_{i,\Lambda(g,Z)}^{Q'Q''Q'''Q}(r) = \int_0^{r} r'^2 {\rm d}r'\, g_{Q'Q''}^{0,Z}(z;r')\; b_{i,\Lambda}(r')\; g_{Q'''Q}^{Z}(z;r') \quad , \tag{11.66}$$

$$\widetilde{v}_{\Lambda(f,Z)}^{Q'Q''Q'''Q}(r) = \int_0^{r} r'^2 {\rm d}r'\, f_{Q'Q''}^{0,Z}(z;r')\; v_\Lambda(r')\; f_{Q'''Q}^{Z}(z;r') \quad , \tag{11.67}$$

$$\widetilde{b}_{i,\Lambda(f,Z)}^{Q'Q''Q'''Q}(r) = \int_0^{r} r'^2 {\rm d}r'\, f_{Q'Q''}^{0,Z}(z;r')\; b_{i,\Lambda}(r')\; f_{Q'''Q}^{Z}(z;r') \quad . \tag{11.68}$$

For the irregular solution similar expressions can be derived:

$$\begin{aligned} C_{Q'Q}(z;r) = \delta_{Q'Q} - \sum_{\Lambda\neq(0,0)} \sum_{Q''Q'''} \Bigg\{ & v_{\Lambda(g,I)}^{Q'Q''Q'''Q}(r)\; \langle \chi_{Q''} | Y_\Lambda | \chi_{Q'''} \rangle \\ & + \sum_{i=x,y,z} b_{i,\Lambda(g,I)}^{Q'Q''Q'''Q}(r)\; \langle \chi_{Q''} | \sigma_i\, Y_\Lambda | \chi_{Q'''} \rangle \\ & + v_{\Lambda(f,I)}^{Q'Q''Q'''Q}(r)\; \left\langle \chi_{\overline{Q}''} | Y_\Lambda | \chi_{\overline{Q}'''} \right\rangle \\ & - \sum_{i=x,y,z} b_{i,\Lambda(f,I)}^{Q'Q''Q'''Q}(r)\; \left\langle \chi_{\overline{Q}''} | \sigma_i\, Y_\Lambda | \chi_{\overline{Q}'''} \right\rangle \Bigg\} \quad , \end{aligned} \tag{11.69}$$

and

$$\begin{aligned} D_{Q'Q}(z;r) = \sum_{\Lambda\neq(0,0)} \sum_{Q''Q'''} \Bigg\{ & \widetilde{v}_{\Lambda(g,I)}^{Q'Q''Q'''Q}(r)\; \langle \chi_{Q''} | Y_\Lambda | \chi_{Q'''} \rangle \\ & + \sum_{i=x,y,z} \widetilde{b}_{i,\Lambda(g,I)}^{Q'Q''Q'''Q}\; \langle \chi_{Q''} | \sigma_i\, Y_\Lambda | \chi_{Q'''} \rangle \\ & + \widetilde{v}_{\Lambda(f,I)}^{Q'Q''Q'''Q}(r)\; \left\langle \chi_{\overline{Q}''} | Y_\Lambda | \chi_{\overline{Q}'''} \right\rangle \\ & - \sum_{i=x,y,z} \widetilde{b}_{i,\Lambda(f,I)}^{Q'Q''Q'''Q}(r)\; \left\langle \chi_{\overline{Q}''} | \sigma_i\, Y_\Lambda | \chi_{\overline{Q}'''} \right\rangle \Bigg\} \quad . \end{aligned} \tag{11.70}$$

The corresponding integrals are now:

$$v_{\Lambda(g,I)}^{Q'Q''Q'''Q}(r) = \int_r^{r_{\mathrm{BS}}} r'^2 \mathrm{d}r'\, g_{Q'Q''}^{0,Z}(z;r')\, v_{\Lambda}(r')\, g_{Q'''Q}^{I}(z;r') \quad , \tag{11.71}$$

$$b_{i,\Lambda(g,I)}^{Q'Q''Q'''Q}(r) = \int_r^{r_{\mathrm{BS}}} r'^2 \mathrm{d}r'\, g_{Q'Q''}^{0,Z}(z;r')\, b_{i,\Lambda}(r')\, g_{Q'''Q}^{I}(z;r') \quad , \tag{11.72}$$

$$v_{\Lambda(f,I)}^{Q'Q''Q'''Q}(r) = \int_r^{r_{\mathrm{BS}}} r'^2 \mathrm{d}r'\, f_{Q'Q''}^{0,Z}(z;r')\, v_{\Lambda}(r')\, f_{Q'''Q}^{I}(z;r') \quad , \tag{11.73}$$

$$b_{i,\Lambda(f,I)}^{Q'Q''Q'''Q}(r) = \int_r^{r_{\mathrm{BS}}} r'^2 \mathrm{d}r'\, f_{Q'Q''}^{0,Z}(z;r')\, b_{i,\Lambda}(r')\, f_{Q'''Q}^{I}(z;r') \quad , \tag{11.74}$$

$$\widetilde{v}_{\Lambda(g,I)}^{Q'Q''Q'''Q}(r) = \int_r^{r_{\mathrm{BS}}} r'^2 \mathrm{d}r'\, g_{Q'Q''}^{0,I}(z;r')\, v_{\Lambda}(r')\, g_{Q'''Q}^{I}(z;r') \quad , \tag{11.75}$$

$$\widetilde{b}_{i,\Lambda(g,I)}^{Q'Q''Q'''Q}(r) = \int_r^{r_{\mathrm{BS}}} r'^2 \mathrm{d}r'\, g_{Q'Q''}^{0,I}(z;r')\, b_{i,\Lambda}(r')\, g_{Q'''Q}^{I}(z;r') \quad , \tag{11.76}$$

$$\widetilde{v}_{\Lambda(f,I)}^{Q'Q''Q'''Q}(r) = \int_r^{r_{\mathrm{BS}}} r'^2 \mathrm{d}r'\, f_{Q'Q''}^{0,I}(z;r')\, v_{\Lambda}(r')\, f_{Q'''Q}^{I}(z;r') \quad , \tag{11.77}$$

$$\widetilde{b}_{i,\Lambda(f,I)}^{Q'Q''Q'''Q}(r) = \int_r^{r_{\mathrm{BS}}} r'^2 \mathrm{d}r'\, f_{Q'Q''}^{0,I}(z;r')\, b_{i,\Lambda}(r')\, f_{Q'''Q}^{I}(z;r') \quad . \tag{11.78}$$

It should be noted that in using the local spin density functional in (11.59)–(11.60) and (11.69)–(11.70) only the term $i = z$ has to be taken into account, because an artificial z-axis of quantization can be assumed.

11.1.7 Single-site Green's function

In terms of the so found regular and (reformulated in (11.13)–(11.17)) irregular scattering solutions the single-site Green's function in (11.18) can formally now be written as a 2×2 matrix

$$G(z;\mathbf{r},\mathbf{r}') = \sum_{QQ'} \begin{pmatrix} G_{QQ'}^{++}\, \chi_Q(\hat{\mathbf{r}})\, \chi_{Q'}(\hat{\mathbf{r}}')^{\dagger} & -\mathrm{i}G_{QQ'}^{+-}\, \chi_Q(\hat{\mathbf{r}})\, \chi_{\overline{Q}'}(\hat{\mathbf{r}}')^{\dagger} \\ \mathrm{i}G_{QQ'}^{-+}\, \chi_{\overline{Q}}(\hat{\mathbf{r}})\, \chi_{Q'}(\hat{\mathbf{r}}')^{\dagger} & G_{QQ'}^{--}\, \chi_{\overline{Q}}(\hat{\mathbf{r}})\, \chi_{\overline{Q}'}(\hat{\mathbf{r}}')^{\dagger} \end{pmatrix} \tag{11.79}$$

of elements

$$G^{++}_{QQ'} = \Theta\left(r'-r\right)\sum_{Q''} g^{Z}_{QQ''}\left(z;r\right)\, g^{I}_{Q'Q''}\left(z;r'\right) + \Theta\left(r-r'\right)\sum_{Q''} g^{I}_{QQ''}\left(z;r\right)\, g^{Z}_{Q'Q''}\left(z;r'\right) \quad , \tag{11.80}$$

$$G^{+-}_{QQ'} = \Theta\left(r'-r\right)\sum_{Q''} g^{Z}_{QQ''}\left(z;r\right)\, f^{I}_{QQ''}\left(z;r'\right) + \Theta\left(r-r'\right)\sum_{Q''} g^{I}_{QQ''}\left(z;r\right)\, f^{Z}_{Q'Q''}\left(z;r'\right) \quad , \tag{11.81}$$

$$G^{-+}_{QQ'} = \Theta\left(r'-r\right)\sum_{Q''} f^{Z}_{QQ''}\left(z;r\right)\, g^{I}_{Q'Q''}\left(z;r'\right) + \Theta\left(r-r'\right)\sum_{Q''} f^{I}_{QQ''}\left(z;r\right)\, g^{Z}_{Q'Q''}\left(z;r'\right) \quad , \tag{11.82}$$

$$G^{--}_{QQ'} = \Theta\left(r'-r\right)\sum_{Q''} f^{Z}_{QQ''}\left(z;r\right)\, f^{I}_{Q'Q''}\left(z;r'\right) + \Theta\left(r-r'\right)\sum_{Q''} f^{I}_{QQ''}\left(z;r\right)\, f^{Z}_{Q'Q''}\left(z;r'\right) \quad . \tag{11.83}$$

11.2 Direct numerical solution of the coupled radial differential equations

The Kohn-Sham-Dirac Hamiltonian can be rewritten as [1] [2] [3]

$$\mathcal{H}\left(\mathbf{r}\right) = c\,\boldsymbol{\alpha}\cdot\mathbf{p} + \beta mc^2 + u\left(\mathbf{r}\right) \quad , \tag{11.84}$$

with

$$u\left(\mathbf{r}\right) = \begin{pmatrix} u^{+}\left(\mathbf{r}\right) & 0 \\ 0 & u^{-}\left(\mathbf{r}\right) \end{pmatrix} \quad , \tag{11.85}$$

and

$$u^{+}\left(\mathbf{r}\right) = \upsilon\left(\mathbf{r}\right) + \boldsymbol{\Sigma}\cdot\,\mathbf{b}\left(\mathbf{r}\right) \quad , \tag{11.86}$$

$$u^{-}\left(\mathbf{r}\right) = \upsilon\left(\mathbf{r}\right) - \boldsymbol{\Sigma}\cdot\,\mathbf{b}\left(\mathbf{r}\right) \quad . \tag{11.87}$$

The potential $\upsilon\left(\mathbf{r}\right)$, as defined in (9.2), and the magnetic field $\mathbf{b}\left(\mathbf{r}\right) = \left(b_x(\mathbf{r}), b_y(\mathbf{r}), b_z(\mathbf{r})\right)$, which is also confined to the Wigner-Seitz cell, have to be now expanded as follows

$$\upsilon\left(\mathbf{r}\right)=V(\mathbf{r})\sigma(\mathbf{r})=\sum_{\Lambda}\upsilon_{\Lambda}(r)Y_{\Lambda}(\hat{\mathbf{r}})=\sum_{\Lambda\Lambda'\Lambda''}C_{\Lambda'\Lambda''}^{\Lambda}Y_{\Lambda}(\hat{\mathbf{r}})V_{\Lambda'}(r)\sigma_{\Lambda''}(r)\quad , \tag{11.88}$$

$$b_i(\mathbf{r})=B_i(\mathbf{r})\sigma(\mathbf{r})=\sum_{\Lambda}b_{i,\Lambda}(r)Y_{\Lambda}(\hat{\mathbf{r}})=\sum_{\Lambda\Lambda'\Lambda''}C_{\Lambda'\Lambda''}^{\Lambda}Y_{\Lambda}(\hat{\mathbf{r}})B_{i,\Lambda'}(r)\sigma_{\Lambda''}(r)\quad , \tag{11.89}$$

$V(\mathbf{r})$ and $B(\mathbf{r})$ being the untruncated potential and magnetic field, respectively.

After rewriting the Hamiltonian in spherical coordinates and making the following Ansatz for the wave functions

$$\psi_Q(\mathbf{r})=\sum_{Q'}\begin{pmatrix} g_{Q'Q}(r)\,\chi_{Q'}\left(\hat{\mathbf{r}}\right) \\ \mathrm{i}f_{Q'Q}(r)\,\chi_{\bar{Q}'}\left(\hat{\mathbf{r}}\right)\end{pmatrix}\quad , \tag{11.90}$$

where $Q=(\kappa,\mu)$ and $\bar{Q}=(-\kappa,\mu)$, one arrives at the below system of coupled radial equations by making use of the orthonormality of the spin spherical harmonics $\chi_Q\left(\hat{\mathbf{r}}\right)$ and performing the angular integrations:

$$\begin{bmatrix} W-mc^2 & -\mathrm{i}\hbar c[\frac{\mathrm{d}}{\mathrm{d}r}+\frac{1}{r}-\frac{\kappa}{r}] \\ -\mathrm{i}\hbar c[\frac{\mathrm{d}}{\mathrm{d}r}+\frac{1}{r}+\frac{\kappa}{r}] & W+mc^2\end{bmatrix}\begin{bmatrix} g_{Q'Q}(r) \\ \mathrm{i}f_{Q'Q}(r)\end{bmatrix}=$$

$$=\sum_{Q''}\begin{bmatrix} u_{Q'Q''}^{+}(r)g_{Q''Q}(r) \\ \mathrm{i}u_{\bar{Q}'Q''}^{-}(r)f_{Q''Q}(r)\end{bmatrix}\quad . \tag{11.91}$$

The quantities $u_{QQ'}^{+}(r)$ and $u_{\bar{Q}Q'}^{-}(r)$ are given by

$$u_{QQ'}^{+}(r)=\langle\chi_Q|\upsilon\left(\mathbf{r}\right)+\boldsymbol{\Sigma}\cdot\mathbf{b}(\mathbf{r})|\chi_{Q'}\rangle \tag{11.92}$$

$$=\upsilon_{QQ'}^{+}(r)+\langle\chi_Q|\boldsymbol{\Sigma}\cdot\mathbf{b}(\mathbf{r})|\chi_{Q'}\rangle \tag{11.93}$$

$$=\upsilon_{QQ'}^{+}(r)+\sum_{i=x,y,z}\langle\chi_Q|\sigma_i b_i(\mathbf{r})|\chi_{Q'}\rangle \tag{11.94}$$

$$=\upsilon_{QQ'}^{+}(r)+\sum_{i=x,y,z}\sum_{\Lambda}b_{i,\Lambda}(r)\,\langle\chi_Q|\sigma_i Y_{\Lambda}(\hat{\mathbf{r}})|\chi_{Q'}\rangle \tag{11.95}$$

$$=\upsilon_{QQ'}^{+}(r)+\sum_{i=x,y,z}b_{i,QQ'}^{+}(r)\quad , \tag{11.96}$$

$$u_{\bar{Q}Q'}^{-}(r)=\upsilon_{\bar{Q}Q'}^{-}(r)-\sum_{i=x,y,z}\sum_{\Lambda}b_{i,\Lambda}(r)\,\langle\chi_{\bar{Q}}|\sigma_i Y_{\Lambda}(\hat{\mathbf{r}})|\chi_{\bar{Q}'}\rangle \tag{11.97}$$

$$=\upsilon_{\bar{Q}Q'}^{-}(r)-\sum_{i=x,y,z}b_{i,QQ'}^{-}(r)\quad . \tag{11.98}$$

The matrix elements $\langle \chi_Q | \sigma_i Y_\Lambda(\hat{\mathbf{r}}) | \chi_{\bar{Q}'} \rangle$ and $\langle \chi_{\bar{Q}} | \sigma_i Y_\Lambda(\hat{\mathbf{r}}) | \chi_{\bar{Q}'} \rangle$ are evaluated in (11.49) and (11.50), whereas $v^+_{QQ'}(r)$ and $v^-_{\bar{Q}\bar{Q}'}(r)$ were defined in (9.7) and (9.9). Furthermore, the following matrices for the components of the magnetic field have been defined:

$$\begin{aligned}
b^+_{x,QQ'}(r) &= \sum_{s=\pm 1/2} C\left(\ell, j, 1/2 \middle| (\mu - s)\ s\right) \\
&\times\ C\left(\ell', j', 1/2 \middle| (\mu' - s^*)\ s^*\right) b_{x,LL'}(r) \quad , \qquad (11.99) \\
b^+_{y,QQ'}(r) &= i \sum_{s=\pm 1/2} C\left(\ell, j, 1/2 \middle| (\mu - s)\ s\right) \\
&\times\ C\left(\ell', j', 1/2 \middle| (\mu' - s^*)\ s^*\right) b_{y,LL'}(r) \quad , \qquad (11.100) \\
b^+_{z,QQ'}(r) &= \sum_{s=\pm 1/2} 2sC\left(\ell, j, 1/2 \middle| (\mu - s)\ s\right) \\
&\times\ C\left(\ell', j', 1/2 \middle| (\mu' - s^*)\ s^*\right) b_{z,LL'}(r) \quad , \qquad (11.101) \\
b^-_{x,QQ'}(r) &= \sum_{s=\pm 1/2} C\left(\bar{\ell}, j, 1/2 \middle| (\mu - s)\ s\right) \\
&\times\ C\left(\bar{\ell}', j', 1/2 \middle| (\mu' - s^*)\ s^*\right) b_{x,\bar{L}\bar{L}'}(r) \quad , \qquad (11.102) \\
b^-_{y,QQ'}(r) &= i \sum_{s=\pm 1/2} C\left(\bar{\ell}, j, 1/2 \middle| (\mu - s)\ s\right) \\
&\times\ C\left(\bar{\ell}', j', 1/2 \middle| (\mu' - s^*)\ s^*\right) b_{y,\bar{L}\bar{L}'}(r) \quad , \qquad (11.103) \\
b^-_{z,QQ'}(r) &= \sum_{s=\pm 1/2} 2sC\left(\bar{\ell}, j, 1/2 \middle| (\mu - s)\ s\right) \\
&\times\ C\left(\bar{\ell}', j', 1/2 \middle| (\mu' - s^*)\ s^*\right) b_{z,\bar{L}\bar{L}'}(r) \quad , \qquad (11.104)
\end{aligned}$$

with

$$b_{i,LL'}(r) = \sum_\Lambda C^L_{\Lambda L'} b_{i,\Lambda}(r) \quad , \qquad (11.105)$$

$$b_{i,\bar{L}\bar{L}'}(r) = \sum_\Lambda C^{\bar{L}}_{\Lambda \bar{L}'} b_{i,\Lambda}(r) \quad . \qquad (11.106)$$

Using atomic units ($\hbar = 1$, $m = 1/2$) and the below definitions

$$P_{QQ'}(r) = r g_{QQ'}(r)\,, \quad Q_{QQ'}(r) = cr f_{QQ'}(r) \quad ,$$

the radial Dirac (11.91) transforms to

$$\frac{\mathrm{d}}{\mathrm{d}r}Q_{Q'Q}(r) = \frac{\kappa}{r}\,Q_{Q'Q}(r) - \sum_{Q''}\left[\epsilon\delta_{Q'Q''} - u^{+}_{Q'Q''}(r)\right]P_{Q''Q}(r) \quad , \tag{11.107}$$

$$\frac{\mathrm{d}}{\mathrm{d}r}P_{Q'Q}(r) = -\frac{\kappa}{r}\,P_{Q'Q}(r) + \sum_{Q''}\left\{\frac{1}{c^2}\left[\epsilon\delta_{Q'Q''} - u^{-}_{Q'Q''}(r)\right] + \delta_{Q'Q''}\right\}Q_{Q''Q}(r) \quad . \tag{11.108}$$

where $\epsilon = W - mc^2$ and $\left(W + mc^2\right)/c^2 = \epsilon/c^2 + 1$.

11.2.1 Starting values

In changing variables, $x = \ln r$, one obtains

$$\frac{\mathrm{d}}{\mathrm{d}x}Q_{Q'Q}(x) = \kappa\,Q_{Q'Q}(x) - \sum_{Q''}e^{x}\left[\epsilon\delta_{Q'Q''} - u^{+}_{Q'Q''}(x)\right]P_{Q''Q}(x) \tag{11.109}$$

$$\frac{\mathrm{d}}{\mathrm{d}x}P_{Q'Q}(x) = -\kappa\,P_{Q'Q}(x) + \sum_{Q''}e^{x}\left\{\frac{1}{c^2}\left[\epsilon\delta_{Q'Q''} - u^{-}_{Q'Q''}(x)\right] + \delta_{Q'Q''}\right\}Q_{Q''Q}(x) \quad . \tag{11.110}$$

As in the vicinity of the origin the potentials are spherical symmetric the starting values turn out to be (c.f., Sect. 10.1.3)

$$P_{QQ}(x_1) = 10^{-20} \quad , \tag{11.111}$$

$$Q_{QQ}(x_1) = \frac{\kappa + \sqrt{\kappa^2 - b^2}}{b/c}\,P_{QQ}(x_1) \quad , \tag{11.112}$$

$$\frac{\mathrm{d}}{\mathrm{d}x}P_{QQ}(x_1) = -\kappa\,P_{QQ}(x_1) + e^{x_1}\left[\frac{\epsilon - u^{-}_{QQ}(x_1)}{c^2} + 1\right]Q_{QQ}(x_1) \quad , \tag{11.113}$$

$$\frac{\mathrm{d}}{\mathrm{d}x}Q_{QQ}(x_1) = \kappa\,Q_{QQ}(x_1) - e^{x_1}\left[\epsilon - u^{+}_{QQ}(x_1)\right]P_{QQ}(x_1) \quad . \tag{11.114}$$

Noting that

$$\lim_{x\to-\infty} e^{x}b_{i,QQ'}(x) = 0 \quad , \tag{11.115}$$

one can approximate $u^{\pm}_{QQ}(x_1)$ in (11.114) and (11.113) by

$$u^{\pm}_{QQ}(x) \underset{x\to-\infty}{\longrightarrow} v^{\pm}_{QQ}(x) \tag{11.116}$$

11.2.2 Runge–Kutta extrapolation

The extrapolation for a few radial mesh points works exactly as discussed in Sects. 5.1.2 and 8.1.2 except that the function $\mathbf{P}(x_i)$ and $\mathbf{Q}(x_i)$ are now given by $P_{QQ'}(x_i)$ and $Q_{QQ'}(x_i)$, respectively,

$$P_{QQ'}(x_{i+1}) = P_{QQ'}(x_i) + \frac{\Delta x}{6}\left(k_1 + 2k_2 + 2k_3 + k_4\right) \tag{11.117}$$

$$Q_{QQ'}(x_{i+1}) = Q_{QQ'}(x_i) + \frac{\Delta x}{6}\left(m_1 + 2m_2 + 2m_3 + m_4\right) \tag{11.118}$$

and that (11.109) and (11.110) have to be used in order to calculate k_1 and m_1:

$$\begin{aligned} k_1 = &-\kappa\, P_{Q'Q}(x) \\ &+ \sum_{Q''} e^x \left\{ \frac{1}{c^2}\left[\epsilon\delta_{Q'Q''} - u^-_{Q'Q''}(x)\right] + \delta_{Q'Q''} \right\} Q_{Q''Q}(x) \end{aligned} \tag{11.119}$$

$$m_1 = \kappa\, Q_{Q'Q}(x) - \sum_{Q''} e^x \left[\epsilon\delta_{Q'Q''} - u^+_{Q'Q''}(x)\right] P_{Q''Q}(x) \quad . \tag{11.120}$$

The other coefficients k_i and m_i have to be evaluated in the usual manner according to table 5.1.

11.2.3 Predictor-corrector algorithm

The predictor–corrector scheme works like in the case of spherical symmetric potentials and is discussed in Sect. 8.1.3. The function $f(x_i)$ is represented either by $P_{QQ'}(x_i)$ or $Q_{QQ'}(x_i)$, and the predictors are calculated from (5.38); for the correctors (5.40) has to be used and the function $f^{1\prime}(x_i)$ is obtained from (11.109) and (11.110) in analogy to (8.41) and (8.42). The function $f^{1\prime}(x_i)$ refers to

$$\begin{aligned} \frac{\mathrm{d}}{\mathrm{d}x} P^1_{QQ}(x_i) = &-\kappa\, P^0_{Q'Q}(x_i) \\ &+ \sum_{Q''} e^{x_i} \left\{ \frac{1}{c^2}\left[\epsilon\delta_{Q'Q''} - u^-_{Q'Q''}(x_i)\right] + \delta_{Q'Q''} \right\} Q^0_{Q''Q}(x_i) \quad , \end{aligned} \tag{11.121}$$

or

$$\frac{\mathrm{d}}{\mathrm{d}x} Q^1_{QQ}(x_i) = \kappa\, Q^0_{Q'Q}(x_i) - \sum_{Q''} e^{x_i} \left[\epsilon\delta_{Q'Q''} - u^+_{Q'Q''}(x_i)\right] P^0_{Q''Q}(x_i) \quad .$$

In order to evaluate the irregular solutions the same procedure can be utilized, except that now an inward integration has to be performed. The starting values refer in this case to the values at the bounding sphere radius as discussed in Sect. 11.2.6.

11.2.4 Normalization of regular solutions

A general regular solution of the Dirac equation in (11.2) is of the form

$$\Psi_Q(z;\mathbf{r}) = \sum_{Q'} \begin{pmatrix} g^{\mathrm{r}}_{Q'Q}(z;r)\,\chi_{Q'}(\hat{\mathbf{r}}) \\ \\ \mathrm{i} f^{\mathrm{r}}_{Q'Q}(z;r)\,\chi_{\overline{Q}'}(\hat{\mathbf{r}}) \end{pmatrix} \quad , \tag{11.122}$$

which multiplied by a normalization factor $a_{Q'Q}$ then yields a proper regular scattering solution $Z_Q\,(z;\mathbf{r})$:

$$Z_Q\,(z;\mathbf{r}) = \sum_{Q'} \Psi_{Q'}(z;\mathbf{r})\,a_{Q'Q} \quad , \tag{11.123}$$

i.e.,

$$\sum_{Q'} \begin{pmatrix} g^{Z}_{Q'Q}(z;r)\,\chi_{Q'}(\hat{\mathbf{r}}) \\ \\ \mathrm{i} f^{Z}_{Q'Q}(z;r)\,\chi_{\overline{Q}'}(\hat{\mathbf{r}}) \end{pmatrix} = \sum_{Q',Q''} \begin{pmatrix} g^{\mathrm{r}}_{Q'Q''}(z;r)\,\chi_{Q'}(\hat{\mathbf{r}})\,a_{Q''Q} \\ \\ \mathrm{i} f^{\mathrm{r}}_{Q'Q''}(z;r)\,\chi_{\overline{Q}'}(\hat{\mathbf{r}})\,a_{Q''Q} \end{pmatrix} \quad . \tag{11.124}$$

At $|\mathbf{r}| = r_{\mathrm{BS}}$ by using (11.3) this leads to two sets of equations from which the inverse of the reactance and the normalization factors can be determined:

$$\begin{aligned} &\sum_{Q'} j_{\ell'}(pr_{\mathrm{BS}})\,\chi_{Q'}(\hat{\mathbf{r}})\,K^{-1}_{Q'Q} + \delta_{Q'Q}\,p\,n_{\ell'}(pr_{\mathrm{BS}})\,\chi_{Q'}(\hat{\mathbf{r}}) \\ &= \sum_{Q'Q''} g^{\mathrm{r}}_{Q'Q''}(z;r_{\mathrm{BS}})\,\chi_{Q'}(\hat{\mathbf{r}})\,a_{Q''Q} \quad , \end{aligned} \tag{11.125}$$

$$\begin{aligned} &\sum_{Q'} \frac{S_{\kappa'}p}{c} \left(j_{\bar{\ell}'}(pr_{\mathrm{BS}})\,\chi_{\overline{Q}'}(\hat{\mathbf{r}})\,K^{-1}_{Q'Q} + \delta_{Q'Q}\,p\,n_{\bar{\ell}'}(pr_{\mathrm{BS}})\,\chi_{\overline{Q}'}(\hat{\mathbf{r}}) \right) \\ &= \sum_{Q'Q''} f^{\mathrm{r}}_{Q'Q''}(z;r_{\mathrm{BS}})\,\chi_{\overline{Q}'}(\hat{\mathbf{r}})\,a_{Q''Q} \quad , \end{aligned} \tag{11.126}$$

i.e.,

$$j_{\ell'}(pr_{\mathrm{BS}})\,K^{-1}_{Q'Q} + \delta_{Q'Q}\,p\,n_{\ell'}(pr_{\mathrm{BS}}) = \sum_{Q''} g^{\mathrm{r}}_{Q'Q''}(z;r_{\mathrm{BS}})\,a_{Q''Q} \quad , \tag{11.127}$$

$$\frac{S_{\kappa'}p}{c} \left(j_{\bar{\ell}'}(pr_{\mathrm{BS}})\,K^{-1}_{Q'Q} + \delta_{Q'Q}\,p\,n_{\bar{\ell}'}(pr_{\mathrm{BS}}) \right) = \sum_{Q''} f^{\mathrm{r}}_{Q'Q''}(z;r_{\mathrm{BS}})\,a_{Q''Q} \quad . \tag{11.128}$$

11.2.5 Reactance and single-site t matrix

Adopting for matters of simplification the following matrix notation

$$\begin{aligned}
\mathbf{j} &= \{\delta_{QQ'}\, j_{\ell'}(pr_{\mathrm{BS}})\} \quad , \\
\mathbf{n} &= \{\delta_{QQ'}\, p\, n_{\ell'}(pr_{\mathrm{BS}})\} \quad , \\
\bar{\mathbf{j}} &= \{\delta_{QQ'}\ (S_{\kappa'}p/c)\ j_{\ell'}(pr_{\mathrm{BS}})\} \quad , \\
\bar{\mathbf{n}} &= \left\{\delta_{QQ'}\ \left(S_{\kappa'}p^2/c\right)\ n_{\ell'}(pr_{\mathrm{BS}})\right\} \quad , \\
\mathbf{K}^{-1} &= \left\{K^{-1}_{QQ'}\right\} \quad , \\
\mathbf{t} &= \{t_{QQ'}\} \quad , \\
\mathbf{a} &= \{a_{QQ'}\} \quad , \\
\mathbf{p} &= \{\delta_{QQ'}\, ip\} \quad , \\
\mathbf{f}_{\mathrm{r}} &= \left\{f^{\mathrm{r}}_{QQ'}(z; r_{\mathrm{BS}})\right\} \quad , \\
\mathbf{g}_{\mathrm{r}} &= \left\{g^{\mathrm{r}}_{QQ'}(z; r_{\mathrm{BS}})\right\} \quad ,
\end{aligned}$$

(11.127) and (11.128) can be written compactly as

$$\mathbf{j} \circ \mathbf{K}^{-1} + \mathbf{n} = \mathbf{g}_{\mathrm{r}} \circ \mathbf{a} \quad , \tag{11.129}$$

$$\bar{\mathbf{j}} \circ \mathbf{K}^{-1} + \bar{\mathbf{n}} = \mathbf{f}_{\mathrm{r}} \circ \mathbf{a} \quad , \tag{11.130}$$

where for a better visibility matrix multiplications are explicitly marked ($\circ$). From these two equations the matrices $\mathbf{K}^{-1}$ and $\mathbf{a}$ can be evaluated

$$\mathbf{K}^{-1} = (\mathbf{s} \circ \mathbf{j} - \bar{\mathbf{j}})^{-1} \circ (\bar{\mathbf{n}} - \mathbf{s} \circ \mathbf{n}) \quad , \tag{11.131}$$

$$\mathbf{a} = (\mathbf{r} \circ \mathbf{g}_{\mathrm{r}} - \mathbf{f}_{\mathrm{r}})^{-1} \circ (\mathbf{r} \circ \mathbf{n} - \bar{\mathbf{n}}) \quad , \tag{11.132}$$

or,

$$\mathbf{a} = \mathbf{g}_{\mathrm{r}}^{-1} \circ (\mathbf{j} \circ \mathbf{K}^{-1} + \mathbf{n}) \quad , \tag{11.133}$$

where

$$\mathbf{s} = \mathbf{f}_{\mathrm{r}} \circ \mathbf{g}_{\mathrm{r}}^{-1} \quad , \tag{11.134}$$

$$\mathbf{r} = \bar{\mathbf{j}} \circ \mathbf{j}^{-1} \quad , \tag{11.135}$$

The single-site t-matrix is then given by:

$$\mathbf{t}^{-1} = \mathbf{K}^{-1} + \mathbf{p} \quad , \tag{11.136}$$

$$\mathbf{t} = \left(\mathbf{K}^{-1} + \mathbf{p}\right)^{-1} \quad . \tag{11.137}$$

11.2.6 Normalization of the irregular solution

In general a proper irregular scattering solution can be defined in terms of a superposition of regular (r) and irregular solutions (i) of (11.2):

$$J_Q(z;\mathbf{r}) = \sum_{Q'} \Phi^{\mathrm{r}}_{Q'}(z;\mathbf{r})\, b_{Q'Q} + \Phi^{\mathrm{i}}_{Q'}(z;\mathbf{r})\, c_{Q'Q} \quad , \tag{11.138}$$

$$\Phi^{\alpha}_{Q'}(z;\mathbf{r}) = \sum_{Q'} \begin{pmatrix} g^{\alpha}_{Q'Q}(z;r)\, \chi_{Q'}(\hat{\mathbf{r}}) \\ \mathrm{i} f^{\alpha}_{Q'Q}(z;r)\, \chi_{\overline{Q}'}(\hat{\mathbf{r}}) \end{pmatrix} \quad , \quad \alpha = \mathrm{r}, \mathrm{i} \quad . \tag{11.139}$$

From the matching condition for the irregular solution $J_Q(z;\mathbf{r})$ given in (11.4) then follows:

$$\begin{aligned} &\sum_{Q'Q''} g^{\mathrm{r}}_{Q'Q''}(z;r_{\mathrm{BS}})\, \chi_{Q'}(\hat{\mathbf{r}})\, b_{Q''Q} + g^{\mathrm{i}}_{Q'Q''}(z;r_{\mathrm{BS}})\, \chi_{Q'}(\hat{\mathbf{r}})\, c_{Q''Q} \\ &= \sum_{Q'} \delta_{Q'Q}\, j_{\ell'}(pr_{\mathrm{BS}})\, \chi_{Q'}(\hat{\mathbf{r}}) \quad , \end{aligned} \tag{11.140}$$

$$\begin{aligned} &\sum_{Q'Q''} f^{\mathrm{r}}_{Q'Q''}(z;r_{\mathrm{BS}})\, \chi_{\overline{Q}'}(\hat{\mathbf{r}})\, b_{Q''Q} + f^{\mathrm{i}}_{Q'Q''}(z;r_{\mathrm{BS}})\, \chi_{\overline{Q}'}(\hat{\mathbf{r}})\, c_{Q''Q} \\ &= \sum_{Q'} \delta_{Q'Q}\, \frac{S_{\kappa' p}}{c}\, j_{\bar{\ell}'}(pr_{\mathrm{BS}})\, \chi_{\overline{Q}'}(\hat{\mathbf{r}}) \quad , \end{aligned} \tag{11.141}$$

and, consequently therefore,

$$\begin{aligned} &\sum_{Q''} g^{\mathrm{r}}_{Q'Q''}(z;r_{\mathrm{BS}})\, b_{Q''Q} + g^{\mathrm{i}}_{Q'Q''}(z;r_{\mathrm{BS}})\, c_{Q''Q} \\ &= \delta_{Q'Q}\, j_{\ell'}(pr_{\mathrm{BS}}) \quad , \end{aligned} \tag{11.142}$$

$$\begin{aligned} &\sum_{Q''} f^{\mathrm{r}}_{Q'Q''}(z;r_{\mathrm{BS}})\, b_{Q''Q} + f^{\mathrm{i}}_{Q'Q''}(z;r_{\mathrm{BS}})\, c_{Q''Q} \\ &= \delta_{Q'Q}\, \frac{S_{\kappa' p}}{c}\, j_{\bar{\ell}'}(pr_{\mathrm{BS}}) \quad . \end{aligned} \tag{11.143}$$

Introducing the following additional matrices,

$$\begin{aligned} \mathbf{g}_{\mathrm{i}} &= \left\{ g^{\mathrm{i}}_{QQ'}(z;r_{\mathrm{BS}}) \right\} \quad , \\ \mathbf{f}_{\mathrm{i}} &= \left\{ f^{\mathrm{i}}_{QQ'}(z;r_{\mathrm{BS}}) \right\} \quad , \\ \mathbf{b} &= \left\{ b_{QQ'} \right\} \quad , \\ \mathbf{c} &= \left\{ c_{QQ'} \right\} \quad , \end{aligned}$$

(11.142)–(11.143) reduce to

$$\mathbf{g}_{\mathrm{r}} \cdot \mathbf{b} + \mathbf{g}_{\mathrm{i}} \cdot \mathbf{c} = \mathbf{j} \quad , \tag{11.144}$$

$$\mathbf{f}_{\mathrm{r}} \cdot \mathbf{b} + \mathbf{f}_{\mathrm{i}} \cdot \mathbf{c} = \bar{\mathbf{j}} \quad , \tag{11.145}$$

$$\mathbf{c} = (\mathbf{f}_{\mathrm{i}} - \mathbf{s} \circ \mathbf{g}_{\mathrm{i}})^{-1} \circ (\bar{\mathbf{j}} - \mathbf{s} \circ \mathbf{j}) \quad , \tag{11.146}$$

$$\mathbf{b} = (\mathbf{f}_{\mathrm{r}} - \bar{\mathbf{s}} \circ \mathbf{g}_{\mathrm{r}})^{-1} \circ (\bar{\mathbf{j}} - \bar{\mathbf{s}} \circ \mathbf{j}) \quad , \tag{11.147}$$

where

$$\bar{\mathbf{s}} = \mathbf{f}_{\mathrm{i}} \circ \mathbf{g}_{\mathrm{i}}^{-1} \quad . \tag{11.148}$$

References

1. P. Weinberger, *Electron Scattering Theory of Ordered and Disordered Matter* (Clarendon Press, Oxford 1992)
2. M.E. Rose, *Relativistic Electron Theory* (Wiley, New York 1961)
3. P. Strange, *Relativistic Quantum Mechanics* (Cambridge University Press, Cambridge, England 1998)

12 Scalar-relativistic single-site scattering for spherically symmetric potentials

This chapter is devoted to the derivation of the scalar-relativistic radial differential equations. By *scalar-relativistic* usually an approach is meant in which the *spin-orbit coupling term* is neglected while the *mass velocity term* and the *Darwin shift* is retained, see also Chap. 3. If one primarily wants to calculate the total energy of a system this approximation usually is rather accurate. Furthermore, in calculating charge densities the small component of the wave-functions is not used, which implies that the non-relativistic and the scalar-relativistic problem can be treated on the same numerical footing.

12.1 Derivation of the scalar-relativistic differential equation

In omitting the energy argument in the radial amplitudes the radial Dirac equations, see Chap. 8, are given by

$$\frac{\mathrm{d}}{\mathrm{d}r}Q_\kappa(r) = \frac{\kappa}{r}Q_\kappa(r) - [\epsilon - V(r)]\,P_\kappa(r) \quad , \tag{12.1}$$

$$\frac{\mathrm{d}}{\mathrm{d}r}P_\kappa(r) = -\frac{\kappa}{r}P_\kappa(r) + \left[\frac{\epsilon - V(r)}{c^2} + 1\right] Q_\kappa(r) \quad . \tag{12.2}$$

Since $B(r)$,

$$B(r) = \frac{\epsilon - V(r)}{c^2} + 1 \quad , \tag{12.3}$$

goes to 1 as $c \to \infty$, it follows from (12.2) that

$$Q_\kappa(r) = B^{-1}(r)\left[P'_\kappa(r) + \frac{\kappa}{r}\,P_\kappa(r)\right] \quad . \tag{12.4}$$

In forming the derivative $\mathrm{d}Q_\kappa(r)/\mathrm{d}r = Q'_\kappa(r)$,

$$\begin{aligned} Q'_\kappa(r) &= -B^{-2}(r)B'(r)\left[P'_\kappa(r) + \frac{\kappa}{r}\,P_\kappa(r)\right] \\ &\quad + B^{-1}(r)\left[P''_\kappa(r) + \frac{\kappa}{r}\,P'_\kappa(r) - \frac{\kappa}{r^2}\,P_\kappa(r)\right] \qquad (12.5) \\ &= B^{-1}(r)\left[\frac{\kappa}{r}\,P'_\kappa(r) + \frac{\kappa^2}{r^2}\,P_\kappa(r)\right] - [\epsilon - V(r)]\,P_\kappa(r) \quad , \qquad (12.6) \end{aligned}$$

one obtains

$$B^{-1}(r)P''_\kappa(r) - B^{-2}(r)B'(r)P'_\kappa(r) \\ -\Big[B^{-2}(r)B'(r)\frac{\kappa}{r} + B^{-1}(r)\frac{\kappa}{r^2} + B^{-1}(r)\frac{\kappa^2}{r^2} - (\epsilon - V(r))\Big]P_\kappa(r) = 0 \quad . \tag{12.7}$$

Because of the identity

$$\kappa^2 + \kappa = \ell(\ell+1) \quad , \tag{12.8}$$

one can write

$$B^{-1}(r)P''_\kappa(r) - B^{-2}(r)B'(r)\left[P'_\kappa(r) + \frac{\kappa}{r}P_\kappa(r)\right] \\ -B^{-1}(r)\frac{\ell(\ell+1)}{r^2}P_\kappa(r) + [\epsilon - V(r)]P_\kappa(r) = 0 \quad . \tag{12.9}$$

The derivative of $B(r)$ is then simply given by

$$\frac{\mathrm{d}}{\mathrm{d}r}B(r) = -\frac{1}{c^2}\frac{\mathrm{d}}{\mathrm{d}r}V(r) = -\frac{1}{c^2}V'(r) \quad . \tag{12.10}$$

Adding and subtracting the term $B^{-2}(r)V'(r)/(c^2 r)P(r)$ yields the below equation,

$$B^{-1}(r)P''_\kappa(r) + \frac{1}{c^2}B^{-2}(r)V'(r)\left[P'_\kappa(r) - \frac{1}{r}P_\kappa(r)\right] \\ + \frac{1}{c^2}B^{-2}(r)V'(r)\frac{\kappa+1}{r}P_\kappa(r) \\ - \Big[B^{-1}(r)\frac{\ell(\ell+1)}{r^2} + V(r) - \epsilon\Big]P_\kappa(r) = 0 \quad ,$$

which can be rewritten in the following way:

$$-P''_\kappa(r) + \left[\frac{\ell(\ell+1)}{r^2} + V(r) - \epsilon\right]P_\kappa(r) = \frac{1}{c^2}B^{-2}(r)V'(r)\frac{\kappa+1}{r}P_\kappa(r) \\ + \frac{1}{c^2}\left[\epsilon - V(r)\right]B^{-1}\left[-P''_\kappa(r) + \frac{\ell(\ell+1)}{r^2}P_\kappa(r)\right] \\ + \frac{1}{c^2}B^{-2}(r)V'(r)\left[P'_\kappa(r) - \frac{1}{r}P_\kappa(r)\right] \quad , \tag{12.11}$$

where now the three terms on the right hand side are the spin-orbit coupling term, the mass velocity term and the Darwin shift, respectively. By neglecting finally the spin-orbit coupling term,

$$\frac{1}{c^2}B^{-2}(r)V'(r)\frac{\kappa+1}{r}P_\kappa(r) \quad , \tag{12.12}$$

the radial differential equation in the scalar-relativistic approximation is given by

$$B^{-1}(r)\left[P_\ell''(r)-\frac{\ell(\ell+1)}{r^2}\,P_\ell(r)\right]+[\epsilon-V(r)]\,P_\ell(r) \\ -B^{-2}(r)B'(r)\left[P_\ell'(r)-\frac{1}{r}\,P_\ell(r)\right]=0 \quad . \tag{12.13}$$

12.1.1 Transformation to first order coupled differential equations

In using the following Ansatz,

$$B(r)Q_\ell(r)=P_\ell'(r)-\frac{1}{r}\,P_\ell(r) \quad , \tag{12.14}$$

and by forming the corresponding derivative of $Q(r)$,

$$\begin{aligned} Q_\ell'(r)=&-B^{-2}(r)B'(r)P_\ell'(r)+B^{-1}(r)P_\ell''(r)-\frac{1}{r}\,B^{-1}(r)P_\ell'(r) \\ &+\frac{1}{r^2}\,B^{-1}(r)P_\ell(r)+\frac{1}{r}\,B^{-2}(r)B'(r)P_\ell(r) \qquad (12.15)\\ =&B^{-1}(r)P_\ell''(r)-B^{-2}(r)B'(r)\left[P_\ell'(r)-\frac{1}{r}\,P_\ell(r)\right] \\ &-\frac{1}{r}\,B^{-1}(r)\left[P_\ell'(r)-\frac{1}{r}\,P_\ell(r)\right] \\ =&B^{-1}(r)P_\ell''(r)-B^{-1}(r)B'(r)Q_\ell(r)-\frac{1}{r}\,Q_\ell(r) \quad , \qquad (12.16)\end{aligned}$$

one gets

$$B^{-1}(r)P_\ell''(r)=Q_\ell'(r)+B^{-1}(r)B'(r)Q_\ell(r)+\frac{1}{r}\,Q_\ell(r) \quad , \tag{12.17}$$

which inserted into (12.13) yields

$$Q_\ell'(r)+B^{-1}(r)B'(r)Q_\ell(r)+\frac{1}{r}\,Q_\ell(r) \\ -B^{-1}(r)\frac{\ell(\ell+1)}{r^2}\,P_\ell(r) \\ +[\epsilon-V(r)]\,P_\ell(r)-B^{-1}(r)B'(r)Q_\ell(r)=0 \quad .$$

The two terms involving $B^{-1}(r)B'(r)$ now cancel and after rearrangement of terms one obtains the following system of coupled differential equations:

$$\frac{\mathrm{d}}{\mathrm{d}r}Q_\ell(r)=-\frac{1}{r}\,Q_\ell(r)+\left[\frac{\ell(\ell+1)}{r^2B(r)}-\epsilon+V(r)\right]P_\ell(r) \quad , \tag{12.18}$$

$$\frac{\mathrm{d}}{\mathrm{d}r}P_\ell(r)=\frac{1}{r}\,P_\ell(r)+B(r)Q_\ell(r) \quad . \tag{12.19}$$

These equations are identical to those in the non-relativistic case if $B(r) = 1$, i.e., if $c \to \infty$. Therefore the numerical treatment is the same as in the non-relativistic case except that one has to provide different boundary conditions for $r \to 0$, which will be discussed below.

12.2 Numerical solution of the coupled radial differential equations

12.2.1 Starting values

In changing variables, $x = \ln r$, yields

$$\frac{\mathrm{d}}{\mathrm{d}x} Q_\ell(x) = -\,Q_\ell(x) + \left[\frac{\ell(\ell+1)}{e^x B(x)} + e^x\,(V(x) - \epsilon)\right] P_\ell(x) \quad , \tag{12.20}$$

$$\frac{\mathrm{d}}{\mathrm{d}x} P_\ell(x) = P_\ell(x) + e^x B(x) Q_\ell(x) \quad , \tag{12.21}$$

with

$$e^x B(x) = e^x \left[1 + \frac{\epsilon - V(x)}{c^2}\right] \underset{x \to -\infty}{\longrightarrow} \frac{2Z}{c^2} = \frac{b}{c} \quad . \tag{12.22}$$

For small radial values the above coupled equations are of the form

$$\frac{\mathrm{d}}{\mathrm{d}x} Q_\ell(x) = -Q(x) + \left[\frac{\ell(\ell+1)}{b/c} - bc\right] P(x) \quad , \tag{12.23}$$

$$\frac{\mathrm{d}}{\mathrm{d}x} P_\ell(x) = \frac{b}{c}\, Q_\ell(x) + P(x) \quad , \tag{12.24}$$

From the last equation, however, also follows that

$$Q(x) = \frac{c}{b}\,\left[P'(x) - P(x)\right] \quad , \tag{12.25}$$

$$Q'(x) = \frac{c}{b}\,\left[P''(x) - P'(x)\right] \quad , \tag{12.26}$$

where $f'(x) = \mathrm{d}f(x)/\mathrm{d}x$. Equations (12.23) and (12.24) can therefore be rewritten as

$$\frac{c}{b}\,\left[P''(x) - P'(x)\right] = -\frac{c}{b}\,\left[P'(x) - P(x)\right] + \frac{\ell(\ell+1)}{b/c}\,P(x) - bcP(x) \quad , \tag{12.27}$$

$$P''(x) = \left[1 + \ell(\ell+1) - b^2\right] P(x) \quad . \tag{12.28}$$

In making the Ansatz

$$P(x) = e^{Ax} \quad , \tag{12.29}$$

one finds for A

$$A = \sqrt{\ell(\ell+1)+1-b^2} \quad , \tag{12.30}$$

and the start values can be chosen as follows

$$P(x_1) = 10^{-20} \quad , \tag{12.31}$$

$$Q(x_1) = \left[\frac{-1+\sqrt{\ell(\ell+1)+1-b^2}}{b/c}\right] P(x_1) \quad , \tag{12.32}$$

where as should be recalled the value of $P(x_1)$ of course refers to an arbitrarily chosen small number. The derivatives follow then according to (12.20) and (12.21).

The Runge–Kutta procedure and predictor–corrector algorithm can be performed in exactly in the same way as in the non-relativistic case, the reader is therefore referred to Sects. 5.1.2 and 5.1.3.

Reference

1. J.S. Faulkner, Solid State Comm. **90**, 791 (1994)

13 Scalar-relativistic full potential single-site scattering

13.1 Derivation of the scalar-relativistic differential equation

In this particular case one has to derive from the radial Dirac equation,

$$\frac{\mathrm{d}}{\mathrm{d}r}Q_{Q'Q}(r) = \frac{\kappa}{r}\,Q_{Q'Q}(r) - \sum_{Q''}\left[\epsilon\delta_{Q'Q''} - v^{+}_{Q'Q''}(r)\right]P_{Q''Q}(r) \quad , \tag{13.1}$$

$$\begin{aligned}\frac{\mathrm{d}}{\mathrm{d}r}P_{Q'Q}(r) = &-\frac{\kappa}{r}\,P_{Q'Q}(r) \\ &+\sum_{Q''}\left\{\frac{1}{c^2}\left[\epsilon\delta_{Q'Q''} - v^{-}_{Q'Q''}(r)\right] + \delta_{Q'Q''}\right\}Q_{Q''Q}(r) \quad ,\end{aligned} \tag{13.2}$$

the radial differential equations for full potentials in the scalar relativistic approximation. By defining

$$B_{QQ'}(r) = \left[\frac{\epsilon}{c^2} + 1\right]\delta_{QQ'} - \frac{1}{c^2}\,v^{-}_{QQ'}(r) \quad , \tag{13.3}$$

and by introducing for matters of simplicity the matrix notation:

$$\mathbf{M} = \{M_{QQ'}(r)\} \quad , \tag{13.4}$$

one then can write

$$\mathbf{Q} = \mathbf{B}^{-1}\left[\mathbf{P}' + \frac{\kappa}{r}\,\mathbf{P}\right] \quad . \tag{13.5}$$

In forming the derivative $\mathrm{d}\mathbf{Q}/\mathrm{d}r = \mathbf{Q}'$ this yields

$$\mathbf{Q}' = -\mathbf{B}^{-2}\mathbf{B}'\left[\mathbf{P}' + \frac{\kappa}{r}\,\mathbf{P}\right] + \mathbf{B}^{-1}\left[\mathbf{P}'' + \frac{\kappa}{r}\,\mathbf{P}' - \frac{\kappa}{r^2}\,\mathbf{P}\right] \tag{13.6}$$

$$= \mathbf{B}^{-1}\left[\frac{\kappa}{r}\,\mathbf{P}' + \frac{\kappa^2}{r^2}\,\mathbf{P}\right] - \left[\epsilon - v^{+}\right]\mathbf{P} \quad . \tag{13.7}$$

from which then the following equation is obtained

$$\mathbf{B}^{-1}\mathbf{P}'' - \mathbf{B}^{-2}\mathbf{B}'\mathbf{P}' - \left[\mathbf{B}^{-2}\mathbf{B}'\frac{\kappa}{r} + \mathbf{B}^{-1}\frac{\kappa}{r^2} + \mathbf{B}^{-1}\frac{\kappa^2}{r^2} - \left(\epsilon - v^{+}\right)\right]\mathbf{P} = 0 \quad .$$

By using

$$\kappa^2 + \kappa = \ell(\ell+1) \quad , \tag{13.8}$$

one therefore can write

$$\mathbf{B}^{-1}\mathbf{P}'' - \mathbf{B}^{-2}\mathbf{B}'\left[\mathbf{P}' + \frac{\kappa}{r}\mathbf{P}\right] - \mathbf{B}^{-1}\frac{\ell(\ell+1)}{r^2}\mathbf{P} + \left[\epsilon - \upsilon^+\right]\mathbf{P} = 0 \quad .$$

Adding and subtracting now the term $\mathbf{B}^{-2}\mathbf{B}'\mathbf{P}/r$ leads to

$$\begin{aligned}\mathbf{B}^{-1}\mathbf{P}'' - \mathbf{B}^{-2}\mathbf{B}'&\left[\mathbf{P}' - \frac{1}{r}\mathbf{P}\right] \\ -\mathbf{B}^{-2}\mathbf{B}'&\frac{\kappa+1}{r}\mathbf{P} - \mathbf{B}^{-1}\frac{\ell(\ell+1)}{r^2}\mathbf{P} + \left[\epsilon - \upsilon^+\right]\mathbf{P} = 0 \quad .\end{aligned} \tag{13.9}$$

In neglecting the spin-orbit coupling term,

$$\frac{1}{c^2}\mathbf{B}^{-2}\upsilon^{-\prime}\frac{\kappa+1}{r}\mathbf{P} \quad , \tag{13.10}$$

the radial differential equation in the scalar relativistic approximation are given by:

$$\mathbf{B}^{-1}\left[\mathbf{P}'' - \frac{\ell(\ell+1)}{r^2}\mathbf{P}\right] + \left[\epsilon - \upsilon^+\right]\mathbf{P} - \mathbf{B}^{-2}\mathbf{B}'\left[\mathbf{P}' - \frac{1}{r}\mathbf{P}\right] = 0 \quad . \tag{13.11}$$

It should be noted that the occurring matrices in the above equation all carry relativistic (κ, μ) indices and therefore have to be transformed in a (ℓ, m) representation in terms of Clebsch-Gordan coefficients. As will be shown in the following this then leads to two identical equations in spin-space.

Recalling that the potential $\upsilon^+_{QQ'}(r)$ is given by

$$\upsilon^+_{QQ'}(r) = \sum_{s=\pm\frac{1}{2}} C(\ell, j, \frac{1}{2} \,|\, \mu - s, s)\, \upsilon_{LL'}(r)\, C(\ell', j', \frac{1}{2} \,|\, \mu' - s, s) \tag{13.12}$$

$$= \sum_{s=\pm\frac{1}{2}} C^\dagger_{QL}(s)\, \upsilon_{LL'}(r)\, C_{L'Q'}(s) \quad . \tag{13.13}$$

after multiplication with Clebsch-Gordan coefficients from the left and the right, one clearly enough obtains

$$C_{LQ}(s)\upsilon^+_{QQ'}(r)C^\dagger_{Q'L'}(s') = \sum_{s''=\pm\frac{1}{2}} C_{LQ}(s)C^\dagger_{QL}(s'')\upsilon_{LL'}(r)C_{L'Q'}(s'')C^\dagger_{Q'L'}(s') \tag{13.14}$$

$$= \sum_{s''=\pm\frac{1}{2}} \delta_{ss''}\, \upsilon_{LL'}(r)\, \delta_{s's''} \tag{13.15}$$

$$= \upsilon_{LL'}(r)\, \delta_{ss'} \quad . \tag{13.16}$$

Furthermore, because the following identity is valid

$$\langle \chi_Q | \chi_{Q'} \rangle = \langle \chi_{\bar{Q}} | \chi_{\bar{Q}'} \rangle \quad , \tag{13.17}$$

one gets

$$v^{+}_{QQ'}(r) = v^{-}_{\bar{Q}\bar{Q}'}(r) \quad . \tag{13.18}$$

All other matrices can be transformed to a LL'-representation in a similar manner:

$$C_{LQ}(s)\, M_{QQ'}(r)\, C^{\dagger}_{Q'L'}(s') = M_{LL'}(r)\delta_{ss'} \quad . \tag{13.19}$$

The radial differential equations for the scalar relativistic approximation in (ℓ, m) representation are therefore identical for each of the two components in spin-space, and consequently are given by

$$\begin{aligned} \sum_{L''} \Bigg\{ & B^{-1}_{LL''}(r) \left[P''_{L''L'}(r) - \frac{\ell''(\ell''+1)}{r^2}\, P_{L''L'}(r) \right] \\ & + \Big[\epsilon\, \delta_{LL''} - v_{LL''}(r) \Big] P_{L''L'}(r) \\ & - \left[B^{-2}(r) B'(r) \right]_{LL''} \left[P'_{L''L'}(r) - \frac{1}{r}\, P_{L''L'}(r) \right] \Bigg\} = 0 \end{aligned} \tag{13.20a}$$

13.1.1 Transformation to first order coupled differential equations

In the following once again the matrix notation from above is used in order to simplify the derivation as much as possible. It has to be recalled, however, that all matrices now carry LL' indices such as $v = \{v_{LL'}(r)\}$. In defining

$$\mathbf{Q} = \mathbf{B}^{-1} \left[\mathbf{P}' - \frac{1}{r}\, \mathbf{P} \right] \tag{13.21}$$

and forming the corresponding derivative of Q:

$$\mathbf{Q}' = -\mathbf{B}^{-2}\mathbf{B}'\mathbf{P}' + \mathbf{B}^{-1}\mathbf{P}'' - \frac{1}{r}\, \mathbf{B}^{-1}\mathbf{P}' + \frac{1}{r}\, \mathbf{B}^{-2}\mathbf{B}'\mathbf{P} + \frac{1}{r^2}\, \mathbf{P} \tag{13.22}$$

$$= \mathbf{B}^{-1}\mathbf{P}'' - \mathbf{B}^{-2}\mathbf{B}' \left(\mathbf{P}' - \frac{1}{r}\, \mathbf{P} \right) - \frac{1}{r}\, \mathbf{B}^{-1} \left(\mathbf{P}' - \frac{1}{r}\, \mathbf{P} \right) \tag{13.23}$$

$$= \mathbf{B}^{-1}\mathbf{P}'' - \mathbf{B}^{-2}\mathbf{B}'\mathbf{B}\mathbf{Q} - \frac{1}{r}\, \mathbf{Q} \quad , \tag{13.24}$$

one obtains

$$\mathbf{B}^{-1}\mathbf{P}'' = \mathbf{Q}' + \mathbf{B}^{-2}\mathbf{B}'\mathbf{B}\mathbf{Q} + \frac{1}{r}\, \mathbf{Q} \quad . \tag{13.25}$$

Insertion into (13.11),

$$\mathbf{Q}' + \mathbf{B}^{-2}\mathbf{B}'\mathbf{B}\mathbf{Q} + \frac{1}{r}\, \mathbf{Q} - \mathbf{B}^{-1}\frac{\ell(\ell+1)}{r^2}\, \mathbf{P} + [\epsilon - v]\, \mathbf{P} - \mathbf{B}^{-2}\mathbf{B}'\mathbf{B}\mathbf{Q} = 0 \quad , \tag{13.26}$$

finally yields the following two first order coupled differential equations

$$\mathbf{Q}' = -\frac{1}{r}\,\mathbf{Q} + \left[\mathbf{B}^{-1}\frac{\ell(\ell+1)}{r^2} - (\epsilon - \upsilon)\right]\mathbf{P} \quad , \tag{13.27}$$

$$\mathbf{P}' = \mathbf{B}\mathbf{Q} + \frac{1}{r}\,\mathbf{P} \quad . \tag{13.28}$$

Considering finally all angular momentum indices and arguments explicitly these two equations read as follows

$$\frac{\mathrm{d}}{\mathrm{d}r}Q_{LL'}(r) = -\frac{1}{r}\,Q_{L''L'}(r) + \sum_{L''} U_{LL''}(r)P_{L''L'}(r) \quad , \tag{13.29}$$

$$\frac{\mathrm{d}}{\mathrm{d}r}P_{LL'}(r) = \sum_{L''} B_{LL''}(r)\,Q_{L''L'}(r) + \frac{1}{r}\,P_{LL'}(r) \quad . \tag{13.30}$$

where

$$U_{LL'}(r) = \sum_{L''} B^{-1}_{LL''}\delta_{L''L'}\frac{\ell''(\ell''+1)}{r^2} - [\epsilon\,\delta_{LL'} - \upsilon_{LL'}(r)] \quad . \tag{13.31}$$

In the limit of $c \to \infty$, i.e. $B \to 1$, (13.29) and (13.30) reduce to the non-relativistic equations for full-potentials.

13.2 Numerical solution of the coupled radial differential equations

To solve these equations one can make use of the same start values as in the case of spherical potentials. Subsequently (13.29) and (13.30) have to be used for the Runge–Kutta and the predictor–corrector scheme applies in the same manner as described in Sects. 5.1.2 and 5.1.3.

14 Phase shifts and resonance energies

In order to illustrate the various types of single-site scattering discussed up-to-now in the following the probably most well-known single-site scattering properties, namely *phase shifts* and *resonance energies* are introduced and examples thereof shown.

14.1 Non-spin-polarized approaches

The asymptotic form of the regular radial wave function differs from the free space solution only by a phase factor – the phase shift $\delta_\ell(\varepsilon)$. From the relation between the scattering cross section $\sigma(\varepsilon)$ and the phase shifts for a spherical symmetric scatterer,

$$\sigma(\varepsilon) = \frac{4\pi}{\varepsilon} \sum_\ell (2\ell + 1) \sin^2 \delta_\ell(\varepsilon) \quad , \tag{14.1}$$

one can see immediately that a phase shift near 0 or π gives rise to weak and around $\pi/2$ to strong scattering.

The phase shifts are related in turn to the so-called Wigner delay time,

$$t_W \sim \frac{\mathrm{d}}{\mathrm{d}\varepsilon} \delta_\ell(\varepsilon) \quad , \tag{14.2}$$

which – colloquially expressed – means that electrons that have a resonance at a certain energy spend a long time around a scattering center. Since resonances occur predominantly for $\ell = 2$ this is compatible with the picture of localized d electrons in transition metals.

As discussed in Chap. 5, for spherically symmetric potentials the single-site t matrix is diagonal in angular momentum space and the phase shifts can directly be obtained from the below well-known equation,

$$\tan \delta_\ell(\varepsilon) = \frac{L_\ell(\varepsilon; r_S)\ j_\ell(pr_S) - p j'_\ell(pr_S)}{L_\ell(\varepsilon; r_S)\ n_\ell(pr_S) - p n'_\ell(pr_S)} \quad , \tag{14.3}$$

where $p = \sqrt{\varepsilon}$, $L_\ell(\varepsilon; r_S)$ is the logarithmic derivative of the regular radial wave-function at the muffin-tin or ASA radius, and $j_\ell(pr)$ and $n_\ell(pr)$ are spherical Bessel and Neumann functions, respectively.

Table 14.1. Non-zero elements of the reactance matrix up to $\ell = 2$ in a fcc(100) or bcc(100) lattice. These elements are determined by the non-zero components of the shape functions and hence by the symmetry of the system.

$K_{LL'}(\varepsilon)$		ℓ'	0	1	1	1	2	2	2	2	2
		m'	0	-1	0	1	-2	-1	0	1	2
ℓ	m	LL'	1	2	3	4	5	6	7	8	9
0	0	1	11								
1	-1	2		22							
1	0	3			33						
1	1	4				44					
2	-2	5					55				59
2	-1	6						66			
2	0	7							77		
2	1	8								88	
2	2	9					95				99

In the general full-potential case (see Chap. 6) the single-site t matrix $\mathbf{t}(\varepsilon)$ obviously has off-diagonal elements, therefore the phase shifts can not be directly related to scattering channels characterized by angular momentum quantum numbers. Since, however, for real energies the reactance matrix, $\mathbf{K}(\varepsilon)$,

$$\mathbf{K}(\varepsilon) = \left(\mathbf{t}(\varepsilon)^{-1} - \mathrm{i}p\mathbf{I}\right)^{-1} \quad , \tag{14.4}$$

is hermitean,

$$\mathbf{K}(\varepsilon) = \mathbf{K}(\varepsilon)^{+} \quad , \tag{14.5}$$

the so-called S matrix, $\mathbf{S}(\varepsilon)$

$$\mathbf{S}(\varepsilon) = \left(\mathbf{I} - \mathrm{i}p\mathbf{K}(\varepsilon)\right)\left(\mathbf{I} + \mathrm{i}p\mathbf{K}(\varepsilon)\right)^{-1} \tag{14.6}$$

$$= \left(\mathbf{t}(\varepsilon)^{-1}\right)^{+} \mathbf{t}(\varepsilon) \quad , \tag{14.7}$$

is a unitary matrix:

$$\mathbf{S}(\varepsilon)^{-1} = \mathbf{S}(\varepsilon)^{+} \quad . \tag{14.8}$$

Thus, by employing a unitary transformation of the basis $\{Y_L\,(\widehat{\mathbf{r}})\}$,

$$Y_L\,(\widehat{\mathbf{r}}) = \sum_{\lambda} U_{L\lambda} X_\lambda\,(\widehat{\mathbf{r}}) \quad , \tag{14.9}$$

$$\mathbf{U}^{-1} = \mathbf{U}^{+} \quad , \tag{14.10}$$

that diagonalizes $\mathbf{S}(\varepsilon)$,

$$\mathbf{S}'(\varepsilon) = \mathbf{U}^{-1}\mathbf{S}(\varepsilon)\mathbf{U} = \{S'_\lambda(\varepsilon)\,\delta_{\lambda\lambda'}\} \quad , \tag{14.11}$$

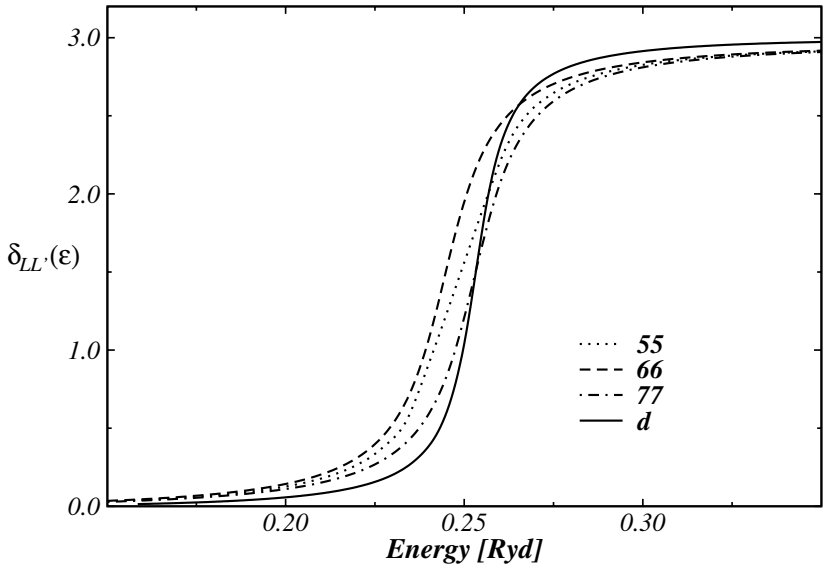

Fig. 14.1. Phase shifts in fcc-Ag for $\ell = 2$ (ASA calculation), and $\ell = 2$, $m = -2, -1, 0$ (full-potential calculation). The phase shift $\delta_{\ell=2}(\varepsilon)$ is labelled by d, while $\delta_{LL}(\varepsilon)$ is denoted by LL with the composite index $L = (\ell, m) = \ell(\ell+1) + m + 1$. Note that due to the symmetry of the system $\delta_{55}(\varepsilon) = \delta_{99}(\varepsilon)$ and $\delta_{66}(\varepsilon) = \delta_{88}(\varepsilon)$, see also Table 14.1.

where

$$|S'_\lambda(\varepsilon)| = 1 \quad , \tag{14.12}$$

so-called *generalized phase shifts,* $\delta'_\lambda(\varepsilon)$ can be defined as

$$S'_\lambda(\varepsilon) = \exp\left(\mathrm{i}2\delta'_\lambda(\varepsilon)\right) \quad . \tag{14.13}$$

Returning to the original angular momentum representation, in principle, a *phase shift matrix,* $\boldsymbol{\delta}(\varepsilon)$ can be introduced

$$\boldsymbol{\delta}(\varepsilon) = \mathbf{U}^{-1}\boldsymbol{\delta}'(\varepsilon)\mathbf{U} \quad , \tag{14.14}$$

with $\boldsymbol{\delta}'(\varepsilon) = \left\{\delta'_\lambda(\varepsilon)\,\delta_{\lambda\lambda'}\right\}$, such that

$$\mathbf{S}(\varepsilon) = \exp\left(\mathrm{i}2\boldsymbol{\delta}(\varepsilon)\right) \quad . \tag{14.15}$$

Inserting (14.15) into the inverse relationship of (14.6),

$$\mathbf{K}(\varepsilon) = -\frac{\mathrm{i}}{p}\left(\mathbf{I} + \mathbf{S}(\varepsilon)\right)^{-1}\left(\mathbf{I} - \mathbf{S}(\varepsilon)\right) \quad , \tag{14.16}$$

the below expression can be obtained

$$\tan\boldsymbol{\delta}(\varepsilon) = -p\mathbf{K}(\varepsilon) \quad , \tag{14.17}$$

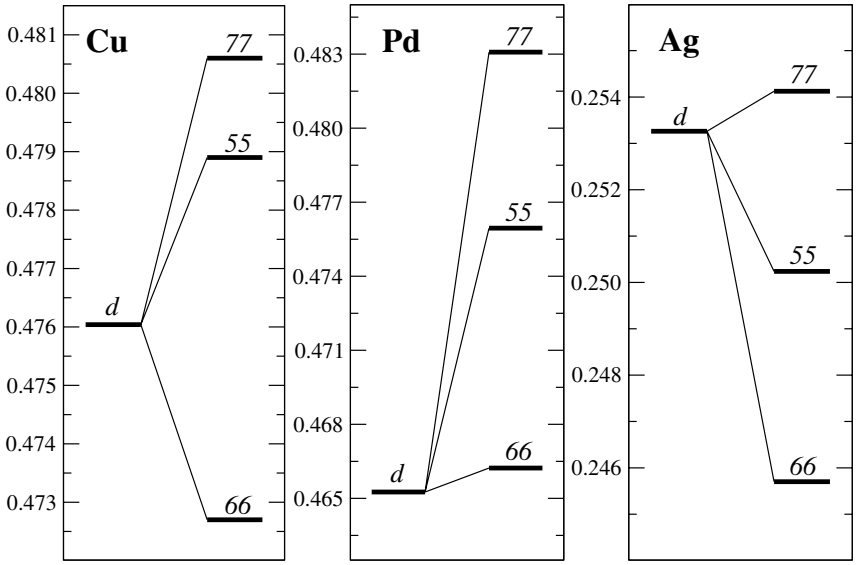

Fig. 14.2. Resonance energies of fcc-Cu, Pd, and Ag for non-relativistic ASA and full-potential calculations. The d like resonant energies for ASA are denoted by d, while those corresponding to the phase shifts δ_{LL} for the full-potential calculations are labelled by LL; $L = (\ell, m) = \ell(\ell+1) + m + 1$, see also Table 14.1.

where the tangent of a matrix $\mathbf{a}$ is defined as

$$\tan \mathbf{a} = -\mathrm{i}\frac{\exp(\mathrm{i}\mathbf{a}) - \exp(-\mathrm{i}\mathbf{a})}{\exp(\mathrm{i}\mathbf{a}) + \exp(-\mathrm{i}\mathbf{a})} \quad . \tag{14.18}$$

Clearly enough, (14.17) is an extension of (14.3) for the case of spherical symmetry. Since in all the cases investigated the off-diagonal elements of $\mathbf{K}(\varepsilon)$ turned to be of orders of magnitude less than the diagonal elements, in the following for *illustrative purposes* the diagonal elements of the phase shift matrix are calculated from the corresponding diagonal elements of the reactance or the single-site t matrix,

$$\delta_{LL}(\varepsilon) \simeq \arctan\left[-pK_{LL}(\varepsilon)\right] \tag{14.19}$$

$$\simeq \arctan\left[-pt_{LL}(\varepsilon)\left(1 - \mathrm{i}pt_{LL}(\varepsilon)\right)^{-1}\right] \quad . \tag{14.20}$$

In Fig. 14.1 one can see the resonance energies of three fcc-metals – Cu, Pd, and Ag. The resonance energy is defined as that energy where the phase shift passes through $\pi/2$. In transition metals this occurs for spherical symmetric potentials only for $\ell = 2$. In the case of full potential calculations there is more than one resonance because the phase shifts split up with respect to the quantum number m. One now finds different resonances for $m = 0, \pm 1, \pm 2$

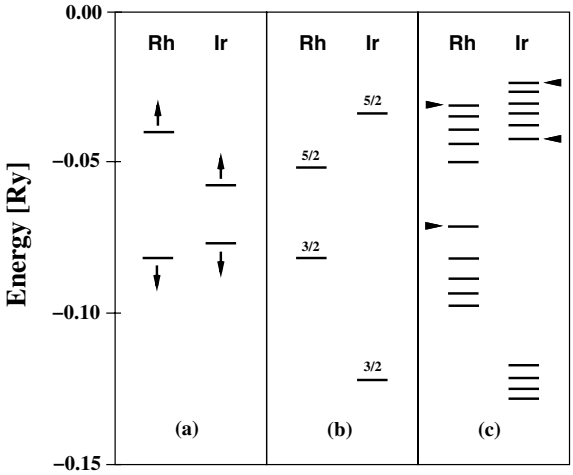

Fig. 14.3. Calculated positions of d–like resonances of a Rh and an Ir overlayer for the case of a Ag(001) substrate. The potentials from the scalar–relativistic spin–polarized calculations were used for the different single–site scattering schemes. Panel (a) refers to the scalar–relativistic spin–polarized case, where the spin–up and spin–down channels are denoted by up and down arrows. The relativistic non–magnetic case is shown in panel (b) illustrating the spin–orbit splitting between the j=3/2 and 5/2 resonances. The relativistic spin–polarized case is displayed in panel (c) and shows a total of ten different resonance energies for each case. The uncoupled resonances corresponding to (j, μ) = (5/2,-5/2) (upper ones) and (5/2,5/2) (lower ones) are indicated by small horizontal arrows. From [3].

in the diagonal of the phase shift matrix $\delta_{LL}(\varepsilon)$, see Table 14.1). The variation of the $\ell = 2$ phase shifts with energy is plotted in Fig. 14.2, in which the energy scale is positive relative to the maximum of the potential.

14.2 Spin-polarized approaches

For the spin-polarized and the relativistic cases analogous formulations for the phase shifts as above can be derived using, e.g., the expression for the reactance in the corresponding chapters.

The d–like resonances for various kinds of spin-polarized single–site scattering are presented in Fig. 14.3 for the case of Rh and Ir monolayers on Ag(001). In this figure, panel (a) refers to the non–relativistic spin–polarized case, and shows an exchange splitting that is approximately twice as large for Rh as for Ir. In panel (b) the resonance energies corresponding to a fully relativistic non–magnetic approach are shown. Quite clearly, the spin–orbit splitting of Ir, i.e., the splitting between the $d^{3/2}$ and $d^{5/2}$ resonance energy, is about three times larger than that of Rh. As compared to panel

(a), the spin–orbit splitting of Rh amounts to only about 70 % of the corresponding exchange splitting, while the spin–orbit splitting of Ir is more than four times larger than the corresponding exchange splitting. The fully relativistic spin-polarized case is shown in panel (c). Here, Rh represents the "strong magnetic case", in which the scattering channels corresponding to different j but to the same μ quantum numbers, namely $-3/2 \leq \mu \leq 3/2$ and $j = 3/2, 5/2$, are strongly coupled, while the two uncoupled resonances, $(j, \mu) = (5/2, -5/2), (5/2, 5/2)$ are energetically separated approximately by the exchange splitting as shown in panel (a). For Rh this coupling obviously leads to an "upper" and a "lower" set of resonances, each of them consisting of five levels. By transforming the single–site t–matrices from the (κ, μ) representation to the (ℓ, m, σ) representation, one can rather safely associate the lower and the upper sets of resonances with the $\sigma = -\frac{1}{2}$ and $\sigma = \frac{1}{2}$ channels, respectively, although, the resonances corresponding to different values of the spin quantum number σ are still slightly coupled. In the case of Ir, the small exchange coupling results into an almost "classical" *Zeeman–type splitting* of the $d^{3/2}$ and $d^{5/2}$ levels. Since, here the levels corresponding to the same j but to the opposite μ quantum numbers, like e.g. $(3/2, -3/2)$ and $(1/2, -1/2)$, are split only very weakly, a decreased magnetism has to be expected.

References

1. B.L. Gyorffy and G.M. Stocks, in *Electrons in finite and infinite structures*, ed by P. Phariseau and L. Scheire (Plenum Press, New York 1977)
2. P. Lloyd and P.V. Smith, Adv. Phys. **21**, 69 (1972).
3. B. Újfalussy, L. Szunyogh and P. Weinberger, Phys. Rev. **B51**, 12 836 (1995).

15 Structure constants

15.1 Real space structure constants

The real space structure constants were already discussed in the chapter introducing the concept of multiple scattering (Chap. 3), and for matters of completeness are repeated below. Provided that

$$\mathbf{r} = \mathbf{r}_n + \mathbf{R}_n \quad , \quad \mathbf{r}' = \mathbf{r}'_m + \mathbf{R}_m \quad , \tag{15.1}$$

$$n \neq m \quad ; \quad |\mathbf{r}_n - \mathbf{r}'_m| < |\mathbf{R}_{nm}| \quad , \quad \mathbf{R}_{nm} = \mathbf{R}_m - \mathbf{R}_n \quad , \tag{15.2}$$

the free space Green's functions for an in general complex energy $z = \epsilon + \mathrm{i}\delta$ (partial wave representation of the resolvent for a free travelling particle) is given according to (3.95) by

$$G_0\left(z; \mathbf{r}_n + \mathbf{R}_n, \mathbf{r}'_m + \mathbf{R}_m\right) = \sum_{LL'} j_L\left(z; \mathbf{r}_n\right) G^{nm}_{0,LL'}\left(z\right) \; j_{L'}\left(z; \mathbf{r}'_m\right)^{\times} \quad , \tag{15.3}$$

or, written in matrix notation as

$$G_0\left(z; \mathbf{r}_n + \mathbf{R}_n, \mathbf{r}'_m + \mathbf{R}_m\right) = \mathrm{j}\left(z; \mathbf{r}_n\right) \underline{G}^{nm}_0\left(z\right) \mathrm{j}\left(z; \mathbf{r}'_m\right)^{\times} \quad , \tag{15.4}$$

where

$$\underline{G}^{nm}_0\left(z\right) = \left\{G^{nm}_{0,LL'}\left(z\right)\right\} \quad , \tag{15.5}$$

with the matrix elements $G^{nm}_{0,LL'}\left(\varepsilon\right)$ usually referred to as *real space structure constants*

$$G^{nm}_{0,LL'}\left(z\right) = -4\pi p \mathrm{i} \sum_{L''} \mathrm{i}^{\ell - \ell' - \ell''} \, h^{+}_{L''}(z; \mathbf{R}_{nm}) \, C^{L'}_{LL''} \quad , \; p = \sqrt{z} \quad . \tag{15.6}$$

It is worthwhile to recall that again in here the below notation

$$j_L\left(z; \mathbf{r}_n\right) = \; j_\ell\left(p\left|\mathbf{r}_n\right|\right) Y_L(\hat{\mathbf{r}}_n) \quad , \tag{15.7}$$

$$h^{+}_L(z; \mathbf{R}_{nm}) = h^{+}_\ell(p\left|\mathbf{R}_{nm}\right|) Y_L(\hat{\mathbf{R}}_{nm}) \quad , \tag{15.8}$$

is used and that, e.g., $\mathrm{j}\left(z; \mathbf{r}_n\right)$ is a vector of properly arranged elements $j_L\left(z; \mathbf{r}_n\right)$. Including formally also the on-site term, the free space Green's function can be written according to (3.105) as

$$G_0\left(z;\mathbf{r}_n+\mathbf{R}_n,\mathbf{r}'_m+\mathbf{R}_m\right)=\delta_{nm}\,\mathsf{j}\left(z;\mathbf{r}_<\right)\left(-\mathrm{i}p\right)\,\mathsf{h}^+\left(z;\mathbf{r}_>\right)^\times + \left(1-\delta_{nm}\right)\mathsf{j}\left(z;\mathbf{r}_n\right)\underline{G}_0^{nm}\left(z\right)\,\mathsf{j}\left(z;\mathbf{r}'_m\right)^\times \quad . \tag{15.9}$$

As easily can be seen from (15.6) for a numerical evaluation of the structure constants corresponding to an arbitrarily arranged ensemble of scatterers only three kinds of well-established procedures are needed, namely for (1) spherical Hankel functions of complex argument, $h_\ell^+(x)$, (2) complex spherical harmonics, $Y_L(\hat{\mathbf{x}})$, and (3) Gaunt integrals, $C_{LL''}^{L'}$.

15.2 Two-dimensional translational invariance

15.2.1 Complex "square" lattices

Suppose that the potential is given as a superposition of individual ("non-overlapping") potentials such that

$$V(\mathbf{r})=\sum_{s=1}^{m}\sum_i V_i^s(\mathbf{r}_i) \quad , \tag{15.10}$$

$$\mathbf{r}_i\in D_{V_i^s} \quad ; \quad D_{V_i^s}\cap D_{V_j^{s'}}=0\,,\forall i\neq j \quad ; \quad \forall s\neq s' \quad , \tag{15.11}$$

where the $\mathbf{c}_{s,\parallel}$ are the so-called non-primitive translations, m is the number of sublattices, the $\mathbf{R}_{i,\parallel}$ refer to location vectors of Coulomb singularities in a particular sublattice, and $R_{i,z}\hat{\mathbf{z}}$ fixes the position of such a plane of atoms in the configuration space**.** As was pointed out in Chap. 2, a complex two-dimensional lattice is defined by the following translational invariance condition

$$\mathcal{L}(R_{i,z})=\left\{\mathbf{R}_{j,\parallel}\mid V(\mathbf{r}_i+\mathbf{R}_{i,\parallel}-\mathbf{R}_{j,\parallel}+R_{i,z}\hat{\mathbf{z}}+\mathbf{c}_{s,\parallel})=V_i^s(\mathbf{r}_i)\right\} \tag{15.12}$$

$$\equiv\left\{\mathbf{t}_{j,\parallel}\mid V_i^s(\mathbf{r}_i-\mathbf{t}_{j,\parallel})=V_i^s(\mathbf{r}_i)\right\} \quad , \tag{15.13}$$

and the corresponding translational group as

$$\mathcal{T}(R_{i,z})=\left\{\left[E\mid\mathbf{t}_{i,\parallel}\right]\right\} \quad ; \quad \left[E\mid\mathbf{t}_{i,\parallel}\right]^{|\mathcal{T}|}=\left[E\mid\mathbf{0}\right] \quad , \tag{15.14}$$

where $|\mathcal{T}|$ denotes the group order. It should be noted that in (15.12) for a particular sublattice s an arbitrary "in-plane" site $\mathbf{R}_{i,\parallel}$ serves as the origin of $\mathcal{L}(R_{i,z})$, and that the following definition of the vectors $\mathbf{c}_s$

$$\mathbf{c}_s=\mathbf{c}_{s,\parallel}+R_{i,z}\hat{\mathbf{z}} \;\equiv\; \mathbf{c}_{s,\parallel}+c_{s,\perp}\hat{\mathbf{z}} \quad . \tag{15.15}$$

is used. A simple two-dimensional lattice refers "simply" to the case of $m=1$ and $\mathbf{c}_{s,\parallel}=0$, i.e., trivially $\mathbf{c}_{s,\parallel}-\mathbf{c}_{s',\parallel}=0$.

15.2.2 Multilayer systems

Assuming now that in a multilayer system one and the same translational symmetry applies in all layers, i.e.,

$$\mathcal{L}(R_{i,z}) = \mathcal{L} \quad ; \quad \mathcal{T}(R_{i,z}) = \mathcal{T} \quad ; \forall R_{i,z} \quad , \tag{15.16}$$

a difference vector in configuration space can be written as

$$\begin{aligned} \mathbf{r} - \mathbf{r}' &= \mathbf{r}_i - \mathbf{r}_j + \mathbf{R}_{i,\parallel} - \mathbf{R}_{j,\parallel} + \mathbf{c}_{s,\parallel} - \mathbf{c}_{s',\parallel} + (c_{s,\perp} - c_{s',\perp})\,\hat{\mathbf{z}} & (15.17)\\ &= \mathbf{r}_i - \mathbf{r}_j + \mathbf{R}_{i,\parallel} - \mathbf{R}_{j,\parallel} + \mathbf{c}_{ss'} \quad , & (15.18) \end{aligned}$$

where in general $(c_{s,\perp} - c_{s',\perp}) \equiv (R_{i,z} - R_{j,z})$, and

$$\mathbf{c}_{ss'} = \mathbf{c}_{s,\parallel} - \mathbf{c}_{s',\parallel} + (c_{s,\perp} - c_{s',\perp})\,\hat{\mathbf{z}} \equiv \mathbf{c}_{ss',\parallel} + c_{ss',\perp}\hat{\mathbf{z}} \quad . \tag{15.19}$$

It should be noted that for a multilayer system corresponding to a simple two-dimensional lattice, the difference vector $\mathbf{c}_{ss'}$ reduces to

$$\mathbf{c}_{ss'} = c_{ss',\perp}\hat{\mathbf{z}} = (R_{i,z} - R_{j,z})\hat{\mathbf{z}} \quad . \tag{15.20}$$

15.2.3 Real and reciprocal two-dimensional lattices

As is well-known the translations $\mathbf{t}_{i,\parallel} \in \mathcal{L}$, $\mathcal{L} \equiv \mathcal{L}^{(2)}$, can be written as linear combinations of primitive two-dimensional lattice vectors $\mathbf{a}_1$ and $\mathbf{a}_2$,

$$\mathbf{t}_{i,\parallel} \equiv \mathbf{R}_{i,\parallel} = n_1\mathbf{a}_1 + n_2\mathbf{a}_2 \quad , \tag{15.21}$$

the (unit) surface area A being defined as

$$A = |\mathbf{a}_1 \times \mathbf{a}_2| \quad . \tag{15.22}$$

The corresponding reciprocal lattice, $\mathcal{L}^{-1} \equiv \mathcal{L}^{(2d)}$, is then given by

$$\mathcal{L}^{-1} = \left\{\mathbf{b}_{j,\parallel} \mid \mathbf{t}_{i,\parallel} \cdot \mathbf{b}_{j,\parallel} = 2\pi\delta_{ij} \ , \forall \mathbf{t}_{i,\parallel} \in \mathcal{L}\right\} \quad . \tag{15.23}$$

For matters of convenience in the following

$$I(\mathcal{L}) = \left\{i \mid \mathbf{t}_{i,\parallel} V_j^s(\mathbf{r}_j) = V_j^s(\mathbf{r}_j)\right\} \tag{15.24}$$

denotes the set of indices referring to $\mathcal{L}$ and

$$I(\mathcal{L}^{-1}) = \left\{j \mid \mathbf{b}_{j,\parallel} \cdot \mathbf{t}_{i,\parallel} = 2\pi\delta_{ij}, \forall \mathbf{t}_{i,\parallel} \in \mathcal{L}\right\} \tag{15.25}$$

the corresponding set for $\mathcal{L}^{-1}$.

15.2.4 The "Kambe" structure constants

By assuming two-dimensional translational symmetry as specified in (15.16) the configuration space representation of the free particle Green's function $G_0(\epsilon;\mathbf{r},\mathbf{r}')$ can be *lattice Fourier transformed* by formally using the following projection operator,

$$P_{\mathbf{k}_\parallel} = \frac{1}{|\mathcal{T}|}\sum_{i\in I(\mathcal{L})} \exp\left(-\mathrm{i}\mathbf{k}_\parallel\cdot\mathbf{R}_{i,\parallel}\right)\left[E \mid \mathbf{R}_{i,\parallel}\right] \quad , \tag{15.26}$$

such that

$$\begin{aligned} P_{\mathbf{k}_\parallel} G^0(\epsilon;\mathbf{r},\mathbf{r}')P_{\mathbf{k}'_\parallel} &= P_{\mathbf{k}_\parallel}P_{\mathbf{k}'_\parallel}G^0(\epsilon;\mathbf{r},\mathbf{r}')\delta_{\mathbf{k}_\parallel\mathbf{k}'_\parallel} = P^2_{\mathbf{k}_\parallel}G^0(\epsilon;\mathbf{r},\mathbf{r}')\delta_{\mathbf{k}_\parallel\mathbf{k}'_\parallel} \\ &= P_{\mathbf{k}_\parallel}G^0(\epsilon;\mathbf{r},\mathbf{r}')\delta_{\mathbf{k}_\parallel\mathbf{k}'_\parallel} \quad . \end{aligned} \tag{15.27}$$

The matrix of structure constants,

$$\mathbf{A}(\mathbf{k}_\parallel,z) = \left\{\underline{A}^{ss'}(\mathbf{k}_\parallel,z)\right\} \quad , \quad \underline{A}^{ss'}(\mathbf{k}_\parallel,z) = \left\{A^{ss'}_{LL'}(\mathbf{k}_\parallel,z)\right\} \quad , \tag{15.28}$$

is then related to the $\mathbf{k}_\parallel$ - projected unperturbed Green's function ("structural Green's function") as follows

$$\begin{aligned} G^0(\mathbf{r}_s,\mathbf{r}'_{s'};\mathbf{k}_\parallel,z) = \sum_{L,L'}\Big\{ & j_\ell(z;\mathbf{r}_{0s})A^{ss'}_{LL'}(\mathbf{k}_\parallel;z)j_{\ell'}(z;\mathbf{r}'_{0s'}) \\ & + \delta_{ss'}\delta_{LL'}\sqrt{z}j_\ell(z;\mathbf{r}_{0s,<})n_{\ell'}(z;\mathbf{r}'_{0s',>})\Big\} \quad , \end{aligned} \tag{15.29}$$

or,

$$\begin{aligned} G^0(\mathbf{r}_s,\mathbf{r}'_{s'};\mathbf{k}_\parallel,z) = {} & \mathsf{j}(z;\mathbf{r}_{0s})\underline{A}^{ss'}(\mathbf{k}_\parallel;z)\mathsf{j}(z;\mathbf{r}'_{0s'}) \\ & + \delta_{ss'}\sqrt{z}\mathsf{j}(z;\mathbf{r}_{0s,<})\mathsf{n}(z;\mathbf{r}'_{0s',>}) \quad , \end{aligned} \tag{15.30}$$

where

$$\mathbf{r}_s = \mathbf{r}_{0s} + \mathbf{c}_s \quad , \quad \mathbf{r}'_{s'} = \mathbf{r}'_{0s'} + \mathbf{c}_{s'} \quad , \tag{15.31}$$

$$z = \epsilon + \mathrm{i}\delta \quad , \quad \mathrm{Im}z > 0 \quad . \tag{15.32}$$

It should be noted that in (15.31) the sites $0s$ and $0s'$ serve as origins of their respective lattices. Clearly enough a summation over all $\mathbf{k}_\parallel$ - projections yields $G^0(\mathbf{r}_s,\mathbf{r}'_{s'};z)$

$$\begin{aligned} G^0(\mathbf{r}_s,\mathbf{r}'_{s'};z) &= |\mathcal{T}|^{-1}\sum_{\mathbf{k}_\parallel\ \in\ \mathrm{SBZ}} G^0(\mathbf{r}_s,\mathbf{r}'_{s'};\mathbf{k}_\parallel,z) \\ &\simeq \Omega^{-1}_{\mathrm{SBZ}}\int G^0(\mathbf{r}_s,\mathbf{r}'_{s'};\mathbf{k}_\parallel,z)\mathrm{d}\mathbf{k}_\parallel \quad ., \end{aligned} \tag{15.33}$$

where $\Omega_{\rm SBZ}^{-1}$ is the unit area ("volume") of the first Surface Brillouin zone (SBZ) and $\mathbf{k}_\parallel \in$ SBZ.

Defining the following quantities

$$\mathbf{K}_{m,\parallel} = \mathbf{k}_\parallel + \mathbf{b}_{m,\parallel} \quad , \quad \mathbf{b}_{m,\parallel} \in \mathcal{L}^{-1} \quad , \tag{15.34}$$

$$K_{m,\perp} = \begin{cases} \sqrt{\epsilon - \left|\mathbf{K}_{m,\parallel}\right|^2} \; ; \epsilon > \left|\mathbf{K}_{m,\parallel}\right|^2 \\ \mathrm{i}\sqrt{\left|\mathbf{K}_{m,\parallel}\right|^2 - \epsilon} \; ; \epsilon < \left|\mathbf{K}_{m,\parallel}\right|^2 \end{cases} , \tag{15.35}$$

$\mathbf{k}_\parallel \in$ SBZ, the limiting procedure and contour integration originally discussed by Segall [7] for three-dimensional lattices has to be applied (Kambe [1], [2] and [3]) now to the structure constants $A_{LL'}^{ss'}(\mathbf{k}_\parallel, \epsilon)$ for a multilayer system corresponding to an in general complex two-dimensional lattice. For this purpose the structure constants $A_{LL'}^{ss'}(\mathbf{k}_\parallel, z)$ are split up into three contributions,

$$A_{LL'}^{ss'}(\mathbf{k}_\parallel, \epsilon) = 4\pi \mathrm{i}^{(\ell - \ell')} \sum_{L''} \mathrm{i}^{-\ell''} C_{LL'}^{L''} \quad \Big\{ D_{L''}^{ss',(1)}(\mathbf{k}_\parallel, z) + D_{L''}^{ss',(2)}(\mathbf{k}_\parallel, z) + \delta_{ss'} \delta_{0\ell} \delta_{0m} D_{00}^{ss,(3)}(z) \Big\} \quad , \tag{15.36}$$

where the $C_{LL'}^{L''}$ refer to the by now familiar Gaunt integrals.

15.2.5 The layer- and sublattice off-diagonal case ($s \neq s'$)

The $D^{ss',(1)}$ term: $c_{ss',\perp} \neq 0$

Following Kambe for $\mathbf{c}_{ss'} \neq 0$ **and** $c_{ss',\perp} \neq 0$, the first $\mathbf{k}_\parallel$ - dependent term in (15.36) is given by

$$\begin{aligned} D_L^{ss',(1)}(\mathbf{k}_\parallel, z) = -\frac{1}{A\sqrt{\epsilon}} F_{\ell m} \sum_{m \,\in\, I(\mathcal{L}^{-1})} \Big\{ & \exp\left[\mathrm{i}\left(\mathbf{K}_{m,\parallel} \cdot \mathbf{c}_{ss',\parallel} - m\Phi(\mathbf{K}_{m,\parallel})\right)\right] \\ & \times \sum_{n=0}^{\ell - |m|} \left(\frac{1}{n!}\right) \left(K_{m,\perp}/\sqrt{z}\right)^{2n-1} \Delta_n^{ss'}(K_{m,\perp}) \\ & \times \Bigg[\sum_{s=n}^{\min(2n, \ell - |m|)} \left[\binom{n}{2n-s} \right. \\ & \left. \times \frac{\left(-\sqrt{\epsilon} c_{ss',\perp}\right)^{2n-s} \left(\left|\mathbf{K}_{m,\parallel}\right| / \sqrt{z}\right)^{\ell - s}}{[(\ell - |m| - s)/2]!\,[(\ell + |m| - s)/2]!} \right] \Bigg] \Big\} \quad , \end{aligned} \tag{15.37}$$

where

$$F_{\ell m} = \mathrm{i}^{|m|+1} 2^{-\ell} \sqrt{(2\ell+1)\,(\ell+|m|)!(\ell-|m|)!} \quad , \tag{15.38}$$

$$\Delta_n^{ss'}(K_{m,\perp}) = \int_x^\infty \eta^{\left(-\frac{1}{2}-n\right)} \exp\left[-\eta + \frac{y^2}{4\eta}\right] \mathrm{d}\eta \quad , \tag{15.39}$$

and

$$x = \exp\left[-\mathrm{i}\pi\right] K_{m,\perp}^2 \omega/2 \quad , \quad y^2 = \left(K_{m,\perp} c_{ss',\perp}\right)^2 \quad , \tag{15.40}$$

with ω being a complex number such that $Re(\omega)$ and $|\omega| < \infty$. In (15.37) $\Phi(\mathbf{K}_{m,\parallel})$ refers to the polar coordinates of the $\mathbf{K}_{m,\parallel}$,

$$\mathbf{K}_{m,\parallel} = \left|\mathbf{K}_{m,\parallel}\right| \cos\left(\Phi(\mathbf{K}_{m,\parallel})\right) \quad . \tag{15.41}$$

It should be noted that (15.37) applies to different sublattices in different layers ($c_{ss',\perp} = R_{i,z} - R_{j,z} \neq 0$)!

The $D^{ss',(1)}$ term: $c_{ss',\perp} = 0$

For $\mathbf{c}_{ss'} \neq 0$ **and** $c_{ss',\perp} = 0$, the form in the second paper by Kambe [2] has to be used, namely

$$\begin{aligned} D_L^{ss',(1)}(\mathbf{k}_\parallel, \epsilon) = -\frac{1}{A\sqrt{\epsilon}} F_{\ell m} \sum_{m \,\in\, I(\mathcal{L}^{-1})} \Bigg\{ & \exp\left[\mathrm{i}\left(\mathbf{K}_{m,\parallel} \cdot \mathbf{c}_{ss',\parallel} - m\Phi(\mathbf{K}_{m,\parallel})\right)\right] \\ & \times \sum_{n=0}^{(\ell-|m|)/2} \Bigg[\left(\frac{1}{n!}\right) \frac{(K_{m,\perp}/\sqrt{\epsilon})^{2n-1} \left(\left|\mathbf{K}_{m,\parallel}\right|/\sqrt{\epsilon}\right)^{\ell-2n}}{[(\ell-|m|-2n)/2]!\,[(\ell+|m|-2n)/2]!} \\ & \times \Gamma\left(\frac{1}{2}-n, x\right) \Bigg] \Bigg\} \quad , \end{aligned} \tag{15.42}$$

where $\Gamma(\frac{1}{2}-n, x)$ is an incomplete $\Gamma-$function, which can be evaluated recursively using standard numerical recipes, and x is defined in (15.40).

According to Appendix 3 [3] the integral in (15.39) can also be obtained in a recursive manner, namely

$$\left(\frac{y}{2}\right)^2 \Delta_{n+1} = (\frac{1}{2}-n)\Delta_n + \Delta_{n-1} - x^{\left(\frac{1}{2}-n\right)} \exp\left[\frac{y^2}{4x} - x\right] \quad , \tag{15.43}$$

with

$$\begin{aligned} \Delta_0 = \frac{\sqrt{\pi}}{2} \exp\left[\frac{y^2}{4x} - x\right] \Bigg\{ & \mathrm{erf}\left(-\frac{y}{2\sqrt{x}} + \mathrm{i}\sqrt{x}\right) \\ & + \mathrm{erf}\left(\frac{y}{2\sqrt{x}} + \mathrm{i}\sqrt{x}\right) \Bigg\} \quad , \end{aligned} \tag{15.44}$$

$$\Delta_1 = \frac{\sqrt{\pi}}{2\mathrm{i}} \left(\frac{2}{y}\right) \exp\left[\frac{y^2}{4x} - x\right] \left\{ \mathrm{erf}\left(-\frac{y}{2\sqrt{x}} + \mathrm{i}\sqrt{x}\right) - \mathrm{erf}\left(\frac{y}{2\sqrt{x}} + \mathrm{i}\sqrt{x}\right)\right\} \tag{15.45}$$

where in here $\mathrm{erf}(\xi)$ is the complex error function:

$$\mathrm{erf}(\xi) = \exp\left[-\xi^2\right] \left(1 + \frac{2\mathrm{i}}{\sqrt{\pi}} \int_0^{\xi} \exp\left[t^2\right] \mathrm{d}t\right) \quad , \tag{15.46}$$

and x and y are defined in (15.40).

It is useful to recall that (15.42) applies to different sublattices in one and the same layer.

The $D^{ss',(1)}$ term: $\left|\mathbf{K}_{m,\parallel}\right| = 0$

For the special case of $\left|\mathbf{K}_{m,\parallel}\right| = 0$, $\mathbf{c}_{ss'} \neq 0$, $D_L^{ss',(1)}(\mathbf{k}_\parallel, z)$ reduces for (a) $m \neq 0$ or (b) $m = 0$ **and** odd ℓ to

$$D_L^{ss',(1)}(\mathbf{k}_\parallel, z) = 0 \quad , \tag{15.47}$$

while for $m = 0$ and even ℓ one gets:

$$D_L^{ss',(1)}(\mathbf{k}_\parallel, z) = \sum_n \frac{1}{n!} (K_{m,\perp}/\sqrt{z})^{2n-1} \binom{n}{2n-\ell} \times \Delta_n^{ss'}(K_{m,\perp}) \left(-\sqrt{z} c_{ss',\perp}\right)^{2n-\ell} \quad . \tag{15.48}$$

The $D^{ss',(2)}$ term

For $\mathbf{c}_{ss'} \neq 0$, the second $k_\parallel$ - dependent term in (15.36) is given [3] by

$$D_L^{ss',(2)}(\mathbf{k}_\parallel, z) = -\sqrt{\frac{z}{4\pi}} \sum_{\mathbf{j} \in I(\mathcal{L})} \left\{ \exp\left[-\mathrm{i}\left(\mathbf{k}_\parallel \cdot \mathbf{t}_{j,\parallel}\right)\right] \times \left(-\sqrt{z}\left|\mathbf{t}_{j,\parallel} + \mathbf{c}_{ss'}\right|^{\ell}\right) Y_L(\widehat{\mathbf{t}_{j,\parallel} + \mathbf{c}_{ss'}}) \Lambda_\ell(z) \right\} \quad , \tag{15.49}$$

where

$$\Lambda_\ell(\epsilon) = \int_0^{\eta} u^{-\frac{3}{2}-\ell} \exp\left[u - u^{-1}\left(\sqrt{z}\left|\mathbf{t}_{j,\parallel} + \mathbf{c}_{ss'}\right|/2\right)^2\right] \mathrm{d}u \quad , \tag{15.50}$$

$$\eta = z\omega/2 \quad , \tag{15.51}$$

and ω is again an arbitrary complex number such that $Re(\omega) > 0$ and $|\omega| < \infty$. It is worthwhile to mention that the quantity η in (15.51) usually is also called "Ewald parameter".

Note that (15.47), (15.48) and (15.49) apply to different sublattices in different layers as well as to different sublattices in one and the same layer.

15.2.6 The layer- and sublattice diagonal case ($s = s'$)

The $D^{ss,(1)}$ term: $\mathbf{c}_{ss'} = 0$

For $\mathbf{c}_{ss'} = 0$, the $D^{ss,(1)}$ term is very similar to the one in (15.42), namely

$$D_L^{ss,(1)}(\mathbf{k}_\parallel, z) = -\frac{1}{A\sqrt{z}} F_{\ell m} \sum_{m \,\in\, I(\mathcal{L}^{-1})} \Bigg\{ \exp\left[-\mathrm{i} m \Phi(\mathbf{K}_{m,\parallel})\right] \times \sum_{n=0}^{(\ell-|m|)/2} \Bigg\{ \left(\frac{1}{n!}\right) \frac{(K_{m,\perp}/\sqrt{z})^{2n-1} \left(\left|\mathbf{K}_{m,\parallel}\right|/\sqrt{z}\right)^{\ell-2n}}{[(\ell-|m|-2n)/2]!\,[(\ell+|m|-2n)/2]!} \times \Gamma(\frac{1}{2} - n, x) \Bigg\} \Bigg\} \quad , \tag{15.52}$$

i.e., only the term $\exp[\mathrm{i}(\mathbf{K}_{m,\parallel} \cdot \mathbf{c}_{ss',\parallel})]$ in (15.42) is missing.

The $D^{ss,(2)}$ term: $\mathbf{c}_{ss'} = 0$

The second term is very much related to (15.49), since for odd $\ell - |m|$

$$D_L^{ss,(2)}(\mathbf{k}_\parallel, z) = 0 \quad , \tag{15.53}$$

while for even $\ell - |m|$:

$$D_L^{ss,(2)}(\mathbf{k}_\parallel, z) = -\overline{F}_{\ell m} \sqrt{\frac{z}{4\pi}} \sum_{\mathbf{j} \,\in\, I(\mathcal{L}) \,;\, j \neq 0} \Bigg\{ \exp\left[-\mathrm{i}\left(\mathbf{k}_\parallel \cdot \mathbf{t}_{j,\parallel} + m\Phi(\mathbf{K}_{m,\parallel})\right)\right] \times \left(-\sqrt{z}\left|\mathbf{t}_{j,\parallel}\right|^{\ell}\right) Y_L(\hat{\mathbf{t}}_{j,\parallel}) \Lambda_\ell(z) \Bigg\} \quad , \tag{15.54}$$

where now

$$\Lambda_\ell(z) = \int_0^\eta u^{-\frac{3}{2}-\ell} \exp\left[u - u^{-1}\left(\sqrt{z}\left|\mathbf{t}_{j,\parallel}\right|/2\right)^2\right] \mathrm{d}u \quad , \tag{15.55}$$

with η being defined in (15.51), and the following abbreviation was used

$$\overline{F}_{\ell m} = \frac{(-1)^\ell (-1)^{(\ell-|m|)/2}}{2^{2\ell}\,((\ell-|m|)/2)!\,((\ell+|m|)/2)!} \sqrt{(2\ell+1)\,(\ell+|m|)!(\ell-|m|)!} \quad . \tag{15.56}$$

The excluded contribution $\mathbf{t}_{j,\parallel} = 0$ in (15.54) is then taken care off by the last term, $D_{00}^{ss,(3)}(\epsilon)$, which is explicitly $\mathbf{k}_\parallel-$independent, and is quite familiar also from the structure constants for a simple three-dimensional lattice, see the following section,

$$D_{00}^{ss,(3)}(z) = -\frac{\sqrt{z}}{4\pi}\sum_{n=0}^{\infty}\frac{\eta^{n-\frac{1}{2}}}{n!(n-\frac{1}{2})}$$
$$= -\frac{\sqrt{z}}{2\pi}\left(2\int_0^{\sqrt{\eta}}\exp\left[t^2\right]\mathrm{d}t - \frac{\exp\left[\eta\right]}{\sqrt{\eta}}\right) \quad . \tag{15.57}$$

It should be recalled that $\mathbf{c}_{ss'} = 0$ implies that $\mathbf{c}_{ss',\parallel} = 0$ **and** $c_{ss',\perp} = 0$, i.e., (15.52)–(15.54) and (15.57) apply only to the sublattice-diagonal case in one and the same layer.

15.2.7 Simple two-dimensional lattices

For multilayer systems corresponding to a simple two-dimensional lattice such that

$$\mathcal{L}(R_{i,z}) = \mathcal{L} \quad , \quad \forall R_{i,z} \quad , \tag{15.58}$$

the **layer-off-diagonal** elements of the structure constants can be evaluated according to Kambe [1] [2] directly in momentum space, since

$$c_{ss',\perp} = R_{i,z} - R_{j,z} \neq 0 \quad , \forall i \neq j \quad , \tag{15.59}$$

namely by

$$A_{LL'}^{ss'}(\mathbf{k}_\parallel,\epsilon) = \frac{(4\pi)^2}{A}\mathrm{i}^{(\ell-\ell')}\sum_{m\ \in\ I(\mathcal{L}^{-1})}\left\{\frac{1}{2\mathrm{i}K_{m,\perp}}\exp\left[\mathrm{i}\mathfrak{K}_m\cdot\mathbf{c}_{ss'}\right]\right.$$
$$\left.\times\, Y_{\ell-m}(\widehat{\mathfrak{K}}_m^{\pm})^* Y_{\ell m}(\widehat{\mathfrak{K}}_m^{\pm})\right\} \tag{15.60}$$

where

$$\mathfrak{K}_m^{\pm} = \mathbf{K}_{m,\parallel} \ \pm\ (c_{ss',\perp}K_{m,\perp})\hat{\mathbf{z}} \quad . \tag{15.61}$$

In here the plus (minus) sign applies for $c_{s,\perp} > c_{s',\perp}$ ($c_{s,\perp} < c_{s',\perp}$). Equations (15.52)–(15.54) and (15.57) refer then to the special **layer-diagonal case**!

Table 15.1. Simple two-dimensional lattices: matrix structure

	$R_{i,z}$	$R_{j,z}$
$R_{i,z}$	A	B
$R_{j,z}$	B'	A

Table 15.2. Simple two-dimensional lattices: equation numbers corresponding to the matrix elements

	A	B, B'
D^1	(15.52)	
D^2	(15.53, 15.54)	
D^3	(15.57)	
direct		(15.60)

Table 15.3. Complex two-dimensional lattices: matrix structure

		$R_{i,z}$			$R_{j,z}$	
		$\mathbf{c}_{ss,\parallel}$	$\mathbf{c}_{ss',\parallel}$		$\mathbf{c}_{ss,\parallel}$	$\mathbf{c}_{ss',\parallel}$
$R_{i,z}$	$\mathbf{c}_{ss,\parallel}$	A	B	$\mathbf{c}_{ss,\parallel}$	B	B
	$\mathbf{c}_{ss',\parallel}$	B'	A	$\mathbf{c}_{ss',\parallel}$	B	B
		$\mathbf{c}_{ss,\parallel}$	$\mathbf{c}_{ss',\parallel}$		$\mathbf{c}_{ss,\parallel}$	$\mathbf{c}_{ss',\parallel}$
$R_{j,z}$	$\mathbf{c}_{ss,\parallel}$	B'	B'	$\mathbf{c}_{ss,\parallel}$	A	B
	$\mathbf{c}_{ss',\parallel}$	B'	B'	$\mathbf{c}_{ss',\parallel}$	B'	A

Table 15.4. Complex two-dimensional lattices: equation numbers corresponding to the matrix elements

	A	B, B'
D^1	(15.52)	(15.37)
D^2	(15.53, 15.54)	(15.49)
D^3	(15.57)	–

15.2.8 Note on the "Kambe structure constants"

It is important to note that for the "Kambe structure constants" not necessarily a "parent" three-dimensional lattice [10] has to be assumed, i.e., the distances between layers can vary in an appropriate manner such as for example in a multilayer system showing **surface (interface) relaxation**.

From the above tables one can see that the structure constants can be viewed as supermatrices with rows and columns labelled by atomic layers. In the case of a simple two-dimensional lattice each matrix element is a matrix in L and L',

$$\mathbf{A}(\mathbf{k}_\parallel,\epsilon)=\left\{\underline{A}^{ss'}(\mathbf{k}_\parallel,\epsilon)\right\}\quad,\quad \underline{A}^{ss'}(\mathbf{k}_\parallel,\epsilon)=\left\{A^{ss'}_{LL'}(\mathbf{k}_\parallel,\epsilon)\right\}\quad. \tag{15.62}$$

In the case of a complex two-dimensional lattice each such element is itself a supermatrix labelled by sublattices, the elements thereof being matrices in L and L'.

Furthermore, it should be noted that because of, e.g., (15.60)–(15.61) in general

$$\underline{A}^{ss'}(\mathbf{k}_\parallel,\epsilon)\neq\underline{A}^{s's}(\mathbf{k}_\parallel,\epsilon)\quad, \tag{15.63}$$

which was indicated by using B' in the above tables.

Although the analytical form of the structure constants for two-dimensional invariant systems appears rather complicated, for their numerical evaluation again only a few procedures are needed: besides the by now familiar procedures for complex spherical harmonics and Gaunt numbers, in particular only routines for evaluating (1) complex error and incomplete $\Gamma-$functions, (2) factorials, and (3) simple integrals of one variable of the type as specified in (15.55) are required. For the evaluation of complex error and incomplete $\Gamma-$functions, e.g., respective numerical recipes from Abramowitz and Stegun [11] can readily be picked up.

15.3 Three-dimensional translational invariance

15.3.1 Three-dimensional structure constants for simple lattices

Let $\mathcal{L}=\mathcal{L}^{(3)}=\{\mathbf{R}_i\}$ be the set of real space lattice vectors, $\mathcal{L}^{-1}=\mathcal{L}^{(3d)}=\{\mathbf{K}_n\}$ the respective set of reciprocal lattice vectors, and $\mathcal{T}=\left\{[E\mid\mathbf{R}_i];[E\mid\mathbf{R}_i]^{|T|}=[E\mid\mathbf{0}]\right\}$ the corresponding translational group. It was originally Kohn and Rostoker [4], who suggested to write the $\mathbf{k}$-th projection of the free space Green's function $G_0(\mathbf{r},\mathbf{r}',z)$, where $\mathbf{k}$ is a vector of the first Brillouin zone, either in terms of reciprocal lattice vectors,

$$G_0(\mathbf{r},\mathbf{r}',\mathbf{k},z)=-\Omega^{-1}\sum_{K_n\in\mathcal{L}^{-1}}\frac{\exp\left[\mathrm{i}\left(\mathbf{K}_n+\mathbf{k}\right)\cdot\left(\mathbf{r}-\mathbf{r}'\right)\right]}{\left(\mathbf{K}_n+\mathbf{k}\right)^2-z}\quad, \tag{15.64}$$

where Ω is the volume of the unit cell, or in terms of real space vectors,

$$G_0^+(\mathbf{r},\mathbf{r}',\mathbf{k},z)=-(4\pi)^{-1}\sum_{\mathbf{R}_i\in\mathcal{L}}\frac{\exp\left(\mathrm{i}p\left|\mathbf{r}-\mathbf{r}'-\mathbf{R}_i\right|\right)}{\left|\mathbf{r}-\mathbf{r}'-\mathbf{R}_i\right|}\exp\left(\mathrm{i}\mathbf{k}\cdot\mathbf{R}_i\right)\quad, \tag{15.65}$$

$$z=\epsilon+\mathrm{i}\delta\quad,\quad p=\sqrt{z}\quad,\quad \mathrm{Im}z>0\quad. \tag{15.66}$$

Since (15.64) is a very slowly converging series it was suggested by Ham and Segall [8] that Ewald's method could be applied in (15.65). Abbreviating $\mathbf{r}-\mathbf{r}'$ by $\mathbf{R}$, the $\mathbf{R}$-dependent factors in (15.65) can be written as the following contour integral:

$$\frac{\exp\left(\mathrm{i}p\left|\mathbf{R}-\mathbf{R}_i\right|\right)}{\left|\mathbf{R}-\mathbf{R}_i\right|}=2\pi^{-1/2}\int_0^\infty \exp\left[-\left(\mathbf{R}-\mathbf{R}_i\right)^2\xi^2+p^2/4\xi^2\right]\mathrm{d}\xi \quad . \tag{15.67}$$

This integral can be broken up into two parts corresponding to the intervals $\left[0,\frac{1}{2}\sqrt{\eta}\right]$ and $\left[\frac{1}{2}\sqrt{\eta},+\infty\right]$, respectively, with $\eta>0$, such that $G_0\left(\mathbf{R},\mathbf{k},z\right)$ is given by

$$G_0\left(\mathbf{R},\mathbf{k},z\right)=G_1\left(\mathbf{R},\mathbf{k},z\right)+G_2\left(\mathbf{R},\mathbf{k},z\right) \quad , \tag{15.68}$$

with η being usually being referred to as *Ewald parameter*. Using the identity

$$\begin{aligned}&\sum_{\mathbf{R}_i\in L}\exp\left[-\left(\mathbf{R}-\mathbf{R}_i\right)^2\xi^2+\mathrm{i}\mathbf{k}\cdot\left(\mathbf{R}_i-\mathbf{R}\right)\right]\\&=\left[\pi^{3/2}/\left(\Omega\xi^3\right)\right]\sum_{K_n\in\mathcal{L}^{-1}}\exp\left[-\left(\mathbf{K}_n+\mathbf{k}\right)^2/4\xi^2+\mathrm{i}\mathbf{K}_n\cdot\mathbf{R}\right] \quad ,\end{aligned} \tag{15.69}$$

which is valid for each point along the contour in the interval $\left[0,\frac{1}{2}\sqrt{\eta}\right]$, one gets

$$G_1\left(\mathbf{R},\mathbf{k},z\right)=-\frac{1}{\Omega}\sum_{K_n\in\mathcal{L}^{-1}}\frac{\exp\left[\mathrm{i}\left(\mathbf{K}_n+\mathbf{k}\right)\cdot\mathbf{R}\right]\exp\left\{\left[-\left(\mathbf{K}_n+\mathbf{k}\right)^2+z\right]/\eta\right\}}{\left(\mathbf{K}_n^2+\mathbf{k}^2\right)-z} \tag{15.70}$$

$$G_2\left(\mathbf{R},\mathbf{k},z\right)=-\frac{\pi^{-3/2}}{2}\int_{1/2\sqrt{\eta}}^\infty\sum_{\mathbf{R}_i\in\mathcal{L}}\exp\left[\mathrm{i}\mathbf{k}\cdot\mathbf{R}_i-\left(\mathbf{R}_i-\mathbf{R}\right)^2\xi^2+z/4\xi^2\right]\mathrm{d}\xi \tag{15.71}$$

The series in (15.69) is (now) absolute convergent for any finite $\eta>0$. $G_0\left(\mathbf{R},z\right)$ is an analytical function of z in the whole complex plane with the exception of the simple poles in $G_0\left(\mathbf{R},\epsilon\right)$ for $\epsilon=\left(\mathbf{K}_n+\mathbf{k}\right)^2$. By analytic continuation, however, the sum of the series represents $G_0\left(\mathbf{R},z\right)$ for all energies z.

As suggested by Kohn and Rostoker in their original paper [4], $G_0\left(\mathbf{R},\epsilon\right)$ can be expanded into spherical harmonics

$$\begin{aligned}G_0\left(\mathbf{R},\mathbf{k},z\right)=G_0\left(\mathbf{r},\mathbf{r}',\mathbf{k},z\right)=\sum_{L,L'}\Big[&\mathrm{i}^{\ell-\ell'}B_{LL'}\left(\mathbf{k},z\right)j_\ell\left(pr\right)j_{\ell'}\left(pr'\right)\\&+\;p\boldsymbol{\delta}_{LL'}j_\ell\left(pr\right)n_{\ell'}\left(pr'\right)\Big]Y_L(\hat{\mathbf{r}})Y_{L'}^*(\hat{\mathbf{r}}') \quad ,\end{aligned} \tag{15.72}$$

with $r<r'<r_{\mathrm{MT}}$ (muffin-tin radius). Note that in their formulation the authors used spherical Neumann functions as irregular functions. Written in matrix notation the above equation reads

$$G_0^+\left(\mathbf{r},\mathbf{r}',\mathbf{k},z\right)=\mathsf{j}\left(z;\mathbf{r}\right)\underline{B}(\mathbf{k},z)\mathsf{j}\left(z;\mathbf{r}\right)^\times+p\;\mathsf{j}\left(z;\mathbf{r}_<\right)\mathsf{n}\left(z;\mathbf{r}_>\right)^\times \tag{15.73}$$

$$\underline{B}(\mathbf{k},z)=\left\{\mathrm{i}^{\ell-\ell'}B_{LL'}\left(\mathbf{k},z\right)\right\} \quad . \tag{15.74}$$

According to Ham and Segall [8] – as discussed above – the structure constants $B_{LL'}(\mathbf{k}, z)$ can be written as

$$B_{LL'}(\mathbf{k}, z) = 4\pi \mathrm{i}^{\ell - \ell'} \sum_{L''} \mathrm{i}^{-\ell''} C_{LL'}^{L''} D_{L''}(\mathbf{k}, z) \quad , \tag{15.75}$$

where

$$D_L(\mathbf{k}, z) = D_L^{(1)}(\mathbf{k}, z) + D_L^{(2)}(\mathbf{k}, z) + D_{00}^{(3)}(z)\, \delta_{\ell 0} \delta_{m0} \quad . \tag{15.76}$$

Since $\mathbf{R}$ may be chosen arbitrarily in evaluating the $D_L(\mathbf{k}, z)$, one can also take the limit of $|\mathbf{R}| \to 0$ and obtain

$$D_L^{(1)}(\mathbf{k}, z) = -(4\pi/\Omega)\, \mathrm{i}^{\ell} p^{-\ell} \exp(z/\eta) \times \sum_{K_n \in \mathcal{L}^{-1}} \frac{|\mathbf{K}_n + \mathbf{k}|^{\ell} \exp\left[-(\mathbf{K}_n + \mathbf{k})^2/\eta\right]}{(\mathbf{K}_n + \mathbf{k})^2 - z} Y_L^*(\widehat{\mathbf{K} + \mathbf{k}}) \quad , \tag{15.77}$$

$$D_L^{(2)}(\mathbf{k}, z) = \left[(-2)^{\ell+1}/\sqrt{\pi}\right] p^{-\ell} \sum_{\substack{\mathbf{R}_i \in \mathcal{L} \\ (\mathbf{R}_i \neq 0)}} |\mathbf{R}_i|^{\ell} \exp(\mathrm{i}\mathbf{k} \cdot \mathbf{R}_i)\, Y_L^*(\hat{\mathbf{R}}_i) \times \int_{1/2\sqrt{\eta}}^{\infty} \xi^{2\ell} \exp\left[-\xi^2 \left|\hat{\mathbf{R}}_i\right|^2 + z/4\xi^2\right] \mathrm{d}\xi \quad , \tag{15.78}$$

$$D_{00}^{(3)}(z) = -\frac{\sqrt{\eta}}{2\pi} \sum_{n=0}^{\infty} \frac{(z/\eta)^n}{(2n-1)\, n!} \quad . \tag{15.79}$$

15.3.2 Three-dimensional structure constants for complex lattices

Suppose there are m atoms per unit cell with corresponding non-primitive translations $\mathbf{a}_1, \mathbf{a}_2, ..., \mathbf{a}_m$. The explicit form of the Green function $G_0(\mathbf{r}, \mathbf{r}', z)$ is easily obtained when it is recalled that $\mathbf{r}$ and $\mathbf{r}'$ can be measured either from one and the same origin $\mathbf{a}_i$ or from two different origins $\mathbf{a}_i$ and $\mathbf{a}_j$. $G_0(\mathbf{r}, \mathbf{r}', \epsilon)$ can therefore be viewed as a matrix with respect to the different sublattices involved, i.e. as a matrix in which rows and columns refer to sublattices,

$$\underline{G}_0(\mathbf{r}, \mathbf{r}', \epsilon) = \begin{pmatrix} G_0(\mathbf{r}_i, \mathbf{r}'_i, \epsilon) & G_0(\mathbf{r}_i, \mathbf{r}'_j, \epsilon) \\ G_0(\mathbf{r}_j, \mathbf{r}'_i, \epsilon) & G_0(\mathbf{r}_j, \mathbf{r}'_j, \epsilon) \end{pmatrix} \quad , \tag{15.80}$$

for $i, j = 1, ..., m$. Note that contrary to the notation used in (15.80) the subscripts i and j refer to the origins of the sublattices and not to sites in a real space description. The advantage of (15.80) is obvious once angular momentum representations are formed, since a particular element (in momentum representation) is given by [7] as

$$G_0\left(\mathbf{r}_i,\mathbf{r}'_j,z\right) = -\Omega^{-1}\sum_{K_n\in\mathcal{L}^{-1}}\frac{\exp\left[\mathrm{i}\left(\mathbf{K}_n+\mathbf{k}\right)\cdot\left(\mathbf{a}_i-\mathbf{a}_j\right)\right]\exp\left[\mathrm{i}\left(\mathbf{K}_n+\mathbf{k}\right)\cdot\left(\mathbf{r}_i-\mathbf{r}'_i\right)\right]}{\left(\mathbf{K}_n+\mathbf{k}\right)^2-z} \quad , \tag{15.81}$$

where for $i=j: r_i < r_{\mathrm{MT}}^i$ and $i\neq j: \left(r_i+r'_j\right) < |\mathbf{a}_i-\mathbf{a}_j|$ each such element can be transformed into a partial wave representation

$$G_0\left(\mathbf{r}_i,\mathbf{r}'_j,\mathbf{k},z\right) = \mathsf{j}\left(z;\mathbf{r}_i\right)\underline{B}^{ij}\left(\mathbf{k},z\right)\mathsf{j}\left(z;\mathbf{r}'_j\right)^{\times} + \delta_{ij}p\;\mathsf{j}\left(z;\mathbf{r}_{i,<}\right)\mathsf{n}\left(z;\mathbf{r}_{j,>}\right)^{\times} \quad , \tag{15.82}$$

$$\underline{B}^{ij}\left(\mathbf{k},z\right) = \left\{B^{ij}_{LL'}(\mathbf{k},z)\right\} \quad . \tag{15.83}$$

The structure constants $B^{ij}_{LL'}(\mathbf{k},z)$ can again be expressed in coefficients $D^{ij}_L\left(\mathbf{k},z\right)$ in the following way:

$$B^{ij}_{LL'}\left(\mathbf{k},z\right) = 4\pi\mathrm{i}^{\ell-\ell'}\sum_{L''}\mathrm{i}^{-\ell''}C^{L''}_{LL'}D^{ij}_{L''}\left(\mathbf{k},z\right) \quad , \tag{15.84}$$

$$D^{ij}_L\left(\mathbf{k},z\right) = D^{ij,(1)}_L\left(\mathbf{k},z\right) + D^{ij,(2)}_L\left(\mathbf{k},z\right) + \delta_{ij}\delta_{\ell 0}\delta_{m0}D^{(3)}_{00}\left(z\right) \quad , \tag{15.85}$$

with

$$D^{ij,(1)}_L\left(\mathbf{k},z\right) = \left(4\pi/\Omega\right)\mathrm{i}^{\ell}p^{-\ell}\exp\left(z/\eta\right) \times\sum_{K_n\in\mathcal{L}^{-1}}\left\{\frac{\left|\mathbf{K}_n+\mathbf{k}\right|^{\ell}\exp\left[-\left(\mathbf{K}_n+\mathbf{k}\right)^2/\eta\right]}{\left|\mathbf{K}_n+\mathbf{k}\right|^2-z} \times\exp\left[\mathrm{i}\left(\mathbf{K}_n+\mathbf{k}\right)\cdot\left(\mathbf{a}_i-\mathbf{a}_j\right)\right]Y^*_L(\widehat{\mathbf{K}_n+\mathbf{k}})\right\} \quad , \tag{15.86}$$

$$D^{ij,(2)}_L\left(\mathbf{k},z\right) = \frac{(-2)^{\ell+1}}{\sqrt{\pi}}p^{-\ell}\sum_{\substack{\mathbf{R}_s\in\mathcal{L}\\(\mathbf{R}_s\neq 0)}}\left\{\left|\mathbf{R}_s-\mathbf{a}_i+\mathbf{a}_j\right|^{\ell} \times\exp\left[\mathrm{i}\left(\mathbf{k}\cdot\mathbf{R}_s\right)\right]Y_L(\widehat{\mathbf{R}_s-\mathbf{a}_i}+\mathbf{a}_j)^* \times\int_{\frac{1}{2}\sqrt{\eta}}^{\infty}\xi^{2\ell}\exp\left[-\xi^2\left(\mathbf{R}_s-\mathbf{a}_i+\mathbf{a}_j\right)^2+z/4\xi^2\right]\mathrm{d}\xi\right\} \quad . \tag{15.87}$$

and $D^{(3)}_{00}\left(z\right)$ being defined in (15.79). As one can see from (15.77)–(15.78) for $i=j$ these equations reduce to the case of a simple lattice. The diagonal blocks in the structure constants refer therefore to a "propagation" within a particular sublattice, whereas the off-diagonal blocks refer to a "propagation" between sublattices.

15.3.3 Note on the structure constants for three-dimensional lattices

A numerical evaluation of the structure constants in the case of three-dimensional lattices requires only very simple procedures, namely summations and an easy integral of one (complex) variable. It turns out that the choice of the so-called Ewald parameter, namely η, is – as it should – numerically of little importance.

15.4 Relativistic structure constants

The relativistic structure constants were first derived and discussed by Onodera and Okazaki [5] and by Takada [6]. They can be written in terms of their non-relativistic analogues, see (15.84), and Clebsch-Gordan coefficients, see also Chap. 3, equation (3.216),

$$B^{ij}_{QQ'}(\mathbf{k},\epsilon) = \sum_{s=\pm 1/2} c(\ell j 1/2; \mu - s, s)\, B^{ij}_{LL'}(\mathbf{k},\epsilon)\, c(\ell' j' 1/2; \mu' - s, s)\,, \tag{15.88}$$

$$\begin{aligned} Q &= (\kappa\mu) \quad , \quad Q' = (\kappa'\mu') \quad , \\ L &= (\ell, \mu - s)\,, \quad , \quad L' = (\ell', \mu' - s) \quad . \end{aligned} \tag{15.89}$$

Clearly enough the same kind of transformation with Clebsch-Gordan coefficients applies also to the Kambe structure constants.

15.5 Structure constants and Green's function matrix elements

In all the "classical" approaches, see (15.30), (15.73) and (15.82), partial wave representations of $\mathcal{G}_0(z)$ of the type

$$G_0\left(\mathbf{r}_i, \mathbf{r}'_j, \mathbf{k}, z\right) = \mathsf{j}(z;\mathbf{r}_i)\, \underline{B}^{ij}(\mathbf{k},z)\, \mathsf{j}\left(z;\mathbf{r}'_j\right)^{\times} + \delta_{ij} p\, \mathsf{j}(z;\mathbf{r}_{i,<})\, \mathsf{n}(z;\mathbf{r}_{j,>})^{\times} \quad , \tag{15.90}$$

were used with the matrix $\underline{B}^{ij}(\mathbf{k},z)$ traditionally being called structure constants. However, from the below representation

$$G_0\left(\mathbf{r}_i, \mathbf{r}'_j, \mathbf{k}, z\right) = \mathsf{j}(z;\mathbf{r}_i)\, \underline{G}^{ij}(\mathbf{k},z)\, \mathsf{j}\left(z;\mathbf{r}'_j\right)^{\times} - \mathrm{i}p\delta_{ij}\, (z;\mathbf{r}_{i,<})\, \mathsf{h}^{+}(z;\mathbf{r}_{j,>})^{\times} \quad , \tag{15.91}$$

namely the representation that directly enters the description of the scattering path operators, see the chapter on multiple scattering, follows immediately that

$$\underline{G}^{ij}\left(\mathbf{k},\epsilon\right) = \underline{B}^{ij}\left(\mathbf{k},\epsilon\right) + \mathrm{i}p\boldsymbol{\delta}_{ij} \quad . \tag{15.92}$$

References

1. K. Kambe, Z. Naturforschung **22a**, 322 (1967).
2. K. Kambe, Z. Naturforschung **22a**, 422 (1967).
3. K. Kambe, Z. Naturforschung **23a**, 1280 (1968).
4. W. Kohn and N. Rostoker, Phys. Rev. **94**, 1111 (1954).
5. Y. Onodera and M. Okazaki, J. Phys. Soc. Jap. **21**, 1273 (1966).
6. S. Takada, Progr. Theoret. Phys. (Kyoto) **36**, 224 (1966).
7. B. Segall, Phys. Rev. **105**, 108 (1957)
8. F.S. Ham and B. Segall, Phys. Rev. **124**, 1786 (1961).
9. P. Weinberger, *Electron Scattering Theory of Ordered and Disordered Matter* (Clarendon Press, Oxford 1992)
10. P. Weinberger, Phil. Mag. B **75**, 509–533 (1997).
11. M. Abramowitz and I. Stegun, *Handbook of Mathematical Functions* (Dover Publ., New York 1973)

16 Green's functions: an in-between summary

Since in the previous chapters a rather detailed description of particular properties or schemes was given, it is perhaps appropriate to summarize in a very short chapter achievements obtained up-to-now. Quite clearly all theoretical developments were devoted to arrive at practical schemes in order to numerically evaluate the single-particle Green's function $G(\epsilon; \mathbf{r}, \mathbf{r}')$,

$$\boxed{\begin{aligned} G(\epsilon; \mathbf{r}_n + \mathbf{R}_n, \mathbf{r}'_m + \mathbf{R}_m) = \; & \mathbf{Z}^n(\epsilon; \mathbf{r}_n)\tau(\epsilon)\mathbf{Z}(\epsilon; \mathbf{r}'_m) \\ & -\boldsymbol{\delta}_{nm}\mathbf{Z}^n(\epsilon; \mathbf{r}_{n,<})\mathbf{J}^n(\epsilon; \mathbf{r}_{n,>}) \end{aligned}}$$

in terms of the so-called scattering path operator $\tau(\epsilon)$,

$$\boxed{\tau(\epsilon) = \left[\mathbf{t}^{-1}(\epsilon) - \mathbf{G}(\epsilon)\right]^{-1}}$$

which essentially consists of two parts, namely single-site t-matrices and structure constants:

$$\boxed{\left.\begin{matrix} \mathbf{t}(\epsilon) \\ \mathbf{G}(\epsilon) \end{matrix}\right\} \rightarrow \tau(\epsilon) \rightarrow G(\epsilon; \mathbf{r}, \mathbf{r}')}$$

Tables (16.1)–(16.3) are meant to give an easy access to the various cases discussed or different levels of sophistication that can be used.

It should be noted that up to this point all formal descriptions refer to the *classical* formulation of scattering theory (*classical KKR-method*). The following chapter is now to introduce *screened scattering theory*, in particular

Table 16.1. Abbreviations

acronym	meaning
NR	non-relativistic
SR	semi-relativistic
R	relativistic
NS-	non-spinpolarized
S-	spin-polarized
SSP	spherical symmetric potential
FP	full potential

Table 16.2. Single site quantities:

$$\mathbf{t}(\epsilon), \mathbf{Z}^n(\epsilon; \mathbf{r}_n), \mathbf{J}^n(\epsilon; \mathbf{r}_n)$$

type	potential	Chapter
NR	NS-SSP	5
	NS-FP	6
	S-SSP, S-FP	7
R	NS-SSP	8
	S-SSP	10
	NS-FP	9
	S-FP	11
SR	NS-SSP	12
	NS-FP	13

Table 16.3. Structure constants:

$$\mathbf{G}(\epsilon)$$

type	dimensionality	Section
NR	2	15.2
	3	15.3
R	2,3	15.4

as applied for two-dimensional translationally invariant systems, i.e., systems with a surface and/or interfaces, which in turn places the KKR-approach in the category of *Order-N* methods for determining the electronic structure of matter. All further conceptual chapters will deal with either formal or practical aspects related to Density Functional Theory (total energies, self-consistency, etc.), or will introduce variations of scattering theory (embedded clusters) and additional concepts such as the Coherent Potential Approximation in order to deal with disordered systems.

17 The Screened KKR method for two-dimensional translationally invariant systems

17.1 "Screening transformations"

Suppose that the potential $\mathcal{V}$ in the (relativistic or non-relativistic) Kohn-Sham Hamiltonian $\mathcal{H} = \mathcal{H}_0 + \mathcal{V}$ is represented by a superposition of non-overlapping functions (individual potentials with or without shape corrections),

$$V(\mathbf{r}) = \sum_i V_i(\mathbf{r}_i) \quad . \tag{17.1}$$

The Green's function matrix $\mathbf{G}(\epsilon)$ corresponding to $\mathcal{G}(z) = (z - \mathcal{H})^{-1}$ is then related to the scattering path operator $\tau(\epsilon)$,

$$\tau(\epsilon) = \left(\mathbf{t}(\epsilon)^{-1} - \mathbf{G}_0(\epsilon)\right)^{-1} \quad , \tag{17.2}$$

$$\tau(\epsilon) = \left\{\underline{\tau}^{ij}(\epsilon)\right\} \quad , \quad \underline{\tau}^{ij}(\epsilon) = \left\{\tau^{ij}_{LL'}(\epsilon)\right\} \quad , \tag{17.3}$$

e.g., by the expression in (3.133)

$$\mathbf{G}(\epsilon) = \mathbf{G}_0(\epsilon)\left(\mathbf{I} - \mathbf{t}(\epsilon)\mathbf{G}_0(\epsilon)\right)^{-1} \quad , \tag{17.4}$$

where

$$\mathbf{G}(\epsilon) = \left\{\underline{G}^{ij}(\epsilon)\right\} \quad , \quad \underline{G}^{ij}(\epsilon) = \left\{G^{ij}_{LL'}(\epsilon)\right\} \quad , \tag{17.5}$$

and $\mathbf{I}$ denotes a unit matrix.

Returning now to the section on "scaling transformations" in Chap. 3, see (3.30)–(3.34), it shall be assumed that the perturbation $\mathcal{W}$ in (3.30) is also a superposition of individual (non-overlapping) potentials,

$$W(\mathbf{r}) = \sum_i W_i(\mathbf{r}_i) \quad , \tag{17.6}$$

with

$$W_i(\mathbf{r}_i) = \begin{cases} W_{\mathrm{r}} & |\mathbf{r}_i| \le b \\ 0 & ;\text{otherwise} \end{cases} \quad , \tag{17.7}$$

where W_{r} is a suitable constant, b denotes now a suitable radius such as e.g. the respective inscribed (muffin-tin-) sphere radius and the index r stands for *reference system*.

If the single-site t matrices corresponding to $W_{\rm r}$ are denoted by $\underline{t}^{\rm r}(\epsilon)$, the respective Green's function matrix, $\mathbf{G}^{\rm r}(\epsilon)$,

$$\mathbf{G}^{\rm r}(\epsilon) = \{\underline{G}^{{\rm r},ij}(\epsilon)\} \quad , \quad \underline{G}^{{\rm r},ij}(\epsilon) = \{G^{{\rm r},ij}_{LL'}(\epsilon)\} \quad , \tag{17.8}$$

see in particular (3.132)–(3.133), is given by

$$\mathbf{G}^{\rm r}(\epsilon) = \mathbf{G}^{0}(\epsilon)\left[\mathbf{I} - \mathbf{t}^{\rm r}(\epsilon)\mathbf{G}^{0}(\epsilon)\right]^{-1} \ . \tag{17.9}$$

By introducing the following difference,

$$\mathbf{t}_{\Delta}(\epsilon) = \mathbf{t}(\epsilon) - \mathbf{t}^{\rm r}(\epsilon) \quad , \tag{17.10}$$

where $\mathbf{t}(\epsilon)$ and $\mathbf{t}^{\rm r}(\epsilon)$ are of the form

$$\mathbf{t}(\epsilon) = \{\underline{t}^{i}(\epsilon)\delta_{ij}\} \quad , \quad \underline{t}^{i}(\epsilon) = \{t^{i}_{LL'}(\epsilon)\delta_{\ell\ell'}\delta_{mm'}\} \quad , \tag{17.11}$$

one obtains for $\mathbf{G}(\epsilon)$:

$$\mathbf{G}(\epsilon) = \mathbf{G}^{\rm r}(\epsilon)\left[\mathbf{I} - \mathbf{t}_{\Delta}(\epsilon)\mathbf{G}^{\rm r}(\epsilon)\right]^{-1} \ . \tag{17.12}$$

Defining finally the following scattering-path operator,

$$\tau_{\Delta}(\epsilon) = \left[\mathbf{t}_{\Delta}(\epsilon)^{-1} - \mathbf{G}^{\rm r}(\epsilon)\right]^{-1} \quad , \tag{17.13}$$

$\mathbf{G}(\epsilon)$ can also be expressed as

$$\begin{aligned} \mathbf{G}(\epsilon) &= \mathbf{G}^{\rm r}(\epsilon) + \mathbf{G}^{\rm r}(\epsilon)\tau_{\Delta}(\epsilon)\mathbf{G}^{\rm r}(\epsilon) \\ &= \mathbf{t}_{\Delta}(\epsilon)^{-1}\tau_{\Delta}(\epsilon)\mathbf{t}_{\Delta}(\epsilon)^{-1} - \mathbf{t}_{\Delta}(\epsilon)^{-1} \ . \end{aligned} \tag{17.14}$$

Therefore, once $\mathbf{t}^{\rm r}(\epsilon)$ and $\mathbf{G}^{\rm r}(\epsilon)$ are known, (17.12)–(17.14) represent an equivalent set of equations to (17.2)–(17.5). Combining (17.2) with (17.13) the below relation can easily be read off,

$$\tau(\epsilon) = \mathbf{t}(\epsilon)\left[\mathbf{t}_{\Delta}(\epsilon)^{-1}\tau_{\Delta}(\epsilon)\mathbf{t}_{\Delta}(\epsilon)^{-1} + \left(\mathbf{t}(\epsilon)^{-1} - \mathbf{t}_{\Delta}(\epsilon)^{-1}\right)\right]\mathbf{t}(\epsilon) \quad . \tag{17.15}$$

By choosing a suitable $W_{\rm r}$ (17.9) can be solved such that

$$\underline{G}^{{\rm r},ij}(\epsilon) \sim \underline{0} \qquad \text{for :} \qquad \forall \ |\mathbf{R}_i - \mathbf{R}_j| \geq \ d \quad , \tag{17.16}$$

where the distance d has to be viewed as the radius of a sphere that comprises only a few types of "neighboring" sites such as e.g. first- and second-nearest neighbors. The matrix $\underline{G}^{{\rm r},ij}(\epsilon)$ is usually called *screened structure constants*.

17.2 Two-dimensional translational symmetry

Suppose now that the potential in the (relativistic or non-relativistic) Kohn-Sham Hamiltonian $\mathcal{H} = \mathcal{H}_0 + \mathcal{V}$ for a *system with only two-dimensional translational symmetry* is a superposition of non-overlapping functions,

$$V(\mathbf{r}) = \sum_i V_i(\mathbf{r}_i + \mathbf{R}_{i,\parallel} + R_{i,z}\hat{\mathbf{z}}) = \sum_i V_i(R_{i,z}) \quad , \tag{17.17}$$

$$\mathbf{R}_i = (\mathbf{R}_{i,\parallel}, R_{i,z}\hat{\mathbf{z}}) \quad , \quad \mathbf{R}_{i,\parallel} \in \mathcal{L}^{(2)} \quad , \tag{17.18}$$

such that one and the same two-dimensional lattice $\mathcal{L}^{(2)}$ applies in all atomic layers under consideration and for matters of simplification $\mathcal{L}^{(2)}$ refers to a simple two-dimensional lattice. In order to simplify the notation, in the following position vectors shall be denoted by $\mathbf{R}_{pi}$,

$$\mathbf{R}_{pi} = \mathbf{C}_p + \mathbf{R}_{i,\parallel} \quad ; \quad \mathbf{R}_{i,\parallel} \in \mathcal{L}^{(2)} \quad , \quad \mathbf{C}_p = R_{i,z}\mathbf{z} \quad , \tag{17.19}$$

where $\mathbf{C}_p$ is sometimes referred to as the *spanning vector* of a particular layer p. According to (17.16) for the lattice Fourier transformed screened structure constants,

$$\underline{G}^{\mathrm{r},pq}(\mathbf{k}_\parallel;\epsilon) = \sum_{\mathbf{R}_\parallel \in \mathcal{L}^{(2)}} \exp\left[\mathrm{i}\mathbf{k}_\parallel \cdot \mathbf{R}_\parallel\right] \underline{G}^{\mathrm{r}}(\mathbf{C}_p + \mathbf{R}_\parallel, \mathbf{C}_q;\epsilon) \ ; \tag{17.20}$$

$$p, q = 1, \ldots, n \quad , \tag{17.21}$$

where $\mathbf{k}_\parallel$ belongs to the Surface Brillouin zone corresponding to $\mathcal{L}^{(2)}$, therefore the following assumption can be made:

$$\underline{G}^{\mathrm{r},pq}(\mathbf{k}_\parallel;\epsilon) = 0 \quad , \quad \text{if} \quad \mid p - q \mid > N \quad , \tag{17.22}$$

with N denoting a suitably chosen parameter. It should be noted that in (17.21) n refers to the number of considered atomic layers.

A non-vanishing block of dimension N of elements $\underline{G}^{\mathrm{r},pq}(\mathbf{k}_\parallel;\epsilon)$, $\mid p - q \mid \leq N$, can now be viewed as one particular element of a tridiagonal supermatrix with rows and columns labelled by P and Q (*principal layers*):

$$\mathbf{G}^{\mathrm{r}}(\mathbf{k}_\parallel;\epsilon) = \{\underline{G}^{\mathrm{r},pq}(\mathbf{k}_\parallel;\epsilon)\} \equiv \{\underline{\mathbf{G}}^{\mathrm{r},PQ}(\mathbf{k}_\parallel;\epsilon)\} \quad , \tag{17.23}$$

i.e., $\mathbf{G}^{\mathrm{r}}(\mathbf{k}_\parallel;\epsilon)$ is of the form

$$\mathbf{G}^{\mathrm{r}}(\mathbf{k}_\parallel;\epsilon) = \begin{pmatrix} \underline{\mathbf{G}}^{P,P} & \underline{\mathbf{G}}^{P,P+1} & 0 & 0 \\ \underline{\mathbf{G}}^{P+1,P} & \underline{\mathbf{G}}^{P+1,P+1} & \underline{\mathbf{G}}^{P+1,P+2} & 0 \\ 0 & \underline{\mathbf{G}}^{P+2,P+1} & \underline{\mathbf{G}}^{P+2,P+2} & \underline{\mathbf{G}}^{P+2,P+3} \end{pmatrix} \quad . \tag{17.24}$$

For example for $|q - p| \leq 2$ the matrices $\underline{\mathbf{G}}^{P,Q}$ comprise the following elements $\underline{G}^{\mathrm{r},pq}(\mathbf{k}_\parallel;\epsilon)$:

$$\underline{\mathbf{G}}^{P,P} = \begin{pmatrix} G^{p,p} & G^{p,p+1} \\ G^{p+1,p} & G^{p+1,p+1} \end{pmatrix}, \quad \underline{\mathbf{G}}^{P,P+1} = \begin{pmatrix} G^{p,p+2} & 0 \\ G^{p+1,p+2} & G^{p+1,p+3} \end{pmatrix} \quad ,$$

$$\underline{\mathbf{G}}^{P+1,P} = \begin{pmatrix} G^{p+2,p} & G^{p+2,p+1} \\ 0 & G^{p+3,p+1} \end{pmatrix}, \quad \underline{\mathbf{G}}^{P+1,P+1} = \begin{pmatrix} G^{p+2,p+2} & G^{p+2,p+3} \\ G^{p+3,p+2} & G^{p+3,p+3} \end{pmatrix} \quad ,$$

$$\underline{\mathbf{G}}^{P,P+2} = \underline{\mathbf{G}}^{P+2,P} = \begin{pmatrix} 0 & 0 \\ 0 & 0 \end{pmatrix} \quad .$$

It should be noted that formally in (17.23) only the indexing of the matrix is changed by collapsing a regime of indices into one index such that $\mathbf{G}^{\mathrm{r}}(\mathbf{k}_{\parallel};\epsilon)$ can be viewed as a tridiagonal matrix!

Furthermore, if a parent three-dimensional lattice can be assumed, i.e., if all interlayer distances are equal (no layer relaxation), then obviously the elements of this tridiagonal matrix are of the following form:

$$\underline{\mathbf{G}}^{\mathrm{r},PQ}(\mathbf{k}_{\parallel};\epsilon) = \begin{cases} \underline{\mathbf{G}}^{\mathrm{r},00}(\mathbf{k}_{\parallel};\epsilon) \; ; \; P = Q \\ \underline{\mathbf{G}}^{\mathrm{r},01}(\mathbf{k}_{\parallel};\epsilon) \; ; \; P = Q-1 \\ \underline{\mathbf{G}}^{\mathrm{r},10}(\mathbf{k}_{\parallel};\epsilon) \; ; \; P = Q+1 \\ 0 \qquad\qquad\quad ; \text{otherwise} \end{cases} \quad , \tag{17.25}$$

where the index zero refers to an arbitrarily *principle layer*. Of course in the case of layer relaxations in principle all $\underline{G}^{\mathrm{r},PQ}(\mathbf{k}_{\parallel};\epsilon)$ are different, although $\mathbf{G}^{\mathrm{r}}(\mathbf{k}_{\parallel};\epsilon)$ is still formally tridiagonal. In using the so-called Kambe structure constants discussed earlier (Chap. 15), screened structure constants for layered systems with or without layer relaxation can be obtained. As easily can be checked within atomic layers these structure constants are exact, the screening procedure is confined to the number of neighboring atomic planes considered: the parameter d in (17.16) obviously refers to a typical interlayer distance beyond which the $\underline{G}^{\mathrm{r},pq}(\mathbf{k}_{\parallel};\epsilon)$ vanish.

The $\mathbf{k}_{\parallel}$-th projection of $\tau_{\Delta}(\epsilon)$, see (17.13), is then given by

$$\tau_{\Delta}(\mathbf{k}_{\parallel};\epsilon) = \left[\mathbf{t}_{\Delta}(\epsilon)^{-1} - \mathbf{G}^{\mathrm{r}}(\mathbf{k}_{\parallel};\epsilon)\right]^{-1} \quad , \tag{17.26}$$

where

$$\mathbf{t}_{\Delta}(\epsilon) = \{\underline{t}^{P}_{\Delta}(\epsilon)\,\delta_{PQ}\} \quad , \quad \underline{t}^{P}_{\Delta}(\epsilon) = \{t^{p}_{\Delta}(\epsilon)\,\delta_{pq}\} \quad , \tag{17.27}$$

$$\tau_{\Delta}(\mathbf{k}_{\parallel};\epsilon) = \{\underline{\tau}^{PQ}_{\Delta}(\mathbf{k}_{\parallel};\epsilon)\} \quad , \quad \underline{\tau}^{PQ}_{\Delta}(\epsilon) = \{\tau^{pq}_{\Delta}(\epsilon)\} \quad . \tag{17.28}$$

Quite clearly, since $\mathbf{t}_{\Delta}(\epsilon)$ formally is a diagonal supermatrix, the inverse of $\tau_{\Delta}(\mathbf{k}_{\parallel};\epsilon)$ is also of tridiagonal form.

17.3 Partitioning of configuration space

Usually for a system with a surface or with interfaces three regions of different physical properties can be distinguished, namely a *left semi–infinite system*

(L), a *right semi–infinite system* (R) and an *intermediate region* (I). These regions correspond to the following numbering scheme for principal layers:

$$\begin{array}{ll} \mathrm{L}: & -\infty < P \leq 0 \\ \mathrm{I}: & 1 \leq P \leq \mathrm{n} \\ \mathrm{R}: & \mathrm{n}+1 \leq P < \infty \end{array} \quad , \tag{17.29}$$

which in turn implies, that formally $\left[\tau_{\Delta}(\mathbf{k}_{\parallel};\epsilon)\right]^{-1}$ in (17.26) can be partitioned as follows,

$$\left[\tau_{\Delta}(\mathbf{k}_{\parallel};\epsilon)\right]^{-1} = \begin{pmatrix} \left[\tau_{\Delta}(\mathbf{k}_{\parallel};\epsilon)\right]^{-1}_{\mathrm{L,L}} & \left[\tau_{\Delta}(\mathbf{k}_{\parallel};\epsilon)\right]^{-1}_{\mathrm{L,I}} & \mathbf{0} \\ \left[\tau_{\Delta}(\mathbf{k}_{\parallel};\epsilon)\right]^{-1}_{\mathrm{I,L}} & \left[\tau_{\Delta}(\mathbf{k}_{\parallel};\epsilon)\right]^{-1}_{\mathrm{I,I}} & \left[\tau_{\Delta}(\mathbf{k}_{\parallel};\epsilon)\right]^{-1}_{\mathrm{I,R}} \\ \mathbf{0} & \left[\tau_{\Delta}(\mathbf{k}_{\parallel};\epsilon)\right]^{-1}_{\mathrm{R,I}} & \left[\tau_{\Delta}(\mathbf{k}_{\parallel};\epsilon)\right]^{-1}_{\mathrm{R,R}} \end{pmatrix} \quad . \tag{17.30}$$

In order to evaluate $\tau(\mathbf{k}_{\parallel};\epsilon)_{\mathrm{I,I}}$ use can be made of the so-called *surface scattering path operators*, which in turn refer to the so-called "missing elements" in the above tridiagonal matrix,

$$\begin{aligned} \underline{\tau}^{00}_{\Delta,\mathrm{L}}(\mathbf{k}_{\parallel};\epsilon) = \big[& \underline{\mathbf{t}}^{\mathrm{L}}_{\Delta}(\epsilon)^{-1} - \underline{\mathbf{G}}^{\mathrm{r},\,00}(\mathbf{k}_{\parallel};\epsilon) - \underline{\mathbf{G}}^{\mathrm{r},\,10}(\mathbf{k}_{\parallel};\epsilon)\underline{\tau}^{00}_{\Delta,\mathrm{L}}(\mathbf{k}_{\parallel};\epsilon)\underline{\mathbf{G}}^{\mathrm{r},\,01}(\mathbf{k}_{\parallel};\epsilon) \\ & - \underline{\mathbf{G}}^{\mathrm{r},\,10}(\mathbf{k}_{\parallel};\epsilon)\underline{\tau}^{00}_{\Delta,\mathrm{L}}(\mathbf{k}_{\parallel};\epsilon)\underline{\mathbf{G}}^{\mathrm{r},\,01}(\mathbf{k}_{\parallel};\epsilon)\big]^{-1} \quad , \end{aligned} \tag{17.31}$$

$$\begin{aligned} \underline{\tau}^{00}_{\Delta,\mathrm{R}}(\mathbf{k}_{\parallel};\epsilon) = \big[& \underline{\mathbf{t}}^{\mathrm{R}}_{\Delta}(\epsilon)^{-1} - \underline{\mathbf{G}}^{\mathrm{r},\,00}(\mathbf{k}_{\parallel};\epsilon) - \underline{\mathbf{G}}^{\mathrm{r},\,01}(\mathbf{k}_{\parallel};\epsilon)\underline{\tau}^{00}_{\Delta,\mathrm{R}}(\mathbf{k}_{\parallel};\epsilon)\underline{\mathbf{G}}^{\mathrm{r},\,10}(\mathbf{k}_{\parallel};\epsilon) \\ & - \underline{\mathbf{G}}^{\mathrm{r},\,01}(\mathbf{k}_{\parallel};\epsilon)\underline{\tau}^{00}_{\Delta,\mathrm{R}}(\mathbf{k}_{\parallel};\epsilon)\underline{\mathbf{G}}^{\mathrm{r},\,10}(\mathbf{k}_{\parallel};\epsilon)\big]^{-1} \quad , \end{aligned} \tag{17.32}$$

which – as can be seen – have to be calculated recursively by making use of the fact that in the left (L) or right (R) semi-infinite system corresponding to a simple two-dimensional lattice all (atomic) layers have to be identical. It should be noted that in (17.31)–(17.32) and in the following equation a parent three-dimensional lattice is assumed. In terms of these two quantities, the PQ-th element of the scattering path operator in the interface region is then given by

$$\begin{aligned} \left[\left[\tau_{\Delta}(\mathbf{k}_{\parallel};\epsilon)\right]^{-1}_{\mathrm{I,I}}\right]^{PQ} = & \left(\underline{t}^{P}_{\Delta}(\epsilon)^{-1} - \underline{G}^{\mathrm{r},\,00}(\mathbf{k}_{\parallel};\epsilon)\right)\delta_{PQ} \\ & - \underline{G}^{\mathrm{r},\,01}(\mathbf{k}_{\parallel};\epsilon)\delta_{P,\,Q-1} - \underline{G}^{\mathrm{r},\,10}(\mathbf{k}_{\parallel};\epsilon)\delta_{P,\,Q+1} \\ & - \underline{G}^{\mathrm{r},\,10}(\mathbf{k}_{\parallel};\epsilon)\underline{\tau}^{00}_{\Delta,\mathrm{L}}(\mathbf{k}_{\parallel};\epsilon)\underline{G}^{\mathrm{r},\,01}(\mathbf{k}_{\parallel};\epsilon)\ \delta_{P,\,1}\delta_{Q,\,1} \\ & - \underline{G}^{\mathrm{r},\,01}(\mathbf{k}_{\parallel};\epsilon)\underline{\tau}^{00}_{\Delta,\mathrm{R}}(\mathbf{k}_{\parallel};\epsilon)\underline{G}^{\mathrm{r},\,10}(\mathbf{k}_{\parallel};\epsilon)\ \delta_{P,\,n}\delta_{Q,\,n} \quad . \end{aligned} \tag{17.33}$$

If layer relaxation occurs then care has to be taken that the intermediate region includes enough atomic layers with bulk-like properties (no layer relaxation), i.e., enough layers from the left and the right semi-finite system. In the case of layer relaxation(s) the above equation has to be modified in the following manner

$$\begin{aligned}\left[\left[\tau_{\Delta}(\mathbf{k}_{\parallel};\epsilon)\right]^{-1}_{\mathrm{I,I}}\right]^{PQ} &= \left(\underline{t}^{P}_{\Delta}(\epsilon)^{-1} - \underline{G}^{\mathrm{r},\,PP}(\mathbf{k}_{\parallel};\epsilon)\right)\boldsymbol{\delta}_{PQ} \\ &- \underline{G}^{\mathrm{r},\,PQ}(\mathbf{k}_{\parallel};\epsilon)\boldsymbol{\delta}_{P,\,Q-1} - \underline{G}^{\mathrm{r},\,QP}(\mathbf{k}_{\parallel};\epsilon)\boldsymbol{\delta}_{P,\,Q+1} \\ &- \underline{G}^{\mathrm{r},\,10}(\mathbf{k}_{\parallel};\epsilon)\underline{\tau}^{00}_{\Delta,\mathrm{L}}(\mathbf{k}_{\parallel};\epsilon)\underline{G}^{\mathrm{r},\,01}(\mathbf{k}_{\parallel};\epsilon)\;\boldsymbol{\delta}_{P,\,1}\boldsymbol{\delta}_{Q,\,1} \\ &- \underline{G}^{\mathrm{r},\,01}(\mathbf{k}_{\parallel};\epsilon)\underline{\tau}^{00}_{\Delta,\mathrm{R}}(\mathbf{k}_{\parallel};\epsilon)\underline{G}^{\mathrm{r},\,10}(\mathbf{k}_{\parallel};\epsilon)\;\boldsymbol{\delta}_{P,\,n}\boldsymbol{\delta}_{Q,\,n}\quad,\end{aligned} \tag{17.34}$$

where now the $\underline{G}^{\mathrm{r},\,PQ}(\mathbf{k}_{\parallel};\epsilon)$ refer to relaxed layers and $\underline{G}^{\mathrm{r},\,10}(\mathbf{k}_{\parallel};\epsilon)$ and $\underline{G}^{\mathrm{r},\,01}(\mathbf{k}_{\parallel};\epsilon)$ to unrelaxed layers.

Finally, with respect to two given sites, $\mathbf{R}_n = \mathbf{R}_{n,\parallel} + \mathbf{C}_p$ and $\mathbf{R}_n = \mathbf{R}_{n,\parallel} + \mathbf{C}_q$, respectively, $\mathbf{R}_{n,\parallel}\,, \mathbf{R}_{m,\parallel} \in \mathcal{L}^{(2)}$, the so-called *site representation* of $\tau_{\Delta}(\mathbf{k}_{\parallel};\epsilon)$ in the interface region can be obtained by means of the following Surface Brillouin Zone integral,

$$\tau^{nm}_{\Delta}(\varepsilon) = \frac{1}{\Omega_{\mathrm{SBZ}}}\int \exp\left[-\mathrm{i}\mathbf{k}_{\parallel}\cdot(\mathbf{R}_{n,\parallel} - \mathbf{R}_{m,\parallel})\right]\tau^{pq}_{\Delta}(\mathbf{k}_{\parallel};\epsilon)\mathrm{d}\mathbf{k}_{\parallel}\quad, \tag{17.35}$$

where Ω_{SBZ} is the unit area of the two–dimensional Surface Brillouin Zone (SBZ). The "unscreened" scattering path operator $\tau^{nm}(\varepsilon)$ is then obtained from $\tau^{nm}_{\Delta}(\varepsilon)$ via (17.15).

17.4 Numerical procedures

The main advantage of the Screened KKR method is of course the tridiagonalization of the inverse of the scattering path operator. Tridiagonalization implies that an originally $O(N^3)$ problem reduces to an $O(N)$ method which numerically implemented is very fast indeed. Screening in one direction is sufficient to achieve this tridiagonalization: this is an ideal set-up for layered systems such as solid systems with a surface or with interfaces.

17.4.1 Inversion of block tridiagonal matrices

Following the method proposed by Godfrin [1] the inverse τ of a block tridiagonal matrix $\mathbf{M}$ of order N

$$\mathbf{M}\tau = \mathbf{I} \quad , \tag{17.36}$$

$$\mathbf{M} = \begin{pmatrix} \underline{M}_{1,-1} & \underline{M}_{1,1} & \underline{M}_{1,2} & 0 & 0 & 0 & 0 \\ 0 & \underline{M}_{2,1} & \underline{M}_{2,2} & \underline{M}_{2,3} & 0 & 0 & 0 \\ 0 & 0 & \underline{M}_{2,3} & \underline{M}_{3,3} & \underline{M}_{3,4} & 0 & 0 \\ & & & & \ddots & & \\ 0 & 0 & 0 & 0 & \underline{M}_{N,N-1} & \underline{M}_{N,N} & \underline{M}_{N,N+1} \end{pmatrix} \quad , \tag{17.37}$$

can be calculated by means of the following auxiliary blocks of matrices

$$\begin{aligned} \underline{X}_N &= 0 \quad , \\ \underline{X}_{N-i} &= \underline{M}_{N-i+1,N-i} \left[\underline{M}_{N-i+1} - \underline{X}_{N-i+1}\right]^{-1} \underline{M}_{N-i+1,N-i} \quad , \\ \underline{Y}_1 &= 0 \quad , \\ \underline{Y}_{i+1} &= \underline{M}_{i+1,i} \left[\underline{M}_{ii} - Y_i\right]^{-1} \underline{M}_{i+1,i} \quad , \\ \underline{C}_i &= -\left[\underline{M}_{i,i} - \underline{X}_i\right]^{-1} \underline{M}_{i,i-1} \quad , \\ \underline{D}_i &= -\left[\underline{M}_{i,i} - \underline{Y}_i\right]^{-1} \underline{M}_{i+1,i} \quad . \end{aligned} \tag{17.38}$$

The blocks of τ are then obtained as follows

$$\begin{aligned} \underline{\tau}_{i,i} &= \left[\underline{M}_{i,i} - \underline{X}_i - \underline{Y}_i\right]^{-1} \quad , \\ \underline{\tau}_{i,j} &= \underline{C}_i \underline{\tau}_{i-1,j} \quad , \quad i > j \quad , \quad 1 \le i \le N-1 \quad , \\ \underline{\tau}_{i,j} &= \underline{D}_i \underline{\tau}_{i+1,j} \quad , \quad i < j \quad , \quad 2 \le i \le N \quad . \end{aligned} \tag{17.39}$$

17.4.2 Evaluation of the surface scattering path operators

Starting again formally from (17.36), namely

$$\mathbf{M}\tau = \mathbf{I} \quad , \tag{17.40}$$

where for a parent three-dimensional lattice

$$\mathbf{M} = \left\{\underline{M}_{i,j}\right\} \quad , \quad \underline{M}_{i,j} = \underline{M}_{0,0}\delta_{i,j} + \underline{M}_{1,0}\delta_{i,j+1} + \underline{M}_{0,1}\delta_{i,j-1} \quad , \tag{17.41}$$

then in this particular case (17.40) corresponds to the following set of equations

$$\begin{aligned} \underline{M}_{0,0}\underline{\tau}_{0,0} + \underline{M}_{0,1}\underline{\tau}_{1,0} &= \underline{1} \quad , \\ \underline{M}_{1,0}\underline{\tau}_{0,0} + \underline{M}_{0,0}\underline{\tau}_{1,0} + \underline{M}_{0,1}\underline{\tau}_{2,0} &= 0 \quad , \\ \underline{M}_{1,0}\underline{\tau}_{1,0} + \underline{M}_{0,0}\underline{\tau}_{2,0} + \underline{M}_{0,1}\underline{\tau}_{3,0} &= 0 \quad , \\ &\vdots \\ \underline{M}_{N,0}\underline{\tau}_{N-1,0} + \underline{M}_{0,0}\underline{\tau}_{N,0} + \underline{M}_{0,1}\underline{\tau}_{N+1,0} &= 0 \quad , \end{aligned} \tag{17.42}$$

from which $\underline{\tau}_{0,0}$ has to be extracted. By defining initially

$$\underline{\alpha}_0 = -\underline{M}_{0,1} \quad , \quad \underline{\beta}_0 = -\underline{M}_{1,0} \quad , \quad \underline{\epsilon}_0 = M_{0,0} \quad , \quad \underline{\epsilon}_0^s = \underline{M}_{0,0} \quad , \tag{17.43}$$

the set of equations in (17.40) can be rewritten as

$$\begin{aligned} \underline{\epsilon}_0^s &= \underline{1} + \underline{\alpha}_0 \tau_{1,0} \quad , \quad n = 1 \quad , \\ \underline{\epsilon}_0 \underline{\tau}_{n,0} &= \underline{\beta}_0 \underline{\tau}_{n-1,0} + \underline{\alpha}_0 \underline{\tau}_{n+1,0} \quad , \quad n \geq 1 \quad . \end{aligned} \tag{17.44}$$

Similarly, by replacing $\underline{\tau}_{n-1,0}$ and $\underline{\tau}_{n+1,0}$ in the corresponding equation in (17.40), for $\underline{\tau}_{n,0}$ one obtains a relation between $\underline{\tau}_{n,0}$ and $\underline{\tau}_{n-2,0}$, $\underline{\tau}_{n+2,0}$. Proceeding along these lines one arrives by successive iteration at the following identities

$$\begin{aligned} \underline{\alpha}_{i+1} &= \underline{\alpha}_i \underline{\epsilon}_i^{-1} \underline{\alpha}_i \quad , \\ \underline{\beta}_{i+1} &= \underline{\beta}_i \underline{\epsilon}_i^{-1} \underline{\beta}_i \quad , \\ \underline{\epsilon}_{i+1} &= \underline{\epsilon}_i - \underline{\beta}_i \underline{\epsilon}_i^{-1} \underline{\alpha}_i - \underline{\alpha}_i \underline{\epsilon}_i^{-1} \underline{\beta}_i \quad , \\ \underline{\epsilon^s}_{i+1} &= \underline{\epsilon}_i^s - \underline{\alpha}_i \underline{\epsilon}_i^{-1} \underline{\beta}_i \quad , \end{aligned} \tag{17.45}$$

where

$$\begin{aligned} \underline{\epsilon}_{i+1}^s \underline{\tau}_{0,0} &= \underline{1} + \underline{\alpha}_{i+1} \underline{\tau}_{2^{(i+1)},0} \quad , \\ \underline{\epsilon}_{i+1} \underline{\tau}_{n,0} &= \beta_{i+1} \underline{\tau}_{n-2^{(i+1)},0} + \underline{\alpha}_{i+1} \underline{\tau}_{n+2^{(i+1)},0} \quad , \quad n \geq 2^{(i+1)} \quad . \end{aligned} \tag{17.46}$$

In the limit of $i \to \infty$,

$$\lim_{i \to \infty} \underline{\alpha}_i = 0 \quad , \tag{17.47}$$

from which follows that

$$\underline{\tau}_{0,0} = \left[\lim_{i \to \infty} \underline{\epsilon}_i^s \right]^{-1} \quad . \tag{17.48}$$

Usually this procedure, which very often is termed *decimation technique* (López Sancho et al. [2]) turns out to be quite fast: only about 10–20 iterations are necessary to reach sufficient accuracy for $\underline{\tau}_{0,0}$, the quantity required in (17.31) and (17.32).

17.4.3 Practical evaluation of screened structure constants

In practice, three methods are used in order to calculate the $\underline{G}^{\mathrm{r},pq}(\mathbf{k}_\parallel; \epsilon)$ defined in (17.20).

Real space evaluation

The conceptually simplest way is to perform the screening transformation, (17.9), in real space, i.e., for a finite number of sites (cluster). Let a cluster $\mathcal{C}$ consist of N suitably chosen sites,

$$\mathcal{C} = \{\mathbf{R}_i \mid i = 1, \ldots, N\} \quad , \tag{17.49}$$

which comprise also a limited number of sites from different layers, say $p_1 \leq p \leq p_2$,

$$\mathcal{C} = \bigcup_{p_1 \leq p \leq p_2} \mathcal{C}_p \quad , \tag{17.50}$$

where

$$\mathcal{C}_p = \mathcal{C} \cap \mathcal{L}_p^{(2)} \quad . \tag{17.51}$$

Furthermore, let $I(\mathcal{C})$ and $I(\mathcal{C}_p)$ denote the corresponding set of indices. Equation (17.9) is then solved for matrices confined to cluster $\mathcal{C}$,

$$\mathbf{G}_{\mathcal{C}}^{\mathrm{r}}(\epsilon) = \mathbf{G}_{\mathcal{C}}^{0}(\epsilon) \left[\mathbf{I}_{\mathcal{C}} - \mathbf{t}_{\mathcal{C}}^{\mathrm{r}}(\epsilon)\mathbf{G}_{\mathcal{C}}^{0}(\epsilon)\right]^{-1} \quad , \tag{17.52}$$

where for $i, j \in I(\mathcal{C})$,

$$[\mathbf{I}_{\mathcal{C}}]_{ij} = \underline{I}\delta_{i,j} \ , \ \left[\mathbf{G}_{\mathcal{C}}^{0}(\epsilon)\right]_{ij} = \underline{G}_{ij}^{0}(\epsilon)\,(1 - \delta_{ij}) \ \text{ and } \ [\mathbf{t}_{\mathcal{C}}^{\mathrm{r}}(\epsilon)]_{ij} = \underline{t}_i^{\mathrm{r}}(\epsilon)\delta_{i,j} \quad . \tag{17.53}$$

The condition

$$[\mathbf{G}_{\mathcal{C}}^{\mathrm{r}}(\epsilon)]_{ij} = \underline{G}_{ij}^{\mathrm{r}}(\epsilon) \quad , \quad i, j \in I(\mathcal{C}) \quad , \tag{17.54}$$

is obviously not satisfied because of the finite size of $\mathcal{C}$. Nevertheless, if the size of the cluster exceeds the range of screening, d, $\underline{G}_{\mathcal{C},ij}^{\mathrm{r}}(\epsilon)$ approaches $\underline{G}_{ij}^{\mathrm{r}}(\epsilon)$ at least for pair of sites well inside the cluster. Usually, one fixes one particular site i at the center of $\mathcal{C}$, and chooses sites j within a distance d. For close-packed fcc or bcc lattices, one gets converged values for $\underline{G}_{ij}^{\mathrm{r}}(\epsilon)$ by considering clusters of less than 100 sites.

For complex lattices and in the case of lattice relaxations, however, one has to take great care when performing a real space evaluation of $\underline{G}_{ij}^{\mathrm{r}}(\epsilon)$, since in principle for each non-equivalent site in the lattice a specific cluster has to be chosen with a given non-equivalent site being at the center of the cluster. Once $\mathbf{G}_{\mathcal{C}}^{\mathrm{r}}(\epsilon)$ is obtained, a two-dimensional Fourier representation of the screened structure constants can directly be calculated,

$$\underline{G}^{\mathrm{r},pq}(\mathbf{k}_{\parallel};\epsilon) = \sum_{\mathbf{R}_j \in \mathcal{C}_q} \exp\left[\mathrm{i}\mathbf{k}_{\parallel} \cdot \left(\mathbf{R}_{j,\parallel} - \mathbf{R}_{i,\parallel}\right)\right] \underline{G}_{\mathcal{C},ij}^{\mathrm{r}}(\epsilon) \quad , \quad \mathbf{R}_i \in \mathcal{C}_p \quad . \tag{17.55}$$

Beyond its conceptual simplicity an obvious advantage of a real space evaluation of $\underline{G}_{ij}^{\mathrm{r}}(\epsilon)$ is that for a given energy the lattice Fourier transform, $\underline{G}^{\mathrm{r},pq}(\mathbf{k}_{\parallel};\epsilon)$ can quickly be obtained, and therefore (17.52) is in particular useful for calculations for which a large number of $\mathbf{k}_{\parallel}$ points is needed.

Two-dimensional reciprocal space evaluation

Finite size effects can considerably be reduced when making use of a two-dimensional Fourier representation of the bare structure constants discussed in Sect. 15.2, since it is straightforward to show that (17.9) factorizes due

to the orthogonality of the irreducible representations of the translational group,

$$\mathbf{G}^{\mathrm{r}}(\mathbf{k}_{\parallel};\epsilon) = \mathbf{G}^{0}(\mathbf{k}_{\parallel};\epsilon)\left[\mathbf{I} - \mathbf{t}^{\mathrm{r}}(\epsilon)\mathbf{G}^{0}(\mathbf{k}_{\parallel};\epsilon)\right]^{-1} \quad . \tag{17.56}$$

All matrices in the above equation carry now layer indices; due to translational invariance $\underline{t}^{\mathrm{r},pi}(\epsilon) = \underline{t}^{\mathrm{r},pj}(\epsilon) = \underline{t}^{\mathrm{r},p}(\epsilon)$. In order to get numerically reliable values of $\underline{G}^{\mathrm{r},pq}(\mathbf{k}_{\parallel};\epsilon)$ for a system of n layers, when solving (17.56) one needs to add a few layers, usually not more than two principal layers, from the semi-infinite regions. Therefore, although the screening transformation has to be carried out for each energy and $\mathbf{k}_{\parallel}$ point separately, this technique is in particular suitable for complex lattices and in the case of layer relaxations.

Three-dimensional reciprocal space evaluation

When layer relaxations need not be considered, that means, a perfect three-dimensional parent lattice [6] applies, an alternative method can be used which excludes any finite size effects induced by the screening transformation. In that case, similar to (17.55), one can write

$$\underline{G}^{\mathrm{r}}(\mathbf{k};\epsilon) = \underline{G}^{0}(\mathbf{k};\epsilon)\left[\underline{I} - \underline{t}^{\mathrm{r}}(\epsilon)\underline{G}^{0}(\mathbf{k};\epsilon)\right]^{-1} \quad , \tag{17.57}$$

where $\mathbf{k}$ is a vector in the three-dimensional Brillouin zone and the angular momentum matrices $\underline{G}^{0}(\mathbf{k};\epsilon)$ can be calculated directly in terms of Ewald summation, see Sect. 15.3.

Clearly enough with regard to the different approaches of performing screening transformations, namely (17.52), (17.56) and (17.57), the last one involves the smallest size of matrices and does not suffer from finite size effects. "Two-dimensional" screened structure constants can then be obtained by the below folding procedure,

$$\underline{G}^{\mathrm{r},pq}(\mathbf{k}_{\parallel};\epsilon) = \frac{2\pi}{d_{\perp}} \int_{-\pi/d_{\perp}}^{\pi/d_{\perp}} \mathrm{d}k_{\perp} \exp\left[-\mathrm{i}k_{\perp}\left(C_{p,\perp} - C_{q,\perp}\right)\right] \underline{G}^{\mathrm{r}}(\mathbf{k}_{\parallel}, k_{\perp};\epsilon) \quad , \tag{17.58}$$

where $d_{\perp}$ denotes the layer spacing. It should be noted that (17.58) can be extended in a straightforward manner to the case of complex three-dimensional parent lattices.

17.4.4 Relativistic screened structure constants

In principle the above methods can be applied in the relativistic case by taking the relativistic counterparts of the "bare structure constants" ,

$$G^{0,ij}_{QQ'}(\varepsilon) = \sum_{s=\pm\frac{1}{2}} C\left(\ell j 1/2; \mu - s, s\right) G^{0,ij}_{\ell(\mu-s),\ell'(\mu'-s)}(\varepsilon)\, C\left(\ell' j' 1/2; \mu' - s, s\right) \tag{17.59}$$

(real space evaluation), of $G^{0,pq}_{QQ'}\left(\mathbf{k}_{\parallel};\varepsilon\right)$ (two-dimensional reciprocal space evaluation), or of $G^{0}_{QQ'}\left(\mathbf{k};\varepsilon\right)$ (three-dimensional reciprocal space evaluation), and the relativistic single-site t-matrices corresponding to the reference system, $\underline{t}^{\mathrm{r},i}(\epsilon) = \left\{ t^{\mathrm{r},i}_{QQ'}\left(\varepsilon\right) \right\}$.

Since in this case the corresponding matrix equations are doubled in dimension as compared to the non-relativistic case have to be solved, it is advisable to solve first the screening transformation for the non-relativistic structure constants and then make use of the orthogonality relations of the Clebsch-Gordan coefficients and the fact that

$$t^{\mathrm{r},i}_{QQ'}\left(\varepsilon\right) = t^{\mathrm{r},i}_{\ell}\left(\varepsilon\right)\, \delta_{\ell\ell'}\delta_{jj'}\delta_{\mu\mu'} \quad . \tag{17.60}$$

It easily can be shown that e.g. (17.59) applies also for the screened structure constants,

$$G^{\mathrm{r},ij}_{QQ'}\left(\varepsilon\right) = \sum_{s=\pm\frac{1}{2}} C\left(\ell j 1/2; \mu - s, s\right)\, G^{\mathrm{r},ij}_{\ell(\mu-s),\ell'(\mu'-s)}\left(\varepsilon\right)\, C\left(\ell' j' 1/2; \mu' - s, s\right) \tag{17.61}$$

where the non-relativistic screened structure constants $G^{\mathrm{r},ij}_{Ll'}\left(\varepsilon\right)$ are derived from a screening transformation using either of (17.52), (17.56), or (17.57) and the reference t-matrices, $\underline{t}^{\mathrm{r},i}(\epsilon) = \left\{ t^{\mathrm{r},i}_{\ell}\left(\varepsilon\right)\, \delta_{LL'} \right\}$.

17.4.5 Decaying properties of screened structure constants

The decaying properties of screened structure constants are in the following illustrated in terms of real-space structure constants $\underline{G}^{\mathrm{r},ij}$ by using finite clusters of sites in appropriate neighboring shells of an *fcc* lattice and by choosing $W_{\mathrm{r}} = 2$ Ry. In order to visualize the decay of $\underline{G}^{\mathrm{r},ij}$ as a function of $|\mathbf{R}_i - \mathbf{R}_j|$, the following "partial norm" is evaluated:

$$N_{\ell\ell'}(|\mathbf{R}_i - \mathbf{R}_j|;\epsilon) = \frac{|\epsilon|^{(\ell+\ell')/2}}{(2\ell+1)!!(2\ell'+1)!!} \left[\sum_{mm'} |G^{\mathrm{r},ij}_{\ell m,\ell' m'}(\epsilon)|^2 \right]^{1/2} \tag{17.62}$$

which at a given distance $|\mathbf{R}_i - \mathbf{R}_j|$ does not show any angular dependence.

For $\epsilon = 0.65$ Ry (about the Fermi energy of Cu) these partial norms as evaluated using a cluster with a total of 225 sites are displayed for $\ell = \ell'$ in Fig. (17.1, left panel) as function of the distance $|\mathbf{R}_i - \mathbf{R}_j|$ together with the corresponding norms of their unscreened counterparts (right panel).

It is obvious from this figure that the partial norms corresponding to the screened structure constants $\underline{G}^{\mathrm{r},ij}$ decay rapidly (essentially exponentially), whereas the unscreened norms typically decrease by less than a factor of ten in the range of distances: the screened norms decrease to about 10^{-5} of their nearest-neighbor values.

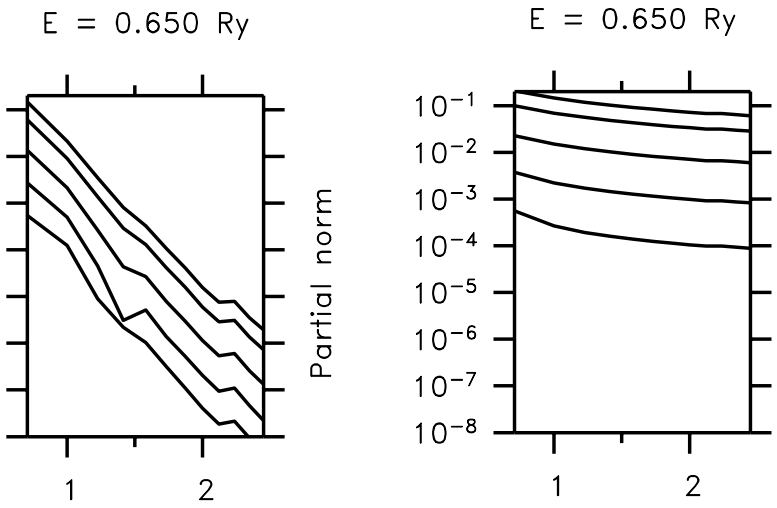

Fig. 17.1. Screened (left panel) and unscreened (right panel) partial norms for $\ell = \ell'$ and $\epsilon = 0.65$ Ry as function of the distance in units of the lattice constant. The results for $\ell = 0, 1, 2, 3, 4$ are shown from top to bottom. From [5].

If the screened partial norms are plotted as function of energy (see Fig. (17.2) for $\ell = \ell' = 0$ and Fig. (17.3) for $\ell = \ell' = 2$), two observations can be made: (1) the decay of the screened structure constants is very similar in the relevant positive energy range of about one Rydberg and calculations with clusters of 79 or 225 repulsive muffin-tin potentials lead to almost indistinguishable results, and (2) if ϵ approaches the energy bottom, ϵ_{bot}, which is about 1.38 Ry for $W_{\rm r} = 2$ Ry, then the exponential decay breaks down and the screened structure constants become strongly energy dependent. However, such energies usually do not occur in self-consistent density-functional calculations for occupied states and, if they do, one could increase $V^{\rm r}$ to, say, 3 or 4 Ry to extend the energy range of fast decaying and smoothly varying screened structure constants. Since the curves in Fig. (17.2) and Fig. (17.3) are plotted on a logarithmic scale covering several orders of magnitude, the small differences obtained between the clusters of 79 or 225 repulsive potentials are difficult to trace: both curves practically coincide.

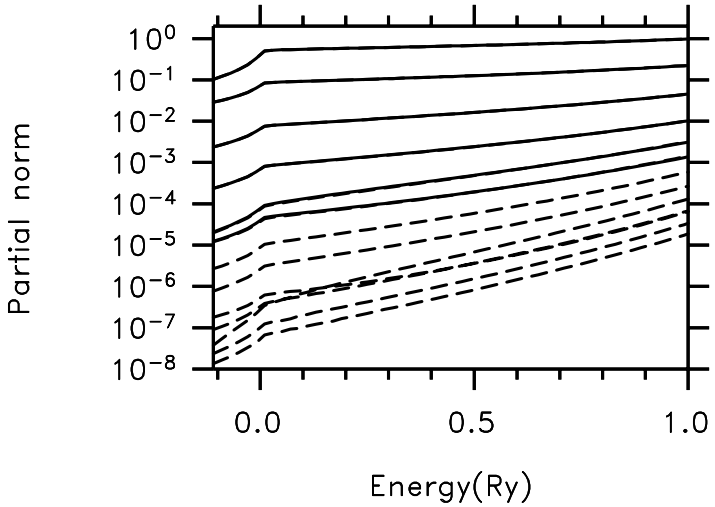

Fig. 17.2. Screened partial norms for $\ell = \ell' = 0$ as function of energy. From top to bottom on-site results and the ones for twelve neighboring shells with increasing distance from the central site are given. The six solid curves are calculated with repulsive potentials on 79 sites, the thirteen broken curves with 225 sites. The six upper broken curves practically coincide with the solid ones. From [5]

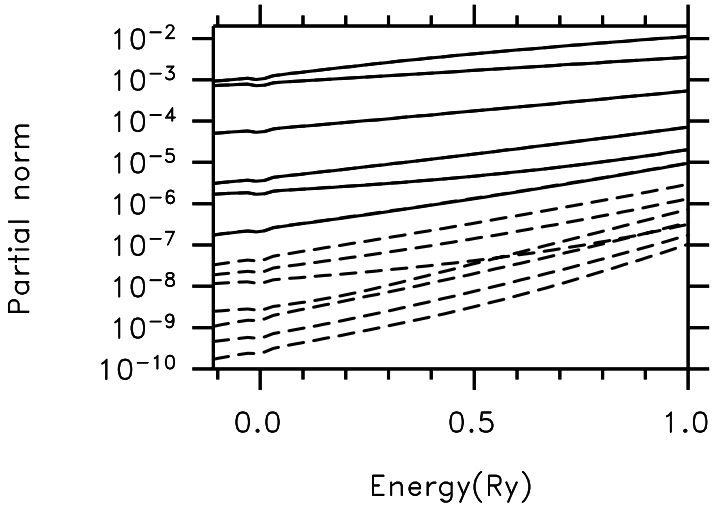

Fig. 17.3. Screened partial norms for $\ell = \ell' = 2$ as function of energy. From top to bottom on-site results and the ones for twelve neighboring shells with increasing distance from the central site are given. The six solid curves are calculated with repulsive potentials on 79 sites, the thirteen broken curves with 225 sites. The six upper broken curves practically coincide with the solid ones. From [5]

References

1. E.M. Godfrin, J. Phys.: Condens. Matter **3**, 7843 (1991).
2. M.P. López Sancho, J.M. López Sancho, and J. Rubio, J. Phys. C.: **18**, 1803 (1985).
3. L. Szunyogh, B. Újfalussy, P. Weinberger and J. Kollar, Phys. Rev. **B49**, 2721 (1994).
4. R. Zeller, P.H. Dederichs, B. Újfalussy, L. Szunyogh and P. Weinberger,Phys. Rev. **B52**, 8807 (1995).
5. C. Uiberacker, L. Szunyogh, B. Újfalussy, P. Weinberger, A. Ernst, and P.H. Dederichs, Phil. Mag. B **78**, 423 (1998).
6. P. Weinberger, Phil. Mag. B **75**, 509–533 (1997).

18 Charge and magnetization densities

18.1 Calculation of physical observables

For a system of independent fermions, the statistical average of a one-particle observable, say A, is given by

$$\mathsf{A} = \sum_n f(\varepsilon_n) \langle\varphi_n| \mathcal{A} |\varphi_n\rangle \quad , \tag{18.1}$$

where $\mathcal{A}$ is the Hermitian operator related to A and the Fermi-Dirac distribution function $f(\varepsilon)$ is given by

$$f(\varepsilon) = \frac{1}{\exp\left[(\varepsilon - \mu)/k_\mathrm{B}T\right] + 1} \quad , \tag{18.2}$$

T being the temperature, μ the chemical potential and k_B the Boltzmann constant. In (18.1) the $|\varphi_n\rangle$ and ε_n refer to the the eigenstates and the eigenvalues of the one-particle Hamilton operator, $\mathcal{H}$, respectively,

$$\mathcal{H} |\varphi_n\rangle = \varepsilon_n |\varphi_n\rangle \quad . \tag{18.3}$$

By using the spectral resolution of the resolvent,

$$\mathcal{G}(z) = \sum_n \frac{|\varphi_n\rangle\langle\varphi_n|}{z - \varepsilon_n} \quad , \tag{18.4}$$

one can write

$$f(z)\ \mathrm{Tr}\left(\mathcal{A}\mathcal{G}(z)\right) = \sum_n \frac{f(z) \langle\varphi_n| \mathcal{A} |\varphi_n\rangle}{z - \varepsilon_n} \quad ,$$

which with respect to (18.1) has to be integrated over a closed contour in the complex plane comprising the spectrum of $\mathcal{H}$. In terms of Cauchy's theorem this yields for a closed counterclockwise contour,

$$-\frac{1}{2\pi\mathrm{i}} \int_{\circlearrowleft} \mathrm{d}z \frac{g(z)}{z - a} = \begin{cases} g(a) \text{ , if } a \text{ is within the contour} \\ \\ 0 \quad \text{ , if } a \text{ is outside of the contour} \end{cases} \quad , \tag{18.5}$$

where it is supposed that the function g has no poles within the contour, implying therefore that also the poles of the Fermi-Dirac distribution, the so-called *Matsubara poles*, z_k,

$$z_k = \mu + \mathrm{i}\,(2k+1)\,\pi k_{\mathrm{B}} T \quad , \quad k \in \mathbb{Z} \quad , \tag{18.6}$$

$\mathbb{Z}$ denoting the field of integer numbers, have to be taken into account. Consequently (18.1) can be written as

$$\mathsf{A} = -\frac{1}{2\pi\mathrm{i}} \int_{\circlearrowleft} \mathrm{d}z\, f\,(z)\, \mathrm{Tr}\,(\mathcal{A}\mathcal{G}\,(z)) - k_{\mathrm{B}} T \sum_k \mathrm{Tr}\,(\mathcal{A}\mathcal{G}\,(z_k)) \quad , \tag{18.7}$$

such that only the Matsubara poles within the contour have to be considered. By splitting the contour into parts lying in the upper and lower complex semi-planes (18.7) can further be transformed to

$$\begin{aligned}
\mathsf{A} = &-\frac{1}{2\pi\mathrm{i}} \left[\int_{\curvearrowright} \mathrm{d}z\, f\,(z)\, \mathrm{Tr}\,(\mathcal{A}\mathcal{G}\,(z)) - \int_{\curvearrowright} \mathrm{d}z^*\, f\,(z^*)\, \mathrm{Tr}\,(\mathcal{A}\mathcal{G}\,(z^*)) \right] \\
&\qquad - k_{\mathrm{B}} T \sum_{\mathrm{Im} z_k > 0} \left[\mathrm{Tr}\,(\mathcal{A}\mathcal{G}\,(z_k)) + \mathrm{Tr}\,(\mathcal{A}\mathcal{G}\,(z_k^*)) \right] \\
= &-\frac{1}{2\pi\mathrm{i}} \left[\int_{\curvearrowright} \mathrm{d}z\, f\,(z)\, \mathrm{Tr}\,(\mathcal{A}\mathcal{G}\,(z)) - \left(\int_{\curvearrowright} \mathrm{d}z\, f\,(z)\, \mathrm{Tr}\,(\mathcal{A}\mathcal{G}\,(z)) \right)^* \right] \\
&\qquad - k_{\mathrm{B}} T \sum_{\mathrm{Im} z_k > 0} \left[\mathrm{Tr}\,(\mathcal{A}\mathcal{G}\,(z_k)) + \mathrm{Tr}\,(\mathcal{A}\mathcal{G}\,(z_k))^* \right] \\
= &-\frac{1}{\pi} \mathrm{Im} \int_{\curvearrowright} \mathrm{d}z\, f\,(z)\, \mathrm{Tr}\,(\mathcal{A}\mathcal{G}\,(z)) - 2 k_{\mathrm{B}} T\, \mathrm{Re} \sum_{\mathrm{Im} z_k > 0} \mathrm{Tr}\,(\mathcal{A}\mathcal{G}\,(z_k)) \quad .
\end{aligned} \tag{18.8}$$

In here use was made of the analyticity of the resolvent

$$\mathcal{G}\,(z^*) = \mathcal{G}\,(z)^\dagger \quad . \tag{18.9}$$

Equation (18.8) is particularly useful for practical calculations since the Green function has to be evaluated only for energies z with finite imaginary parts. This in turn implies a "damping" of the Green's function which has simple poles on the real energy axis. By deforming the contour to the real axis, the below expression is obtained:

$$\mathsf{A} = -\frac{1}{\pi} \mathrm{Im} \int_{-\infty}^{\infty} \mathrm{d}\varepsilon\, f\,(\varepsilon)\, \mathrm{Tr}\left(\mathcal{A}\mathcal{G}^+\,(\varepsilon)\right) = \frac{1}{\pi} \mathrm{Im} \int_{-\infty}^{\infty} \mathrm{d}\varepsilon\, f\,(\varepsilon)\, \mathrm{Tr}\left(\mathcal{A}\mathcal{G}^-\,(\varepsilon)\right) \quad , \tag{18.10}$$

Furthermore, *at zero temperature* the expectation value of $\mathcal{A}$ can be written as

$$\mathsf{A} = -\frac{1}{\pi}\mathrm{Im}\int_{\curvearrowright} \mathrm{d}z\,\mathrm{Tr}\left(\mathcal{A}\mathcal{G}\left(z\right)\right) = -\frac{1}{\pi}\mathrm{Im}\int_{-\infty}^{\varepsilon_\mathrm{F}} \mathrm{d}\varepsilon\,\mathrm{Tr}\left(\mathcal{A}\mathcal{G}^{+}\left(\varepsilon\right)\right) \quad , \tag{18.11}$$

where ε_F denotes the Fermi energy. Usually the lower limit of the above integration is chosen below the valence band and well above the lowest lying core states. In particular, the number of electrons can be calculated by choosing $\mathcal{A} = \mathcal{I}$,

$$N = \int_{-\infty}^{\varepsilon_\mathrm{F}} \mathrm{d}\varepsilon\; n\left(\varepsilon\right) \quad , \tag{18.12}$$

where, omitting the subscript for $\mathcal{G}^{+}\left(\varepsilon\right)$, $n\left(\varepsilon\right)$, the *density of states* (DOS), is given by

$$n\left(\varepsilon\right) = -\frac{1}{\pi}\mathrm{Im}\mathrm{Tr}\mathcal{G}\left(\varepsilon\right) \quad . \tag{18.13}$$

Expressing the trace in configuration space, a so-called *real-space density* $\mathsf{A}\left(\mathbf{r}\right)$ can be defined as

$$\mathsf{A} = \int \mathsf{A}\left(\mathbf{r}\right)\mathrm{d}\mathbf{r} \quad , \tag{18.14}$$

$$\mathsf{A}\left(\mathbf{r}\right) = -\frac{1}{\pi}\mathrm{Im}\int_{\curvearrowright} \mathrm{d}z\,\mathrm{tr}\left(AG\left(z;\mathbf{r},\mathbf{r}\right)\right) = -\frac{1}{\pi}\mathrm{Im}\int_{-\infty}^{\varepsilon_\mathrm{F}} \mathrm{d}\varepsilon\,\mathrm{tr}\left(AG\left(\varepsilon;\mathbf{r},\mathbf{r}\right)\right) \quad , \tag{18.15}$$

where tr denotes a trace with respect to further coordinates of the Green's function, e.g., spin-coordinates. As multiple scattering theory is based on a partitioning of the configuration space into cells related to atoms, the observables and their densities can naturally be decomposed into cell-like contributions,

$$\mathsf{A} = \sum_i \mathsf{A}_i \quad , \tag{18.16}$$

$$\mathsf{A}_i = \int_{D_i} \mathsf{A}_i\left(\mathbf{r}_i\right)\mathrm{d}\mathbf{r}_i \quad , \tag{18.17}$$

and

$$\mathsf{A}_i\left(\mathbf{r}_i\right) = -\frac{1}{\pi}\mathrm{Im}\int_{\curvearrowright} \mathrm{d}z\,\mathrm{tr}\left(AG\left(z;\mathbf{r}_i+\mathbf{R}_i,\mathbf{r}_i+\mathbf{R}_i\right)\right) \; . \tag{18.18}$$

Since in Density Functional Theory (DFT) charge and the magnetization densities are key quantities, in the next sections explicit expressions for these quantities are given. It should be noted that for matters of brevity in the following the cell-index (i) is dropped.

18.2 Non-relativistic formulation

Starting from the expression in (3.156) the Green's function $G(z; \mathbf{r}+\mathbf{R}, \mathbf{r}+\mathbf{R})$ can be expanded in terms of spherical harmonics

$$G\left(z; \mathbf{r}+\mathbf{R}, \mathbf{r}+\mathbf{R}\right) = \sum_{LL'} Y_L(\hat{\mathbf{r}}) G_{LL'}(z;r) Y^*_{L'}(\hat{\mathbf{r}}) \quad , \tag{18.19}$$

where

$$\begin{aligned} G_{LL'}(z;r) = & \sum_{L''L'''} Z_{LL''}\left(z;r\right) \tau_{L''L'''}\left(z\right) Z_{L'L'''}\left(z;r\right) \\ & - \sum_{L''} J_{LL''}\left(z;r\right) Z_{L'L''}\left(z;r\right) \quad . \end{aligned} \tag{18.20}$$

18.2.1 Charge density

The charge density confined to a particular cell is defined as

$$\rho(\mathbf{r}) = -\frac{2}{\pi} \mathrm{Im} \int_{\curvearrowright} \mathrm{d}z \, G\left(z; \mathbf{r}+\mathbf{R}, \mathbf{r}+\mathbf{R}\right) \quad , \tag{18.21}$$

where a factor of two accounts for the spin-degeneracy. Inserting (18.19) into (18.21) then yields

$$\rho(\mathbf{r}) = -\frac{2}{\pi} \mathrm{Im} \sum_{LL'} Y_L(\hat{\mathbf{r}}) G_{LL'}\left(r\right) Y^*_{L'}(\hat{\mathbf{r}}) \tag{18.22}$$

$$= -\frac{1}{\pi \mathrm{i}} \sum_{LL'} \left(G_{LL'}\left(r\right) - G_{L'L}\left(r\right)^* \right) Y_L(\hat{\mathbf{r}}) Y^*_{L'}(\hat{\mathbf{r}}) \quad , \tag{18.23}$$

where

$$G_{LL'}\left(r_i\right) = \int_{\curvearrowright} \mathrm{d}z \, G_{LL'}\left(z;r\right) \quad . \tag{18.24}$$

By using the identity

$$Y_L(\hat{\mathbf{r}}) \, Y^*_{L'}(\hat{\mathbf{r}}) = \sum_{L''} C^{L'}_{LL''} \, Y^*_{L''}(\hat{\mathbf{r}}) \quad , \tag{18.25}$$

$C^{L'}_{LL''}$ being the Gaunt-coefficients,

$$C^{L'}_{LL''} = \int \mathrm{d}\hat{\mathbf{r}} Y_L(\hat{\mathbf{r}}) Y^*_{L'}(\hat{\mathbf{r}}) Y_{L''}(\hat{\mathbf{r}}) \quad , \tag{18.26}$$

the charge density can be expanded as

$$\rho(\mathbf{r}) = \sum_{L} \rho_L(r) Y^*_L(\hat{\mathbf{r}}) \, , \tag{18.27}$$

namely in the form used when solving the Poisson equation, see Chap. 19. The radial functions $\rho_L(r)$ can be written as follows,

$$\rho_L(r) = -\frac{1}{\pi \mathrm{i}} \sum_{L'L''} C_{LL'}^{L''} \left(G_{L'L''}(r) - G_{L''L'}(r)^* \right) \quad . \tag{18.28}$$

Because the charge density is confined to a polyhedral Wigner-Seitz cell (WSC) it has to be multiplied by the shape function,

$$\sigma(\mathbf{r}) = \sum_L \sigma_L(r)\, Y_L(\hat{\mathbf{r}}) \quad , \tag{18.29}$$

in order to meet the requirement of non-overlapping domains,

$$\rho(\mathbf{r})\, \sigma(\mathbf{r}) = \sum_{LL'} \rho_L(r)\, \sigma_{L'}(r)\, Y_L^*(\hat{\mathbf{r}}) = \sum_L \bar{\rho}_L(r)\, Y_L^*(\hat{\mathbf{r}}) \quad , \tag{18.30}$$

with

$$\bar{\rho}_L(r) = \sum_{L'L''} C_{L''L}^{L'}\, \rho_{L'}(r)\, \sigma_{L''}(r) \quad . \tag{18.31}$$

18.2.2 Charges

The charge corresponding to the charge distribution inside a WSC is given by

$$Q = \int_\Omega \mathrm{d}\mathbf{r}\, \rho(\mathbf{r}) \quad . \tag{18.32}$$

By multiplying the integrand with the corresponding shape function the above integral can be evaluated as

$$Q = \int_{\mathrm{BS}} \mathrm{d}\mathbf{r}\, \rho(\mathbf{r})\, \sigma(\mathbf{r}) \quad , \tag{18.33}$$

where BS refers to the bounding sphere around the WSC. In using the angular momentum expansion in (18.30) one obtains

$$Q = \sqrt{4\pi} \int_0^{r_{\mathrm{BS}}} \mathrm{d}r\, r^2\, \bar{\rho}_{(0,0)}(r) = \sum_L \int_0^{r_{\mathrm{BS}}} \mathrm{d}r\, r^2\, \rho_L(r)\, \sigma_L(r) \quad , \tag{18.34}$$

where r_{BS} denotes the radius of the bounding sphere. Since for a muffin-tin sphere of radius r_{MT}

$$\sigma_L(r) = \sqrt{4\pi}\delta_{L,(0,0)} \quad , \quad r \le r_{\mathrm{MT}} \quad , \tag{18.35}$$

one finally can write

$$Q = \sqrt{4\pi} \int_0^{r_{\mathrm{MT}}} \mathrm{d}r\, r^2\, \rho_{(0,0)}(r) + \int_{r_{\mathrm{MT}}}^{r_{\mathrm{BS}}} \mathrm{d}r\, r^2 \sum_L \rho_L(r)\, \sigma_L(r) \quad . \tag{18.36}$$

18.2.3 Partial local density of states

Similar to the charge density the density of states related to cell i can be computed by integrating over the corresponding Wigner-Seitz cell,

$$n(\varepsilon) = -\frac{2}{\pi}\,\mathrm{Im}\int\limits_{\Omega} \mathrm{d}\mathbf{r}\, G(\varepsilon;\mathbf{r}+\mathbf{R},\mathbf{r}+\mathbf{R}) \tag{18.37}$$

$$= -\frac{2}{\pi}\mathrm{Im}\int\limits_{\mathrm{BS}} \mathrm{d}\mathbf{r}\, G(\varepsilon;\mathbf{r}+\mathbf{R},\mathbf{r}+\mathbf{R})\,\sigma(\mathbf{r}) \quad . \tag{18.38}$$

Inserting the expansions in (18.19) and (18.29) yields

$$n(\varepsilon) = -\frac{2}{\pi}\,\mathrm{Im}\sum_{LL'L''}\int\limits_{0}^{r_{\mathrm{BS}}} \mathrm{d}r\, r^2\, G_{LL'}(\varepsilon;r)\, C^{L'}_{LL''}\,\sigma_{L''}(r) \tag{18.39}$$

$$= -\frac{2}{\pi}\,\mathrm{Im}\sum_{LL'}\int\limits_{0}^{r_{\mathrm{BS}}} \mathrm{d}r\, r^2\, G_{LL'}(\varepsilon;r)\,\sigma_{L'L}(r) \quad , \tag{18.40}$$

where

$$\sigma_{L'L}(r) = \sum_{L''} C^{L'}_{LL''}\,\sigma_{L''}(r) \quad . \tag{18.41}$$

By defining the angular momentum representation of the local densities of states (*density matrix*) in the following manner,

$$n_{LL'}(\varepsilon) = -\frac{2}{\pi}\,\mathrm{Im}\sum_{L''}\int\limits_{0}^{r_{\mathrm{BS}}} \mathrm{d}r\, r^2\, G_{LL''}(\varepsilon;r)\,\sigma_{L''L'}(r) \quad , \tag{18.42}$$

(18.40) can simply be expressed as

$$n(\varepsilon) = \mathrm{Tr}\big\{n_{LL'}(\varepsilon)\big\} = \sum_{L} n_{LL}(\varepsilon) \quad . \tag{18.43}$$

Denoting finally the diagonal elements of the local density matrix by $n_L(\varepsilon)$, $n_L(\varepsilon) \equiv n_{LL}(\varepsilon)$, the local densities of states can be sorted into s-, p-, d-like (and so forth) partial components,

$$n(\varepsilon) = \sum_{L} n_L(\varepsilon) = \sum_{\ell m} n_{\ell m}(\varepsilon) = \sum_{\ell} n_{\ell}(\varepsilon) \quad , \tag{18.44}$$

where

$$n_{\ell}(\varepsilon) = \sum_{m=-\ell}^{\ell} n_{\ell m}(\varepsilon) \quad . \tag{18.45}$$

It should be noted that only $n(\varepsilon)$ is well-defined, although colloquially very often partial densities of states are used as if they would be"physical quantities".

Obviously because of (18.12) also the (valence) charge can be decomposed into partial (valence) charges, Q_ℓ,

$$Q = \sum_\ell Q_\ell \quad , \quad Q_\ell = \int_{\varepsilon_\mathrm{B}}^{\varepsilon_\mathrm{F}} \mathrm{d}\varepsilon \, n_\ell(\varepsilon) \quad , \tag{18.46}$$

ε_B referring to the bottom of the valence band.

18.2.4 The spin-polarized non-relativistic case

As in the (collinear) spin-polarized non-relativistic formalism the Green's function is diagonal in spin-space all the above physical quantities can naturally be decomposed into spin-up ($s =\uparrow$) and spin-down ($s =\downarrow$) components,

$$\rho(\mathbf{r}) = \sum_{s=\uparrow,\downarrow} \rho_s(\mathbf{r}) \quad , \tag{18.47}$$

$$n(\varepsilon) = \sum_{s=\uparrow,\downarrow} n_s(\varepsilon) = \sum_{s=\uparrow,\downarrow} \sum_\ell n_{\ell,s}(\varepsilon) \quad , \tag{18.48}$$

$$Q = \sum_{s=\uparrow,\downarrow} Q_s = \sum_{s=\uparrow,\downarrow} \sum_\ell Q_{\ell,s} \quad , \tag{18.49}$$

whereby the definition of the spin-resolved charge densities, $\rho_s(\mathbf{r})$, partial local DOS, $n_{\ell,s}(\varepsilon)$, and partial local charges, $Q_{\ell,s}$, deserve no special attention since merely the matrices of the spin-dependent Green's functions, $G_{LL',s}(\varepsilon; r)$, have to be used in the corresponding expressions. The magnetic moments, M, can then be calculated as

$$M = \mu_\mathrm{B}(Q_\uparrow - Q_\downarrow) \quad , \tag{18.50}$$

while the magnetization density, $m(\mathbf{r})$ follows from the spin-resolved charge densities,

$$m(\mathbf{r}) = \mu_\mathrm{B}(\rho_\uparrow(\mathbf{r}) - \rho_\downarrow(\mathbf{r})) \quad . \tag{18.51}$$

18.3 Relativistic formulation

Starting from the expression in (3.255) the Green's function $G(z; \mathbf{r}+\mathbf{R}, \mathbf{r}+\mathbf{R})$ can be written as

$$G\left(z;\mathbf{r}+\mathbf{R},\mathbf{r}+\mathbf{R}\right)= \sum_{QQ'} Z_Q\left(z;\mathbf{r}\right)\,\tau_{QQ'}\left(z\right)\,\widetilde{Z}_{Q'}\left(z;\mathbf{r}\right)^{\dagger} - \sum_{Q} J_Q\left(z;\mathbf{r}\right)\,\widetilde{Z}_Q\left(z;\mathbf{r}\right)^{\dagger} \quad , \tag{18.52}$$

where the four-component scattering functions

$$Z_Q\left(z;\mathbf{r}\right)=\sum_{Q'}\begin{pmatrix} g^{Z}_{Q'Q}\left(z;r\right)\chi_{Q'}\left(\hat{\mathbf{r}}\right) \\ \mathrm{i}f^{Z}_{Q'Q}\left(z;r\right)\chi_{\bar{Q}'}\left(\hat{\mathbf{r}}\right)\end{pmatrix} \quad , \tag{18.53}$$

$$J_Q\left(z;\mathbf{r}\right)=\sum_{Q'}\begin{pmatrix} g^{J}_{Q'Q}\left(z;r\right)\chi_{Q'}\left(\hat{\mathbf{r}}\right) \\ \mathrm{i}f^{J}_{Q'Q}\left(z;r\right)\chi_{\bar{Q}'}\left(\hat{\mathbf{r}}\right)\end{pmatrix} \quad , \tag{18.54}$$

$$\widetilde{Z}_Q\left(z;\mathbf{r}\right)=\sum_{Q'}\begin{pmatrix} g^{\widetilde{Z}}_{Q'Q}\left(z;r\right)\chi_{Q'}\left(\hat{\mathbf{r}}\right) \\ \mathrm{i}f^{Z}_{Q'Q}\left(z;r\right)\chi_{\bar{Q}'}\left(\hat{\mathbf{r}}\right)\end{pmatrix} \quad , \tag{18.55}$$

are defined by their respective normalization conditions, see (3.230), (3.232) and (3.245). Note that for the case of a uniform (effective) magnetic field pointing along the z axis of the local frame of reference – as assumed in the local density functional theory – the following relationship applies, see also Chap. 3,

$$g^{\widetilde{Z}}_{Q'Q}\left(z;r\right)=g^{Z}_{Q'Q}\left(z;r\right)^{*} \quad , \tag{18.56}$$

$$f^{\widetilde{Z}}_{Q'Q}\left(z;r\right)=f^{Z}_{Q'Q}\left(z;r\right)^{*} \quad . \tag{18.57}$$

The Green's function in (18.52) can then be written in the following blockwise form,

$$G\left(z;\mathbf{r}+\mathbf{R},\mathbf{r}+\mathbf{R}\right)= \tag{18.58}$$

$$\sum_{QQ'}\begin{pmatrix} G^{11}_{QQ'}\left(z;r\right)\,\chi_Q\left(\hat{\mathbf{r}}\right)\chi_{Q'}\left(\hat{\mathbf{r}}\right)^{\dagger} & G^{12}_{QQ'}\left(z;r\right)\,\chi_Q\left(\hat{\mathbf{r}}\right)\chi_{\overline{Q}'}\left(\hat{\mathbf{r}}\right)^{\dagger} \\ G^{21}_{QQ'}\left(z;r\right)\,\chi_{\overline{Q}}\left(\hat{\mathbf{r}}\right)\chi_{Q'}\left(\hat{\mathbf{r}}\right)^{\dagger} & G^{22}_{QQ'}\left(z;r\right)\,\chi_{\overline{Q}}\left(\hat{\mathbf{r}}\right)\chi_{\overline{Q}'}\left(\hat{\mathbf{r}}\right)^{\dagger}\end{pmatrix} \quad ,$$

where

$$G^{11}_{QQ'}\left(z;r\right)=\sum_{Q''Q'''}\Big\{g^{Z}_{QQ''}\left(z;r\right)\tau_{Q''Q'''}\left(z\right)g^{\widetilde{Z}}_{Q'Q'''}\left(z;r\right)^{*} - \delta_{Q''Q'''}\,g^{J}_{QQ''}\left(z;r\right)g^{\widetilde{Z}}_{Q'Q'''}\left(z;r\right)^{*}\Big\} \quad , \tag{18.59}$$

$$G^{12}_{QQ'}\left(z;r\right)=-\mathrm{i}\sum_{Q''Q'''}\Big\{g^{Z}_{QQ''}\left(z;r\right)\tau_{Q''Q'''}\left(z\right)f^{\widetilde{Z}}_{Q'Q'''}\left(z;r\right)^{*} - \delta_{Q''Q'''}\,g^{J}_{QQ''}\left(z;r\right)f^{\widetilde{Z}}_{Q'Q'''}\left(z;r\right)^{*}\Big\} \quad , \tag{18.60}$$

$$G^{21}_{QQ'}(z;r) = \mathrm{i}\sum_{Q''Q'''}\Big\{f^{Z}_{QQ''}(z;r)\,\tau_{Q''Q'''}(z)\,g^{\tilde{Z}}_{Q'Q'''}(z;r)^{*} - \delta_{Q''Q'''}\,f^{J}_{QQ''}(z;r)\,g^{\tilde{Z}}_{Q'Q'''}(z;r)^{*}\Big\} \quad , \tag{18.61}$$

and

$$G^{22}_{QQ'}(z;r) = \sum_{Q''Q'''}\Big\{f^{Z}_{QQ''}(z;r)\,\tau_{Q''Q'''}(z)\,f^{\tilde{Z}}_{Q'Q'''}(z;r)^{*} - \delta_{Q''Q'''}\,f^{J}_{QQ''}(z;r)\,f^{\tilde{Z}}_{Q'Q'''}(z;r)^{*}\Big\} \quad . \tag{18.62}$$

18.3.1 Charge density

The charge density confined to a cell centered around the lattice position $\mathbf{R}$ is given as

$$\rho(\mathbf{r}) = -\frac{1}{\pi}\mathrm{Im}\int_{\curvearrowright}\mathrm{d}z\,\mathrm{Tr}G(z;\mathbf{r}+\mathbf{R},\mathbf{r}+\mathbf{R}) \ , \tag{18.63}$$

where Tr stands now for the trace over a 4×4 matrix. By using (18.58), (18.59) and (18.62) yields

$$\rho(\mathbf{r}) = -\frac{1}{\pi}\mathrm{Im}\sum_{QQ'}\left[G^{11}_{QQ'}(r)+G^{22}_{QQ'}(r)\right]\,\chi_{Q'}(\hat{\mathbf{r}})^{\dagger}\,\chi_{Q}(\hat{\mathbf{r}}) \tag{18.64}$$

$$= \sum_{QQ'}\left[I^{11}_{QQ'}(r)+I^{22}_{QQ'}(r)\right]\,\chi_{Q'}(\hat{\mathbf{r}})^{\dagger}\,\chi_{Q}(\hat{\mathbf{r}}) \quad , \tag{18.65}$$

where use was made of the identity,

$$\chi_{Q'}(\hat{\mathbf{r}})^{\dagger}\,\chi_{Q}(\hat{\mathbf{r}}) = \chi_{\overline{Q}'}(\hat{\mathbf{r}})^{\dagger}\,\chi_{\overline{Q}}(\hat{\mathbf{r}}) \quad , \tag{18.66}$$

and

$$G^{ij}_{QQ'}(r) = \int_{\curvearrowright}\mathrm{d}z\,G^{ij}_{LL'}(z;r) \quad , \quad i,j=1,2 \quad , \tag{18.67}$$

$$I^{ij}_{QQ'}(r) = -\frac{1}{2\pi\mathrm{i}}\left[G^{ij}_{QQ'}(r)-G^{ij}_{Q'Q}(r)^{*}\right] \quad , \quad i,j=1,2 \quad . \tag{18.68}$$

The radial functions $\rho_L(r)$ can easily be obtained in terms of the following integral,

$$\rho_L(r) = \int \mathrm{d}\hat{\mathbf{r}}\,\rho(\mathbf{r})Y_L(\hat{\mathbf{r}}) \ , \tag{18.69}$$

which by using (18.65) can be expressed as

$$\rho_L(r) = \sum_{i=1,2}\sum_{Q'Q''} I^{ii}_{Q''Q'}(r)\,\langle\chi_{Q'}|Y_L|\chi_{Q''}\rangle \ . \tag{18.70}$$

The occurring angular integrals $\langle\chi_{Q'}|Y_L|\chi_{Q''}\rangle$ are discussed in Sect. 11.1.5.

18.3.2 Spin and orbital magnetization densities

The "real-space" spin magnetization density $m_i^{\rm sp}(\mathbf{r})$, $i = x, y, z$, is defined by

$$m_i^{\rm sp}(\mathbf{r}) = -\frac{\mu_{\rm B}}{\pi}{\rm Im}\int\limits_{\curvearrowright} {\rm d}z\ {\rm Tr}\ \{\beta\Sigma_i G\,(z;\mathbf{r}+\mathbf{R},\mathbf{r}+\mathbf{R})\} \quad , \tag{18.71}$$

where as should be recalled

$$\beta = \begin{pmatrix} \mathsf{I}_2 & \\ & -\mathsf{I}_2 \end{pmatrix} \quad , \quad \Sigma_i = \begin{pmatrix} \sigma_i & \\ & \sigma_i \end{pmatrix} \quad , \tag{18.72}$$

I_2 is the 2×2 unity matrix and the σ_i are the Pauli matrices. Inserting again (18.58), (18.59) and (18.62) one obtains

$$\begin{aligned} m_i^{\rm sp}(\mathbf{r}) = -\frac{\mu_{\rm B}}{\pi}{\rm Im}\sum_{QQ'}\Big\{ & G^{11}_{QQ'}\,(r)\ \chi_{Q'}\,(\hat{\mathbf{r}})^\dagger\,\sigma_i\chi_Q\,(\hat{\mathbf{r}}) \\ & - G^{22}_{QQ'}\,(r)\ \chi_{\overline{Q}'}\,(\hat{\mathbf{r}})^\dagger\,\sigma_i\chi_{\overline{Q}}\,(\hat{\mathbf{r}})\Big\} \qquad (18.73) \\ = \mu_{\rm B}\sum_{QQ'}\Big\{ & I^{11}_{QQ'}\,(r)\ \chi_{Q'}\,(\hat{\mathbf{r}})^\dagger\,\sigma_i\chi_Q\,(\hat{\mathbf{r}}) \\ & - I^{22}_{QQ'}\,(r)\ \chi_{\overline{Q}'}\,(\hat{\mathbf{r}})^\dagger\,\sigma_i\chi_{\overline{Q}}\,(\hat{\mathbf{r}})\Big\} \quad . \qquad (18.74) \end{aligned}$$

The coefficients of the expansion,

$$m_i^{\rm sp}(\mathbf{r}) = \sum_L m_{i,L}^{\rm sp}(r)Y_L(\hat{\mathbf{r}})^* \quad , \tag{18.75}$$

can be found in a similar manner as in the case of the charge density:

$$\begin{aligned} m_{i,L}^{\rm sp}(r) &= \int {\rm d}\hat{\mathbf{r}}\, m_i^{\rm sp}(\mathbf{r})Y_L(\hat{\mathbf{r}}) \qquad (18.76) \\ &= \mu_{\rm B}\sum_{Q'Q''}\Big\{ I^{11}_{Q''Q'}\,(r)\ \langle\chi_{Q'}|\sigma_i Y_L|\chi_{Q''}\rangle \\ &\qquad - I^{22}_{Q''Q'}\,(r)\ \Big\langle\chi_{\overline{Q}'}|\sigma_i Y_L|\chi_{\overline{Q}''}\Big\rangle\Big\} \quad . \qquad (18.77) \end{aligned}$$

Since the density of the orbital magnetization, $m_i^{\rm orb}(\mathbf{r})$, $i = x, y, z$, is defined similar to that of the spin magnetization,

$$m_i^{\rm orb}(\mathbf{r}) = -\frac{\mu_{\rm B}}{\pi}{\rm Im}\int\limits_{\curvearrowright} {\rm d}z\ {\rm Tr}\ \{\beta L_i G\,(z;\mathbf{r}+\mathbf{R},\mathbf{r}+\mathbf{R})\} \quad , \tag{18.78}$$

with $\boldsymbol{L} = \boldsymbol{r}\times\boldsymbol{p}$ being the angular momentum operator, the derivation of the corresponding expansion,

$$m_i^{\rm orb}(\mathbf{r}) = \sum_L m_{i,L}^{orb}(r) Y_L(\hat{\mathbf{r}})^* \quad , \tag{18.79}$$

with

$$m_{i,L}^{\rm orb}(r) = \mu_{\rm B} \sum_{Q'Q''} \Big\{ I^{11}_{Q''Q'}(r) \, \langle \chi_{Q'} | L_i Y_L | \chi_{Q''} \rangle - I^{22}_{Q''Q'}(r) \left\langle \chi_{\overline{Q}'} | L_i Y_L | \chi_{\overline{Q}''} \right\rangle \Big\} \quad , \tag{18.80}$$

is straightforward; the evaluation of the matrix elements $\langle \chi_{Q'} | L_i Y_L | \chi_{Q''} \rangle$ will be described at the end of this section.

Integrated quantities like the charge, the spin and the orbital magnetic moments can be calculated in analogy to (18.36) by using the expressions for $\rho_L(r)$, $m_{i,L}^{\rm sp}(r)$ and $m_{i,L}^{\rm orb}(r)$, respectively.

18.3.3 Density of States

The local density of states $n(\varepsilon)$ is now defined by the below expression,

$$n(\varepsilon) = -\frac{1}{\pi} \, {\rm Im} \int\limits_{\Omega} {\rm d}\mathbf{r}_i \, {\rm Tr} G(\varepsilon; \mathbf{r}+\mathbf{R}, \mathbf{r}+\mathbf{R}) \tag{18.81}$$

$$= -\frac{1}{\pi} \, {\rm Im} \int\limits_{\rm BS} {\rm d}\mathbf{r}_i \, {\rm Tr} G(\varepsilon; \mathbf{r}+\mathbf{R}, \mathbf{r}+\mathbf{R}) \, \sigma(\mathbf{r}) \quad . \tag{18.82}$$

Inserting the angular momentum expansion of the shape function in (18.29) and using (18.58) for the Green's function yields

$$n(\varepsilon) = -\frac{1}{\pi} \, {\rm Im} \sum_{QQ'} \sum_{\Lambda} \langle \chi_{Q'} | Y_\Lambda | \chi_Q \rangle \int\limits_0^{r_{\rm BS}} {\rm d}r \, r^2 \, \left(G^{11}_{QQ'}(\varepsilon; r) + G^{22}_{QQ'}(\varepsilon; r) \right) \sigma_\Lambda(r) \quad , \tag{18.83}$$

where $\Lambda = (\lambda, m_\lambda)$ is a composite index of non-relativistic angular momentum quantum numbers.

In terms of (18.59) and (18.62), $n(\varepsilon)$ can then be written in the form of

$$n(\varepsilon) = -\frac{1}{\pi} \, {\rm Im} \sum_{QQ'} \left(\mathsf{N}^{ZZ}_{Q'Q}(\varepsilon) \, \tau_{QQ'}(\varepsilon) - \delta_{QQ'} \, \mathsf{N}^{JZ}_{Q'Q}(\varepsilon) \right) \quad , \tag{18.84}$$

with

$$\mathsf{N}^{ZZ}_{Q'Q}(\varepsilon) = \sum_{Q''Q'''} \sum_{\Lambda} \langle \chi_{Q'''} | Y_\Lambda | \chi_{Q''} \rangle \int\limits_0^{r_{\rm BS}} {\rm d}r \, r^2 \left(g^{Z}_{Q''Q}(\varepsilon; r) \, g^{\widetilde{Z}}_{Q'''Q'}(\varepsilon; r)^* + f^{Z}_{Q''Q}(\varepsilon; r) \, f^{\widetilde{Z}}_{Q'''Q'}(\varepsilon; r)^* \right) \sigma_\Lambda(r) \quad , \tag{18.85}$$

and

$$\mathsf{N}^{JZ}_{Q'Q}(\varepsilon) = \sum_{Q''Q'''} \sum_{\Lambda} \langle \chi_{Q''} | Y_\Lambda | \chi_{Q'''} \rangle \int_0^{r_{\rm BS}} \mathrm{d}r\, r^2 \tag{18.86}$$
$$\left(g^J_{Q''Q}(\varepsilon;r)\, g^{\tilde{Z}}_{Q'''Q'}(\varepsilon;r)^* + f^J_{Q''Q}(\varepsilon;r)\, f^{\tilde{Z}}_{Q'''Q'}(\varepsilon;r)^* \right) \sigma_\Lambda(r) \quad ,$$

or, by utilizing (18.35),

$$\mathsf{N}^{ZZ}_{Q'Q}(\varepsilon) = \sqrt{4\pi} \sum_{Q''} \int_0^{r_{\rm MT}} \mathrm{d}r\, r^2 \tag{18.87}$$
$$\left(g^Z_{Q''Q}(\varepsilon;r_i)\, g^{\tilde{Z}}_{Q''Q'}(\varepsilon;r)^* + f^Z_{Q''Q}(\varepsilon;r)\, f^{\tilde{Z}}_{Q''Q'}(\varepsilon;r)^* \right)$$
$$+ \sum_{Q''Q'''} \sum_{\Lambda} \langle \chi_{Q'''} | Y_\Lambda | \chi_{Q''} \rangle \int_{r_{\rm MT}}^{r_{\rm BS}} \mathrm{d}r\, r^2$$
$$\left(g^Z_{Q''Q}(\varepsilon;r)\, g^{\tilde{Z}}_{Q'''Q'}(\varepsilon;r)^* + f^Z_{Q''Q}(\varepsilon;r)\, f^{\tilde{Z}}_{Q'''Q'}(\varepsilon;r)^* \right) \sigma_\Lambda(r) \ ,$$

with similar expressions pertaining for $\mathsf{N}^{JZ}_{Q'Q}(\varepsilon)$. It is tempting to introduce again the concept of a density matrix, $\{n_{QQ'}(\varepsilon)\}$,

$$n_{QQ'}(\varepsilon) = -\frac{1}{\pi}\, \mathrm{Im} \left\{ \sum_{Q''} \mathsf{N}^{ZZ}_{QQ''}(\varepsilon)\, \tau_{Q''Q'}(\varepsilon) - \delta_{QQ'}\, \mathsf{N}^{JZ}_{QQ'}(\varepsilon) \right\} \quad , \tag{18.88}$$

according to which

$$n(\varepsilon) = \mathrm{Tr}\{n_{QQ'}(\varepsilon)\} = \sum_Q n_{QQ}(\varepsilon) \quad , \tag{18.89}$$

and accordingly the $\kappa\mu-$like partial local DOS can be defined as

$$n_{\kappa\mu}(\varepsilon) = n_{\kappa\mu,\kappa\mu}(\varepsilon) \quad , \tag{18.90}$$

while the $\kappa-$like partial local DOS is given by

$$n_\kappa(\varepsilon) = \sum_{\mu=-j}^{j} n_{\kappa\mu}(\varepsilon) \quad . \tag{18.91}$$

By using the transformation between the $\kappa\mu$-representation and the ℓms-representation, see (3.173), a ℓms-like partial DOS can be defined as follows,

$$n_{\ell ms,\ell' m' s'}(\varepsilon) = \sum_{j=\ell\pm\frac{1}{2}} \sum_{j'=\ell'\pm\frac{1}{2}} C(\ell j 1/2; m+s, s) \tag{18.92}$$
$$n_{\ell j(m+s),\ell' j'(m'+s')}(\varepsilon)\, C(\ell' j' 1/2; m'+s', s') \quad ,$$

such that

$$n_{\ell ms}(\varepsilon) \equiv n_{\ell ms,\ell ms}(\varepsilon) \quad , \tag{18.93}$$

and

$$n(\varepsilon) \equiv \sum_{\ell ms} n_{\ell ms}(\varepsilon) \quad . \tag{18.94}$$

However, since the density matrix is not diagonal in spin-space, an interpretation of the DOS with respect to "spin-channels" is rather limited within a relativistic theory. Treating the spin-orbit coupling as a second (or higher order) perturbation clearly causes mixing of the "spin-channels" that in turn gives rise, e.g., to the magnetocrystalline anisotropy not present within a non-relativistic theory.

18.3.4 Angular momentum operators and matrix elements

For matters of convenience in the following the notation and the basic properties of spin spherical harmonics are repeated ($\hbar = 1$):

$$|\chi_Q\rangle = |\ell j \mu\rangle \quad , \tag{18.95}$$

$$J_z\ |\ell j \mu\rangle = \mu\ |\ell j \mu\rangle \quad , \tag{18.96}$$

$$J_\pm\ |\ell j \mu\rangle = \sqrt{j(j+1) - \mu(\mu \pm 1)}\ |\ell j (\mu \pm 1)\rangle \quad , \tag{18.97}$$

where

$$J_\pm = J_x \pm i\, J_y \quad , \tag{18.98}$$

and $\boldsymbol{J}$,

$$\boldsymbol{J} = \boldsymbol{L} + \boldsymbol{S} \quad , \tag{18.99}$$

is the total angular momentum operator. Since

$$J_x = \frac{1}{2}\,(J_+ + J_-) \quad , \quad J_y = \frac{1}{2\mathrm{i}}\,(J_+ - J_-) \quad , \tag{18.100}$$

the matrix elements $\langle \ell j \mu | J_i\, Y_\Lambda | \ell' j' \mu' \rangle$ can easily be expressed as a combination of the matrix elements of the type $\langle \ell j \mu | Y_\Lambda | \ell' j' \mu' \rangle$,

$$\begin{aligned} \langle \ell j \mu | J_x\, Y_\Lambda | \ell' j' \mu' \rangle = {} & \frac{1}{2}\sqrt{j'(j'+1) - \mu'(\mu'+1)}\ \langle \ell j \mu | Y_\Lambda | \ell' j' (\mu'+1) \rangle \\ & + \frac{1}{2}\sqrt{j'(j'+1) - \mu'(\mu'-1)}\ \langle \ell j \mu | Y_\Lambda | \ell' j' (\mu'-1) \rangle \end{aligned} \tag{18.101}$$

$$\begin{aligned} \langle \ell j \mu | J_y\, Y_\Lambda | \ell' j' \mu' \rangle = {} & \frac{1}{2\mathrm{i}}\sqrt{j'(j'+1) - \mu'(\mu'+1)}\ \langle \ell j \mu | Y_\Lambda | \ell' j' (\mu'+1) \rangle \\ & - \frac{1}{2\mathrm{i}}\sqrt{j'(j'+1) - \mu'(\mu'-1)}\ \langle \ell j \mu | Y_\Lambda | \ell' j' (\mu'-1) \rangle \end{aligned} \tag{18.102}$$

$$\langle \ell j \mu | J_z\, Y_\Lambda | \ell' j' \mu' \rangle = \mu'\ \langle \ell j \mu | Y_\Lambda | \ell' j' \mu' \rangle \quad . \tag{18.103}$$

The matrix elements $\langle \ell j \mu | L_i \, Y_\Lambda | \ell' j' \mu' \rangle$ are then given by

$$\langle \ell j \mu | L_i \, Y_\Lambda | \ell' j' \mu' \rangle = \langle \ell j \mu | J_i \, Y_\Lambda | \ell' j' \mu' \rangle - \frac{1}{2} \, \langle \, \ell j \mu | \sigma_i \, Y_\Lambda | \ell' j' \mu' \rangle \quad . \tag{18.104}$$

18.4 2D Brillouin zone integrations

Calculations of surfaces or interfaces require to average periodic functions over the two-dimensional Brillouin zone. These averages involve sampling over specific sets of k-points and a summation with appropriate weighting factors for each k. Methods of choosing such sets for three-dimensional Brillouin zones are discussed in [1]– [8]. In here the discussion of [9] is summarized for the two-dimensional cases with special emphasis to fcc and bcc lattices.

In principle, a periodic function $f(\mathbf{k})$ can be expanded as

$$f(\mathbf{k}) = f_0 + \sum_{m \, = \, 1}^{\infty} f_m \, A_m(\mathbf{k}) \quad , \tag{18.105}$$

with

$$A_m(\mathbf{k}) = \sum_{|\mathbf{R}| \, = \, c_m} e^{\mathrm{i}\mathbf{k}\cdot\mathbf{R}} \, , \quad m = 1, 2, \ldots \quad , \tag{18.106}$$

where $\mathbf{k}$ is a vector in the Brillouin zone. The summation in (18.106) is performed over equivalent lattice vectors $\mathbf{R} \in \mathcal{L}^{(2)}$, i.e., vectors of equal magnitude c_m. Thus the $A_m(\mathbf{k})$ can be ordered according to increasing magnitudes of $\mathbf{R}$: each $A_m(\mathbf{k})$ can then be associated with a particular shell of lattice vectors.

Since f_0 is the exact average of $f(\mathbf{k})$ over the two-dimensional Brillouin zone, the second term in (18.105) has to vanish, which in turn implies that the best set of points $\{k_i\}$ and weighting factors $\{w_i\}$ need to be found in order to yield the most accurate approximation to f_0.

Defining for a chosen set of points $\mathbf{k}_i$ the following quantities

$$\sum_i w_i A_m(\mathbf{k}_i) \, , \quad m = 1, 2, \ldots, N \quad , \tag{18.107}$$

where N is the number of functions $A_m(\mathbf{k})$ and

$$\sum_i w_i = 1 \quad , \tag{18.108}$$

it is obvious from (18.105) that

$$f_0 = \sum_i w_i f(\mathbf{k}_i) - \sum_{m \, > \, N}^{\infty} f_m \sum_i w_i A_m(\mathbf{k}_i) \quad . \tag{18.109}$$

As the coefficients f_m usually decrease quickly with increasing m, for a sufficiently large N the exact average f_0 can be approximated by

$$f_0 = \sum_i w_i f(\mathbf{k}_i) \quad . \tag{18.110}$$

Suppose that $\mathbf{k}_1$ satisfies the condition $A_m(\mathbf{k}_1) = 0$ for several values of m belonging to the set $\{N_1\}$, and $\mathbf{k}_2$ the condition $A_m(\mathbf{k}_2) = 0$ for certain values of m from the set $\{N_2\}$. With $\mathbf{k}_1$ and $\mathbf{k}_2$ a new set of points can be generated that satisfies (18.107) for m being in either from $\{N_1\}$ or $\{N_2\}$. The new points $\mathbf{k}_i$ are related to $\mathbf{k}_1$ and $\mathbf{k}_2$ via

$$\mathbf{k}_i = \mathbf{k}_1 + D(S_i)\mathbf{k}_2 \,, \quad i = 1, 2, \ldots, n_G \quad , \tag{18.111}$$

where i varies over all symmetry operations S_i of the point group G corresponding to the chosen lattice and the $D(S_i)$ are the corresponding irreducible representations in $\mathbb{R}^3$. The weighting factor is then given by

$$w_i = |G|^{-1} \quad , \tag{18.112}$$

where $|G|$ is the order of G. The vectors obtained thus can be used to generate further vectors by means of the below equations,

$$\mathbf{k}_n = \mathbf{k}_i + D(S_j)\mathbf{k}_3 \,, \quad i = 1, 2, \ldots, n_G \quad , \tag{18.113}$$

$$w_n = |G|^{-2} \quad , \tag{18.114}$$

provided that for m in $\{N_3\}$ the condition $A_m(\mathbf{k}_3) = 0$ is fulfilled.

The *generating vectors* are chosen in the following manner. Initially a vector $\mathbf{k}_1$ is selected such that functions of the type $A_1(\mathbf{k}_1) = 0$ corresponding thus to all those $\mathbf{R} \in \mathcal{L}^{(2)}$ of equal length which are closest to the lattice point of interest ($m = 1$). Then, by varying m as many other functions $A_m(\mathbf{k}_1)$, $A_m(\mathbf{k}_1) = 0$, as possible are evaluated. For the first function $A_m(\mathbf{k}_1)$, $A_m(\mathbf{k}_1) \neq 0$, a second vector $\mathbf{k}_2$ is determined such that for functions of the type $A_m(\mathbf{k}_2)$, $A_m(\mathbf{k}_2) = 0$. Again m is varied in search of vanishing functions $A_m(\mathbf{k}_2)$. By applying finally (18.111) a particular set of k-points, $\{k_i\}$, is found. The last steps, i.e., finding an appropriate $\mathbf{k}_3, \mathbf{k}_4$, etc., are then repeated several times until the set of k-points needed is generated.

In the following a distinction between sets of generating vectors $\mathbf{k}_1$, $\mathbf{k}_2$, ..., and particular sets of special points $\{k_i\}$ will be made, which eventually are used for evaluating Brillouin zone integrals. These sets can be large in number, whereas the sets of generating vectors are rather small.

18.5 Primitive vectors in two-dimensional lattices

Generally, the two basis vectors forming a primitive cell in direct space are given by

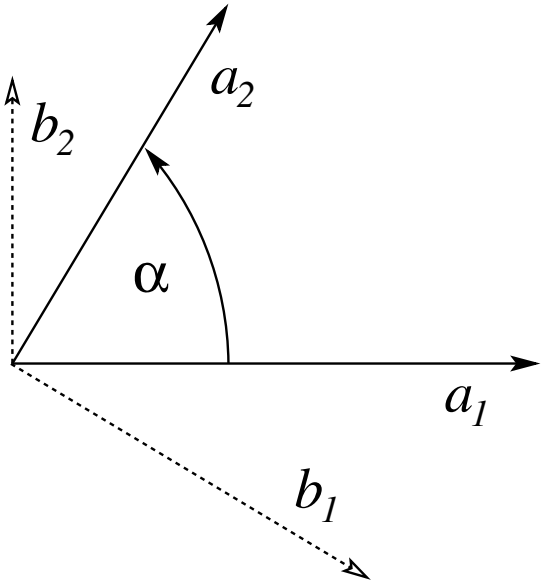

Fig. 18.1. The two-dimensional real space primitive vectors $\mathbf{a}_1$, $\mathbf{a}_2$ and the corresponding vectors in reciprocal space, labelled by $\mathbf{b}_1$, $\mathbf{b}_2$. One can see that $\mathbf{b}_1$ ($\mathbf{b}_2$) is perpendicular to $\mathbf{a}_2$ ($\mathbf{a}_1$).

$$\mathbf{a}_1 = a_{2\mathrm{D}} \begin{pmatrix} 1 \\ 0 \end{pmatrix} , \quad \mathbf{a}_2 = \beta\, a_{2\mathrm{D}} \begin{pmatrix} \cos\alpha \\ \sin\alpha \end{pmatrix} \quad , \tag{18.115}$$

where α is the angle between $\mathbf{a}_1$ and $\mathbf{a}_2$, and β is the so-called *asymmetry ratio* of the primitive cell: $\beta = 1$, if $\mathbf{a}_1$ and $\mathbf{a}_2$ are of the same length. Any arbitrary vector $\mathbf{R} \in \mathcal{L}^{(2)}$ is then given by

$$\mathbf{R} = l\mathbf{a}_1 + n\mathbf{a}_2 \quad , \quad l, n \in \mathbb{Z} \quad , \tag{18.116}$$

where $\mathbb{Z}$ is the field of integer numbers, see also Chap. 2. Because of the relation

$$\mathbf{a}_i \cdot \mathbf{b}_j = 2\pi\, \delta_{ij} , \quad i, j = 1, 2 \quad , \tag{18.117}$$

the primitive vectors in $\mathcal{L}^{(2d)}$, $\mathbf{b}_1$ and $\mathbf{b}_2$, are given by

$$\mathbf{b}_1 = \frac{2\pi}{a_{2\mathrm{D}} \sin\alpha} \begin{pmatrix} \sin\alpha \\ -\cos\alpha \end{pmatrix} , \quad \mathbf{b}_2 = \frac{2\pi}{\beta\, a_{2\mathrm{D}} \sin\alpha} \begin{pmatrix} 0 \\ 1 \end{pmatrix} \quad . \tag{18.118}$$

18.6 Oblique lattice

A general oblique lattice can be defined in terms of the following primitive vectors:

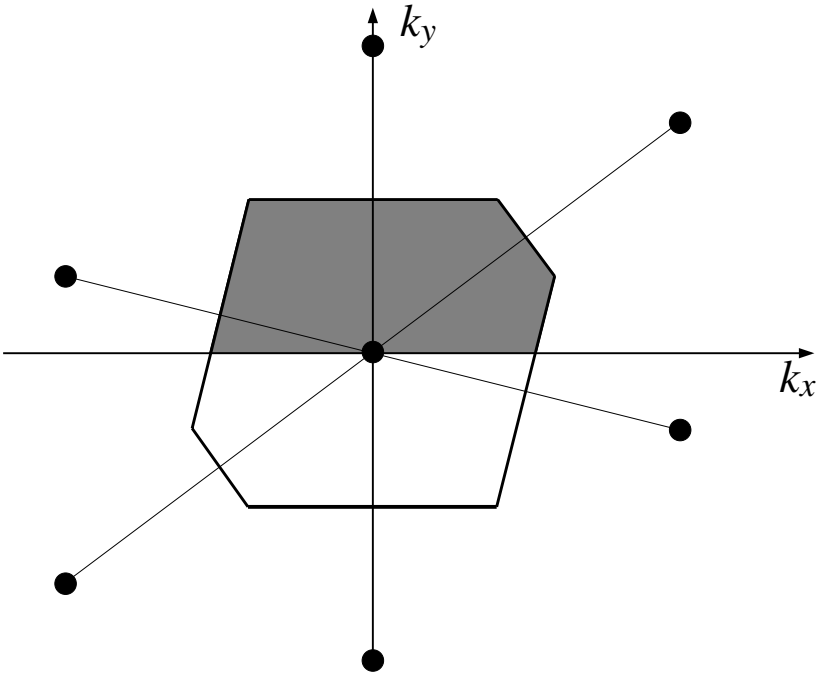

Fig. 18.2. Brillouin zone of an oblique lattice and its irreducible wedge (shaded) for the case $\delta = 1/4$ and $\beta = 1/2$.

$$\mathbf{a}_1 = a_{2\mathrm{D}} \begin{pmatrix} 1 \\ 0 \end{pmatrix} , \quad \mathbf{a}_2 = a_{2\mathrm{D}} \begin{pmatrix} \delta \\ \beta \end{pmatrix} \quad , \tag{18.119}$$

where $|\delta| \leq 1/2$ and $\beta < 1/2$. An arbitrary lattice vector refers then to the position

$$\mathbf{R} = a_{2\mathrm{D}} \begin{pmatrix} l + n\delta \\ n\beta \end{pmatrix} \quad , \quad l, n \in \mathbb{Z} \quad , \tag{18.120}$$

and the primitive vectors in $\mathcal{L}^{(2d)}$ are given by

$$\mathbf{b}_1 = \frac{2\pi}{a_{2\mathrm{D}}} \begin{pmatrix} 1 \\ -\delta/\beta \end{pmatrix} , \quad \mathbf{b}_2 = \frac{2\pi}{a_{2\mathrm{D}}} \begin{pmatrix} 0 \\ 1/\beta \end{pmatrix} \quad . \tag{18.121}$$

Fig. 18.2 shows the Brillouin zone of this lattice type for $\delta = 1/4$ and $\beta = 1/2$.

The functions $A_m(\mathbf{k})$ are now of the general form

$$A_m(\mathbf{k}) = 2 \cos a \left[k_x \left(l + n\delta \right) + k_y n\beta \right] \quad . \tag{18.122}$$

For $\beta > 1/2$ a good choice for $\mathbf{k}_1$ is the following one,

$$\mathbf{k}_1 = \frac{\pi}{a_{2\mathrm{D}}} \begin{pmatrix} 0 \\ 1/(2\beta) \end{pmatrix} \quad , \tag{18.123}$$

as all $A_1(\mathbf{k}_1) = 0$ for all pairs of indices (l, n) for which $l = 0$ and n is an odd integer. The first non-vanishing function $A_2(\mathbf{k}_1)$ contains the lattice point $\mathbf{R} = a_{2D}(1, 0)$. The vector $\mathbf{k}_2$ for which $A_2(\mathbf{k}_2) = 0$ is then given by

$$\mathbf{k}_2 = \frac{\pi}{a_{2D}} \begin{pmatrix} 1/2 \\ 0 \end{pmatrix} \quad , \tag{18.124}$$

for which all functions with odd l and $n = 0$ vanish.

In order to construct a particular set of k-points, $\{k_i\}$, (18.111) has to be applied. Since the point group of the oblique lattice consists only of the identity and a rotation by π, one obtains only two special points, namely

$$\mathbf{k} = \frac{\pi}{a_{2D}} \begin{pmatrix} 1/2 \\ 1/(2\beta) \end{pmatrix}, \quad \mathbf{k}' = \frac{\pi}{a_{2D}} \begin{pmatrix} -1/2 \\ 1/(2\beta) \end{pmatrix} \quad , \tag{18.125}$$

with identical weights $w = 1/2$. By determining the next function $A_3(\mathbf{k}_2)$, $A_3(\mathbf{k}_2) \neq 0$, and a vector $\mathbf{k}_3$ such that $A_3(\mathbf{k}_2) = 0$, one obtains a set of three generating vectors, and so forth.

18.7 Centered rectangular lattice

This is a special case of the oblique lattice type with $\delta = 1/2$ and $\beta < 1$. The primitive vectors are given by

$$\mathbf{a}_1 = a_{2D} \begin{pmatrix} 1 \\ 0 \end{pmatrix}, \quad \mathbf{a}_2 = a_{2D} \begin{pmatrix} 1/2 \\ 1/2\beta \end{pmatrix} \quad . \tag{18.126}$$

and in $\mathcal{L}^{(2d)}$ by

$$\mathbf{b}_1 = \frac{2\pi}{a_{2D}} \begin{pmatrix} 1 \\ -1/\beta \end{pmatrix}, \quad \mathbf{b}_2 = \frac{2\pi}{a_{2D}} \begin{pmatrix} 0 \\ 2/\beta \end{pmatrix} \quad , \tag{18.127}$$

see also Fig. 18.3. The real space lattice vectors are defined by

$$\mathbf{R} = a_{2D} \begin{pmatrix} l + 1/2n \\ 1/2n\beta \end{pmatrix} \quad , \quad l, n \in \mathbb{Z} \quad , \tag{18.128}$$

and the functions $A_m(\mathbf{k})$ by

$$A_m(\mathbf{k}) = \sum_{l,m} e^{\mathrm{i}a[k_x(l+1/2n)+k_y 1/2n\beta]} \quad . \tag{18.129}$$

For any ring of lattice vectors of equal length corresponding to an odd n or odd $n/2 \in \mathbb{Z}$ for all values of l the first generating vector $\mathbf{k}_1$ is given by

$$\mathbf{k}_1 = \frac{\pi}{a_{2D}} \begin{pmatrix} 1 \\ 1/\left(2\beta\right) \end{pmatrix} \quad , \tag{18.130}$$

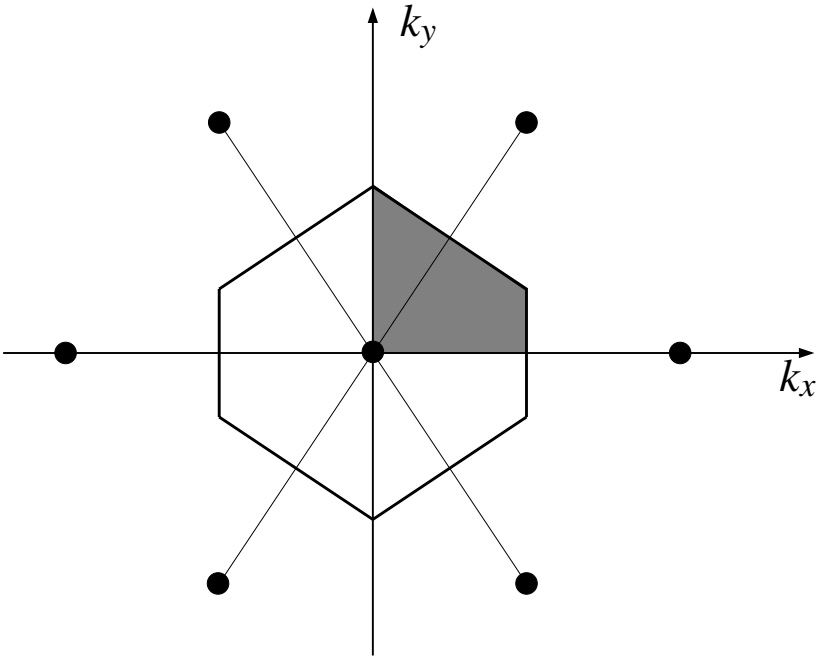

Fig. 18.3. Brillouin zone of a centered rectangular lattice and its irreducible wedge (shaded) for the case $\beta = 2/3$.

and $\mathbf{k}_2$ by

$$\mathbf{k}_2 = \frac{\pi}{a_{2\mathrm{D}}} \begin{pmatrix} 1/2 \\ 1/\left(4\beta\right) \end{pmatrix} \quad . \tag{18.131}$$

Because the point group of this lattice is of order four, from (18.111) four special k-points result, each having a weight $w = 1/4$. If a third generating vector $\mathbf{k}_3$ is used, 16 special k-points can be generated.

This particular two-dimensional lattice refers to bcc (110) structures, where

$$a_{2\mathrm{D}} = a\sqrt{2} \tag{18.132}$$

$\beta = 1/\sqrt{2}$ and a is the lattice constant of the three-dimensional lattice.

18.8 Primitive rectangular lattice

The primitive (real space) vectors are now given by

$$\mathbf{a}_1 = a_{2\mathrm{D}} \begin{pmatrix} 1 \\ 0 \end{pmatrix} , \quad \mathbf{a}_2 = a_{2\mathrm{D}} \begin{pmatrix} 0 \\ \beta \end{pmatrix} \quad , \tag{18.133}$$

the real space lattice by

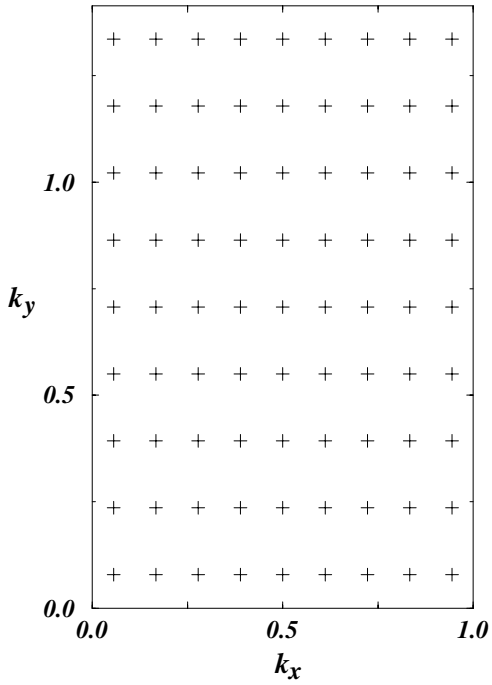

Fig. 18.4. Distribution of a set of 81 k points in the irreducible part of the Brillouin zone of a two-dimensional rectangular lattice for a fcc (110) plane.

$$\mathbf{R} = a_{2\mathrm{D}} \begin{pmatrix} l \\ n\beta \end{pmatrix} \quad , \quad l, n \in \mathbb{Z} \quad , \tag{18.134}$$

and the (primitive) reciprocal vectors are defined by

$$\mathbf{b}_1 = \frac{2\pi}{a_{2\mathrm{D}}} \begin{pmatrix} 1 \\ 0 \end{pmatrix} , \quad \mathbf{b}_2 = \frac{2\pi}{a_{2\mathrm{D}}} \begin{pmatrix} 0 \\ 1/\beta \end{pmatrix} \quad , \tag{18.135}$$

with $\beta < 1$. Consequently the functions $A_m(\mathbf{k})$ are given by

$$A_m(\mathbf{k}) = \sum_{l,n} e^{\mathrm{i}a(k_x l + k_y n\beta)} \quad , \tag{18.136}$$

and the first generating vector $\mathbf{k}_1$ by

$$\mathbf{k}_1 = \frac{\pi}{a_{2\mathrm{D}}} \begin{pmatrix} 1/2 \\ 1/(2\beta) \end{pmatrix} \quad , \tag{18.137}$$

for which $A_m(\mathbf{k}_1) = 0$ for any ring of lattice vectors with odd l or odd n. The second generating vector is found to be

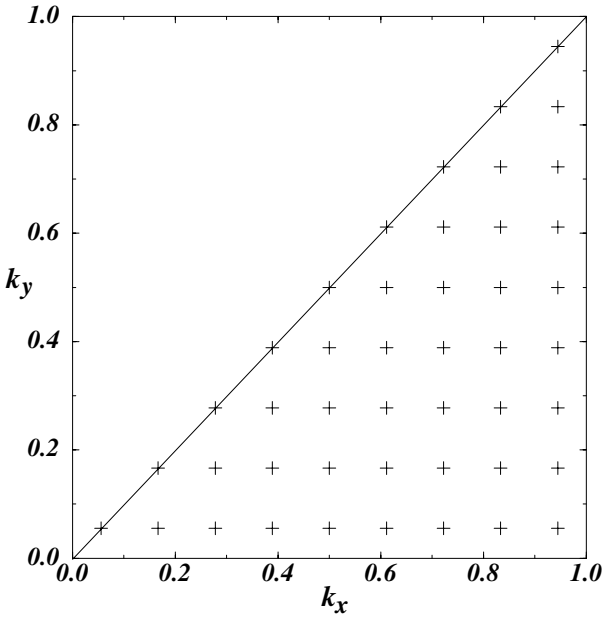

Fig. 18.5. Distribution of a set of 45 k points in the irreducible part of the Brillouin zone of a two-dimensional square lattice for a fcc or bcc (001) plane.

$$\mathbf{k}_2 = \frac{\pi}{a_{2\mathrm{D}}} \begin{pmatrix} 1/4 \\ 1/\left(4\beta\right) \end{pmatrix} \quad , \tag{18.138}$$

for which all $A_m(\mathbf{k}_2) = 0$ corresponding to an odd $l/2$ or odd $n/2 \in \mathbb{Z}$. Together with a third generating vector this results in a set of 16 special k-points.

This type of lattice refers for example to fcc(110) structures and is displayed in Fig. 18.4, where the two-dimensional lattice constant $a_{2\mathrm{D}} = a$ and $\beta = 1/\sqrt{2}$.

18.9 Square lattice

This is a special case of a primitive rectangular lattice with $\beta = 1$. According to (18.115) the primitive vectors are given by

$$\mathbf{a}_1 = a_{2\mathrm{D}} \begin{pmatrix} 1 \\ 0 \end{pmatrix}, \quad \mathbf{a}_2 = a_{2\mathrm{D}} \begin{pmatrix} 0 \\ 1 \end{pmatrix} \quad , \tag{18.139}$$

$\mathcal{L}^{(2)}$ consists of vectors of the form

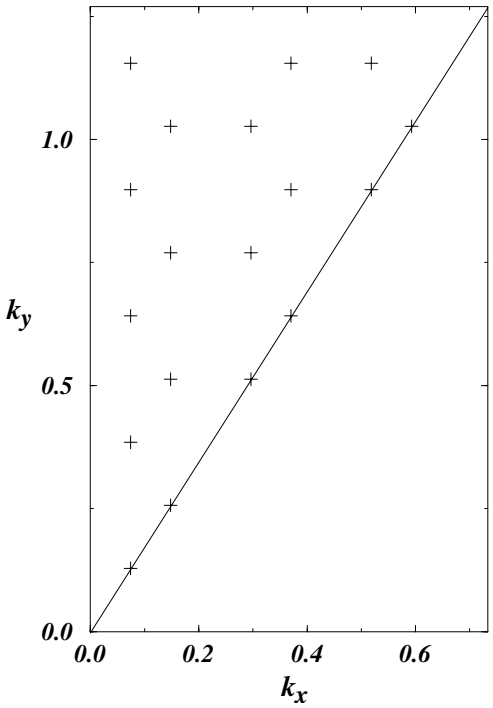

Fig. 18.6. Distribution of k points in the irreducible part of the Brillouin zone of a two-dimensional hexagonal lattice for a fcc or bcc (111) plane.

$$\mathbf{R} = a_{2\mathrm{D}} \begin{pmatrix} l \\ n \end{pmatrix} \quad , \quad l, n \in \mathbb{Z} \quad , \tag{18.140}$$

and the basis vectors in reciprocal space are defined by

$$\mathbf{b}_1 = \frac{2\pi}{a_{2\mathrm{D}}} \begin{pmatrix} 1 \\ 0 \end{pmatrix} , \quad \mathbf{b}_2 = \frac{2\pi}{a_{2\mathrm{D}}} \begin{pmatrix} 0 \\ 1 \end{pmatrix} \quad , \tag{18.141}$$

see (18.118).

The generating vectors $\mathbf{k}_1$ and $\mathbf{k}_2$ for this lattice are the same as for the primitive rectangular lattice by setting $\beta = 1$. The irreducible segment of the Brillouin zone, however, is smaller than for a rectangular lattice, $\beta \neq 1$, and therefore only a reduced number of wave vectors is needed, see Fig. 18.5. This kind of lattice refers, e.g., to fcc or bcc (001) planes. The two-dimensional lattice constant is related to the three-dimensional constant a via $a_{2\mathrm{D}} = a/\sqrt{2}$.

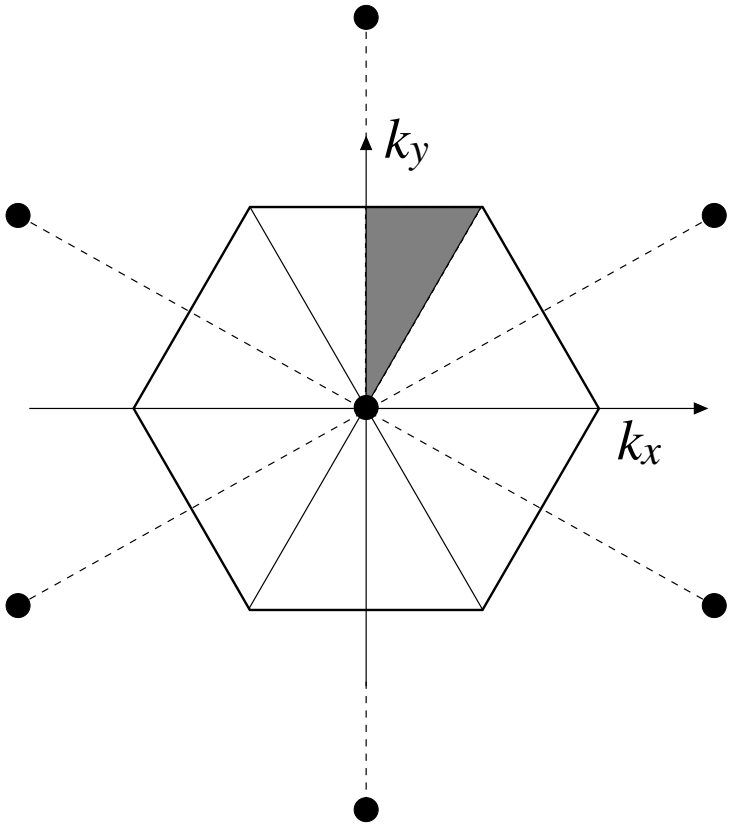

Fig. 18.7. First Brillouin zone in a two-dimensional hexagonal lattice with the lattice points indicated by filled circles.

18.10 Hexagonal lattice

Fcc or bcc planes perpendicular to the (111) direction, see Fig. 18.7, correspond to a two-dimensional hexagonal lattice with $a_{2\mathrm{D}} = a/\sqrt{2}$. The spanning vectors of the two-dimensional primitive cell are given by (18.115) using $\beta = 1$ and $\alpha = \pi/3$, namely by

$$\mathbf{a}_1 = a_{2\mathrm{D}} \begin{pmatrix} 1 \\ 0 \end{pmatrix} , \quad \mathbf{a}_2 = a_{2\mathrm{D}} \begin{pmatrix} 1/2 \\ \sqrt{3}/2 \end{pmatrix} \quad . \tag{18.142}$$

$\mathcal{L}^{(2)}$ refers to vectors of the type

$$\mathbf{R} = a_{2\mathrm{D}} \begin{pmatrix} l + 1/2n \\ \sqrt{3}/2n\beta \end{pmatrix} \quad , \quad l, n \in \mathbb{Z} \quad , \tag{18.143}$$

and the reciprocal primitive vectors are defined as

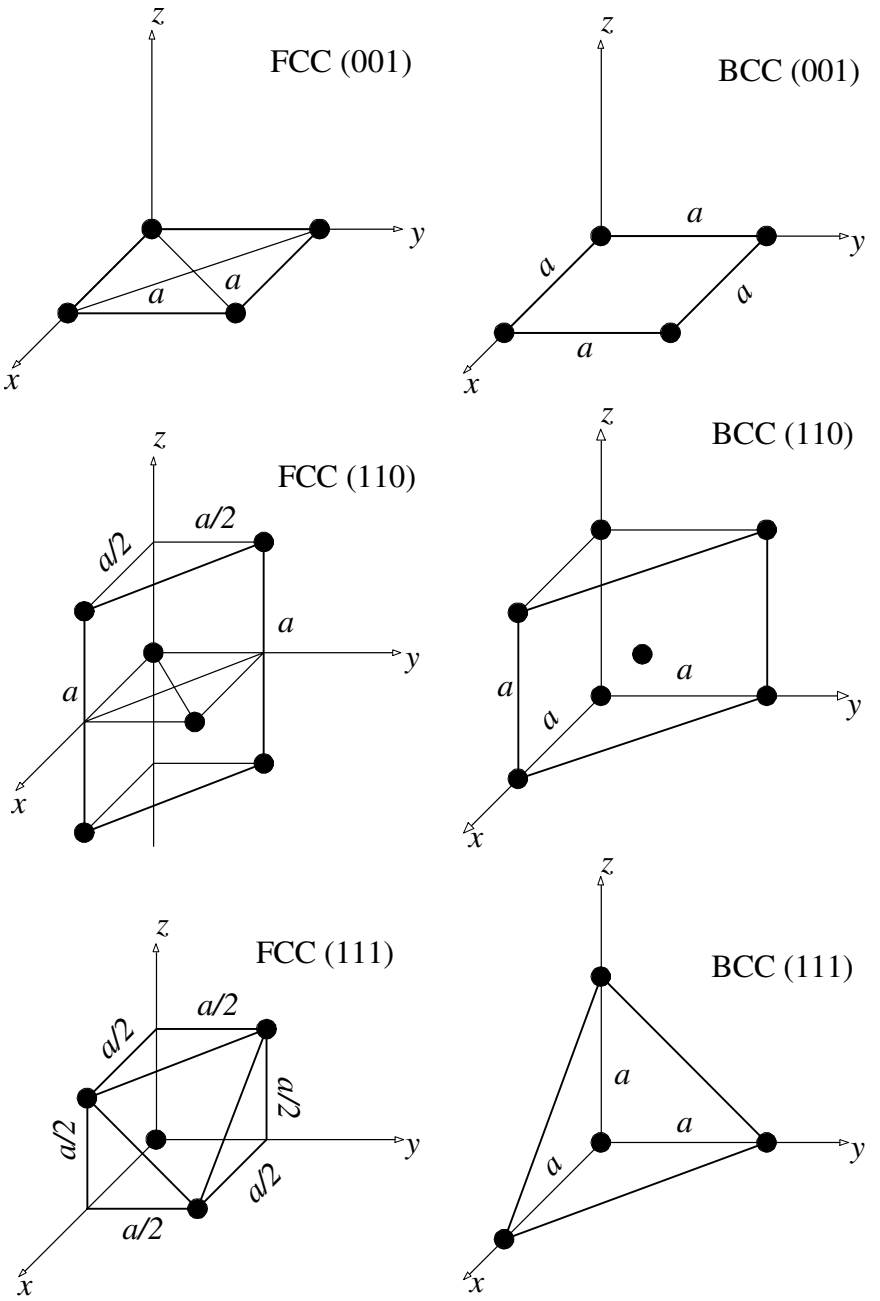

Fig. 18.8. Fcc and bcc (001), (110) and (111) planes. Indicated are the relations to the three-dimensional lattice constant a.

$$\mathbf{b}_1 = \frac{2\pi}{a_{2\mathrm{D}}} \begin{pmatrix} 1 \\ -1/\sqrt{3} \end{pmatrix}, \quad \mathbf{b}_2 = \frac{2\pi}{a_{2\mathrm{D}}} \begin{pmatrix} 0 \\ 2/\sqrt{3} \end{pmatrix} \quad . \tag{18.144}$$

The functions $A_m(\mathbf{k})$ are then given by

$$A_m(\mathbf{k}) = \sum_{l,n} e^{\mathrm{i}a\left[k_x(l+1/2n)+k_y\sqrt{3}/2n\beta\right]} \quad . \tag{18.145}$$

For $(l, n) = (0, 1)$, $(1, 0)$, $(1, -1)$, generating the first ring of lattice vectors, $A_1(\mathbf{k})$ is of the general form

$$\begin{aligned} A_1(\mathbf{k}) &= 2\cos\left(a_{2\mathrm{D}}k_x\right) + 2\cos\left(a_{2\mathrm{D}}\left(\frac{1}{2}k_x + \frac{\sqrt{3}}{2}k_y\right)\right) \\ &\quad + 2\cos\left(a_{2\mathrm{D}}\left(\frac{1}{2}k_x - \frac{\sqrt{3}}{2}k_y\right)\right) \qquad (18.146) \\ &= 2\cos\left(a_{2\mathrm{D}}k_x\right) + 4\cos\left(\frac{1}{2}k_x a_{2D}\right)\cos\left(\frac{\sqrt{3}}{2}k_y a_{2\mathrm{D}}\right) \quad . \qquad (18.147) \end{aligned}$$

The first four generating vectors are then given by

$$\mathbf{k}_1 = \frac{\pi}{a_{2\mathrm{D}}} \begin{pmatrix} 2/3 \\ 2\sqrt{3}/3 \end{pmatrix} \tag{18.148}$$

$$\mathbf{k}_2 = \frac{\pi}{a_{2\mathrm{D}}} \begin{pmatrix} 4/9 \\ 0 \end{pmatrix} \tag{18.149}$$

$$\mathbf{k}'_1 = \frac{\pi}{a_{2\mathrm{D}}} \begin{pmatrix} 2/9 \\ 2\sqrt{3}/9 \end{pmatrix} \tag{18.150}$$

$$\mathbf{k}'_2 = \frac{\pi}{a_{2\mathrm{D}}} \begin{pmatrix} 4/27 \\ 0 \end{pmatrix} \quad . \tag{18.151}$$

which then generate a set of 18 special k-points. In Fig. 18.6 an example of the distribution of k points in the irreducible segment of the first Brillouin zone, see Fig. 18.7, is displayed.

References

1. G. Lehmann and M. Taut, Phys. Status Solidi B **54**, 469 (1972).
2. W.R. Fehlner and S.H. Vosko, Can. J. Phys. **54**, 2159 (1976).
3. A. Bansil, Solid State Commun. **16**, 885 (1975).
4. L. Kleinman, Phys. Rev. B **28**, 1139 (1983).
5. C.B. Haselgrove, Math. Comput. **15**, 323 (1961).
6. J. Hama, M. Watanabe and T. Kato, J. Phys. Cond. Matter **2**, 7445 (1990).
7. M. Hanke, W. Kühn and R. Strehlow, Phys. Status Solidi B **123**, K39 (1984).
8. D.J. Chadi and M.L. Cohen, Phys. Rev. B **8**, 5747 (1973).
9. S.L. Cunningham, , Phys. Rev. B **10**, 4988 (1974).

19 The Poisson equation and the generalized Madelung problem for two- and three-dimensional translationally invariant systems

As most of the formal developments in this chapter have not been published elsewhere, a rather detailed discussion of the various conceptual steps is presented. For this reason at the end of this chapter the main relations are compiled in a summary that references also the key equations or main analytical results.

19.1 The Poisson equation: basic definitions

Using atomic Rydberg units ($m = \frac{1}{2}, \hbar = 1, e^2 = 2$) the (now dimensionless) Poisson equation is given by

$$\Delta V(\mathbf{r}) = -8\pi\rho(\mathbf{r}) \quad , \tag{19.1}$$

and the corresponding Green's function

$$G(\mathbf{r}, \mathbf{r}') = G_0(\mathbf{r}, \mathbf{r}') + F(\mathbf{r}, \mathbf{r}') \quad , \tag{19.2}$$

$$G_0(\mathbf{r}, \mathbf{r}') = \frac{1}{|\mathbf{r} - \mathbf{r}'|} \quad \text{and} \quad \Delta F(\mathbf{r}, \mathbf{r}') = 0 \quad , \tag{19.3}$$

fulfills

$$\Delta G(\mathbf{r}, \mathbf{r}') = -4\pi\delta(\mathbf{r} - \mathbf{r}') \quad . \tag{19.4}$$

Thus,

$$V(\mathbf{r}) = 2\int \mathrm{d}\mathbf{r}' G(\mathbf{r}, \mathbf{r}')\rho(\mathbf{r}') = 2\int \mathrm{d}\mathbf{r}' \frac{\rho(\mathbf{r}')}{|\mathbf{r} - \mathbf{r}'|} + 2\int \mathrm{d}\mathbf{r}' F(\mathbf{r}, \mathbf{r}')\rho(\mathbf{r}') \quad . \tag{19.5}$$

It should be noted that in using the boundary condition,

$$\lim_{r\to\infty} V(\mathbf{r}) = 0 \quad , \tag{19.6}$$

the second term can be neglected. At a particular lattice site $\mathbf{R}$ the *intercell* contribution to the electrostatic potential is then given by

$$V_{\mathbf{R}}(\mathbf{r}) = 2 \sum_{\substack{\mathbf{R}' \\ (\mathbf{R}' \neq \mathbf{R})}} \int_{\Omega_{\mathbf{R}'}} \mathrm{d}\mathbf{r}' G_0(\mathbf{r}+\mathbf{R}, \mathbf{r}'+\mathbf{R}') \rho_{\mathbf{R}'}(\mathbf{r}') \quad ; \quad \mathbf{r} \in \Omega_{\mathbf{R}} \quad , \tag{19.7}$$

and the *intracell contribution* to the electrostatic potential by

$$V_{\mathbf{R}}(\mathbf{r}) = 2 \int_{\Omega_{\mathbf{R}}} \mathrm{d}\mathbf{r}' G_0(\mathbf{r}, \mathbf{r}') \rho_{\mathbf{R}}(\mathbf{r}') \quad ; \quad \mathbf{r} \in \Omega_{\mathbf{R}} \quad , \tag{19.8}$$

where $\Omega_{\mathbf{R}} \equiv D_{V_{\mathbf{R}}}$ refers to the domain of the potential centered in $\mathbf{R}$.

19.2 Intracell contribution

Let $\bar{\rho}(\mathbf{r})$ be the (shape truncated) charge density in the cell of a chosen origin $\mathbf{R}_0$ of a given lattice or of a particular site in an arbitrary ensemble of scatterers,

$$\bar{\rho}(\mathbf{r}) = \rho(\mathbf{r}) \sigma_{\Omega_{\mathbf{0}}}(\mathbf{r}) = \sum_L \bar{\rho}_L(r) Y_L^*(\hat{\mathbf{r}}) \quad , \tag{19.9}$$

where the index $\Omega_0 = \Omega_{\mathbf{R}_0}$ refers to the domain in this cell, i.e., for $\mathbf{r} \in \Omega_{\mathbf{0}} \Rightarrow |\mathbf{r}| = r \leq r_{\mathrm{BS}}$. By using the well-known expansion (A.3) in the Appendix for $1/|\mathbf{r}-\mathbf{r}'|$, the corresponding potential,

$$V_{\mathrm{Intra}}(\mathbf{r}) = 2 \int_{\Omega_0} \frac{1}{|\mathbf{r}-\mathbf{r}'|} \bar{\rho}(\mathbf{r}') \mathrm{d}\mathbf{r}' \quad , \tag{19.10}$$

can be written as

$$V_{\mathrm{Intra}}(\mathbf{r}) = \sum_L \frac{8\pi}{2\ell+1} \left[r^\ell \left(\int_r^{r_{\mathrm{BS}}} \frac{\bar{\rho}_L(r')}{(r')^{\ell-1}} \mathrm{d}r' \right) + \frac{1}{r^{\ell+1}} \left(\int_0^r (r')^{\ell+2} \bar{\rho}_L(r') \mathrm{d}r' \right) \right] Y_L^*(\hat{\mathbf{r}}) \quad . \tag{19.11}$$

It should be noted that because in (19.9) $\bar{\rho}(\mathbf{r})$ is a real function, in (19.11) one needs to evaluate only terms $\overline{\rho}_{\ell,m}(r)$ for $m \geq 0$ and then make use of the relation

$$\overline{\rho}_{\ell,-m}(r) = (-1)^m \left(\overline{\rho}_{\ell,m}(r) \right)^* \quad . \tag{19.12}$$

Furthermore, for a system with inversion symmetry with respect to $\mathbf{R}_0$,

$$\overline{\rho}_{\ell m}(r) = 0 \quad , \quad \forall \ell \text{ odd} \quad . \tag{19.13}$$

If the z axis of the coordinate system is a n-fold rotational symmetry axis the following selection rule,

$$m = \ldots, -n, 0, n, \ldots \quad , \tag{19.14}$$

applies, which in turn implies e.g. that for simple cubic systems there are only very few non-vanishing terms, namely

plane n two-dimensional lattice
(100) 4 quadratic lattice
(110) 2 rectangular lattice
(111) 3 hexagonal lattice

Since in (19.11) the $\bar{\rho}_L(r)$ are the coefficients of the shape truncated charge density,

$$\bar{\rho}_L(r) = \sum_{L',L''} C^{L'}_{L''L} \rho_{L'}(r) \sigma_{L''}(r) \quad , \tag{19.15}$$

(19.11) can also be written as

$$V_{\mathrm{Intra}}(\mathbf{r}) = \sum_L V_{\mathrm{Intra},L}(r) Y_L(\hat{\mathbf{r}}) \quad , \tag{19.16}$$

where

$$V_{\mathrm{Intra},L}(r) = \frac{8\pi}{2l+1} \left[r^\ell \int_r^{r_{\mathrm{BS}}} \frac{1}{(r')^{\ell-1}} \left(\sum_{L'L''} C^{L'}_{L''L} \rho_{L'}(r') \sigma_{L''}(r') \right) \mathrm{d}r' \right.$$
$$\left. + \frac{1}{r^{\ell+1}} \int_0^r (r')^{\ell+2} \left(\sum_{L'L''} C^{L'}_{L''L} \rho_{L'}(r') \sigma_{L''}(r') \right) \mathrm{d}r' \right]^* \quad . \tag{19.17}$$

19.3 Multipole expansion in real-space

19.3.1 Charge density

Clearly enough the total charge density is the sum over all local densities $\bar{\rho}_{\mathbf{R}_i}(\mathbf{r})$ centered at positions $\mathbf{R}_i$

$$\rho(\mathbf{r}) = \sum_i \bar{\rho}_{\mathbf{R}_i}(\mathbf{r}) \quad , \quad \bar{\rho}_{\mathbf{R}_i}(\mathbf{r}) = \rho(\mathbf{R}_i + \mathbf{r}) \sigma_{\Omega_{\mathbf{R}_i}}(\mathbf{R}_i + \mathbf{r}) \quad , \tag{19.18}$$

which can be expanded as

$$\bar{\rho}_{\mathbf{R}_i}(\mathbf{r}) = \sum_L \bar{\rho}_{\mathbf{R}_i,L}(r) Y^*_L(\hat{\mathbf{r}}) \quad . \tag{19.19}$$

The spherical multipole moments thereof are then defined by

$$Q^L_{\mathbf{R}_i} = \frac{\sqrt{4\pi}}{2\ell+1} \int_{\Omega_{\mathbf{R}_i}} r^\ell \bar{\rho}_{\mathbf{R}_i}(\mathbf{r}) Y_L(\hat{\mathbf{r}}) \mathrm{d}\mathbf{r} \quad , \tag{19.20}$$

or, expressed in terms of the expansion coefficients of the untruncated charge density, $\rho_{\mathbf{R}_i,L}(r)$, by

$$Q^L_{\mathbf{R}_i} = \frac{\sqrt{4\pi}}{2\ell+1} \sum_{L',L''} C^{L'}_{L''L} \left(\int_0^\infty r^{\ell+2} \rho_{\mathbf{R}_i,L'}(r) \sigma_{\mathbf{R}_i,L''}(r) \mathrm{d}r \right) \quad . \tag{19.21}$$

The $\ell = 0$ like multipole moment, $Q^{00}_{\mathbf{R}_i} = Q_{\mathbf{R}_i}$, simply is the charge of the cell centered at $\mathbf{R}_i$. Because $\bar{\rho}(\mathbf{r})$ is real,

$$Q^{\ell,-m}_{\mathbf{R}_i} = (-1)^m (Q^{\ell m}_{\mathbf{R}_i})^* \quad . \tag{19.22}$$

In the following between two cases will be distinguished, namely

(1) **three-dimensional (complex) lattices** in which atomic positions $\mathbf{R}_\alpha$ are defined by

$$\mathbf{R}_\alpha \equiv \mathbf{R}_{i\mu} = \mathbf{t}_i + \mathbf{a}_\mu \quad , \mathbf{t}_i \in \mathcal{L}^{(3)} \quad , \tag{19.23}$$

where the $\mathbf{a}_\mu$ refer to non-primitive translations, and

(2) **two-dimensional (complex) lattices,**

$$\mathbf{R}_\alpha = \mathbf{R}_{ip} = \mathbf{t}_i + \mathbf{c}_p \quad , \mathbf{t}_i \in \mathcal{L}^{(2)} \quad , \tag{19.24}$$

where the $\mathbf{c}_p$ refer not only to non-primitive translations, but also to the position vectors of atomic planes (see also the corresponding chapter on the structure constants).

19.3.2 Green's functions and Madelung constants

Using from the Appendix expansions (A.3) and (A.4), the Green's function $G_0(\mathbf{r}+\mathbf{R}, \mathbf{r}'+\mathbf{R}')$,

$$G_0(\mathbf{r}+\mathbf{R}, \mathbf{r}'+\mathbf{R}') = \frac{1}{|\mathbf{r}+\mathbf{R}-\mathbf{r}'-\mathbf{R}'|} \quad , \tag{19.25}$$

can be written for $r < |\mathbf{r}'-\mathbf{R}+\mathbf{R}'|$ and $r' < |\mathbf{R}-\mathbf{R}'|$ as

$$\begin{aligned} G_0(\mathbf{r}+\mathbf{R}, \mathbf{r}'+\mathbf{R}') &= \sum_L \frac{4\pi}{2\ell+1} r^\ell Y^*_L(\widehat{\mathbf{r}}) \frac{Y_L(\widehat{\mathbf{r}'-\mathbf{R}+\mathbf{R}'})}{|\mathbf{r}'-\mathbf{R}+\mathbf{R}'|^{\ell+1}} = \\ &= \sum_{L,L'} r^\ell Y^*_L(\widehat{\mathbf{r}}) \left\{ (-1)^\ell \frac{(4\pi)^2 [2(\ell+\ell')-1]!!}{(2\ell+1)!!(2\ell'+1)!!} C^{\ell'm'}_{\ell m,(\ell+\ell')(m'-m)} \right. \\ &\quad \left. \times \frac{Y^*_{(\ell+\ell')(m'-m)}(\widehat{\mathbf{R}-\mathbf{R}'})}{|\mathbf{R}-\mathbf{R}'|^{\ell+\ell'+1}} \right\} (r')^{\ell'} Y_{\ell'm'}(\widehat{\mathbf{r}}') \quad . \end{aligned} \tag{19.26}$$

In combining this equation with (19.20), namely the one for the spherical multipole moments of the charge density, $G_0(\mathbf{r}+\mathbf{R}, \mathbf{r}'+\mathbf{R}')$ can be reformulated as

$$G_0(\mathbf{r}+\mathbf{R},\mathbf{r}'+\mathbf{R}') = \sum_{L,L'} \frac{\sqrt{4\pi}}{2\ell+1} r^{\ell} Y_L^*(\widehat{\mathbf{r}})\, A^{LL'}_{\mathbf{R}\mathbf{R}'} \frac{\sqrt{4\pi}}{2\ell'+1} (r')^{\ell'} Y_{L'}(\widehat{\mathbf{r}}') \quad , \tag{19.27}$$

where the matrix elements $A^{LL'}_{\mathbf{R}\mathbf{R}'}$,

$$A^{LL'}_{\mathbf{R}\mathbf{R}'} = (-1)^{\ell} \frac{4\pi[2(\ell+\ell')-1]!!}{(2\ell-1)!!(2\ell'-1)!!} C^{\ell' m'}_{\ell m,(\ell+\ell')(m'-m)} \frac{Y^*_{(\ell+\ell')(m'-m)}(\widehat{\mathbf{R}-\mathbf{R}'})}{|\mathbf{R}-\mathbf{R}'|^{\ell+\ell'+1}} \quad , \tag{19.28}$$

are usually called *real-space Madelung constants*. The assumption made, namely $r < |\mathbf{r}' - \mathbf{R} + \mathbf{R}'|$ and $r' < |\mathbf{R} - \mathbf{R}'|$, implies that the bounding spheres of the cells at $\mathbf{R}$ and $\mathbf{R}'$ must not overlap. By neglecting so-called *near-field corrections* for such neighboring cells, see also the following chapter, the *intercell potential* in (19.7) can then be expressed as

$$\begin{aligned} V_{\mathbf{R}}(\mathbf{r}) &= 2 \sum_{\mathbf{R}'(\neq\mathbf{R})} \sum_{L,L'} \frac{\sqrt{4\pi}}{2\ell+1} r^{\ell} Y_L^*(\widehat{\mathbf{r}})\, A^{LL'}_{\mathbf{R}\mathbf{R}'}\, Q^{L'}_{\mathbf{R}'} \\ &= \sum_{L} V_{\mathbf{R},L}(r)^* Y_L^*(\widehat{\mathbf{r}}) = \sum_{L} V_{\mathbf{R},L}(r) Y_L(\widehat{\mathbf{r}}) \quad , \end{aligned} \tag{19.29}$$

where

$$V_{\mathbf{R},L}(r) = \frac{4\sqrt{\pi}}{2\ell+1} \left(\sum_{\mathbf{R}'(\neq\mathbf{R})} \sum_{L'} A^{LL'}_{\mathbf{R}\mathbf{R}'}\, Q^{L'}_{\mathbf{R}'} \right)^* r^{\ell} \quad . \tag{19.30}$$

If one considers only spherically symmetric potentials (ASA), i.e., takes only the $\ell = 0$ term in (19.29), this expression reduces to a constant value, although all higher multipole moments of the charge densities are still taken into account.

$$V^{\mathrm{ASA}}_{\mathbf{R}} = 2 \sum_{\mathbf{R}'(\neq\mathbf{R})} \sum_{L'} A^{00,L'}_{\mathbf{R}\mathbf{R}'}\, Q^{L'}_{\mathbf{R}'} \quad . \tag{19.31}$$

19.3.3 Green's functions and reduced Madelung constants

Since the Green's function $G_0(\mathbf{r}+\mathbf{R},\mathbf{r}'+\mathbf{R}')$ depends only on the difference vector $\mathbf{r}-\mathbf{r}'$,

$$G_0(\mathbf{r}+\mathbf{R},\mathbf{r}'+\mathbf{R}') = G_0(\mathbf{r}-\mathbf{r}'+\mathbf{R}-\mathbf{R}') \quad , \tag{19.32}$$

it can be expanded for $|\mathbf{r}-\mathbf{r}'| < |\mathbf{R}-\mathbf{R}'|$ as

$$\begin{aligned} G_0(\mathbf{r}+\mathbf{R},\mathbf{r}'+\mathbf{R}') &= \sum_{L} |\mathbf{r}-\mathbf{r}'|^{\ell} Y_L(\widehat{\mathbf{r}-\mathbf{r}'}) \frac{4\pi}{2\ell+1} \frac{Y_L^*(\widehat{\mathbf{R}'-\mathbf{R}})}{|\mathbf{R}-\mathbf{R}'|^{\ell+1}} \\ &= \sum_{L} |\mathbf{r}-\mathbf{r}'|^{\ell} Y_L(\widehat{\mathbf{r}-\mathbf{r}'}) G^{L}_{\mathbf{R}\mathbf{R}'} \quad . \end{aligned} \tag{19.33}$$

The matrix elements $G^L_{\mathbf{R}\mathbf{R}'}$ in this equation are usually termed *reduced Madelung constants*.

Inserting from the Appendix (A.5) for $|\mathbf{r}-\mathbf{r}'|^\ell Y_L(\widehat{\mathbf{r}-\mathbf{r}'})$ into (19.33) yields

$$G_0(\mathbf{r}+\mathbf{R},\mathbf{r}'+\mathbf{R}') = \sum_{L,L'} r^\ell Y^*_L(\widehat{\mathbf{r}})\,\frac{4\pi(-1)^{\ell'}[2(\ell+\ell')+1]!!}{(2\ell+1)!!(2\ell'+1)!!}C^{\ell'm'}_{\ell m,(\ell+\ell')(m'-m)} \times G^{(\ell+\ell')(m'-m)}_{\mathbf{R}\mathbf{R}'}\,(r')^{\ell'}Y_{L'}(\widehat{\mathbf{r}}') \quad . \tag{19.34}$$

Comparing now (19.27) with (19.34) implies the following relationship between the *Madelung constants* and their *reduced counterparts*

$$\begin{aligned} A^{LL'}_{\mathbf{R}\mathbf{R}'} &= (-1)^{\ell'}\,\frac{[2(\ell+\ell')+1]!!}{(2\ell-1)!!(2\ell'-1)!!}C^{\ell'm'}_{\ell m,(\ell+\ell')(m'-m)}G^{(\ell+\ell')(m'-m)}_{\mathbf{R}\mathbf{R}'} \\ &= 2\sqrt{\pi}(-1)^{\ell'}\,\frac{\Gamma(\ell+\ell'+\frac{3}{2})}{\Gamma(\ell+\frac{1}{2})\Gamma(\ell'+\frac{1}{2})}C^{\ell'm'}_{\ell m,(\ell+\ell')(m'-m)}G^{(\ell+\ell')(m'-m)}_{\mathbf{R}\mathbf{R}'} \quad , \end{aligned} \tag{19.35}$$

which evidently also follows from (19.28), since

$$G^L_{\mathbf{R}\mathbf{R}'} = \frac{4\pi}{2\ell+1}\frac{Y^*_L(\widehat{\mathbf{R}'-\mathbf{R}})}{|\mathbf{R}-\mathbf{R}'|^{\ell+1}} = \frac{4\pi\,(-1)^\ell}{2\ell+1}\frac{Y^*_L(\widehat{\mathbf{R}-\mathbf{R}'})}{|\mathbf{R}-\mathbf{R}'|^{\ell+1}} \quad . \tag{19.36}$$

In principle one could calculate the coefficients $V_{\mathbf{R},L}(r)$ in (19.30) by means of a direct space summation, which, however, leads to a (if at all) slowly converging series. In the following therefore use of possibly underlying two- or three-dimensional translational invariance is made. Because of the relationship (19.35) all expressions will be formulated in terms of *reduced Madelung constants* $G^L_{\mathbf{R}\mathbf{R}'}$.

19.4 Three-dimensional complex lattices

Let $\mathbf{R}_{n\mu}$ denote the positions in a (in general) complex three-dimensional lattice,

$$\mathbf{R}_{n\mu} = \mathbf{t}_n + \mathbf{a}_\mu \quad , \quad \mathbf{t}_n \in \mathcal{L}^{(3)} \quad , \tag{19.37}$$

where the $\mathbf{a}_\mu$ refer to inequivalent atomic positions. The total electrostatic potential then obviously depends only on the sublattice index μ,

$$\begin{aligned} V(\mathbf{R}_{n\mu}+\mathbf{r}) &= V(\mathbf{a}_\mu+\mathbf{r}) = V_\mu(\mathbf{r}) \\ &= 2\sum_{n,\nu}\int_{\Omega_\nu} \mathrm{d}\mathbf{r}' G_0(\mathbf{a}_\mu+\mathbf{r},\mathbf{a}_\nu+\mathbf{t}_n+\mathbf{r}')\rho_\nu(\mathbf{r}') \quad , \quad \mathbf{r}\in\Omega_\mu \quad , \end{aligned} \tag{19.38}$$

where

$$\rho_\mu(\mathbf{r}) = \rho_{\mathbf{R}_{n\mu}}(\mathbf{r}) \quad . \tag{19.39}$$

It should be recalled that Ω_μ in this case picks up the meaning of a periodically repeated cell.

19.4.1 Evaluation of the Green's function for three-dimensional lattices

In order to separate those parts in (19.38) that are independent of the charge density, one first performs the summation over all n, i.e., for all $\mathbf{t}_n \in \mathcal{L}^{(3)}$,

$$G_{\mu\nu}(\mathbf{r},\mathbf{r}') = \sum_{\substack{n \\ (\mu=\nu, n\neq 0)}} G_0(\mathbf{r}+\mathbf{a}_\mu, \mathbf{r}'+\mathbf{t}_n+\mathbf{a}_\nu) \quad , \tag{19.40}$$

and only then sums over all sublattices

$$V_\mu(\mathbf{r}) = 2\sum_\nu \int_{\Omega_\nu} \mathrm{d}\mathbf{r}' G_{\mu\nu}(\mathbf{r},\mathbf{r}')\rho_\nu(\mathbf{r}') \quad , \quad \mathbf{r}\in\Omega_\mu \quad . \tag{19.41}$$

In the following two conceptually different methods for evaluating $G_{\mu\nu}(\mathbf{r},\mathbf{r}')$ are discussed, which – as will be shown – lead to the same final expressions for $G_{\mu\nu}(\mathbf{r},\mathbf{r}')$.

Method A

(19.40) can be reformulated as a sum over all cells minus the intracell contribution

$$G_{\mu\nu}(\mathbf{r},\mathbf{r}') = D_{\mu\nu}(\mathbf{r},\mathbf{r}') - \delta_{\mu\nu}G_0(\mathbf{r},\mathbf{r}') \quad , \tag{19.42}$$

where

$$D_{\mu\nu}(\mathbf{r},\mathbf{r}') = D(\mathbf{r}+\mathbf{a}_\mu-\mathbf{r}'-\mathbf{a}_\nu) \quad , \tag{19.43}$$

and

$$D(\mathbf{r}) \equiv \sum_n G_0(\mathbf{r}-\mathbf{t}_n) = \sum_n \frac{1}{|\mathbf{r}-\mathbf{t}_n|} \quad . \tag{19.44}$$

Because of long-range contributions the above infinite sum is trivially divergent to $+\infty$. Furthermore, it does not exist for all $\mathbf{r}$ equal to a lattice translation $\mathbf{t}_n$. However, since D has to be evaluated only at $(\mathbf{r}+\mathbf{a}_\mu)-(\mathbf{r}'+\mathbf{a}_\nu)$, which can be chosen in the same unit cell of the translational lattice, such a singularity can only occur at $\mathbf{t}_n = 0$.

By using (A.19) from the Appendix in (19.44), $D(\mathbf{r})$ can be split up into two parts,

$$D(\mathbf{r}) = D_1(\mathbf{r}) + D_2(\mathbf{r}) \quad , \tag{19.45}$$

where

$$D_1(\mathbf{r}) = \frac{2}{\sqrt{\pi}} \sum_n \int_0^{1/2\sigma} \mathrm{d}x \exp(-|\mathbf{r}-\mathbf{t}_n|^2 x^2) \quad , \tag{19.46}$$

$$D_2(\mathbf{r}) = \frac{2}{\sqrt{\pi}} \sum_n \int_{1/2\sigma}^{\infty} \mathrm{d}x \exp(-|\mathbf{r}-\mathbf{t}_n|^2 x^2) \quad , \tag{19.47}$$

and σ is the so-called *Ewald parameter*.

With the exception of $r = 0$, a case that will be considered further on, $D_2(\mathbf{r})$ in (19.47) can now easily be evaluated:

$$\begin{aligned} D_2(\mathbf{r}) &= \sum_n \frac{1}{|\mathbf{r}-\mathbf{t}_n|} \left\{ \frac{2}{\sqrt{\pi}} \int_{|\mathbf{r}-\mathbf{t}_n|/2\sigma}^{\infty} \mathrm{d}x \exp(-x^2) \right\} \\ &= \sum_n \frac{1}{|\mathbf{r}-\mathbf{t}_n|} \mathrm{erfc}(|\mathbf{r}-\mathbf{t}_n|/2\sigma) \quad , \end{aligned} \tag{19.48}$$

i.e., results in a rapidly converging sum, since

$$\lim_{z\to\infty} \mathrm{erfc}(z) = e^{-z^2}/(\sqrt{\pi}z) \quad . \tag{19.49}$$

In using (A.7) from the Appendix (19.46) can be rewritten as

$$D_1(\mathbf{r}) = \frac{2\pi}{V} \sum_j \exp(\mathrm{i}\mathbf{G}_j \cdot \mathbf{r}) \int_0^{1/2\sigma} \frac{\mathrm{d}x}{x^3} \exp(-\mathbf{G}_j^2/4x^2) \quad , \tag{19.50}$$

where the $\mathbf{G}_j$ denote reciprocal lattice vectors. The above mentioned divergence appears now for the $\mathbf{G}_j = \mathbf{0}$ term. Excluding therefore explicitly the singularity arising from this term,

$$D_1(\mathbf{r}) = \frac{2\pi}{V} \sum_{\substack{j \\ (\mathbf{G}_j \neq \mathbf{0})}} \exp(\mathrm{i}\mathbf{G}_j \cdot \mathbf{r}) \int_0^{1/2\sigma} \frac{\mathrm{d}x}{x^3} \exp(-\mathbf{G}_j^2/4x^2) - \frac{4\pi\sigma^2}{V} \quad . \tag{19.51}$$

the integral occurring in (19.51) can easily be evaluated

$$\int_0^{1/2\sigma} \frac{1}{x^3} \exp(-\mathbf{G}_j^2/4x^2)\mathrm{d}x = \frac{2}{\mathbf{G}_j^2} \int_{-\infty}^{-\mathbf{G}_j^2\sigma^2} \mathrm{d}y \exp(y) = \frac{2\exp(-\mathbf{G}_j^2\sigma^2)}{\mathbf{G}_j^2} \quad , \tag{19.52}$$

and $D_1(\mathbf{r})$ reduces to

$$D_1(\mathbf{r}) = \frac{4\pi}{V} \sum_{\substack{j \\ (\mathbf{G}_j \neq \mathbf{0})}} \exp(\mathrm{i}\mathbf{G}_j \cdot \mathbf{r}) \frac{\exp(-\mathbf{G}_j^2\sigma^2)}{\mathbf{G}_j^2} - \frac{4\pi\sigma^2}{V} \quad . \tag{19.53}$$

Replacing now in (19.48) and (19.51) $\mathbf{r}$ by $\mathbf{r} + \mathbf{a}_{\mu\nu}$ and $\mathbf{a}_\mu - \mathbf{a}_\nu$ by $\mathbf{a}_{\mu\nu}$ yields

$$D_{1,\mu\nu}(\mathbf{r}) = \frac{4\pi}{V} \sum_{\substack{j \\ (\mathbf{G}_j \neq \mathbf{0})}} \exp(\mathrm{i}\mathbf{G}_j \cdot \mathbf{r}) \exp(\mathrm{i}\mathbf{G}_j \cdot \mathbf{a}_{\mu\nu}) \frac{\exp(-\mathbf{G}_j^2\sigma^2)}{\mathbf{G}_j^2} - \frac{4\pi\sigma^2}{V} \quad , \tag{19.54}$$

$$D_{2,\mu\nu}(\mathbf{r}) = \sum_{\substack{n \\ (\mathbf{t}_n - \mathbf{a}_{\mu\nu} \neq \mathbf{0})}} \frac{1}{|\mathbf{r} + \mathbf{a}_{\mu\nu} - \mathbf{t}_n|} \mathrm{erfc}(|\mathbf{r} + \mathbf{a}_{\mu\nu} - \mathbf{t}_n| / 2\sigma) \quad , \tag{19.55}$$

Finally by taking into account the last term in (19.42), namely $\delta_{\mu\nu} G_0(\mathbf{r}, \mathbf{r}')$, together with the term left out in the sum (19.55) an additional term, $D_{3,\mu\nu}(\mathbf{r})$, can be defined,

$$D_{3,\mu\nu}(\mathbf{r}) = \delta_{\mu\nu} \frac{\mathrm{erfc}(|\mathbf{r}| / 2\sigma) - 1}{|\mathbf{r}|} = -\delta_{\mu\nu} \frac{\mathrm{erf}(|\mathbf{r}| / 2\sigma)}{|\mathbf{r}|} \quad , \tag{19.56}$$

$$\lim_{r \to 0} D_{3,\mu\nu}(\mathbf{r}) = -\delta_{\mu\nu} \frac{1}{\sqrt{\pi}\sigma} \quad , \tag{19.57}$$

such that now for any $\mathbf{r}, \mathbf{r}'$, see also the comment before (19.48),

$$G_{\mu\upsilon}(\mathbf{r}, \mathbf{r}') = D_{1,\mu\upsilon}(\mathbf{r} - \mathbf{r}') + D_{2,\mu\nu}(\mathbf{r} - \mathbf{r}') + D_{3,\mu\nu}(\mathbf{r} - \mathbf{r}') \quad . \tag{19.58}$$

Method B

From (19.7) it is clear that the potential produced by point charges Q_μ,

$$\rho(\mathbf{r}) = \sum_\mu \sum_n Q_\mu \delta(\mathbf{r} - \mathbf{a}_\mu - \mathbf{t}_n) \quad , \tag{19.59}$$

is given by

$$V_\mu(\mathbf{r}) = 2 \sum_\nu \sum_n Q_\nu G_0(\mathbf{r} + \mathbf{a}_\mu, \mathbf{a}_\nu + \mathbf{t}_n) = 2 \sum_\nu Q_\nu G_{\mu\nu}(\mathbf{r}) + \frac{2Q_\mu}{|\mathbf{r}|} \quad . \tag{19.60}$$

Thus, the problem of calculating $G_{\mu\nu}(\mathbf{r})$ leads to solving the Poisson equation under the condition of charge neutrality, i.e.,

$$\sum_\mu Q_\mu = 0 \quad . \tag{19.61}$$

Adding and subtracting from the charge density a charge distribution $\rho_{\mathrm{I}}(\mathbf{r})$ of the form

$$\rho_{\mathrm{I}}(\mathbf{r}) = \sum_\mu \sum_n Q_\mu \frac{1}{8\sigma^3\pi^{3/2}} \exp\left(-(\mathbf{r} - \mathbf{a}_\mu - \mathbf{t}_n)^2 / 4\sigma^2\right) \quad , \tag{19.62}$$

$$\int \mathrm{d}\mathbf{r}\rho_{\mathrm{I}}(\mathbf{r}) = \sum_{\mu}\sum_{n} Q_{\mu} = 0 \quad , \tag{19.63}$$

the Poisson equation can be solved for $\rho_{\mathrm{I}}(\mathbf{r})$ and $\rho_{\mathrm{S}}(\mathbf{r})$,

$$\rho_{\mathrm{S}}(\mathbf{r}) = \sum_{\mu}\sum_{n} Q_{\mu}\left(\delta(\mathbf{r}-\mathbf{a}_{\mu}-\mathbf{t}_{n}) - \frac{1}{8\sigma^{3}\pi^{3/2}}\exp\left(-(\mathbf{r}-\mathbf{a}_{\mu}-\mathbf{t}_{n})^{2}/4\sigma^{2}\right)\right) \quad , \tag{19.64}$$

separately, since

$$\rho(\mathbf{r}) = \rho_{\mathrm{S}}(\mathbf{r}) + \rho_{\mathrm{I}}(\mathbf{r}) \quad . \tag{19.65}$$

Furthermore, from the relation

$$\Delta V_{\mathrm{S}}(\mathbf{r}) = -8\pi\rho_{\mathrm{S}}(\mathbf{r}) \quad , \tag{19.66}$$

it is easy to show that

$$V_{\mathrm{S}}(\mathbf{r}) = \sum_{\mu}\sum_{n} 2Q_{\mu}\frac{\mathrm{erfc}(|\mathbf{r}-\mathbf{a}_{\mu}-\mathbf{t}_{n}|/2\sigma)}{|\mathbf{r}-\mathbf{a}_{\mu}-\mathbf{t}_{n}|} + C \quad , \tag{19.67}$$

where C is an integration constant.

By expressing the potential $V_{\mathrm{I}}(\mathbf{r})$ and the charge density $\rho_{\mathrm{I}}(\mathbf{r})$ in lattice Fourier series

$$V_{\mathrm{I}}(\mathbf{r}) = \sum_{j} V_{\mathrm{I}}(\mathbf{G}_{j})\exp\left(\mathrm{i}\mathbf{G}_{j}\cdot\mathbf{r}\right) \quad , \tag{19.68}$$

$$\rho_{\mathrm{I}}(\mathbf{r}) = \sum_{j} \rho_{\mathrm{I}}(\mathbf{G}_{j})\exp\left(\mathrm{i}\mathbf{G}_{j}\cdot\mathbf{r}\right) \quad , \tag{19.69}$$

the Poisson equation in (19.1) implies that

$$V_{\mathrm{I}}(\mathbf{G}_{j}) = -\frac{8\pi}{\mathbf{G}_{j}^{2}}\rho_{\mathrm{I}}(\mathbf{G}_{j}) \quad . \tag{19.70}$$

The lattice Fourier transform of $\rho_{\mathrm{I}}(\mathbf{r})$ can be reformulated as

$$\begin{aligned}\rho_{\mathrm{I}}(\mathbf{G}_{j}) &= \frac{1}{NV}\int \mathrm{d}\mathbf{r}\,\rho_{\mathrm{I}}(\mathbf{r})\exp\left(-\mathrm{i}\mathbf{G}_{j}\cdot\mathbf{r}\right) \\ &= \frac{1}{V}\sum_{\mu} Q_{\mu}\exp\left(-\mathrm{i}\mathbf{G}_{j}\cdot\mathbf{a}_{\mu}\right) \\ &\qquad \times \frac{1}{\pi^{3/2}}\int \mathrm{d}\mathbf{u}\exp\left(-u^{2}\right)\exp\left(-\mathrm{i}2\sigma\mathbf{G}_{j}\cdot\mathbf{u}\right) \quad .\end{aligned} \tag{19.71}$$

where V is the volume of the unit cell.

Furthermore, since

$$\frac{1}{\pi^{3/2}} \int \mathrm{d}\mathbf{u} \exp\left(-\mathbf{u}^2\right) \exp\left(-\mathrm{i}2\sigma \mathbf{G}_j \cdot \mathbf{u}\right) = \exp(-\mathbf{G}_j^2 \sigma^2) \quad , \tag{19.72}$$

$\rho_{\mathrm{I}}(\mathbf{G}_j)$ reduces to

$$\rho_{\mathrm{I}}(\mathbf{G}_j) = \frac{1}{V} \sum_{\mu} Q_\mu \exp\left(-\mathrm{i}\mathbf{G}_j \cdot \mathbf{a}_\mu\right) \exp(-\mathbf{G}_j^2 \sigma^2) \quad , \tag{19.73}$$

i.e.,

$$\rho_{\mathrm{I}}\left(\mathbf{G}_j = \mathbf{0}\right) = 0 \quad . \tag{19.74}$$

Consequently, one gets

$$V_{\mathrm{I}}(\mathbf{G}_j) = -\frac{8\pi}{V} \sum_{\mu} Q_\mu \frac{\exp\left(-\mathrm{i}\mathbf{G}_j \cdot \mathbf{a}_\mu\right) \exp(-\mathbf{G}_j^2 \sigma^2)}{\mathbf{G}_j^2} \quad , \tag{19.75}$$

and

$$V_{\mathrm{I}}(\mathbf{r}) = -\frac{4\pi}{V} \sum_{\mu} 2Q_\mu \sum_{j \neq 0} \frac{\exp\left(\mathrm{i}\mathbf{G}_j \cdot (\mathbf{r} - \mathbf{a}_\mu)\right) \exp(-\mathbf{G}_j^2 \sigma^2)}{\mathbf{G}_j^2} \quad . \tag{19.76}$$

Therefore, one finally obtains

$$V(\mathbf{r}) = \sum_{\nu} 2Q_\nu \left\{ -\frac{4\pi}{V} \sum_{j \neq 0} \frac{\exp\left(\mathrm{i}\mathbf{G}_j \cdot (\mathbf{r} - \mathbf{a}_\nu)\right) \exp(-\mathbf{G}_j^2 \sigma^2)}{\mathbf{G}_j^2} + \sum_{n} \frac{\operatorname{erfc}(|\mathbf{r} - \mathbf{a}_\nu - \mathbf{t}_n| / 2\sigma)}{|\mathbf{r} - \mathbf{a}_\nu - \mathbf{t}_n|} + C \right\} \quad , \tag{19.77}$$

where, in order to ensure independence of the ν-like terms (sublattice contributions) from the parameter σ, for the integration constant C the value $-4\pi\sigma^2/V$ has to be chosen. Replacing $\mathbf{r}$ by $\mathbf{r}+\mathbf{a}_\mu$ and comparing with (19.60), one can see immediately that both methods proposed, namely methods A and B, yield an identical final expression for $V(\mathbf{r})$.

19.4.2 Derivation of Madelung constants for three-dimensional lattices

According to (19.25)–(19.33) for small r the terms in (19.58), namely $D_{i,\mu\nu}(\mathbf{r})$, $i = 1, 2, 3$, have to be expanded as

$$D_{i,\mu\nu}(\mathbf{r}) = \sum_{L} r^\ell Y_L(\widehat{\mathbf{r}}) D_{i,\mu\nu}^L \quad . \tag{19.78}$$

whereby the coefficients $D_{i,\mu\nu}^L$ are conveniently defined by the following limit

$$D_{i,\mu\nu}^L = \lim_{r \to 0} \frac{1}{r^\ell} \int \mathrm{d}\widehat{\mathbf{r}} D_{i,\mu\nu}(\mathbf{r}) Y_L^*(\widehat{\mathbf{r}}) \quad . \tag{19.79}$$

The reciprocal sum components $D^L_{1,\mu\nu}$

By using (A.6) from the Appendix in (19.54) one immediately obtains

$$\int \mathrm{d}\widehat{\mathbf{r}} D_{1,\mu\nu}(\mathbf{r}) Y_L^*(\widehat{\mathbf{r}}) = \frac{(4\pi)^2 \mathrm{i}^\ell}{V} \sum_{j\neq 0} \Big\{ j_\ell(G_j r) Y_L^*(\widehat{\mathbf{G}}_j) \times \exp(\mathrm{i}\mathbf{G}_j \cdot \mathbf{a}_{\mu\nu}) \frac{\exp(-\mathbf{G}_j^2\sigma^2)}{\mathbf{G}_j^2} - \delta_{L,00} \frac{(4\pi)^{3/2}\sigma^2}{V} \Big\} \quad , \tag{19.80}$$

which by recalling the properties of spherical Bessel functions for small argument,

$$\lim_{z\to 0} j_\ell(z) = \frac{z^\ell}{(2\ell+1)!!} = \frac{\sqrt{\pi}}{2^{\ell+1}\Gamma(\ell+\frac{3}{2})} z^\ell \quad , \tag{19.81}$$

yields

$$D^L_{1,\mu\nu} = \frac{(4\pi)^2 \sqrt{\pi} \mathrm{i}^\ell}{V 2^{\ell+1}\Gamma(\ell+\frac{3}{2})} \sum_{j\neq 0} Y_L^*(\widehat{\mathbf{G}}_j) \exp(\mathrm{i}\mathbf{G}_j \cdot \mathbf{a}_{\mu\nu}) G_j^{\ell-2} \exp(-\mathbf{G}_j^2\sigma^2) - \delta_{L,00} \frac{(4\pi)^{3/2}\sigma^2}{V} \quad . \tag{19.82}$$

The direct sum components $D^L_{2,\mu\nu}$

In order to evaluate $D^L_{2,\mu\nu}$ one returns to the integral representation in (19.48),

$$D_{2,\mu\nu}(\mathbf{r}) = \frac{2}{\sqrt{\pi}} \sum_{\substack{n \\ (\mathbf{t}_n - \mathbf{a}_{\mu\nu} \neq \mathbf{0})}} \int_{1/2\sigma}^\infty \mathrm{d}x \exp(-|\mathbf{r} + \mathbf{a}_{\mu\nu} - \mathbf{t}_n|^2 x^2) \quad , \tag{19.83}$$

and expands the integrand as follows

$$\exp(-|\mathbf{r} + \mathbf{a}_{\mu\nu} - \mathbf{t}_n|^2 x^2) = \exp(-r^2x^2) \exp(-|\mathbf{a}_{\mu\nu} - \mathbf{t}_n|^2 x^2) \times 4\pi \sum_L \mathrm{i}^\ell j_\ell(\mathrm{i}2r|\mathbf{a}_{\mu\nu} - \mathbf{t}_n| x^2) Y_L^*(\widehat{\mathbf{a}_{\mu\nu} - \mathbf{t}_n}) Y_L(\widehat{\mathbf{r}}) \quad , \tag{19.84}$$

such that – although $j_\ell(\mathrm{i}x)$ is exponentially increasing with x – the integral in (19.83) is still converging. One therefore gets

$$\int \mathrm{d}\widehat{\mathbf{r}} D_{2,\mu\nu}(\mathbf{r}) Y_L^*(\widehat{\mathbf{r}}) = 8\sqrt{\pi}\mathrm{i}^\ell \sum_{|\mathbf{a}_\mu - \mathbf{a}_\nu - \mathbf{t}_n| \neq 0} Y_L^*(\widehat{\mathbf{a}_{\mu\nu} - \mathbf{t}_n}) \times \int_{1/2\sigma}^\infty \mathrm{d}x\, j_\ell(\mathrm{i}2r|\mathbf{a}_{\mu\nu} - \mathbf{t}_n| x^2) \exp(-r^2x^2) \exp(-|\mathbf{a}_{\mu\nu} - \mathbf{t}_n|^2 x^2) \quad , \tag{19.85}$$

and consequently by taking the limit according to (19.79) for $r \to 0$ the direct sum components $D^L_{2,\mu\nu}$ are given by

$$\begin{aligned} D^L_{2,\mu\nu} &= \frac{4\pi(-1)^\ell}{\Gamma(\ell+\frac{3}{2})} \sum_{|\mathbf{a}_\mu - \mathbf{a}_\nu - \mathbf{t}_n| \neq 0} Y^*_L(\widehat{\mathbf{a}_{\mu\nu} - \mathbf{t}_n})\, |\mathbf{a}_{\mu\nu} - \mathbf{t}_n|^\ell \\ &\qquad \times \int_{1/2\sigma}^{\infty} \mathrm{d}x\, x^{2\ell} \exp(-|\mathbf{a}_{\mu\nu} - \mathbf{t}_n|^2 x^2) \\ &= \frac{4\pi(-1)^\ell}{\Gamma(\ell+\frac{3}{2})} \sum_{\substack{n \\ (\mathbf{t}_n - \mathbf{a}_{\mu\nu} \neq \mathbf{0})}} \frac{Y^*_L(\widehat{\mathbf{a}_{\mu\nu} - \mathbf{t}_n})}{|\mathbf{a}_{\mu\nu} - \mathbf{t}_n|^{\ell+1}} \int_{|\mathbf{a}_{\mu\nu} - \mathbf{t}_n|/2\sigma}^{\infty} \mathrm{d}x\, x^{2\ell} \exp(-x^2) \quad , \end{aligned} \tag{19.86}$$

or, by using the incomplete Γ function, see Appendix,

$$D^L_{2,\mu\nu} = \frac{2\pi(-1)^\ell}{\Gamma(\ell+\frac{3}{2})} \sum_{\substack{n \\ (\mathbf{t}_n - \mathbf{a}_{\mu\nu} \neq \mathbf{0})}} Y^*_L(\widehat{\mathbf{a}_{\mu\nu} - \mathbf{t}_n}) \frac{\Gamma(\ell+\frac{1}{2}, |\mathbf{a}_{\mu\nu} - \mathbf{t}_n|^2 / 4\sigma^2)}{|\mathbf{a}_{\mu\nu} - \mathbf{t}_n|^{\ell+1}} \quad . \tag{19.87}$$

The third term in (19.58) follows then immediately from (19.56):

$$D^L_{3,\mu\nu} = -\delta_{\mu\nu}\delta_{L,00}\frac{2}{\sigma} \quad . \tag{19.88}$$

19.4.3 Reduced Madelung constants for three-dimensional lattices

In terms of the *reduced Madelung constants* $G^L_{\mu\nu}$,

$$G^L_{\mu\nu} = D^L_{1,\mu\nu} + D^L_{2,\mu\nu} + D^L_{3,\mu\nu} \quad , \tag{19.89}$$

the potential can now be written as

$$V_\mu(\mathbf{r}) = \sum_L V_{\mu,L}(r) Y_L(\hat{\mathbf{r}}) \quad , \tag{19.90}$$

where the coefficients $V_{\mu,L}(r) = V_{\mu,\ell m}(r)$ are given by

$$\begin{aligned} V_{\mu,\ell m}(r) = \frac{4\pi}{\Gamma(\ell+\frac{3}{2})} &\left(\sum_{L'} \frac{(-1)^{\ell'}\Gamma(\ell+\ell'+\frac{3}{2})}{\Gamma(\ell'+\frac{1}{2})} C^{\ell' m'}_{\ell m,(\ell+\ell')(m'-m)} \right. \\ &\left. \times \left(\sum_\nu G^{\ell+\ell',m'-m}_{\mu\nu} Q^{L'}_\nu \right) \right)^* r^\ell \quad . \end{aligned} \tag{19.91}$$

It should be recalled that one only needs to evaluate the coefficients $V_{\mu,\ell m}(r)$ for $m \geq 0$, since the intercell potential $V_\mu(\mathbf{r})$ is real. Furthermore, in case one is only interested in the ASA potential, (19.90) reduces to

$$V_{\mathrm{ASA},\mu} = \sum_{L'} (-1)^{\ell'} \frac{2\ell'+1}{\sqrt{\pi}} \left(\sum_{\nu} G_{\mu\nu}^{\ell',m'} Q_{\nu}^{L'} \right) \quad . \tag{19.92}$$

19.5 Complex two-dimensional lattices

In the case of two-dimensional translational invariance all atomic positions can be written in the following manner

$$\mathbf{R}_{np} = \mathbf{t}_n + \mathbf{c}_p,\ \mathbf{t}_n \in \mathcal{L}^{(2)},\ \mathbf{c}_p \notin \mathcal{L}^{(2)} \quad , \tag{19.93}$$

and the charge density is independent of a lattice translation

$$\rho_{\mathbf{R}_{np}}(\mathbf{r}) = \rho_p(\mathbf{r}) \quad , \forall \mathbf{t}_n \in \mathcal{L}^{(2)} \quad . \tag{19.94}$$

19.5.1 Evaluation of the Green's function for two-dimensional lattices

Since obviously the potential depends only on the layer index p,

$$V_p(\mathbf{r}) = V(\mathbf{c}_p + \mathbf{r}) = 2 \sum_q \int_{\Omega_q} \mathrm{d}\mathbf{r}' G_{pq}(\mathbf{r}, \mathbf{r}') \rho_q(\mathbf{r}') \quad , \quad \mathbf{r} \in \Omega_p \quad , \tag{19.95}$$

where the Green's functions $G_{pq}(\mathbf{r}, \mathbf{r}')$ are given in this case by the following lattice sum, see also (19.42) –(19.44),

$$G_{pq}(\mathbf{r}, \mathbf{r}') = D_{pq}(\mathbf{r}, \mathbf{r}') - \delta_{pq} G_0(\mathbf{r}, \mathbf{r}') \quad , \tag{19.96}$$

and the $D_{pq}(\mathbf{r}, \mathbf{r}')$ are defined as

$$D_{pq}(\mathbf{r}, \mathbf{r}') = D(\mathbf{r} + \mathbf{c}_p - \mathbf{r}' - \mathbf{c}_q) = \sum_n G_0(\mathbf{r} + \mathbf{c}_p, \mathbf{r}' + \mathbf{t}_n + \mathbf{c}_q) \quad . \tag{19.97}$$

In using the notation $\mathbf{r} = (\mathbf{r}_\parallel, z)$ – in analogy to (19.46)–(19.47) – one can write

$$\begin{aligned} D(\mathbf{r}) &= \frac{2}{\sqrt{\pi}} \sum_n \int_0^\infty \mathrm{d}x \exp(-|\mathbf{r} - \mathbf{t}_n|^2 x^2) \ = \\ &= \frac{2}{\sqrt{\pi}} \int_0^\infty \mathrm{d}x \exp(-z^2 x^2) \sum_n \exp(-|\mathbf{r}_\parallel - \mathbf{t}_n|^2 x^2) \\ &= \frac{2}{\sqrt{\pi}} \int_0^\infty \mathrm{d}x \exp(-z^2 x^2) \frac{\pi}{A x^2} \sum_j \exp\left(-\mathbf{G}_j^2/4x^2 + \mathrm{i}\mathbf{G}_j \cdot \mathbf{r}_\parallel\right) \\ &= \frac{2\sqrt{\pi}}{A} \sum_j \left(\exp\left(\mathrm{i}\mathbf{G}_j \cdot \mathbf{r}_\parallel\right) \int_0^\infty \mathrm{d}x \frac{1}{x^2} \exp(-z^2 x^2 - \mathbf{G}_j^2/4x^2) \right) \quad , \end{aligned} \tag{19.98}$$

with the $\mathbf{G}_j$ referring to two-dimensional reciprocal lattice vectors and A to the area of the translational lattice unit cell.

The integral in (19.98) is finite for $\forall \mathbf{G}_j \neq \mathbf{0}$, see also (A.20), but divergent for $\mathbf{G}_j = \mathbf{0}$. It will be shown further on that the $\mathbf{G}_j = \mathbf{0}$ term corresponds to a one-dimensional (normal to the planes of atoms) Poisson equation. Quite obviously the $\mathbf{G}_j = \mathbf{0}$ term has to be treated separately and eventually will be used for imposing boundary conditions for the potential as $z \to \pm\infty$. Omitting for the time being the $\mathbf{G}_j = \mathbf{0}$ term in (19.98), this equation can be rewritten in the following way

$$D(\mathbf{r}) = \frac{2\sqrt{\pi}}{A} \sum_{j \neq 0} \exp\left(\mathrm{i}\mathbf{G}_j \cdot \mathbf{r}_\parallel\right) \int_0^\infty \mathrm{d}x \frac{1}{x^2} \exp(-z^2 x^2 - \mathbf{G}_j^2/4x^2) \tag{19.99}$$

$$= \frac{2\pi}{A} \sum_{j \neq 0} \frac{1}{G_j} \exp\left(\mathrm{i}\mathbf{G}_j \cdot \mathbf{r}_\parallel\right) \exp(-G_j\,|z|) \quad . \tag{19.100}$$

Since the sum in (19.100) converges very weakly for small z, especially for $z = 0$, similar to the three-dimensional case, the integral in (19.99) is split into two parts,

$$D(\mathbf{r}) = D_1(\mathbf{r}) + D_2(\mathbf{r}) \quad , \tag{19.101}$$

$$D_1(\mathbf{r}) = \frac{2\sqrt{\pi}}{A} \sum_{j \neq 0} \exp\left(\mathrm{i}\mathbf{G}_j \cdot \mathbf{r}_\parallel\right) \int_0^{1/2\sigma} \mathrm{d}x \frac{1}{x^2} \exp(-z^2 x^2 - \mathbf{G}_j^2/4x^2) \quad , \tag{19.102}$$

$$D_2(\mathbf{r}) = \frac{2\sqrt{\pi}}{A} \sum_{j \neq 0} \exp\left(\mathrm{i}\mathbf{G}_j \cdot \mathbf{r}_\parallel\right) \int_{1/2\sigma}^\infty \mathrm{d}x \frac{1}{x^2} \exp(-z^2 x^2 - \mathbf{G}_j^2/4x^2) \quad . \tag{19.103}$$

It is easy to see that the infinite sum involved in $D_1(\mathbf{r})$ is now well-converging, since

$$|D_1(\mathbf{r})| \leq \frac{2\sqrt{\pi}}{A} \sum_{j \neq 0} \int_0^{1/2\sigma} \mathrm{d}x \frac{1}{x^2} \exp(-\mathbf{G}_j^2/4x^2)$$

$$= \frac{2\pi}{A} \sum_{j \neq 0} \frac{1}{G_j} \mathrm{erfc}(G_j \sigma) < \infty \quad , \tag{19.104}$$

and

$$D_1(\mathbf{r}_\parallel, z = 0) = \frac{2\pi}{A} \sum_{j \neq 0} \frac{1}{G_j} \exp\left(\mathrm{i}\mathbf{G}_j \cdot \mathbf{r}_\parallel\right) \mathrm{erfc}(G_j \sigma) \quad . \tag{19.105}$$

By changing the integration variable in the integral on the rhs of (19.102) to $y = x^{-2}$ one gets,

$$D_1(\mathbf{r}) = \frac{\sqrt{2\pi}}{A} \sum_{j \neq 0} \exp\left(\mathrm{i}\mathbf{G}_j \cdot \mathbf{r}_\parallel\right) \int_{2\sigma^2}^{\infty} y^{-\frac{1}{2}} \exp\left(-\frac{1}{2}(z^2/y + \mathbf{G}_j^2 y)\right) \mathrm{d}y \quad . \tag{19.106}$$

Returning now to the real lattice summation in (19.103) the $G_j = 0$ term has to be added and subtracted

$$\begin{aligned} D_2(\mathbf{r}) = {} & \frac{2\sqrt{\pi}}{A} \int_{1/2\sigma}^{\infty} \mathrm{d}x \exp(-z^2x^2) \frac{1}{x^2} \sum_j \exp\left(\mathrm{i}\mathbf{G}_j \cdot \mathbf{r}_\parallel - \mathbf{G}_j^2/4x^2\right) \\ & - \frac{2\sqrt{\pi}}{A} \int_{1/2\sigma}^{\infty} \mathrm{d}x \frac{1}{x^2} \exp(-z^2x^2) \quad , \end{aligned} \tag{19.107}$$

and recalling that

$$\frac{1}{x^2} \sum_j \exp\left(\mathrm{i}\mathbf{G}_j \cdot \mathbf{r}_\parallel - \mathbf{G}_j^2/4x^2\right) = \frac{A}{\pi} \sum_n \exp(-\left|\mathbf{r}_\parallel - \mathbf{t}_n\right|^2 x^2) \quad , \tag{19.108}$$

one therefore gets for $D_2(\mathbf{r})$:

$$D_2(\mathbf{r}) = \sum_n \frac{1}{|\mathbf{r} - \mathbf{t}_n|} \mathrm{erfc}(|\mathbf{r} - \mathbf{t}_n| / 2\sigma) - \frac{2\sqrt{\pi}}{A} \int_{1/2\sigma}^{\infty} \mathrm{d}x \frac{1}{x^2} \exp(-z^2x^2) \quad . \tag{19.109}$$

Finally, because of (A.22) in the Appendix, the second term on the rhs of the last equation reduces to

$$\begin{aligned} -\frac{2\sqrt{\pi}}{A} \int_{1/2\sigma}^{\infty} \mathrm{d}x \frac{1}{x^2} \exp(-z^2x^2) = {} & -\frac{4\sqrt{\pi}\sigma}{A} \exp\left(-\frac{z^2}{4\sigma^2}\right) \\ & - \frac{2\pi\,|z|}{A} \mathrm{erf}\left(\frac{|z|}{2\sigma}\right) + \frac{2\pi\,|z|}{A} \quad . \end{aligned} \tag{19.110}$$

Without the $\mathbf{G}_j = \mathbf{0}$ contribution, the Green's function for a two-dimensional translational invariant system can then be written as

$$G_{pq}(\mathbf{r}, \mathbf{r}') = D_{1,pq}(\mathbf{r} - \mathbf{r}') + D_{2\mathrm{a},pq}(\mathbf{r} - \mathbf{r}') + D_{2\mathrm{b},pq}(\mathbf{r} - \mathbf{r}') + D_{3,pq}(\mathbf{r} - \mathbf{r}') \quad , \tag{19.111}$$

where

$$\begin{aligned} D_{1,pq}(\mathbf{r}) = {} & \frac{\sqrt{2\pi}}{A} \sum_{\substack{j \\ (\mathbf{G}_j \neq \mathbf{0})}} \exp\left(\mathrm{i}\mathbf{G}_j \cdot \mathbf{r}_\parallel\right) \exp\left(\mathrm{i}\mathbf{G}_j \cdot \mathbf{c}_{pq\parallel}\right) \\ & \times \int_{2\sigma^2}^{\infty} y^{-\frac{1}{2}} \exp\left(-\frac{1}{2}\left[(z + c_{pq\perp})^2/y + \mathbf{G}_j^2 y\right]\right) \mathrm{d}y \quad , \end{aligned} \tag{19.112}$$

$$D_{2\mathrm{a},pq}(\mathbf{r}) = \sum_{\substack{n \\ (\mathbf{t}_n - \mathbf{c}_{pq} \neq \mathbf{0})}} \frac{1}{|\mathbf{r} + \mathbf{c}_{pq} - \mathbf{t}_n|} \mathrm{erfc}(|\mathbf{r} + \mathbf{c}_{pq} - \mathbf{t}_n| / 2\sigma) \quad , \tag{19.113}$$

$$D_{2\mathrm{b},pq}(\mathbf{r}) = -\left(1-\delta_{c_{pq\perp},0}\right)\frac{2\sqrt{\pi}}{A}\int_{1/2\sigma}^{\infty}\mathrm{d}x\frac{1}{x^2}\exp\left[-\left(z+c_{pq\perp}\right)^2x^2\right] - \delta_{c_{pq\perp},0}\left[\frac{4\sqrt{\pi}\sigma}{A}\exp\left(-\frac{z^2}{4\sigma^2}\right)+\frac{2\pi\left|z\right|}{A}\mathrm{erf}\left(\frac{\left|z\right|}{2\sigma}\right)\right] \quad , \tag{19.114}$$

$$D_{3,pq}(\mathbf{r}) = \delta_{pq}\frac{1}{\left|\mathbf{r}\right|}\left(\mathrm{erfc}(\left|\mathbf{r}\right|/2\sigma)-1\right) = -\delta_{pq}\frac{\mathrm{erf}(\left|\mathbf{r}\right|/2\sigma)}{\left|\mathbf{r}\right|} \quad , \tag{19.115}$$

with $\mathbf{c}_{pq}$ being $\mathbf{c}_p - \mathbf{c}_q$. It should be noted that for $D_{2,pq}(\mathbf{r})$ two forms are given and that the missing term $(2\pi\left|z\right|/A)\,\delta_{c_{pq\perp},0}$ in (19.114), see (19.110), will be included in the $\mathbf{G}_j = 0$ contribution to the Green's function to be discussed in the following.

The $\mathbf{G}_j = 0$ contribution for two-dimensional lattices

Using in (19.1) a two-dimensional lattice Fourier representation for the potential and the charge density,

$$V(\mathbf{r}) = \sum_j V_{\mathbf{G}_j}(z)\exp(\mathrm{i}\mathbf{G}_j\cdot\mathbf{r}_\parallel) \quad , \tag{19.116}$$

$$\rho(\mathbf{r}) = \sum_j \rho_{\mathbf{G}_j}(z)\exp(\mathrm{i}\mathbf{G}_j\cdot\mathbf{r}_\parallel) \quad , \tag{19.117}$$

one gets

$$\left(\frac{\mathrm{d}^2}{\mathrm{d}z^2}-\mathbf{G}_j^2\right)V_{\mathbf{G}_j}(z) = -8\pi\rho_{\mathbf{G}_j}(z) \quad , \tag{19.118}$$

which for $\mathbf{G}_j = 0$ simply reduces to

$$\frac{\mathrm{d}^2}{\mathrm{d}z^2}V_0(z) = -8\pi\rho_0(z) \quad , \tag{19.119}$$

where

$$\rho_0(z) = \rho_{(00)}(z) = \frac{1}{A}\int_{\Omega_{2\mathrm{D}}}\mathrm{d}\mathbf{r}_\parallel\rho(\mathbf{r}_\parallel,z) \quad , \tag{19.120}$$

with $\Omega_{2\mathrm{D}}$ denoting the 2D Wigner-Seitz cell of unit area A. The Green's function corresponding to (19.119), as defined by

$$\frac{\mathrm{d}^2}{\mathrm{d}z^2}G_0(z,z') = -4\pi\delta(z-z') \quad , \tag{19.121}$$

is then given by

$$G_0(z,z') = -2\pi\left|z-z'\right| \quad . \tag{19.122}$$

Since two-dimensional translational invariance of $\rho(\mathbf{r})$ applies, $V_0(z)$, namely the term that corresponds to $\mathbf{G}_j = 0$, can be written as

$$V_{0,p}(z) = V_0(\mathbf{c}_p + z) = 2\sum_q \int_{\Omega_q} \mathrm{d}\mathbf{r}' G_{0,pq}(z,z')\rho_q(\mathbf{r}') + \mathcal{A}\,(z + c_{p\perp}) + \mathcal{B} \quad , \tag{19.123}$$

where

$$G_{0,pq}(z,z') = -\frac{2\pi}{A}\,|z - z' + c_{pq\perp}| \quad . \tag{19.124}$$

It should be noted that in (19.123) $\mathbf{r}' \in \Omega_q$, z is measured with respect to a particular (layer position vector) $\mathbf{c}_p$ and an integration constant $\mathcal{A}\,z + \mathcal{B}$ has been added in order to satisfy appropriate boundary conditions.

Returning finally to (19.114) and adding the term left out there one can define a term $D_{0,pq}(z)$,

$$D_{0,pq}(z) = -\left(1 - \delta_{c_{pq\perp},0}\right)\frac{2\pi}{A}\,|z + c_{pq\perp}| \quad , \tag{19.125}$$

from which for $|c_{pq\perp}| \to \infty$ the only non-vanishing Madelung constants can be derived.

19.5.2 Derivation of the Madelung constants for two-dimensional lattices

The L-like expansion coefficients of $D_{i,\mu\nu}(\mathbf{r})$ ($i = 0, 1, 2\mathrm{a}, 2\mathrm{b}, 3$) in (19.112)–(19.115) can again be obtained using the below relation

$$D^L_{i,pq} = \lim_{r\to 0}\left(\frac{1}{r^\ell}\int \mathrm{d}\widehat{\mathbf{r}} D_{i,pq}(\mathbf{r}) Y^*_L(\widehat{\mathbf{r}})\right) \quad . \tag{19.126}$$

The reciprocal sum terms $D^L_{1,pq}$

By inserting the following Taylor expansion,

$$\begin{aligned}\exp\left(-\frac{1}{2}(z + c_{pq\perp})^2/y\right) &= \exp\left(-\frac{1}{2}c^2_{pq\perp}/y\right)\exp\left(-\frac{1}{2}(z^2 + 2zc_{pq\perp})/y\right)\\ &= \exp\left(-\frac{1}{2}c^2_{pq\perp}/y\right)\\ &\quad\times\sum_{n=0}^{\infty}\frac{1}{n!}\left(-\frac{1}{2}(z^2 + 2zc_{pq\perp})\right)^n y^{-n} \quad ,\end{aligned} \tag{19.127}$$

in (19.112) yields

$$D_{1,pq}(\mathbf{r}) = \frac{\sqrt{2\pi}}{A} \sum_{\substack{j \\ (\mathbf{G}_j \neq \mathbf{0})}} \exp\left(\mathrm{i}\mathbf{G}_j \cdot \mathbf{r}_\parallel\right) \exp\left(\mathrm{i}\mathbf{G}_j \cdot \mathbf{c}_{pq\parallel}\right)$$
$$\times \left[\sum_{n=0}^{\infty} \frac{1}{n!} \left(-\frac{1}{2}\right)^n (z^2 + 2zc_{pq\perp})^n \right.$$
$$\left. \times \int_{2\sigma^2}^{\infty} y^{-\frac{1}{2}-n} \exp\left(-\frac{1}{2}(c_{pq\perp}^2/y + \mathbf{G}_j^2 y)\right) \mathrm{d}y \right] \quad . \qquad (19.128)$$

Introducing now polar coordinates,

$$\mathbf{r}_\parallel = (r\sin(\Theta)\cos(\phi), r\sin(\Theta)\sin(\phi)) \quad , \quad z = r\cos(\Theta) \quad ,$$
$$\mathbf{G}_j = (G_j\cos(\phi_j), G_j\sin(\phi_j)) \quad ,$$
$$\mathbf{G}_j \cdot \mathbf{r}_\parallel = G_j r\sin(\Theta)\cos(\phi_j - \phi) \quad ,$$

in the corresponding expression for $D_{1,pq}^L$,

$$D_{1,pq}^L = \lim_{r\to 0} \frac{1}{r^\ell} \int \mathrm{d}\widehat{\mathbf{r}} D_{1,pq}(\mathbf{r}) Y_L^*(\widehat{\mathbf{r}})$$
$$= \frac{\mathrm{i}^{m+|m|}}{A} \sqrt{\frac{2\ell+1}{2} \frac{(\ell-|m|)!}{(\ell+|m|)!}} \sum_{\substack{j \\ (\mathbf{G}_j \neq \mathbf{0})}} \exp\left(\mathrm{i}\mathbf{G}_j \cdot \mathbf{c}_{pq\parallel}\right) \sum_{n=0}^{\infty} \frac{1}{n!} \left(-\frac{1}{2}\right)^n$$
$$\times \left\{ \int_{2\sigma^2}^{\infty} y^{-\frac{1}{2}-n} \exp\left(-\frac{1}{2}(c_{pq\perp}^2/y + \mathbf{G}_j^2 y)\right) \mathrm{d}y \right\}$$
$$\times \left\{ \lim_{r\to 0} \frac{1}{r^\ell} \int_0^\pi \sin(\Theta)\mathrm{d}\Theta \right.$$
$$\left. \times \int_0^{2\pi} \mathrm{d}\phi \exp\left(\mathrm{i}\mathbf{G}_j \cdot \mathbf{r}_\parallel\right) P_\ell^{|m|}(\cos(\Theta)) \exp(-\mathrm{i}m\phi)(z^2 + 2zc_{pq\perp})^n \right\} \quad , \qquad (19.129)$$

the integral with respect to ϕ reduces to

$$\int_0^{2\pi} \exp(-\mathrm{i}m\phi + \mathrm{i}G_j r\sin(\Theta)\cos(\phi_j - \phi))\mathrm{d}\phi$$
$$= 2\pi\,\mathrm{i}^{|m|} \exp(-\mathrm{i}m\phi_j)\, J_{|m|}(G_j r\sin(\Theta)) \quad . \qquad (19.130)$$

Equation (19.129) can therefore be written as

$$D_{1,pq}^{L} = \frac{2\pi \mathrm{i}^{-m}}{A} \sqrt{\frac{2\ell+1}{2} \frac{(\ell-|m|)!}{(\ell+|m|)!}} \sum_{\substack{j \\ (\mathbf{G}_j \neq \mathbf{0})}} \exp(-\mathrm{i}m\phi_j) \exp\left(\mathrm{i}\mathbf{G}_j \cdot \mathbf{c}_{pq\|}\right)$$
$$\times \sum_{n=0}^{\infty} \frac{1}{n!} \left(-\frac{1}{2}\right)^n \left\{ \int_{2\sigma^2}^{\infty} y^{-\frac{1}{2}-n} \exp\left(-\frac{1}{2}(c_{pq\perp}^2/y + \mathbf{G}_j^2 y)\right) \mathrm{d}y \right\}$$
$$\times \lim_{r\to 0} \frac{1}{r^\ell} I_n \quad , \tag{19.131}$$

where the I_n refer to the integrals with respect to Θ,

$$I_n = \int_0^{\pi} \sin(\Theta) \mathrm{d}\Theta P_\ell^{|m|}(\cos(\Theta)) J_{|m|}(G_j r \sin(\Theta))$$
$$\times (r^2 \cos^2(\Theta) + 2r c_{pq\perp} \cos(\Theta))^n \quad . \tag{19.132}$$

Furthermore, by expanding the Bessel functions into a power series, see (A.35) in the Appendix, and using the binomial theorem, namely (A.36) from the Appendix, it can be shown that

$$\lim_{r\to 0} \frac{1}{r^\ell} I_n = \sum_{k=0}^{\infty} \binom{n}{\ell - |m| - n - 2k} \frac{\sqrt{\pi} 2^{2n-2\ell}}{k!(|m|+k)!} \frac{\Gamma(\ell+|m|+1)}{\Gamma(l+\frac{3}{2})}$$
$$\times G_j^{|m|+2k} c_{pq\perp}^{2n-\ell+|m|+2k} \quad , \tag{19.133}$$

which inserted into (19.131) yields

$$D_{1,pq}^{L} = \frac{\pi^{\frac{3}{2}} \mathrm{i}^{-m}}{2^{2\ell-1} A} \frac{\sqrt{(2\ell+1)\,\Gamma(\ell+|m|+1)\,\Gamma(\ell-|m|+1)}}{\Gamma\left(\ell+\frac{3}{2}\right)}$$
$$\times \sum_{\substack{j \\ (\mathbf{G}_j \neq \mathbf{0})}} \Bigg\{ \exp(-\mathrm{i}m\phi_j) \exp\left(\mathrm{i}\mathbf{G}_j \cdot \mathbf{c}_{pq\|}\right)$$
$$\times \sum_{k=0}^{\frac{\ell-|m|}{2}} \sum_{n=\frac{\ell-|m|}{2}-k}^{\ell-|m|-2k} I_n\left(G_j\sigma, \frac{|c_{pq\perp}|\, G_j}{2}\right)$$
$$\times \frac{(-1)^n\, c_{pq\perp}^{2n-\ell+|m|+2k}}{\Gamma\left(2n-\ell+|m|+2k+1\right)\Gamma\left(\ell-|m|-n-2k+1\right)}$$
$$\times \frac{G_j^{2n+|m|+2k-1}}{\Gamma\left(k+1\right)\Gamma\left(|m|+k+1\right)} \Bigg\} \quad . \tag{19.134}$$

It should be noted that as indicated in (A.28) in the Appendix, the occurring integral,

$$I_n(G_j\sigma, \frac{|c_{pq\perp}|\, G_j}{2}) = \int_{G_j^2\sigma^2}^{\infty} x^{-\frac{1}{2}-n} \exp\left(-\frac{c_{pq\perp}^2 G_j^2}{4x} - x\right) \mathrm{d}x \;, \qquad (19.135)$$

can be evaluated recursively in terms of error functions.

For $c_{pq\perp} = 0$ the only non-vanishing terms correspond to $n = (\ell - |m|)/2 - k$, which in turn is only the case for even $\ell - |m|$. Then:

$$\begin{aligned} D_{1,pq}^L = {} & \frac{\pi^{\frac{3}{2}} \mathrm{i}^{\ell-m-|m|}}{2^{2\ell-1}A} \frac{\sqrt{(2\ell+1)\,\Gamma(\ell+|m|+1)\,\Gamma(\ell-|m|+1)}}{\Gamma\left(\ell+\frac{3}{2}\right)} \\ & \times \sum_{\substack{j \\ (\mathbf{G}_j \neq \mathbf{0})}} \exp(-\mathrm{i}m\phi_j) \exp\left(\mathrm{i}\mathbf{G}_j \cdot \mathbf{c}_{pq\parallel}\right) G_j^{\ell-1} \\ & \times \sum_{k=0}^{\frac{\ell-|m|}{2}} \frac{(-1)^k \Gamma(\frac{1}{2} - \frac{\ell-|m|}{2} + k, \mathbf{G}_j^2\sigma^2)}{(|m|+k)!k!(\frac{\ell-|m|}{2}-k)!} \quad . \end{aligned} \qquad (19.136)$$

The direct sum terms $D_{2\mathrm{a},pq}^L$

The expression for the direct sum terms $D_{2\mathrm{a},pq}^L$ is analogous to the one in (19.87) for three-dimensional lattices with the exception that now $\mathbf{t}_n \in \mathcal{L}^{(2)}$ and that in general $\mathbf{c}_{pq}$ is a three-dimensional vector:

$$D_{2\mathrm{a},pq}^L = \frac{2\pi(-1)^\ell}{\Gamma(\ell+\frac{3}{2})} \sum_{\substack{n \\ (\mathbf{t}_n - \mathbf{c}_{pq} \neq \mathbf{0})}} Y_L^*(\widehat{\mathbf{c}_{pq} - \mathbf{t}_n}) \frac{\Gamma(\ell+\frac{1}{2}, |\mathbf{c}_{pq} - \mathbf{t}_n|^2/4\sigma^2)}{|\mathbf{c}_{pq} - \mathbf{t}_n|^{\ell+1}} \quad . \qquad (19.137)$$

The $D_{0,pq}^L$ terms

Since for small z, $|z + c_{pq\perp}| = |c_{pq\perp}| + \mathrm{sign}(c_{pq\perp})z, c_{pq\perp} \neq 0$, one can immediately derive the below expression

$$D_{0,pq}^L = -\left(1 - \delta_{c_{pq\perp},0}\right) \delta_{m0} \frac{4\pi}{A} \left(\delta_{\ell 0}\sqrt{\pi}\,|c_{pq\perp}| + \delta_{\ell 1}\frac{\sqrt{3\pi}}{3}\mathrm{sign}(c_{pq\perp})\right) \quad . \qquad (19.138)$$

The direct sum $D_{2\mathrm{a},pq}^L$ terms, $c_{pq\perp} \neq 0$

In order to evaluate $D_{2\mathrm{b},pq}^L$ for $c_{pq\perp} \neq 0$ one can use the following expansion

$$\exp(-\left(z+c_{pq\perp}\right)^2 x^2) = \exp(-c_{pq\perp}^2 x^2)\exp(-\left(z^2+2c_{pq\perp}z\right)x^2)$$
$$= \sum_{\ell=0}^{\infty}\left(\exp(-c_{pq\perp}^2 x^2)\right.$$
$$\left.\times \sum_{\frac{\ell}{2}\leq n\leq \ell} \frac{(-1)^n\, 2^{2n-\ell} c_{pq\perp}^{2n-\ell} x^{2n}}{\Gamma\left(\ell-n+1\right)\Gamma\left(2n-\ell+1\right)}\right) z^{\ell} \quad , \quad (19.139)$$

from which one obtains

$$D_{2\mathrm{b},pq}^{L} = -\,\delta_{m0}\,\mathrm{sign}\left(c_{pq\perp}\right)\frac{2\pi}{A}\frac{\sqrt{\pi\left(2\ell+1\right)}}{4^{\ell}c_{pq\perp}^{\ell-1}}\frac{\Gamma(\ell+1)}{\Gamma(\ell+\frac{3}{2})}$$
$$\times \sum_{\frac{\ell}{2}\leq n\leq \ell}\frac{(-1)^n\,4^n}{\Gamma\left(\ell-n+1\right)\Gamma\left(2n-\ell+1\right)}\int_{|c_{pq\perp}|/2\sigma}^{\infty}\mathrm{d}x\, x^{2n-2}\exp(-x^2)$$
$$= -\,\delta_{m0}\,\mathrm{sign}\left(c_{pq\perp}\right)\frac{\pi}{A}\frac{\sqrt{\pi\left(2\ell+1\right)}}{4^{\ell}c_{pq\perp}^{\ell-1}}\frac{\Gamma(\ell+1)}{\Gamma(\ell+\frac{3}{2})}$$
$$\times \sum_{\frac{\ell}{2}\leq n\leq \ell}\frac{(-1)^n\,4^n}{\Gamma\left(\ell-n+1\right)\Gamma\left(2n-\ell+1\right)}\Gamma\left(n-\frac{1}{2}, c_{pq\perp}^2/4\sigma^2\right) \quad . \quad (19.140)$$

The direct sum $D_{2\mathrm{a}pq}^{L}$ terms, $c_{pq\perp}=0$

In using Taylor series expansions and rearranging corresponding terms, one can show that

$$-\frac{4\sqrt{\pi}\sigma}{A}\exp\left(-\frac{z^2}{4\sigma^2}\right)-\frac{2\pi\,|z|}{A}\mathrm{erf}\left(\frac{|z|}{2\sigma}\right)=\frac{4\sqrt{\pi}\sigma}{A}\sum_{n=0}^{\infty}\frac{(-1)^n}{n!\left(2n-1\right)\left(2\sigma\right)^{2n}}z^{2n} \quad , \quad (19.141)$$

which yields

$$D_{2\mathrm{b},pq}^{L} = \begin{cases} \delta_{m0}\left(2\pi/A\right)\left[(-1)^n\sqrt{4n+1}/\left(4^n\sigma^{2n-1}\right)\right] & \\ \qquad \times\,\Gamma(n-\frac{1}{2})/\Gamma(2n+\frac{3}{2}) & , \ \ell \text{ even} \\ 0 & , \ \ell \text{ odd} \end{cases} \quad . \quad (19.142)$$

The $D_{3,pq}^{L}$ terms

Finally, similar to (19.88), for the $D_{3,pq}^{L}$ terms the below expression is found:

$$D_{3,pq}^{L} = -\delta_{pq}\delta_{L,00}\frac{2}{\sigma} \quad . \quad (19.143)$$

19.5.3 The intercell potential

In terms of the reduced Madelung constants G^L_{pq},

$$G^L_{pq} = \sum_{i=0,1,2a,2b,3} D^L_{i,pq} \ , \tag{19.144}$$

and G_{00}, the potential can finally be written in the following compact form as

$$V_p(\mathbf{r}) = \sum_L \overline{V}_{p,\ell m}(r) Y_L(\hat{\mathbf{r}}) + \mathcal{A}\sqrt{\frac{4\pi}{3}} r Y_{10}(\hat{\mathbf{r}}) + (\mathcal{A} c_{p\perp} + \mathcal{B})\sqrt{4\pi} Y_{00}(\hat{\mathbf{r}}) \quad , \tag{19.145}$$

where for matters of similarity with the three-dimensional translationally invariant case the expansion coefficients $V_{p,\ell m}(r)$ are regrouped such that

$$\overline{V}_{p,\ell m}(r) = \frac{4\pi}{\Gamma(\ell+\frac{3}{2})} \left(\sum_{L'} \frac{(-1)^{\ell'}\Gamma(\ell+\ell'+\frac{3}{2})}{\Gamma(\ell'+\frac{1}{2})} C^{\ell' m'}_{\ell m,(\ell+\ell')(m'-m)} \right.$$
$$\left. \times \sum_q G^{\ell+\ell',m'-m}_{pq} Q^{L'}_q \right)^* r^\ell \quad . \tag{19.146}$$

In the case of an ASA potential , (19.145) simply reduces to

$$V_{\mathrm{ASA},p} = \sum_{L'} \frac{(-1)^{\ell'}(2\ell'+1)}{\sqrt{\pi}} \left(\sum_q G^{\ell',m'}_{pq} Q^{L'}_q \right) + \mathcal{A} c_{p\perp} + \mathcal{B} \quad . \tag{19.147}$$

19.5.4 Determination of the constants $\mathcal{A}$ and $\mathcal{B}$

In order to use the same kind of identification of the Madelung constants $A^{LL'}_{pq}$ in terms of their reduced counterparts $G^{LL'}_{pq}$ as in (19.35), namely

$$A^{LL'}_{i,pq} = (-1)^{\ell'} \frac{[2(\ell+\ell')+1]!!}{(2\ell-1)!!(2\ell'-1)!!} C^{\ell' m'}_{\ell m,(\ell+\ell')(m'-m)} G^{(\ell+\ell')(m'-m)}_{i,pq} \quad , \tag{19.148}$$

and since (19.145) is valid for all $\mathbf{r} \in \Omega_p$, for a determination of the constants $\mathcal{A}$ and $\mathcal{B}$ one just as well can choose $\mathbf{r} = 0$ and therefore $L = (00)$. Denoting $V_p(\mathbf{r} = \mathbf{0})$ simply by V_p, this quantity can be split up into two terms,

$$V_p = \widehat{V}_p + V_{\perp,p} \quad , \tag{19.149}$$

where

$$\widehat{V}_p = 2 \sum_{i=1,2a,2b,3} \sum_L \sum_q A^{00,L}_{i,pq} Q^L_q \quad , \tag{19.150}$$

with

$$A_{i,pq}^{00,L} = (-1)^{\ell} \frac{\ell + \frac{1}{2}}{\sqrt{\pi}} D_{i,pq}^{L} \qquad (i = 0, 1, 2\mathrm{a}, 2\mathrm{b}, 3) \quad , \tag{19.151}$$

and where $V_{\perp,p}$ refers to the remaining part for $p \to \infty$:

$$V_{\perp,p} = 2 \sum_{L} \sum_{q} A_{0,pq}^{00,L} Q_q^L + \mathcal{A} c_{p\perp} + \mathcal{B} \quad . \tag{19.152}$$

In particular, by using (19.138) yields

$$A_{0,pq}^{00,L} = -\left(1 - \delta_{c_{pq\perp},0}\right) \delta_{m0} \frac{2\pi}{A} \left(\delta_{\ell 0} \left|c_{pq\perp}\right| - \delta_{\ell 1} \sqrt{3} \mathrm{sign}(c_{pq\perp})\right) \quad , \tag{19.153}$$

and, consequently,

$$V_{\perp,p} = -\frac{4\pi}{A} \sum_{q} \left(\left|c_{pq\perp}\right| Q_q^{00} - \mathrm{sign}(c_{pq\perp}) \sqrt{3} Q_q^{10}\right) + \mathcal{A} c_{p\perp} + \mathcal{B} \quad , \tag{19.154}$$

where by using the convention $\mathrm{sign}(0) = 0$ the restriction for $D_{0,pq}^{L}$, namely, $|c_{pq\perp}| \neq 0$ is automatically fulfilled.

Numbering of layers

Suppose that in a typical layered system in all layers $p \leq 0$ all local physical quantities (charges, magnetic moments, potentials, etc.) are identical to those in the corresponding (in general complex) three-dimensional translationally invariant system ("bulk", substrate; *left semi-infinite region*: L), while for $p \geq N+1$ (*right semi-infinite system*: R) these quantities are again identical to those in an (in general complex) three-dimensional translationally invariant ("bulk", substrate) system, or, in order to mimic vacuum, the charge density is zero. This region shall be called in the following *right semi-infinite region*, R. Layers $1 \leq p \leq N$ then form the so-called *interface* or *intermediate region*, to be abbreviated by I. As continuity for the Madelung potential between all these regions has to be required, the constants $\mathcal{A}$ and $\mathcal{B}$ can uniquely be determined.

The layer numbering indices is conveniently chosen such that

$$c_{p\perp} \geq c_{q\perp} \quad \text{if} \quad p > q \quad , \tag{19.155}$$

$$c_{0\perp} < c_{1\perp} \quad \text{and} \quad c_{N\perp} < c_{N+1,\perp} \quad . \tag{19.156}$$

It should be noted that in the case that $(c_{p\perp} - c_{q\perp}) = 0$ the corresponding difference vector $\mathbf{c}_p - \mathbf{c}_q$ not necessarily has to be zero, since in general in the $\mathbf{c}_p$ also the non-primitive translations are absorbed, i.e., those vectors that generate possibly present sublattices. If, however, $\mathbf{c}_p - \mathbf{c}_q = 0$, this implies that $p = q$. The index p can therefore be used for an unambiguous numbering of both, atomic planes and sublattices.

"Bulk" from the left

If $V_{\rm Left}$ is the value of the intercell potential in that "bulk" layer labelled by $p = 0$, then continuity between regions L and I implies for the Madelung potentials

$$V_{\rm Left} = V_{p=0} = \widehat{V}_0 - \frac{4\pi}{A}\sum_q \left(|c_{0q\perp}|\, Q_q^{00} - \mathrm{sign}(c_{0q\perp})\sqrt{3}Q_q^{10}\right) + \mathcal{A}c_{0\perp} + \mathcal{B} \quad , \tag{19.157}$$

from which the constant $\mathcal{B}$ can be expressed as,

$$\mathcal{B} = V_{\rm Left} - 2\sum_L \sum_q \frac{(-1)^\ell\,(2\ell+1)}{\sqrt{\pi}} G_{0q}^L Q_q^L \quad , \tag{19.158}$$

and inserted into (19.154) for $p \geq 0$ yields

$$V_{\perp,p} = -\frac{4\pi}{A}\sum_q \Bigg(Q_q^{00}\left(|c_{pq\perp}| - |c_{0q\perp}|\right) - \sqrt{3}Q_q^{10}\left(\mathrm{sign}(c_{pq\perp}) - \mathrm{sign}(c_{0q\perp})\right)\Bigg) + \mathcal{A}c_{p0\perp} + V_{\rm Left} - \widehat{V}_0 \quad . \tag{19.159}$$

It should be noted that for $p \geq 1$ the following relations apply

$$|c_{pq\perp}| - |c_{0q\perp}| = \begin{cases} c_{p0\perp} & ;\, q \leq 0 \\ c_{pq\perp} - c_{q0\perp} = c_{p0\perp} - 2c_{q0\perp} & ;\, 1 \leq q \leq p \\ -c_{p0\perp} & ;\, p < q \end{cases} \quad , \tag{19.160}$$

$$\mathrm{sign}(c_{pq\perp}) - \mathrm{sign}(c_{0q\perp}) = \begin{cases} 0\ ;\, c_{q\perp} < c_{0\perp} \\ 1\ ;\, c_{q\perp} = c_{0\perp} \\ 2\ ;\, q \geq 1 \text{ and } c_{q\perp} < c_{p\perp} \\ 1\ ;\, q \geq 1 \text{ and } c_{q\perp} = c_{p\perp} \\ 0\ ;\, q \geq 1 \text{ and } c_{q\perp} > c_{p\perp} \end{cases} \quad . \tag{19.161}$$

where again the convention $\mathrm{sign}(0) = 0$ is used.

Because of charge neutrality in the "bulk", one thus gets

$$V_{\perp,p} = -\frac{4\pi}{A}\sum_{q\geq 1} Q_q^{00}\left(|c_{pq\perp}| - c_{q0\perp}\right) + \frac{4\pi}{A}\sum_{\substack{q\leq 0 \\ (c_{q0\perp}=0)}} \sqrt{3}Q_q^{10} + \frac{8\pi}{A}\sum_{\substack{q\geq 1 \\ (c_{q\perp}<c_{p\perp})}} \sqrt{3}Q_q^{10} + \frac{4\pi}{A}\sum_{\substack{q\geq 1 \\ (c_{q\perp}=c_{p\perp})}} \sqrt{3}Q_q^{10} + \mathcal{A}c_{p0\perp} + V_{\rm Left} - \widehat{V}_0 \quad . \tag{19.162}$$

"Vacuum" from the right

Suppose

$$\rho_p(\mathbf{r}) = 0 \quad ; \quad \mathbf{r} \in \Omega_p \quad ; \quad p \geq N+1 \quad , \tag{19.163}$$

which in turn implies that

$$V_p(\mathbf{r}) = V_p = const. \quad ; \quad \mathbf{r} \in \Omega_p \quad ; \quad p \geq N+1 \quad . \tag{19.164}$$

Therefore, in this case for layers $p \geq N+1$, the following boundary condition can be imposed

$$\frac{\mathrm{d}}{\mathrm{d}c_{p\perp}} V_{\perp,p} = 0 \quad . \tag{19.165}$$

Recalling now that $c_{N+1,\perp} > c_{p\perp},\ p \leq N$, this implies in (19.162) that for $p > N$

$$V_{\perp,p} = \left(-\frac{4\pi}{A} \sum_{q=1}^{N} Q_q^{00} + \mathcal{A} \right) c_{p0\perp} + \frac{8\pi}{A} \sum_{q=1}^{N} Q_q^{00} c_{q0\perp} + \frac{4\pi}{A} \sum_{\substack{q \leq 0 \\ (c_{q0\perp}=0)}} \sqrt{3} Q_q^{10} + \frac{8\pi}{A} \sum_{q=1}^{N} \sqrt{3} Q_q^{10} + V_{\mathrm{Left}} - \widehat{V}_0 \quad . \tag{19.166}$$

Therefore, one obtains

$$\mathcal{A} = \frac{4\pi}{A} \sum_{q=1}^{N} Q_q^{00} \quad , \tag{19.167}$$

and

$$\begin{aligned} V_{\mathrm{vac}} \equiv V_{\perp,p>N} &= \frac{8\pi}{A} \sum_{q=1}^{N} \left(Q_q^{00} c_{q0\perp} + \sqrt{3} Q_q^{10} \right) + \frac{4\pi}{A} \sum_{\substack{q \leq 0 \\ (c_{q0\perp}=0)}} \sqrt{3} Q_q^{10} \\ &\quad + V_{\mathrm{Left}} - \widehat{V}_0 \\ &= \frac{4\pi}{A} \sum_{q} \left(Q_q^{00} c_{q0\perp} + \sqrt{3} Q_q^{10} \right) + \mathcal{B} \quad . \end{aligned} \tag{19.168}$$

Furthermore, for the intermediate regime, namely for $1 \leq p \leq N$, one gets

$$V_{\perp,p} = V_{L,1} - \widehat{V}_0 + \frac{8\pi}{A} \sum_{q=1}^{N} Q_q^{00} \min(c_{p0\perp}, c_{q0\perp}) + \frac{4\pi}{A} \sum_{\substack{q \leq 0 \\ (c_{q0\perp}=0)}} \sqrt{3} Q_q^{10} + \frac{4\pi}{A} \sum_{\substack{q \geq 1 \\ (c_{q\perp}=c_{p\perp})}} \sqrt{3} Q_q^{10} \quad . \tag{19.169}$$

"Bulk" from the right

Continuity between the regions I and R then implies that

$$\begin{aligned} V_{\text{Right}} = V_{N+1} = \widehat{V}_{N+1} - \frac{4\pi}{A}\sum_{q=1}^{N} Q_q^{00}\left(c_{N+1,0\perp} - 2c_{q0\perp}\right) \\ + \frac{4\pi}{A}\sum_{\substack{q\le 0 \\ (c_{q0\perp}=0)}} \sqrt{3}Q_q^{10} + \frac{8\pi}{A}\sum_{q=1}^{N}\sqrt{3}Q_q^{10} \\ + \frac{4\pi}{A}\sum_{\substack{q\ge N+1 \\ (c_{q\perp}=c_{N+1,\perp})}} \sqrt{3}Q_q^{10} + \mathcal{A}c_{N+1,0\perp} + V_{\text{Left}} - \widehat{V}_0 \quad , \end{aligned} \tag{19.170}$$

where use has been made of (19.162) *and* the condition of charge neutrality in the right "bulk" region (R) was assumed. Thus, in this particular case

$$\begin{aligned} \mathcal{A} = \frac{1}{c_{N+1,0\perp}}\Bigg(V_{\text{Right}} - V_{\text{Left}} + \widehat{V}_0 - \widehat{V}_{N+1} + \frac{4\pi}{A}\sum_{q=1}^{N} Q_q^{00}\left(c_{N+1,0\perp} - 2c_{q0\perp}\right) \\ - \frac{4\pi}{A}\sum_{\substack{q\le 0 \\ (c_{q0\perp}=0)}} \sqrt{3}Q_q^{10} - \frac{8\pi}{A}\sum_{q=1}^{N}\sqrt{3}Q_q^{10} - \frac{4\pi}{A}\sum_{\substack{q\ge N+1 \\ (c_{q\perp}=c_{N+1,\perp})}} \sqrt{3}Q_q^{10} \Bigg) \quad , \end{aligned} \tag{19.171}$$

which inserted into (19.162) yields:

$$\mathcal{A} = \frac{1}{c_{N+1,0\perp}}\left(V_{\text{Right}} - V_{\text{Left}} + \sum_{L}\sum_{q}\frac{(-1)^{\ell}(2\ell+1)}{\sqrt{\pi}}\left(G_{0q}^{L} - G_{N+1q}^{L}\right)Q_q^{L}\right) . \tag{19.172}$$

Slabs (thin films)

Finally considering a *slab,* namely a finite number of (atomic) layers with vacuum on both sides, i.e.,

$$Q_p^{L} = 0 \qquad \text{for} \quad p \le 0 \quad \text{and} \quad p > N\,, \quad \forall L \quad . \tag{19.173}$$

from (19.154) one arrives in this case at

$$V_{\perp,p} = -\frac{4\pi}{A}\sum_{q=1}^{N}\left(|c_{pq\perp}|\,Q_q^{00} - \text{sign}(c_{pq\perp})\sqrt{3}Q_q^{10}\right) + \mathcal{A}c_{p\perp} + \mathcal{B} \quad . \tag{19.174}$$

One boundary condition is again set by vacuum on the left hand side. Consequently for $p > N$ one gets

$$\begin{aligned} V_{\perp,p} &= -\frac{4\pi}{A}\sum_{q=1}^{N}\left(c_{pq\perp}Q_q^{00} - \sqrt{3}Q_q^{10}\right) + \mathcal{A}c_{p\perp} + \mathcal{B} \\ &= \left(-\frac{4\pi}{A}\sum_{q=1}^{N}Q_q^{00} + \mathcal{A}\right)c_{p\perp} + \frac{4\pi}{A}\sum_{q=1}^{N}Q_q^{00}c_{q\perp} + \frac{4\pi}{A}\sum_{q=1}^{N}\sqrt{3}Q_q^{10} + \mathcal{B} \quad , \end{aligned} \tag{19.175}$$

The constant $\mathcal{A}$ is therefore given by

$$\mathcal{A} = \frac{4\pi}{A}\sum_{q=1}^{N}Q_q^{00} \quad , \tag{19.176}$$

and, consequently, for $p \leq N$ one obtains

$$\begin{aligned} V_p = &-\frac{4\pi}{A}\sum_{q=1}^{N}\left(\left(|c_{pq\perp}| - c_{p\perp}\right)Q_q^{00} - \mathrm{sign}(c_{pq\perp})\sqrt{3}Q_q^{10}\right) \\ &+\mathcal{B} + \widehat{V}_p \quad . \end{aligned} \tag{19.177}$$

The constant $\mathcal{B}$ can then be determined by fixing the Madelung potential in *one* particular layer of the slab.

19.6 A remark: density functional requirements

Since Density Functional Theory describes ground states in terms of a self-consistent process it is clear that by keeping two boundary conditions fixed as is the case of two "bulk" systems in the left and right region, or, in the case of a slab the actual variation parameter is the Fermi energy, i.e., the chemical potential at $T = 0\ K$, which of course can only assume one particular value that has to apply for the whole system. This implies that in the case of two bulk systems in the left and right region in both bulk systems one and the same Fermi energy has to apply. For freestanding thin films (slabs) this causes the Fermi energy to vary with the film thickness. In the case of a left "bulk" system and a right "vacuum" system the Fermi energy is that of the left "bulk" system and the actual variation parameter turns out to be V_{vac}.

19.7 Summary

Definitions

$$\boxed{V_{\mathbf{R}}(\mathbf{r}) = V_{\mathbf{R},\mathrm{Intra}}(\mathbf{r}) + V_{\mathbf{R},\mathrm{Inter}}(\mathbf{r}) \quad , \quad \mathbf{r} \in \Omega_R}$$

Three-dimensional lattices:

$$\boxed{Q_\mu = \int\limits_{\Omega_\mu} \mathrm{d}\mathbf{r} \rho_\mu(\mathbf{r})}$$

$$\boxed{V_\mu(\mathbf{r}) = \sum_L V_{\mu,L}(r) Y_L(\widehat{\mathbf{r}}) = \sum_L V_{\mu,\ell m}(r) Y_{\ell m}(\widehat{\mathbf{r}})}$$

$$\boxed{G^L_{\mu\nu} = \sum_{i=1,2,3} D^L_{i,\mu\nu} \quad , \quad D_{i,\mu\nu}(\mathbf{r}) = \sum_L r^\ell D^L_{i,\mu\nu} Y_L(\widehat{\mathbf{r}})}$$

$$\boxed{V^{\mathrm{Inter}}_{\mu,\ell m}(r) = \left[\sum_{L'} X_{LL'} \sum_{\upsilon} \left(G^{\ell+\ell',m'-m}_{\mu\nu} Q^{L'}_{\upsilon} \right) \right]^* r^\ell}$$

$$\boxed{X_{LL'} = \left(4\pi/\Gamma(\ell+\tfrac{3}{2})\right) \left((-1)^{\ell'} \Gamma(\ell+\ell'+\tfrac{3}{2}) / \Gamma(\ell'+\tfrac{1}{2}) \right) C^{\ell' m'}_{\ell m,(\ell+\ell')(m'-m)}}$$

Two-dimensional lattices

$$\boxed{Q_p = \int\limits_{\Omega_p} \mathrm{d}\mathrm{r} \rho_p(\mathbf{r})}$$

Table 19.1. The Poisson equation and the generalized Madelung problem: equation numbers corresponding to the various quantities

case	**quantity**	**Equation number**
Real space	$V_{\rm Intra}(\mathbf{r})$	(19.16), (19.17)
	$V_{\rm Inter}(\mathbf{r})$	(19.29), (19.30)
3D-invariant	$V(\mathbf{r})$	(19.38), (19.90)
	$V_{\mu}(\mathbf{r})$	(19.60)
	$V_{\mu,L}(r)$	(19.91)
	$D^{L}_{1,\mu\nu}$	(19.54); (19.82)
	$D^{L}_{2,\mu\nu}$	(19.55); (19.87)
	$D^{L}_{3,\mu\nu}$	(19.56); (19.88)
2D-invariant	$V_p(\mathbf{r})$,$\overline{V}_p(\mathbf{r})$	(19.145)
	$\overline{V}_{p,L}(r)$	(19.146)
	$D_{1,pq}$	(19.134)
	$D_{2\mathrm{a},pq}$	(19.137)
	$D_{2\mathrm{b},pq}$	(19.142)
	$D_{3,pq}$	(19.143)
	$D_{0,pq}$	(19.138)

$$V_p(\mathbf{r}) = \sum_L V_{p,L}(r) Y_L(\widehat{\mathbf{r}}) = \sum_L V_{p,\ell m}(r) Y_{\ell m}(\widehat{\mathbf{r}})$$

$$G^L_{pq} = \sum_{i=0,1,2a,2b,3} D^L_{i,pq} \quad , \quad D_{i,pq}(\mathbf{r}) = \sum_L r^\ell D^L_{i,pq} Y_L(\widehat{\mathbf{r}})$$

$$V_p^{\rm Inter}(\mathbf{r}) = \sum_L \overline{V}_{p,L}(r) Y_L(\widehat{\mathbf{r}}) + \mathcal{A}\sqrt{\tfrac{4\pi}{3}} r Y_{10}(\widehat{\mathbf{r}}) + (\mathcal{A} c_{p\perp} + \mathcal{B})\sqrt{4\pi} Y_{00}(\widehat{\mathbf{r}})$$

$$\overline{V}_{p,\ell m}(r) = \left[\sum_{L'} X_{LL'} \left(\sum_q G^{\ell+\ell',m'-m}_{pq} Q^{L'}_q \right) \right]^* r^\ell$$

Table 19.2. Boundary conditions for the intercell potential in the case of two-dimensional translational symmetry: equation numbers

Left	**Right**	$\mathcal{A}$	$\mathcal{B}$
"bulk"	"vac"	(19.167)	(19.158)
"bulk"	"bulk"	(19.172)	(19.158)
"vac"	"vac"	(19.167)	(19.177)

Table 19.3. Definitions of Madelung constants and their reduced counterparts: equation numbers

Real space definitions	**Equation number**
Madelung constants	(19.28)
Reduced Madelung constants	(19.36)
Relation between both	(19.35)

References

1. I.S. Gradshteyn and I.M. Ryzhik, *Table of Integrals, Series and Products*, Corrected and Enlarged Edition (Academic Press Inc., 1980)
2. M. Abramowitz and I. Stegun, *Handbook of Mathematical Functions* (Dover Publ., New York 1973)
3. R. Hammerling: Aspects of dispersion interactions and of the full-potential Korringa–Kohn–Rostoker (KKR) method for semi-infinite systems. PHD Thesis, Technical University, Vienna (2003). http://www.cms.tuwien.ac.at/PhD_Theses

20 “Near field” corrections

The problem of “near field” corrections arises from the fact that by solving the Poisson equation in terms of classical electrodynamics, which describes the potential due to a charge distribution by an expansion in terms of multipole moments [1], this expansion no longer is valid for neighboring or – better – near cells in the case of a space filling geometry, i.e., when using Wigner Seitz cells. By definition a cell centered at position $\mathbf{R}'$ is called a near cell of a cell centered at $\mathbf{R}$ if

$$|\mathbf{R} - \mathbf{R}'| < r_{\mathrm{BS}} + r'_{\mathrm{BS}} \quad , \tag{20.1}$$

where r_{BS} denotes the radius of the bounding sphere. In the following two different methods are presented in order to circumvent this problem.

20.1 Method 1: shifting bounding spheres

In this particular case one has to consider what has been called by Gonis [2] the *moon region*, namely the complement of the Wigner-Seitz cell and its circumscribed sphere.

In order to treat also nearest neighbors rigorously, a special reformulated multipole expansion of the inverse of the difference vector $\mathbf{r}_R - \mathbf{r}'_R$ has to be used.

Let $\mathbf{b}$ denote a vector for which the relation $b < |\mathbf{r}_R - \mathbf{R}'_R - \mathbf{b}|$ is always true. Adding and subtracting this vector one can make use of the below identity,

$$\frac{1}{|\mathbf{r}_R - \mathbf{r}'_R|} = \frac{1}{|-\mathbf{b} - (\mathbf{r}_R - \mathbf{r}'_R - \mathbf{b})|} \quad , \tag{20.2}$$

where

$$\mathbf{r}_R = \mathbf{r} - \mathbf{R} \quad , \tag{20.3}$$

$$\mathbf{r}'_R = \mathbf{r}' - \mathbf{R}' \quad . \tag{20.4}$$

It is advantageous to choose $\mathbf{b}$ in the direction of $\mathbf{R} - \mathbf{R}'$. This particular choice of $\mathbf{b}$ will be denoted in the following by $\mathbf{b}_{RR'}$. Making use of the expansion in (A.3) of the Appendix yields:

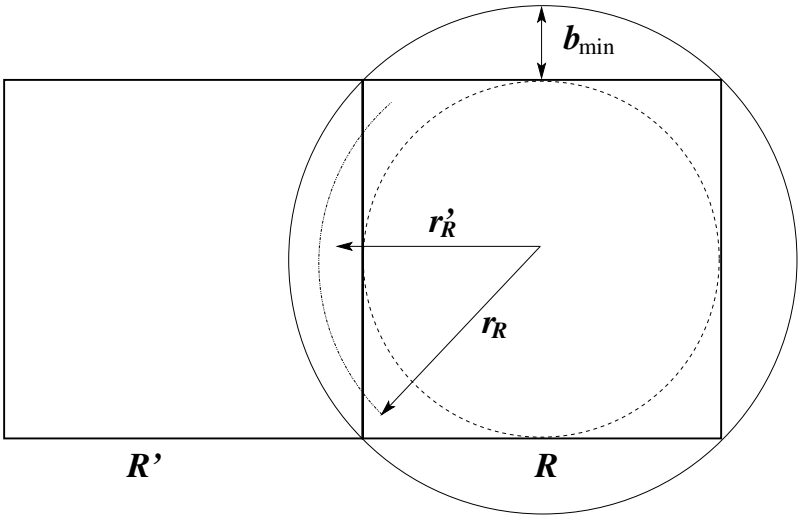

Fig. 20.1. The moon region of two adjacent cells for which the muffin tin condition is not satisfied. It can be seen from this sketch that the vector r'_R, even though it extends into the neighboring cell, R', can be shorter than the vector r_R in cell R. The minimum length of the displacement vector is indicated by $b_{\min}$.

$$\frac{1}{|-\mathbf{b}_{RR'} - (\mathbf{r}_R - \mathbf{r}'_R - \mathbf{b}_{RR'})|} = \sum_L \frac{4\pi}{2\ell+1}\, b^\ell_{RR'}\, Y^*_{\ell m}(-\hat{\mathbf{b}}_{RR'})\, \frac{Y_{\ell m}(\mathbf{r}_R - \widehat{(\mathbf{r}'_R + \mathbf{b}_{RR'})})}{|\mathbf{r}_R - (\mathbf{r}'_R + \mathbf{b}_{RR'})|^{\ell+1}} \quad . \tag{20.5}$$

In order to proceed, one condition has to be imposed on the minimum length of the vector $\mathbf{b}_{RR'}$: it has to be at least as large as the difference between the radius of the circumscribing sphere and the inscribed sphere, see also Fig. 20.1. This implies that $r_R < |\mathbf{r}'_R + \mathbf{b}_{RR'}|$, and therefore the expansion in (A.4) of the Appendix can be applied:

$$\begin{aligned}\frac{1}{|-\mathbf{b}_{RR'} - (\mathbf{r}_R - \mathbf{r}'_R - \mathbf{b}_{RR'})|} = \sum_L \frac{(-1)^\ell\,(4\pi)^2}{2\ell+1}\, b^\ell_{RR'}\, Y^*_{\ell m}(\hat{\mathbf{b}}_{RR'}) \\ \times \sum_{L'} (-1)^\ell\, \frac{(2(\ell+\ell')-1)!!}{(2\ell-1)!!\,(2\ell'+1)!!}\, C^{\ell' m'}_{\ell m,(\ell+\ell')(m'-m)} \\ \times \frac{Y^*_{(\ell+\ell')(m'-m)}(\widehat{\mathbf{r}'_R + \mathbf{b}_{RR'}})}{|\mathbf{r}'_R + \mathbf{b}_{RR'}|^{\ell+\ell'+1}}\, r^{\ell'}_R\, Y_{\ell' m'}(\hat{\mathbf{r}}_R) \quad .\end{aligned} \tag{20.6}$$

The summations over L and L' in this equation are both infinite. Because the inner sum over L' depends on the value of L, the double summation is (only) conditionally convergent and its order cannot be interchanged.

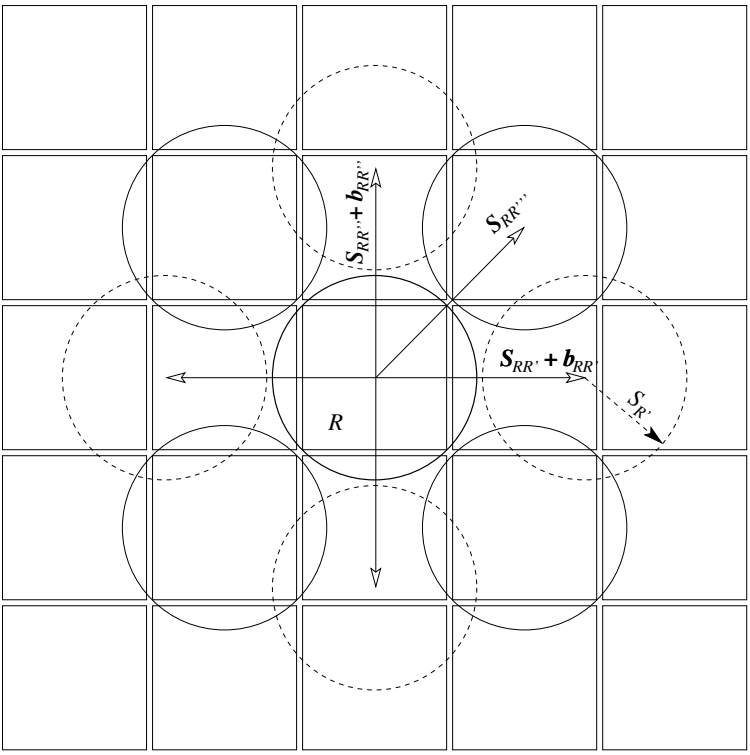

Fig. 20.2. The bounding spheres of neighboring cells, which would overlap with the bounding sphere of the cell at R are shifted away along the direction of $S_{RR'}$. From this illustration it is clear that it is of advantage to align $S_{RR'}$ and $b_{RR'}$ parallel.

Using however the below identity,

$$\mathbf{r}'_R + \mathbf{b}_{RR'} = \mathbf{r}'_{R'} - (\mathbf{S}_{R'R} - \mathbf{b}_{RR'}) \quad , \tag{20.7}$$

with

$$\mathbf{S}_{RR'} = \mathbf{R}' - \mathbf{R} \quad , \tag{20.8}$$

in terms of (A.4) in the Appendix the following expansion is found:

$$\frac{Y^*_{(\ell+\ell')(m'-m)}(\widehat{\mathbf{r}'_R + \mathbf{b}_{RR'}})}{|\mathbf{r}'_R + \mathbf{b}_{RR'}|^{\ell+\ell'+1}} =$$
$$\sum_{L''}(-1)^{\ell+\ell'} 4\pi \frac{(2(\ell+\ell'+\ell'')-1)!!}{(2(\ell+\ell')-1)!!\,(2\ell''+1)!!} C^{\ell''m''}_{(\ell+\ell')(m'-m),(\ell+\ell'+\ell'')(m''-m'+m)}$$
$$\times \frac{Y_{(\ell+\ell'+\ell'')(m''-m'+m)}(\widehat{\mathbf{S}_{R'R} - \mathbf{b}_{RR'}})}{|\mathbf{S}_{R'R} - \mathbf{b}_{RR'}|^{\ell+\ell'+\ell''+1}} r'^{\ell''}_{R'} Y^*_{\ell''m''}(\hat{\mathbf{r}}'_{R'}) \quad , \tag{20.9}$$

which requires $r'_{R'} < |\mathbf{S}_{RR'} + \mathbf{b}_{RR'}|$. This expansion can now be inserted into (20.6).

Making use of the following identity, where for simplicity the arguments are left out and the definitions $m''' = m' - m$, $m^{iv} = m'' - m' + m$, and $\{m\} = mm'm''m'''m^{iv}$ are used,

$$\sum_{\{m\}} Y^*_{\ell m}\, Y_{\ell' m'}\, Y^*_{\ell'' m''}\, Y_{(\ell+\ell'+\ell'')m^{iv}}\, C^{\ell' m'}_{\ell m,(\ell+\ell')m'''}\, C^{\ell'' m''}_{(\ell+\ell')m''',(\ell+\ell'+\ell'')m^{iv}} = \sum_{\{m\}} Y_{\ell m}\, Y_{\ell' m'}\, Y^*_{\ell'' m''}\, Y^*_{(\ell+\ell'+\ell'')m^{iv}}\, C^{(\ell+\ell')m'''}_{\ell m,\ell' m'}\, C^{(\ell+\ell')m'''}_{\ell'' m'',(\ell+\ell'+\ell'')m^{iv}} \quad , \tag{20.10}$$

in combining (20.6) and (20.9), one arrives at the below final expression

$$\frac{1}{|\mathbf{r}_R - \mathbf{r}'_R|} = 2\pi \sum_L b^\ell\, Y_{\ell m}(\hat{\mathbf{b}}_{RR'}) \sum_{L'} r'^{\ell'}_R\, Y_{\ell' m'}(\hat{\mathbf{r}}_R)\, C^{(\ell+\ell')(m+m')}_{\ell m,\ell' m'} \times \sum_{L''} B_{LL'L''}(\mathbf{S}_{RR'} + \mathbf{b}_{RR'})\, \sqrt{4\pi}\, r'^{\ell''}_{R'}\, Y^*_{\ell'' m''}(\hat{\mathbf{r}}'_{R'}) \quad , \tag{20.11}$$

in which the coefficients $B_{LL'L''}(\mathbf{S}_{RR'} + \mathbf{b}_{RR'})$ are defined by

$$B_{LL'L''}(\mathbf{S}_{RR'} + \mathbf{b}_{RR'}) = (-1)^{\ell''}\, \frac{8\pi\ (2(\ell+\ell'+\ell'')-1)!!}{(2\ell+1)!!\,(2\ell'+1)!!\,(2\ell''+1)!!} \times \sqrt{4\pi}\, C^{(\ell+\ell')(m+m')}_{\ell' m',(\ell+\ell'+\ell'')(m+m'-m'')}\, \frac{Y^*_{(\ell+\ell'+\ell'')(m+m'-m'')}(\widehat{\mathbf{S}_{RR'} + \mathbf{b}_{RR'}})}{|\mathbf{S}_{RR'} + \mathbf{b}_{RR'}|^{\ell+\ell'+\ell''+1}} \quad . \tag{20.12}$$

An interpretation of the derivation of (20.11) is the following. Initially the neighboring cells are displaced by the vector $\mathbf{b}_{RR'}$ until the bounding spheres are no longer overlapping. This can be expressed in terms of the multipole moments of the undisplaced cell which corresponds to the inner summation over L'' in (20.11). The outer sum (over L) can then be interpreted as a shift of the cell back to its original position [3].

The convergence of the summations in (20.11) depends sensitively on $\mathbf{b}_{RR'}$. Different authors gave different prescriptions of how the vectors $\mathbf{b}_{RR'}$ should be chosen. According to Gonis, its length should be approximately of the size of the inter-cell vector, however, Vitos et al. [4] found that the displacement vectors $\mathbf{b}_{RR'}$ are related to the radii of the circumscribed spheres of the neighboring cells by

$$|\mathbf{S}_{RR'} + \mathbf{b}_{RR'}| = (1+\alpha)(r_{\mathrm{BS}} + r'_{\mathrm{BS}}) \quad , \tag{20.13}$$

where the parameter α is the ratio between $\ell_{\max}$ and $\ell'_{\max}$, i.e.

$$\alpha = \frac{\ell_{\max}}{\ell'_{\max}} \quad , \tag{20.14}$$

and r_{BS} is the radius of the circumscribed sphere.

The near field corrections to the intercell potential $V^{\mathrm{nf}}(\mathrm{r})$ induced by a charge distribution of a specific near cell can be expressed with the help of (20.11) as

$$V^{\mathrm{nf}}_{\mathbf{R}\mathbf{R}'}(\mathbf{r}) = 2 \int\limits_{\Omega} \mathrm{d}\mathbf{r}' \, \frac{\rho(\mathbf{r}')}{|\mathbf{r}-\mathbf{r}'|} = 4\pi \sum_{LL'L''} b^{\ell} \, Y_L(\hat{\mathbf{b}}) r^{\ell'} \, Y_{L'}(\hat{\mathbf{r}}) \, C^{(\ell+\ell')(m+m')}_{\ell m, \ell' m'} B_{LL'L''}(\mathbf{S}+\mathbf{b}) Q_{\mathbf{R}',L''} \quad , \tag{20.15}$$

where the vector $\mathbf{S}$ connects the two cell centers, the displacement vector aligned parallel to it is denoted by $\mathbf{b}$, and the multipole moments of the near cells, see Chap. 19, are defined by

$$Q_{\mathbf{R},L} = \sqrt{4\pi} \int\limits_{\Omega_{\mathbf{R}}} \mathrm{d}\mathbf{r} \, r^{\ell} \, Y^{*}_{L}(\hat{\mathbf{r}}) \rho_{\mathbf{R}}(\mathbf{r}) \quad . \tag{20.16}$$

Summing up the contributions of all near cells the near field potential is given by

$$V^{\mathrm{nf}}_{\mathbf{R}}(\mathbf{r}) = \sum_{\mathbf{R}' \in \mathrm{nc}} V^{\mathrm{nf}}_{\mathbf{R}\mathbf{R}'}(\mathbf{r}) \quad . \tag{20.17}$$

Since (20.15) contains internal sums that are only conditionally convergent, in the next section an alternative approach is presented which avoids this kind of numerical difficulties.

20.2 Method 2: direct evaluation of the near field corrections

A real-space method which yields the exact intercell potential of neighboring or near cells is the following: one first has to compute the contributions to the intercell potential arising from near cells via a coordinate transformation of their intracell potentials. Then the sum over all near cells is performed and the expansion coefficients of the angular momentum series is evaluated by means of a numerical angular integration.

The intracell potential of a particular charge distribution inside a cell with respect to the coordinate system centered in that cell is given by

$$V^{\mathrm{intra}}(\mathbf{r}) = \sum_{L} \frac{8\pi}{2\ell+1} \left(r^{\ell} \int\limits_{r}^{r_{\mathrm{BS}}} \mathrm{d}r' \; (r')^{-\ell+1} \, \bar{\rho}_L(r') + r^{-\ell-1} \int\limits_{0}^{r} \mathrm{d}r' \; (r')^{\ell+2} \, \bar{\rho}_L(r') \right)^{*} Y_L(\hat{\mathbf{r}}) \quad , \tag{20.18}$$

where the expansion coefficients of the shape truncated charge density are of the form

$$\bar{\rho}_L(r) = \sum_{L'L''} C^{L'}_{L''L} \rho_{L'}(r) \sigma_{L''}(r) \quad . \tag{20.19}$$

For values of $\mathbf{r}$ beyond the bounding sphere radius this potential can be written in terms of multipole moments Q_L:

$$V^{\rm intra}(\mathbf{r}) = \sum_L \frac{4\sqrt{\pi}}{r^{\ell+1}} Q^*_L \, Y_L(\hat{\mathbf{r}}) \,, \quad r > r_{\rm BS} \quad , \tag{20.20}$$

see also Chap. 19.

The intracell potential of a cell Ω' centered at position $\mathbf{R}'$ contributes then to the intercell potential of a cell Ω centered at $\mathbf{R}$ as follows

$$V^{\rm nf}_{\mathbf{R}\mathbf{R}'}(\mathbf{r}) = V^{\rm intra}_{\mathbf{R}'}(\mathbf{R} - \mathbf{R}' + \mathbf{r}) \tag{20.21}$$

$$= \sum_L \frac{8\pi}{2\ell+1} \Bigg(|\mathbf{R} - \mathbf{R}' + \mathbf{r}|^{\ell} \int\limits_{|\mathbf{R}-\mathbf{R}'+\mathbf{r}|}^{r_{\rm BS}} {\rm d}r' \; (r')^{-\ell+1} \, \bar{\rho}_{\mathbf{R}'L}(r') + |\mathbf{R} - \mathbf{R}' + \mathbf{r}|^{-\ell-1} \int\limits_0^{|\mathbf{R}-\mathbf{R}'+\mathbf{r}|} {\rm d}r' \; (r')^{\ell+2} \, \bar{\rho}_{\mathbf{R}'L}(r') \Bigg)^* Y_L(\widehat{\mathbf{R} - \mathbf{R}' + \mathbf{r}}) \tag{20.22}$$

$$= \sum_L V^{\rm intra}_{\mathbf{R}',L}(|\mathbf{R} - \mathbf{R}' + \mathbf{r}|) Y_L(\widehat{\mathbf{R} - \mathbf{R}' + \mathbf{r}}) \quad , \tag{20.23}$$

which reduces outside the bounding sphere of cell Ω' to the below expression

$$V^{\rm nf}_{\mathbf{R}\mathbf{R}'}(\mathbf{r}) = \sum_L \frac{4\sqrt{\pi}}{|\mathbf{R} - \mathbf{R}' + \mathbf{r}|^{\ell+1}} \, Q^*_{\mathbf{R}',L} \, Y_L(\widehat{\mathbf{R} - \mathbf{R}' + \mathbf{r}}) \,, \quad |\mathbf{R} - \mathbf{R}' + \mathbf{r}| > r'_{\rm BS} \,. \tag{20.24}$$

Needed, however, is the expansion of $V^{\rm nf}_{\mathbf{R}\mathbf{R}'}(\mathbf{r})$ into an angular momentum series,

$$V^{\rm nf}_{\mathbf{R}\mathbf{R}'}(\mathbf{r}) = \sum_L V^{\rm nf}_{\mathbf{R}\mathbf{R}',L}(r) Y_L(\hat{\mathbf{r}}) \quad , \tag{20.25}$$

the coefficients of which have to be obtained by an integration over the unit sphere (for every radius r):

$$V^{\rm nf}_{\mathbf{R}\mathbf{R}',L}(r) = \int\limits_\Omega {\rm d}\hat{\mathbf{r}} \, V^{\rm nf}_{\mathbf{R}\mathbf{R}'}(\mathbf{r}) \, Y^*_L(\hat{\mathbf{r}}) \tag{20.26}$$

$$= \int\limits_\Omega {\rm d}\hat{\mathbf{r}} \left(\sum_{L'} V^{\rm intra}_{\mathbf{R}'L'}(|\mathbf{R} - \mathbf{R}' + \mathbf{r}|) Y_{L'}(\widehat{\mathbf{R} - \mathbf{R}' + \mathbf{r}}) \, Y^*_L(\hat{\mathbf{r}}) \right) \quad . \tag{20.27}$$

By applying a rotation of the coordinate system such that the z-axis points in the direction of the respective near cell the above two-dimensional angular integral can be reduced to a one-dimensional integral.

Then by summing up the contributions from all near cells a formally exact expression for the near field corrections is found:

$$V^{\mathrm{nf}}_{\mathbf{R},L}(r) = \int\limits_{\Omega} \mathrm{d}\hat{\mathbf{r}} \sum_{L'} \sum_{\mathbf{R}'\in \mathrm{nc}} V^{\mathrm{intra}}_{\mathbf{R}'L'}(|\mathbf{R}-\mathbf{R}'+\mathbf{r}|) Y_{L'}(\widehat{\mathbf{R}-\mathbf{R}'+\mathbf{r}})\, Y^*_L(\hat{\mathbf{r}}) \quad . \tag{20.28}$$

In Fig. 20.3 the geometrical arrangement is illustrated: one can see that in this case the corrections arise only outside a sphere of radius $r_{\mathrm{cor}} = |\mathbf{R}-\mathbf{R}'|-r'_{\mathrm{BS}}$. For a less symmetric neighborhood, however, one has to use

$$r_{\mathrm{cor}} = \min_{\mathbf{R}'} (|\mathbf{R}-\mathbf{R}'| - r'_{\mathrm{BS}}) \quad . \tag{20.29}$$

Consequently the quantities $V^{\mathrm{nf}}_L(r)$ have to be calculated only for points r outside that sphere (and inside a sphere of radius r_{BS}).

Another method to treat near field corrections has been given by Schadler [5] and may equally well be applicable.

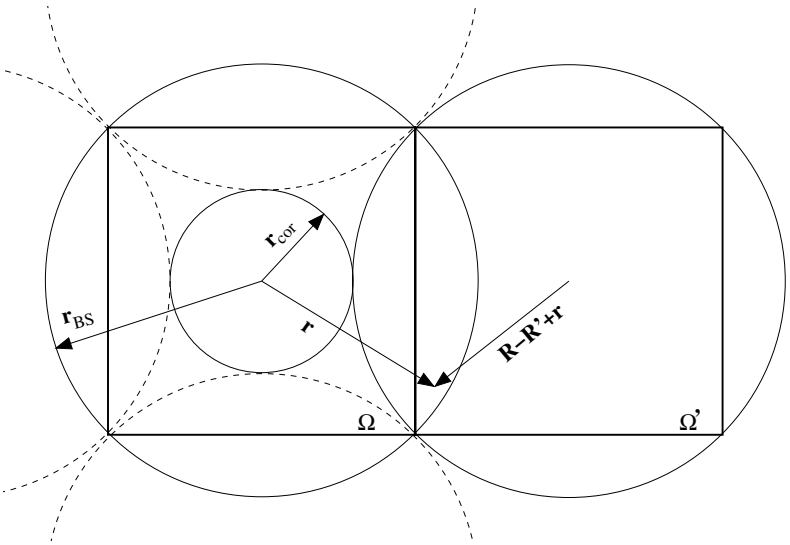

Fig. 20.3. Illustration of two near cells with overlapping bounding spheres. Dashed circles denote bounding spheres of other near cells. Also indicated is the radius r_{cor} outside which the near field corrections have to be calculated.

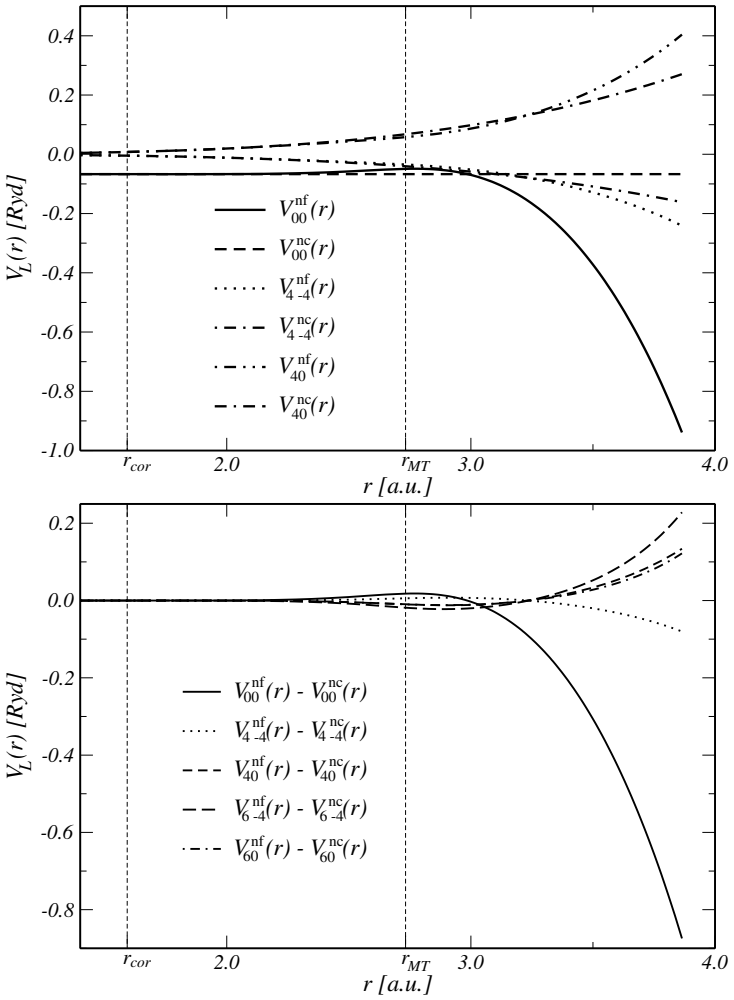

Fig. 20.4. Top: the first three non-vanishing angular momentum components of the near field potential $V_{\ell m}^{\rm nf}(r)$ and the near cell potential $V_{\ell m}^{\rm nc}(r)$ for fcc bulk Ag. The dashed vertical lines indicate the muffin-tin and $r_{\rm cor}$ radius, respectively. Note the different behaviour of the spherically symmetric components between the muffin-tin and the bounding sphere radius, whereas inside the muffin tin the differences are quite small. Inside a sphere of radius $r_{\rm cor}$ the components are identical. **Bottom:** angular momentum components of the near field corrections $V_{\ell m}^{\rm nf}(r) - V_{\ell m}^{\rm nc}(r)$ for fcc bulk Ag. For radii smaller than $r_{\rm cor}$ the corrections are vanishing.

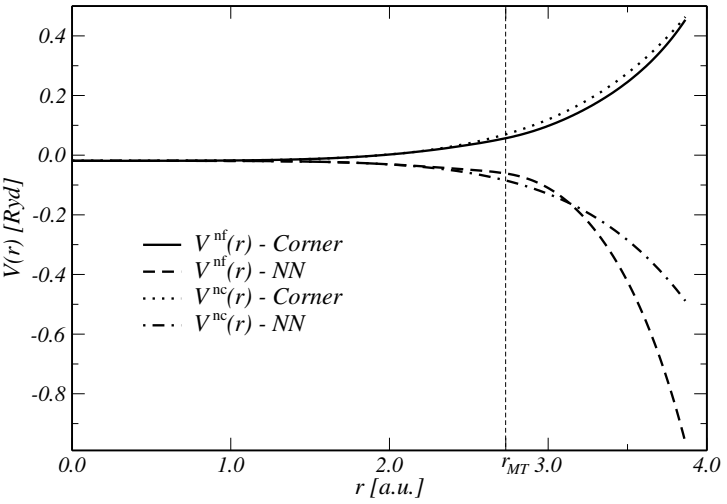

Fig. 20.5. Near field potential $V^{\mathrm{nf}}(\mathbf{r})$ and the incorrect potential from near cells $V^{\mathrm{nc}}(\mathbf{r})$ plotted towards the farthest corner of the cell (Corner) and along the nearest neighbor direction (NN).

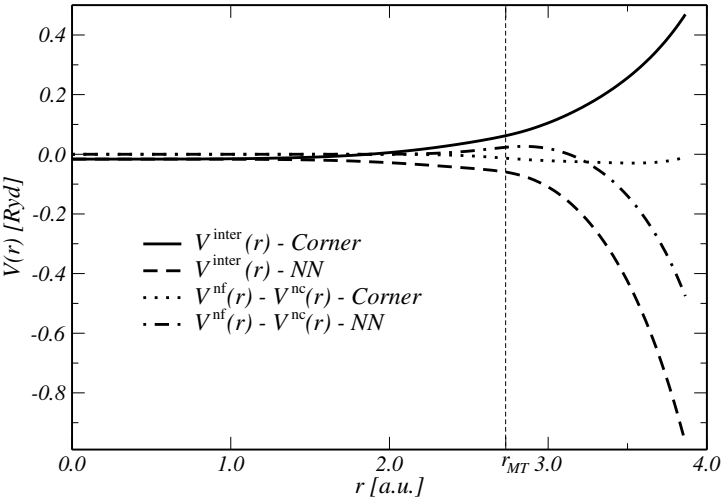

Fig. 20.6. Intercell potential including the near field corrections plotted along two different directions of an fcc Wigner-Seitz cell for the case of bulk Ag. The full line illustrates the potential towards the farthest corner (Corner) and the dashed line in nearest neighbor (NN) direction. Also shown are the near field corrections $V^{\mathrm{nf}}(\mathbf{r}) - V^{\mathrm{nc}}(\mathbf{r})$ along the same directions.

20.3 Corrections to the intercell potential

The correct intercell potential results then from adding the near field correction term and subtracting the (incorrect) contributions from the near cells (nc), implicitly contained in the previously derived Madelung potential results, see Chap. 19,

$$\tilde{V}_{\mathbf{R}}^{\text{inter}}(\mathbf{r}) = V_{\mathbf{R}}^{\text{inter}}(\mathbf{r}) + \left(V_{\mathbf{R}}^{\text{nf}}(\mathbf{r}) - V_{\mathbf{R}}^{\text{nc}}(\mathbf{r})\right) \quad , \tag{20.30}$$

where the differences $V_{\mathbf{R}}^{\text{nf}}(\mathbf{r}) - V_{\mathbf{R}}^{\text{nc}}(\mathbf{r})$ are the actual near field corrections to the intercell potential. In order to calculate the potential of near cells $V_{\mathbf{R}}^{\text{nc}}(\mathbf{r})$ the following real-space sum has to be evaluated:

$$V_{\mathbf{R}}^{\text{nc}}(\mathbf{r}) = 2 \sum_{\mathbf{R}' \in \text{nc}} \sum_{L} \frac{\sqrt{4\pi}}{2\ell+1} \left(\sum_{L'} A_{\mathbf{R}\mathbf{R}'}^{LL'} Q_{\mathbf{R}'}^{L'} \right)^{*} r^{\ell} Y_L(\hat{\mathbf{r}}) \quad , \tag{20.31}$$

where the real space summation runs over all near cells and the $A_{\mathbf{R}\mathbf{R}_{nc}}^{LL'}$ are the corresponding *real space Madelung* constants,

$$A_{\mathbf{R}\mathbf{R}'}^{LL'} = (-1)^{\ell} \frac{4\pi[2(\ell+\ell')-1]!!}{(2\ell-1)!!(2\ell'-1)!!} C_{\ell m,(\ell+\ell')(m'-m)}^{\ell' m'} \frac{Y_{(\ell+\ell')(m'-m)}^{*}(\widehat{\mathbf{R}-\mathbf{R}'})}{|\mathbf{R}-\mathbf{R}'|^{\ell+\ell'+1}} \quad . \tag{20.32}$$

Fig. 20.4 illustrates the angular momentum components of the potential arising from the near field corrections derived from (20.28) and the near cell potential as implicit in (20.31) for the case of fcc bulk Ag. If the differences of the respective angular momentum components are plotted, the results show that the corrections in fact vanish below the radius r_{cor} and all components are rather small up to the muffin-tin radius. Beyond the muffin-tin region the spherical symmetric component picks up the character of the intracell potential of a near cell. This feature is also reflected in Fig. 20.6 where the near field corrected intercell potential of (20.30) and the near field corrections are plotted along two directions in the Wigner-Seitz cell. If drawn in the nearest neighbor direction the corrections are small up to the muffin-tin radius and then diverge in the same manner as the intracell potential of the neighboring cell. If shape functions are applied this behavior is suppressed as they force the potential to jump to zero at the cell boundary. If plotted in the direction of the farthest corner of the cell the corrections are small with respect to the magnitude of the intercell potential up to the bounding sphere radius.

References

1. J.D. Jackson, *Classical Electrodynamics* (Wiley, New York 1992)
2. A. Gonis, *Green Functions for Ordered and Disordered Systems* (Elsevier Science Publishers B.V., New York 1992)

3. A. Gonis, E.C. Sowa, and P.A. Sterne, Phys. Rev. Lett. **66**, 2207 (1991).
4. L. Vitos, and J. Kollar, Phys. Rev. B **51**, 4074 (1995).
5. G.H. Schadler, Phys. Rev. B **45**, 11314 (1992).

21 Practical aspects of full-potential calculations

In this short chapter first an unpleasant side-effect of having to deal with shape functions in full potential calculations, namely their slow convergence properties, shall be investigated, and an approach is suggested to reduce some of the inherent computational problems. This will be followed by a discussion of the effect of the maximum orbital angular momentum quantum number $\ell_{\max}$ included in self-consistent calculations.

21.1 Influence of a constant potential shift

The shape or characteristic function $\sigma(\mathbf{r})$ of a cell has the purpose to cut off the (single-site) potential at the cell boundary. Ideally this means that the potential has a discontinuity there and jumps to zero beyond. Because the angular momentum expansion has to be limited, this jump of the shape truncated potential $\upsilon(\mathbf{r})$ at the cell boundary is only crudely approximated. The potential leaves the cell with a finite slope and is even slightly positive before finally dropping to zero, see Fig. 21.1. This "deficiency" leads not only to inaccuracies, e.g., in integrals over the Wigner-Seitz cell, but also produces an unphysical charge accumulation in the corners of the Wigner-Seitz cell. In order to circumvent such difficulties one can make use of the fact that a global constant added to the potential in all layers can be chosen freely:

$$V^{\text{shift}}(\mathbf{r}) = V^{\text{noshift}}(\mathbf{r}) + C \quad , \tag{21.1}$$

such that

$$\upsilon^{\text{shift}}(\mathbf{r}) = V^{\text{shift}}(\mathbf{r})\,\sigma(\mathbf{r}) \quad , \tag{21.2a}$$

$$\upsilon^{\text{noshift}}(\mathbf{r}) = V^{\text{noshift}}(\mathbf{r})\,\sigma(\mathbf{r}) \quad . \tag{21.2b}$$

In a bulk system one can, e.g., shift the potential to zero at the muffin-tin radius in the nearest neighbor direction, a procedure, which in turn reduces substantially the number of self-consistent iterations needed to converge the potential. This shifted potential should – in principle – leave the charge density unchanged but for reasons mentioned above this is in fact not the case [2]. The accuracy of the charge density, however, is improved, as can be seen from Fig. 21.1.

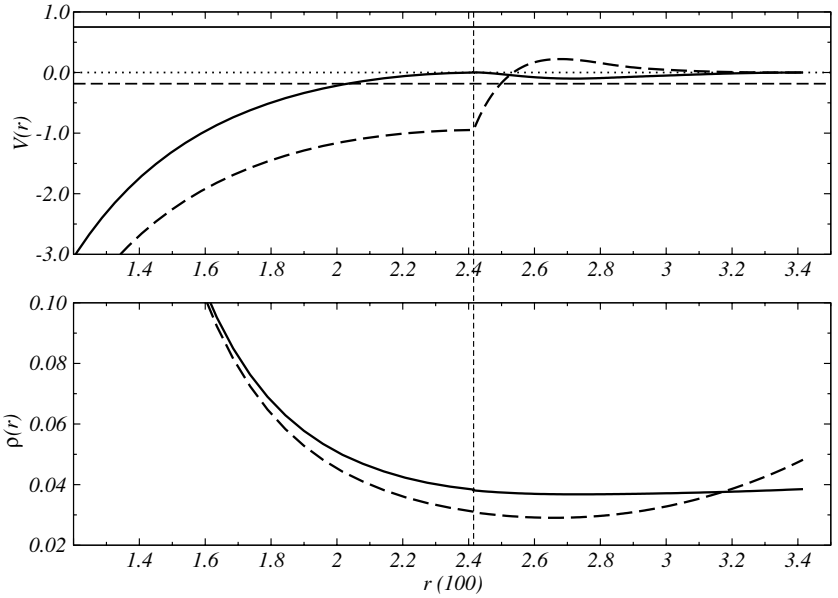

Fig. 21.1. Shifted and unshifted charge densities (in a.u.), and shifted and unshifted shape truncated potentials (in Ryd) of fcc bulk Cu for $\ell_{\max} = 6$ plotted in the direction of a nearest neighbor. Upper panel: $v^{\text{shift}}(\mathbf{r})$ full line, $v^{\text{noshift}}(\mathbf{r})$ dashed line, in the nearest neighbor direction. The horizontal lines are the Fermi energy of the shifted (full line) and unshifted (dashed line) potentials. Lower panel: charge density of the shifted (full line) and unshifted (dashed line) potential. The vertical dashed line marks the muffin tin radius.

Ultimately, however, also the self-consistent potential is calculated more accurately as can be seen from Fig. (21.2), in which the three components of the total (untruncated) potential $V^{\text{xc}}(\mathbf{r})$, $V^{\text{intra}}(\mathbf{r})$, and $V^{\text{inter}}(\mathbf{r})$ are shown for a shifted and an unshifted potential. The intra-cell and the exchange-correlation potential which have discontinuous derivatives at the cell boundary in a calculation with an unshifted potential become smooth functions at that point if a shifted potential is used. Furthermore, the peak of the inter-cell potential there, which is a result of insufficient angular momentum convergence as will be shown below, is decreased approximately by a factor of two.

Because of the strong anisotropic properties of a full-potential, see also Fig. 21.5, one can propose even better ways of how to shift the potential. If the shift potential is chosen such that the spherical symmetric expansion coefficient is zero at the muffin-tin radius,

$$v_{00}^{\text{shift}}(r_{\text{MT}}) = 0 \quad , \tag{21.3}$$

the effect of the shape functions is equally reduced in the nearest neighbor as well as in the corner direction.

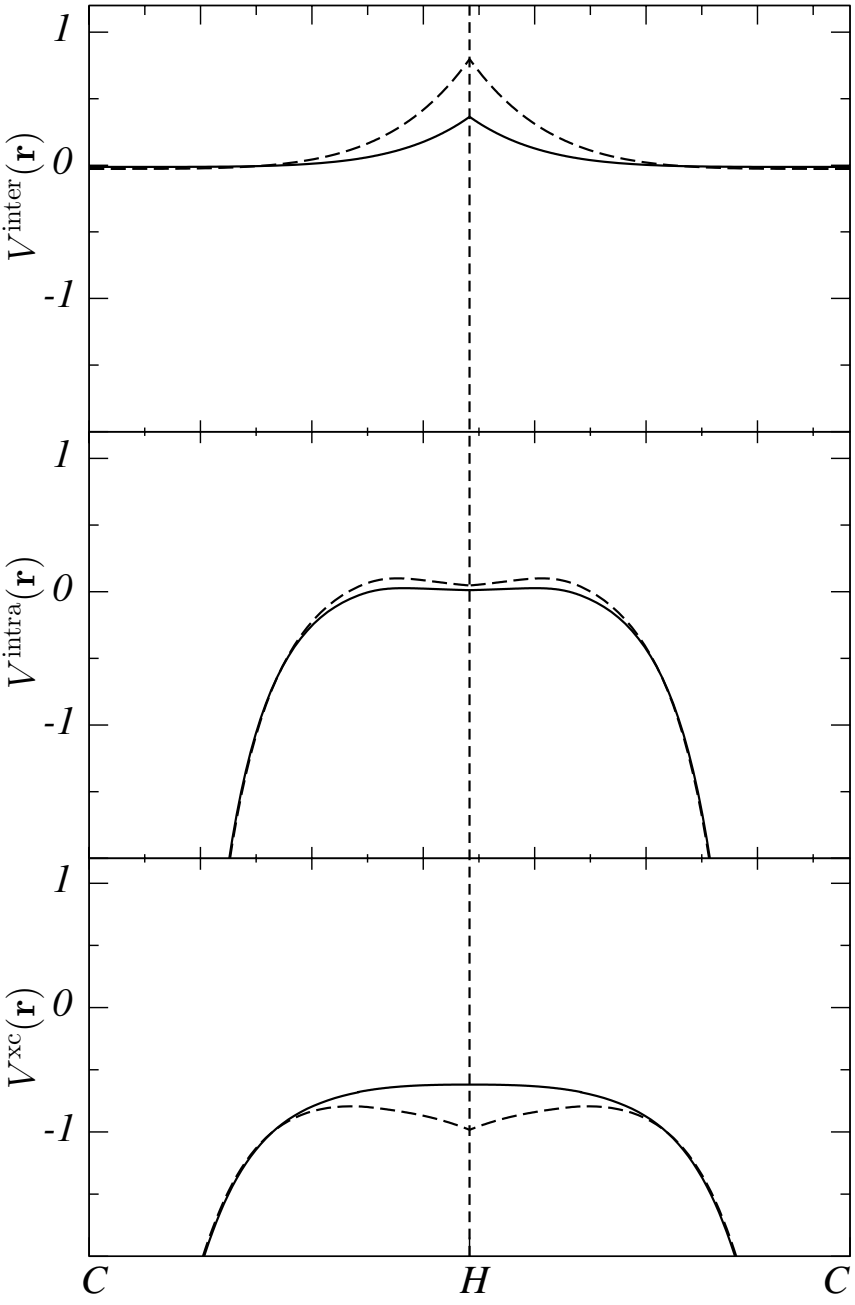

Fig. 21.2. Contributions to a converged bulk Cu potentials for $\ell_{\max} = 6$ between two Coulomb singularities. Dashed lines refer to the contributions to V^{noshift}, full lines to components of V^{shift}. The vertical dashed line marks the cell boundary.

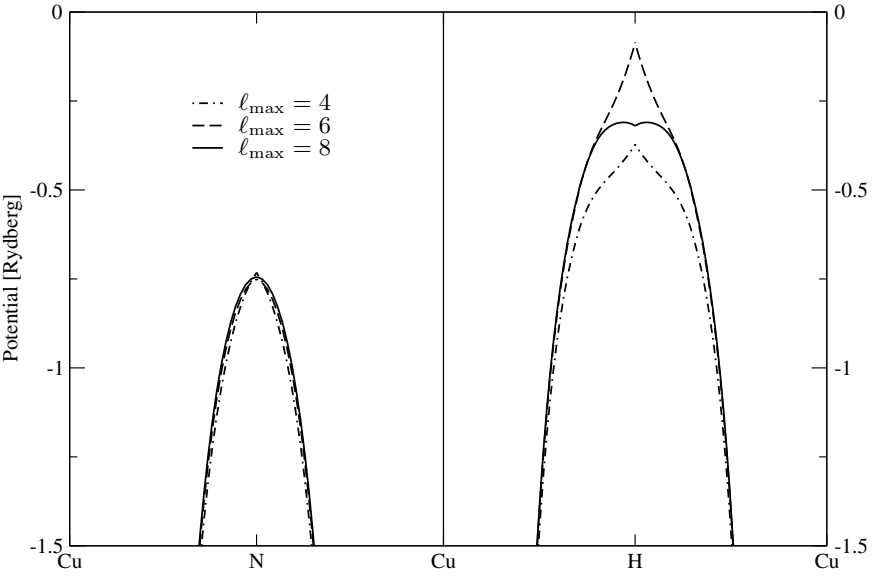

Fig. 21.3. Converged bulk Cu potentials (plotted with respect to their respective Fermi energies) between three Coulomb singularities for three different $\ell_{\max}$ for the potential. The label "H" marks a cell corner and "N" the center of a boundary plane.

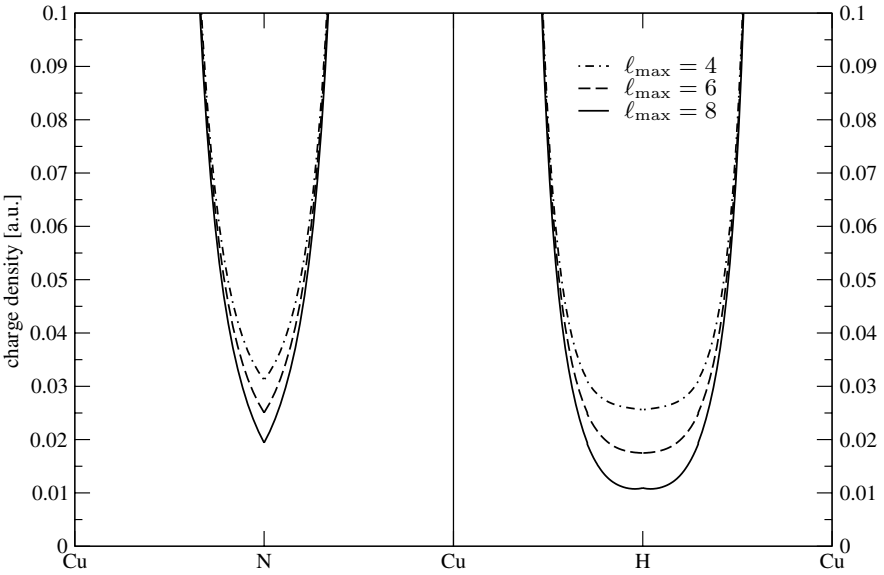

Fig. 21.4. Converged bulk Cu charge densities between three Coulomb singularities for three different $\ell_{\max}$ for the potential. The label "H" marks a cell corner and "N" the center of a boundary plane.

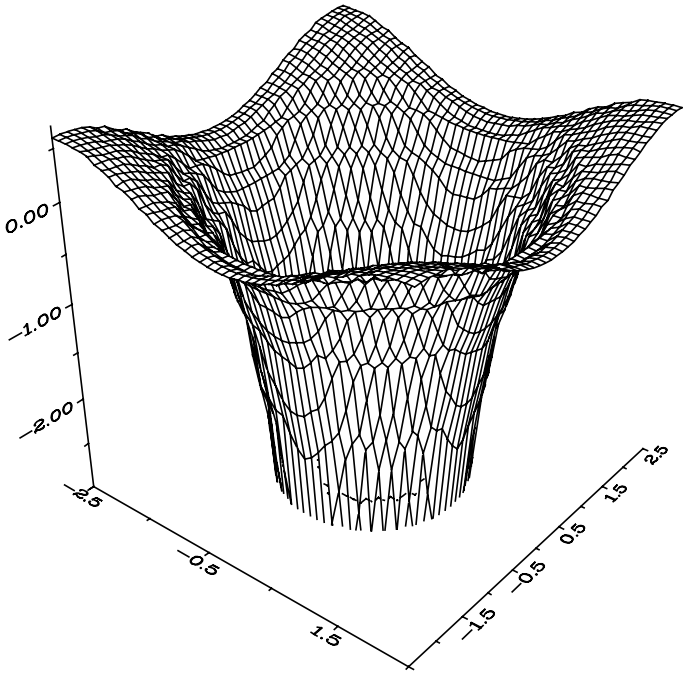

Fig. 21.5. Three-dimensional plot of an ideally shape truncated potential. Displayed is a cut through the center of an fcc cell oriented in the (001) direction.

Obviously in a surface calculation the zero of energy is determined by the preceding bulk calculation, and consequently it is not possible to shift the potential by another constant.

21.2 ℓ-convergence

As mentioned before if the scattering path operator is calculated up to an orbital momentum quantum number $\ell_{\max}$ then the expansion coefficients of the potentials and charge densities have to be evaluated up to $2\ell_{\max}$. Hence in Figs. 21.3 and 21.4 the reference value of $\ell_{\max} = 4$ corresponds to the use of $\ell_{\max} = 2$ for the scattering path operator.

In Fig. 21.3 the potential for fcc-Cu is plotted in the nearest neighbor direction and in the direction of a cell corner. In the former case no significant change in the potential can be detected with increasing $\ell_{\max}$. However, in the latter case the potential has prominent peaks for $\ell_{\max} = 4$ and 6 which arise from the inter-cell part of the potential, see also Fig. 21.2, and only vanishes if $\ell_{\max}$ is increased to 8. As a consequence the maximum of the potential is also shifted by a significant amount. Taking now a closer look at the charge density, which is plotted in Fig. 21.4 along the same directions

as the potential, one can see that with increasing angular momentum the charge density near the cell boundary is reduced. In full-potential calculations it is therefore not sufficient [1] to simply include the "physically relevant" (say "spd" or "spdf" angular momentum components as is the case in ASA calculations.

References

1. S. Bei der Kellen, Yoonsik Oh, E. Badralexe, and A.J. Freeman, Phys. Rev. B **51**, 9560 (1995).
2. R. Zeller, M. Asato, T. Hoshino, J. Zabloudil, P. Weinberger, and P.H. Dederichs, Phil. Mag. B **78**, 417 (1998).

22 Total energies

22.1 Calculation of the total energy

According to density functional theory the total energy is defined as the sum of a universal functional $G[\rho]$ that contains the kinetic energy $T[\rho]$ of non-interacting particles of density ρ and the exchange-correlation energy $E_{\rm xc}[\rho]$, and a functional $F[\rho]$, which includes all Coulomb contributions [2],

$$E[\rho] \equiv G[\rho] + F[\rho] \quad , \tag{22.1}$$

$$G[\rho] \equiv T[\rho] + E_{\rm xc}[\rho] \quad , \tag{22.2}$$

and the Coulomb contribution to the total energy is in general given by (using Rydberg units, i.e. $e^2 = 2$):

$$F[\rho] \equiv \int {\rm d}\mathbf{r}\, \rho(\mathbf{r})\, v(\mathbf{r}) + U[\rho] \quad , \tag{22.3}$$

In the above equation $v(\mathbf{r})$ is an external potential and $U[\rho]$ the Coulomb energy,

$$U[\rho] = \iint {\rm d}\mathbf{r}\, {\rm d}\mathbf{r}'\, \frac{\rho(\mathbf{r})\, \rho(\mathbf{r}')}{|\mathbf{r} - \mathbf{r}'|} \quad . \tag{22.4}$$

In the absence of an external potential the total energy obviously is nothing but the sum of the kinetic, exchange-correlation and Coulomb energy,

$$E_{\rm tot}[\rho] = T[\rho] + E_{\rm xc}[\rho] + U[\rho] \quad . \tag{22.5}$$

The three terms that add up to the total energy, will be separately discussed in the following sections, as each of them requires special considerations.

22.2 Kinetic energy

From the Kohn-Sham equations follows that the kinetic energy functional is given by

$$T[\rho] = E_{\rm one} - \int {\rm d}\mathbf{r}\, \rho(\mathbf{r})\, V(\mathbf{r}) \quad , \tag{22.6}$$

Table 22.1. *Comparison of atomic Hartree and Rydberg units.*

	Hartree	Rydberg
$\hbar$	1	1
m	1	1/2
e^2	1	2
c	137.036	274.072

where $V(\mathbf{r})$ refers to the effective potential in the Kohn-Sham equations which contains the Coulomb potential, exchange-correlation, and the external potential, if present.

The *one-electron energy*, $E_{\rm one}$, can be split up into a contribution arising from the core and the valence electrons:

$$E_{\rm one} = E_{\rm c} + E_{\rm v} \quad . \tag{22.7}$$

22.3 Core energy

The core contribution is given simply as the sum over the eigenvalues of the electron states in the core region,

$$E_{\rm c} = \sum_j \epsilon_j \quad , \tag{22.8}$$

where j runs over all core orbitals.

22.3.1 Radial Dirac equations

The core energies are obtained from a numerical solution of the Dirac equation with *atomic boundary conditions*, and is based on a procedure developed by J. P. Desclaux and described in [7]. One of the crucial questions to be discussed in this context is which potential should be used for the calculation of the core wave-functions.

The term *atomic boundary conditions* implies that the core wave-functions do not result from solving a scattering problem but are computed as atomic like states. If – which often happens – higher lying core levels have wave-functions extending significantly outside of the muffin-tin region of the Wigner-Seitz cell, they will have to be treated as *semi-core states* in a similar manner as valence states.

The coupled first order differential equations to be solved are given in atomic Hartree (!) units (see Tab. 22.1) as:

$$\frac{\mathrm{d}}{\mathrm{d}r}P_\kappa(r) = -\frac{\kappa}{r}\,P_\kappa(r) + \left[\frac{\epsilon - 2V(r)}{2c} - 2c\right] Q_\kappa(r) \quad , \tag{22.9}$$

$$\frac{\mathrm{d}}{\mathrm{d}r}Q_\kappa(r) = \frac{\kappa}{r}\,Q_\kappa(r) - \left[\frac{\epsilon - 2V(r)}{2c}\right] P_\kappa(r) \quad , \tag{22.10}$$

where $P_\kappa(r)$ and $Q_\kappa(r)$ are defined as

$$P_\kappa(r) = r g_\kappa(r) \quad , \quad Q_\kappa(r) = r f_\kappa(r) \quad , \tag{22.11}$$

and $\epsilon = 2(W - mc^2)$.

22.3.2 Numerical solution

It is convenient to define an equally spaced radial mesh by introducing $x = \ln r$, which in turn leads to the following coupled equations,

$$\frac{\mathrm{d}}{\mathrm{d}x}P_\kappa(x) = -\kappa\,P_\kappa(x) + e^x \left[\frac{\epsilon - 2V(x)}{2c} - 2c\right] Q_\kappa(x) \quad , \tag{22.12}$$

$$\frac{\mathrm{d}}{\mathrm{d}x}Q_\kappa(x) = \kappa\,Q_\kappa(x) - e^x \left[\frac{\epsilon - 2V(x)}{2c}\right] P_\kappa(x) \quad , \tag{22.13}$$

In order to obtain solutions to these equations first an outwards integration is performed using (for example) a five point Adams predictor–corrector method, chosen because of its stability properties. The predictor at the $(n{+}1)$-th mesh point p_{n+1} is given by

$$p_{n+1} = f_n + \frac{h}{720}\left(1901\,f'_n - 2774\,f'_{n-1} + 2616\,f'_{n-2} - 1274\,f'_{n-3} + 251\,f'_{n-4}\right) \tag{22.14}$$

and the corrector c_{n+1} by

$$c_{n+1} = f_n + \frac{h}{720}\left(251\,p'_n + 646\,f'_n - 264\,f'_{n-1} + 106\,f'_{n-2} - 19\,f'_{n-3}\right) \quad , \tag{22.15}$$

where h denotes the constant step size, and the resulting function at that mesh point is obtained from the below expression

$$f_{n+1} = \frac{1}{502}\left(475\,c_{n+1} + 27\,p_{n+1}\right) \quad . \tag{22.16}$$

Here the functions f_n and their derivatives f'_n denote the the radial solutions $P(x_n)$ and $Q(x_n)$ and their respective derivatives at the mesh point n. For this scheme at least five start values are needed, e.g., by a simple power series expansion [8].

Then an inwards integration is started at a point determined by the condition

$$[V(r) - \epsilon]\,r^2 \geq 300 \quad , \tag{22.17}$$

which for all practical purposes can be considered to represent infinity, and carried out up to the classical turning point. This is the point where the wave-functions changes from an oscillating to a monotonic behavior, which in turn can be determined by analyzing the number of nodes in the wave-functions. In other words, the oscillating function from the outwards integration has to be matched smoothly to the monotonous function due to the inwards integration.

The asymptotic forms of the relativistic wave-functions for $r \longrightarrow \infty$ are given by

$$P_\kappa(r) = pe^{-\mu r} \quad , \tag{22.18}$$

$$Q_\kappa(r) = qe^{-\mu r} \quad , \tag{22.19}$$

with

$$\mu = \sqrt{\epsilon - \frac{\epsilon^2}{4c^2}} \quad , \tag{22.20}$$

$$\frac{p}{q} = \frac{2c - \epsilon/2c}{\mu} \quad , \tag{22.21}$$

and are used to start the inwards integration, again carried out using the Adams predictor–corrector method. The one-electron energy ϵ has to be varied (readjusted) until the inward and outward integrations give identical values at the matching radius.

The procedure described above has to be repeated for each core orbital and yields an energy eigenvalue ϵ_j for each orbital in turn.

22.3.3 Core charge density

Once the radial wave-functions for all core orbitals are known the core charge density can be calculated from the below expression,

$$\rho_{\rm c}(r) = \sum_j n_j \frac{P_j(r)^2 + Q_j(r)^2}{r^2 N_j} \quad , \tag{22.22}$$

where n_j is the occupation number and N_j the normalization factor of orbital j as obtained from an integration over the Wigner-Seitz cell,

$$N_j = \int_\Omega {\rm d}\mathbf{r} \, \left[P_j(r)^2 + Q_j(r)^2\right] \sigma(\mathbf{r}) \tag{22.23}$$

$$= \frac{1}{\sqrt{4\pi}} \int_0^{r_{\rm BS}} {\rm d}r \, \left[P_j(r)^2 + Q_j(r)^2\right] \sigma_{00}(r) \quad , \tag{22.24}$$

such that each orbital j contains exactly n_j states.

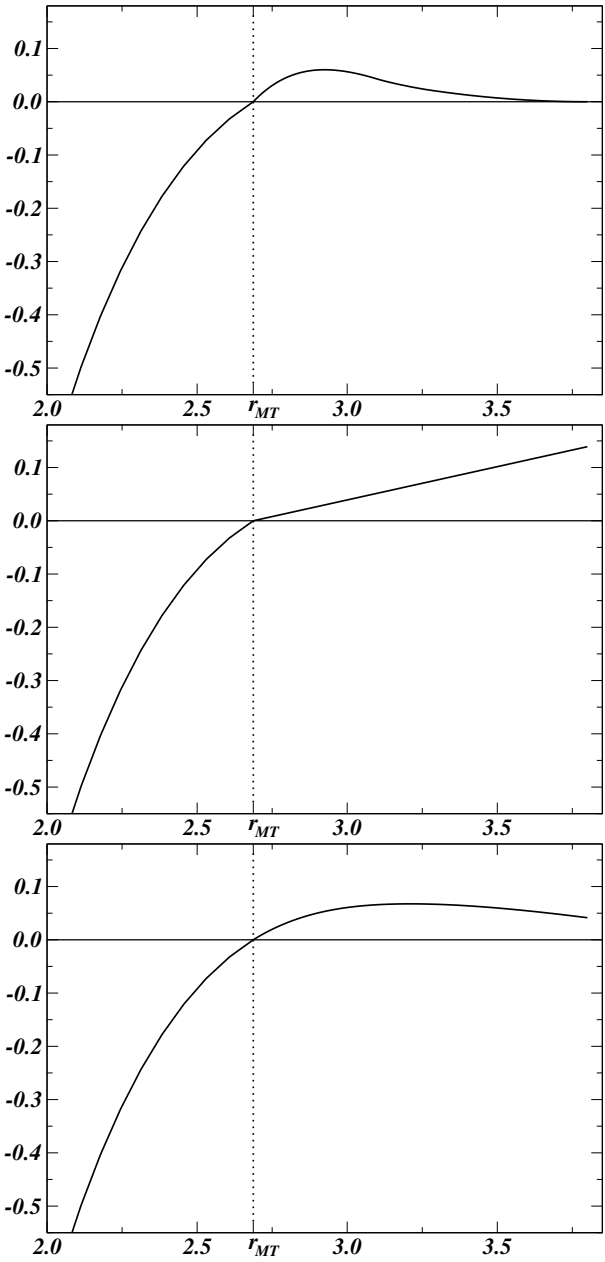

Fig. 22.1. Top: $v_{00}(r)$ serving as potential for the core calculation. Center: choosing $V_{00}(r)$ as potential for the core calculation. Beyond the muffin tin radius the potential is extrapolated using a constant line with an appropriately chosen slope. Bottom: $V_{00}(r)$ as potential for the core calculation. Beyond the bounding sphere radius the potential is extrapolated with a constant. (r in atomic units and $V(r)$ in Rydberg.)

22.3.4 Core potential

Clearly enough the method of numerically solving the radial Dirac equations is limited to spherically symmetric potentials. For the lower lying core states this is no serious limitation since they are well within a region of the potential where this condition is well satisfied. If, however, heavier atoms have to be considered or situations apply where the distance between adjacent atomic centers is reduced due to lattice distortions (such as in the case of layer relaxations) there may be energetically higher lying core states with wave-functions that significantly extend beyond the muffin-tin region. Such states will have to be treated as so-called *semi-core states*, i.e., have to augment the valence region.

For not too heavy atoms such higher core states can have wave-functions which are mostly confined to the muffin-tin sphere, but extend slightly into the interstitial region (this is the region between the muffin-tin and the bounding sphere radius). In order to treat these states correctly care has to be taken concerning the appropriate choice of the potential.

Since only potentials with spherical symmetry can be dealt with in the above described procedures, one possibility is to use the $L = (0, 0)$ component of the shape truncated potential. This core potential is given as

$$V_{\mathrm{c}}(r) = \begin{cases} 1/\sqrt{4\pi}\, v_{00}(r) & r \leq r_{\mathrm{BS}} \\ \\ 0 & r > r_{\mathrm{BS}} \end{cases} , \tag{22.25}$$

and plotted in Fig. 22.1. However, when trying to calculate an equilibrium lattice constant using this potential one fails to produce a minimum in the total energy curve. The reason is that the core electrons must not be treated on the same footing as valence states and hence the shape truncated single-site potential is not an appropriate choice. While for valence electrons a scattering problem has to be solved, where the single-site potential results from separating the (periodic crystal) potential into a sum over potentials confined to a (non-spherical) region in real space, the core electrons are treated as if belonging to an individual atom, i.e., reflect a proper atomic boundary condition for $r \longrightarrow \infty$. Therefore it leads to an erroneous result if a potential with a polyhedral shape is used (even by using only its leading expansion term).

A better choice for $V_{\mathrm{c}}(r)$ is to use the leading expansion term of the untruncated potential

$$V_{\mathrm{c}}(r) = \begin{cases} 1/\sqrt{4\pi}\, V_{00}(r) & r \leq r_{\mathrm{BS}} \\ \\ 1/\sqrt{4\pi}\, V_{00}(r_{\mathrm{BS}}) & r > r_{\mathrm{BS}} \end{cases} , \tag{22.26}$$

which is displayed in the bottom part of Fig. 22.1. With such a potential an equilibrium volume of a bulk system is readily obtained. The same minimum

can be found when one uses a linear continuation of the potential outside the muffin-tin:

$$V_{\rm c}(r) = \begin{cases} 1/\sqrt{4\pi}\, V_{00}(r) & r \le r_{\rm MT} \\ 1/\sqrt{4\pi}\, V_{00}(r_{\rm MT}) + k\,(r - r_{\rm MT}) & r > r_{\rm MT} \end{cases} \quad , \tag{22.27}$$

as indicated in the middle part of Fig. 22.1, where k is an appropriately chosen positive slope. Note that inside the muffin-tin region all three potentials are identical.

An interesting account on the various core approximations can be found in [21]. There the authors also find that the results for the equilibrium volumes is insensitive to the specific kind of extrapolation used for the potential outside the muffin-tin sphere.

22.4 Band energy

The second contribution to the one-electron energy in (22.7) is often referred to as *band energy* and can be evaluated by means of the following integral (along the real energy axis)

$$E_{\rm v} = \int_{-\infty}^{E_{\rm F}} {\rm d}\epsilon\, \epsilon\, n(\epsilon) \quad , \tag{22.28}$$

where $n(\epsilon)$ is the density of states for the valence electrons.

22.4.1 Contour integration

In using complex energies it is advisable to apply a Gaussian quadrature [1] for the occurring integral for which a special parameterization can be chosen such that the complex energies follow a semicircular contour and the mesh becomes exponentially denser when approaching the Fermi energy. The integral to be evaluated is of the form [3]

$$I = \int_{E_{\rm B}}^{E_{\rm F}} f(z)\, {\rm d}z \quad , \tag{22.29}$$

where z is some complex energy, $E_{\rm B}$ denotes the bottom of the valence band, which in practical calculations is a (real) energy well below the valence band, and $E_{\rm F}$ is the Fermi energy. A parameterization of complex energies can, e.g., consists of an angle φ and a radius r, see Fig. 22.3. In terms of the radius r,

$$r = \frac{E_{\rm F} - E_{\rm B}}{2} \quad , \tag{22.30}$$

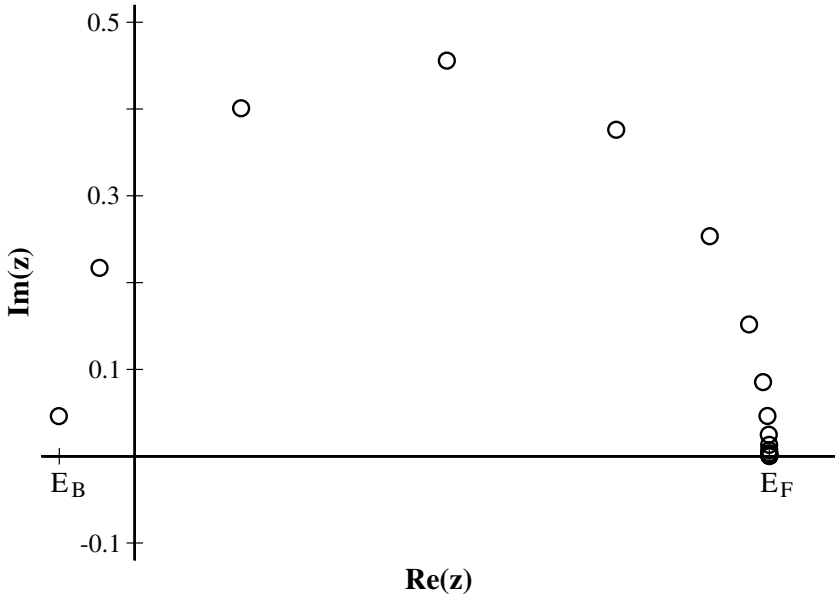

Fig. 22.2. Actual distribution of 16 energy points on a contour in the complex plane.

and by defining $z_0 = E_\mathrm{B} + r$, a particular complex energy is given by

$$z = z_0 + r\, e^{\mathrm{i}\varphi} \quad . \tag{22.31}$$

In order to obtain the desired distribution of complex energy points, φ is chosen such that

$$\varphi = \varepsilon \left(e^{-y} - 1 \right) \quad , \tag{22.32}$$

where ε is some small number and y is defined by

$$y = \frac{1}{2} \left(y_2 - y_1 \right) x_k + \frac{1}{2} \left(y_2 + y_1 \right) \quad . \tag{22.33}$$

In here the x_k are the zeros of Legendre polynomials, and y_1 and y_2 define the first and the last point on the contour as obtained from the conditions

$$y_1 = -\ln \left(\frac{\varepsilon + \varphi_1}{\varepsilon} \right) \quad , \tag{22.34}$$

$$y_2 = -\ln \left(\frac{\varepsilon + \varphi_2}{\varepsilon} \right) \quad , \tag{22.35}$$

In considering $\varphi_1 = \pi$ and $\varphi_2 = 0$ it easily can be checked that with $x_k = -1$ one gets $z = z_0 - r$ and with $x_k = 1$ one obtains $z = z_0 + r$. With this parameterization the integral to be solved can be evaluated by means of the below expression,

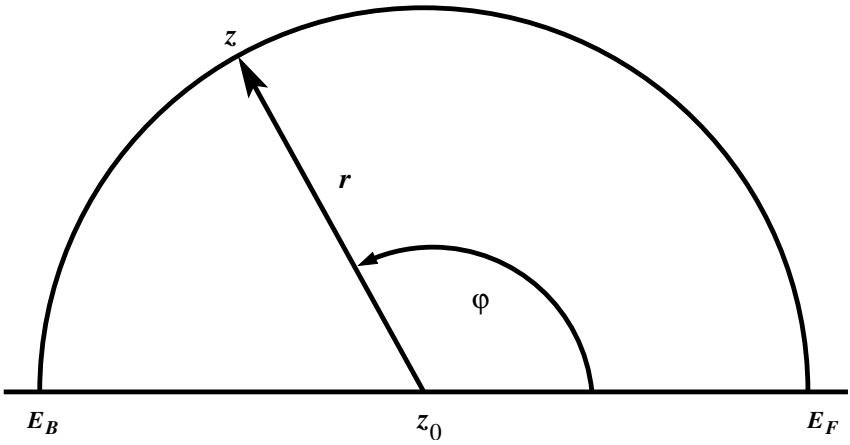

Fig. 22.3. Parameterization of the semicircular contour for the complex energy integration.

$$I = \sum_{k=1}^{n} \rho_k \, f(z_k) \quad , \tag{22.36}$$

where the parametrized weights, ρ_k, and the nodes, z_k, are given by

$$\rho_k = -\mathrm{i}\,\frac{\varepsilon\, e^{-y}\,(y_2 - y_1)\,(z_k - z_0)\,w_k}{2} \quad , \tag{22.37}$$

$$z_k = r\, e^{\mathrm{i}\varphi} + z_0 \quad . \tag{22.38}$$

22.5 Potential energy

The evaluation of the one-electron energies is rather straightforward, whereas the computation of the integral in (22.6) requires some consideration. Denoting the region of a particular Wigner Seitz cell centered at position $\mathbf{R}_i$ by Ω_i, the charge density can be written as a sum of localised cell contributions

$$\rho(\mathbf{r}) = \sum_i \overline{\rho}_i(\mathbf{r}_i) \quad , \quad \mathbf{r}_i = \mathbf{r} - \mathbf{R}_i \quad , \tag{22.39}$$

and the effective potential $V(\mathbf{r})$ by

$$V(\mathbf{r}) = \sum_i \upsilon_i(\mathbf{r}_i) \quad , \tag{22.40}$$

such that $\overline{\rho}_i(\mathbf{r}_i) = \upsilon_i(\mathbf{r}_i) = 0$ for $\mathbf{r}_i \notin \Omega_i$.

For a particular Wigner Seitz cell, the integral in (22.6) can be rewritten by making use of the shape functions as

$$\int\limits_{\Omega_i} \mathrm{d}\mathbf{r}_i \, \rho(\mathbf{r}_i) \, V(\mathbf{r}_i) = \int\limits_{\mathrm{BS}} \mathrm{d}\mathbf{r}_i \, \sigma(\mathbf{r}_i) \, \rho(\mathbf{r}_i) \, V(\mathbf{r}_i) \quad . \tag{22.41}$$

Employing now the following expansions in terms of complex spherical harmonics,

$$\rho(\mathbf{r}) = \sum_L \rho_L(r) \, Y_L^*(\hat{\mathbf{r}}) \quad , \tag{22.42}$$

$$V(\mathbf{r}) = \sum_L V_L(r) \, Y_L(\hat{\mathbf{r}}) \quad , \tag{22.43}$$

$$\sigma(\mathbf{r}) = \sum_L \sigma_L(r) \, Y_L(\hat{\mathbf{r}}) \quad , \tag{22.44}$$

where as should be recalled the charge density is expanded in terms of complex conjugated spherical harmonics, see also Chap. 19, one obtains from (22.41)

$$\begin{aligned} \int\limits_{\mathrm{BS}} \mathrm{d}\mathbf{r} \, \sigma(\mathbf{r}) \, \rho(\mathbf{r}) \, V(\mathbf{r}) &= \int\limits_{\mathrm{BS}} \mathrm{d}\mathbf{r} \sum_{LL'L''} Y_L(\hat{\mathbf{r}}) \, Y_{L'}^*(\hat{\mathbf{r}}) \, Y_{L''}(\hat{\mathbf{r}}) \, \sigma_L(r) \, \rho_{L'}(r) \, V_{L''}(r) \\ &= \int\limits_0^{r_{\mathrm{BS}}} r^2 \, \mathrm{d}r \sum_{LL'L''} C_{LL''}^{L'} \, \sigma_L(r) \, \rho_{L'}(r) \, V_{L''}(r) \quad . \end{aligned}$$

The coefficients of the shape truncated charge density $\overline{\rho}_L(r)$ are given by

$$\overline{\rho}_L(r) = \sum_{L'L''} C_{LL''}^{L'} \, \rho_{L'}(r) \, \sigma_{L''}(r) \quad . \tag{22.45}$$

By renaming indices, one finally arrives at

$$\int\limits_{\mathrm{BS}} \mathrm{d}\mathbf{r} \, \sigma(\mathbf{r}) \, \rho(\mathbf{r}) \, V(\mathbf{r}) = \int\limits_0^{r_{\mathrm{BS}}} r^2 \, \mathrm{d}r \sum_L \overline{\rho}_L(r) \, V_L(r) \quad . \tag{22.46}$$

In summary therefore the kinetic energy for a particular cell centered at position $\mathbf{R}_i$ can be evaluated in terms of the following expression

$$T[\rho] = \sum_j \epsilon_j + \int\limits_{-\infty}^{E_{\mathrm{F}}} \mathrm{d}\epsilon \, \epsilon \, n(\epsilon) - \int\limits_0^{r_{\mathrm{BS}}} r^2 \, \mathrm{d}r \sum_L \overline{\rho}_L(r) \, V_L(r) \quad . \tag{22.47}$$

22.6 Exchange and correlation energy

If $\rho(\mathbf{r})$ is varying sufficiently slowly, the exchange-correlation energy is given [2] by

$$E_{\rm xc} = \int\limits_{\Omega} {\rm d}\mathbf{r}\, \rho(\mathbf{r})\, \varepsilon_{\rm xc}[\rho(\mathbf{r})] \quad , \tag{22.48}$$

where $\epsilon_{\rm xc}[\rho(\mathbf{r})]$ is the exchange-correlation energy per electron of a uniform electron gas and is assumed to be known from some approximation. In computing $\epsilon_{\rm xc}[\rho(\mathbf{r})]$ per Wigner Seitz cell in terms of an expansion in complex spherical harmonics,

$$\varepsilon_{\rm xc}[\rho(\mathbf{r})] = \sum_{L} \varepsilon_L^{\rm xc}(r)\, Y_L(\hat{\mathbf{r}}) \quad , \tag{22.49}$$

one immediately can see that the expansion coefficients $\varepsilon_L^{\rm xc}(r)$ have to be obtained from an angular integration,

$$\varepsilon_L^{\rm xc}(r) = \int {\rm d}\hat{\mathbf{r}}\, \varepsilon_{\rm xc}[\rho(\mathbf{r})]\, Y_L^*(\hat{\mathbf{r}}) \quad , \tag{22.50}$$

which has to be evaluated numerically by means of, e.g., a Gauss quadrature as shall be explained in detail in Sect. 22.6.1. The energy $E_{\rm xc}$ is then given by

$$E_{\rm xc} = \int\limits_{\rm BS} {\rm d}\mathbf{r} \sum_{LL'L''} \rho_L(r)\, \varepsilon_{L'}^{\rm xc}(r)\, \sigma_{L''}(r)\, Y_L^*(\hat{\mathbf{r}})\, Y_{L'}(\hat{\mathbf{r}})\, Y_{L''}(\hat{\mathbf{r}}) \tag{22.51}$$

$$= \int\limits_{0}^{r_{\rm BS}} r^2\, {\rm d}r \sum_{LL'L''} C_{L'L''}^{L}\, \rho_L(r)\, \varepsilon_{L'}^{\rm xc}(r)\, \sigma_{L''}(r) \tag{22.52}$$

$$= \int\limits_{0}^{r_{\rm BS}} r^2\, {\rm d}r \sum_{L} \overline{\rho}_L(r)\, \varepsilon_L^{\rm xc}(r) \quad , \tag{22.53}$$

whereby for $r \leq r_{\rm MT}$ this expression simplifies to:

$$E_{\rm xc} = \int\limits_{0}^{r_{\rm MT}} r^2\, {\rm d}r \sum_{L} \rho_L(r)\, \varepsilon_L^{\rm xc}(r) \quad . \tag{22.54}$$

22.6.1 Numerical angular integration – Gauss quadrature

In order to perform the integration in (22.50) one has to recall the very meaning of an angular integration, namely

$$\int {\rm d}\hat{\mathbf{r}} = \int\limits_{0}^{\pi} \sin\theta\, {\rm d}\theta \int\limits_{0}^{2\pi} {\rm d}\varphi \quad , \tag{22.55}$$

and that the occurring integration regimes $[a, b]$ can be mapped in turn into the interval $[-1, 1]$ via a suitable coordinate transformation [1]:

$$\int_a^b f(\xi)\,\mathrm{d}\xi \longrightarrow \int_{-1}^{1} f(x)\,\mathrm{d}x \quad , \tag{22.56}$$

$$\xi = \frac{b-a}{2}\,x + \frac{a+b}{2} \quad . \tag{22.57}$$

Investigating first the integration over θ with $\xi = \cos\theta$ one gets the following integral,

$$-\int_0^{\pi} f(\cos\theta)\,\mathrm{d}(\cos\theta) = \int_{-1}^{1} f(x)\,\mathrm{d}x \tag{22.58}$$

which can be solved numerically by means of *Gauss' Formula* [4]

$$\int_{-1}^{1} f(x)\,\mathrm{d}x = \sum_{i=1}^{n} w_i\, f(x_i) \quad , \tag{22.59}$$

where x_i is the i^{th} zero of the Legendre polynomial $P_n(x)$. The weights w_i are obtained from the condition

$$w_i = \frac{2}{(1-x_i^2)[P_n'(x_i)]^2} \quad . \tag{22.60}$$

In order to find the zeros of $P_n(x)$ *Newton's rule* [4] is applied. Within this scheme the roots are found by repeatedly using the following sequence

$$x_{l+1} = x_l - \frac{P_n(x_l)}{P_n'(x_l)} \quad . \tag{22.61}$$

For the integration over θ one therefore gets

$$-\int_0^{\pi} f(\cos\theta)\,\mathrm{d}(\cos\theta) = \sum_{i=1}^{n} w_i\, f(x_i) \quad . \tag{22.62}$$

Turning now to the numerical evaluation of the integral over φ, the same steps as before are performed

$$\int_0^{2\pi} f(\theta,\varphi)\,\mathrm{d}\varphi = \pi \int_{-1}^{1} f(\theta,y)\,\mathrm{d}y \quad , \tag{22.63}$$

with

$$\varphi = \pi\,(y+1) \quad . \tag{22.64}$$

which result in the below expression,

$$\pi \int_{-1}^{1} f(\theta, y)\, \mathrm{d}y = \pi \sum_{k=1}^{m} w_k\, f(\theta, y_k) \quad . \tag{22.65}$$

Finally, in putting (22.65) and (22.62) together one gets

$$\int_0^{\pi} \int_0^{2\pi} f(\theta, \varphi) \sin\theta \, \mathrm{d}\theta \, \mathrm{d}\varphi = \pi \sum_{i=1}^{n} \sum_{k=1}^{m} w_i\, w_k\, f(x_i, y_k) \quad . \tag{22.66}$$

22.7 The Coulomb energy

In order to arrive at a formulation for the Coulomb energy in terms of the Coulomb potential the following general expression can serve as a starting point:

$$U[\rho] = \int\int \mathrm{d}\mathbf{r}\, \mathrm{d}\mathbf{r}' \frac{\Big(\rho(\mathbf{r}) - \sum\limits_i Z_i\, \delta(\mathbf{r} - \mathbf{R}_i)\Big)\Big(\rho(\mathbf{r}') - \sum\limits_j Z_j\, \delta(\mathbf{r}' - \mathbf{R}_j)\Big)}{|\mathbf{r} - \mathbf{r}'|} \quad , \tag{22.67}$$

where $\rho(\mathbf{r})$ refers to the full electron charge density and Z_i (atomic number) specifies the Coulomb singularity at a particular atomic position $\mathbf{R}_i$. In separating the Coulomb energy into three terms

$$\begin{aligned} U[\rho] = & \int\int \mathrm{d}\mathbf{r}\, \mathrm{d}\mathbf{r}' \frac{\rho(\mathbf{r})\, \rho(\mathbf{r}')}{|\mathbf{r} - \mathbf{r}'|} \\ & - 2 \int\int \mathrm{d}\mathbf{r}\, \mathrm{d}\mathbf{r}' \rho(\mathbf{r}) \sum_i Z_i\, \frac{\delta(\mathbf{r}' - \mathbf{R}_i)}{|\mathbf{r} - \mathbf{r}'|} \\ & + \int\int \mathrm{d}\mathbf{r}\, \mathrm{d}\mathbf{r}' \sum_{i,j} Z_i\, Z_j \frac{\delta(\mathbf{r} - \mathbf{R}_i)\, \delta(\mathbf{r}' - \mathbf{R}_j)}{|\mathbf{r} - \mathbf{r}'|} \quad . \end{aligned} \tag{22.68}$$

this equation can be rewritten as

$$U[\rho] = \int \mathrm{d}\mathbf{r}\, \rho(\mathbf{r}) \left[\int \mathrm{d}\mathbf{r}' \frac{\rho(\mathbf{r}')}{|\mathbf{r} - \mathbf{r}'|} - \sum_i \frac{2Z_i}{|\mathbf{r}_i|} \right] + \sum_{\substack{i,j \\ i \neq j}} \frac{Z_i\, Z_j}{|\mathbf{R}_i - \mathbf{R}_j|} \quad . \tag{22.69}$$

Comparison of this equation with the general expression for the Coulomb potential $V^{\mathrm{c}}(\mathbf{r})$, which is given by

$$V^{\mathrm{c}}(\mathbf{r}) = 2 \int \mathrm{d}\mathbf{r}' \frac{\rho(\mathbf{r}')}{|\mathbf{r} - \mathbf{r}'|} - \sum_i \frac{2Z_i}{|\mathbf{r}_i|} \quad , \tag{22.70}$$

see also chapter 19, yields

$$U[\rho] = \frac{1}{2}\int \mathrm{d}\mathbf{r}\,\rho(\mathbf{r})\,V^{\mathrm{c}}(\mathbf{r}) - \sum_i Z_i \left[\int \mathrm{d}\mathbf{r}\,\frac{\rho(\mathbf{r})}{|\mathbf{r}_i|} - \sum_{\substack{j\\ j\neq i}} \frac{Z_j}{|\mathbf{R}_i - \mathbf{R}_j|}\right] \quad . \tag{22.71}$$

In rewriting the terms inside the bracket by means of the below relations,

$$\mathbf{r}_i = \mathbf{r}_j + \mathbf{S}_{ij} \quad , \tag{22.72}$$

$$\mathbf{S}_{ij} = \mathbf{R}_j - \mathbf{R}_i \quad . \tag{22.73}$$

one obtains

$$\int \mathrm{d}\mathbf{r}\,\frac{\rho(\mathbf{r})}{|\mathbf{r}_i|} - \sum_{\substack{j\\ j\neq i}} \frac{Z_j}{|\mathbf{R}_i - \mathbf{R}_j|} = \sum_j \int_{\Omega_j} \mathrm{d}\mathbf{r}_j\,\frac{\rho(\mathbf{r}_j)}{|\mathbf{r}_i|} - \sum_{\substack{j\\ j\neq i}} \frac{Z_j}{|\mathbf{R}_i - \mathbf{R}_j|} \tag{22.74}$$

$$= \sum_j \int_{\Omega_j} \mathrm{d}\mathbf{r}_j\,\frac{\rho(\mathbf{r}_j)}{|\mathbf{r}_j + \mathbf{S}_{ij}|} - \sum_{\substack{j\\ j\neq i}} \frac{Z_j}{|\mathbf{S}_{ij}|} \tag{22.75}$$

$$= \int_{\Omega_i} \mathrm{d}\mathbf{r}_i\,\frac{\rho(\mathbf{r}_i)}{|\mathbf{r}_i|} + \sum_{\substack{j\\ j\neq i}} \left[\int_{\Omega_j} d\mathbf{r}_j\,\frac{\rho(\mathbf{r}_j)}{|\mathbf{r}_j + \mathbf{S}_{ij}|} - \frac{Z_j}{|\mathbf{S}_{ij}|}\right] \quad . \tag{22.76}$$

By recalling the expression for the intercell potential, see Chap. 19,

$$V^{\mathrm{inter}}(\mathbf{r}_i) = 2\sum_{\substack{j\\ j\neq i}} \left[\int_{\Omega_j} \mathrm{d}\mathbf{r}'_j\,\frac{\rho(\mathbf{r}'_j)}{|\mathbf{r}_j - \mathbf{r}'_j|} - \frac{Z_j}{|\mathbf{r}_j|}\right] \quad , \tag{22.77}$$

which can be rewritten in the following way,

$$V^{\mathrm{inter}}(\mathbf{r}_i) = 2\sum_{\substack{j\\ j\neq i}} \left[\int_{\Omega_j} \mathrm{d}\mathbf{r}'_j\,\frac{\rho(\mathbf{r}'_j)}{|\mathbf{r}_i - \mathbf{r}'_j - \mathbf{S}_{ij}|} - \frac{Z_j}{|\mathbf{r}_i - \mathbf{S}_{ij}|}\right] \quad , \tag{22.78}$$

for $\mathbf{r}_i = 0$, i.e., for the intercell potential at the origin, one obtains

$$V^{\mathrm{inter}}(0) = 2\sum_{\substack{j\\ j\neq i}} \left[\int_{\Omega_j} \mathrm{d}\mathbf{r}_j\,\frac{\rho(\mathbf{r}_j)}{|\mathbf{r}_j + \mathbf{S}_{ij}|} - \frac{Z_j}{|\mathbf{S}_{ij}|}\right] \quad . \tag{22.79}$$

Comparison with (22.76) then yields

$$\int \mathrm{d}\mathbf{r}\,\frac{\rho(\mathbf{r})}{|\mathbf{r}_i|} - \sum_{\substack{j\\ j\neq i}} \frac{Z_j}{|\mathbf{R}_i - \mathbf{R}_j|} = \int_{\Omega_i} \mathrm{d}\mathbf{r}_i\,\frac{\rho(\mathbf{r}_i)}{|\mathbf{r}_i|} + \frac{1}{2}\,V^{\mathrm{inter}}(0) \quad . \tag{22.80}$$

Thus the Coulomb energy is finally given by

$$U[\rho] = \frac{1}{2}\int \mathrm{d}\mathbf{r}\,\rho(\mathbf{r})\,V^{\mathrm{c}}(\mathbf{r}) - \sum_i Z_i \left[\int\limits_{\Omega_i} \mathrm{d}\mathbf{r}_i\,\frac{\rho(\mathbf{r}_i)}{|\mathbf{r}_i|} + \frac{1}{2}\,V^{\mathrm{inter}}(0)\right] \quad , \quad (22.81)$$

and consequently the Coulomb energy per unit cell by

$$U_i[\rho] = \frac{1}{2}\int\limits_{\Omega_i} \mathrm{d}\mathbf{r}_i\,\rho(\mathbf{r}_i)\,\left(V^{\mathrm{c}}(\mathbf{r}_i) - \frac{2Z_i}{|\mathbf{r}_i|}\right) - \frac{1}{2}\,Z_i\,V^{\mathrm{inter}}(0) \quad . \quad (22.82)$$

22.8 A computationally efficient expression for the total energy

For matters of computational efficiency a compact expression for the total energy is needed. Since as was discussed in Sect. 22.1 the total energy per unit cell is the sum of the kinetic, the Coulomb, and the exchange-correlation terms, in summary therefore one can write

$$\begin{aligned} E_{\mathrm{tot}} = E_{\mathrm{c}} + E_{\mathrm{v}} &- \int\limits_{\Omega_i} \mathrm{d}\mathbf{r}_i\,\rho(\mathbf{r}_i)\,V_i(\mathbf{r}_i) \\ &+ \frac{1}{2}\int\limits_{\Omega_i} \mathrm{d}\mathbf{r}_i\,\rho(\mathbf{r}_i)\,\left(V^{\mathrm{c}}(\mathbf{r}_i) - \frac{2Z_i}{|\mathbf{r}_i|}\right) - \frac{1}{2}\,Z_i\,V^{\mathrm{inter}}(0) \\ &+ \int\limits_{\Omega_i} \mathrm{d}\mathbf{r}_i\,\rho(\mathbf{r}_i)\,\epsilon_{\mathrm{xc}}\left[\rho(\mathbf{r}_i)\right] \quad , \end{aligned} \quad (22.83)$$

where $V(\mathbf{r})$ represents the sum of the Coulomb and the exchange-correlation potential,

$$V(\mathbf{r}) = V^{\mathrm{c}}(\mathbf{r}) + V^{\mathrm{xc}}(\mathbf{r}) \quad . \quad (22.84)$$

Obviously the total energy is then of following (final) form:

$$\begin{aligned} E_{\mathrm{tot}} = E_{\mathrm{c}} + E_{\mathrm{v}} &- \frac{1}{2}\int\limits_{\Omega_i} \mathrm{d}\mathbf{r}_i\,\rho(\mathbf{r}_i)\,\left(V^{\mathrm{c}}(\mathbf{r}_i) + \frac{2Z_i}{|\mathbf{r}_i|}\right) \\ &- \frac{1}{2}\,Z_i\,V^{\mathrm{inter}}(0) + \int\limits_{\Omega_i} \mathrm{d}\mathbf{r}_i\,\rho(\mathbf{r}_i)\left(\epsilon_{\mathrm{xc}}\left[\rho(\mathbf{r}_i)\right] - V^{\mathrm{xc}}(\mathbf{r}_i)\right) \quad . \end{aligned} \quad (22.85)$$

22.9 Illustration of total energy calculations

In making use of only two-dimensional translational invariance, which of course applies especially to semi-infinite systems (systems with a surface

and/or interfaces), it is an excellent test for the correctness of the suggested numerical procedures to calculate for illustrative purposes typical bulk properties such as equilibrium lattice constants and bulk moduli. Clearly enough the results cannot be expected to be identical to those when using a true "bulk" approach in terms of three-dimensional cyclic boundary conditions. One can mimic, however, bulk-like behavior by "gluing" together two semi-infinite systems of the same material with identical lattice constants. As will be shown the thus obtained results are qualitatively in very good agreement with and quantitatively close to those based on three-dimensional translational invariance [11] [12] [13] [14] [15], which in turn indicates the precision that can be asked for in describing structural properties of semi-infinite systems.

The examples shown refer to "mimicked" bulk calculations using the ASA and the full potential (FP) scheme non-relativistically and scalar relativistically for $\ell_{\max}$ ranging from 2 to 4. As a first approximation for the transition from ASA to full potentials also calculations based only on the use of full charge densities (FCD) are displayed. In this particular scheme the radial Schrödinger equation is solved only for the spherically symmetric part of the full potential (i.e., the scattering solutions and the t matrices are all diagonal) but computing all angular momentum components of the charge density and when solving the Poisson equation all components of the potential are stored. Furthermore, all real space integrations are performed in this case over the

Table 22.2. Equilibrium lattice constant a0 (a.u.) and bulk modulus B (MBar), for fcc Cu, Pd, and Ag. The experimental values are taken from Kittel (1986).

	Cu		Pd		Ag	
	a_0	B	a_0	B	a_0	B
ASA NR ($\ell_{\max} = 2$)	6.81	1.78	7.59	1.88	7.94	1.08
ASA NR ($\ell_{\max} = 3$)	6.68	1.90	7.41	1.79	7.71	1.27
ASA SR ($\ell_{\max} = 2$)	6.73	1.84	7.41	2.09	7.73	1.29
ASA SR ($\ell_{\max} = 3$)	6.62	2.03	7.24	2.90	7.51	1.59
FCD NR ($\ell_{\max} = 3$)	6.79	1.63	7.53	1.74	7.88	1.02
FCD NR ($\ell_{\max} = 4$)	6.74	1.73	7.47	1.80	7.80	1.12
FCD SR ($\ell_{\max} = 4$)	6.67	1.84	7.29	2.14	7.60	1.35
FP NR ($\ell_{\max} = 3$)	6.78	1.67	7.51	1.73	7.86	1.05
Experiment	6.82	1.37	7.35	1.81	7.73	1.01

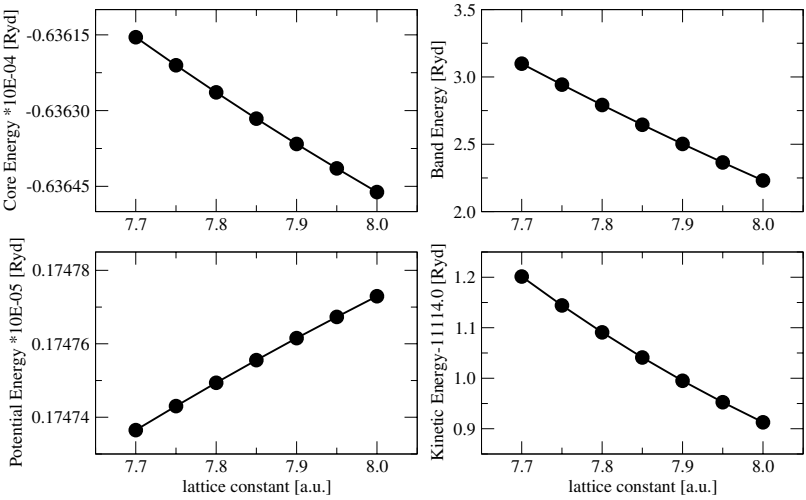

Fig. 22.4. Kinetic Energy and its separate contributions for Ag(100) versus the lattice parameter, $\ell_{\max} = 4$.

polyhedral Wigner-Seitz cell instead of over a spherical region as would be the case in ASA calculations. It turns out that the resulting bulk properties in the FCD case are very close to those in the FP case.

22.9.1 Computational details

The number of atomic layers in one principle layer, see Chap. 17 is 4 in the FCD and FP calculations and 3 in the ASA calculation, since in calculating the structure constants and consequently the scattering path operator three layers turned out to be not sufficient to obtain converged results in the FCD and FP case. In these cases, e.g., the $(\ell, m) = (2, 0)$ components in the expansion coefficient of the charge density $\rho_{(2,0)}(r)$ or in the potential $v_{(2,0)}(r)$, which have to vanish in a cubic bulk system, are not sufficiently small. In an ASA calculation this problem never arises as no component other than the spherically symmetric one is calculated.

In the following results for bulk fcc Ag, Cu, and Pd are displayed, all of them based on the local density approximation (LDA) using the functional of Ceperley and Alder in the parametrization of Perdew and Zunger and by choosing the (100) direction. Clearly enough the choice of this direction then determines the k-set necessary for the two-dimensional Brillouin zone integrations, see Chap. 18. In particular 45 points in the irreducible part of the Brillouin zone are used and in applying (17.58) 20 mesh points. All energy integrations are performed on a semi-circular contour using 16 complex energy points; all radial quantities like the expansion coefficients of the charge density or the potential refer to a radial mesh consisting of 510 points in

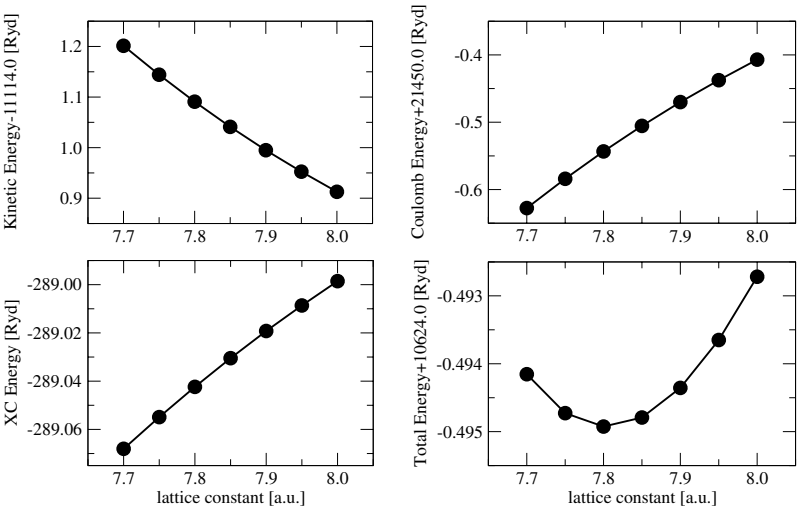

Fig. 22.5. Total energy of Ag(100) and its separate contributions versus the lattice parameter, $\ell_{\max} = 4$.

order to reproduce the correct number of core electrons for each core level up to 10^{-8}. In this radial mesh 120 radial points correspond to the region between the muffin-tin and the bounding sphere radius, the remaining 390 points are inside the muffin-tin.

In each iteration the potential was shifted such that the spherical component $V_{(0,0)}(r) = 0$ at $r = r_{\mathrm{MT}}$. This – as already was mentioned in Chap. 21 – is not only advantageous to minimize the effect of the shape functions, but also leads to a faster convergence of the self-consistent calculations.

22.9.2 Results

As already discussed in the previous sections the total energy is the sum of the kinetic, the Coulomb, and the exchange-correlation energy:

$$E_{\mathrm{tot}} = E_{\mathrm{kin}} + E_{\mathrm{coul}} + E_{\mathrm{xc}} \quad . \tag{22.86}$$

Contrary to the Coulomb and the exchange-correlation energy the kinetic energy has more than one contribution and is the sum of the core, band, and the so called potential energy:

$$E_{\mathrm{kin}} = E_{\mathrm{core}} + E_{\mathrm{band}} + E_{\mathrm{pot}} \quad . \tag{22.87}$$

An example for the change in the kinetic energy and its contributions with varying lattice parameter a is displayed in Fig. 22.4 for fcc-Ag(100). As can be seen the dominant contributions are the core and potential energy, while the band energy only adds a minor contribution. The two dominant energies are

of opposite behavior as the lattice constant is changed: while the core energy decreases, the potential energy increases with the size of the Wigner-Seitz cell such that in total the kinetic energy also decreases.

Fig. 22.5 shows the corresponding changes in the Coulomb and the exchange-correlation energy. The Coulomb energy goes to minus infinity when the size of the cell tends towards zero, and to zero for an infinitely extended cell. Since the exchange-correlation energy is a functional of the charge density it also diverges if the cell size decreases.

In summing up all energy contributions the total energy has a minimum at a certain equilibrium volume. The change of the total energy is of the order of 10^{-3} Rydberg when the lattice parameter varied by about 1%, although the change in each separate term to the total energy is of the order 10^{-1}.

Clearly enough such small energy differences in the total energy imply to evaluate each energy contribution very accurately. It is for example of crucial importance to carefully compute the core energies. As discussed in Sect. 22.3, one has to use the correct potential with the proper boundary conditions and to make sure that the inwards integration of the wave-function starts sufficiently far outside of the bounding sphere. Small changes in the core energies can produce a completely erroneous minimum in the total energy.

Fig. 22.6 illustrates the total energy for fcc Ag, Cu, and Pd for different values of $\ell_{\max}$ as a function of the lattice spacing. Generally one sees that the equilibrium volume and the energy decrease for higher angular momentum quantum numbers. The value of $\ell_{\max}$ refers to the number of angular moments used for the scattering path operator, which in turn implies that for the potential $2\ell_{\max}$ and for the shape functions $4\ell_{\max}$ had to be used. Obviously the calculated quantities are not fully converged [16] with respect to $\ell_{\max}$.

Shifting the potential by a constant as explained in Chap. 21 does not change the position of the energy minimum and in principle also the total energy values should remain unchanged. However, in practical calculations, mainly due to an insufficient angular momentum convergence it does in fact change.

In the literature on calculated bulk properties [11] [15] [17] [18] one finds that ASA calculations in the local density approximation (LDA) reproduce closely the full-potential generalized gradient approximation (GGA) results (independent of whether the APW, LMTO, or KKR method is used) because of an error cancellation between the LDA and the overlap of atomic spheres. When using a full-potential scheme the error due to the ASA is removed and the equilibrium volumes decrease because of the "overbinding" inherent to the LDA, which can be "corrected" for by making use of the GGA.

Fig. 22.7 shows how the total energy curve for fcc Pd is altered when switching from an ASA to a FCD description. From the non-relativistic ASA calculations one can see that for $\ell_{\max} = 3$ both the energy minimum and the position of the curve is completely changed when compared to the case of $\ell_{\max} = 2$. From Table 22.2 one can see that the lattice constant is 7.41 a.u.

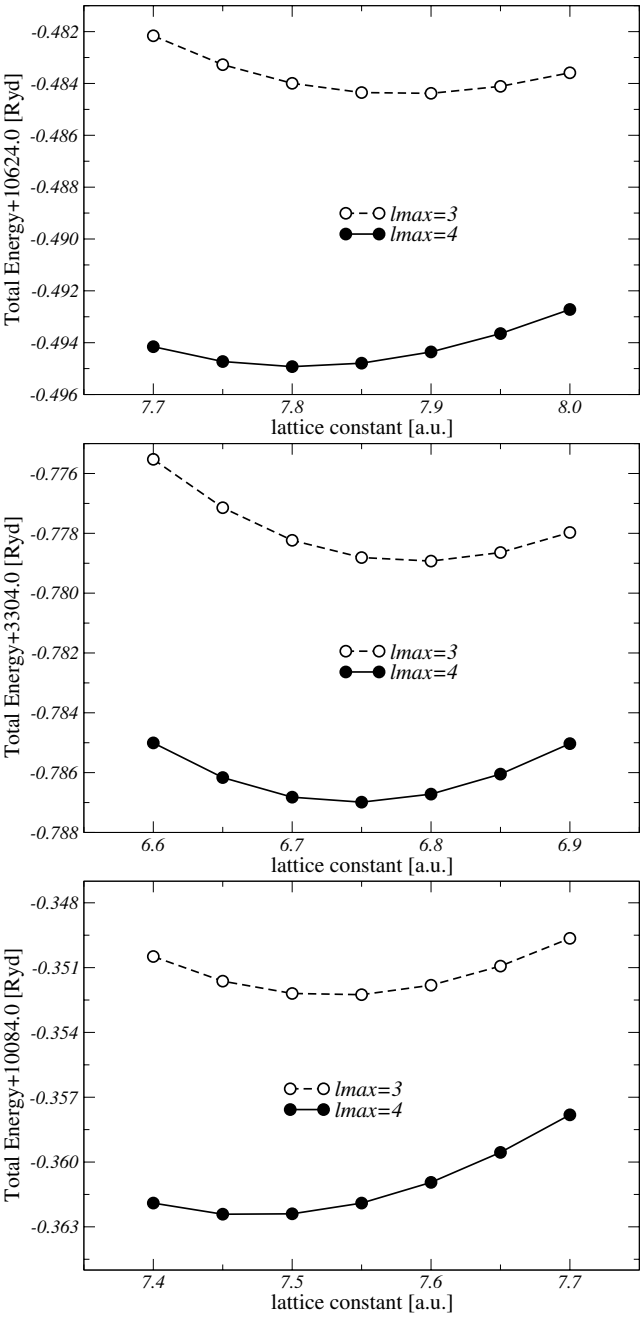

Fig. 22.6. Lattice constant of fcc Ag (top), Cu (center), and Pd (bottom) from non-relativistic calculations using $\ell_{\max} = 3, 4$.

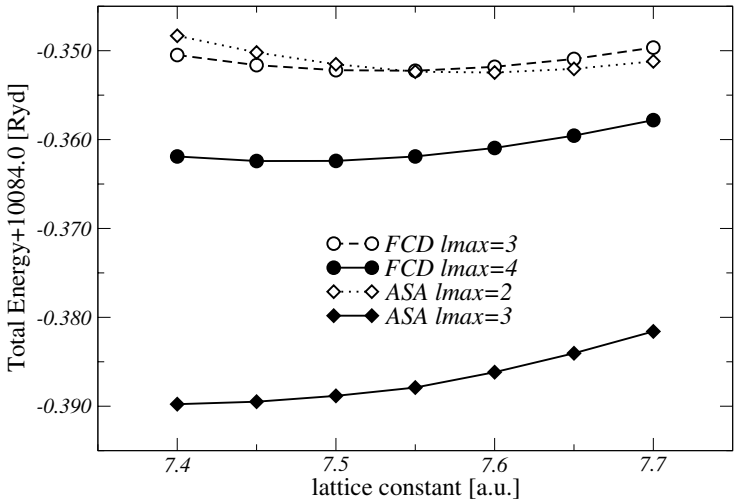

Fig. 22.7. Lattice constant of Pd from non-relativistic ASA calculations with $\ell_{\max} = 2, 3$ and FCD calculations with $\ell_{\max} = 3, 4$.

in the ASA and 7.53 a.u. in the FCD calculation, while the bulk modulus is almost unchanged when for both calculations $\ell_{\max} = 3$ is used. Comparing the $\ell_{\max} = 3$ FCD result with the $\ell_{\max} = 2$ ASA calculation it is obvious that the equilibrium lattice constant and the bulk modulus are reduced. Hence one arrives at the conclusion that within the LDA the resulting equilibrium volume not only depends on whether spherical or full potentials (or full charge densities) are used [17], [18], but also on $\ell_{\max}$.

The bulk moduli mentioned above were obtained by calculating total energies for about seven lattice parameters and then applying a fit to the Birch-Murnaghan equation of state [19]:

$$E_{\text{tot}} = p_0 a^2 + p_1 + p_2 a^4 + p_3 a^6 \quad . \tag{22.88}$$

Here a is the lattice constant and the p_i are the fitting parameters. The second derivative of this expression with respect to the lattice parameter defines then the bulk modulus B as

$$B = \frac{a_0^2}{9V} \frac{\mathrm{d}^2}{\mathrm{d}a^2} E_{\text{tot}} \quad . \tag{22.89}$$

where a_0 is the equilibrium lattice constant and V the unit cell volume. In order to obtain values in MBar B has to be multiplied by a factor of 147.24.

References

1. H.R. Schwarz, *Numerische Mathematik* (B.G. Teubner, Stuttgart 1997)
2. W. Kohn and L.J. Sham, Phys. Rev. **140**, 1133 (1965)

3. I. Turek, V. Drchal, J. Kudrnovsky, M. Sob, and P. Weinberger, *Electronic structure of disordered alloys, surfaces, and interfaces* (Kluwer Academic Publishers, Boston London Dordrecht 1997)
4. M. Abramowitz and I. Stegun, *Handbook of mathematical functions* (Dover Publ., New York 1973)
5. J.P. Desclaux, Comp. Phys. Commun. **1**, 216 (1969)
6. J.P. Desclaux, Comp. Phys. Commun. **9**, 31 (1975)
7. J.P. Desclaux, D. F. Mayers, and F. O'Brien, J. Phys. B **4**, 631 (1971)
8. H. Ebert, J. Phys. Cond. Matter **1**, 9111 (1989)
9. D.M. Ceperley, and B.J. Alder, Phys. Rev. Lett. **45**, 566 (1980)
10. J.P. Perdew, and A. Zunger, Phys. Rev. B **23**, 5048-5079 (1981)
11. M. Asato, A. Settels, T. Hoshino, T. Asada, S. Blügel, R. Zeller, and P.H. Dederichs, Phys. Rev. B **60**, 8, 5202 (1999)
12. R. Zeller, M. Asato, T. Hoshino, J. Zabloudil, P. Weinberger, and P.H. Dederichs, Phil. Mag. B **78**, 417 (1998)
13. R. Zeller, Phys. Rev. B **55**, 9400 (1997)
14. S. Bei der Kellen, Yoonsik Oh, E. Badralexe, and A.J. Freeman, Phys. Rev. B **51**, 9560 (1995)
15. L. Vitos, J. Kollar, and H.L. Skriver, Phys. Rev. B **55**, 13521 (1997)
16. Nassrin Y. Moghadam, G.M. Stocks, X.-G. Zhang, D.M.C. Nicholson, W. A. Shelton, Yang Wang, and J. S. Faulkner, J. Phys. Condens. Matter **13**, 3073 (2001)
17. V. Ozolins, and M. Körling, Phys. Rev. B **48**, 18304 (1993)
18. K.B. Hathaway, H.J.F. Jansen, and A.J. Freeman, Phys. Rev. B **31**, 7603 (1985)
19. F. Birch, J. Geophys. Res. **83**, 1257 (1978)
20. C. Kittel, *Introduction to Solid State Physics*, 6th edn (Wiley, New York 1986)
21. S. Wei, H. Krakauer, and M. Weinert, Phys. Rev. B **32**, 7792 (1985)

23 The Coherent Potential Approximation

23.1 Configurational averages

Suppose a binary bulk alloy is of composition A_cB_{1-c} with $c_A = c$ being the concentration of species A and $c_B = (1-c)$ the concentration of species B. If the diffraction patterns of the system are characterized by sharp Bragg maxima, positional disorder is of little importance. Positional disorder would imply the displacement of atoms from the positions of an underlying ideal lattice $\mathcal{L} = \mathcal{L}^{(3)}$. Assuming that there is no positional disorder and for matters of simplicity $\mathcal{L}$ refers to a simple lattice and $I(\mathcal{L})$ denotes the set of indices i of $\mathcal{L}$, the potential can be written as

$$V(\mathbf{r}) = \sum_{i \in I(\mathcal{L})} V_i(\mathbf{r}_i) \quad , \tag{23.1}$$

$$V_i(\mathbf{r}_i) = \xi_i V_A(\mathbf{r}_i) + (1-\xi_i) V_B(\mathbf{r}_i) \quad , \tag{23.2}$$

where ξ_i is an occupational variable such that $\xi_i = 1$ if site $\mathbf{R}_i$ is occupied by species A and $\xi_i = 0$ if this site is occupied by species B. For a completely random alloy the probability for ξ_i being 1 is c_A and correspondingly for $\xi_i = 0$ the probability is c_B. In (23.2) $V_A(\mathbf{r}_i)$ and $V_B(\mathbf{r}_i)$ are the individual (effective) potentials of species A and B at the site $\mathbf{R}_i$, respectively. Then $\{\xi_i \mid i \in I(\mathcal{L})\}$ is one particular arrangement of atoms A and B on the positions of $\mathcal{L}$. Such an arrangement is called a *configuration*.

Quite clearly for one particular configuration $(V(\mathbf{r}) = V(\mathbf{r}, \{\xi_i\}))$ the Kohn-Sham equations can be solved,

$$\mathcal{H}\{\xi_i\}\ \psi_n(\mathbf{r}, \{\xi_i\}) = \epsilon_n\{\xi_i\}\, \psi_n(\mathbf{r}, \{\xi_i\}) \quad , \tag{23.3}$$

where $\mathcal{H}$ can be relativistic or non-relativistic and n labels the eigenstates. Observables, however, in general do not map a particular configuration but an average over all configurations. Let $\langle \mathcal{O}_{nn'} \rangle$ be the configurationally averaged matrix element of some (Hermitian) operator $\mathcal{O}$. Then

$$\langle \mathcal{O}_{nn'} \rangle = \sum_{\{\xi_i\}} P(\{\xi_i\}) \langle \psi_n\{\xi_i\} | \mathcal{O} | \psi_{n'}\{\xi_i\} \rangle \quad , \tag{23.4}$$

where the $P(\{\xi_i\})$ are microcanonical probabilities for a particular configuration. Obviously the calculation of such averages is greatly simplified by directly calculating the configurationally averaged Green function $\langle G^+(\mathbf{r},\mathbf{r}',\epsilon)\rangle$ from which typical one-particle physical properties such as e.g. the configurationally averaged density of states $\langle n(\epsilon)\rangle$ or the configurationally averaged charge density $\langle \rho(\mathbf{r})\rangle$ can immediately be calculated:

$$\langle n(\epsilon)\rangle = -\frac{1}{\pi}\mathrm{Im}\left[\mathrm{Tr}\left\langle \mathcal{G}^+(\epsilon)\right\rangle\right] = -\frac{1}{\pi}\int \mathrm{Im}\left\langle G^+(\mathbf{r},\mathbf{r},\epsilon)\right\rangle \mathrm{d}\mathbf{r} \quad , \tag{23.5}$$

$$\langle \rho(\mathbf{r})\rangle = -\frac{1}{\pi}\int_{-\infty}^{E_\mathrm{F}} \mathrm{Im}\left\langle G^+(\mathbf{r},\mathbf{r},\epsilon)\right\rangle \mathrm{d}\epsilon \quad , \tag{23.6}$$

where Tr denotes the trace and E_F the Fermi energy.

In the following it shall be assumed that the occupational probabilities for different sites are independent from each other, i.e., that

$$P(\{\xi_i\}) = \prod_i P_i(\xi_i) \quad , \tag{23.7}$$

$$\sum_{\xi_i=0,1} P_i(\xi_i) = P_i(0) + P_i(1) = 1 \quad , \tag{23.8}$$

$$\langle \xi_i\rangle \equiv P_i(1) = c \; , \; \langle 1-\xi_i\rangle \equiv P_i(0) = 1-c \quad . \tag{23.9}$$

Suppose the total number of atoms in a binary bulk system $\mathrm{A}_c\mathrm{B}_{1-c}$ is N and the number of A atoms and B atoms is N_A and N_B, respectively,

$$N = N_A + N_B \quad , \quad N_A = \sum_i P_i(1) = cN \quad ,$$
$$N_B = \sum_i P_i(0) = (1-c)\,N \quad . \tag{23.10}$$

23.2 Restricted ensemble averages – component projected densities of states

Let $\mathcal{P}_{iA}$ and $\mathcal{P}_{iB}$ be projection operators corresponding to unit cell i of the following form:

$$\langle \mathbf{r}_i|\,\mathcal{P}_{i\alpha}\,|\mathbf{r}_i'\rangle = P_{i\alpha}(\mathbf{r}_i,\mathbf{r}_i') = P_{i\alpha}(\mathbf{r}_i)\,\delta(\mathbf{r}_i - \mathbf{r}_i') \quad , \quad \alpha = A,B \quad , \tag{23.11}$$

$$P_{i\alpha}(\mathbf{r}_i) = \begin{cases} 1; \text{ if species } \alpha \text{ is in the unit cell } i \\ 0; \text{ if species } \alpha \text{ is } \mathbf{not} \text{ in the unit cell } i \end{cases} \quad , \tag{23.12}$$

and $P_{i\alpha}(\mathbf{r}_i) = 0$ for $\mathbf{r}_i \notin D_i$. According to (23.5), the component-like densities of states related to unit cell i are given by

$$\langle n_{iA}(\epsilon)\rangle = -\frac{1}{\pi}\mathrm{Im}\left[\mathrm{Tr}\left\langle \mathcal{P}_{iA}\mathcal{G}^{+}(\epsilon)\right\rangle\right] \quad , \tag{23.13}$$

$$\langle n_{iB}(\epsilon)\rangle = -\frac{1}{\pi}\mathrm{Im}\left[\mathrm{Tr}\left\langle \mathcal{P}_{iB}\mathcal{G}^{+}(\epsilon)\right\rangle\right] \quad . \tag{23.14}$$

Because of the below properties of the projection operators,

$$\mathcal{P}_{iA}+\mathcal{P}_{iB}=\mathcal{P}_{i} \quad , \quad \langle \mathbf{r}_i|\,\mathcal{P}_{iA}+\mathcal{P}_{iB}\,|\mathbf{r}'_i\rangle = \delta(\mathbf{r}_i-\mathbf{r}'_i) \quad , \quad \mathbf{r}_i,\mathbf{r}'_i\notin D_i \quad , \tag{23.15}$$

$$\sum_i \mathcal{P}_i = \mathcal{I} \quad , \tag{23.16}$$

trivially the following equation also holds true:

$$\mathrm{Im}\left[\mathrm{Tr}\left\langle \mathcal{G}^{+}(\epsilon)\right\rangle\right] = \sum_i \left(\mathrm{Im}\left[\mathrm{Tr}\left\langle \mathcal{P}_{iA}\mathcal{G}^{+}(\epsilon)\right\rangle\right] + \mathrm{Im}\left[\mathrm{Tr}\left\langle \mathcal{P}_{iB}\mathcal{G}^{+}(\epsilon)\right\rangle\right]\right) \quad , \tag{23.17}$$

and therefore a comparison with (23.5), (23.13) and (23.14) yields the below expression for the density of states *per site*,

$$\langle n(\epsilon)\rangle = \frac{1}{N}\sum_i \left[\langle n_{iA}(\epsilon)\rangle + \langle n_{iB}(\epsilon)\rangle\right] \quad . \tag{23.18}$$

Written explicitly, the corresponding averages, see (23.4) and (23.7), are given by

$$\begin{aligned}\langle n_{iA}(\epsilon)\rangle &= -\frac{1}{\pi}\sum_{\xi_i} P_i(\xi_i)\,\mathrm{ImTr}\left[\mathcal{P}_{iA}\prod_{j(\neq i)}\sum_{\xi_j} P_j(\xi_j)\,\mathcal{G}^{+}(\epsilon)\right] = \\ &= -\frac{1}{\pi}c\,\mathrm{ImTr}\left[\mathcal{P}_{iA}\prod_{j(\neq i)}\sum_{\xi_j} P_j(\xi_j)\,\mathcal{G}^{+}(\epsilon)\right] \\ &= -\frac{1}{\pi}c\,\mathrm{ImTr}\left[\mathcal{P}_{i}\left\langle \mathcal{G}^{+}(\epsilon)\right\rangle_{(i=A)}\right] \quad ,\end{aligned} \tag{23.19}$$

where the so-called *restricted ensemble average*, $\langle \mathcal{G}^{+}(\epsilon)\rangle_{(i=A)}$, has the following meaning: in cell i the occupation is fixed to atom A and the averaging is restricted to all configurations for the remaining $N-1$. Similarly,

$$\langle n_{iB}(\epsilon)\rangle = -\frac{1}{\pi}(1-c)\,\mathrm{ImTr}\left[\mathcal{P}_{i}\left\langle \mathcal{G}^{+}(\epsilon)\right\rangle_{(i=B)}\right] \quad . \tag{23.20}$$

Since $\langle n_{i\alpha}(\epsilon)\rangle$ is obviously independent of site i, one gets

$$\langle n(\epsilon)\rangle = c\,n_A(\epsilon) + (1-c)\;n_B(\epsilon) \quad , \tag{23.21}$$

with

$$n_\alpha(\epsilon) = -\frac{1}{\pi}\mathrm{ImTr}\left[\mathcal{P}_0\left\langle \mathcal{G}^+(\epsilon)\right\rangle_{(0=\alpha)}\right] = -\frac{1}{\pi}\mathrm{Im}\left(\int_{D_0} \mathrm{d}\mathbf{r}_0 \left\langle G^+(\mathbf{r}_0,\mathbf{r}_0,\epsilon)\right\rangle_{(0=\alpha)}\right) \quad , \tag{23.22}$$

where the index 0 labels an arbitrarily chosen unit cell (domain D_0).

By using restricted ensemble averages the configurational average is partitioned into two subsets, whereas the following condition has to be satisfied, see also (23.21),

$$c\left\langle G^+(\mathbf{r}_0,\mathbf{r}_0,\epsilon)\right\rangle_{(0=A)} + (1-c)\left\langle G^+(\mathbf{r}_0,\mathbf{r}_0,\epsilon)\right\rangle_{(0=B)} = \left\langle G^+(\mathbf{r}_0,\mathbf{r}_0,\epsilon)\right\rangle \quad , \tag{23.23}$$

$$(\mathbf{r}_0 \in D_0) \quad .$$

23.3 The electron self-energy operator

The averaged resolvent $\langle \mathcal{G}(z)\rangle$ of the Hamiltonian $\mathcal{H}$ in (23.3) can formally be written as

$$\langle \mathcal{G}(z)\rangle = \left\langle (z-\mathcal{H})^{-1}\right\rangle = [z-\mathcal{H}_0-\Sigma(z)]^{-1} \quad , \tag{23.24}$$

with $\Sigma(z)$ being the so-called *electron self-energy operator*. If $\Sigma(z)$ is a translationally invariant effective medium, i.e., assuming that the system under consideration is characterized by sharp (diffraction) Bragg maxima (no structural disorder), then $\mathcal{H}$ can formally be rewritten as

$$\mathcal{H} = \mathcal{H}_0 + \mathcal{V} - \mathcal{W}(z) + \mathcal{W}(z) = \mathfrak{H}(z) + \mathcal{V} - \mathcal{W}(z) \quad , \qquad \mathfrak{H}(z) = \mathcal{H}_0 + \mathcal{W}(z) \quad , \tag{23.25}$$

where $\mathcal{V}$ is given by a superposition of (real) individual site potentials $\mathcal{V}_i$, see, e.g., (23.1)), and $\mathcal{W}(z)$ as a superposition of energy-dependent translationally invariant site quantities $\mathcal{W}_i(z)$:

$$\mathcal{V} = \sum_i \mathcal{V}_i \quad , \quad \mathcal{W}(z) = \sum_i \mathcal{W}_i(z) \quad , \tag{23.26}$$

$$[E \mid \mathbf{R}_i]\, W_i(\mathbf{r},z) = W_i(\mathbf{r},z) \quad ; \quad \forall [E \mid \mathbf{R}_i] \in T \quad , \tag{23.27}$$

$$\mathfrak{V}(z) = \sum_i \mathfrak{V}_i(z) = \sum_i (\mathcal{V}_i - \mathcal{W}_i(z)) \quad . \tag{23.28}$$

Using $\mathfrak{V}(z)$ as a yet-to-be-specified approximation for $\Sigma(z)$ the resolvent $\mathcal{G}(z)$ within this particular approximation can be written as

$$\mathcal{G}(z) = [z-\mathfrak{H}(z)-\mathfrak{V}(z)]^{-1} \quad . \tag{23.29}$$

Let $\mathfrak{G}(z)$ be the resolvent of $\mathfrak{H}(z)$,

$$\mathfrak{G}(z) = [z - \mathfrak{H}(z)]^{-1} \quad , \tag{23.30}$$

the resolvent $\mathcal{G}(z)$ and the corresponding $\mathcal{T}$ operator $\mathcal{T}(z)$ are then given by the below Dyson equations,

$$\mathcal{G}(z) = \mathfrak{G}(z)[1 + \mathfrak{V}(z)\mathfrak{G}(z)] \quad , \tag{23.31}$$

$$\mathcal{T}(z) = \mathfrak{V}(z) + \mathfrak{V}(z)\mathfrak{G}(z)\mathfrak{V}(z) \quad , \tag{23.32}$$

$$\mathcal{G}(z) = \mathfrak{G}(z) + \mathfrak{G}(z)\mathcal{T}(z)\mathfrak{G}(z) \quad . \tag{23.33}$$

Since $\mathfrak{V}(z)$ is a superposition of site-dependent quantities (23.24), in (23.27) or (23.28) multiple scattering expansions can immediately be applied. One has to bear in mind, however, that the scattering processes are now much more complicated because the scattering from the individual site terms $\mathfrak{V}_i(z)$ is in relation to a generally non-hermitean reference medium.

It should be noted that, because of (23.27), $\mathfrak{G}(z)$ is translationally invariant and therefore no longer is configuration dependent. Averaging (23.28) over all configurations therefore gives

$$\begin{aligned} \langle \mathcal{G}(z) \rangle &\equiv \mathfrak{G}(z) + \mathfrak{G}(z) \langle \mathcal{T}(z) \rangle \mathfrak{G}(z) \\ &\equiv [1 + \mathfrak{G}(z) \langle \mathcal{T}(z) \rangle] \mathfrak{G}(z) \quad . \end{aligned} \tag{23.34}$$

23.4 The coherent potential approximation

Let $\langle \mathcal{T}(z; \mathcal{W}(z)) \rangle$ denote the averaged $\mathcal{T}$ operator for such a particularly chosen medium $\mathcal{W}(z)$and let $\mathfrak{G}(z; \mathcal{W}(z))$ be the corresponding resolvent of $\mathfrak{H}(z) = \mathcal{H}_0 + \mathcal{W}(z)$. Then from (23.34) one can see immediately that

$$\langle \mathcal{G}(z) \rangle = \mathfrak{G}(z; \mathcal{W}(z)) \quad , \tag{23.35}$$

if and only if

$$\langle \mathcal{T}(z; \mathcal{W}(z)) \rangle = 0 \quad , \tag{23.36}$$

and consequently the self-energy operator $\Sigma(z)$, defined in (23.24), is simply given by

$$\Sigma(z) = \mathcal{W}(z) \quad . \tag{23.37}$$

Equations (23.35) and (23.36) serve both as definitions and as practical tools: if on average there is no additional scattering because of $\mathcal{W}(z)$, i.e., the condition in (23.36)) is met, then the averaged resolvent $\langle \mathcal{G}(z) \rangle$ is indeed the translationally invariant resolvent $\mathfrak{G}(z)$ of an (in general non-hermitean) operator $\mathfrak{H}(z) = \mathcal{H}_0 + \mathcal{W}(z)$ corresponding to the *complex potential operator* $\mathcal{W}(z)$. Therefore, in order to fulfil (23.35), (23.36) has to be solved self-consistently. The condition in (23.36) is usually called the *Coherent Potential Approximation* (CPA).

23.5 Isolated impurities

23.5.1 Single impurities

Consider again a lattice $\mathcal{L} = \mathcal{L}^{(3)}$ with only one atom per unit cell and suppose there is a single impurity of species α ($\alpha = A$ or B) at the origin of this host lattice of atoms h (host). Then for the single-site t-matrices obviously the following situation pertains:

$$\underline{t}_i(\epsilon) = \underline{t}_\alpha(\epsilon) \quad ; \quad i = 0 \quad , \tag{23.38}$$

$$\underline{t}_i(\epsilon) = \underline{t}_h(\epsilon) \quad ; \quad \forall i \neq 0 \quad , \quad i \in I(\mathcal{L}) \quad . \tag{23.39}$$

As should be recalled the scattering path operator is in principle given by

$$\underline{\tau}^{ij}(\epsilon) = \underline{t}_i(\epsilon)\,\delta_{ij} + \sum_{k\neq i} \underline{t}_i(\epsilon)\,\underline{G}^{ik}(\epsilon)\,\underline{\tau}^{kj}(\epsilon) \quad , \tag{23.40}$$

which, taking (23.38) and (23.39) explicitly into account, can be written as

$$\begin{aligned}\underline{\tau}^{ij}(\epsilon) = \underline{t}_h(\epsilon) &\left[\delta_{ij} + \sum_{k\neq i} \underline{G}^{ik}(\epsilon)\,\underline{\tau}^{kj}(\epsilon)\right] \\ &+ \delta_{i0}\left((\underline{t}_\alpha(\epsilon) - \underline{t}_h(\epsilon))\left[\delta_{0j} + \sum_{k\neq 0} \underline{G}^{0k}(\epsilon)\,\underline{\tau}^{kj}(\epsilon)\right]\right) \quad .\end{aligned} \tag{23.41}$$

For translationally invariant systems one can make use of the properties of the projection operator $P_{\mathbf{k}}$ of the translational group,

$$P_{\mathbf{k}} P_{\mathbf{k}'} = P_{\mathbf{k}}\delta_{\mathbf{k}\mathbf{k}'} \quad , \quad \sum_{\mathbf{k}} P_{\mathbf{k}} = I \quad , \tag{23.42}$$

where I is the identity operator. For the present case, however, the key equation of translational invariance no longer holds true. Therefore one has to use the following lattice Fourier transformations

$$\underline{\tau}(\mathbf{k}, \mathbf{k}', \epsilon) = |T|^{-1} \sum_{\mathbf{R}_i, \mathbf{R}_j \,\in\, \mathcal{L}} \exp(-\mathrm{i}\mathbf{k}\cdot\mathbf{R}_i)\,\underline{\tau}^{ij}(\epsilon)\exp(\mathrm{i}\mathbf{k}'\cdot\mathbf{R}_j) \quad , \tag{23.43}$$

$$\begin{aligned}\underline{\tau}^{ij}(\epsilon) &= \sum_{\mathbf{k},\ \mathbf{k}'} P^i_{\mathbf{k}}\,\underline{\tau}(\mathbf{k}, \mathbf{k}', \epsilon)\,P^j_{\mathbf{k}'} = \\ &= |T|^{-1} \sum_{\mathbf{k},\ \mathbf{k}'} \exp(\mathrm{i}\mathbf{k}\cdot\mathbf{R}_i)\,\underline{\tau}(\mathbf{k}, \mathbf{k}', \epsilon)\exp(-\mathrm{i}\mathbf{k}'\cdot\mathbf{R}_j) \quad ,\end{aligned} \tag{23.44}$$

where trivially because of (23.42)

$$|T|^{-1}\sum_{\mathbf{k}}\exp\left(-\mathrm{i}\mathbf{k}\cdot\mathbf{R}_i\right)\exp\left(\mathrm{i}\mathbf{k}\cdot\mathbf{R}_i\right)=1 \quad ; \quad \forall i\in I\left(\mathcal{L}\right) \quad , \tag{23.45}$$

and $|T|$ is the order of the translational group of the lattice consisting of host (h) atoms only.

Multiplying (23.41) from the right and left by $\exp\left(\mathrm{i}\mathbf{k}\cdot\mathbf{R}_i\right)$ and $\exp\left(-\mathrm{i}\mathbf{k}'\cdot\mathbf{R}_j\right)$ respectively, summing over $\forall\mathbf{R}_i,\mathbf{R}_j\in\mathcal{L}$, and using (23.43) - (23.45) one gets [2]

$$\begin{aligned}\underline{\tau}\left(\mathbf{k},\mathbf{k}',\epsilon\right)&=\underline{t}_h\left(\epsilon\right)\left[\delta_{\mathbf{k}\mathbf{k}'}+\underline{G}\left(\mathbf{k},\epsilon\right)\underline{\tau}\left(\mathbf{k},\mathbf{k}',\epsilon\right)\right]\\&+|T|^{-1}\left(\underline{t}_\alpha\left(\epsilon\right)-\underline{t}_h\left(\epsilon\right)\right)\left[1+\sum_{\mathbf{k}_1}\underline{G}\left(\mathbf{k}_1,\epsilon\right)\underline{\tau}\left(\mathbf{k}_1,\mathbf{k}',\epsilon\right)\right] \quad .\end{aligned} \tag{23.46}$$

Defining now the following quantities ($\mathbf{R}_0=0$, where $\mathbf{R}_0$ refers to the origin of the lattice):

$$\underline{\tau}_h\left(\mathbf{k},\epsilon\right)=\left[\underline{t}_h^{-1}\left(\epsilon\right)-\underline{G}\left(\mathbf{k},\epsilon\right)\right]^{-1} \quad , \tag{23.47}$$

$$\underline{\tau}_h^{00}\left(\epsilon\right)=|T|^{-1}\sum_{\mathbf{k}}\underline{\tau}_h\left(\mathbf{k},\epsilon\right) \quad , \tag{23.48}$$

(23.46) can be rewritten as [2] [4]

$$\begin{aligned}\underline{\tau}\left(\mathbf{k},\mathbf{k}',\epsilon\right)&=\underline{t}_h\left(\epsilon\right)\delta_{\mathbf{k}\mathbf{k}'}\\&-|T|^{-1}\underline{\tau}_h\left(\mathbf{k},\epsilon\right)\underline{D}_\alpha^{00}\left(\epsilon\right)\left(\underline{t}_\alpha^{-1}\left(\epsilon\right)-\underline{t}_h^{-1}\left(\epsilon\right)\right)\underline{\tau}_h\left(\mathbf{k}',\epsilon\right) \quad ,\end{aligned} \tag{23.49}$$

$$\underline{D}_\alpha^{00}\left(\epsilon\right)=\left[\underline{1}+\underline{\tau}_h^{00}\left(\epsilon\right)\left(\underline{t}_\alpha^{-1}\left(\epsilon\right)-\underline{t}_h^{-1}\left(\epsilon\right)\right)\right]^{-1} \quad . \tag{23.50}$$

The site-diagonal scattering path operator for $i=0$ (origin of the lattice) is then obtained from (23.43) as

$$\underline{\tau}^{00}\left(\epsilon\right)=|T|^{-1}\sum_{\mathbf{k},\mathbf{k}'}\underline{\tau}\left(\mathbf{k},\mathbf{k}',\epsilon\right)=\underline{D}_\alpha^{00}\left(\epsilon\right)\underline{\tau}_h^{00}\left(\epsilon\right) \quad . \tag{23.51}$$

The matrix $\underline{D}_\alpha^{00}\left(\epsilon\right)$ usually is called *impurity matrix*. Clearly, $\underline{\tau}^{00}\left(\epsilon\right)$ can also be written as

$$\underline{\tau}^{00}\left(\epsilon\right)=\underline{\tau}_h^{00}\left(\epsilon\right)\widetilde{\underline{D}}_\alpha^{00}\left(\epsilon\right) \quad , \tag{23.52}$$

with

$$\widetilde{\underline{D}}_\alpha^{00}\left(\epsilon\right)=\left[\underline{1}+\left(\underline{t}_\alpha^{-1}\left(\epsilon\right)-\underline{t}_h^{-1}\left(\epsilon\right)\right)\underline{\tau}_h^{00}\left(\epsilon\right)\right]^{-1} \quad . \tag{23.53}$$

23.5.2 Double impurities

Consider again a simple lattice of host atoms h. The diagonal- and off-diagonal elements of the scattering path operator are then given by

$$\underline{\tau}_h^{ii}\left(\epsilon\right)=\Omega_{\mathrm{BZ}}^{-1}\int\left[\underline{t}_h^{-1}\left(\epsilon\right)-\underline{G}\left(\mathbf{k},\epsilon\right)\right]^{-1}\mathrm{d}\mathbf{k}=\underline{\tau}_h^{00}\left(\epsilon\right), \quad \forall i\in I\left(\mathcal{L}\right) \quad , \tag{23.54}$$

and

$$\underline{\tau}_h^{ij}(\epsilon) = |T|^{-1} \sum_{\mathbf{k}} \exp(-\mathrm{i}\mathbf{k}\cdot(\mathbf{R}_i - \mathbf{R}_j))\underline{\tau}_h(\mathbf{k},\epsilon)$$
$$= \Omega_{\mathrm{BZ}}^{-1} \int \exp(-\mathrm{i}\mathbf{k}\cdot(\mathbf{R}_i - \mathbf{R}_j)) \left[\underline{t}_h^{-1}(\epsilon) - \underline{G}(\mathbf{k},\epsilon)\right]^{-1} \mathrm{d}\mathbf{k} \quad , \tag{23.55}$$

where $\underline{t}_h(\epsilon)$ is the single-site matrix of the host atoms. Furthermore, consider that two sites, say i and j, $i \neq j$, are occupied by impurity atoms of type α and β

$$\underline{t}_i(\epsilon) = \underline{t}_\alpha(\epsilon) \quad ; \quad \underline{t}_j(\epsilon) = \underline{t}_\beta(\epsilon) \quad , \tag{23.56}$$
$$\underline{t}_k(\epsilon) = \underline{t}_h(\epsilon) \quad ; \quad \forall k \neq i,j \quad , \quad k \in I(\mathcal{L}) \quad . \tag{23.57}$$

Using similar arguments as before it can be shown that by *neglecting backscattering effects* [1] for the chosen values of i and j the corresponding scattering path operator is given by

$$\underline{\tau}^{ij}(\epsilon)_{i=\alpha,j=\beta} = \underline{D}_\alpha^i(\epsilon)\,\underline{\tau}_h^{ij}(\epsilon)\,\widetilde{\underline{D}}_\beta^j(\epsilon) \quad , \quad i \neq j \quad , \tag{23.58}$$

with the matrices, $\underline{D}_\alpha^i(\epsilon)$ and $\widetilde{\underline{D}}_\beta^j(\epsilon)$, defined in (23.50) and (23.53), where the symbol t indicates a transposed matrix.

23.6 The single-site coherent potential approximation

The total T matrix $\mathcal{T}(z)$ can be written in terms of quantities $\mathcal{Q}_i(z)$, see also Chap. 3,

$$\mathcal{T}(z) = \sum_i \mathcal{Q}_i(z) \quad , \tag{23.59}$$

$$\mathcal{Q}_i(z) = t_i(z) + t_i(z)\,\mathfrak{G}(z) \sum_{j(\neq i)} \mathcal{Q}_j(z) \quad , \tag{23.60}$$

where in terms of (23.28)–(23.33)

$$t_i(z) = \mathfrak{V}_i(z) + \mathfrak{V}_i(z)\,\mathfrak{G}(z)\,t_i(z) \quad . \tag{23.61}$$

The average of the T matrix, $\langle\mathcal{T}(z)\rangle$, is therefore given by

$$\langle\mathcal{T}(z)\rangle = \sum_i \langle\mathcal{Q}_i(z)\rangle \quad . \tag{23.62}$$

Averaging $\mathcal{Q}_i(z)$ one now gets the relation

$$\begin{aligned}\langle \mathcal{Q}_i(z)\rangle &= \langle t_i(z)\rangle + \left\langle t_i(z)\,\mathfrak{G}(z)\sum_{j(\neq i)}\mathcal{Q}_j(z)\right\rangle \\ &= \langle t_i(z)\rangle\left[1+\mathfrak{G}(z)\sum_{j(\neq i)}\langle \mathcal{Q}_j(z)\rangle\right] \\ &\quad + \left\langle \left[t_i(z)-\langle t_i(z)\rangle\right]\mathfrak{G}(z)\sum_{j(\neq i)}\mathcal{Q}_j(z)\right\rangle \quad . \end{aligned} \tag{23.63}$$

The first term on the right-hand side of (23.63) consists only of single-site quantities, whereas the second term, obviously much more complicated, is a kind of fluctuation or correlation term. The omission of the second term is called the *single-site approximation* for the configurational average. Within the single-site approximation, $\langle \mathcal{Q}_i(z)\rangle$ is given by

$$\langle \mathcal{Q}_i(z)\rangle = \langle t_i(z)\rangle\left[1+\mathfrak{G}(z)\sum_{j(\neq i)}\langle \mathcal{Q}_j(z)\rangle\right] \quad . \tag{23.64}$$

Let $\mathcal{T}(z;\mathcal{W}(z))$ be the T matrix for a given periodic complex function $\mathcal{W}(z)$, see (23.22). Then the CPA equation in (23.36),

$$\langle \mathcal{T}(z;\mathcal{W}(z))\rangle = \sum_i \langle \mathcal{Q}_i(z;\mathcal{W}(z))\rangle = 0 \quad , \tag{23.65}$$

in the *single-site approximation* requires that

$$\langle \mathcal{Q}_i(z;\mathcal{W}(z))\rangle = 0 \quad ; \qquad \forall i \in I(\mathcal{L}) \quad , \quad \mathcal{L} = \mathcal{L}^{(3)} \quad . \tag{23.66}$$

From (23.64), however, one can see that within the single-site approximation the CPA condition is simply reduced to

$$\langle t_i(z;\mathcal{W}(z))\rangle = 0; \qquad \forall i \in I(\mathcal{L}) \quad . \tag{23.67}$$

It should be noted that by omitting the second term on the right-hand side of (23.63) *short-range-order effects* are explicitly excluded. Multiple scattering effects, however, are implicitly included since the single-site approximation is based on the idea of a single scatterer immersed in an average medium, i.e., on the very concept of a 'mean field theory'. It is also worthwhile to mention that by satisfying (23.67) the lowest order correlation in terms of the t-matrices neglected with respect to the condition (23.65) is of fourth order [11].

23.6.1 Single-site CPA and restricted averages

From the definition of the scattering path operator, which for convenience is repeated here,

$$\underline{\tau}^{ij}(\epsilon) = \underline{t}_i(\epsilon)\,\delta_{ij} + \sum_{k\neq i} \underline{t}_i(\epsilon)\,\underline{G}^{ik}(\epsilon)\,\underline{\tau}^{kj}(\epsilon) \quad , \tag{23.68}$$

one can see immediately that within the CPA single-site approximation, because of (23.67), the following condition for the site-diagonal scattering path operator *with the effective medium as reference* has to be fulfilled:

$$\left\langle \underline{\tau}^{ii}(\epsilon; W(\epsilon)) \right\rangle = 0 \quad ; \quad \forall i \in I(\mathcal{L}) \quad . \tag{23.69}$$

From the discussion of restricted averages and the relation of the site-diagonal scattering path operator to the Green function $G(\mathbf{r}, \mathbf{r}', \epsilon)$ with $\mathbf{r}$ and $\mathbf{r}'$ measured from the same origin, it is clear that for a binary system A_cB_{1-c} (simple lattice, one atom per unit cell) the restricted averages $\left\langle \tau^{ii}(\epsilon) \right\rangle_{(i=\alpha)}$, $\alpha = A, B$, have to meet the condition

$$c\left\langle \underline{\tau}^{ii}(\epsilon) \right\rangle_{(i=A)} + (1-c)\left\langle \underline{\tau}^{ii}(\epsilon) \right\rangle_{(i=B)} = \left\langle \underline{\tau}^{ii}(\epsilon) \right\rangle \quad . \tag{23.70}$$

Since (23.69) and (23.70) are valid for all site indices $i \in I(\mathcal{L})$, it is sufficient to restrict (23.70), for example, to $i = 0$, i.e., to the origin of the underlying lattice $\mathcal{L}$. However, before any practical use can be made of these equations methods of calculating the restricted averages $\left\langle \underline{\tau}^{ii}(\epsilon) \right\rangle_{(i=\alpha)}, \alpha = A, B$, must be discussed.

23.7 The single-site CPA equations for three-dimensional translational invariant systems

23.7.1 Simple lattices

Consider a binary (substitutional) bulk alloy A_cB_{1-c} of components A and B occupying statistically a simple lattice $\mathcal{L}$ (one atom per unit cell). Let $\mathbf{t}_c(\epsilon)$ be a guess for the *single-site t matrix for the coherent lattice* $\mathcal{L}$:

$$\underline{t}_i(\epsilon) = \underline{t}_c(\epsilon) \quad ; \quad \forall i \in I(\mathcal{L}) \quad . \tag{23.71}$$

Then the corresponding site-diagonal scattering path operator $\underline{\tau}_c^{00}(\epsilon)$ is given by

$$\underline{\tau}_c^{00}(\epsilon) = \Omega_{\mathrm{BZ}}^{-1} \int \left[\underline{t}_c^{-1}(\epsilon) - \underline{G}(\mathbf{k}, \epsilon)\right]^{-1} \mathrm{d}\mathbf{k} \quad . \tag{23.72}$$

Suppose now that in the unit cell at the origin ($i = 0$) restricted ensemble averages are performed:

$$\left\langle \underline{\tau}_c^{00}(\epsilon) \right\rangle_{(0=\alpha)} \equiv \underline{\tau}_\alpha^{00}(\epsilon) \quad ; \quad \alpha = A, B \quad , \tag{23.73}$$

where

$$\underline{\tau}_\alpha^{00}(\epsilon) = \underline{D}_\alpha^{00}(\epsilon)\,\underline{\tau}_c^{00}(\epsilon) \quad , \tag{23.74}$$

and

$$\underline{D}_{\alpha}^{00}(\epsilon) = \left[\underline{1} + \underline{\tau}_{c}^{00}(\epsilon)\left(\underline{t}_{\alpha}^{-1}(\epsilon) - \underline{t}_{c}^{1}(\epsilon)\right)\right]^{-1} \quad . \tag{23.75}$$

Then in the single-site approximation the CPA condition is given by

$$c\underline{\tau}_{A}^{00}(\epsilon) + (1-c)\,\underline{\tau}_{B}^{00}(\epsilon) = \underline{\tau}_{c}^{00}(\epsilon) \quad , \tag{23.76}$$

or,

$$c\underline{D}_{A}^{00}(\epsilon) + (1-c)\,\underline{D}_{B}^{00}(\epsilon) = \underline{1} \quad . \tag{23.77}$$

It is also straightforward to show that the matrix representation of the single-site T-operator, $t_{\alpha}(z;\mathcal{W}(z))$, called the *excess scattering matrix* (Butler 1985) is given by

$$\underline{X}_{\alpha}(\epsilon) = \left[\left(\underline{t}_{\alpha}^{-1}(\epsilon) - \underline{t}_{c}^{-1}(\epsilon)\right)^{-1} + \underline{\tau}_{c}^{00}(\epsilon)\right]^{-1} \quad , \tag{23.78}$$

for which the following CPA condition applies (see (23.67)),

$$c\underline{X}_{A}^{00}(\epsilon) + (1-c)\,\underline{X}_{B}^{00}(\epsilon) = \underline{0}\,. \tag{23.79}$$

According to the below relation,

$$\underline{D}_{\alpha}^{00}(\epsilon) = \underline{1} + \underline{X}_{\alpha}(\epsilon)\,\underline{\tau}_{c}^{00}(\epsilon) \ , \tag{23.80}$$

the equivalence of the conditions in (23.77) and (23.79) is obvious. Since the single-site t-matrix for the coherent lattice, $\mathbf{t}_{c}(\epsilon)$, is only a guess, the condition in (23.77) or (23.79), usually called the *KKR-CPA equations* (for a simple lattice), has to be solved self-consistently. It should be recalled that these equations are based on the *single-site coherent potential approximation.*

23.7.2 Complex lattices

For complex lattices the *KKR-CPA equations* can conveniently be formulated in terms of a supermatrix notation where the rows and columns are numbered by sublattices. Suppose for example that one particular sublattice is alloyed and all the other sublattices are ordered. Then the supermatrix containing the single-site t matrices is of the form

$$\mathbf{t}_{c}^{-1}(\epsilon) = \begin{pmatrix} \ddots & & & & \\ & \underline{t}_{X}^{i}(\epsilon)^{-1} & \underline{0} & \underline{0} & \\ & \underline{0} & \underline{t}_{c}^{j}(\epsilon)^{-1} & \underline{0} & \\ & \underline{0} & \underline{0} & \underline{t}_{Y}^{k}(\epsilon)^{-1} & \\ & & & & \ddots \end{pmatrix} \quad , \tag{23.81}$$

whereby the ordered sublattice i is occupied by species X, the ordered sublattice k by species Y, and sublattice j statistically by A and B atoms, corresponding to the concentrations c and $(1-c)$, respectively. For a particular choice of $\mathbf{t}_{c}^{j}(\epsilon)$ the *cell-diagonal* scattering path operator is given by

$$\tau_c^{00}(\epsilon) = \Omega_{\mathrm{BZ}}^{-1} \int \left[\mathbf{t}_c^{-1}(\epsilon) - \mathbf{G}(\mathbf{k},\epsilon)\right]^{-1} \mathrm{d}\mathbf{k} \quad , \tag{23.82}$$

$$\tau_c^{00}(\epsilon) = \begin{pmatrix} \vdots & \vdots & \\ \cdots \tau_c^{0i,0i}(\epsilon) & \tau_c^{0i,0j}(\epsilon) & \cdots \\ \cdots \tau_c^{0j,0i}(\epsilon) & \tau_c^{0j,0j}(\epsilon) & \cdots \\ \vdots & \vdots & \end{pmatrix} \quad , \tag{23.83}$$

from which, in turn, the sublattice-diagonal scattering path operator in case of single impurities of atoms A and B on sublattice j in the cell at the origin (the very meaning of (00) in (23.82)) can be obtained as

$$\underline{\tau}_\alpha^{0j,0j}(\epsilon) = \underline{D}_\alpha^{0j,0j}(\epsilon)\,\underline{\tau}_c^{0j,0j}(\epsilon) \quad ; \quad \alpha = A, B \quad , \tag{23.84}$$

$$\underline{D}_\alpha^{0j,0j}(\epsilon) = \left[\underline{1} + \left(\underline{t}_\alpha^j(\epsilon)^{-1} - \underline{t}_c^j(\epsilon)^{-1}\right)\underline{\tau}_c^{0j,0j}(\epsilon)\right]^{-1} \quad . \tag{23.85}$$

The single-site CPA condition, i.e., no additional scattering from sublattice j, is then given by

$$c\tau_A^{0j,0j}(\epsilon) + (1-c)\,\tau_B^{0j,0j}(\epsilon) = \tau_c^{0j,0j}(\epsilon) \quad , \tag{23.86}$$

or

$$c\underline{D}_A^{0j,0j}(\epsilon) + (1-c)\,\underline{D}_B^{0j,0j}(\epsilon) = \underline{1} \quad . \tag{23.87}$$

It is important to repeat that the superscripts (00) in (23.82)–(23.87) refer to cells and not to sites: Ω_{BZ} in (23.82) refers to the volume of the Brillouin zone for the complex lattice under investigation. It is also clear from (23.83) and (23.85) that the ordered sublattices "interfere" with the CPA condition representing the alloy problem on a particular sublattice. In the case that more than one sublattice is alloyed, sublattice dependent concentrations have to be introduced and instead of (23.86) or (23.87) one has to deal with a set of corresponding equations that have to be solved *simultaneously*. Formally, one can then introduce the following sublattice diagonal matrices,

$$\mathbf{D}_\alpha^{00}(\epsilon) = \begin{pmatrix} \ddots & & & & \\ & \underline{D}_\alpha^{0i,0i}(\epsilon) & \underline{0} & \underline{0} & \\ & \underline{0} & \ddots & \underline{0} & \\ & \underline{0} & \underline{0} & \underline{D}_\alpha^{0j,0j}(\epsilon) & \\ & & & & \ddots \end{pmatrix} \quad , \tag{23.88}$$

and

$$\mathbf{c} = \begin{pmatrix} \ddots & & & & \\ & c_i & 0 & 0 & \\ & 0 & \ddots & 0 & \\ & 0 & 0 & c_j & \\ & & & & \ddots \end{pmatrix} \quad , \tag{23.89}$$

and summarize the set of CPA conditions of type of (23.87) as

$$\mathbf{c}\mathbf{D}_A^{00}(\epsilon) + (\mathbf{1} - \mathbf{c})\,\mathbf{D}_B^{00}(\epsilon) = \mathbf{1}\,. \tag{23.90}$$

23.8 The single-site CPA equations for two-dimensional translational invariant systems

23.8.1 Simple parent lattices

For a given set of n layers, see Chap. 17, the elements of the coherent scattering path operator $\tau_c(\epsilon)$ are defined as

$$\underline{\tau}_c^{pi,qj}(\epsilon) = \Omega_{\mathrm{SBZ}}^{-1} \int \exp\left[-\mathrm{i}\mathbf{k}_\parallel \cdot (\mathbf{R}_{i,\parallel} - \mathbf{R}_{j,\parallel})\right] \underline{\tau}_c^{pq}(\mathbf{k}_\parallel, \epsilon)\mathrm{d}\mathbf{k}_\parallel \quad , \tag{23.91}$$

$p, q = 1, \ldots, n$, which implies that in each layer p for the coherent single-site t-matrices the following translational invariance applies,

$$\underline{t}_c^{pi}(\epsilon) = \underline{t}_c^{p}(\epsilon) \quad ; \quad \forall i \in I(\mathcal{L}^{(2)}) \quad . \tag{23.92}$$

In (23.91) it is supposed that in all atomic layers one and the same two-dimensional translational symmetry applies, where $\mathcal{L}^{(2)}$ refers to a simple two-dimensional lattice, and that position vectors are simply denoted by $\mathbf{R}_{pi}$,

$$\mathbf{R}_{pi} = \mathbf{c}_p + \mathbf{R}_{i,\parallel} \quad ; \quad \mathbf{R}_{i,\parallel} \in \mathcal{L}^{(2)} \quad , \quad \mathbf{c}_p = \mathbf{c}_{p,\parallel} + c_{p,z}\mathbf{z} \quad . \tag{23.93}$$

In the following only (super-) matrices, labelled by layers shall be used:

$$\mathbf{t}_c(\epsilon) = \begin{pmatrix} \underline{t}_c^1(\epsilon) & 0 & \cdots & \cdots & 0 \\ \vdots & \ddots & \cdots & \cdots & 0 \\ \vdots & 0 & \underline{t}_c^p(\epsilon) & 0 & \vdots \\ \vdots & \cdots & \cdots & \ddots & \cdots \\ 0 & \cdots & \cdots & 0 & \underline{t}_c^n(\epsilon) \end{pmatrix} \quad , \tag{23.94}$$

$$\tau_c(\epsilon) = \begin{pmatrix} \vdots & \vdots \\ \cdots \underline{\tau}_c^{pp}(\epsilon) \cdots & \underline{\tau}_c^{pq}(\epsilon) \cdots \\ \vdots & \vdots \\ \cdots \underline{\tau}_c^{qp}(\epsilon) \cdots & \underline{\tau}_c^{qq}(\epsilon) \cdots \\ \vdots & \vdots \end{pmatrix} \quad , \tag{23.95}$$

where $p, q = 1, \ldots, n$ and a particular element of $\tau_c(\epsilon)$,

$$\underline{\tau}_c^{pq}(\epsilon) = \underline{\tau}_c^{pi,qi}(\epsilon) = \underline{\tau}_c^{p0,q0}(\epsilon) = \Omega_{\rm SBZ}^{-1} \int \underline{\tau}_c^{pq}(\mathbf{k}_\parallel, \epsilon)\, \mathrm{d}\mathbf{k}_\parallel \quad , \tag{23.96}$$

refers to the unit cells ($i = 0$) at the origin of $\mathcal{L}^{(2)}$ in layers p and q. Suppose now the concentration for constituents A and B in layer p is denoted by c_p^α ($p{=}1, \ldots, n$),

$$\sum_{\alpha=A,B} c_p^\alpha = 1 \, , \tag{23.97}$$

and one specifies the occupation in the unit cell at the origin of $\mathcal{L}^{(2)}$ of a particular layer p in terms of the following impurity matrix,

$$\begin{aligned} \underline{D}_\alpha^p(\epsilon) &\equiv \underline{D}_\alpha^{pi}(\epsilon) = \underline{D}_\alpha^{p0}(\epsilon) \\ &= \left[\underline{1} - \underline{\tau}_c^{p0,p0}(\epsilon) \left(\underline{t}_c^p(\epsilon)^{-1} - \underline{t}_\alpha^p(\epsilon)^{-1}\right)\right]^{-1} \quad , \end{aligned} \tag{23.98}$$

where $\underline{t}_\alpha^p(\epsilon)$ is the single–site t–matrix for constituent α in layer p. The layer-diagonal coherent scattering path operator, $\underline{\tau}_c^{pp}(\epsilon)$, for a given set of atomic layers (multilayer) is therefore obtained from the following *inhomogeneous CPA* condition,

$$\underline{\tau}_c^{pp}(\epsilon) = \sum_{\alpha=A,B} c_p^\alpha \left\langle \underline{\tau}^{pp}(\epsilon) \right\rangle_{p,\alpha} \quad , \tag{23.99}$$

$$\left\langle \underline{\tau}^{pp}(\epsilon) \right\rangle_{p,\alpha} = \underline{\tau}_\alpha^{pp}(\epsilon) = \underline{D}_\alpha^p(\epsilon) \underline{\tau}_c^{pp}(\epsilon) \quad , \tag{23.100}$$

$$p{=}1, \ldots, n \quad ,$$

i.e., from a condition that implies solving *simultaneously* a layer-diagonal CPA condition (in the single-site approximation) for layers $p{=}1, \ldots, n$. Once this condition is met then translational invariance in each layer under consideration is achieved,

$$\left\langle \underline{\tau}^{pp}(\epsilon) \right\rangle_{p,\alpha} \equiv \left\langle \underline{\tau}^{p0,p0}(\epsilon) \right\rangle_{p0,\alpha} = \left\langle \underline{\tau}^{pi,pi}(\epsilon) \right\rangle_{pi,\alpha} \quad , \tag{23.101}$$

$$\forall i \in I(\mathcal{L}^{(2)}) \quad , \quad \alpha = A, B \quad , \quad p{=}1, \ldots, n \quad .$$

Similarly, by specifying the occupation in two different sites, the following restricted averages are obtained,

$$p \neq q: \quad \left\langle \underline{\tau}^{pi,qj}(\epsilon) \right\rangle_{pi\alpha,qj\beta} = \underline{D}^{p}_{\alpha}(\epsilon)\underline{\tau}^{pi,qj}_{c}(\epsilon)\underline{\widetilde{D}}^{q}_{\beta}(\epsilon) \quad , \qquad \forall i,j \in I(\mathcal{L}^{(2)}) \quad , \tag{23.102}$$

$$p = q: \quad = \left\langle \underline{\tau}^{pi,pj}(\epsilon) \right\rangle_{pi\alpha,pj\beta} = \underline{D}^{p}_{\alpha}(\epsilon)\underline{\tau}^{pi,pj}_{c}(\epsilon)\underline{\widetilde{D}}^{p}_{\beta}(\epsilon) \quad , \qquad \forall\,(i \neq j) \in I(\mathcal{L}^{(2)}) \quad , \tag{23.103}$$

where $\left\langle \underline{\tau}^{pi,qj}_{c}(\epsilon) \right\rangle_{pi\alpha,qj\beta}$ has the meaning that site (cell) pi is occupied by species α and site (cell) qj by species β, and

$$\begin{aligned} \underline{\widetilde{D}}^{p}_{\alpha}(\epsilon) &\equiv \underline{\widetilde{D}}^{pi}_{\alpha}(\epsilon) = \underline{\widetilde{D}}^{p0}_{\alpha}(\epsilon) \\ &= \left[1 - \left(\underline{t}^{p}_{c}(\epsilon)^{-1} - \underline{t}^{p}_{\alpha}(\epsilon)^{-1}\right)\underline{\tau}^{p0,p0}_{c}(\epsilon)\right]^{-1} \quad . \end{aligned} \tag{23.104}$$

23.8.2 Complex lattices

In principle the elements of the coherent scattering path operator $\underline{\tau}_{c}(z)$ are now defined by

$$\underline{\tau}^{psi,qs'i'}_{c}(\epsilon) = \Omega^{-1}_{\mathrm{SBZ}} \int \exp\left(-\mathrm{i}\mathbf{k}_{\parallel}\cdot\left(\mathbf{R}_{i,\parallel} - \mathbf{R}_{i',\parallel}\right)\right)\underline{\tau}^{ps,qs'}_{c}(\mathbf{k}_{\parallel},\epsilon)\mathrm{d}\mathbf{k}_{\parallel} \quad , \tag{23.105}$$

a site index psi refers to the $i-th$ site of sublattice s, defined by the non-primitive translation $\mathbf{a}_s$, in layer p. Clearly enough again the notation of supermatrices is of great help as was already pointed out several times: matrix elements become matrices, and on so on. For example, for complex two-dimensional lattices the coherent scattering path operator can be written as

$$\underline{\tau}_{c}(\epsilon) = \begin{pmatrix} \vdots & \vdots \\ \cdots\ \tau^{pp}_{c}(\epsilon) & \cdots\ \tau^{pq}_{c}(\epsilon)\ \cdots \\ \vdots & \vdots \\ \cdots\ \tau^{qp}_{c}(\epsilon) & \cdots\ \tau^{qq}_{c}(\epsilon)\ \cdots \\ \vdots & \vdots \end{pmatrix} \quad , \tag{23.106}$$

$$\tau^{pq}_{c}(\epsilon) = \begin{pmatrix} \vdots & \vdots \\ \cdots\ \underline{\tau}^{ps,qs}_{c}(\epsilon) & \underline{\tau}^{ps,qs'}_{c}(\epsilon)\ \cdots \\ \\ \cdots\ \underline{\tau}^{ps',qs}(\epsilon) & \underline{\tau}^{ps',qs'}_{c}(\epsilon)\ \cdots \\ \vdots & \vdots \end{pmatrix} \quad , \tag{23.107}$$

and the various concentrations will have to carry in addition to a layer index also a sublattice index. Furthermore, Ω_{SBZ} refers now to the unit area of the

complex two-dimensional lattice and an element $\underline{\tau}_c^{ps,qs'}(\epsilon)$ in (23.90) is given by

$$\begin{aligned}\underline{\tau}_c^{ps,qs'}(\epsilon) &= \underline{\tau}_c^{ps,qs'}(\epsilon) = \underline{\tau}_c^{ps0,qs'0}(\epsilon) \\ &= \Omega_{\mathrm{SBZ}}^{-1} \int \exp\left(-\mathrm{i}\mathbf{k}_\parallel \cdot (\mathbf{a}_s - \mathbf{a}_{s'})\right) \underline{\tau}_c^{ps,qs'}(\mathbf{k}_\parallel, \epsilon)\, \mathrm{d}\mathbf{k}_\parallel \quad . \end{aligned} \tag{23.108}$$

The single-site CPA condition is then formally similar to (23.99) considering however an additional sublattice index.

23.9 Numerical solution of the CPA equations

An efficient numerical solution of the CPA condition, (23.79) generalized for m components,

$$\sum_{\alpha=1}^{m} c_\alpha \underline{X}_\alpha(\epsilon) = \underline{0} \quad , \quad \sum_{\alpha=1}^{m} c_\alpha = 1 \quad , \tag{23.109}$$

$$\underline{X}_\alpha(\epsilon) = \left[\left(\underline{t}_\alpha(\epsilon)^{-1} - \underline{t}_c(\epsilon)^{-1}\right)^{-1} + \underline{\tau}_c^{00}(\epsilon)\right]^{-1} \quad , \tag{23.110}$$

was originally proposed by Mills et al. [10] and then implemented first by Ginatempo and Staunton [6]. Suppose the condition in (23.109) is not satisfied in the n-th step of the iteration. One then can define the matrix, $\underline{X}_c^{(n)}(\epsilon)$,

$$\underline{X}_c^{(n)}(\epsilon) \equiv \sum_{\alpha=1}^{m} c_\alpha \underline{X}_\alpha^{(n)}(\epsilon) \neq \underline{0} \quad , \tag{23.111}$$

where

$$\underline{X}_\alpha^{(n)}(\epsilon) = \left[\left(\underline{t}_\alpha(\epsilon)^{-1} - \underline{t}_c^{(n)}(\epsilon)^{-1}\right)^{-1} - \underline{\tau}_c^{00(n)}(\epsilon)\right]^{-1} \quad . \tag{23.112}$$

The subsequent guess for $\underline{t}_c(\epsilon)$ can be estimated as follows,

$$\underline{X}_c^{(n)}(\epsilon) = \left[\left(\underline{t}_c^{(n)}(\epsilon)^{-1} - \underline{t}_c^{(n+1)}(\epsilon)^{-1}\right)^{-1} - \underline{\tau}_c^{00(n)}(\epsilon)\right]^{-1} \quad , \tag{23.113}$$

therefore,

$$\underline{t}_c^{(n+1)}(\epsilon)^{-1} = \underline{t}_c^{(n)}(\epsilon)^{-1} - \left[\underline{X}_c^{(n)}(\epsilon)^{-1} + \underline{\tau}_c^{00(n)}(\epsilon)\right]^{-1} \quad , \tag{23.114}$$

which can be used to calculate the next guess for $\underline{\tau}_c^{00}(\epsilon)$. As was shown by Mills et al. [10] the above iterative scheme guarantees a stable convergency for $\underline{t}_c(\epsilon)$ when starting with the initial guess,

$$\underline{t}_c^{(0)}(\epsilon) = \sum_{\alpha=1}^{m} c_\alpha \underline{t}_\alpha(\epsilon) \quad , \tag{23.115}$$

the so-called average t-matrix approximation (ATA).

References

1. W.H. Butler, Phys. Rev. B **31**, 3260 (1985)
2. H. Ehrenreich, and L.M. Schwartz, Solid State Physics **31**, 149-286 (1976)
3. R.J. Elliott, J.A. Krummhansl, and P.L. Leath, Review of Modern Physics **46**, 465 (1974)
4. J.S. Faulkner, Progress in Materials Science **27**, 1-87 (1982)
5. J.S. Faulkner, and G.M. Stocks, Phys. Rev. **B23**, 5623 (1981)
6. B. Ginatempo and J.B. Staunton, J. Phys. F: Met. Phys. **18**, 1827 (1988)
7. B.L. Györffy, Phys. Rev. **B5**, 2382 (1972)
8. B.L. Györffy, and G.M. Stocks, In: *Electrons in finite and infinite structures*, ed by P. Phariseau and L. Scheire (NATO ASI Series, Physics, **B24**. Plenum Press, New York 1977)
9. B.L. Györffy, and G.M. Stocks, In: *Electrons in disordered metals and at metallic surfaces*, ed by P. Phariseau, B.L. Györffy, and L. Scheire (NATO ASI Series, Physics, **B42**. Plenum Press, New York 1979)
10. R. Mills, L.J. Gray, and T. Kaplan, Phys. Rev. B **27**, 3252 (1983)
11. P. Soven, Phys. Rev. **156**, 809 (1967)
12. D.W. Taylor, Phys. Rev. **156**, 1017 (1967)
13. B. Velicky, S. Kirkpatrik, and H. Ehrenreich, Phys. Rev. **175**, 747 (1968)
14. P. Weinberger, *Electron Scattering Theory of Ordered and Disordered Matter* (Clarendon Press, Oxford 1992)
15. P. Weinberger, Philos. Mag. **B75**, 509 (1997)
16. P. Weinberger, P.M. Levy, J. Banhart, L. Szunyogh, and B. Újfalussy, J. Phys. Cond. Matt. **8**, 7677 (1996)

24 The embedded cluster method

24.1 The Dyson equation of embedding

Let $\tau(\epsilon)$ be the scattering path operator for a given system

$$\tau(\epsilon) = [\mathbf{t}^{-1}(\epsilon) - \mathbf{G}(\epsilon)]^{-1} \quad , \quad \tau(\epsilon) = \{\underline{\tau}^{nm}(\epsilon)\} = \{\tau^{nm}_{QQ'}(\epsilon)\} \quad , \tag{24.1}$$

where $\mathbf{t}(\epsilon)$ is a diagonal (super-) matrix whose elements are the single-site t-matrices corresponding to sites $\mathbf{R}_n$,

$$\mathbf{t}(\epsilon) = \{\underline{t}^n(\epsilon)\,\delta_{nm}\} = \{t^n_{QQ'}(\epsilon)\,\delta_{nm}\} \quad , \tag{24.2}$$

and $\mathbf{G}(\epsilon)$ contains the respective structure constants:

$$\mathbf{G}(\epsilon) = \{\underline{G}^{nm}(\epsilon)\} = \{G^{nm}_{QQ'}(\epsilon)\} \quad . \tag{24.3}$$

Assuming that this system is two-dimensional translationally invariant, i.e., is a system in which the atomic positions $\mathbf{R}_m$ are defined by

$$\mathbf{R}_m = \mathbf{t}_i + \mathbf{c}_p \quad , \quad \mathbf{t}_i \in \mathcal{L}^{(2)} \quad , \mathbf{c}_p \notin \mathcal{L}^{(2)} \quad , \tag{24.4}$$

then the elements of the scattering path operator in (24.1) are given by

$$\underline{\tau}^{mn}_{\rm h}(\epsilon) = \frac{1}{\Omega_{\rm SBZ}} \int\limits_{\rm SBZ} e^{-{\rm i}\mathbf{k}_\parallel\cdot(\mathbf{t}_i-\mathbf{t}_j)}\,\underline{\tau}^{pq}_{\rm h}(\mathbf{k}_\parallel,\epsilon){\rm d}\mathbf{k}_\parallel \quad , \tag{24.5}$$

where $\Omega_{\rm SBZ}$ is the unit area of the surface Brillouin zone, see in particular also (17.35), and the index h simply indicates that this system is intended to serve as host for a collection of impurities. It should be recalled that the $\mathbf{c}_p$ are so–called layer–generating vectors, in which – in general – also the non-primitive translations are absorbed.

Let $\mathcal{C}$ be a finite set of the sites in the chosen system occupied by either impurities or interacting host atoms

$$\mathcal{C} = \{\mathbf{R}_n\} \quad , \tag{24.6}$$

such that

$$\underline{t}^n(\epsilon) = \begin{cases} \underline{t}^n(\epsilon)\,;\mathbf{R}_n \in \mathcal{C} \\ \underline{t}_{\rm h}(\epsilon)\,;\mathbf{R}_n \notin \mathcal{C} \end{cases} \quad . \tag{24.7}$$

Furthermore, let $\mathbf{t}_{\rm h}(\epsilon)$ denote a diagonal (super-) matrix of single-site t-matrices in the case that only unperturbed host atoms *would* occupy $\mathcal{C}$

$$\mathbf{t}_{\rm h}(\epsilon) = \{\underline{t}^n(\epsilon)\delta_{nm} \mid \underline{t}^n(\epsilon) = \underline{t}_{\rm h}(\epsilon) \quad , \quad \forall \mathbf{R}_n \in \mathcal{C}\} \quad , \tag{24.8}$$

whereas $\mathbf{t}_{\mathcal{C}}(\epsilon)$ refers to the actual occupation of sites in $\mathcal{C}$

$$\mathbf{t}_{\mathcal{C}}(\epsilon) = \{\underline{t}^n(\epsilon)\delta_{nm} \mid \underline{t}^n(\epsilon) \neq \underline{t}_{\rm h}(\epsilon) \quad , \quad \forall \mathbf{R}_n \in \mathcal{C}\} \quad , \tag{24.9}$$

then the scattering path operator $\tau_{\mathcal{C}}(\epsilon)$ comprising all sites in $\mathcal{C}$ is given by the following Dyson like equation,

$$\tau_{\mathcal{C}}(\epsilon) = \tau_{\rm h}(\epsilon)\left[1 - (\mathbf{t}_{\rm h}^{-1}(\epsilon) - \mathbf{t}_{\mathcal{C}}^{-1}(\epsilon))\tau_{\rm h}(\epsilon)\right]^{-1} \quad , \tag{24.10}$$

from which in turn all corresponding local quantities, i.e., charge and magnetization densities, spin– and orbital moments, as well as total energies can be calculated. If N denotes the number of sites in $\mathcal{C}$, then the dimension of the supermatrix $\tau_{\mathcal{C}}(\epsilon)$ is N; the actual matrix size is therefore given by $2 \times N \times \ell_{\max}$, where $\ell_{\max}$ refers to the maximal ℓ quantum number used in the angular momentum representations and the factor two applies only in the case of a relativistic description.

24.2 An embedding procedure for the Poisson equation

In order to solve the Poisson equation, see (19.1), the configurational space is partitioned again into non-overlapping cells centered at atomic sites and the potential with respect to one particular site is split into two parts, namely an *intercell*, see (19.7)–(19.8), and an *intracell* contribution. Obviously for embedded clusters only the *intracell* part needs special care. Let $\mathbf{R}_n$ be the position vector of a chosen site within the cluster and considering for matters of simplicity only ASA-type potentials, then the *intracell potential* for this site is given by (19.31), namely by

$$V_{\rm inter}(r) \equiv V_{\mathbf{R}_n}^{\rm ASA} \equiv V_n^{\rm M} = 2 \sum_{\mathbf{R}_m \neq \mathbf{R}_n} \sum_{L'} A_{\mathbf{R}_n \mathbf{R}_m}^{00,L'} Q_{\mathbf{R}_m}^{L'} \quad , \tag{24.11}$$

where the $A_{\mathbf{R}_n \mathbf{R}_m}^{00,L'}$ are real space Madelung constants as defined in (20.32) and the $Q_{\mathbf{R}_m}^{L'}$ multipole moments, see (19.21). Clearly enough the above equation can be rewritten as

$$\begin{aligned} V_n^{\rm M} &= 2 \sum_{\substack{\mathbf{R}_m \neq \mathbf{R}_n \\ \mathbf{R}_m \in \mathcal{C}}} \sum_{L'} A_{\mathbf{R}_n \mathbf{R}_m}^{00,L'} Q_{\mathbf{R}_m}^{L'} + 2 \sum_{\substack{\mathbf{R}_m \neq \mathbf{R}_n \\ \mathbf{R}_m \in \mathcal{S}}} \sum_{L'} A_{\mathbf{R}_n \mathbf{R}_m}^{00,L'} Q_{\mathbf{R}_m}^{L'} \\ &= V_{\mathcal{C},n}^{\rm M} + V_{\mathcal{S},n}^{M} \quad , \end{aligned} \tag{24.12}$$

where $\mathcal{S}$ simply denotes the set of all position vectors of sites not contained in $\mathcal{C}$.

Assuming now that the single particle properties of the scattering sites in $\mathcal{S}$ are independent of $\mathcal{C}$ implies that $V^{\mathrm{M}}_{\mathcal{S},n}$ has to be independent of the type of the atoms in $\mathcal{C}$. Replacing therefore formally the atoms in $\mathcal{C}$ by those of the unperturbed host, one can write

$$V^{\mathrm{M}}_{\mathcal{S},n} = V^{\mathrm{M,h}}_{n} - V^{\mathrm{M,h}}_{\mathcal{C},n} \quad , \tag{24.13}$$

where $V^{\mathrm{M,h}}_{n}$ denotes the Madelung potential of site $\mathbf{R}_n$ for the unperturbed two-dimensional translational invariant host, see for example (19.147), and – in analogy to (24.12) – $V^{\mathrm{M,h}}_{\mathcal{C},n}$ denotes the contribution to the Madelung potential of site $\mathbf{R}_n$ if the cluster $\mathcal{C}$ would be occupied by unperturbed host atoms. Combining now (24.13) with (24.12) yields

$$V^{\mathrm{M}}_{n} = V^{\mathrm{M}}_{\mathcal{C},n} - V^{\mathrm{M,h}}_{\mathcal{C},n} + V^{\mathrm{M,h}}_{n} \quad , \tag{24.14}$$

which can be regarded as an embedding equation for the intercell potential resulting from the boundary condition set by the size of $\mathcal{C}$. Obviously, by using (24.14) the problem of summing up the contributions from region $\mathcal{S}$ to the *intercell* potential is properly solved.

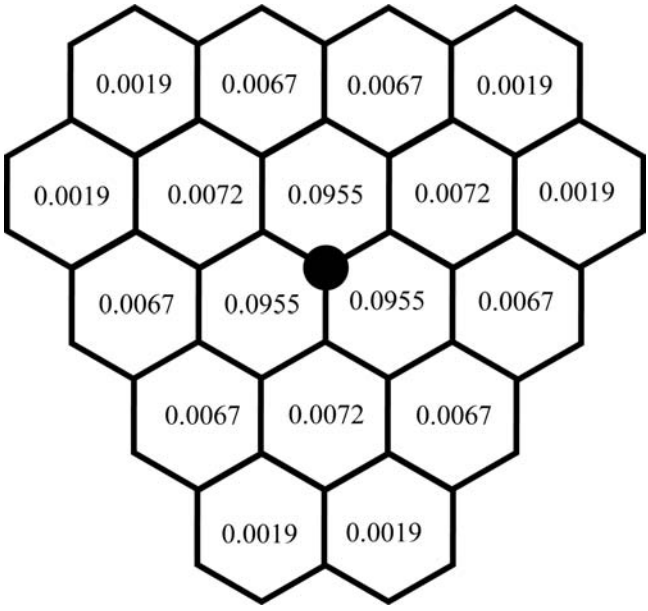

Fig. 24.1. Induced spin-only magnetic moments [μ_{B}] in the surface layer of an fcc(111) Pt substrate caused by a single adatom of Co deposited on top of the surface.

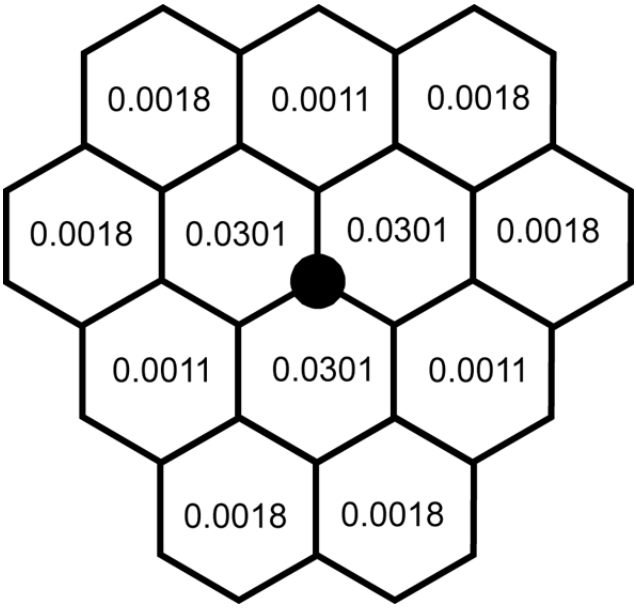

Fig. 24.2. Induced spin-only magnetic moments [μ_B] in the subsurface layer of an fcc(111) Pt substrate caused by a single adatom of Co deposited on top of the surface.

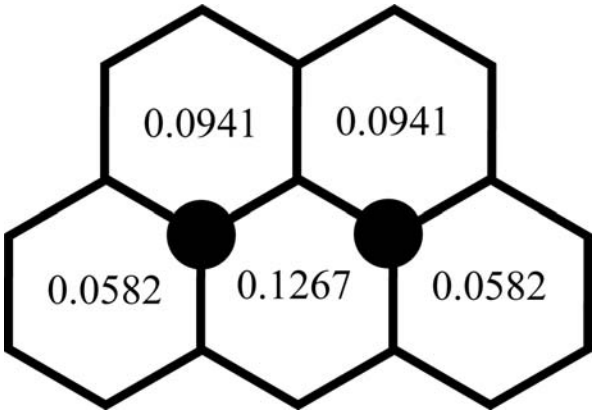

Fig. 24.3. Induced spin-only magnetic moments [μ_B] in the surface layer of an fcc(111) Pt substrate caused by a dimer of Co deposited on the surface.

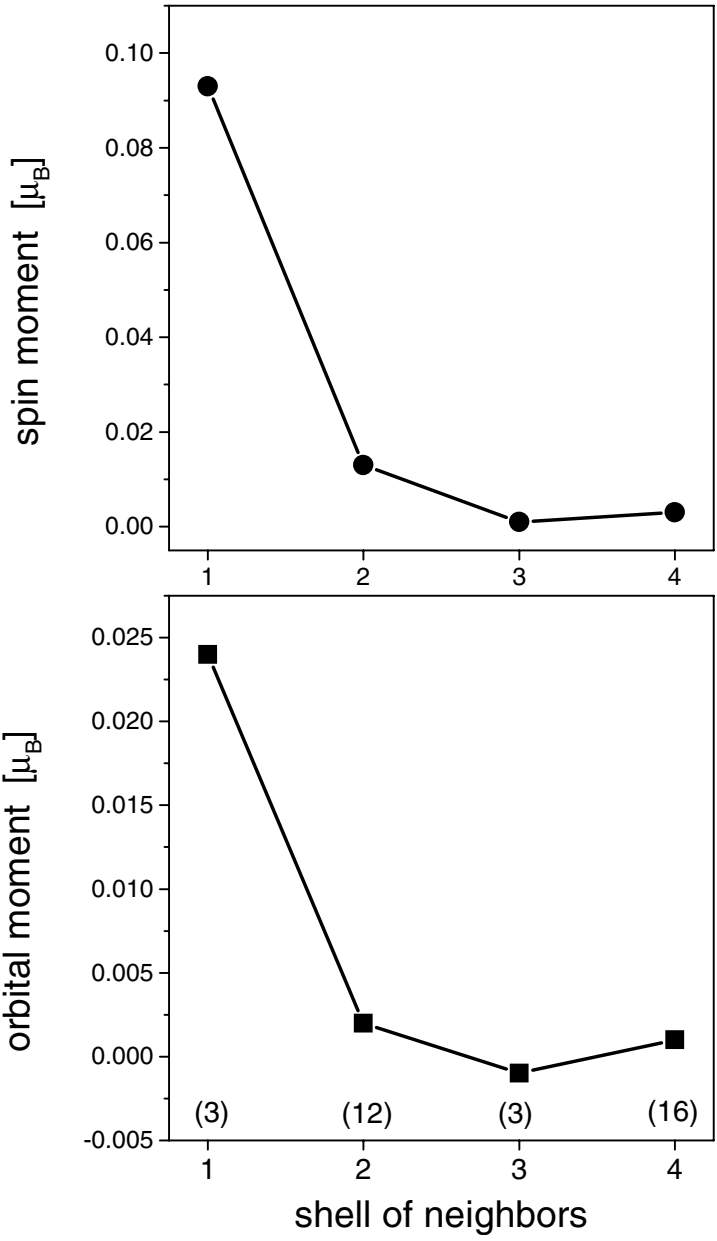

Fig. 24.4. Induced spin-and orbital magnetic moments of Pt atoms in a cluster with one Co atom on top of Pt(111). The number of neighbors in each shell is indicated in brackets. Top: spin moments, bottom: orbital moments.

24.3 Convergence with respect to the size of the embedded cluster

Quite clearly, although the Dyson equation in (24.10) and the above expression for the intercell potential are in principle exact, the size of the cluster, i.e., the number of included "perturbed" host atoms into the cluster is important. Suppose the position vector of a particular site in $\mathcal{C}$ is denoted by $\mathbf{R}_0$ and the distances to the various neighbors, $d_n = |\mathbf{R}_n - \mathbf{R}_0|$, are ordered according to size,

$$d_n < d_{n+1} < d_{n+2} < \ \ldots$$

then a condition for including (excluding) another shell of host atoms at a distance d_n in (from) the cluster can e.g. be of the following kind

$$|\underline{t}^n(\epsilon) - \underline{t}_{\rm h}(\epsilon)| \leq a \quad ,$$

where a is a sufficiently small number guaranteeing that the multipole moments and other relevant one-particle properties are very close to those of the unperturbed host.

As an example for this kind of necessary convergence tests for embedded clusters in Figs. (24.1) and (24.2) the "induced" magnetic moments for Pt atoms in Pt(111) are shown for the case that a single Co atom is placed on top of the surface. Fig. (24.3) depicts the case that a dimer of Co atoms is on top of Pt(111), while in Fig. (24.4) the actual convergence of the Pt spin moments in the various neighbor shells of a single Co atom on top of Pt(111) is displayed. Clearly enough Pd and Pt as substrates are very particular cases, since induced moments are very easily formed. Therefore the inclusion of enough "interacting" Pt sites in $\mathcal{C}$ is essential for a proper description of the electronic structure and the magnetic properties of magnetic structures on top of Pd or Pt substrates.

References

1. B. Lazarovits, L. Szunyogh, and P. Weinberger, Phys. Rev. B **65**, 104441 (2003).
2. B. Lazarovits, L. Szunyogh, and P. Weinberger, Phys. Rev. B **67**, 024415 (2003).

25 Magnetic configurations – rotations of frame

25.1 Rotational properties of the Kohn-Sham-Dirac Hamiltonian

The Hamiltonian as given by the local density functional

$$\mathcal{H}(\mathbf{r}) = c\,\boldsymbol{\alpha}\cdot\mathbf{p} + \beta mc^2 + \mathsf{I}_4 V(\mathbf{r}) + \beta\Sigma_z B(\mathbf{r}) \quad , \tag{25.1}$$

refers to the case that the "magnetization" $\mathbf{B}(\mathbf{r})$ points along an arbitrary assumed $z-$direction, i.e., is of the form

$$\mathbf{B}(\mathbf{r}) = B(\mathbf{r})\hat{\mathbf{z}}\ ,\ \hat{\mathbf{z}} = (0,0,1) \quad , \tag{25.2}$$

such that the Hamiltonian in (25.1) can obviously be written as

$$\mathcal{H}(\mathbf{r}) = c\,\boldsymbol{\alpha}\cdot\mathbf{p} + \beta mc^2 + \mathsf{I}_4 V(\mathbf{r}) + \beta\boldsymbol{\Sigma}\cdot\mathbf{B}(\mathbf{r}) \quad . \tag{25.3}$$

Invariance of $\mathcal{H}(\mathbf{r})$ with respect to a rotation $R \in \mathsf{O}(3)$ is given by

$$S(R)\mathcal{H}(R^{-1}\mathbf{r})S^{-1}(R) = \mathcal{H}(\mathbf{r}) \quad , \tag{25.4}$$

where $S(R)$ is a 4×4 matrix transforming the Dirac matrices $\boldsymbol{\alpha}_i$, β, and Σ_i,

$$S(R) = \begin{pmatrix} U(R) & 0 \\ 0 & \det[\pm]U(R) \end{pmatrix} \quad , \tag{25.5}$$

and $U(R)$ is a (unimodular) 2×2 matrix, i.e., $U(R) \in \mathsf{SU}(2)$, while

$$\det[\pm] = \det[D^{(3)}(R)] \quad , \tag{25.6}$$

where $D^{(3)}(R)$ is the corresponding three-dimensional rotation matrix. Note that $\det[\pm] = 1$ and -1 correspond to proper and improper rotations, respectively. The set of elements R that fulfills (25.4) is usually called the (rotational) symmetry group of $\mathcal{H}(\mathbf{r})$, $\mathrm{G}_{\mathcal{H}}$.

Using now the invariance condition in (25.4) explicitly, one can see immediately that the condition

$$S(R)\left[\mathsf{I}_4 V(R^{-1}\mathbf{r})\right]S^{-1}(R) = \mathsf{I}_4 V(R^{-1}\mathbf{r}) = \mathsf{I}_4 V(\mathbf{r}) \tag{25.7}$$

yields the usual *rotational invariance* condition for the potential. Considering the first term in (25.3) one should account for the transformation of the $\mathbf{p}$ operator,

$$S(R)\left[c\boldsymbol{\alpha}\cdot R^{-1}\mathbf{p}\right]S^{-1}(R) = cS(R)\left[D^{(3)}(R)\boldsymbol{\alpha}\right]S^{-1}(R)\cdot\mathbf{p} \quad , \tag{25.8}$$

where

$$\left[D^{(3)}(R)\boldsymbol{\alpha}\right]_i = \sum_j \alpha_j D^{(3)}(R)_{ji} \quad , \tag{25.9}$$

Inserting the expression of the $\boldsymbol{\alpha}_i$ matrices in terms of the σ_i matrices, the invariance condition,

$$S(R)\left[D^{(3)}(R)\boldsymbol{\alpha}\right]S^{-1}(R) = \boldsymbol{\alpha} \quad , \tag{25.10}$$

implies

$$\det[\pm]U(R)\left[D^{(3)}(R)\sigma\right]U^{-1}(R) = \sigma \quad , \tag{25.11}$$

i.e., a similarity transformation of the Pauli matrices. This means that the kinetic energy part of $\mathcal{H}(\mathbf{r})$ is invariant with respect to an arbitrary rotation R. From (25.11) obviously follows,

$$\det[\pm]S(R)\left[D^{(3)}(R)\boldsymbol{\Sigma}\right]S^{-1}(R) = \boldsymbol{\Sigma} \quad , \tag{25.12}$$

therefore, invariance of the last term of $\mathcal{H}(\mathbf{r})$ in (25.3),

$$S(R)\left[\boldsymbol{\beta\Sigma}\cdot\mathbf{B}(R^{-1}\mathbf{r})\right]S^{-1}(R) = \det[\pm]\boldsymbol{\beta\Sigma}\cdot D^{(3)}(R^{-1})\mathbf{B}(R^{-1}\mathbf{r}) \quad , \tag{25.13}$$

implies

$$\det[\pm]D^{(3)}(R^{-1})\mathbf{B}(R^{-1}\mathbf{r}) = \mathbf{B}(\mathbf{r}) \quad . \tag{25.14}$$

Assuming the form for the exchange field (see also (25.2)) of the following kind,

$$\mathbf{B}(\mathbf{r}) = B(\mathbf{r})\mathbf{n} \quad , \tag{25.15}$$

where $\mathbf{n}$ is a unit vector pointing into an arbitrary direction, two conditions, namely,

$$B(R^{-1}\mathbf{r}) = B(\mathbf{r}) \quad , \tag{25.16}$$

and

$$\det[\pm]D^{(3)}(R^{-1})\mathbf{n} = \mathbf{n} \quad , \tag{25.17}$$

have to be met. Clearly enough for spherical symmetric exchange fields condition (25.16) becomes irrelevant, while (25.17) can be viewed also as an *induced* transformation for the orientation of $\mathbf{B}(\mathbf{r})$. *Induced* in this context means that the mapping $\{U(R)\} \longrightarrow \left\{D^{(3)}(R)\right\}$ is not faithful as the conventional (Pauli gauge) $\mathsf{SU(2)}$ unit matrix maps onto both the identity and the inversion in $O\,(3)$, see [1], [2]:

$$U(R) \equiv \begin{pmatrix} 1 & 0 \\ 0 & 1 \end{pmatrix} \longrightarrow D^{(3)}(E) = \begin{pmatrix} 1 & 0 & 0 \\ 0 & 1 & 0 \\ 0 & 0 & 1 \end{pmatrix} \quad , \tag{25.18}$$

and

$$U(R) \equiv \begin{pmatrix} 1 & 0 \\ 0 & 1 \end{pmatrix} \longrightarrow D^{(3)}(i) = \begin{pmatrix} -1 & 0 & 0 \\ 0 & -1 & 0 \\ 0 & 0 & -1 \end{pmatrix} \quad . \tag{25.19}$$

Consequently, the effective exchange field, $\mathbf{B}(\mathbf{r})$, transforms under rotation as an axial- (or pseudo-)vector as is clearly reflected in (25.17). In simple terms, the very reason of the above result is that the orientation of $\mathbf{B}(\mathbf{r})$ is not given *a priori*, rather it is determined by the invariance condition of the Kohn-Sham-Dirac Hamiltonian in (25.3).

25.2 Translational properties of the Kohn-Sham Hamiltonian

Considering for the moment only simple lattices translational invariance of the Kohn-Sham-Dirac Hamiltonian in (25.3),

$$\mathcal{H}(\mathbf{r} + \mathbf{t}_i) = \mathcal{H}(\mathbf{r}) \quad , \quad \mathbf{t}_i \in \mathcal{L}^{(n)} \quad , \tag{25.20}$$

where $\mathcal{L}^{(n)}$ is a n-dimensional lattice, implies – as easily can be checked – that for the orientations $\mathbf{n}_i$ in all lattice positions the following condition has to apply

$$\mathbf{n}_i = \mathbf{n}_0 \quad , \quad \forall i \in I(\mathcal{L}^{(n)}) \quad , n \leq 3 \quad , \tag{25.21}$$

where $I(\mathcal{L}^{(n)})$ denotes the set of indices corresponding to $\mathcal{L}^{(n)}$ and $\mathbf{n}_0$ is some arbitrarily chosen orientation of $\mathbf{B}(\mathbf{r})$ such as for example $\hat{\mathbf{z}}$, since for a translation the matrix $S(R)$ in (25.5) has to be the unit matrix.

The set T of elements $[E|\mathbf{t}_i]$, $\mathbf{t}_i \in \mathcal{L}^{(n)}$, where E denotes an identity rotation, and group closure is ensured such that

$$[E|\mathbf{t}_i]\,[E|\mathbf{t}_j] = [E|\mathbf{t}_i + \mathbf{t}_j] \in T \quad , \tag{25.22}$$

$$[E|\mathbf{t}_i]\,([E|\mathbf{t}_j]\,[E|\mathbf{t}_k]) = ([E|\mathbf{t}_i]\,[E|\mathbf{t}_j])\,[E|\mathbf{t}_k] \quad , \tag{25.23}$$

$$[E|\mathbf{t}_i]\,[E|-\mathbf{t}_i] = [E|-\mathbf{t}_i]\,[E|\mathbf{t}_i] = [E|0] \quad , \tag{25.24}$$

$$[E|\mathbf{t}_i]^{|T|} = [E|0] \in T \quad , \tag{25.25}$$

with $[E|0]$ being the identity element, is usually referred to as the to $\mathcal{L}^{(n)}$ corresponding translational group of order $|T|$:

$$[E|\mathbf{t}_i]\,\mathcal{H}(\mathbf{r}) = S(E)\mathcal{H}([E|\mathbf{t}_i]^{-1}\,\mathbf{r})S(E) = \mathcal{H}(\mathbf{r} - \mathbf{t}_i) = \mathcal{H}(\mathbf{r}) \quad . \tag{25.26}$$

As is well-known only application of this translational group leads then to cyclic boundary conditions for the eigenfunctions of $\mathcal{H}(\mathbf{r})$, i.e., to Bloch functions. Since $|T|$ has to be always finite,

$$|T| = \prod_{i=1}^{n} |T_i| \quad , \tag{25.27}$$

$|T|$ can be interpreted in physical terms as either the Lohschmidt number ($\mathcal{L}^{(3)}$; bulk, infinite system), the number of atoms in a given atomic plane of a layered structure ($\mathcal{L}^{(2)}$; semi-infinite system), the number of atoms in an atomic linear chain ($\mathcal{L}^{(1)}$), or the number of atoms in a magnetic domain. In the latter case this number is still quite large, sufficient, however, to define a uniform direction of the magnetization within such a domain.

25.3 Magnetic ordering and symmetry

25.3.1 Translational restrictions

If translational invariance applies then (25.21) implies that in all lattice positions the orientation of the magnetization has to point along one and the same direction, i.e., have to be *collinear*. It should be noted that (25.20) can easily be extended to complex lattices. From the discussions above it is easy to see that *non-collinearity* can formally only be introduced by either reducing the dimension of the lattice or, in special cases, considering complex lattices.

25.3.2 Rotational restrictions

Clearly enough rotational invariance is closely related to the magnetic ordering of the system. Consider a set of lattice vectors $\{\mathbf{t}_i\}$, or of position vectors $\{\mathbf{R}_i\}$ in a finite cluster, and orientations of the magnetization $\{\mathbf{n}_i\}$. A possibly present **rotational symmetry transformation** R of the system has to meet the invariance conditions for

1. the (effective) potential $V(\mathbf{r})$,
$$V(R^{-1}(\mathbf{r}_i + \mathbf{t}_i)) = V(\mathbf{r}_i + \mathbf{t}_i) \quad , \tag{25.28}$$
2. the (effective) magnetization $B(\mathbf{r})$,
$$B(R^{-1}(\mathbf{r}_i + \mathbf{t}_i)) = B(\mathbf{r}_i + \mathbf{t}_i) \quad , \tag{25.29}$$
3. and, due to the induced rotations defined in (25.14) or (25.17), for the orientations of the (effective) magnetization,
$$\det[\pm] D^{(3)}(R^{-1}\mathbf{n}_i) = \mathbf{n}_i \quad . \tag{25.30}$$
Expressed in colloquial terms this simply means that "spin-orbit-coupling" also enters the definition of the magnetic order of the system.

25.4 Magnetic configurations

25.4.1 Two-dimensional translational invariance

Based on the previous section it is now very easy to describe magnetic structures in layered systems. For a two-dimensional translational invariant system (layered system; one atom per unit cell for matters of simplicity) a particular configuration

$$\mathcal{C}_i = \{\ldots, \mathbf{n}_{k-1}, \mathbf{n}_k, \mathbf{n}_{k+1}, \ldots\} \quad , \tag{25.31}$$

where k numbers atomic layers, is defined by a set of unit vectors $\mathbf{n}_k$ that characterize the orientations of the magnetization in all atomic layers. Obviously, a ferromagnetic configuration can be formulated as

$$\mathcal{C}_0 = \{\mathbf{n}_k | \mathbf{n}_k = \mathbf{n}_0, \forall k\} \quad , \tag{25.32}$$

where $\mathbf{n}_0$ is a prechosen direction such as e.g. within the planes of atoms. In most cases of applications presented in Chap. 26 such a configuration is considered as reference. The configuration

$$\mathcal{C}_j = \{\ldots, \mathbf{n}_{k-1}, -\mathbf{n}_k, \mathbf{n}_{k+1}, \ldots\} \tag{25.33}$$

refers to an arrangement in which with respect to $\mathcal{C}_0$ the orientation of the magnetization is reversed in the $k-th$ atomic layer. Taking also *non-collinear* configurations into account implies that $\mathcal{C}_j$ can be reached in a continuous manner by means of a rotation $U(\Theta_k)$ of $\mathbf{n}_k$, $0 \leq \Theta \leq 2\pi$, around an axis perpendicular to $\mathbf{n}_k$, i.e., by considering configurations of the form

$$\mathcal{C}_i(\Theta) = \{\ldots, \mathbf{n}_{k-1}, U(\Theta_k)\mathbf{n}_k, \mathbf{n}_{k+1}, \ldots\} \quad . \tag{25.34}$$

This implies that although within one atomic layer because of translational symmetry collinearity has to apply, with respect to each other the various layers can be oriented non-collinearly.

25.4.2 Complex lattices

Suppose that a complex three-dimensional lattice is characterized by M sublattices corresponding to the non-primitive translations $\mathbf{a}_m$. Translational invariance implies that

$$\mathcal{H}(\mathbf{r} + \mathbf{a_m} + \mathbf{t}) = \mathcal{H}(\mathbf{r} + \mathbf{a}_m) \quad , \quad t \in \mathcal{L}^{(n)} \quad , \quad \forall m \quad . \tag{25.35}$$

In principle therefore the orientations in the various sublattices can be different from each other. If $\mathbf{n}_0(\mathbf{a}_m)$ denotes the uniform orientation of the magnetization in a particular sublattice then in the simplest case of $M = 2$ the choice $\mathbf{n}_0(\mathbf{a}_1) = \mathbf{n}_0$ and $\mathbf{n}_0(\mathbf{a}_2) = -\mathbf{n}_0$ denotes a so-called antiferromagnetic arrangement. Clearly enough the same arguments hold true for complex two-dimensional lattices.

25.4.3 Absence of translational invariance

If no translational and/or rotational invariance applies than the orientation of the magnetization has to be specified for each scattering site. In this case the various orientations can be completely arbitrary, i.e., arbitrary non-collinear arrangements can be assumed.

25.5 Rotation of frames

Let $S \in \mathsf{O}(3)$ be a rotation, which transforms the direction $\widehat{\mathbf{z}}$ into the orientation of the effective magnetization $\mathbf{n}^{pi}$ of site i in the p-th layer. Furthermore, let $\underline{t}^{pi}(z)$ refer to the single–site t–matrix for a complex energy z if $\mathbf{n}^{pi}$ is parallel to $\hat{\mathbf{z}}$, while $\underline{t}^{pi}_{S}(z)$ refers to the t–matrix if $\mathbf{n}^{pi}$ points along the direction $S\,\widehat{\mathbf{z}}$. From the analytical form of partial wave representation of single-site scattering matrices, see, e.g., (3.111), which for matters of convenience is repeated below, it is easy to see that a transformation of the single-site t-operator by S simply implies a transformation of the basis used to represent this operator,

$$\underline{t}^{n}(z) = \iint\limits_{\{\mathbf{r}_n,\mathbf{r}'_n \in D_{V_n}\}} \mathrm{d}\mathbf{r}\mathrm{d}\mathbf{r}'\ \mathsf{j}(z;\mathbf{r}_n)^{\times}\ t^{n}(z;\mathbf{r}_n,\mathbf{r}'_n)\ \mathsf{j}(z;\mathbf{r}'_n) \quad . \tag{25.36}$$

However, since the basis functions are nothing but a product of a spherical Besselfunctions and spherical harmonics, $j_L(z;\mathbf{r}_n) = j_\ell(\sqrt{z}\,|\mathbf{r}_n|)\,Y_L(\widehat{\mathbf{r}}_n)$, such a transformation invokes only a transformation of spherical harmonics (spin spherical harmonics in a relativistic treatment),

$$\mathsf{j}(z;S\mathbf{r}_n) = \mathsf{j}(z;\mathbf{r}_n)\,\underline{D}(S) \quad , \tag{25.37}$$

$$\mathsf{j}(z;S\mathbf{r}_n)^{\times} = \underline{D}^{\dagger}(S)\mathsf{j}(z;\mathbf{r}_n) \quad , \tag{25.38}$$

where $\underline{D}(S)$ contains blockwise the irreducible (projective irreducible in the case of spin spherical harmonics) representations [1] of S. Writing out explicitly the orientation of the effective field, the single–site t–matrix, $\underline{t}^{pi}_{S}(z)$ with respect to $S \in \mathsf{O}(3)$, can be expressed as

$$\underline{t}_S^{pi}(z) = \iint\limits_{\{\mathbf{r}_{pi},\mathbf{r}'_{pi}\in D_{V_{pi}}\}} \mathrm{d}\mathbf{r}_{pi}\mathrm{d}\mathbf{r}'_{pi}\ \mathrm{j}(z;\mathbf{r}_{pi})^{\times}\ t^n\left(z;\mathbf{r}_{pi},\mathbf{r}'_{pi};S\,\widehat{\mathbf{z}}\right)\ \mathrm{j}\left(z;\mathbf{r}'_{pi}\right) \tag{25.39}$$

$$= \iint\limits_{\{\mathbf{r}_{pi},\mathbf{r}'_{pi}\in D_{V_{pi}}\}} \mathrm{d}\mathbf{r}_{pi}\mathrm{d}\mathbf{r}'_{pi}\ \mathrm{j}(z;\mathbf{r}_{pi})^{\times}\ t^n\left(z;S^{-1}\mathbf{r}_{pi},S^{-1}\mathbf{r}'_{pi};\,\widehat{\mathbf{z}}\right)\ \mathrm{j}\left(z;\mathbf{r}'_{pi}\right) \tag{25.40}$$

$$= \iint\limits_{\{\mathbf{r}_{pi},\mathbf{r}'_{pi}\in D_{V_{pi}}\}} \mathrm{d}\mathbf{r}_{pi}\mathrm{d}\mathbf{r}'_{pi}\ \mathrm{j}(z;S\mathbf{r}_{pi})^{\times}\ t^n\left(z;\mathbf{r}_{pi},\mathbf{r}'_{pi};\,\widehat{\mathbf{z}}\right)\ \mathrm{j}\left(z;S\mathbf{r}'_{pi}\right) \quad , \tag{25.41}$$

and is therefore related to $\underline{t}^{pi}(z)$ by the following similarity transformation,

$$\underline{t}_S^{pi}(z) = \underline{D}^{\dagger}(S)\underline{t}^{pi}(z)\underline{D}(S) \quad . \tag{25.42}$$

Clearly enough two-dimensional translational invariance then implies that

$$\underline{t}_S^{pi}(z) = \underline{t}_S^{p0}(z) \quad , \quad \forall i \in I(\mathcal{L}^{(2)}) \quad , \tag{25.43}$$

where $i = 0$ refers to the origin of $\mathcal{L}^{(2)}$.

25.5.1 Rotational properties of two-dimensional structure constants

Suppose p, q denote layer indices, S is element of the point-group of a simple two-dimensional lattice $\mathcal{L}^{(2)} = \{\mathbf{t}_i\}$,

$$\mathrm{G}_{\mathcal{L}^{(2)}} = \left\{S \mid S\mathbf{t}_i \in \mathcal{L}^{(2)}; \forall \mathbf{t}_i \in \mathcal{L}^{(2)}\right\} \quad , \tag{25.44}$$

and $\mathbf{k}_{\|}$ is a vector from the surface Brillouin zone (SBZ). The lattice Fourier transformation of the structure constants $\underline{G}_0^{pi,q0}(z)$ is then given by

$$\underline{G}_0^{pq}(z;S\mathbf{k}_{\|}) = \sum_{\mathbf{t}_i\in\mathcal{L}^{(2)}} \exp\left[\mathrm{i}\left(\mathbf{t}_i\cdot S\mathbf{k}_{\|}\right)\right]\underline{G}_0^{pi,q0}(z) \quad , \tag{25.45}$$

where the index pi refers to site i in layer p and $q0$ to the origin of $\mathcal{L}^{(2)}$ in layer q. It should be recalled that at a given energy ε, $\underline{G}_0^{pi,q0}(z)$ depends only on the difference between the position vectors for these two sites,

$$\underline{G}_0^{pq}(z) = \underline{G}_0(z;\mathbf{c}_p + \mathbf{t}_i - \mathbf{c}_q) \quad , \tag{25.46}$$

namely on the difference between the layer generating vectors $\mathbf{c}_p$ and $\mathbf{c}_q$, and $\mathbf{t}_i \in \mathcal{L}^{(2)}$. Making use of the property of scalar products

$$\underline{G}_0^{pq}(z;S\mathbf{k}_\parallel) = \sum_{\mathbf{T}_i\in\mathcal{L}^{(2)}} \exp\left[\mathrm{i}S^{-1}\mathbf{t}_i\cdot\mathbf{k}_\parallel\right]\underline{G}_0(z;\mathbf{c}_p+\mathbf{t}_i-\mathbf{c}_q) \quad . \tag{25.47}$$

and using the notation

$$S^{-1}\mathbf{t}_i = \mathbf{t}_i' \quad .$$

(25.46) can be written as

$$\underline{G}_0^{pq}(z;S\mathbf{k}_\parallel) = \sum_{\mathbf{t}_i'\in\mathcal{L}^{(2)}} \exp\left[\mathrm{i}\mathbf{t}_i'\cdot\mathbf{k}_\parallel\right]\underline{G}_0(z;\mathbf{c}_p+S\mathbf{t}_i'-\mathbf{c}_q) \quad . \tag{25.48}$$

In order to discuss the rotational properties of real space structure constants one has to recall that structure constants per definition are partial wave representations of the real space resolvent $\mathcal{G}_0(z)$, see Chap. 3,

$$G_0(z;S(\mathbf{r}_i+\mathbf{R}_i),S(\mathbf{r}_j+\mathbf{R}_j)) = \mathrm{j}(z;S\mathbf{r}_i)\underline{G}_0(z;S(\mathbf{R}_j-\mathbf{R}_i))\mathrm{j}(z;S\mathbf{r}_j)^\times \quad , \tag{25.49}$$

therefore, a transformation of the basis, (25.37) and (25.38), implies

$$\begin{aligned} &G_0(z;S\left(\mathbf{r}_i+\mathbf{R}_i\right),S\left(\mathbf{r}_j+\mathbf{R}_j\right)) = \\ &\quad \mathrm{j}(z;\mathbf{r}_i)\underline{D}(S)\underline{G}_0\left(z;S\left(\mathbf{R}_j-\mathbf{R}_i\right)\right)\underline{D}^\dagger(S)\mathrm{j}(z;\mathbf{r}_j)^\times \quad . \end{aligned} \tag{25.50}$$

However, since the free Green's function is invariant under $\forall S\in \mathrm{G}_{\mathcal{L}^{(2)}}$

$$G_0(z;S(\mathbf{r}_i+\mathbf{R}_i),S(\mathbf{r}_j+\mathbf{R}_j)) = G_0(z;\mathbf{r}_i+\mathbf{R}_i,\mathbf{r}_j+\mathbf{R}_j) \quad , \tag{25.51}$$

one immediately gets

$$\underline{G}_0\left(z;\mathbf{R}_j-\mathbf{R}_i\right) = \underline{D}(S)\underline{G}_0\left(z;S\left(\mathbf{R}_j-\mathbf{R}_i\right)\right)\underline{D}^\dagger(S) \quad , \tag{25.52}$$

and therefore,

$$\underline{G}_0(z;\mathbf{c}_p+S\mathbf{t}_i'-\mathbf{c}_q) = \underline{D}(S^{-1})\underline{G}_0(z;S^{-1}(\mathbf{c}_p-\mathbf{c}_q)+\mathbf{t}_i')\underline{D}^\dagger(S^{-1}) \quad . \tag{25.53}$$

Consequently the lattice Fourier transformation (25.45) can be rewritten as,

$$\underline{G}_0^{pq}(z;S\mathbf{k}_\parallel) = \sum_{\mathbf{t}_i'\in\mathcal{L}_\parallel} \exp\left(\mathrm{i}\mathbf{t}_i'\cdot\mathbf{k}_\parallel\right)\underline{D}(S^{-1})\underline{G}_0(z;S^{-1}(\mathbf{c}_p-\mathbf{c}_q)+\mathbf{t}_i')\underline{D}^\dagger(S^{-1}) \quad . \tag{25.54}$$

Clearly enough when splitting up the vector $S^{-1}(\mathbf{c}_p-\mathbf{c}_q)$ into components perpendicular and parallel to the layers,

$$S^{-1}(\mathbf{c}_p-\mathbf{c}_q) = S^{-1}(\mathbf{c}_p-\mathbf{c}_q)_\perp + S^{-1}(\mathbf{c}_q-\mathbf{c}_q)_\parallel \quad , \tag{25.55}$$

the perpendicular components (parallel to the axis of rotation!) remain unchanged, i.e.,

$$S^{-1}(\mathbf{c}_p-\mathbf{c}_q)_\perp = (\mathbf{c}_p-\mathbf{c}_q)_\perp \quad . \tag{25.56}$$

Defining finally the following difference vector,

$$\Delta\mathbf{c}_{pq,\parallel}^{S^{-1}} \equiv S^{-1}(\mathbf{c}_p - \mathbf{c}_q)_\parallel - (\mathbf{c}_p - \mathbf{c}_q)_\parallel = S^{-1}(\mathbf{c}_p - \mathbf{c}_q) - (\mathbf{c}_p - \mathbf{c}_q) \quad , \tag{25.57}$$

the coordinate arguments in the structure constants can be reformulated as

$$\begin{aligned} S^{-1}(\mathbf{c}_p - \mathbf{c}_q) + \mathbf{t}_i' &= (\mathbf{c}_p - \mathbf{c}_q)_\perp + S^{-1}(\mathbf{c}_p - \mathbf{c}_q)_\parallel + \mathbf{t}_i' \\ &= (\mathbf{c}_p - \mathbf{c}_q) + \mathbf{t}_i' + \Delta\mathbf{c}_{pq,\parallel}^{S^{-1}} \quad . \end{aligned} \tag{25.58}$$

If $\Delta\mathbf{c}_{pq,\parallel}^{S^{-1}} \in \mathcal{L}^{(2)}$, which is the case, e.g., for the (100), (110) and (111) layers of all cubic lattices, $\underline{G}_0^{pi,q0}(z; S\mathbf{k}_\parallel)$ in (25.54) reduces to

$$\underline{G}_0^{pq}(z; S\mathbf{k}_\parallel) =$$

$$= \sum_{\mathbf{t}_i' \in \mathcal{L}^{(2)}} \exp\left[\mathrm{i}\mathbf{t}_i' \cdot \mathbf{k}_\parallel\right] \exp\left[-\mathrm{i}\Delta\mathbf{c}_{pq,\parallel}^{S^{-1}} \cdot \mathbf{k}_\parallel\right] \underline{D}(S^{-1}) \underline{G}_0^{pi,q0}(z) \underline{D}^\dagger(S^{-1}) \tag{25.59}$$

$$= \exp\left[-\mathrm{i}\Delta\mathbf{c}_{pq,\parallel}^{S^{-1}} \cdot \mathbf{k}_\parallel\right] \underline{D}(S^{-1}) \underline{G}_0^{pq}(z; \mathbf{k}_\parallel) \underline{D}^\dagger(S^{-1}) \quad . \tag{25.60}$$

25.6 Rotational properties and Brillouin zone integrations

Going back now to the partial wave representation of the scattering path operator, see in particular (3.132) and (23.96),

$$\underline{\tau}^{pq}(z) = \underline{\tau}^{pi,qi}(z) = \underline{\tau}^{p0,q0}(z) = \Omega_{\mathrm{SBZ}}^{-1} \int \underline{\tau}^{pq}(z; \mathbf{k}_\parallel)\, \mathrm{d}\mathbf{k}_\parallel \quad , \tag{25.61}$$

$$\left[\tau\left(z; \mathbf{k}_\parallel\right)^{-1}\right]^{pq} = \underline{\mathbf{t}}^p\left(z\right)^{-1} \delta_{pq} - \underline{\mathbf{G}}_0^{pq}\left(z; \mathbf{k}_\parallel\right) \quad , \tag{25.62}$$

one immediately can see that the rotational properties discussed above can be of great help in performing the respective Brillouin zone integrals. It should be noted, however, from the Kohn-Sham-Dirac Hamiltonian in (25.3) that the rotational invariance group $\mathrm{G}_\mathcal{H}$ not automatically is identical to the point group $\mathrm{G}_{\mathcal{L}^{(2)}} = \{S\}$ of $\mathcal{L}^{(2)}$, which by definition comprises only unitary symmetry operations, but in principle contains also all antiunitary symmetry operations,

$$\mathrm{G}_\mathcal{H} = \{\mathrm{G}_{\mathcal{L}^{(2)}}, \Theta\mathrm{G}_{\mathcal{L}^{(2)}}\} \quad , \tag{25.63}$$

Θ being the time inversion operator. For a discussion of the group theoretical manipulations necessary to include also antiunitary operators, see [3].

Let for matters of simplicity $\mathrm{G}_\mathcal{H}$ be the point group of the underlying two-dimensional lattice, such as for example C_{4v} in the case of an fcc(001)

surface of a non-magnetic substrate, and suppose $D(S)$ contains blockwise the irreducible projective representations [1] of $S \in \mathrm{G}_{\mathcal{H}}$. If IBZ_1 denotes an irreducible wedge of the SBZ, then any other wedge IBZ_S of the SBZ is defined by

$$\mathrm{IBZ}_S = \{S\mathbf{k}_\parallel \mid \mathbf{k}_\parallel \in \mathrm{IBZ}_1\} \quad ; \quad S \in \mathrm{G}_{\mathcal{H}} \quad , \tag{25.64}$$

such that

$$\mathrm{SBZ} = \sum_{S \in \mathrm{G}_{\mathcal{H}}} \mathrm{IBZ}_{S^{-1}} \quad . \tag{25.65}$$

From (25.42) and (25.60) then follows,

$$\left[\tau\left(z; S^{-1}\mathbf{k}_\parallel\right)^{-1}\right]^{pq} = \underline{\mathbf{t}}^p(z)^{-1}\,\delta_{pq} - \underline{\mathbf{G}}_0^{pq}\left(z; S^{-1}\mathbf{k}_\parallel\right) \tag{25.66}$$

$$= \underline{\mathbf{t}}^p(z)^{-1}\,\delta_{pq} - \exp\left[-\mathrm{i}\Delta\mathbf{c}^S_{pq,\parallel}\cdot\mathbf{k}_\parallel\right]\underline{D}(S)\underline{G}_0^{pq}(z;\mathbf{k}_\parallel)\underline{D}^\dagger(S) \tag{25.67}$$

$$= \exp\left[-\mathrm{i}\Delta\mathbf{c}^S_{pq,\parallel}\cdot\mathbf{k}_\parallel\right]\underline{D}(S)\left[\tau_S\left(z;\mathbf{k}_\parallel\right)^{-1}\right]^{pq}\underline{D}^\dagger(S) \quad , \tag{25.68}$$

where use was made of the unitary property of the irreducible representations,

$$\underline{D}(S)^{-1} = \underline{D}^\dagger(S) \quad , \tag{25.69}$$

and where the below matrix was introduced,

$$\left[\tau_S\left(z;\mathbf{k}_\parallel\right)^{-1}\right]^{pq} = \underline{\mathbf{t}}_S^p(z)^{-1}\,\delta_{pq} - \underline{G}_0^{pq}(z;\mathbf{k}_\parallel) \quad . \tag{25.70}$$

Inverting the above matrix one obviously gets

$$\underline{\tau}^{pq}(z; S\mathbf{k}_\parallel) = \exp\left[\mathrm{i}\Delta\mathbf{c}^S_{pq,\parallel}\cdot\mathbf{k}_\parallel\right]\underline{D}(S)\underline{\tau}_S^{pq}(z;\mathbf{k}_\parallel)\underline{D}^\dagger(S) \quad , \tag{25.71}$$

where – as should be recalled – p, q are layer indices and $\tau_S^{pq}(\mathbf{k}_\parallel;\epsilon)$ refers to the corresponding similarity transformed t–matrix $t_S^{p0}(\epsilon)$ as defined in (25.42).

The SBZ–integral, (25.61), can therefore be expressed as

$$\underline{\tau}^{pq}(z) = |\mathrm{G}_{\mathcal{H}}|^{-1}\sum_{S\in\mathrm{G}_{\mathcal{H}}}\exp\left[\mathrm{i}\Delta\mathbf{c}^S_{pq,\parallel}\cdot\mathbf{k}_\parallel\right]\underline{D}(S)\underline{\tau}^{pq}_{S,\mathrm{IBZ}}(z)\underline{D}^\dagger(S) \quad , \tag{25.72}$$

$$\underline{\tau}^{pq}_{S,\mathrm{IBZ}}(z) = \frac{1}{\Omega_{\mathrm{IBZ}_1}}\int_{\mathrm{IBZ}_1}\underline{\tau}_S^{pq}(z;\mathbf{k}_\parallel)\mathrm{d}\mathbf{k}_\parallel \quad , \tag{25.73}$$

where $|\mathrm{G}_{\mathcal{H}}|$ is the order of the group and Ω_{IBZ_1} denotes the surface area of IBZ_1. Equation (25.72) implies (i) that the structure constants need only be evaluated for a chosen set of $\mathbf{k}_\parallel \in \mathrm{IBZ}_1$ and (ii) that for any pair $S, R \in \mathrm{G}_{\mathcal{H}}$ for which $t_S^p(z) = t_R^p(z)$ for all p the contributions to the sum in (25.72), $\underline{\tau}^{pq}_{S,\mathrm{IBZ}}(z)$, are identical.

Computationally the easiest way to avoid superfluous numerical operations in (25.72) is to split $\mathrm{G}_{\mathcal{H}}$ into the following subsets of order $|C_t|$

$$C_t = \left\{ S_k \mid \underline{t}^p_{S_k}(z) = \underline{t}^p_{S_1}(\epsilon) \quad ; \quad k = 1, \ldots, |C_t| \ , \ \forall p \right\} \quad , \tag{25.74}$$

such that

$$\underline{\tau}^{pq}(z) = |\mathrm{G}_{\mathcal{H}}|^{-1} \sum_t \sum_{S_k \in C_t} \exp\left[\mathrm{i} \Delta \mathbf{c}^{S_k}_{pq,\parallel} \cdot \mathbf{k}_{\parallel} \right] \underline{D}(S_k) \underline{\tau}^{pq}_{S_1,\mathrm{IBZ}}(z) \underline{D}^{\dagger}(S_k) \quad , \tag{25.75}$$

where S_1 is an arbitrary element of a particular subset C_t.

References

1. S.L. Altmann, *Rotations, Quaternions and Double Groups* (Clarendon Press, Oxford, England 1986)
2. S.L. Altmann and P. Herzig, *Point-Group Theory Tables* (Clarendon Press, Oxford, England 1994)
3. G. Hörmandinger and P. Weinberger, J. Phys. Cond. Matt. **4**, 2185 (1992)
4. P. Weinberger, *Electron Scattering Theory of Ordered and Disordered Matter* (Clarendon Press, Oxford 1992)
5. P. Weinberger, Phil. Mag. B **75**, 509 (1997)

26 Related physical properties

26.1 Surface properties

Theoretical investigations of surface properties by means of first-principle calculations is computationally a very demanding task and therefore linked with the availability of high performance computers. For that reason first semi-empirical studies like that of Lang and Kohn [1] [2] have been performed. Their model was based on a uniform, positively charged background jellium which successfully explained qualitative trends of work functions and surface energies of metals with low electron densities. Other authors improved their approach but still failed to obtain quantitative agreement with available experimental data.

It was then a great step forward when due to the development of more sophisticated methods for the calculation of the electronic structure of solids and the availability of faster computer hardware, *ab initio* calculations became possible.

Still various levels of approximations remain present. These approximations include the use of supercell or slab geometries [3] in which two surfaces have to be treated simultaneously. A more natural approach to the study of surfaces (and interfaces) is to use Green's function methods which are capable of treating true semi-infinite systems featuring only one surface [4] [5].

Other parameters are the kind of LDA functional employed or the use of GGA. On the average LDA results for calculated surface energies are about 8% larger and GGA values are 7% lower than experimental values [5]. Some authors use theoretical equilibrium lattice constants while others obtain their results with the experimental values. Sometimes the relaxation of the top surface layers is taken account of [3] while others claim this will not influence the result considerably [6] [7]. The relaxation of the interlayer spacing in the top surface layers ranges from below 1% to more than 10% and depends on the material and surface orientation under consideration.

Last but not least attention has to be paid to the approximation for the potential. Calculations for semi-infinite systems have been performed within the atomic sphere approximation (ASA) [4], full charge density (FCD) [5], and full potential (FP) [3] approaches.

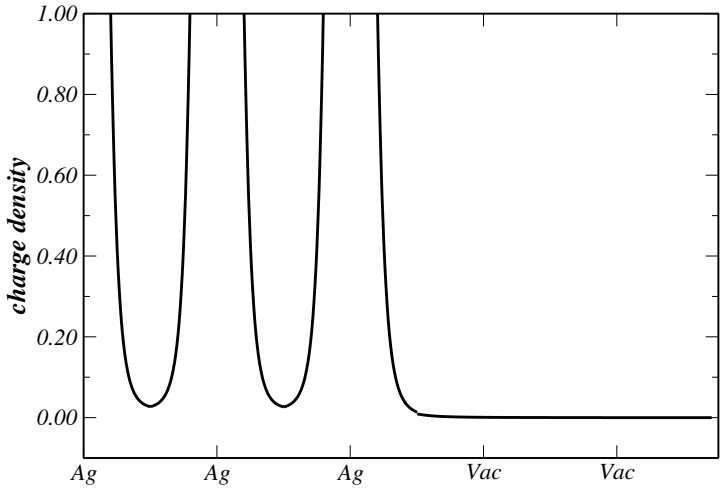

Fig. 26.1. Charge density of Ag (001) plotted along the nearest neighbor direction as indicated in Fig. 26.4.

In the sections below first the properties of the one-electron potentials at surfaces will be addressed, and then a short discussion on the calculation of work functions follows.

26.1.1 Potentials at surfaces

ASA

While for atoms in bulk systems with localized d-electrons and highly isotropic surrounding the ASA is a quite reasonable and an adequate description of the potential, this no longer is the case at surfaces or interfaces. Because of the sudden termination of the crystal the potential has to change from bulk like to a constant vacuum potential level within only a few atomic layers. If described within the ASA the resulting potential acquires the form of a step like function with discontinuous jumps in the vacuum layers as shown in Fig. 26.3.

In order to still obtain a reasonable approximation of the electrostatic potential usually the dipole moment of the charge density is included in the Madelung part of the potential, see Chap. 19. This (constant) intercell potential – as it is also referred to – is then given by

$$V_p^{\text{inter}} = 2 \sum_q \left(A_{pq}^{00,00}\, Q_{q,00} + A_{pq}^{00,10}\, Q_{q,10} \right) + V_p[\bar{\rho}] \quad , \tag{26.1}$$

where $Q_{q,00}$ is the monopole and $Q_{q,10}$ the dipole moment of the charge distribution at site q. In addition to these quantities, the monopole and dipole

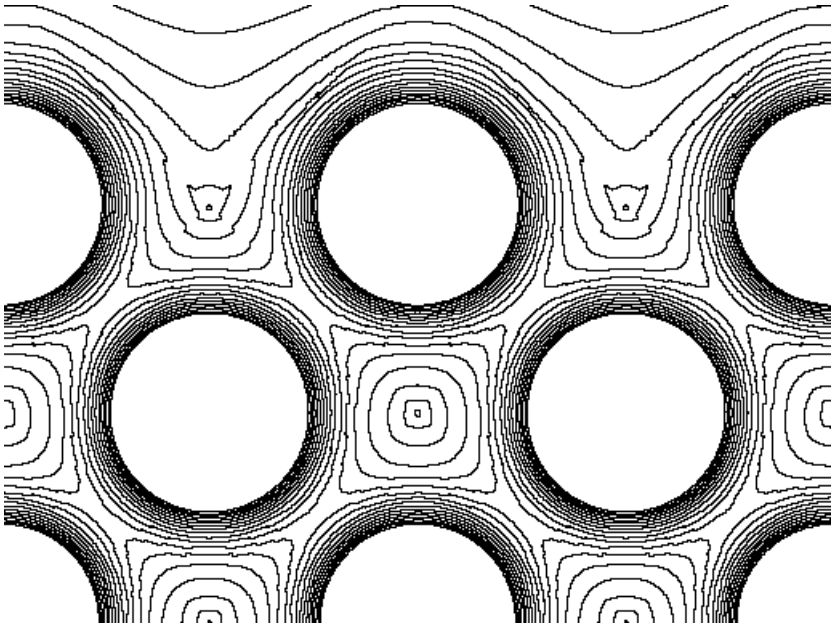

Fig. 26.2. Two dimensional contour plot of the potential at the surface of Ag (001).

Madelung constants, $A_{pq}^{00,00}$ and $A_{pq}^{00,10}$, respectively, have to be evaluated [8]. Finally there is a contribution $V_p[\bar{\rho}]$ attributed to the assumed step like behavior of the interstitial charge density $\bar{\rho}$ perpendicular to the surface.

The second part of the electrostatic potential, the intracell potential is calculated as follows

$$V_p^{\text{intra}}(r) = -2Zr^{-1} + 8\pi\, r^{-1} \int_0^r \mathrm{d}r'\, r'^2 \rho_{00}(r') + 8\pi \int_r^{r_{\text{WS}}} \mathrm{d}r'\, r' \rho_{00}(r') \quad . \tag{26.2}$$

Added together they form the Coulomb potential shown in Fig. 26.3:

$$V_p^{\text{coul}}(r) = V_p^{\text{intra}}(r) + V_p^{\text{inter}} \quad . \tag{26.3}$$

For being able to accurately calculate properties of surfaces such as work functions and therelike, an appropriate exchange-correlation potential has to be added. Some surface properties then crucially depend on the specific LDA functional used.

FCD and FP

In these two cases the anisotropies associated with potentials at surfaces or interfaces can fully taken into account. From self-consistent calculations a

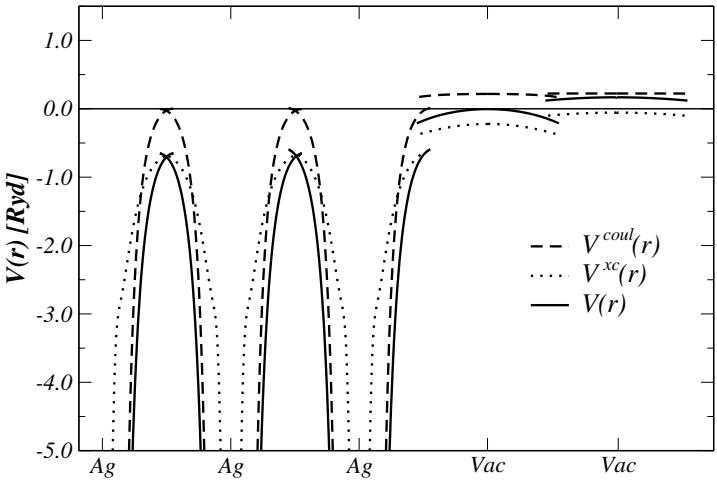

Fig. 26.3. ASA potentials of Ag (001) plotted in the nearest neighbor direction towards the vacuum, see Fig. 26.4. In the ASA calculation the zero of energy coincides with the value of the Coulomb potential in the bulk at the surface of the ASA-sphere.

more or less continuous potential can be obtained limited only by numerics and the chosen angular momentum quantum number, see Chaps. 18 and 21.

The difference between FCD and FP is that in the former case only the spherically symmetric part of the potential is used to compute the solutions of the radial equations, whereas the one electron potential includes the contributions of all multipole moments and all real space integrations are performed over the polyhedral Wigner-Seitz cell. In many relevant cases a FCD description does not lag far behind a complete FP treatment.

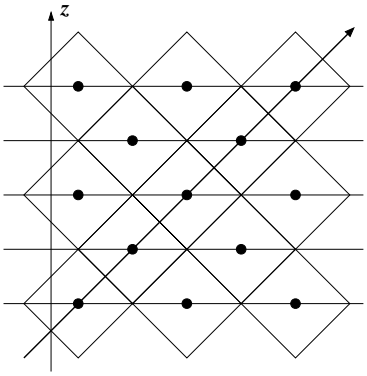

Fig. 26.4. Nearest neighbor direction for an fcc (001) surface.

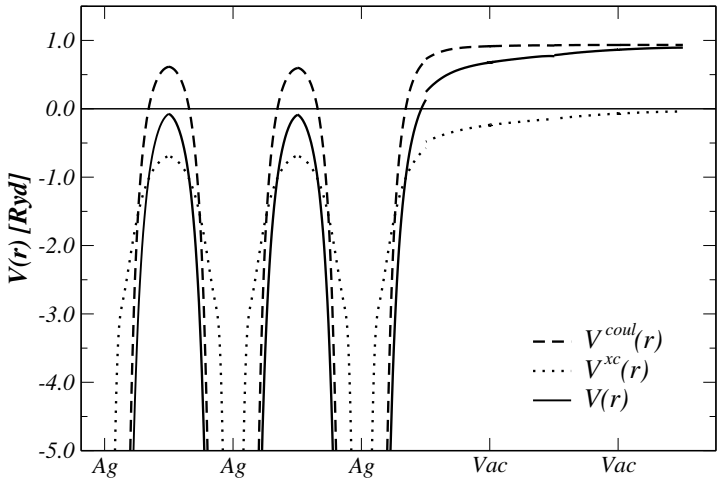

Fig. 26.5. FCD potentials of Ag (001) plotted in the nearest neighbor direction towards the vacuum, see Fig. 26.4. In FCD or FP calculations the energy zero is determined by the value of the spherical symmetric part of the total potential at the muffin-tin radius in the bulk system.

The construction of the potential in the FCD or FP approaches is discussed in detail in Chap. 19. Including the near field corrections as explained in Chap. 20 accounts for the almost perfectly continuous electrostatic (or Coulomb) potential displayed in Fig. 26.5, nearly irrespective of the maximum angular momentum quantum number used.

Small discontinuities of the potential in actual calculations are associated with the evaluation of the exchange-correlation potential $V^{\mathrm{xc}}(\mathbf{r})$,

$$V^{\mathrm{xc}}(\mathbf{r}) = \sum_L V_L^{\mathrm{xc}}(r)\, Y_L(\hat{\mathbf{r}}) \quad , \tag{26.4}$$

since there is no way of knowing the analytic expression for $V^{\mathrm{xc}}(\mathbf{r})$. The occurring expansion coefficients are calculated by numerical integration from:

$$V_L^{\mathrm{xc}}(r) = \int \mathrm{d}\hat{\mathbf{r}}\, V^{\mathrm{xc}}(\mathbf{r})\, Y_L^*(\hat{\mathbf{r}}) \quad . \tag{26.5}$$

At a specific position $\mathbf{r}$ inside the bounding sphere, the angular momentum series of the charge density has to be summed up and the exchange-correlation functional $V^{\mathrm{xc}}(\mathbf{r}) = V^{\mathrm{xc}}[\rho(\mathbf{r})]$ computed from the resulting value.

For very low densities in the vacuum (c.f. Fig. 26.1) this leads to numerical problems not only because the angular momentum series is slowly converging, but also because the complex energy integration is not accurate enough even with 16 points on the semicircular contour. The resulting charge density might be negative at some points in the cell and therefore cause problems

Table 26.1. LDA work functions fcc (001) Ag , Pd, and Cu in various approximations and in comparison to experimental values and calculations of other authors. Values are given in eV. NR refers to non-relativistic and SR to scalar relativistic calculations. The lattice constants [a.u.] in the present calculations were a=7.729 for Ag, a=7.353 for Pd, and a=6.831 for Cu. No layer relaxation has been considered.

	Ag	Pd	Cu
ASA NR ($\ell_{\max} = 2$)	4.73	5.76	5.24
ASA NR ($\ell_{\max} = 3$)	4.64		
ASA SR ($\ell_{\max} = 2$)	5.05	5.96	5.31
ASA SR ($\ell_{\max} = 3$)	4.97		
FCD NR ($\ell_{\max} = 3$)	4.32	5.26	4.55
FCD NR ($\ell_{\max} = 4$)	4.30		
Experiment: [9]	4.64	5.30	4.59
FP LMTO SLAB: [3]	4.43	5.30	
ASA LMTO: [7]	5.02	5.96	5.26

in the calculation of the exchange-correlation potential. To avoid such problems this contribution to the potential can be neglected in vacuum layers of very low charge density. Furthermore, a numerical procedure like a Gaussian quadrature has to be employed for the required angular integration, which can be a numerically tedious task.

26.1.2 Work function

Even though the work function is a fundamental property of a surface there is presently no systematic experimental study available which can serve as a proper reference for theoretical calculations. The work function varies with respect to the surface orientation and depends on sample cleanness and roughness. While experimentally available data mostly refer to polycrystalline samples (the reference usually cited in this context is the study of Michaelson [10]), calculations are performed for different surface orientations of perfect single crystals. It is therefore of great relevance to compare and constantly improve ab-initio calculations.

The work function is defined as the smallest work necessary to remove an electron at the Fermi-level from the crystal to infinity. Hence,

$$W = V_{\text{vac}} - E_{\text{F}} \quad . \tag{26.6}$$

where V_{vac} is the potential level of the semi-infinite vacuum and E_{F} the Fermi energy. In Chap. 19 the calculation of V_{vac} is explained in detail and need not be repeated here.

In Table 26.1 work functions as obtained within SKKR method at various levels of sophistication are compared with available experimental data and with results of other authors. Systematic theoretical studies of work functions for a wide range of metals can be found, e.g., in [6], [7], and [3].

26.2 Applications of the fully relativistic spin-polarized Screened KKR-ASA scheme

It should be noted that in the following sections *exclusively* results of the *fully relativistic spin-polarized Screened KKR-ASA method* are discussed. In all applications shown the calculated Green's functions (GF) for two-dimensional translational invariant systems serve as necessary inputs. The below table gives an overview of the various topics to be mentioned, but indicates also additional approaches that have to be applied.

GF		interlayer exchange coupling
GF		magnetic anisotropies
GF & ECM		Magnetic nanostructures
GF & "Kubo"		electric transport in multilayer systems: GMR, TMR
GF & ECM	& "Kubo"	electric transport for nanostructures (contacts, etc.)
GF & "Kubo"	& optics	magneto-optical transport, Kerr spectroscopy
GF & "Landau –Lifshitz"		spin waves
GF (& "Kubo")		mesoscopic systems: domain walls

26.3 Interlayer exchange coupling, magnetic anisotropies, perpendicular magnetism and reorientation transitions in magnetic multilayer systems

26.3.1 Energy difference between different magnetic configurations

As should be recalled from Chap. 25 in two-dimensional translationally invariant systems magnetic configurations are defined by specifying the orientation of the magnetization in all atomic layers (N), e.g.,

$$\mathcal{C}_i = \{\ldots, \mathbf{n}_{k-1}, \mathbf{n}_k, \mathbf{n}_{k+1}, \ldots, \mathbf{n}_N\} \quad , \tag{26.7}$$

$$\mathcal{C}_j = \left\{ \ldots, \mathbf{n}'_{k-1}, \mathbf{n}'_k, \mathbf{n}'_{k+1}, \ldots, \mathbf{n}'_N \right\} \quad , \tag{26.8}$$

where the $\mathbf{n}_k$ are (classical) unit vectors. For $\mathcal{C}_i \neq \mathcal{C}_j$ the above two magnetic configurations then simply differ in energy by

$$\Delta E = E_j - E_i \quad , \tag{26.9}$$

where E_i and E_j refer to the respective total energies. As this difference requires an accuracy of total energies of 0.1 meV or even less, in most applications up to now the so-called *magnetic force theorem* was applied by considering instead of ΔE the difference in the grand-potentials of the two magnetic configurations,

$$\Delta E_{\mathrm{b}} = E_{\mathrm{b}}(\mathcal{C}_j) - E_{\mathrm{b}}(\mathcal{C}_i) \quad , \tag{26.10}$$

evaluating, however, only one magnetic configuration, e.g., $\mathcal{C}_i$ selfconsistently.

Consider now the most general case, namely that the two-dimensional translationally invariant system is disordered. If c^p_α denotes the respective concentrations of the constituents A and B in layer p then in terms of the (inhomogeneous) CPA for layered systems, see Chap. 23, ΔE_{b} is given by

$$\Delta E_{\mathrm{b}} = \sum_{p=1}^{N} \sum_{\alpha=A,B} c^p_\alpha \Delta E^p_\alpha \quad , \quad \sum_{\alpha=A,B} c^p_\alpha = 1 \quad , \tag{26.11}$$

where the

$$\Delta E^p_\alpha = \int_{\epsilon_b}^{\epsilon_{\mathrm{F}}} \left(n^p_\alpha(\mathcal{C}_j, \epsilon) - n^p_\alpha(\mathcal{C}_i, \epsilon) \right) (\epsilon - \epsilon_{\mathrm{F}}) \mathrm{d}\epsilon \quad , \tag{26.12}$$

refer to component- and layer-resolved contributions to the *grand-potential* at T=0. In (26.12) the $n^p_\alpha(\mathcal{C}, \epsilon)$ are component and layer projected DOS's corresponding to magnetic configuration $\mathcal{C}$, ϵ_b denotes the bottom of the valence band and ϵ_{F} is the Fermi energy of the (nonmagnetic) substrate serving as electron reservoir. Only in the case that (26.11)–(26.12) are used for bulk systems (three-dimensional translational invariance) the Fermi energy becomes configuration dependent. If the substrate (two-dimensional translational invariance) is magnetic then ϵ_{F} simply refers to the chosen magnetic configuration in the substrate, e.g., in-plane or perpendicular to the surface, and remains constant upon deposition of other materials. The energy integral in (26.12) is usually performed in the upper half of the complex plane using a contour starting at ϵ_b and ending at ϵ_{F}, see Chap. 22.

Note that because of the definition given in (26.10) this implies the following energetic order of magnetic configurations

$$\Delta E_{\mathrm{b}} = \begin{cases} > 0; \rightarrow \mathcal{C}_j; \text{ preferred configuration} \\ < 0; \rightarrow \mathcal{C}_i; \text{preferred configuration} \end{cases} \quad , \tag{26.13}$$

i.e., ΔE_{b} serves as approximation for the energy difference defined in (26.9):

$$\Delta E_{\mathrm{b}} \sim \Delta E \quad . \tag{26.14}$$

The numerical advantage of using grand-potentials is that (1) they can be calculated very accurately and (2) only differences of reasonably small numbers have to be taken. The error made by evaluating just one magnetic configuration selfconsistently is usually of the order of 3–5%.

26.3.2 Interlayer exchange coupling (IEC)

Suppose that in a typical trilayer system, $Substrate/X_n/Y_m/X_r$ of N atomic layers, where X refers to a magnetic material such as, e.g., Co and Y (*spacer*) to another material such as, e.g., Cu, $\mathcal{C}_0$ denotes a uniformly parallel arrangement of the orientations of the magnetization in the various layers

$$\mathcal{C}_0 = \{\mathbf{n}_k | \mathbf{n}_k = \mathbf{n}_0, \forall k\} \quad , \quad N = n + m + r \quad , \tag{26.15}$$

and $\mathcal{C}$ to a symmetric antiparallel configuration,

$$\mathcal{C} = \left\{ \underbrace{\mathbf{n}_0, \ldots, \mathbf{n}_0}_{n}, \underbrace{\mathbf{n}_0, \ldots, \mathbf{n}_0}_{m_1}, \underbrace{\mathbf{n}_1, \ldots, \mathbf{n}_1}_{m_2}, \underbrace{\mathbf{n}_1, \ldots, \mathbf{n}_1}_{r} \right\} \quad , \quad \mathbf{n}_1 = -\mathbf{n}_0 \quad , \tag{26.16}$$

where m_1 and m_2 can be chosen such that, e.g.,

$$m_1 = \begin{cases} m/2 & ; m : even \\ (m+1)/2 & ; m : odd \end{cases} \quad , \tag{26.17}$$

$$m_2 = \begin{cases} m/2 & ; m : even \\ (m-1)/2 & ; m : odd \end{cases} \quad . \tag{26.18}$$

In this particular case $\Delta E_{\mathrm{b}} = E_{\mathrm{b}}(\mathcal{C}) - E_{\mathrm{b}}(\mathcal{C}_0)$ is called *interlayer exchange coupling energy*, short *IEC*. It should be noted that as long as the spacer is non-magnetic or the induced magnetic moments of the spacer layers next to the interfaces are very small, a specification of the orientation of the magnetization in the spacer layers obviously seems to be "superfluous", for magnetic spacers, however, the more general form in (26.16) is essential.

Viewed as a function of the number of spacer layers, $\Delta E_{\mathrm{b}}(m)$, the IEC shows characteristic oscillations with respect to m that are now well documented in the literature. Quite clearly in (26.15)–(26.16) $\mathbf{n}_0$ can be, e.g., along the surface normal or perpendicular to it. If $(\mathbf{n}_0 \cdot \mathbf{n}_1) = -1$ one usually speaks of *antiparallel coupling*, if $(\mathbf{n}_0 \cdot \mathbf{n}_1) = 0$ very often the term *perpendicular coupling* is used.

26.3.3 An example: the Fe/Cr/Fe system

As an example in the top part of Fig. 26.6 the (antiparallel) interlayer exchange coupling energy in the system bcc-Fe(100)/Fe_6/Cr_n/Fe_6/Vac is

shown, in the lower part of this figures the case of perpendicular coupling. In this example one can see quite impressively that for both types of coupling not only two kinds of periods of oscillations with respect to the number of Cr layers can be observed, namely a short and a long period, but also a "phase slip", which is quite famous for this particular system.

Figure (26.7) illustrates very nicely the difference between even and odd numbers of Cr layers in terms of Cr magnetic moments, which causes the short period of oscillations with respect to the number of Cr layers. Fig. (26.7) also indicates that from a certain thickness of the Cr spacer on, oscillations in the magnetic moments of Cr set in, whose periods coincide with the long one in the IEC. In the vicinity of the phase slip – about 17 Cr layers, see Fig. (26.7) – the magnetic moments of the Fe leads and the Cr spacer are shown in Fig. (26.8). Quite obviously by going through the critical thickness for the phase slip characteristic frustration effects for the Cr magnetic moments occur, which seem to be at least one of the causes of this phase slip.

Figures (26.7)–(26.8) serve also the purpose to show the enormous richness of variations in magnetic moments when dealing with magnetic multilayer systems.

26.3.4 Magnetic anisotropy energy (E_{a})

Let $\mathcal{C}$ and $\mathcal{C}_0$ refer to a uniform in-plane and a uniform perpendicular to the planes of atoms orientation of the magnetization, respectively. The magnetic anisotropy energy E_{a} is then given as a sum of two contributions,

$$E_{\mathrm{a}} = \Delta E_{\mathrm{b}} + \Delta E_{\mathrm{dd}} \quad , \tag{26.19}$$

the so-called band energy part ΔE_{b}, defined according to (26.10) as

$$\Delta E_{\mathrm{b}} = E_{\mathrm{b}}(\mathcal{C}) - E_{\mathrm{b}}(\mathcal{C}_0) \quad , \tag{26.20}$$

and the (classical) magnetic dipole–dipole interaction, ΔE_{dd}, frequently also called shape anisotropy,

$$\Delta E_{\mathrm{dd}} = E_{\mathrm{dd}}(\mathcal{C}) - E_{\mathrm{dd}}(\mathcal{C}_0) \quad . \tag{26.21}$$

The (classical) magnetostatic dipole–dipole interaction energy for a given magnetic configuration $\mathcal{C}$ appearing in this context is defined (in atomic Rydberg units) by

$$E_{\mathrm{dd}}(\mathcal{C}) = \frac{1}{c^2} \sum_{i,j;i\neq j} \left\{ \frac{\mathbf{m}_i(\mathcal{C}) \cdot \mathbf{m}_j(\mathcal{C})}{|\mathbf{R}_i - \mathbf{R}_j|^3} - 3\frac{[\mathbf{m}_i(\mathcal{C}) \cdot (\mathbf{R}_i - \mathbf{R}_j)][\mathbf{m}_j(\mathcal{C}) \cdot (\mathbf{R}_i - \mathbf{R}_j)]}{|\mathbf{R}_i - \mathbf{R}_j|^5} \right\} \quad , \tag{26.22}$$

where the magnetic moments $\mathbf{m}_i(\mathcal{C})$ are located at sites $\mathbf{R}_i$ and c is the speed of light. In the presence of two-dimensional translational symmetry ($\mathbf{R}_i = \mathbf{R}_{i,\parallel} + \mathbf{R}_{i,z}, \mathbf{R}_{i,\parallel} \in \mathcal{L}^{(2)}$) (26.22) can be evaluated very efficiently using again Ewald's summation technique.

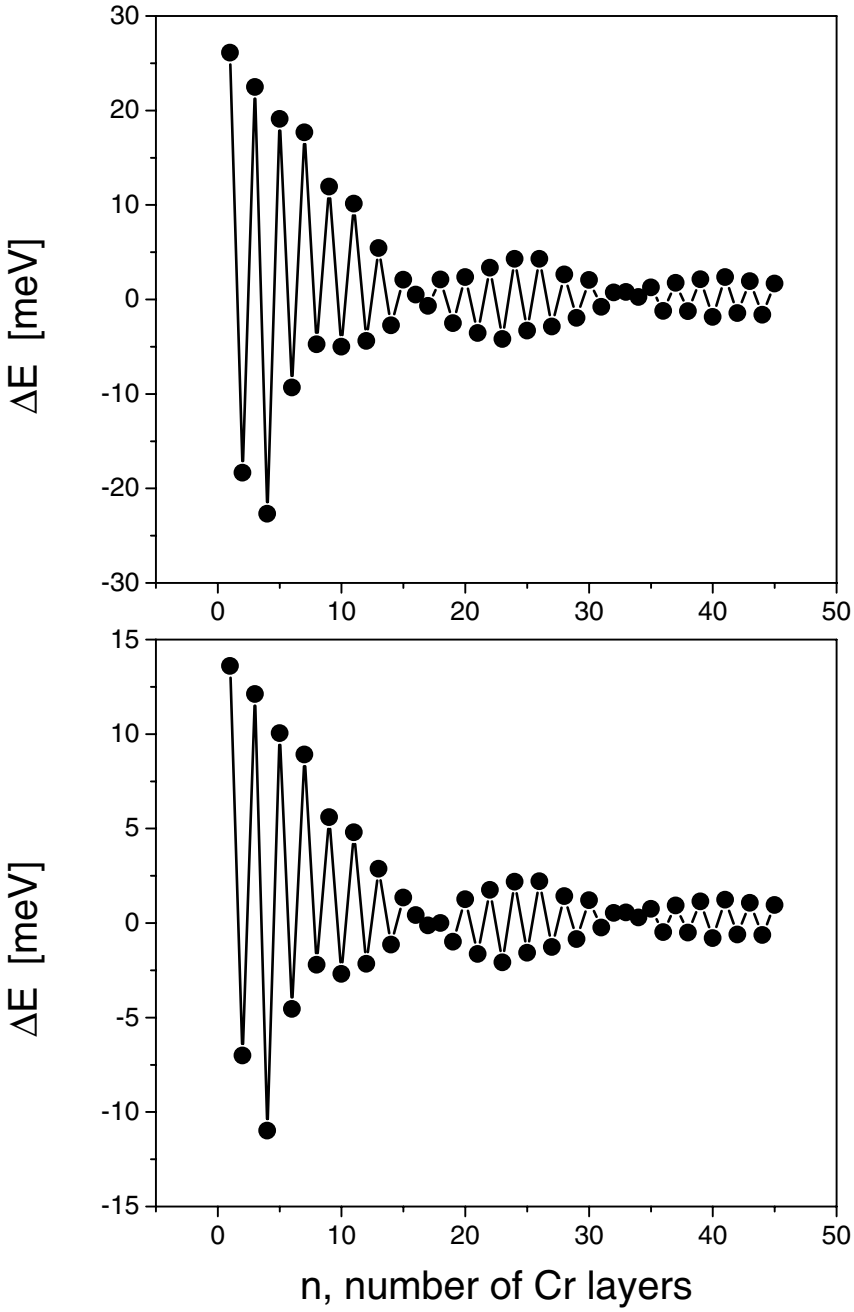

Fig. 26.6. Antiparallel (top) and perpendicular (bottom) interlayer exchange coupling in bcc-Fe(100)/$Fe_6Cr_nFe_6$/Vac. From [13].

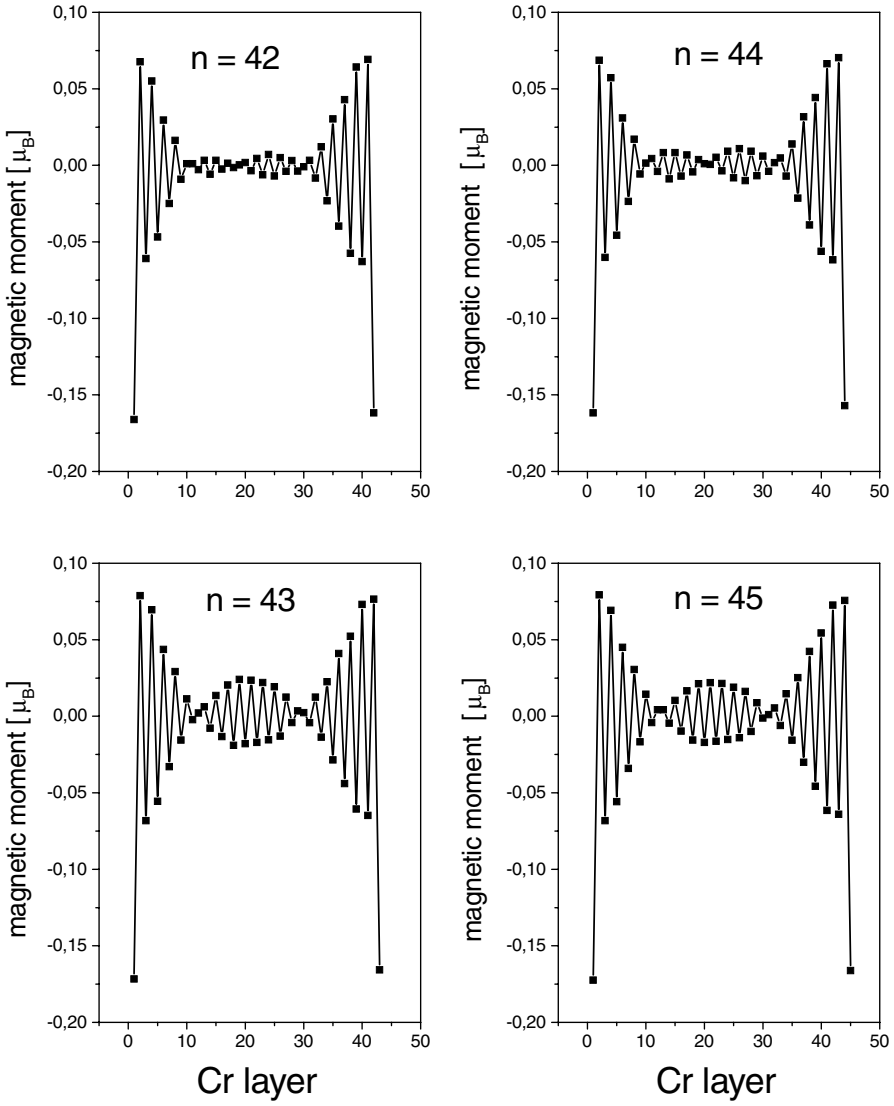

Fig. 26.7. Cr magnetic moments in bcc-Fe(100)/$Fe_6Cr_nFe_6$/Vac for a ferromagnetic configuration with the magnetization parallel to the surface normal. The number of Cr layers is indicated explicitly. From [13].

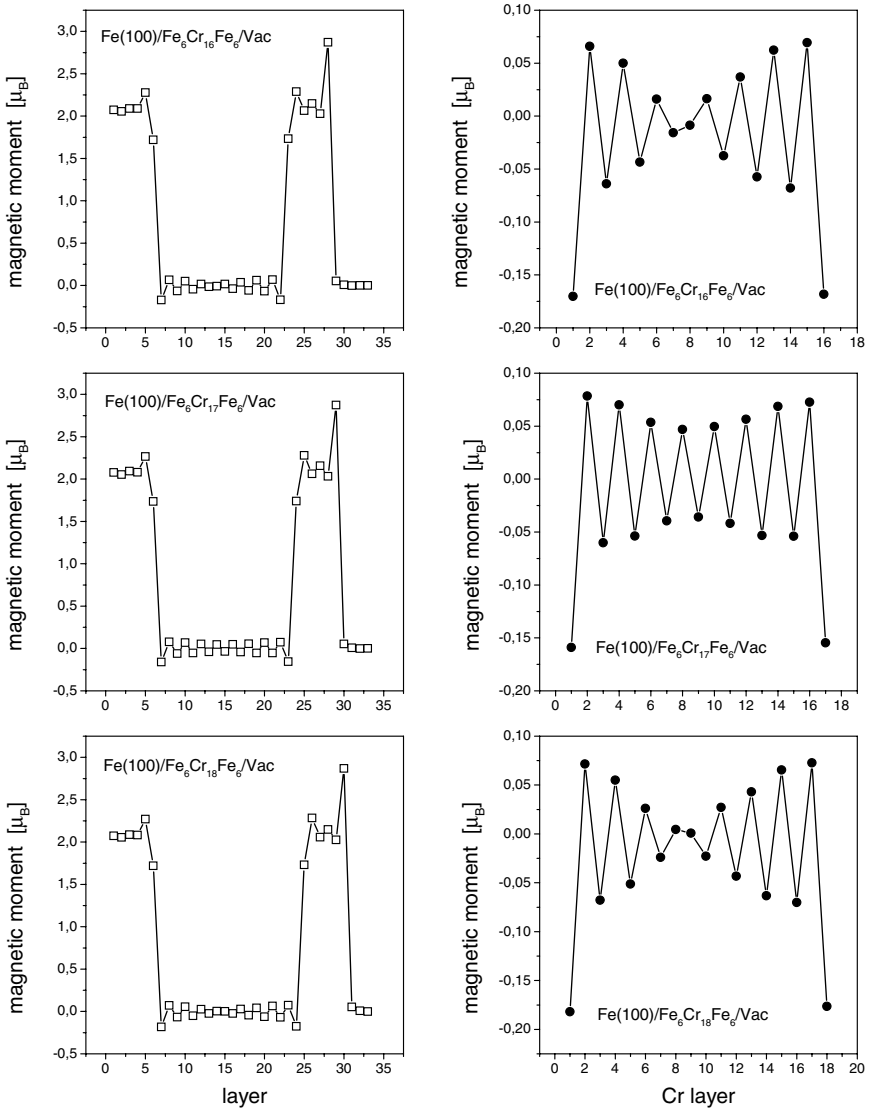

Fig. 26.8. Magnetic moments in bcc-Fe(100)/$Fe_6Cr_nFe_6$Vac, $n = 16, 17, 18$. The right column shows the Cr moments on a blown-up scale. The Fe substrate (origin of counting) is to the left, vacuum to the right. The magnetic configuration is a ferromagnetic configuration with a uniform orientation of the magnetization along the surface normal. From [13].

26.3.5 Disordered systems

In terms of the inhomogeneous CPA for layer-wise, binary substitutionally disordered systems the magnetic moments arising from the constituents have

to be weighted with their respective concentrations such that to each site in a given layer p a uniform magnetic moment applies,

$$\langle \mathbf{m}_p(\mathcal{C}) \rangle = \sum_\alpha c_p^\alpha \, \mathbf{m}_p^\alpha(\mathcal{C}) \quad , \tag{26.23}$$

where $\langle\rangle$ denotes an average over statistical configurations and $\mathbf{m}_p^\alpha(\mathcal{C})$ refers to the magnetic moment of component α in layer p. It should be noted that by using the above averaged magnetic moments in (26.22), one in fact neglects vertex corrections of the kind $\langle \mathbf{m}_i(\mathcal{C}) \cdot \mathbf{m}_j(\mathcal{C}) \rangle - \langle \mathbf{m}_i(\mathcal{C}) \rangle \cdot \langle \mathbf{m}_j(\mathcal{C}) \rangle$, $i \neq j$.

26.3.6 An example: $\mathbf{Ni}_n$/Cu(100) and $\mathbf{Co}_m/\mathbf{Ni}_n$/Cu(100)

While in most magnetic multilayer systems consisting of a (non-magnetic) metallic substrate coated by a thin magnetic film with increasing film thickness a reorientation transition from perpendicular to the planes of atoms to in-plane occurs, multilayers of Ni on Cu(100) exhibit just the opposite behavior: below about 7 monolayers of Ni the orientation of the magnetization is in-plane, then switches with an increasing number of Ni layers to perpendicular (first reorientation transition), and eventually for $n \geq 35$ turns again to in-plane (second reorientation transition). The first reorientation transition is essentially caused by tetragonal distortions with respect to the lattice spacing of the substrate, since with decreasing interlayer distance the band energy contribution is considerably increased. Exactly this is shown in Fig. 26.9. It should be noted that experimentally the first reorientation transition occurs at about 7 monolayers of Ni, the interlayer distances in the Ni-film being contracted by 5.5% as compared to fcc Cu.

The second reorientation transition is even more complicated as with an increasing number of Ni layers also in-plane relaxations occur. Since this implies that no longer it can be assumed that in all atomic planes (including the substrate) one and the same two-dimensional lattice applies, only model-like studies are at present available. Combining systems with respect to n_1 relaxed Ni layers on Cu(100) and n_2 unrelaxed Ni layers on Ni(100), these two systems can be considered to be "stacked together", see Fig. 26.10, in order to predict also the second reorientation transition in the system Cu(100)/Ni_n, $n = n_1 + n_2$. The various cases that have to be taken into account to deal with the occurrence of in-plane relaxations are compiled in Tables (26.2)–(26.3).

In Fig. 26.11 the layer-resolved band energies are displayed for system D. As can be seen from this figure contributions to the total band energy arise only from the first 6–8 Ni layers close to the interface and of course from the Co layers. Figs. 26.10 and 26.11 serve a justification that the band energy of a system of the type

$$Cu(100)/\ldots Cu(a_\parallel^{Cu}, d_\perp^{Cu})_r / Ni_{n_1}(a_\parallel^{Cu}, d_\perp)/Ni_{n_2}(a_\parallel^{Ni}, d_\perp^{Ni})/Co_m(a_\parallel^{Ni}, d_\perp^{Ni})$$

can be obtained by summing up the layer-resolved contributions $\Delta E_{\mathrm{b}}^i(S)$ from two independent systems,

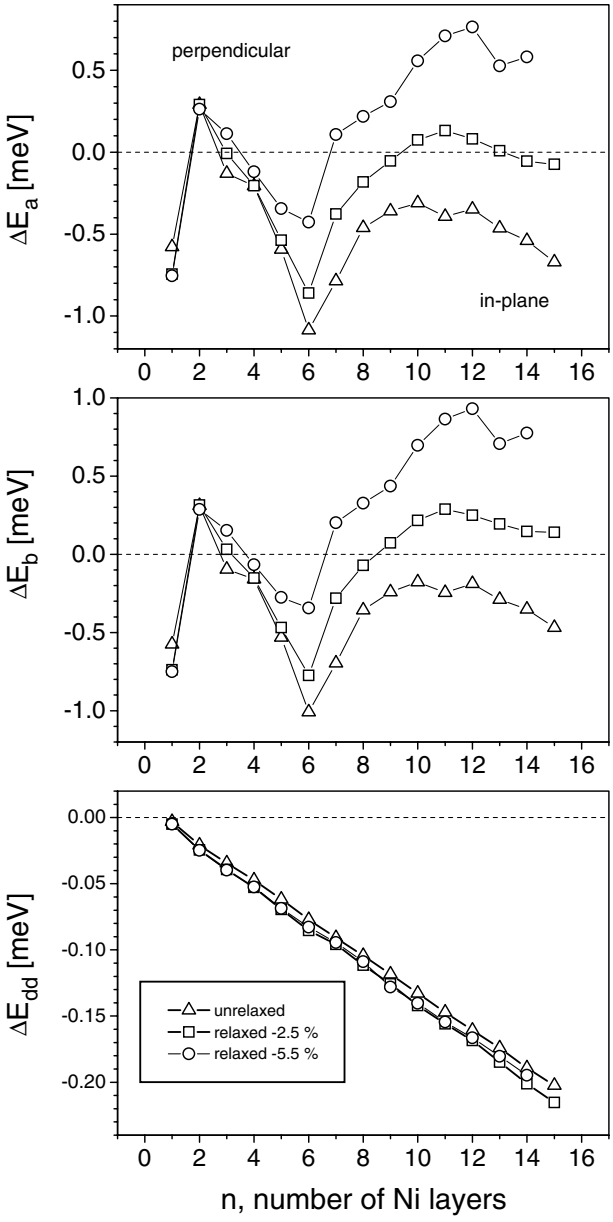

Fig. 26.9. Magnetic anisotropy energy ΔE_{a} (top), band energy difference ΔE_{b} (middle) and magnetic dipole–dipole energy difference ΔE_{dd} (bottom) versus the number of Ni layers on Cu(100). Triangles, squares and circles refer in turn to a uniform relaxation by 0, -2.5 and -5.5%, i.e., to a c/a ratio of 1, 0.975 and 0.945. From [14].

$$\Delta E_{\rm b}(m) = \left(\sum_{i=1}^{r} \Delta E_{\rm b}^{i}(E)\right) + \left(\sum_{i=r+1}^{r+n_1} \Delta E_{\rm b}^{i}(E)\right) + \left(\sum_{i=r+n_1+1}^{r+n_1+1+n_2/2} \Delta E_{\rm b}^{i}(E)\right) + \left(\sum_{i=r+n_1+2+n_2/2}^{r+n_1+n_2+m} \Delta E_{\rm b}^{i}(D)\right)$$
$$= \Delta E_{\rm b}^{(1)} + \Delta E_{\rm b}^{(2)} + \Delta E_{\rm b}^{(3)} + \Delta E_{\rm b}^{(4)} \quad , \tag{26.24}$$

where the arguments E and D refer to the systems listed in Table (26.3). In here $\Delta E_{\rm b}^{(1)}$ is due to contribution from the substrate (r layers with induced magnetic moments), $\Delta E_{\rm b}^{(2)}$ from that part of the Ni film with the in-plane lattice constant of the substrate ($a_{\parallel}^{Cu}$) and an interlayer spacing $d_{\perp} \neq d_{\perp}^{Cu}$, $\Delta E_{\rm b}^{(3)}$ arises from the part of the Ni film with an in-plane lattice constant and an interlayer spacing of the Cu substrate, while for $\Delta E_{\rm b}^{(4)}$ the in-plane lattice constant and the interlayer spacing of pure Ni applies. Quite clearly, as can be seen from Figs. 26.10 and 26.11, the reason for this ad hoc procedure is that in thick Ni films contributions to the band energy from interior layers vanish. Fig. 26.12 finally shows the (total) number of Ni layers at which this reorientation transition occurs as a function of the thickness of a Co cap (m). The different entries refer to different numbers of tetragonally distorted Ni layers (n_1). The results displayed in Fig. 26.12 reflect very closely the experimental evidence in which usually a total of about 12 Ni layers are quoted to be tetragonally distorted.

26.4 Magnetic nanostructures

After having determined for a chosen uniform orientation of the magnetization selfconsistently the potentials and exchange fields for a given cluster of atoms on top of a substrate by means of the Embedded Cluster Method, see Chap. 24, various physical properties of interest in the field of magnetic nanostructures can be evaluated. These are in particular spin- and orbital moments and of course exchange and anisotropy energies.

26.4.1 Exchange energies, anisotropy energies

Suppose the orientation of the magnetization in the selfconsistency procedure has been chosen to point perpendicular to the surface (along the z-axis), then the relevant magnetic anisotropy energies can again be determined in terms of the magnetic force theorem as differences in band-energies,

$$\Delta E_{x-z}^{\rm b} = E_{x}^{\rm b} - E_{z}^{\rm b} \quad , \quad \Delta E_{y-z}^{\rm b} = E_{y}^{\rm b} - E_{z}^{\rm b} \quad , \tag{26.25}$$

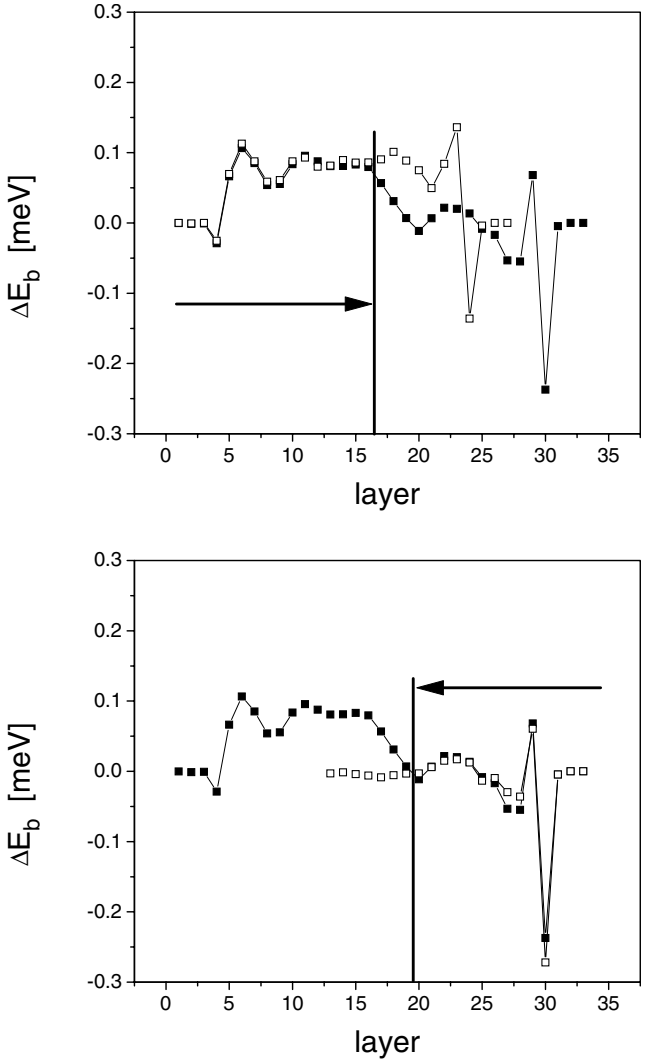

Fig. 26.10. Comparison of the layer-resolved band energy contributions $\Delta E_{\mathrm{b}}^{n}$ of $\mathrm{Cu(100)/Ni_{15}(-5.5\%)/Ni_{12}(0.0\%)}$ (*system A*, squares) with $\mathrm{Cu(100)/Ni_{21}(-5.5\%)}$ (*system B*, open squares, top), and in $\mathrm{Ni(100)/Ni_{18}}$ (*system C*, open squares, bottom). In all cases the first layers to the right denote vacuum layers. In the case of *system A* the first three layers to left refer to Cu layers. The view from the Cu/Ni and from the Ni/Vac interface is indicated by arrows. From [15].

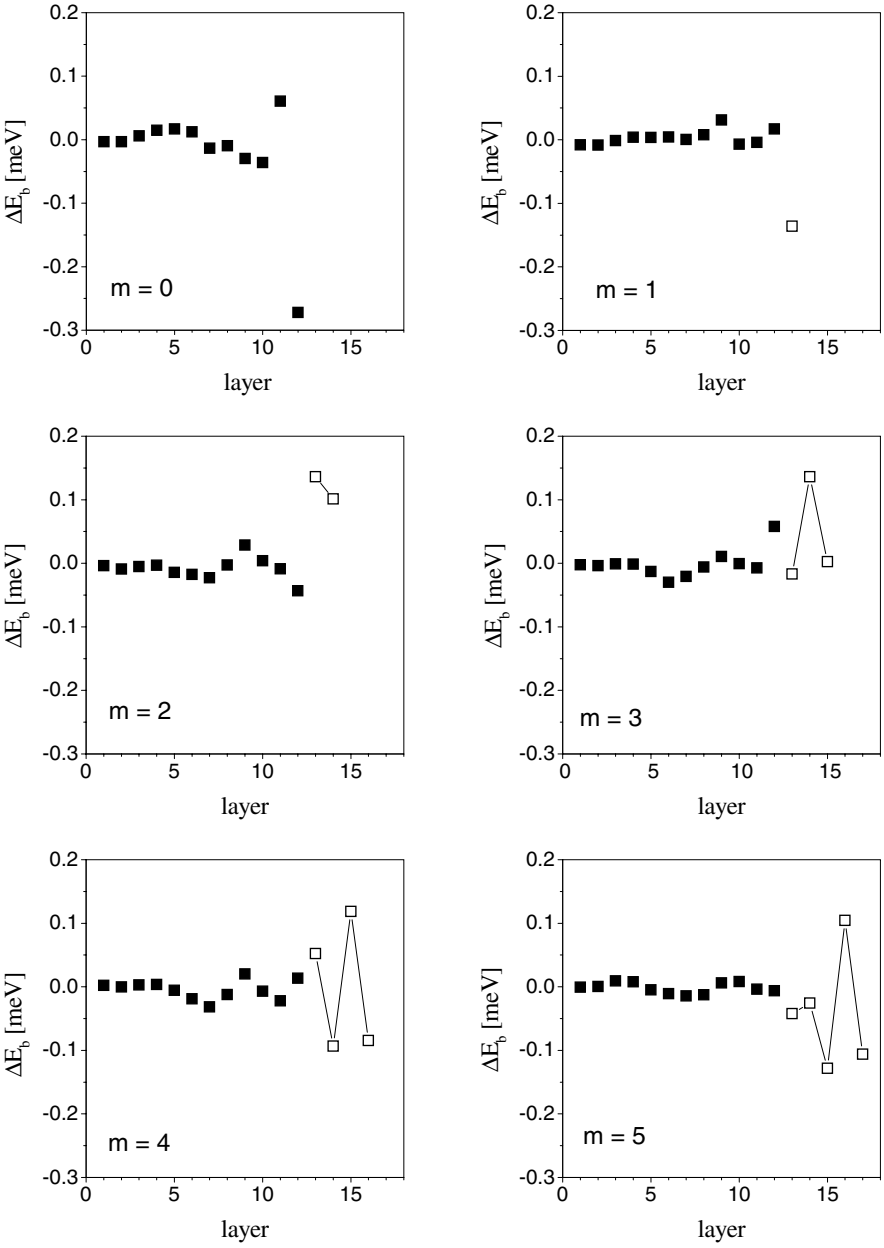

Fig. 26.11. Layer resolved band energy difference $\Delta E_{\mathrm{b}}^{n}$ for 0 to 5 Co layers on Ni(100)/Ni_{12}(0%), system D. Full and open squares denote Ni and Co layers, respectively. From [15].

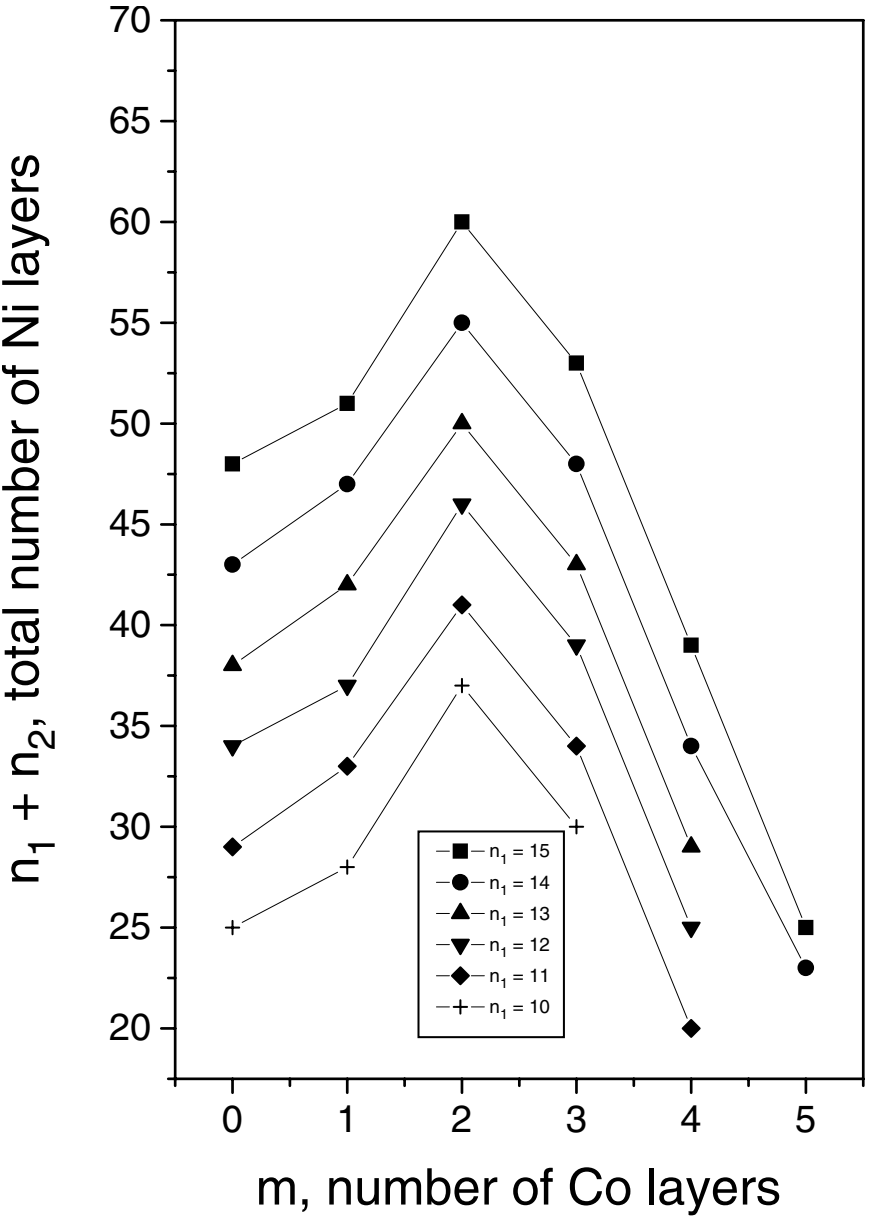

Fig. 26.12. Total number of Ni layers $(n_1 + n_2)$ at which the magnetic anisotropy energy, ΔE_{a} of Cu(100)/Ni$_{n_1}$(-5.5%)/Ni$_{n_2}$(0%)/Co$_m$ changes sign, displayed as a function of the number of Co layers (m). From [15].

Table 26.2. The substrate determines the in-plane lattice constant, the relaxation of the substrate interlayer distance is given in percent.

System A :	*System B :*	*System C :*
[fcc Cu (100)]	[fcc Cu (100)]	[fcc Ni (100)]
$\begin{bmatrix} \mathrm{Cu}_1 \\ \vdots \\ \mathrm{Cu}_3 \end{bmatrix}$ 0%	$\begin{bmatrix} \mathrm{Cu}_1 \\ \vdots \\ \mathrm{Cu}_3 \end{bmatrix}$ 0%	
$\begin{bmatrix} \mathrm{Ni}_1 \\ \vdots \\ \mathrm{Ni}_{15} \end{bmatrix}$ −5.5%	$\begin{bmatrix} \mathrm{Ni}_1 \\ \vdots \end{bmatrix}$ −5.5%	$\begin{bmatrix} \mathrm{Ni}_1 \\ \vdots \end{bmatrix}$ 0%
$\begin{bmatrix} \mathrm{Ni}_1 \\ \vdots \\ \mathrm{Ni}_{12} \end{bmatrix}$ 0%	$\begin{bmatrix} \\ \vdots \\ \mathrm{Ni}_{21} \end{bmatrix}$ −5.5%	$\begin{bmatrix} \vdots \\ \mathrm{Ni}_{18} \end{bmatrix}$ 0%
[vac]	[vac]	[vac]

$$\Delta E^{\mathrm{b}}_{\mu-z} = \begin{cases} > 0, & z \text{ preferred} \\ < 0, & \mu \text{ preferred} \end{cases} \quad ; \quad \mu = x, y \quad , \tag{26.26}$$

where the axes x and y refer to in-plane directions parallel and perpendicular to the chains, respectively, to which in principle the magnetic dipole–dipole interaction energy ΔE_{dd} has to be added. In the following discussion of the anisotropy energy of magnetic nanostructures ΔE_{dd} is neglected, i.e., $E_{\mathrm{a}} \sim \Delta E^{\mathrm{b}}_{\mu-\nu}$.

26.4.2 An example Co clusters on Pt(100)

As an example for magnetic nanostructures and the approach discussed in Chap. 24 self-consistent fully relativistic calculations for finite Co chains along the (110) direction on Pt(111) are chosen. In Fig. 26.13 the spin- (S_z) and orbital (L_z) moment of the central (most symmetric) atom of the monoatomic Co_n wires ($1 \leq n \leq 10$) is displayed. As can be seen for $n > 3$ the spin-moment of the central atom seems to be stabilized at about 2.10 μ_{B}, while the orbital moments oscillates around 0.35 μ_{B}. The spin-moments calculated for each of the Co atoms in the chains are depicted in Fig. 26.14. Apparently, for $n = 3, \ldots, 10$, the spin moments at the end of the chains ($\sim 2.15\ \mu_{\mathrm{B}}$) are systematically higher than those in the middle of the chains ($\sim 2.11\ \mu_{\mathrm{B}}$).

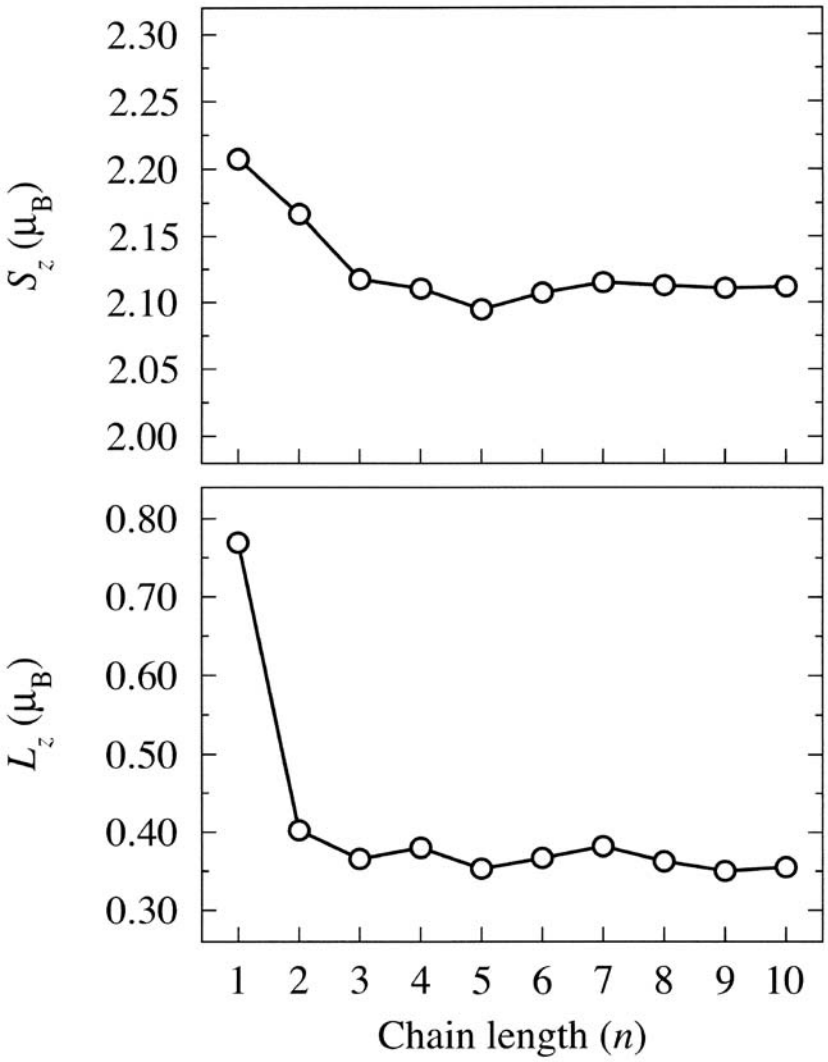

Fig. 26.13. Calculated spin moments (S_z) and orbital moments (L_z) of the central (most symmetric) atom in Co_n ($n = 1, \ldots, 10$) chains oriented along the (110) direction on the top of Pt(111) as a function of the chain length. From [16].

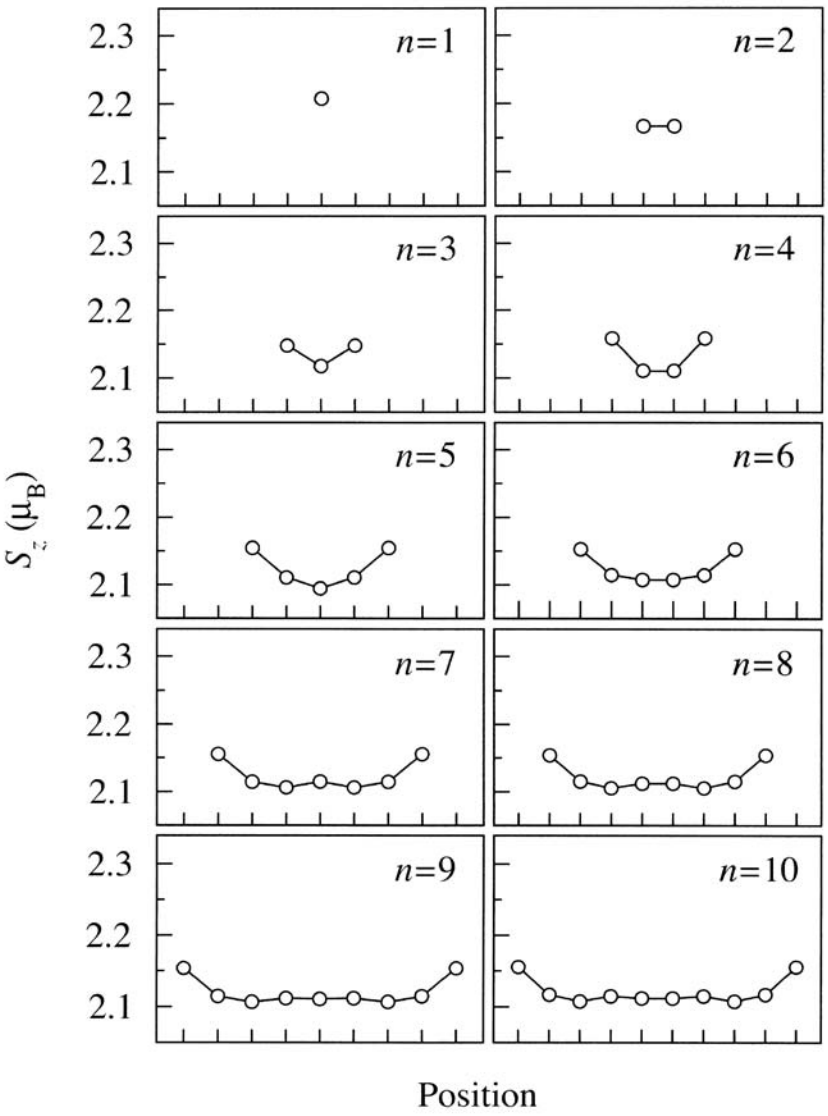

Fig. 26.14. Calculated spin moments (S_z) of the Co atoms in Co_n ($n = 1, \ldots, 10$) chains on Pt(111) with the magnetization pointing perpendicular to the surface. From [16].

Table 26.3. The substrate determines the in-plane lattice constant, the relaxation of the substrate interlayer distance is given in percent

System D :	*System E :*	
[fcc Ni (100)]	[fcc Cu (100)]	
	$\begin{bmatrix} \mathrm{Cu}_1 \\ \vdots \\ \mathrm{Cu}_3 \end{bmatrix}$ 0%	
$\begin{bmatrix} \mathrm{Ni}_1 \\ \vdots \\ \end{bmatrix}$ 0%	$\begin{bmatrix} \mathrm{Ni}_1 \\ \vdots \\ \mathrm{Ni}_{n_1} \end{bmatrix}$ −5.5%	
$\begin{bmatrix} \\ \vdots \\ \mathrm{Ni}_{12} \end{bmatrix}$ 0%	$\begin{bmatrix} \mathrm{Ni}_1 \\ \vdots \\ \mathrm{Ni}_{n_2} \end{bmatrix}$ 0%	$\begin{bmatrix} \text{joining} \\ \text{regime of} \\ \text{layers} \end{bmatrix}$
$\begin{bmatrix} \mathrm{Co}_1 \\ \vdots \\ \mathrm{Co}_m \end{bmatrix}$ 0%	$\begin{bmatrix} \mathrm{Co}_1 \\ \vdots \\ \mathrm{Co}_m \end{bmatrix}$ 0%	
[vac]	[vac]	

Figure 26.15 shows that the fluctuations of the orbital moments within the chains are somewhat larger than for the spin-moments: the orbital moments of the central and the outer atoms can even differ by more than 10%, however, similar to the spin-moments for the inner atoms of the longer chains, a tendency of forming a uniform orbital magnetization can be observed.

In Fig. 26.16 the magnetic anisotropy energies, ΔE_{x-z} and ΔE_{y-z}, including only contributions from the first shell of Pt sites and normalized to a single Co atom are displayed with respect to the length of the Co chains. As can be seen from the positive sign of the MAE, in each case the easy axis points perpendicular to the surface , whereby for $n \geq 2$ there also appears a strong in-plane anisotropy with a preference of the x direction, i.e., parallel to the chains. The huge MAE of a single Co adatom abruptly drops for the dimer and rapidly converges to $\Delta E_{x-z} \simeq 1.5$ meV and $\Delta E_{y-z} \simeq 3.3$ meV for the longer wires. For $n > 3$ the calculated easy axis points out-of-plane and is perpendicular to the chains; the size of the calculated MAE is very close to the experimentally measured value of 2 ± 0.2 meV.

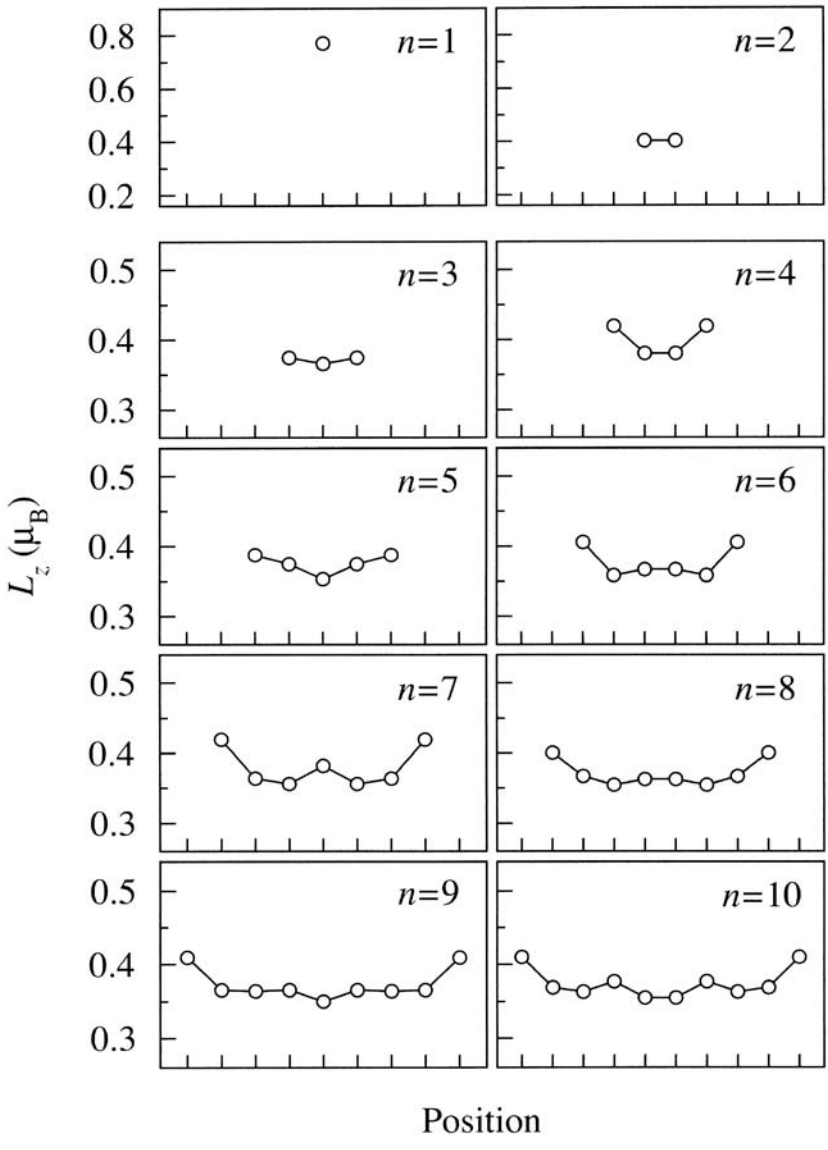

Fig. 26.15. Calculated orbital moments (L_z) of the Co atoms in Co_n ($n = 1, \ldots, 10$) chains on Pt(111) with the magnetization pointing perpendicular to the surface. From [16].

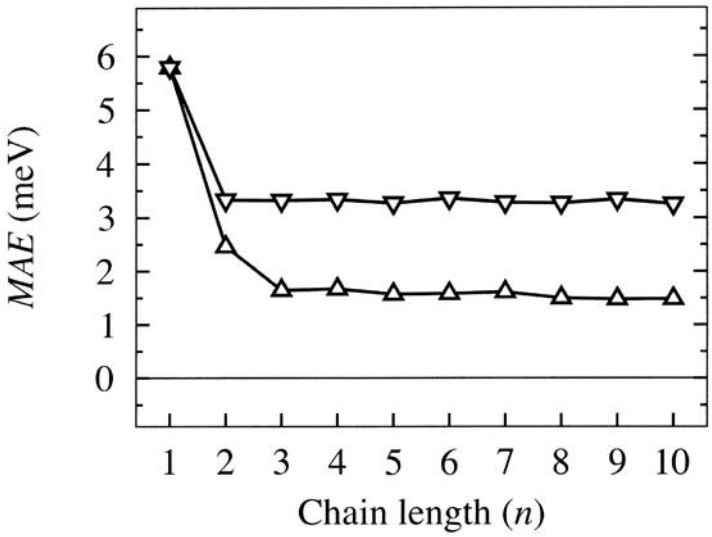

Fig. 26.16. Calculated magnetic anisotropy energies (MAE) for Co_n ($n = 1, \ldots, 10$) chains on Pt(111) including also contributions from nearest neighbor Pt sites and normalized to one Co atom. Up- and down triangles refer to ΔE_{x-z} and ΔE_{y-z}, respectively. From [16].

The contributions of the individual Co atoms, $\Delta E_{x-z}^{\mathrm{Co}_i}$ and $\Delta E_{y-z}^{\mathrm{Co}_i}$ ($i = 1, \ldots, n$), to the MAE are displayed in Fig. 26.17. In the case of $(x - z)$, the largest contributions clearly come from the outer Co atoms, while in the $(y - z)$ case the contribution of the inner atoms to the MAE is nearly as big as the contribution of the outer atoms. In both cases considered namely ΔE_{x-z} and ΔE_{y-z}, only weak oscillations in the MAE can be seen for the longer chains.

The anisotropies of the orbital moments are shown in Fig. 26.18. For a single adatom the anisotropy of the orbital moment $\Delta L_{x(y)-z} = L_{x(y)} - L_z = -0.27\ \mu_{\mathrm{B}}$ follows the qualitative rule that the orbital moment is largest along the easy axis. As can be seen from Fig. 26.18, this rule applies also to the chains since along the y direction (hard axis) the orbital moments of all the Co atoms are by about 0.15 μ_{B} less than along the z direction (easy axis) ($\Delta L_{y-z} = -0.15\ \mu_{\mathrm{B}}$). The anisotropy of the orbital moments of the Co atoms with respect to the x and z directions (ΔL_{x-z}), however, is only a few of 0.01 μ_{B}, and in several cases changes even sign from site to site. This situation is quite unusual since the tiny orbital momentum anisotropies are to be compared with quite sizeable respective magnetic anisotropy energies, ($\Delta E_{x-z}^{\mathrm{Co}_i} \simeq 0.5 - 1.5$ meV. In terms of perturbation theory this implies that

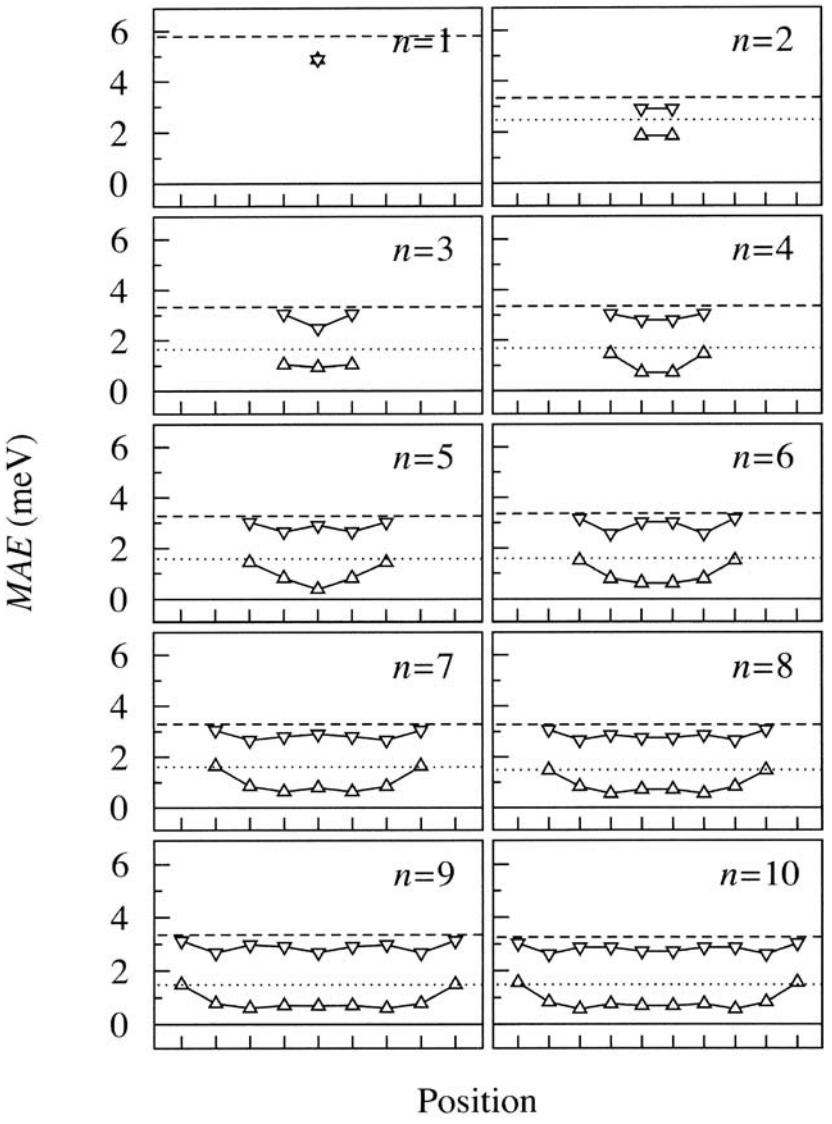

Fig. 26.17. Calculated magnetic anisotropy energies (MAE) for Co_n ($n = 1, \ldots, 10$) chains on Pt(111) including also contributions from nearest neighbor Pt sites and normalized to one Co atom. Up- and down triangles refer to ΔE_{x-z} and ΔE_{y-z}, respectively. From [16].

for the $(x-z)$ case, significant spin-flip coupling induced by the spin-orbit interaction probably contributes to the MAE which, in turn, obscures the simple (inverse) proportionality between the MAE and the anisotropy of the orbital moment.

26.5 Electric transport in semi-inifinite systems

Suppose the diagonal elements of the electrical conductivity tensor of a disordered system, namely $\sigma_{\mu\mu}$, are calculated using the Kubo-Greenwood equation:

$$\sigma_{\mu\mu} = \frac{\pi\hbar}{N_0\Omega_{\rm at}} \left\langle \sum_{m,n} J^{\mu}_{mn} J^{\mu}_{nm} \delta(\epsilon_{\rm F} - \epsilon_m)\delta(\epsilon_{\rm F} - \epsilon_n) \right\rangle \quad . \tag{26.27}$$

In here $\mu \in \{x, y, z\}$, N_0 is the number of atoms, J^{μ} is a representation of the μ-th component of the current operator,

$$J_\mu = \{J^{\mu}_{nm}\} \quad ; \quad J^{\mu}_{nm} = \langle n \mid J_\mu \mid m \rangle \quad , \tag{26.28}$$

$\epsilon_{\rm F}$ is the Fermi energy, $\mid m\rangle$ an eigenstate of a particular configuration of the random system under consideration, $\Omega_{\rm at}$ the atomic volume, and $\langle \cdots \rangle$ denotes an average over configurations. Equation (26.27) can be reformulated in terms of the imaginary part of the (one-particle) Green's function $G(z), z = \epsilon + {\rm i}\delta$,

$$\sigma_{\mu\mu} = \frac{\hbar}{\pi N_0 \Omega_{\rm at}} {\rm Tr} \ \left\langle J_\mu {\rm Im} G^{+}(\epsilon_{\rm F}) J_\mu {\rm Im} G^{+}(\epsilon_F) \right\rangle \quad , \tag{26.29}$$

or, by using "up-" and "down-" side limits as

$$\sigma_{\mu\mu} = \frac{1}{4} \left\{ \widetilde{\sigma}_{\mu\mu}(\epsilon^{+}, \epsilon^{+}) + \widetilde{\sigma}_{\mu\mu}(\epsilon^{-}, \epsilon^{-}) - \widetilde{\sigma}_{\mu\mu}(\epsilon^{+}, \epsilon^{-}) - \widetilde{\sigma}_{\mu\mu}(\epsilon^{-}, \epsilon^{+}) \right\} \quad , \tag{26.30}$$

where $\epsilon^{+} = \epsilon_{\rm F} + {\rm i}\delta$, $\epsilon^{-} = \epsilon_{\rm F} - {\rm i}\delta$; $\delta \to 0$, and

$$\widetilde{\sigma}_{\mu\mu}(\epsilon_1, \epsilon_2) = -\frac{\hbar}{\pi N_0 \Omega_{\rm at}} {\rm Tr} \ \left\langle J_\mu G(\epsilon_1) J_\mu G(\epsilon_2) \right\rangle \quad ; \quad \epsilon_i = \epsilon^{\pm} \quad ; \quad i = 1, 2 \quad . \tag{26.31}$$

26.5.1 Bulk systems

For a two-dimensional translationally invariant system the conductivity for a disordered layered system can be written as

$$\sigma_{\mu\mu}(n; c; \widehat{\mathbf{M}}) = \sum_{p,q=1}^{n} \sigma^{pq}_{\mu\mu}(c; \widehat{\mathbf{M}}) \quad , \tag{26.32}$$

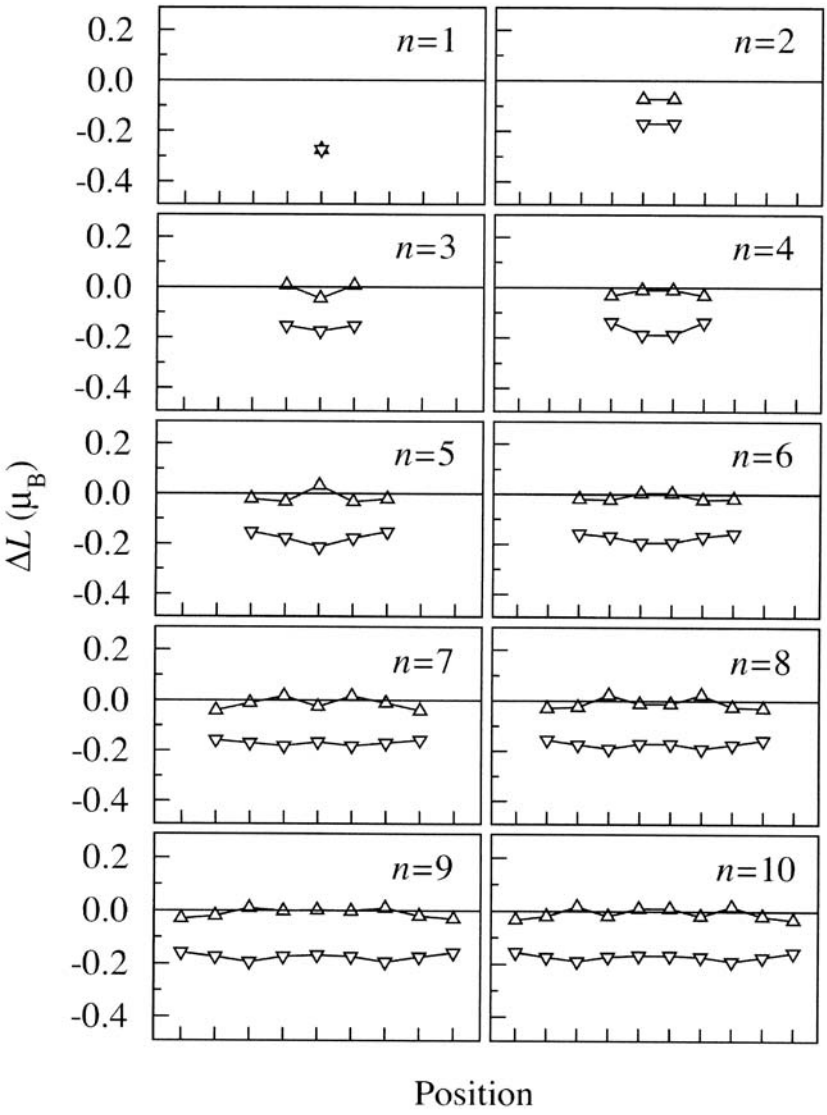

Fig. 26.18. Anisotropy of the orbital moments of the Co sites in Co_n ($n = 1, \ldots, 10$) chains on Pt(111). Up- and down triangles refer to ΔL_{x-z} and ΔL_{y-z}, respectively. From [16].

where n is the number of layers considered, $\mu \in \{x, y, z\}$, c denotes the concentration of one of the constituents of a given binary alloy, and – in general – $\widehat{\mathbf{M}}$ is the direction of the magnetization, both of which, namely c and $\widehat{\mathbf{M}}$, are assumed to be uniform in all layers of the bulk alloy. According to the Kubo-Greenwood equation, the non-local conductivity between layers p and q, $\sigma_{\mu\mu}^{pq} = \sigma_{\mu\mu}^{pq}(c; \widehat{\mathbf{M}})$, is defined as

$$\sigma_{\mu\mu}^{pq} = \frac{\hbar}{\pi N_0 \Omega_{\mathrm{at}}} \mathrm{Tr} \left\langle J_\mu^p \, G^+(\epsilon_\mathrm{F}) \, J_\mu^q \, G^+(\epsilon_F) \right\rangle \quad , \tag{26.33}$$

where the J_μ^p refer to the μ-th component of the current operator in plane p.

Since a bulk system can be viewed as a sequence of identical layers, the corresponding resistivity is given by

$$\rho_{\mu\mu}(n; c; \widehat{\mathbf{M}}) = 1/\sigma_{\mu\mu}(n; c; \widehat{\mathbf{M}}) \quad , \tag{26.34}$$

namely by a relation that in general is only valid in a current-in-plane (CIP) geometry, i.e., for $\mu \in \{x, y\}$). Furthermore, in using the concept of complex Fermi energies, $\epsilon_\mathrm{F} + \mathrm{i}\delta$, a "bulk" resistivity is defined in terms of the following double limit

$$\rho_{\mu\mu}(c; \widehat{\mathbf{M}}) = \lim_{\delta \to 0} \lim_{n \to \infty} \rho_{\mu\mu}^{cal.}(n; c; \widehat{\mathbf{M}}; \delta) \quad . \tag{26.35}$$

26.5.2 An example: the anisotropic magnetoresistance (AMR) in permalloy ($\mathbf{Ni_{1-c}Fe_c}$)

Usually the AMR ratio in bulk alloys is formulated as

$$\frac{\Delta\rho(c)}{\rho_{av}(c)} = \frac{\rho_\parallel(c) - \rho_\perp(c)}{\rho_{av}(c)} \quad , \tag{26.36}$$

where

$$\begin{aligned} \rho_{av}(c) &= 1/3(\rho_\parallel(c) + 2\rho_\perp(c)) \quad , \\ \rho_\parallel(c) &= \rho_{zz}(c; \hat{\mathbf{z}}) \quad , \\ \rho_\perp(c) &= \rho_{zz}(c; \hat{\mathbf{x}}) \quad . \end{aligned} \tag{26.37}$$

As can be seen from Fig. 26.19 the functional shape as well as the magnitude of the calculated concentration dependent AMR ratios are in excellent agreement with the experimental data. The good quantitative description of the AMR in $\mathrm{Ni}_{1-c}\mathrm{Fe}_c$ alloys indicates that effects such as vertex corrections, etc., not explicitly considered, do contribute in equal terms to the average resistivity as well as to $\rho_\parallel$ and $\rho_\perp$, and are therefore not reflected in the AMR ratio.

By varying the direction of the magnetization, the dependence of the resistivity on the angle between the directions of the current and the magnetization can be studied. In the special case, when the direction of the current is

Table 26.4. Fitting parameters for the orientational behavior of the resistivity in permalloy.

	ρ_0	B	C
$Ni_{85}Fe_{15}$	2.693	0.437	0.138
$Ni_{80}Fe_{20}$	2.620	0.315	0.156

The values are given in [μΩcm]. From [18]

fixed along a certain crystallographic axis and the direction of the magnetization is varied between this and another crystallographic axis, this dependency – phenomenologically described – reduces to

$$\rho(\vartheta) = \rho_0 + B\cos^2\vartheta + C\cos^4\vartheta \quad , \tag{26.38}$$

where ϑ is the angle between the magnetization and the current.

In Fig. 26.20 the resistivity for $Ni_{80}Fe_{20}$ and $Ni_{85}Fe_{15}$ fcc-bulk alloys are shown when the direction of the current is along the (001) direction, rotating the magnetization from the (001) to the (110) direction within in the $(1\bar{1}0)$ plane. Note that the cases $\vartheta = 0$ and $\vartheta = \pi/2$ correspond to $\rho_\parallel$ and $\rho_\perp$, respectively. From the fitting parameters listed in Table 26.4, it should be noted that the $\cos^4\vartheta$ term still contributes significantly and can therefore not be omitted in the fitting procedure without a drastic loss in the overall quality of the fit.

26.5.3 Spin valves: the giant magneto-resistance

Electric transport properties in magnetic multilayer systems such as spin valves are theoretically quite demanding not only since at best two-dimensional translational symmetry can be assumed but also since occurring interfaces usually are interdiffused and at least two magnetic configurations have to be taken into account. Interdiffusion implies, e.g., applications of the inhomogeneous CPA equations discussed in Chap. 23.

In the case of a current-in-plane (CIP) geometry the resistivity for a layered system in a particular magnetic configuration $\mathcal{C}$ is given by

$$\rho_{xx}(n;\mathbf{c};\mathcal{C}) = \lim_{\delta\to 0}\rho_{xx}(n;\mathbf{c};\mathcal{C};\delta) \quad , \tag{26.39}$$

where n denotes the number of layers considered, $\mathbf{c} = \{c_1, c_2, \ldots, c_n\}$ is a set containing the layer-wise concentrations, δ is the imaginary part of the complex Fermi energy, $\epsilon_\mathrm{F} + \mathrm{i}\delta$, and $\rho_{xx}(n;\mathbf{c};\mathcal{C})$ is related to the conductivity by

$$\rho_{xx}(n;\mathbf{c};\mathcal{C};\delta) = \sigma_{xx}^{-1}(n;\mathbf{c};\mathcal{C};\delta) \quad , \tag{26.40}$$

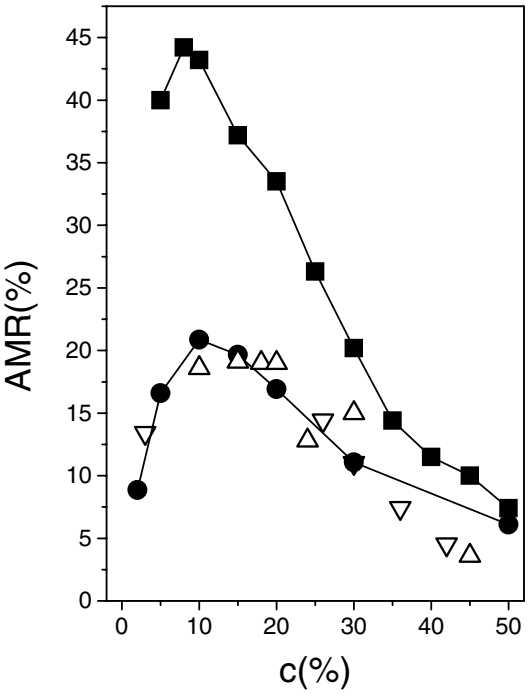

Fig. 26.19. Calculated and experimental AMR ratios of $Ni_{1-c}Fe_c$ alloys. Full circles: see [18] full squares: see [19]; up-triangles: experiment, see [20]; down-triangles: experiment, see [21] and [22].

$$\sigma_{xx}(n;\mathbf{c};\mathcal{C};\delta) = \sum_{i,j=1}^{n} \sigma_{xx}^{ij}(n;\mathbf{c};\mathcal{C};\delta) \quad . \tag{26.41}$$

The (giant) magnetoresistance ratio, usually termed GMR, is then defined by

$$R(n;\mathbf{c}) = \frac{\rho_{xx}(n;\mathbf{c};\mathcal{C}) - \rho_{xx}(n;\mathbf{c};\mathcal{C}_0)}{\rho_{xx}(n;\mathbf{c};\mathcal{C})} \quad , \tag{26.42}$$

where $\mathcal{C}_0$ and $\mathcal{C}$ refer to the *ferro- (parallel)* and *antiferromagnetic (antiparallel)* configuration, respectively, see also (26.15)–(26.16). The advantage of this kind of definition of the GMR is simply that $R(n;\mathbf{c}) \leq 1$. For practical purposes it is useful to define also the below quantity,

$$R(n;\mathbf{c};\delta) = \frac{\rho_{xx}(n;\mathbf{c};\mathcal{C};\delta) - \rho_{xx}(n;\mathbf{c};\mathcal{C}_0;\delta)}{\rho_{xx}(n;\mathbf{c};\mathcal{C};\delta)} \quad , \tag{26.43}$$

$$R(n;\mathbf{c};\delta) \leq R(n;\mathbf{c}) \quad , \tag{26.44}$$

since a finite δ mimics a finite (electronic) temperature and/or structural roughness.

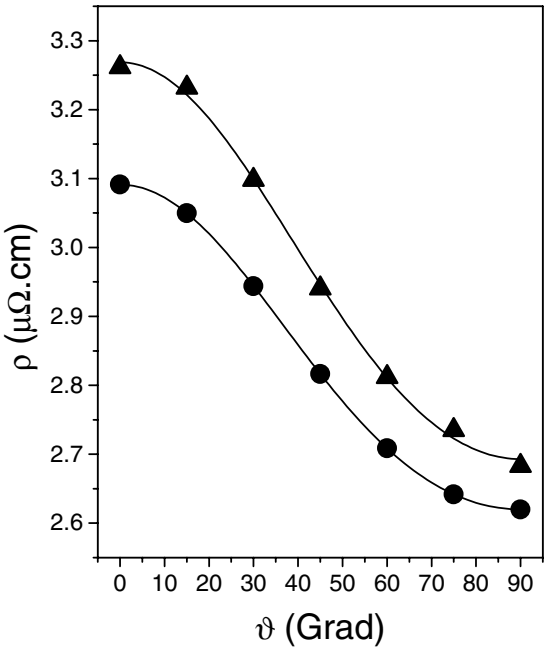

Fig. 26.20. Calculated resistivities with respect to the the angle, ϑ, between the current and the magnetization for $Ni_{85}Fe_{15}$ (triangles) and $Ni_{80}Fe_{20}$ (circles) alloys. Solid lines visualize the results of least square fits according to (26.38), see text.

From (26.42) for illustrative purposes layer-dependent conductivities can be defined

$$\sigma^i_{xx}(n;\mathbf{c};\mathcal{C};\delta) = \sum_{j=1}^{n} \sigma^{ij}_{xx}(n;\mathbf{c};\mathcal{C};\delta) \quad , \tag{26.45}$$

keeping in mind, however, that only the sum over these quantities is well-defined,

$$\sigma_{xx}(n;\mathbf{c};\mathcal{C};\delta) = \sum_{i=1}^{n} \sigma^i_{xx}(n;\mathbf{c};\mathcal{C};\delta) \quad . \tag{26.46}$$

26.5.4 An example: the giant magneto-resistance in Fe/Au/Fe multilayers

Consider the following typical spinvalve system $Au_{20}Fe_{10}Au_7Fe_{28}$/GaAs(100), for which the CIP electric properties shown in Fig. 26.21 were recorded experimentally by placing the contacts on the Au slabs. As in this system three Fe/Au interfaces are present in the theoretical investigations the spin valve system specified in Table 26.5 was considered which not only facilitated a discussion of interdiffusion effects but also addressed the questions of "where" the GMR is "coming from". Fig. 26.22 shows the calculated

Table 26.5. The Fe/Au/Fe magnetic multilayer

Layers	**purpose**
fcc-Au(100)/Au_5/	substrate
$[Au_cFe_{1-c}][Fe_cAu_{1-c}]$/	interdiffused interface
Fe_8	magnetic slab
$[Fe_cAu_{1-c}][Au_cFe_{1-c}]$	interdiffused interface
Au_5	spacer
$[Au_cFe_{1-c}][Fe_cAu_{1-c}]$	interdiffused interface
Fe_{10}	magnetic slab
vac	

resistivities $\rho_{xx}(n;\mathbf{c};\mathcal{C})$ as a function of the interdiffusion concentration c, see Table 26.5, and the corresponding GMR ratios. As can be seen from this figure in the limit of vanishing interdiffusion the calculated values for the resistivities are only about a factor 3–4 smaller than the experimental ones, while the calculated value of the GMR fits the experimental one amazingly well. As the experimental claim of nearly no interdiffusion can be confirmed from the theoretical results, the differences in the resistivities between the theoretical and the experimental values have to be attributed to two facts: (1) in the theoretical evaluations no macroscopical roughness is included, which of course is partially present in experimental samples and which increases both the resistivities in both magnetic configurations in equal terms, and (2) the theoretical descriptions usually yield slightly too low values. Furthermore, in the theoretical calculations no layer relaxation was assumed, i.e., for the whole system the interlayer spacing referred to that in pure fcc Au. Considering, however, that this difference is only of the order of about 4 $\mu\Omega$cm suggests that in principle even for rather complicated systems such as spin valves a realistic description of resistivities resolved with respect to the magnetic configuration can be given.

In Fig. 26.23 the difference between the parallel and the antiparallel layer-resolved conductivities is displayed, see (26.45). Also indicated in this figure are the boundary conditions for (26.41), namely a reflecting boundary condition on the vacuum side of the system and an outgoing boundary condition for electrons moving into or coming from the assumed semi-infinite system Au(100). It is interesting to note that obviously the biggest contribution arises from the two interfaces sandwiching the Au spacer, however, also the contributions from the two Fe slabs are quite big, while the contribution from the interior of the spacer – as to be expected – is very small indeed. Fig. 26.23 gives a very detailed "local" view of all those effects which contribute to the actually observed GMR value.

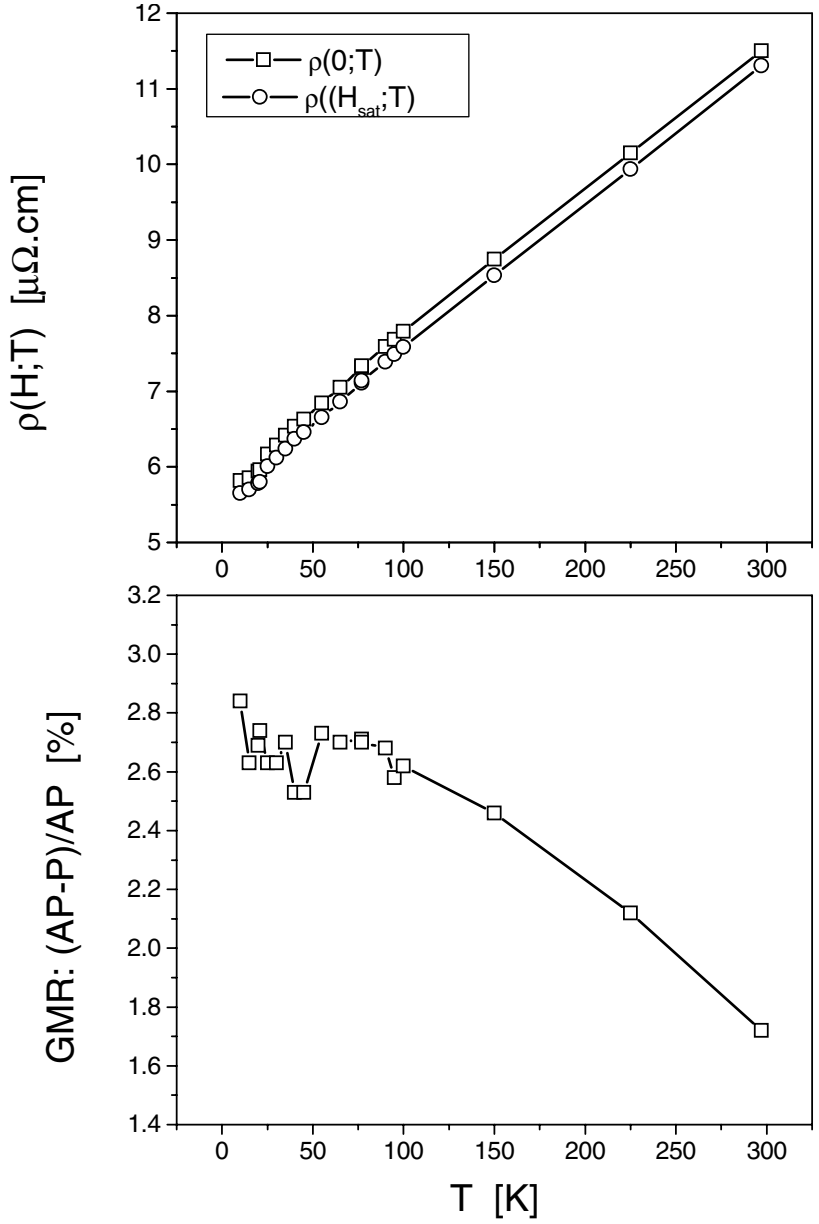

Fig. 26.21. Experimental field and temperature dependent resistivities (top) and temperature dependent giant magnetoresistance (bottom). From [17].

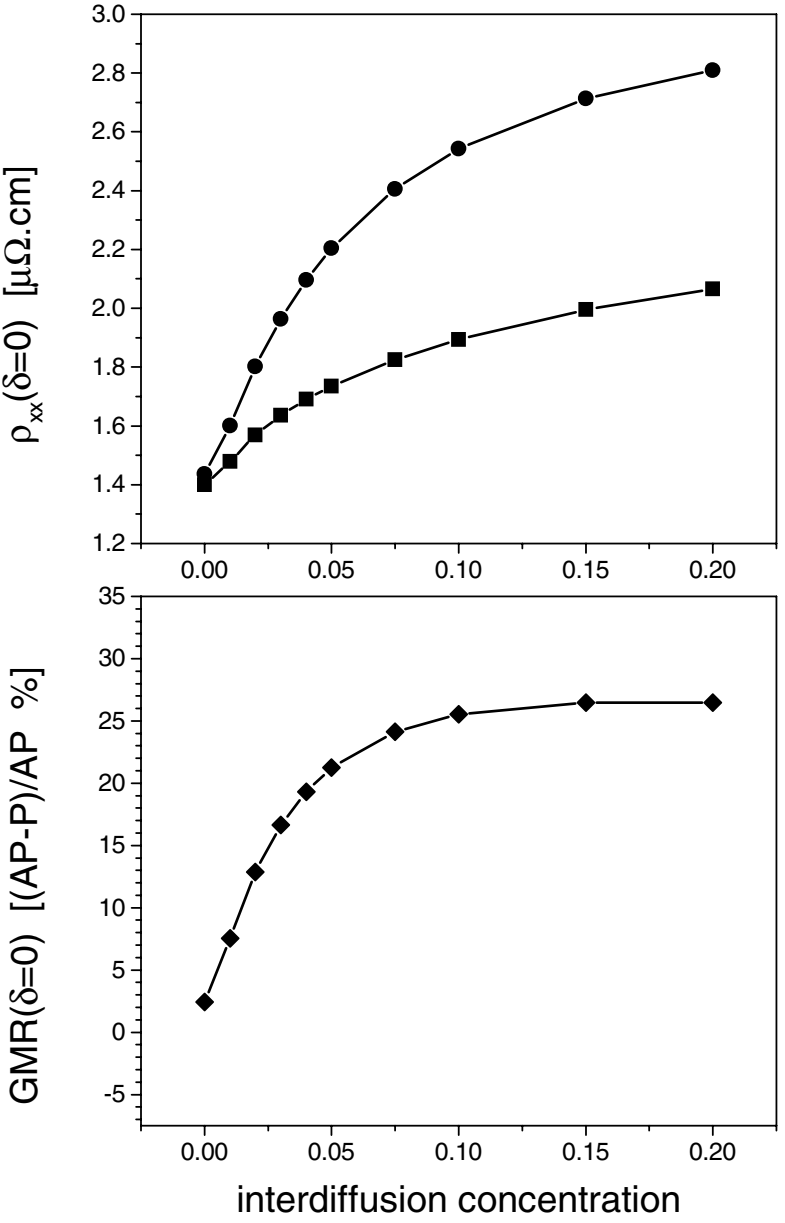

Fig. 26.22. CIP-resistivity and GMR in Fe/Au/Fe multilayers as continued to the real axis. Squares refer to the parallel aligment, circles to the antiparallel aligment. From [17].

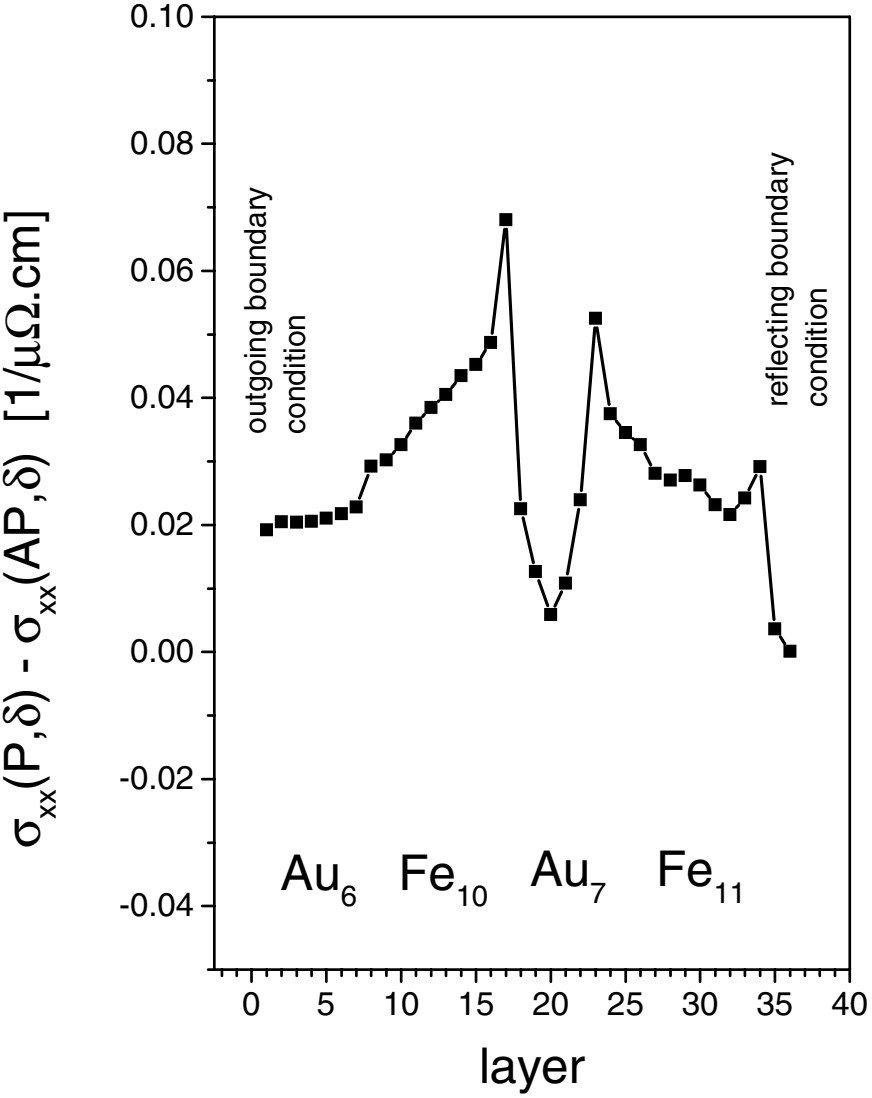

Fig. 26.23. Layer-resolved difference conductivities corresponding to an imaginary part of the Fermi energy of 2 mRyd and an interdiffusion concentration of $c = 0.05$. From [17].

26.6 Magneto-optical transport in semi-infinite systems

26.6.1 The (magneto-) optical tensor

According to Luttinger at finite temperatures the optical conductivity tensor is defined by

$$\Sigma_{\mu\nu}(\omega) = \frac{\sigma_{\mu\nu}(\zeta) - \sigma_{\mu\nu}(0)}{\zeta} \quad , \tag{26.47}$$

where

$$\zeta = \omega + \mathrm{i}\delta/\hbar \quad , \tag{26.48}$$

and

$$\sigma_{\mu\nu}(\zeta) \equiv \sigma_{\mu\nu}(\omega) = \frac{\mathrm{i}}{V} \sum_{m,n} \frac{f(\epsilon_n) - f(\epsilon_m)}{\hbar\zeta + \epsilon_n - \epsilon_m} J^{\mu}_{nm} J^{\nu}_{mn} \quad . \tag{26.49}$$

In (26.49) $f(\epsilon)$ is the Fermi function, V the volume of the system, the $J^{\mu}_{nm} = \langle\ n\ |\ J^{\mu}\ |\ m\ \rangle$ are again the matrix elements of the current density operator J^{μ}, $\mu = x, y, z$, with respect to the eigenfunctions $|n\rangle$ of the one-electron Hamiltonian corresponding to energy eigenvalues ϵ_n. In rewriting this equation in terms of Green's functions and replacing the sums over states by contour integrations, see Figs. 26.24 and 26.25, one obtains

$$\begin{aligned}
\sigma_{\mu\nu}(\omega) = -\frac{1}{2\pi V} \Bigg\{ & \oint_{\mathcal{C}} \mathrm{d}z f(z) \mathrm{Tr}\left[J^{\mu} G(z + \hbar\omega + \mathrm{i}\delta) J^{\nu} G(z)\right] \\
& - \oint_{\mathcal{C}'} \mathrm{d}z f(z) \mathrm{Tr}\left[J^{\mu} G(z) J^{\nu} G(z - \hbar\omega - \mathrm{i}\delta)\right] \Bigg\} \\
& + \mathrm{i}\frac{\delta_T}{\pi V} \Bigg\{ \sum_{k=-N_2+1}^{N_1} \mathrm{Tr}\left[J^{\mu} G(z_k + \hbar\omega + \mathrm{i}\delta) J^{\nu} G(z_k)\right] \\
& + \sum_{k=-N_1+1}^{N_2} \mathrm{Tr}\left[J^{\mu} G(z_k) J^{\nu} G(z_k - \hbar\omega - \mathrm{i}\delta)\right] \Bigg\} \quad ,
\end{aligned} \tag{26.50}$$

where Tr denotes the trace of an operator and where the $z_k = \epsilon_{\mathrm{F}} + \mathrm{i}(2k-1)\delta_T$ (ϵ_F is the Fermi energy, k_{B} the Boltzmann constant, T the temperature and $\delta_T = \pi k_{\mathrm{B}} T$) are the so-called Matsubara-poles, see in particular Chap. 18. In (26.50) it was supposed that N_1 and N_2 Matsubara-poles in the upper and lower semi-plane lie within the contour $\mathcal{C}$, respectively, i.e.,

$$(2N_1 - 1)\delta_T < \delta_1 < (2N_1 + 1)\delta_T \quad , \tag{26.51}$$

$$(2N_2 - 1)\delta_T < \delta_2 < (2N_2 + 1)\delta_T \quad . \tag{26.52}$$

Because of the reflection symmetry for the contours $\mathcal{C}$ and $\mathcal{C}'$, Figs. 26.24 and 26.25, (26.50) can be transformed to

$$\sigma_{\mu\nu}(\omega) = \oint_{\mathcal{C}} \mathrm{d}z f(z)\widetilde{\sigma}_{\mu\nu}(z+\hbar\omega+\mathrm{i}\delta, z) - \left(\oint_{\mathcal{C}} \mathrm{d}z f(z)\widetilde{\sigma}_{\mu\nu}(z-\hbar\omega+\mathrm{i}\delta, z)\right)^* - 2\mathrm{i}\delta_T \sum_{k=-N_2+1}^{N_1} \{\widetilde{\sigma}_{\mu\nu}(z_k+\hbar\omega+\mathrm{i}\delta, z_k) + \widetilde{\sigma}_{\mu\nu}(z_k-\hbar\omega+\mathrm{i}\delta, z_k)^*\} \tag{26.53}$$

where the $\widetilde{\sigma}_{\mu\nu}(z_1, z_2)$ are defined by

$$\widetilde{\sigma}_{\mu\nu}(z_1, z_2) = -\frac{1}{2\pi V}\mathrm{Tr}\left[J^\mu G(z_1) J^\nu G(z_2)\right] \quad , \tag{26.54}$$

for which the following symmetry relations apply,

$$\widetilde{\sigma}_{\nu\mu}(z_2, z_1) = \widetilde{\sigma}_{\mu\nu}(z_1, z_2), \tag{26.55}$$

$$\widetilde{\sigma}_{\mu\nu}(z_1^*, z_2^*) = \widetilde{\sigma}_{\nu\mu}(z_1, z_2)^* = \widetilde{\sigma}_{\mu\nu}(z_2, z_1)^* \quad . \tag{26.56}$$

It should be noted that the $\widetilde{\sigma}_{\mu\nu}(z_1, z_2)$ are exactly of the form as used in the corresponding Kubo-Greenwood approach to electric transport and, e.g., the (inhomogeneous) Coherent Potential Approximation can be applied in order to describe substitutional disorder in layered systems. For a layered system therefore (after augmenting (26.55) with the usual details of multiple scattering theory and performing necessary two-dimensional lattice Fourier transformations) in general the elements of the optical tensor are given by

$$\sigma_{\nu\mu}(n; \mathbf{c}; \widehat{\mathbf{M}}; \omega) = \sum_{p,q=1}^{n} \sigma_{\nu\mu}^{pq}(\mathbf{c}; \widehat{\mathbf{M}}; \omega) \quad , \tag{26.57}$$

where p and q label again atomic layers, $\mathbf{c}$ refers to layer-wise concentrations and $\widehat{\mathbf{M}}$ to a particular magnetic orientation. Equation(26.57) is the frequency-dependent form of (26.32).

26.6.2 An example: the magneto-optical conductivity tensor for Co on Pt(111)

Consider the systems $\mathrm{Co/Pt_5/Pt(111)}$ and $\mathrm{Pt_3/Co/Pt_5/Pt(111)}$, i.e., an fcc-Pt(111) substrate coated with a monolayer of Co and then covered by a cap of three Pt layers. In the particular example five layers of Pt serve as a buffer to the semi-infinite substrate. Figs. 26.26 and 26.27 show the real and imaginary parts of the $\sigma_{\nu\mu}^{pq}(\mathbf{c}; \widehat{\mathbf{M}}; \omega)$ in (26.57) for the uncovered system, Figs. 26.28 and 26.29 for the capped system. In both cases $\widehat{\mathbf{M}}$ refers to a uniform magnetization pointing along the surface normal. It is perhaps surprising to find out that the main contributions to the conductivity arise from the Pt layers and are not due to the Co monolayer. In particular it should be noted that the "ditch" to be seen in Figs. 26.28 and 26.29 corresponds to the contribution from the Co layer.

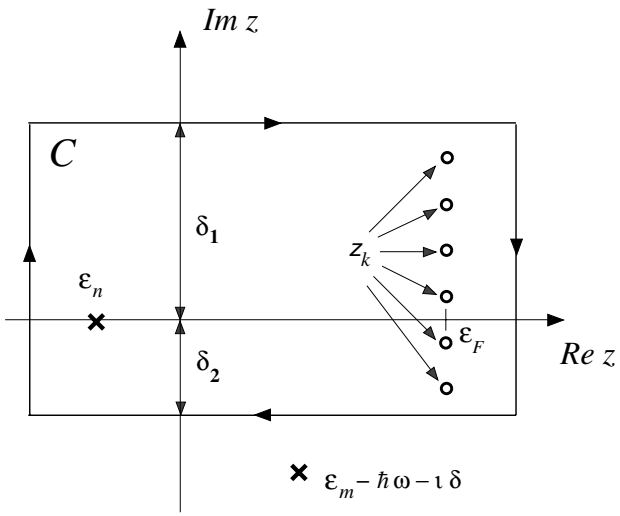

Fig. 26.24. Contour $\mathcal{C}$ in the complex plane corresponding to the integration in (26.50). From [24].

26.6.3 Kerr angles and ellipticities

Clearly enough the optical conductivity tensor is not a quantity directly accessible in experiments, since usually there a "classical optical" recording technique is used that needs to be taken into account in an appropriate manner. In Kerr spectroscopy for example the so-called Kerr angles θ_{K} and ellipticities ε_{K} are measured,

$$\theta_{\mathrm{K}} = -\frac{1}{2}\left(\Delta_{+} - \Delta_{-}\right) \quad , \quad \varepsilon_{\mathrm{K}} = -\frac{|r_{+}| - |r_{-}|}{|r_{+}| + |r_{-}|} \quad , \tag{26.58}$$

where $r_{\pm} = |r_{\pm}|\, e^{\mathrm{i}\Delta_{\pm}}$ is the complex reflectivity of right- and left-handed circularly polarized light, respectively, i.e., in which properties of the in-coming and reflected beam of light are related to each other.

By mapping the $\tilde{\sigma}^{pq}(\omega)$ (for matters of simplicity the concentration and orientational dependency is omitted) onto the corresponding contributions to the permittivity tensor

$$\tilde{\varepsilon}^{pq}(\omega) \Leftarrow \frac{1}{N}\left[1 - \frac{4\pi\mathrm{i}}{\omega}\tilde{\sigma}^{pq}(\omega)\right] \quad , \tag{26.59}$$

one can establish a well-defined macroscopical model for the evaluation of optical spectra. Since a discussion of the various aspects of solving the optical

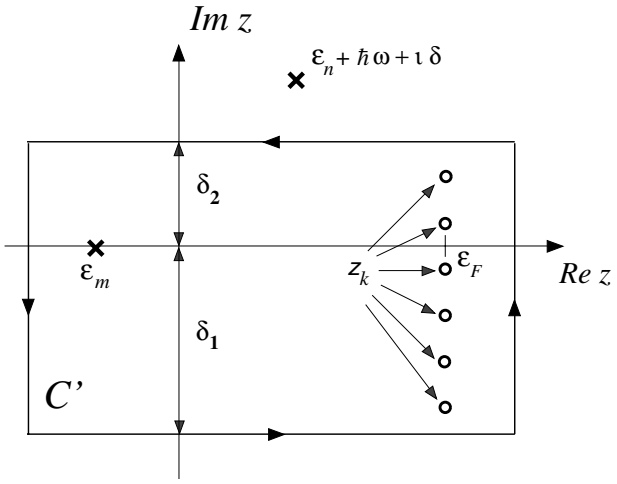

Fig. 26.25. Contour $\mathcal{C}'$ in the complex plane corresponding to the integration in (26.50). From [24].

problem are beyond the scope of this book, in here only the basic steps can be sketched. From the permittivity tensor in (26.59) a corresponding layer-resolved quantity can be obtained by solving the following equation selfconsistently in which $\boldsymbol{E}_p$ denotes the electric field characteristic in layer p and the summation extends over all layers (N) under consideration

$$\tilde{\varepsilon}^{p}\left(\omega\right)\boldsymbol{E}_p = \sum_{q=1}^{N} \tilde{\varepsilon}^{pq}\left(\omega\right)\ \boldsymbol{E}_q \quad . \tag{26.60}$$

With the help of these layer-resolved quantities the Fresnel equation,

$$\left| n_p^2 \delta_{\mu\nu} - n_{p\mu} n_{p\nu} - \tilde{\varepsilon}^{p}_{\mu\nu} \right| = 0 \quad , \quad (\mu, \nu = \mathrm{x}, \mathrm{y}, \mathrm{z}) \quad , \tag{26.61}$$

has to be solved in order to determine the normal modes of the electromagnetic waves in a particular layer p. Then by solving the Helmholtz equation for each normal mode,

$$\sum_{\nu} \left(n_p^2 \delta_{\mu\nu} - n_{p\mu} n_{p\nu} - \tilde{\varepsilon}^{p}_{\mu\nu} \right) \mathcal{E}_{p\nu} = 0 \quad , \quad (\mu, \nu = \mathrm{x}, \mathrm{y}, \mathrm{z}) \quad , \tag{26.62}$$

the corresponding components of the electric field in layer p, $\mathcal{E}_{p\nu}$, are obtained, which in turn provide the amplitudes of the magnetic fields $\boldsymbol{H}_p$ for each normal mode in layer p in terms of the curl Maxwell equation

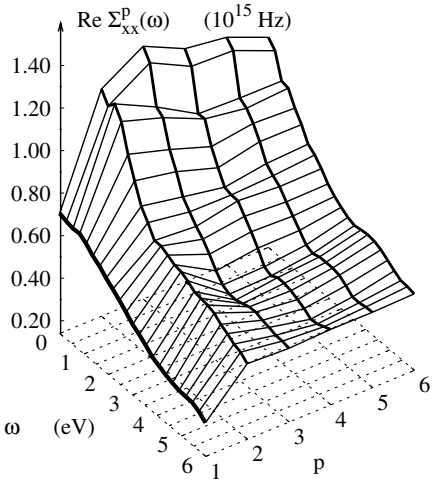

Fig. 26.26. Real (absorptive) parts of the layer-resolved complex optical conductivity $\Sigma^{p}_{\mu\nu}(\omega)$ for $Co/Pt_5/Pt(111)$ as a function of the optical frequency ω and the layer index p. The line at $p = 1$ refers to the Co layer-resolved optical conductivity. From [27].

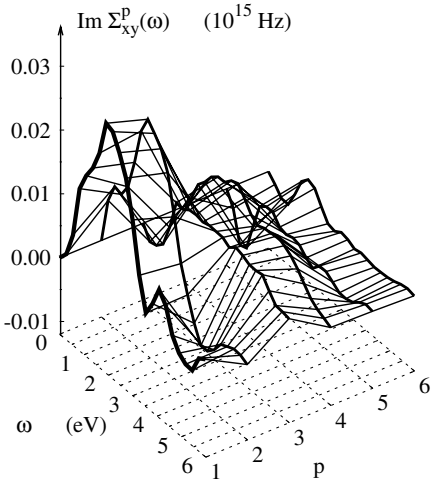

Fig. 26.27. Imaginary (absorptive) parts of the layer-resolved complex optical conductivity $\Sigma^{p}_{\mu\nu}(\omega)$ for $Co/Pt_5/Pt(111)$ as a function of the optical frequency ω and the layer index p. The line at $p = 1$ refers to the Co layer-resolved optical conductivity. From [27].

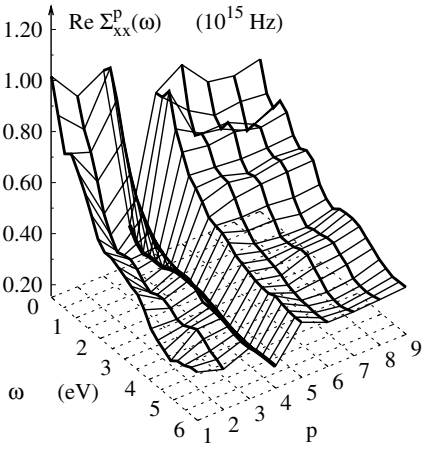

Fig. 26.28. Real (absorptive) parts of the layer-resolved complex optical conductivity $\Sigma^p_{\mu\nu}(\omega)$ for $Pt_3/Co/Pt_5/Pt(111)$ as a function of the optical frequency ω and the layer index p. The line at $p = 4$ refers to the Co layer-resolved optical conductivity. From [27].

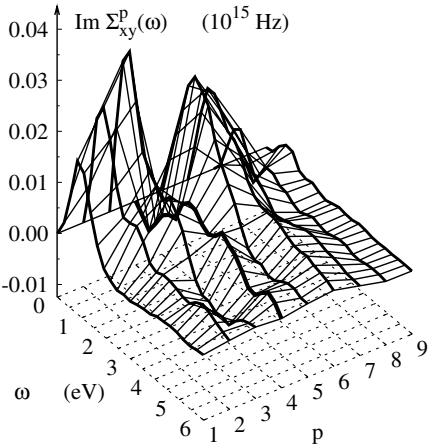

Fig. 26.29. Imaginary (absorptive) parts of the layer-resolved complex optical conductivity $\Sigma^p_{\mu\nu}(\omega)$ for $Pt_3/Co/Pt_5/Pt(111)$ as a function of the optical frequency ω and the layer index p. The line at $p = 4$ refers to the Co layer-resolved optical conductivity. From [27].

$$\boldsymbol{H}_p = \boldsymbol{n}_p \times \boldsymbol{E}_p \quad . \tag{26.63}$$

Continuity of the tangential components of the electric and the magnetic field at the boundary between adjacent layers leads to a set of equations, which has to be solved recursively in order to determine the magneto-optical coefficients of the layered system, such as, e.g., the surface reflectivity.

The reflectivity matrix $\mathcal{R}_p$ is then in general found in terms of the $\boldsymbol{E}_p$ and depends on various geometrical factors such as emission angle, orientation of the magnetization, crystal structures, etc. Finally, by making use of appropriate boundary conditions, namely that (1) inside the semi-infinite substrate the respective reflectivity matrix has to vanish, $\mathcal{R}_0 = 0$, and (2) in the vacuum region $\tilde{\epsilon}_{\mu\mu} = 1$, $\tilde{\epsilon}_{\mu\upsilon} = 0$, where μ, $\nu \in (x, y, z)$, the reflectivity matrix in the surface layer, R_{surf}, can be calculated, the matrix elements of which then determine the Kerr angle and ellipticity.

In the particular case of cubic parent lattices and normal emission R_{surf} reduces to a 2×2 matrix,

$$R_{\mathrm{surf}} = \begin{pmatrix} \tilde{r}_{\mathrm{xx}} & \tilde{r}_{\mathrm{xy}} \\ -\tilde{r}_{\mathrm{xy}} & \tilde{r}_{\mathrm{xx}} \end{pmatrix} \quad , \tag{26.64}$$

which in turn determines the complex Kerr angle Φ_{K},

$$\Phi_{\mathrm{K}} = \theta_{\mathrm{K}} + \mathrm{i}\varepsilon_{\mathrm{K}} \quad , \tag{26.65}$$

with θ_{K} and ϵ_{K}being the Kerr rotation angle and ellipticity, respectively,

$$\theta_{\mathrm{K}} = -\frac{1}{2}\left(\Delta_+ - \Delta_-\right) \quad , \tag{26.66}$$

$$\varepsilon_{\mathrm{K}} = -\frac{r_+ - r_-}{r_+ + r_-} \quad , \tag{26.67}$$

and

$$\tilde{r}_\pm = \tilde{r}_{\mathrm{xx}} \mp \mathrm{i}\tilde{r}_{\mathrm{xy}} = r_\pm \, e^{\mathrm{i}\Delta_\pm} \quad . \tag{26.68}$$

Only in the case that the so-called *two-media approach* applies, which is the case for a homogeneous system of repeated identical atomic layers, Kerr angles and ellipticities can directly be related to the components of the optical conductivity tensor:

$$\Phi_{\mathrm{K}} = \frac{\Sigma_{\mathrm{xy}}(\omega)}{\Sigma_{\mathrm{xx}}(\omega)} \left[1 + \frac{4\pi\mathrm{i}}{\omega}\,\Sigma_{\mathrm{xx}}(\omega)\right]^{-\frac{1}{2}} \quad . \tag{26.69}$$

The term *two-media approach* is derived from assumption that the vacuum region and the solid system form two homogeneous (optical) media.

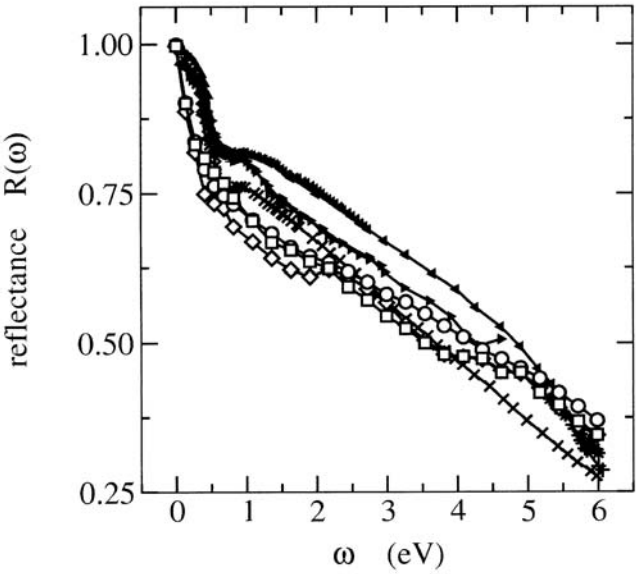

Fig. 26.30. Reflectance of fcc Pt bulk as calculated for the (100), (110) and (111) surface orientation (diamonds, circles and squares). Crosses, pluses, stars, left, right and up- triangles refer to experimental data. From [28].

26.6.4 An example: the optical constants in the "bulk" systems Pt(100), Pt(110), Pt(111)

In Figs. 26.30–26.32 the calculated reflectance, optical constants and the permittivity are displayed together with available experimental data. As can be seen from these three figures for all photon energies larger than the chosen lifetime broadening δ, see 26.48, the theoretical values agree very well indeed with the experimental counterparts.

26.7 Mesoscopic systems: magnetic domain walls

26.7.1 Phenomenological description of domain walls

The phenomenological Landau-Ginzburg theory predicts the following dependence of the Bloch wall energy $E(L)$ on the width of the Bloch Wall L,

$$E(L) = \alpha I_1 \frac{1}{L} + \beta I_2 L \quad , \tag{26.70}$$

where α and β are related to the exchange coupling (spin-stiffness) and the (in-plane) magnetic anisotropy, respectively, while the constants I_1 and I_2

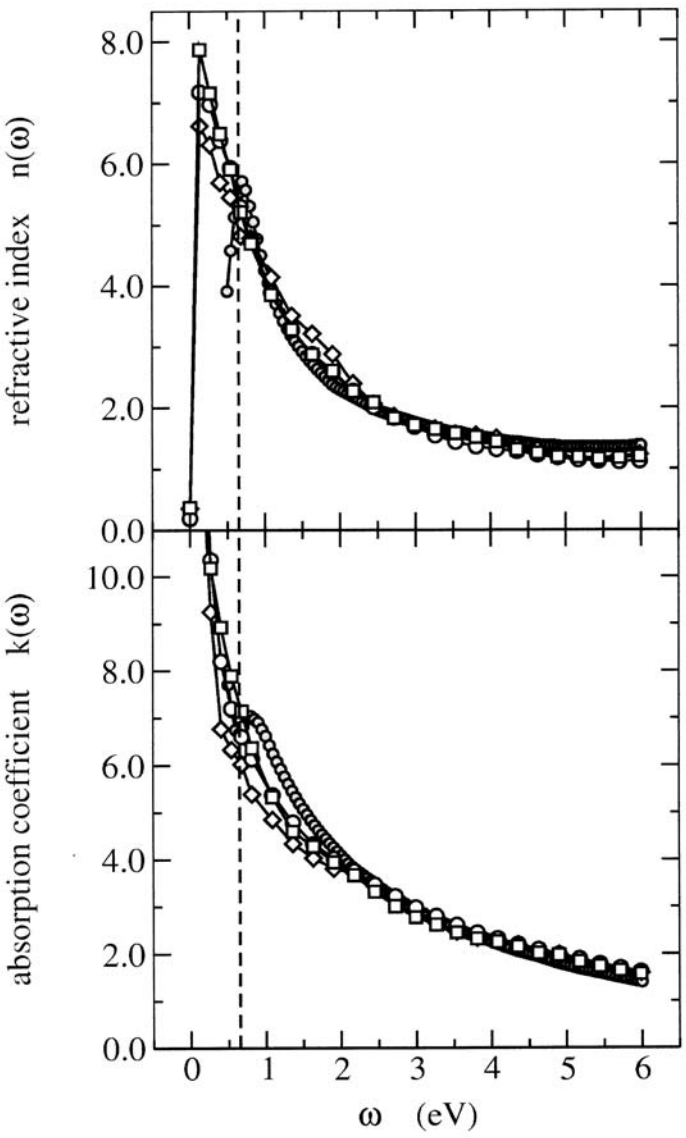

Fig. 26.31. Optical constants of fcc Pt bulk as calculated for the (100), (110) and (111) surface orientation (diamonds, circles and squares). The experimental data are displayed as grey circles. The dotted line marks the photon energy that corresponds to the used lifetime broadening of $\delta = 0.653$ eV. From [28].

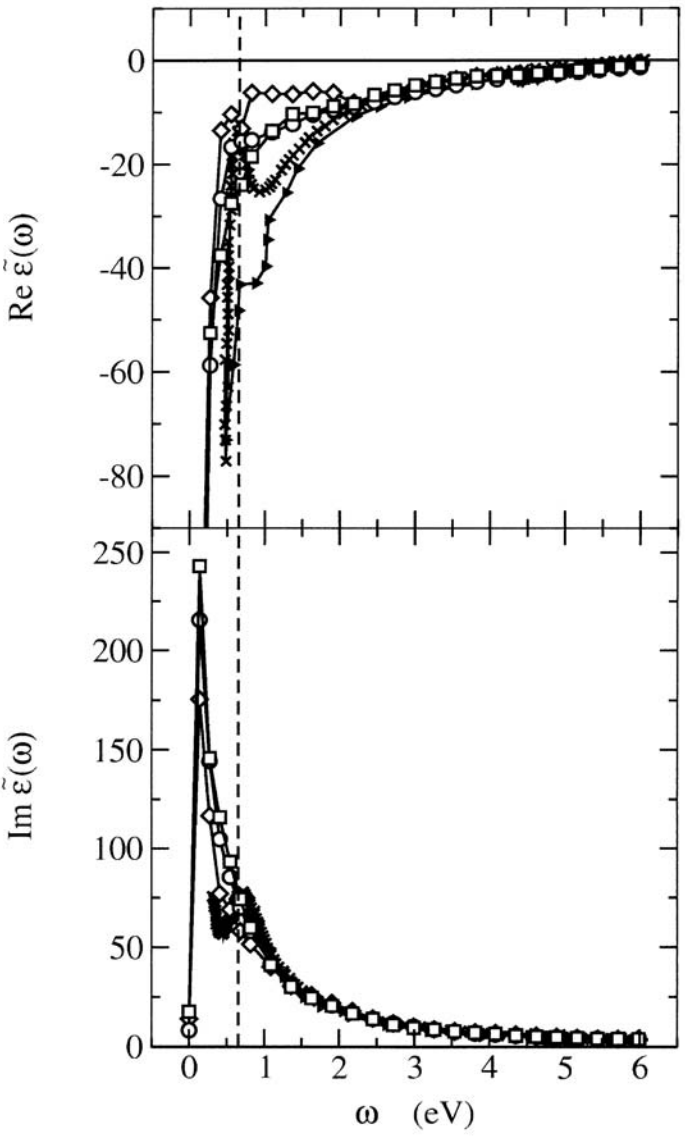

Fig. 26.32. Permittivity of fcc Pt bulk as calculated for the (100), (110) and (111) surface orientation (diamonds, circles and squares). Crosses, pluses, stars, left, right and down- triangles refer to experimental data. The dotted line marks the photon energy that corresponds to the used lifetime broadening of $\delta = 0.653$ eV. From [28].

are integrals depending on the profile of the magnetization direction, $\phi_0(\xi)$ $(0 \leq \xi \leq 1)$ defined as

$$\phi(z) = \phi_0(\frac{z}{L}) \quad , \quad 0 \leq z \leq L \quad , \tag{26.71}$$

$\phi(z)$ denoting the polar angle of the magnetization direction as a function of the position, z across the Bloch wall. Obviously, the function in (26.70) has a minimum at the thickness

$$L_{\mathrm{BW}} = \sqrt{\frac{\alpha}{\beta}\frac{I_1}{I_2}} \quad , \tag{26.72}$$

associated with the (equilibrium) thickness of the Bloch wall. Although the energy has to be minimized with respect to the profile $\phi_0(\xi)$, (26.72) suggests that any profile taken in actual calculations is suitable to predict L_{BW} once the quantity $\sqrt{I_1/I_2}$ is known. It is easy to show that in case of 90° Bloch walls of cubic ferromagnets (e.g. bcc Fe) or 180° Bloch walls of ferromagnets with uniaxial magnetic anisotropy (e.g. hcp Co) the assumption of a simple linear profile

$$\phi_0(\xi) = \begin{cases} 0 & \xi < 0 \\ \xi\Delta\phi & 0 \leq \xi \leq 1 \\ \Delta\phi & \xi \geq 1 \end{cases} \quad , \quad \Delta\phi = \pi \text{ or } \pi/2 \quad , \tag{26.73}$$

results in to an enhancement of L_{BW} by a factor of $\sqrt{2}$ with respect to the exact (soliton) solution.

26.7.2 Ab initio domain wall formation energies

Let $\Delta E(\mathcal{C}_i(L))$ denote the energy difference of a particular magnetic configuration $\mathcal{C}_i(L)$ of L atomic layers (properly embedded inbetween two semi-infinite systems) with respect to a given reference configuration $\mathcal{C}_0(L)$, see 26.10–26.12,

$$\Delta E(\mathcal{C}_i(L)) = E(\mathcal{C}_i(L)) - E(\mathcal{C}_0(L)) \quad . \tag{26.74}$$

It should be recalled that according to the definition given in (26.10) $\Delta E(\mathcal{C}_i(L)) > 0$ implies that $\mathcal{C}_0(L)$ is the preferred configuration, whereas for $\Delta E(\mathcal{C}_i(L)) < 0$, $\mathcal{C}_i(L)$ is preferred.

For a study of 90° and 180° Bloch walls it is useful to define the following magnetic configurations ($\hat{\mathbf{x}}$ and $\hat{\mathbf{y}}$ refer to the in-plane coordinate vectors, $\hat{\mathbf{z}}$ is normal to this plane),

$$\mathcal{C}_0(L) = \{\underbrace{\hat{\mathbf{x}}, \hat{\mathbf{x}}, \ldots, \hat{\mathbf{x}}}_{L}\} \quad , \tag{26.75}$$

and,

$$\mathcal{C}_i(L) \equiv \mathcal{C}_i(L_1; N; L_2; b)$$
$$= \{\underbrace{\hat{\mathbf{n}}_l, \ldots, \hat{\mathbf{n}}_l}_{b}, \hat{\mathbf{n}}_1, \hat{\mathbf{n}}_2, \ldots, \hat{\mathbf{n}}_{L_1}, \underbrace{\hat{\mathbf{y}}, \ldots, \hat{\mathbf{y}}}_{N}, \hat{\mathbf{n}}'_1, \hat{\mathbf{n}}'_2, \ldots, \hat{\mathbf{n}}'_{L_2}, \underbrace{\hat{\mathbf{n}}_r, \ldots, \hat{\mathbf{n}}_r}_{b}\} \quad , \tag{26.76}$$

where $L = N + L_1 + L_2 + 2b$. For matters of simplicity in (26.75) it was assumed that the orientation of the magnetization in the two domains that form the semi-infinite systems is pointing along $\hat{\mathbf{x}}$. The orientation of the magnetization in the individual layers $\hat{\mathbf{n}}_k$ is given by

$$\hat{\mathbf{n}}_{k_1} = R(\Theta_{k_1})\hat{\mathbf{x}} \quad , \quad \hat{\mathbf{n}}'_{k_2} = R(\Theta'_{k_2})\hat{\mathbf{y}} \quad , \tag{26.77}$$

where $R(\Theta_{k_1})$ and $R(\Theta'_{k_2})$ are (clock-wise) rotations around the z-axis, and $k_1(k_2)$ is an integer between 1 and L_1 (L_2). In using a simple model of a "linear" Bloch wall, the angles Θ and Θ' are simply given by

$$\Theta_{k_1} = k_1 \frac{90^0}{L_1} \text{ and } \Theta'_{k_2} = k_2 \frac{90^0}{L_2} \quad . \tag{26.78}$$

In (26.76) the index i denotes different configurations, i.e., different choices of L_1, L_2 and N. This set of atomic layers contains b "buffer-layers" at each end of the wall with orientations $\hat{\mathbf{n}}_l = \hat{\mathbf{x}}$ on the left and $\hat{\mathbf{n}}_r = -\hat{\mathbf{x}}$ or $\hat{\mathbf{n}}_r = \hat{\mathbf{y}}$ on the right. Equation (26.75) refers to a collinear magnetic configuration with the magnetization oriented uniformly in-plane along $\hat{\mathbf{x}}$, while (26.76) specifies a non-collinear magnetic structures in which, however, in each (atomic) plane the orientation of the magnetization is uniform (two-dimensional translational symmetry), but the orientation between different planes can vary in an arbitrary manner.

If in (26.74) $\mathcal{C}_0(L)$ refers to the magnetic ground state configuration and $\mathcal{C}_i(L)$ to a particular choice in (26.76) $\Delta E(\mathcal{C}_i(L))$ can be regarded as the energy of formation for a domain wall; it is a kind of *twisting energy* that is needed to form non-collinear structures. In the following different domain wall configurations $\mathcal{C}_i(L)$ are considered by varying N, L_1 and L_2, see Table 26.6, investigating not only 90° and 180° domains walls, but by increasing N to a sufficiently large number studying also two 90° domain walls separated from one another. For a 180° domain wall, e.g., the domain wall width is given by $L' = L - 2b = L_1 + L_2$; for a 90° domain wall by L_1.

26.7.3 An example: domain walls in bcc Fe and hcp Co

As only negligible changes of the effective potentials and fields across the Bloch wall are to be expected, Bloch walls of bcc Fe and hcp Co by considering the linear profile in (26.73) have been determined varying the width,

Table 26.6. Different types of Bloch walls considered, L'=L-2b.

N	L_1, L_2	**type**
0	$L_1 = L_2 = L'/2$	180° Bloch wall
0	$L_1 = L',\ L_2 = 0$	90° Bloch wall
$\neq 0$	$L_1 = L_2 < L'/2$	two 90° Bloch walls

L of the Bloch wall. The (band) energy difference with respect to the ferromagnetic configuration – to be associated with the energy of the Bloch wall – is shown in Fig. 26.33. As can be seen from this figure the calculated energy data can nicely be fitted to the function in (26.70) (solid lines) giving thus evidence from first principles that the phenomenological Landau-Ginzburg theory applies fairly well to these systems.

It should be mentioned that the Bloch walls investigations shown in Fig. 26.33 comprise about 150 (hcp Co) as well as 800 (bcc Fe) atomic planes. Clearly enough, a self-consistent determination of the magnetization profile and the electronic structure of the Bloch wall are a numerically demanding task. In the case of technologically important ferromagnetic alloys such as FePt or CoPt, however, due to the enhanced magnetic anisotropy the width of the Bloch wall is expected to be of the order of a few tens of atomic planes. This in turn raises the interesting question of the validity of the Landau-Ginzburg theory in such a regime of widths, a question, that only can be answered in terms of self-consistent calculations.

26.7.4 Another example: domain wall formation in permalloy

In order to illustrate the characteristic energy changes caused by changing the profile of the rotation angles Θ and Θ' layer-resolved twisting energies (band energy differences), see (26.12), are useful. In Figs. 26.34 and 26.35 two typical cases are shown for $Ni_{85}Fe_{15}$(100), namely (1) keeping L constant and varying N and (2) keeping N constant and varying L.

In Fig. 26.34 the situation for $L = 42$ is displayed. From this figure one can see, quite impressively, that (1) by increasing N increasingly thinner domain walls between 90° domains are formed and (2) that indeed those layers in which the orientation of the magnetization is along $\hat{\mathbf{y}}$ do not contribute to the total twisting energy (the directions $\hat{\mathbf{x}}$ and $\hat{\mathbf{y}}$ are equivalent). However, one can see another perhaps unanticipated effect; as the domain walls become thinner the Fe-like contribution to the twisting energy increases drastically: when the domain wall is only one ML thick the Fe contributions are almost twice as large as the Ni contribution. Clearly enough such small domain walls are unrealistic, i.e., only academic; however, these cases show in dramatic terms what happens if the domain walls in permalloy shrink. In Fig. 26.35 the opposite behavior is illustrated by keeping N constant and varying $L_1 = L_2$.

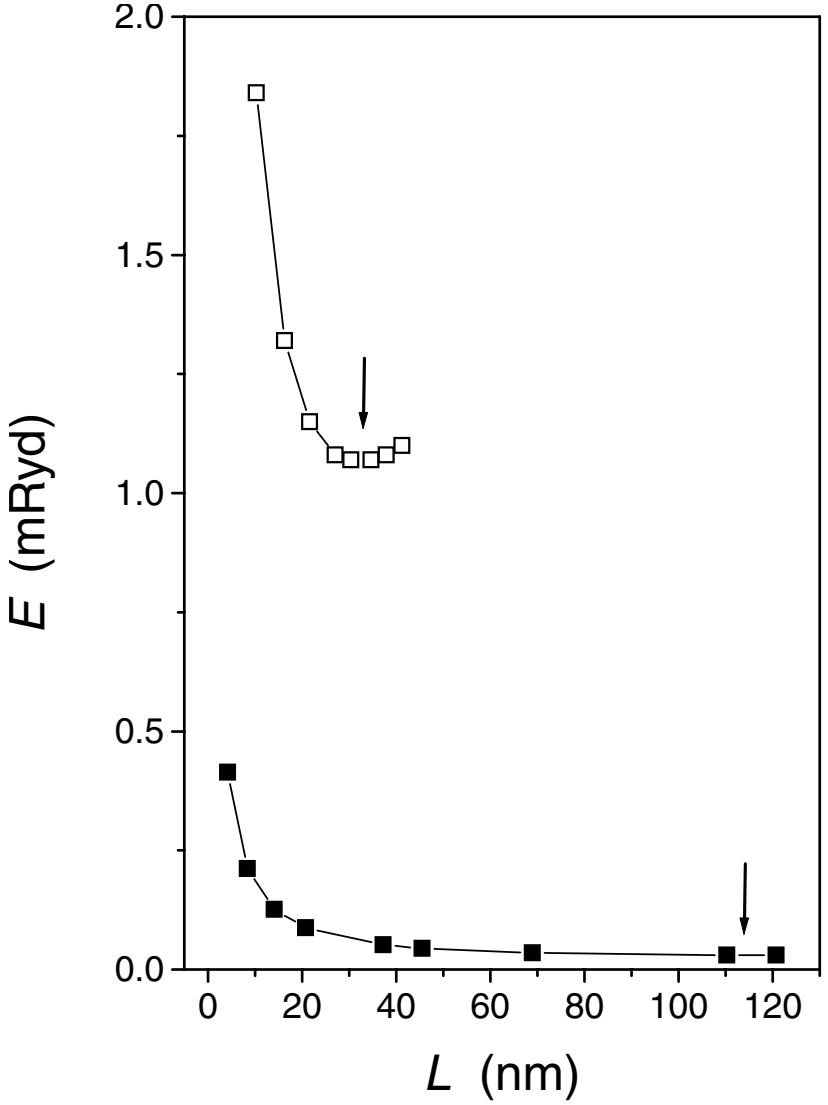

Fig. 26.33. Energy of a 90° Bloch Wall in bcc Fe and of a 180° Bloch Wall in hcp Co as a function of the width L of the Bloch Walls. A linear magnetization profile for the Bloch Wall as described in the text is used. The equilibrium width L_{BW} of the Bloch Wall determined by the minimum of $E(L)$ (labelled by vertical arrows), see also (26.70), is about 113 nm for bcc Fe (experiment: $\sim$ 40 nm) and about 35 nm for hcp Co (experiment: $\sim$ 15 nm). From [29].

Again one sees that in both cases displayed, namely $N = 0$ and $N = 6$, the form of the domain walls are unchanged as $L_1 = L_2$ is increased and N is held constant.

As seen from the changing scales for the different entries in Fig. 26.34 the twisting energy rises sharply with decreasing thickness of the domain wall. Beyond $N = 6$ the layers oriented along $\hat{\mathbf{y}}$ do not contribute to the twisting energy.

In the upper part of Fig. 26.35 the smallest twisting energies for 90° and 180° domain walls are displayed, namely those referring to the linear variation of the rotation angles. It is interesting to note that on the scale shown in this figure there is virtually no difference in the formation energies of two 90° or one 180° domain walls provided the total length is the same. It should be noted that in this figure L ranges from ~ 60 Å to $\sim$320 Å. In the lower half of Fig. 26.35 an interesting situation is addressed, namely the energy needed to split a 180° domain wall in two by inserting a domain of thickness N oriented perpendicular to the outer domains. In defining the energy of formation for two 90°domains in a 180° domain wall as

$$\Delta\varepsilon(L;N) = \Delta E(\mathcal{C}_i(L_1;N;L_2;b)) - \Delta E(\mathcal{C}_i(L_1;0;L_2;b')) \quad , \tag{26.79}$$

one can see from Fig. 26.35 that for

$$L = L_1 + L_2 + N + 2b = L_1 + L_2 + 2b' \quad , \tag{26.80}$$

this quantity is indeed very small and, furthermore, for $N > 6$ remains constant, i.e., in permalloy a 180° wall may easily fractionate into two 90° walls. It will be shown in the following section that at least in the investigated case of CIP the actual width of the domain wall is of little importance for the resistivities and the AMR within the wall.

26.7.5 Domain wall resistivities

For a current in the plane of the layers (CIP) geometry the corresponding element of the resistivity tensor is defined by

$$\rho_{\mu\mu}(L;\mathcal{C}_i(L);\delta) = [\sigma_{\mu\mu}(L;\mathcal{C}_i(L);\delta)]^{-1} \quad , \tag{26.81}$$

$$\rho_{\mu\mu}(L;\mathcal{C}_i(L)) = \lim_{\delta\to 0} \rho_{\mu\mu}(L;\mathcal{C}_i(L);\delta) \quad . \tag{26.82}$$

see 26.39, where L is the total number of atomic layers considered, δ refers to the imaginary part of the complex Fermi energy, $\epsilon_{\mathrm{F}} + \mathrm{i}\delta$, and the argument $\mathbf{c}$ in 26.39 refers to a uniform concentration of 85% Ni (permalloy). When the magnetization in all the layers points along the same direction , e.g., along the x-axis, in the limit of $L \to \infty$, (26.82) corresponds to the so-called residual resistivity of a binary substitutional alloys; in principle this can depend on the orientation of the magnetization chosen, i.e.,

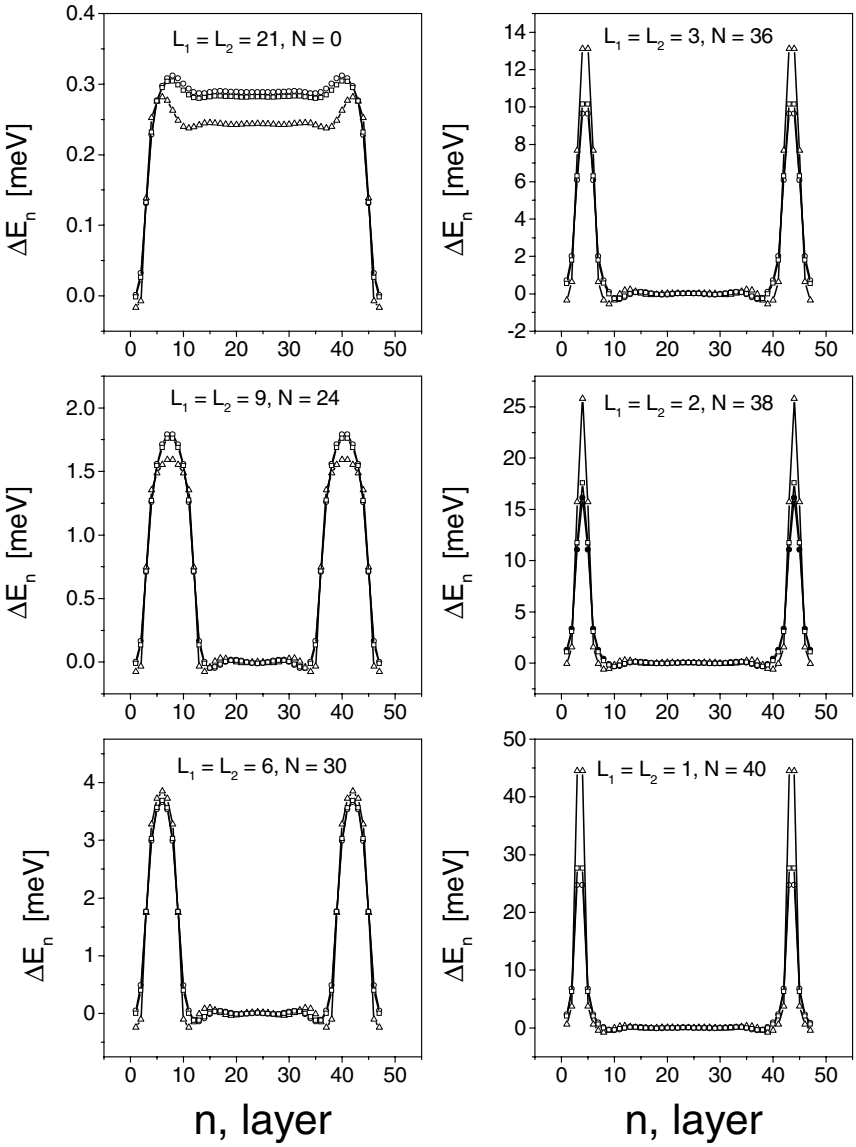

Fig. 26.34. Layer- and component-resolved interlayer exchange or twisting energy for $L = 42$ ML. The various cases of L_1, L_2 and N are indicated. Note that the first and last three layers refer to buffer layers. Circles and triangles refer to Ni and Fe, respectively, squares to the average. From [30].

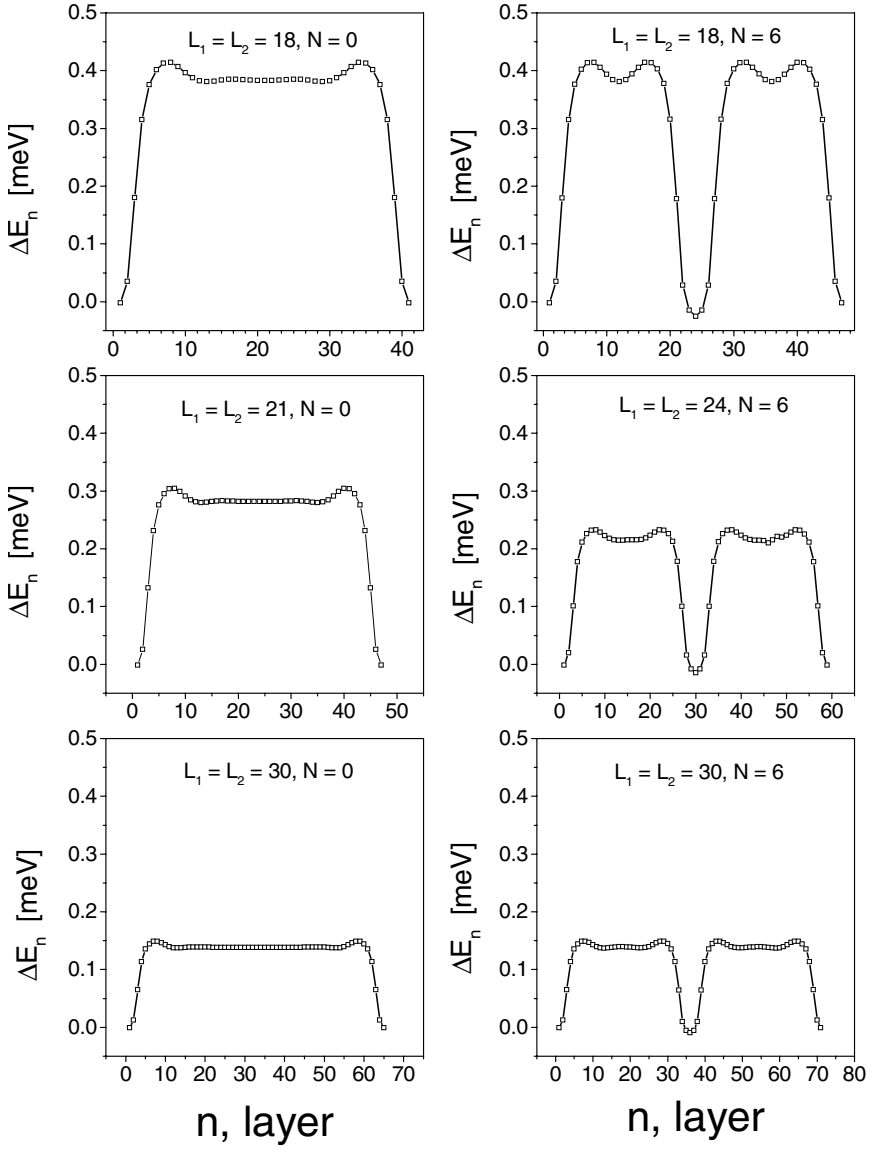

Fig. 26.35. Layer-resolved interlayer exchange or twisting energy for growing values of L. The various cases of L_1, L_2 and N are indicated. Note that the first and last three layers are the buffer layers. From [30].

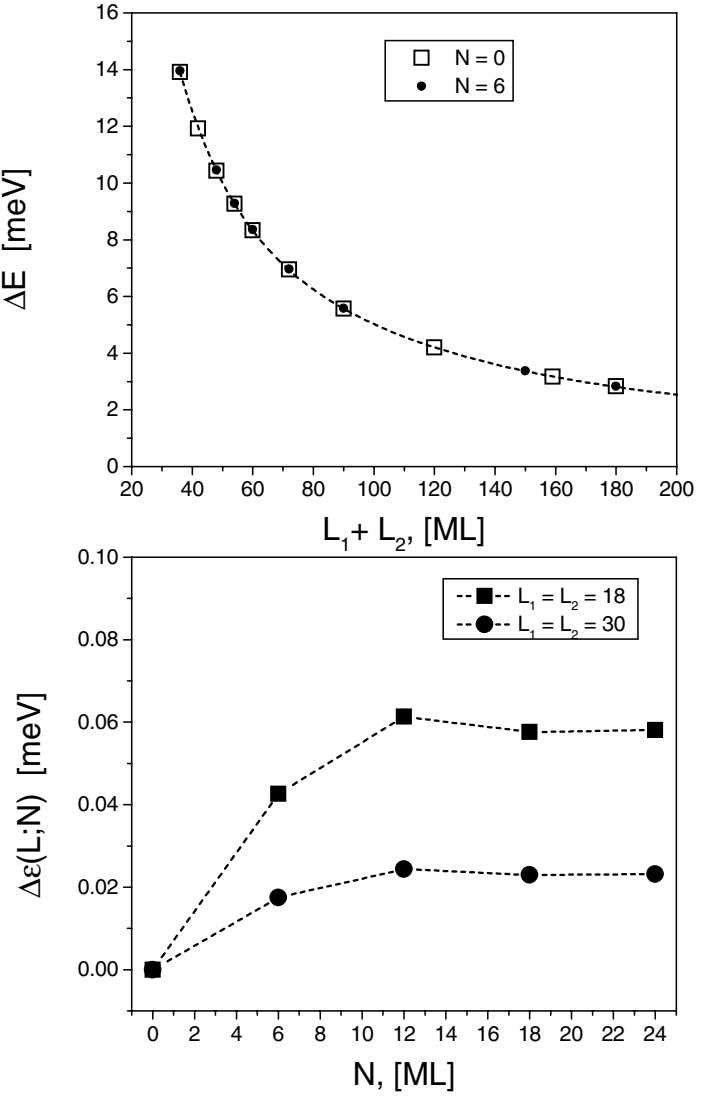

Fig. 26.36. Top: Energy of domain wall formation as a function of $L_1 + L_2$, see 26.75. Bottom: Difference in energy between a single 180° domain wall and when this wall is split into two by inserting a domain of N ML that has its' magnetization pointing at 90° to the two outer domains, see 26.79. From [30].

$$\lim_{L\to\infty}\left[\lim_{\delta\to 0}\rho_{\mu\mu}(L;\mathcal{C}_0(L);\delta)\right]=\rho^0_{\mu\mu}(\mathcal{C}_0)\quad . \tag{26.83}$$

For example, for $\mathcal{C}_0(L)=\{\hat{\mathbf{n}}_i \mid \hat{\mathbf{n}}_i=\hat{\mathbf{z}};1\le i\le L\}$ one gets

$$\rho^0_{xx}(\mathcal{C}_0)=\rho^0_{yy}(\mathcal{C}_0)\neq\rho^0_{zz}(\mathcal{C}_0)\quad , \tag{26.84}$$

while for $\hat{\mathbf{n}}_i = \hat{\mathbf{x}}$,

$$\rho^0_{xx}(\mathcal{C}_0) \neq \rho^0_{yy}(\mathcal{C}_0) = \rho^0_{zz}(\mathcal{C}_0) \quad . \tag{26.85}$$

By taking $\mathcal{C}_0(L) = \{\hat{\mathbf{x}}, \ldots, \hat{\mathbf{x}}\}$, see (26.75), the anisotropic magnetoresistance (AMR) ratio $R(L)$ can be defined in terms of the diagonal elements of the resistivity parallel and perpendicular to the chosen uniform orientation of the magnetization, e.g., by the following ratio

$$R(L) = \frac{\rho_{xx}(\mathcal{C}_0(L)) - \rho_{yy}(\mathcal{C}_0(L))}{\rho_{xx}(\mathcal{C}_0(L))} \quad , \tag{26.86}$$

see also Sect. 26.5. In analogy with (26.86) one can therefore define an anisotropic magnetoresistance for non-collinear structures as

$$R(\mathcal{C}_i(L)) = \frac{\rho_{xx}(\mathcal{C}_i(L)) - \rho_{yy}(\mathcal{C}_i(L))}{\rho_{xx}(\mathcal{C}_i(L))} \quad , \tag{26.87}$$

were $\mathcal{C}_i(L)$ is now a magnetic configuration as given in (26.76). In particular these ρ_{xx}, ρ_{yy}, and $R(\mathcal{C}_i(L))$ characterize the electrical transport properties of domain walls in the case of CIP.

26.7.6 An example: the CIP-AMR in permalloy domain walls

In Fig. 26.37 the CIP resistivities as a function of L for a single domain (corresponding to the magnetic configuration in (26.75), i.e., for a single (infinite) domain with an in-plane orientation of the magnetization), are shown and for a 180° domain wall. As easily can be seen, not only are ρ_{xx} and ρ_{yy} quite a bit larger in a 180° wall compared to the values for a (single) domain, but they are also almost equal in magnitude. It turns out that the products $L\rho_{xx}$ and $L\rho_{yy}$ are linear in L. Therefore the CIP-AMR does not depend on the actual domain wall width. As shown in the lower part of this figure the CIP AMR in the domain wall almost vanishes. The same situation applies to a 90° domain wall. In particular Fig. 26.37 is a clear indication that in using the AMR in permalloy for technological purposes always a CPP geometry should be used, because in this geometry the effect of domain walls on the AMR can be assumed to be rather very small.

26.8 Spin waves in magnetic multilayer systems

Within the *rigid-spin approximation* the adiabatic dynamics of local spin moments is phenomenologically described by the Landau–Lifshitz equation,

$$M_{ri}\,\dot{\sigma}_{ri} = -\frac{2\mu_{\mathrm{B}}}{\hbar}\frac{\delta \mathcal{F}}{\delta \sigma_{ri}} \times \sigma_{ri} \quad , \tag{26.88}$$

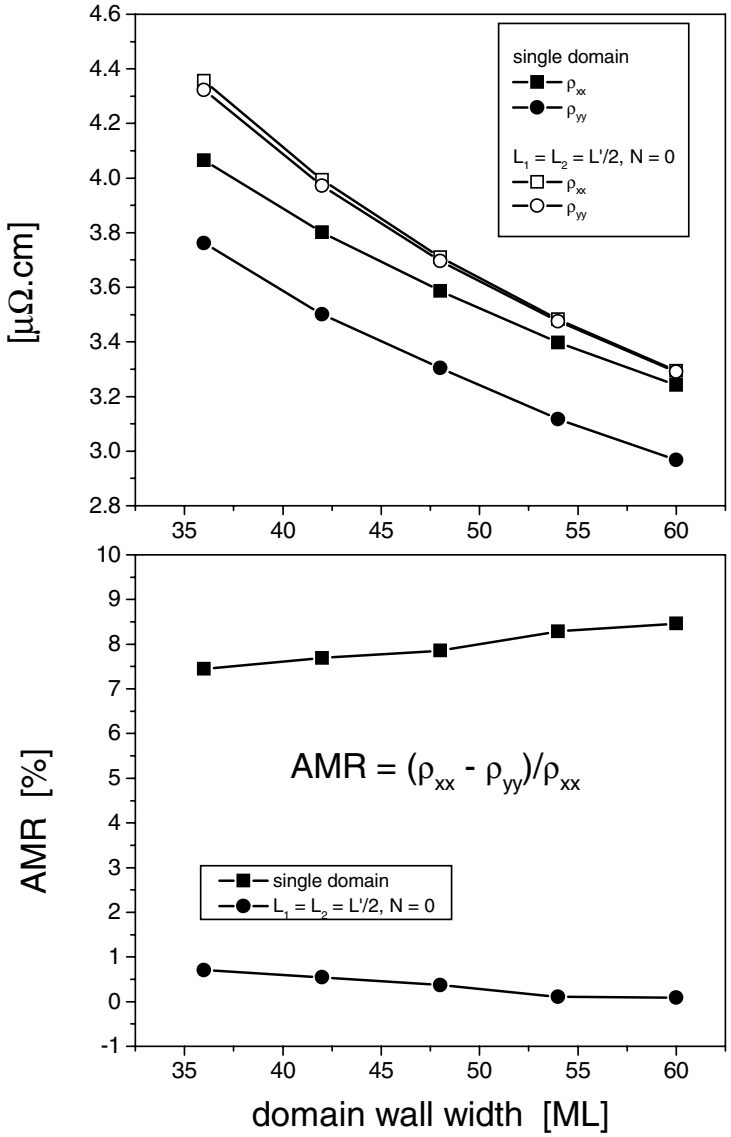

Fig. 26.37. Comparison of resistivities (top) and AMR (bottom) for a single domain (full symbols) and in a 180° domain wall. From [30].

where M_{ri} is the magnitude of the spin-moment and σ_{ri} is a unit vector pointing along the spin–quantization axis in the atomic cell at the site i of layer r,

$$\sigma_{ri} = (\sin\vartheta_{ri}\cos\varphi_{ri}, \sin\vartheta_{ri}\sin\varphi_{ri}, \cos\vartheta_{ri}) \quad , \tag{26.89}$$

with the polar and azimuthal angles ϑ_{ri} and φ_{ri}, respectively, and $\mathcal{F}$ is the free–energy of the system. For the case of transverse magnons, the angles ϑ_{ri} and φ_{ri} depend on time, whereas, by supposing two-dimensional translational invariance for the ground-state, the time independent magnitudes M_{ri} depend only on the layer index, i.e., $M_{ri} = M_r$ for all sites i in a particular layer r.

Rewriting (26.88) into spherical coordinates, the equations of motion for the angles ϑ_{ri} and φ_{ri} are given by

$$M_r \dot{\varphi}_{ri} \sin\vartheta_{ri} = \frac{2\mu_\mathrm{B}}{\hbar} \frac{\partial \mathcal{F}}{\partial \vartheta_{ri}} \quad , \tag{26.90}$$

$$-M_r \dot{\vartheta}_{ri} \sin\vartheta_{ri} = \frac{2\mu_\mathrm{B}}{\hbar} \frac{\partial \mathcal{F}}{\partial \varphi_{ri}} \quad . \tag{26.91}$$

Choosing the polar (z) axis of the reference system to be perpendicular to the magnetization in the ferromagnetic ground-state, (26.90) and (26.91) can easily be linearized,

$$M_r \dot{\varphi}_{ri} = \frac{2\mu_\mathrm{B}}{\hbar} \left. \frac{\partial \mathcal{F}}{\partial \vartheta_{ri}} \right|_{\vartheta=\frac{\pi}{2},\varphi=0} \quad , \tag{26.92}$$

$$-M_r \dot{\vartheta}_{ri} = \frac{2\mu_\mathrm{B}}{\hbar} \left. \frac{\partial \mathcal{F}}{\partial \varphi_{ri}} \right|_{\vartheta=\frac{\pi}{2},\varphi=0} \quad , \tag{26.93}$$

where the constraint $\vartheta = \frac{\pi}{2}, \varphi = 0$ indicates that the partial derivatives have to be taken at $\vartheta_{ri} = \frac{\pi}{2}$ and $\varphi_{ri} = 0$ for all r and i. The linearized version of the Landau–Lifshitz equations, (26.92) and (26.93), are the canonical equations for the generalized coordinates $q_{ri} \equiv (M_r/\mu_\mathrm{B})^{1/2}\varphi_{ri}$ and momenta $p_{ri} \equiv (M_r/\mu_\mathrm{B})^{1/2}\vartheta_{ri}$.

Adopting the *harmonic approximation*, i.e., expanding the free–energy up to second order in the angular variables, the corresponding Hamilton function can be written as

$$\mathcal{H} = \frac{1}{\hbar} \sum_{ri,sj} \left(q_{ri} A_{ri,sj} q_{sj} + q_{ri} B_{ri,sj} p_{sj} + p_{ri} B_{sj,ri} q_{sj} + p_{ri} C_{ri,sj} p_{sj} \right) \quad , \tag{26.94}$$

with

$$A_{ri,sj} = (M_r/\mu_\mathrm{B})^{-1/2} \left. \frac{\partial^2 \mathcal{F}}{\partial \varphi_{ri} \partial \varphi_{sj}} \right|_{\vartheta=\frac{\pi}{2},\varphi=0} (M_s/\mu_\mathrm{B})^{-1/2} \quad , \tag{26.95}$$

$$B_{ri,sj} = (M_r/\mu_\mathrm{B})^{-1/2} \left. \frac{\partial^2 \mathcal{F}}{\partial \varphi_{ri} \partial \vartheta_{sj}} \right|_{\vartheta=\frac{\pi}{2},\varphi=0} (M_s/\mu_\mathrm{B})^{-1/2} \quad , \tag{26.96}$$

$$C_{ri,sj} = (M_r/\mu_\mathrm{B})^{-1/2} \left. \frac{\partial^2 \mathcal{F}}{\partial \vartheta_{ri} \partial \vartheta_{sj}} \right|_{\vartheta=\frac{\pi}{2},\varphi=0} (M_s/\mu_\mathrm{B})^{-1/2} \quad . \tag{26.97}$$

Clearly enough in the case of two-dimensional translational symmetry lattice Fourier transformations can be used in order to reduce the summations

in (26.94). The classical Hamilton function in (26.94) can be quantized by intoducing appropriate bosonic creation and annihilation operators. After diagonalizing this Hamiltonian in terms of a Holstein–Primakoff transformation the corresponding eigenvalue problem can easily be solved, i.e., the spin wave spectrum of the layered system can be calculated [31].

For this purpose, however, the parameters of the Hamiltonian in (26.95)-(26.97) have to be calculated. In using the *magnetic force theorem*, the free–energy (grand potential) at zero temperature can be written as

$$\mathcal{F} = \int_{-\infty}^{\epsilon_{\rm F}} {\rm d}\varepsilon(\varepsilon - E_{\rm F})n(\varepsilon) = -\int_{-\infty}^{\epsilon_F} {\rm d}\varepsilon N(\varepsilon) \quad , \tag{26.98}$$

see Chap. 18, where $\epsilon_{\rm F}$ denotes the Fermi-energy of the system, $n(\varepsilon)$ is the density of states (DOS) and $N(\varepsilon)$ is the integrated DOS. Employing Lloyd's formula [32] for the integral density of states, see Chap. 3, apart from a constant term corresponding to the potential-free system, the free–energy can be written as

$$\mathcal{F} = -\frac{1}{\pi}{\rm Im}\int_{-\infty}^{E_{\rm F}} {\rm d}\varepsilon {\rm Tr}\ln\tau(\varepsilon) \quad , \tag{26.99}$$

where $\tau(\varepsilon) = \{\tau_{ij}\,(\varepsilon)\}$ is the site-representation of the scattering path operator.

The change of the free–energy has to be expressed up to second order with respect to small variations of the orientation of the magnetizations at sites i and j relative to the ferromagnetic ground-state orientation. As was discussed in Chap. 25 the orientational dependence of the single–site t–matrix corresponds to a similarity transformation that rotates the z axis of the reference system to the desired orientation given by the angles ϑ_i and φ_i,

$$t_i^{-1} = m_i = R(\vartheta_i, \varphi_i)\, m_i^0\, R^+(\vartheta_i, \varphi_i) \quad , \tag{26.100}$$

where m_i^0 denotes the inverse of the t–matrix at site i in a local frame in which the z axis coincides with the axis of the spin-quantization (magnetization). Note that for brevity the energy argument in the corresponding matrices has been dropped. The change of m_i up to second order in ϑ_i and φ_i,

$$\Delta m_i^{(1)} = m_i^{\vartheta} d\vartheta_i + m_i^{\varphi} d\varphi_i \quad , \tag{26.101}$$

$$\Delta m_i^{(2)} = \frac{1}{2} m_i^{\vartheta\vartheta} d\vartheta_i d\vartheta_i + m_i^{\varphi\vartheta} d\varphi_i d\vartheta_i + \frac{1}{2} m_i^{\varphi\varphi} d\varphi_i d\varphi_i \quad , \tag{26.102}$$

can easily be expressed by means of the derivatives of the rotation matrices $R(\vartheta_i, \varphi_i)$,

$$m_i^{\vartheta} \equiv \frac{\partial m_i}{\partial \vartheta_i} = \frac{\partial R_i}{\partial \vartheta_i} m_i^0 R_i^+ + R_i m_i^0 \frac{\partial R_i^+}{\partial \vartheta_i} \quad , \tag{26.103}$$

$$m_i^{\varphi} \equiv \frac{\partial m_i}{\partial \varphi_i} = \frac{\partial R_i}{\partial \varphi_i} m_i^0 R_i^+ + R_i m_i^0 \frac{\partial R_i^+}{\partial \varphi_i} \quad , \tag{26.104}$$

$$m_i^{\vartheta\vartheta} \equiv \frac{\partial^2 m_i}{\partial \vartheta_i \partial \vartheta_i} = \frac{\partial^2 R_i}{\partial \vartheta_i^2} m_i^0 R_i^+ + R_i m_i^0 \frac{\partial^2 R_i^+}{\partial \vartheta_i^2} + 2 \frac{\partial R_i}{\partial \vartheta_i} m_i^0 \frac{\partial R_i^+}{\partial \vartheta_i} \quad , \tag{26.105}$$

$$m_i^{\varphi\vartheta} \equiv \frac{\partial^2 m_i}{\partial \varphi_i \partial \vartheta_i} = \frac{\partial^2 R_i}{\partial \varphi_i \partial \vartheta_i} m_i^0 R_i^+ + \frac{\partial R_i}{\partial \varphi_i} m_i^0 \frac{\partial R_i^+}{\partial \vartheta_i} + \frac{\partial R_i}{\partial \vartheta_i} m_i^0 \frac{\partial R_i^+}{\partial \varphi_i} + R_i m_i^0 \frac{\partial^2 R_i^+}{\partial \varphi_i \partial \vartheta_i} \, , \tag{26.106}$$

$$m_i^{\varphi\varphi} \equiv \frac{\partial^2 m_i}{\partial \varphi_i \partial \varphi_i} = \frac{\partial^2 R_i}{\partial \varphi_i^2} m_i^0 R_i^+ + R_i m_i^0 \frac{\partial^2 R_i^+}{\partial \varphi_i^2} + 2 \frac{\partial R_i}{\partial \varphi_i} m_i^0 \frac{\partial R_i^+}{\partial \varphi_i} \quad , \tag{26.107}$$

where for matters of simplicity $R_i \equiv R(\vartheta_i, \varphi_i)$.

By changing the orientation of the magnetization only at site i the logarithm of the transformed scattering path operator can be written as

$$\ln \tau' = \ln(\mathbf{m} + \Delta\mathbf{m}_i - \mathbf{G}_0)^{-1} = \ln \tau - \ln(\mathbf{1} + \tau \Delta \mathbf{m}_i) \quad . \tag{26.108}$$

It should be recalled that in the site-diagonal matrix $\Delta\mathbf{m}_i$ only the block corresponding to site i does not vanish. Expanding the logarithm in (26.108) and keeping the terms up-to second order one obtains,

$$\ln \tau' - \ln \tau = -\tau \Delta \mathbf{m}_i^{(1)} - \tau \Delta \mathbf{m}_i^{(2)} + \frac{1}{2} \tau \Delta \mathbf{m}_i^{(1)} \tau \Delta \mathbf{m}_i^{(1)} \quad . \tag{26.109}$$

The first term on the right hand side of the above equation contributes to the gradient of the free–energy, while the site-diagonal elements of its second derivative tensor are related to the second and third terms of (26.108).

In changing the orientation of the magnetization simultaneously at two different sites, i and j $(i \neq j)$, one gets

$$\ln \tau' = \ln(\mathbf{m} + \Delta\mathbf{m}_i + \Delta\mathbf{m}_j - \mathbf{G}_0)^{-1} = \ln \tau - (\mathbf{1} + \tau(\Delta\mathbf{m}_i + \Delta\mathbf{m}_j)) \quad , \tag{26.110}$$

which can be rewritten into the form,

$$\ln \tau' = \ln \tau - \ln(\mathbf{1} + \tau \Delta \mathbf{m}_i) - \ln(\mathbf{1} + \tau \Delta \mathbf{m}_j) - \ln(\mathbf{1} - \tau \mathbf{\Delta}_i \tau \mathbf{\Delta}_j) \quad , \tag{26.111}$$

where $\mathbf{\Delta}_i \equiv \Delta\mathbf{m}_i(\mathbf{1} + \tau \Delta \mathbf{m}_i)^{-1}$. Expanding (26.111) up to second order gives,

$$\ln \tau' - \ln \tau = -\tau(\Delta \mathbf{m}_i^{(1)} + \Delta \mathbf{m}_j^{(1)}) + \tau \Delta \mathbf{m}_i^{(1)} \tau \Delta \mathbf{m}_j^{(1)} \quad . \tag{26.112}$$

Similar to the site-diagonal case the second derivatives can be deduced from the second term of the right-hand side of (26.112).

Assuming two-dimensional translational symmetry implies that the single-site t-matrix depends only on the layer index. Using finally (26.103)–(26.107) in (26.109) and (26.112), the second derivative tensor of the free-energy with respect to the site-dependent orientations of the magnetization can be written in terms of (26.99) for the *diagonal terms* as,

$$\frac{\partial^2 \mathcal{F}}{\partial \varphi_{ri} \partial \varphi_{ri}} = -\frac{1}{\pi} \mathrm{Im} \int_{-\infty}^{E_\mathrm{F}} \mathrm{d}\varepsilon \mathrm{Tr} \Big(- \tau_{r0,r0}(\varepsilon) m_r^{\varphi\varphi}(\varepsilon) + \tau_{r0,r0}(\varepsilon) m_r^{\varphi}(\varepsilon) \tau_{r0,r0}(\varepsilon) m_r^{\varphi}(\varepsilon) \Big) \quad , \tag{26.113}$$

$$\frac{\partial^2 \mathcal{F}}{\partial \varphi_{ri} \partial \vartheta_{ri}} = -\frac{1}{\pi} \mathrm{Im} \int_{-\infty}^{E_\mathrm{F}} \mathrm{d}\varepsilon \mathrm{Tr} \Big(- \tau_{r0,r0}(\varepsilon) m_r^{\varphi\vartheta}(\varepsilon) + \tau_{r0,r0}(\varepsilon) m_r^{\varphi}(\varepsilon) \tau_{r0,r0}(\varepsilon) m_r^{\vartheta}(\varepsilon) \Big) \quad , \tag{26.114}$$

$$\frac{\partial^2 \mathcal{F}}{\partial \vartheta_{ri} \partial \vartheta_{ri}} = -\frac{1}{\pi} \mathrm{Im} \int_{-\infty}^{E_\mathrm{F}} \mathrm{d}\varepsilon \mathrm{Tr} \Big(- \tau_{r0,r0}(\varepsilon) m_r^{\vartheta\vartheta}(\varepsilon) + \tau_{r0,r0}(\varepsilon) m_r^{\vartheta}(\varepsilon) \tau_{r0,r0}(\varepsilon) m_r^{\vartheta}(\varepsilon) \Big) \quad , \tag{26.115}$$

and for *off-diagonal terms as*

$$\frac{\partial^2 \mathcal{F}}{\partial \varphi_{ri} \partial \varphi_{sj}} = -\frac{1}{\pi} \mathrm{Im} \int_{-\infty}^{E_\mathrm{F}} \mathrm{d}\varepsilon \mathrm{Tr} \Big(\tau_{sj,ri}(\varepsilon) m_r^{\varphi}(\varepsilon) \tau_{ri,sj}(\varepsilon) m_s^{\varphi}(\varepsilon) \Big) \quad , \tag{26.116}$$

$$\frac{\partial^2 \mathcal{F}}{\partial \varphi_{ri} \partial \vartheta_{sj}} = -\frac{1}{\pi} \mathrm{Im} \int_{-\infty}^{E_\mathrm{F}} \mathrm{d}\varepsilon \mathrm{Tr} \Big(\tau_{sj,ri}(\varepsilon) m_r^{\varphi}(\varepsilon) \tau_{ri,sj}(\varepsilon) m_s^{\vartheta}(\varepsilon) \Big) \quad , \tag{26.117}$$

$$\frac{\partial^2 \mathcal{F}}{\partial \vartheta_{ri} \partial \vartheta_{sj}} = -\frac{1}{\pi} \mathrm{Im} \int_{-\infty}^{E_\mathrm{F}} \mathrm{d}\varepsilon \mathrm{Tr} \Big(\tau_{sj,ri}(\varepsilon) m_r^{\vartheta}(\varepsilon) \tau_{ri,sj}(\varepsilon) m_s^{\vartheta}(\varepsilon) \Big) \quad , \tag{26.118}$$

where $\tau_{ri,sj}$ is that block of the real-space scattering path operator that corresponds to site i of layer r and site j of layer s. In (26.113)–(26.118) the trace has to be performed in angular momentum space.

26.8.1 An example: magnon spectra for magnetic monolayers on noble metal substrates

The magnon spectra along high symmetry directions of the Brillouin zone for $\mathrm{Fe_1/Au(001)}$ and $\mathrm{Co_1/Cu(001)}$ as calculated using the fully relativistic

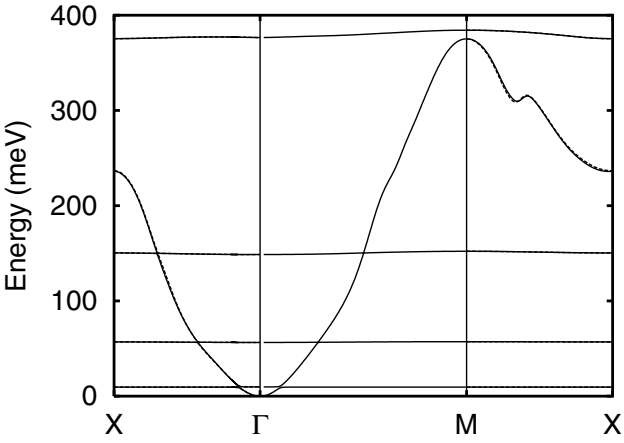

Fig. 26.38. Spin-wave spectrum for $Fe_1/Au(001)$. The almost dispersion-less bands belong to the two Au layers adjacent the Fe monolayer. From [31].

spin-polarized Screened KKR-ASA method are depicted in Figs. 26.38 and 26.39. The almost dispersion-less bands belong to the non-magnetic nearest and next-nearest neighbor layers. There are anti-crossings between the bands which are most pronounced in the case of Co/Cu(001) indicating the largest interactions between the magnetic and the non-magnetic layers. A local minimum observed between the points **X** and **M** is an indication for a so-called Kohn anomaly, which is caused by the long range RKKY like behavior of the exchange interactions. It should be noted that for $Fe_1/Au(001)$ the orientation of the magnetization is along the surface normal, while for $Co_1/Cu(001)$ it is in-plane.

For Fe/Au(001) in the absence of spin–orbit coupling the dispersion curve starts – as to be expected – at zero. Only by including "spin–orbit coupling" opens up a gap of Δ=43 μRyd for the normal-to-plane orientation. For an in-plane magnetization the relativistic calculation resulted into an imaginary magnon energy close to the $\mathbf{\Gamma}$ point indicating that the in-plane ferromagnetic order corresponds to a local maximum in the free–energy and the easy axis is perpendicular to the surface.

In the case of an in-plane magnetization the c_{4v} symmetry of the fcc (001) surface is lifted and the spin–wave spectra for the (001) and (010) directions of the magnetization become different as it is shown in Fig. 26.39 for Co/Cu(001). A splitting of a few meV due to spin–orbit coupling can clearly be seen in the insets in Fig. 26.39.

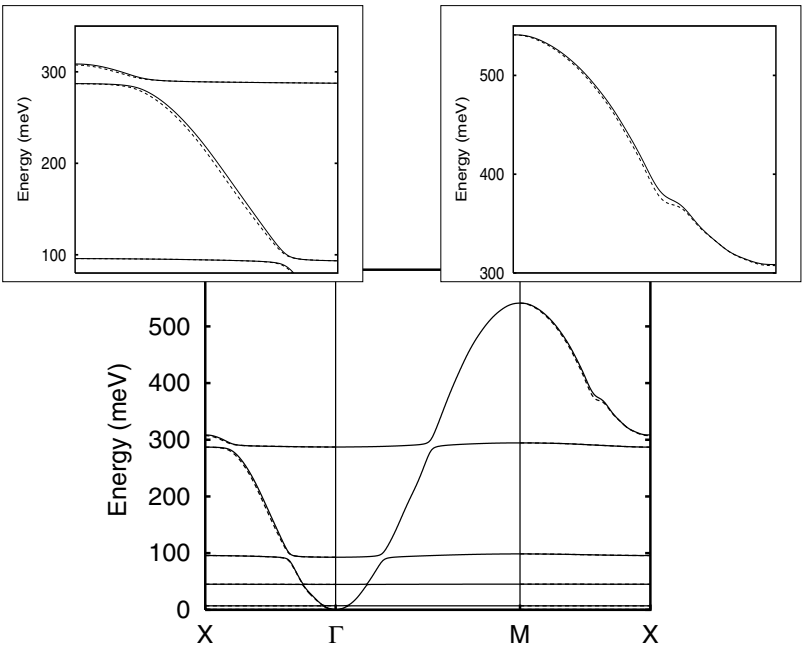

Fig. 26.39. Spin-wave spectrum for $Co_1/Cu(001)$ with an in-plane ground-state magnetization. The four additional Cu layers considered in the calculations are coupled relatively strongly to the Co monolayer as indicated by the non-crossing behavior (hybridization) of the corresponding bands. The solid and dashed lines represent the (100) and (010) directions of the magnetization, respectively. The spectrum between the symmetry points **X** and **Γ** as well as between **M** and **X** are shown on an enlarged scale in the upper left and the upper right inset, respectively. From [31].

References

1. N.D. Lang and W. Kohn, Phys. Rev. B **1**, 4555 (1970)
2. N.D. Lang and W. Kohn, Phys. Rev. B **3**, 1215 (1971)
3. M. Methfessel, D. Hennig, and M. Scheffler, Phys. Rev. B **46**, 4816 (1992)
4. H.L. Skriver and N.M. Rosengaard, Phys. Rev. B **43**, 9538 (1991)
5. L. Vitos, A.V. Ruban, H.L. Skriver, and J. Kollár, Surf. Sci. **411**, 186 (1998)
6. H.L. Skriver and N.M. Rosengaard, Phys. Rev. B **45**, 9410 (1992)
7. H.L. Skriver and N.M. Rosengaard, Phys. Rev. B **46**, 7157 (1992)
8. L. Szunyogh, B. Újfalussy, P. Weinberger, and J. Kollár, Phys. Rev. B **49**, 2721 (1994)
9. C. Kittel, *Introduction to Solid State Physics*, 6th ed (Wiley, New York 1986)
10. H.B. Michaelson, J. Appl. Phys **48**, 4729 (1977)
11. P. Weinberger and L. Szunyogh, Computational Materials Science **17**, 414 (2000)
12. H.J.F. Jansen, Phys. Rev. B **59**, 4699 (1999)

13. A. Vernes, P. Weinberger, P. Mohn, C. Blaas, L. Szunyogh, C. Sommers and P.M. Levy, Phil. Mag. B **82**, 85-104 (2002)
14. C. Uiberacker, J. Zabloudil, P. Weinberger, L. Szunyogh and C. Sommers, Phys. Rev. Lett. **82**, 1289 (1999)
15. C. Uiberacker, J. Zabloudil, P. Weinberger, L. Szunyogh and C. Sommers, Phys. Rev. B **62**, 5305 (2000)
16. B. Lazarovits, L. Szunyogh, and P. Weinberger, Phys. Rev. B **67**, 024415/1-6 (2003)
17. P. Weinberger, L. Szunyogh, J. Zabloudil, R. Hammerling, T.L. Mochesky, and B. Heinrich, Phys. Rev. B **67**, 054404/1-6 (2003)
18. S. Khmelevskii, K. Palotás, P. Weinberger, and L. Szunyogh, Phys. Rev. B **68**, 012402/1-4 (2003)
19. J. Banhart and H. Ebert, Europhys. Lett. **32**, 517 (1995)
20. J. Smith, Physica **16**, 612 (1951)
21. I.A. Campbell, A. Fert, and O. Jaoul, J. Phys. C **3**, S95 (1970)
22. I.A. Campbell, J. Phys. F **4**, L181 (1974)
23. P. Weinberger, Physics Reports **377**, 281–387 (2003)
24. L. Szunyogh and P. Weinberger, J. Phys. Cond. Matt. **11**, 10451 (1999)
25. P. Weinberger, P.M. Levy, J. Banhart, L. Szunyogh and B. Újfalussy, J. Phys. Cond. Matt. **8**, 7677 (1996)
26. K. Palotás, B. Lazarovits, L. Szunyogh, and P. Weinberger, Phys. Rev. B **67**, 174404/1-7 (2003)
27. A. Vernes, L. Szunyogh, L. Udvardi, and P. Weinberger, J. Magn. Magn. Mater. **240**, 215 (2002)
28. A. Vernes, L. Szunyogh and P. Weinberger, Phys. Rev. B **66**, 214404/1-5 (2002)
29. J. Schwitalla, B.L. Györffy, and L. Szunyogh, Phys. Rev. B **63**, 104423 (2001)
30. S. Gallego, P. Weinberger, L. Szunyogh, P.M. Levy, and C. Sommers, Phys. Rev. B **68**, 054406/1-8 (2003)
31. L. Udvardi, L. Szunyogh, K. Palotas, and P. Weinberger, Phys. Rev. B **68**, 104436/1-11 (2003)
32. P. Lloyd, Proc. Phys. Soc. London **90**, 207 (1967)

A Appendix: Useful relations, expansions, functions and integrals

Spherical harmonics (Condon-Shortly phase convention):

$$Y_{\ell m}(\widehat{\mathbf{r}}) = \mathrm{i}^{m+|m|}\sqrt{\frac{2\ell+1}{4\pi}\frac{(\ell-|m|)!}{(\ell+|m|)!}}P_\ell^{|m|}(\cos(\Theta))\exp(\mathrm{i}m\phi) \tag{A.1}$$

Gaunt coefficients:

$$C_{L,L''}^{L'} = \int \mathrm{d}\widehat{\mathbf{r}} Y_L(\widehat{\mathbf{r}})Y_{L'}^*(\widehat{\mathbf{r}})Y_{L''}(\widehat{\mathbf{r}}) \tag{A.2}$$

$1/|\mathbf{r}-\mathbf{r}'|$ type expansions:

$$\frac{1}{|\mathbf{r}-\mathbf{r}'|} = \sum_L \frac{4\pi}{2\ell+1}\frac{r^\ell}{(r')^{\ell+1}}Y_L^*(\widehat{\mathbf{r}})Y_L(\widehat{\mathbf{r}}') \qquad (r<r') \tag{A.3}$$

$$\frac{1}{|\mathbf{r}-\mathbf{r}'|^{\ell+1}}Y_L(\widehat{\mathbf{r}-\mathbf{r}'}) = \sum_{L'}(-1)^\ell \frac{4\pi[2(\ell+\ell')-1]!!}{(2\ell-1)!!(2\ell'+1)!!}C_{\ell m,(\ell+\ell')(m'-m)}^{\ell' m'} \times\frac{r^{\ell'}}{(r')^{\ell+\ell'+1}}Y_{\ell' m'}(\widehat{\mathbf{r}})Y_{(\ell+\ell')(m'-m)}^*(\widehat{\mathbf{r}}') \qquad (r<r') \tag{A.4}$$

$$|\mathbf{r}-\mathbf{r}'|^\ell Y_L(\widehat{\mathbf{r}-\mathbf{r}'}) = \sum_{L',L''}\delta_{\ell,\ell'+\ell''}\delta_{m,m''-m'}\, r^{\ell'}(r')^{\ell''}C_{\ell' m',\ell m}^{\ell'' m''}Y_{L'}^*(\widehat{\mathbf{r}}) \times\frac{4\pi(-1)^{\ell''}[2(\ell'+\ell'')+1]!!}{(2\ell'+1)!!(2\ell''+1)!!}Y_{L''}(\widehat{\mathbf{r}}') \qquad (r<r') \tag{A.5}$$

Plane waves:

$$\begin{aligned}\exp(\mathrm{i}\mathbf{k}\cdot\mathbf{r}) &= 4\pi\sum_L \mathrm{i}^\ell j_\ell(kr)Y_L(\widehat{\mathbf{k}})Y_L^*(\widehat{\mathbf{r}}) \\ &= 4\pi\sum_L \mathrm{i}^\ell j_\ell(kr)Y_L^*(\widehat{\mathbf{k}})Y_L(\widehat{\mathbf{r}})\end{aligned} \tag{A.6}$$

Useful real space summation relations:

$$\sum_n \exp(-\left|\mathbf{r}-\mathbf{t}_n\right|^2 x^2) = \frac{\pi^{d/2}}{Vx^d}\sum_j \exp(-\mathbf{G}_j^2/4x^2 + \mathrm{i}\mathbf{G}_j\cdot\mathbf{r}) \tag{A.7}$$

In here V is the volume of the d-dimensional unit cell in configurational space, and $\mathbf{t}_n$ and $\mathbf{G}_j$ are vectors of the corresponding real and reciprocal lattices, respectively.

Γ-functions:

$$\Gamma(z+1) = z\Gamma(z) \tag{A.8}$$

$$\Gamma(1) = 1 \qquad \Gamma(n) = (n-1)\Gamma(n-1) = (n-1)! \tag{A.9}$$

$$\Gamma\left(\frac{1}{2}\right) = \sqrt{\pi} \qquad \Gamma\left(n+\frac{1}{2}\right) = \frac{2n-1}{2}\Gamma\left(n-\frac{1}{2}\right) = \sqrt{\pi}\frac{(2n-1)!!}{2^n} \tag{A.10}$$

$$\Gamma\left(\frac{1}{2}+\frac{1}{2}n\right)\Gamma\left(1+\frac{1}{2}n\right) = \frac{\sqrt{\pi}}{2^n}\Gamma\left(n+1\right) \tag{A.11}$$

Error- and incomplete Γ-functions:

$$\mathrm{erf}\left(x\right) = \frac{2}{\sqrt{\pi}}\int_0^x e^{-t^2}\mathrm{d}t \tag{A.12}$$

$$\mathrm{erfc}\left(x\right) = \frac{2}{\sqrt{\pi}}\int_x^\infty e^{-t^2}\mathrm{d}t = 1-\mathrm{erf}\left(x\right) \tag{A.13}$$

$$\mathrm{erf}\left(x\right) = \frac{2}{\sqrt{\pi}}\sum_{n=0}^{\infty}\frac{(-1)^n\ x^{2n+1}}{n!\ (2n+1)} = \frac{2}{\sqrt{\pi}}e^{-x^2}\sum_{n=0}^{\infty}\frac{2^n\ x^{2n+1}}{(2n+1)!!} \tag{A.14}$$

$$\Gamma(a,x) = \int_0^x e^{-t}\, t^{a-1} \mathrm{d}t \tag{A.15}$$

$$\Gamma(a,x) = \int_x^\infty e^{-t}\, t^{a-1} \mathrm{d}t = \Gamma(a) - \Gamma(a,x) \tag{A.16}$$

$$\Gamma\left(\frac{1}{2}, x^2\right) = \sqrt{\pi}\mathrm{erf}(x) \ , \quad \Gamma\left(\frac{1}{2}, x^2\right) = \sqrt{\pi}\mathrm{erfc}(x) \tag{A.17}$$

$$\Gamma(a+1,x) = a\Gamma(a,x) - x^a e^{-x} \tag{A.18}$$

Special integrals:

$$\frac{2}{\sqrt{\pi}} \int_0^\infty \mathrm{d}x \exp(-A^2x^2) = \frac{1}{A} \qquad (A>0) \tag{A.19}$$

$$\int_0^\infty \mathrm{d}x \frac{1}{x^2} \exp(-z^2x^2 - \mathbf{G}_j^2/4x^2) = \frac{\sqrt{\pi}}{G_j} \exp\left(-G_j\,|z|\right) \tag{A.20}$$

$$\int_{1/2\sigma}^\infty \mathrm{d}x \frac{1}{x^2} \exp(-z^2x^2) = 2\sigma \exp\left(-\frac{z^2}{4\sigma^2}\right) - 2z^2 \int_{1/2\sigma}^\infty \exp(-z^2x^2)\mathrm{d}x \tag{A.21}$$

$$= 2\sigma \exp\left(-\frac{z^2}{4\sigma^2}\right) - |z|\sqrt{\pi}\mathrm{erfc}\left(\frac{|z|}{2\sigma}\right) \tag{A.22}$$

$$\int_0^\pi \exp(\mathrm{i}\beta\cos(\phi))\cos(m\phi)\mathrm{d}\phi = \pi\,\mathrm{i}^m\, J_m(\beta) = \pi\,\mathrm{i}^{-m}\, J_m(-\beta), \tag{A.23}$$

$$\int_0^\pi \exp(\mathrm{i}\beta\cos(\phi+\pi))\cos(m(\phi+\pi))\mathrm{d}\phi = \pi\,\mathrm{i}^{-m}\, J_m(-\beta) \tag{A.24}$$

$$\int_0^{2\pi} \exp(\mathrm{i}\beta\cos(\phi))\cos(m\phi)\mathrm{d}\phi = 2\pi\,\mathrm{i}^m\, J_m(\beta) \tag{A.25}$$

$$\exp(\mathrm{i}m\phi_j) \int_0^{2\pi} \exp(\mathrm{i}\beta\cos(\phi-\phi_j))\exp(-\mathrm{i}m\phi)\mathrm{d}\phi = 2\pi\,\mathrm{i}^m\, J_m(\beta) \tag{A.26}$$

$$\int_0^1 \mathrm{d}x\, x^s \left(1-x^2\right)^{|m|/2} P_\ell^{|m|}(x) = \frac{2^{-|m|-1}\Gamma\left(\frac{1}{2}+\frac{1}{2}s\right)\Gamma\left(1+\frac{1}{2}s\right)}{\Gamma(1+\ell-|m|)\,\Gamma\left(1+\frac{1}{2}s+\frac{1}{2}|m|-\frac{1}{2}\ell\right)} \times \frac{\Gamma(1+\ell+|m|)}{\Gamma\left(\frac{3}{2}+\frac{1}{2}s+\frac{1}{2}|m|+\frac{1}{2}\ell\right)} \tag{A.27}$$

Recursive evaluation of the integrals $I_n(a,b)$

$$I_n(a,b) \equiv \int_{a^2}^{\infty} x^{-\frac{1}{2}-n} \exp\left(-\frac{b^2}{x} - x\right) \mathrm{d}x \qquad (a,b>0) \tag{A.28}$$

$$I_{n+2}(a,b) = \frac{1}{b^2}\left[\left(n+\frac{1}{2}\right) I_{n+1}(a,b) + I_n(a,b)\right] - \frac{\exp\left(-\frac{b^2}{a^2} - a^2\right)}{a^{2n+1}b^2} \tag{A.29}$$

$$I_0(a,b) = 2\int_a^{\infty} \exp\left(-\frac{b^2}{y^2} - y^2\right) \mathrm{d}y \tag{A.30}$$

$$I_0(0,b) = 2\int_0^{\infty} \exp\left(-\frac{b^2}{y^2} - y^2\right) \mathrm{d}y = \sqrt{\pi}\exp(-2b) \tag{A.31}$$

$$I_0(a,b) = \frac{\sqrt{\pi}}{2}\exp(-2b)\left(\mathrm{erf}\left(\frac{b}{a} - a\right) + 1\right) - \exp(2b)\left(\mathrm{erf}\left(\frac{b}{a} + a\right) - 1\right)\Big] \tag{A.32}$$

$$I_1(a,b) = \frac{\sqrt{\pi}}{2b}\Big[\exp(-2b)\left(\mathrm{erf}\left(\frac{b}{a} - a\right) + 1\right) + \exp(2b)\left(\mathrm{erf}\left(\frac{b}{a} + a\right) - 1\right)\Big] \tag{A.33}$$

Taylor-expansion of Bessel functions and related forms:

$$J_\nu(z) = \sum_{k=0}^{\infty} \frac{(-1)^k}{k!\Gamma(\nu+k+1)}\left(\frac{z}{2}\right)^{2k+\nu} \tag{A.34}$$

$$J_{|m|}(G_j r\sin(\Theta)) = \sum_{k=|m|,|m|+2,\ldots}^{\infty} \frac{(-1)^{(k-|m|)/2}}{2^k\left(\frac{k-|m|}{2}\right)!\left(\frac{k+|m|}{2}\right)!} G_j^k \sin^k(\Theta)\, r^k$$
$$G_j = |\mathbf{G}_j| \quad , \quad \mathbf{G}_j \in \mathcal{L}^{(2)} \tag{A.35}$$

Special polynomial expansions

$$\left(r^2\cos^2(\Theta) + 2rc_{pq\perp}\cos(\Theta)\right)^n = \sum_{s=n}^{2n}\binom{n}{s-n} 2^{2n-s} c_{pq\perp}^{2n-s}\cos^s(\Theta)\, r^s \ . \tag{A.36}$$

Expansions in Legendre polynomials

$$z^n = \sum_{i=0}^{n} c_i^{(n)} P_i(z) \,, \tag{A.37}$$

$$c_{2k}^{(2n)} = \frac{1}{2n+1}\delta_{k0} + (4k+1)\frac{2n(2n-2)\dots(2n-2k+2)}{(2n+1)(2n+3)\dots(2n+2k+1)}\,(1-\delta_{k0}) \tag{A.38}$$

$$c_{2k+1}^{(2n)} = 0 \tag{A.39}$$

$$c_{2k+1}^{(2n+1)} = \frac{3}{2n+3}\delta_{k0} + (4k+3)\frac{2n(2n-2)\dots(2n-2k+2)}{(2n+3)(2n+5)\dots(2n+2k+3)}\,(1-\delta_{k0}) \tag{A.40}$$

$$c_{2k}^{(2n)} = 0 \tag{A.41}$$

$$\int_{-1}^{1} \mathrm{d}x\, x^\ell P_\ell(x) = c_\ell^{(\ell)} = 2\frac{\ell!}{(2\ell+1)!!} = \frac{\sqrt{\pi}\Gamma(\ell+1)}{2^\ell\Gamma(\ell+\frac{3}{2})} \,, \tag{A.42}$$

$$0! = 1! = (-1)!! = 1!! = 1 \tag{A.43}$$

$$\int_{-1}^{1} \mathrm{d}x\, P_0(x) = \int_{-1}^{1} \mathrm{d}x \; = 2 \tag{A.44}$$

$$\int_{-1}^{1} \mathrm{d}x\, xP_1(x) = \int_{-1}^{1} \mathrm{d}x\, x^2 = \frac{2}{3} \tag{A.45}$$

$$\int_{-1}^{1} \mathrm{d}x\, x^2 P_2(x) = \frac{1}{2}\int_{-1}^{1} \mathrm{d}x\, (3x^4 - x^2) = \frac{4}{15} \tag{A.46}$$

$$\int_{-1}^{1} \mathrm{d}x\, x^3 P_3(x) = \frac{1}{2}\int_{-1}^{1} \mathrm{d}x\, (5x^6 - 3x^4) = \frac{4}{35} \tag{A.47}$$

References

1. I.S. Gradshteyn and I.M. Ryzhik, *Table of Integrals, Series and Products*, Corrected and Enlarged Edition (Academic Press Inc. 1980)
2. R. Hammerling: Aspects of dispersion interactions and of the full-potential Korringa–Kohn–Rostoker (KKR) method for semi-infinite systems. PHD Thesis, Technical University, Vienna (2003). http://www.cms.tuwien.ac.at/PhD_Theses
3. M. Abramowitz and I. Stegun, *Handbook of Mathematical Functions* (Dover Publ. New York 1973)

Springer Series in

SOLID-STATE SCIENCES

Series Editors:

M. Cardona P. Fulde K. von Klitzing R. Merlin H.-J. Queisser H. Störmer

90 **Earlier and Recent Aspects of Superconductivity**
Editor: J.G. Bednorz and K.A. Müller

91 **Electronic Properties and Conjugated Polymers III**
Editors: H. Kuzmany, M. Mehring, and S. Roth

92 **Physics and Engineering Applications of Magnetism**
Editors: Y. Ishikawa and N. Miura

93 **Quasicrystals**
Editor: T. Fujiwara and T. Ogawa

94 **Electronic Conduction in Oxides**
2nd Edition By N. Tsuda, K. Nasu, A. Fujimori, and K. Siratori

95 **Electronic Materials**
A New Era in MaterialsScience
Editors: J.R. Chelikowski and A. Franciosi

96 **Electron Liquids**
2nd Edition By A. Isihara

97 **Localization and Confinement of Electrons in Semiconductors**
Editors: F. Kuchar, H. Heinrich, and G. Bauer

98 **Magnetism and the Electronic Structure of Crystals**
By V.A. Gubanov, A.I. Liechtenstein, and A.V. Postnikov

99 **Electronic Properties of High-T_c Superconductors and Related Compounds**
Editors: H. Kuzmany, M. Mehring and J. Fink

100 **Electron Correlations in Molecules and Solids**
3rd Edition By P. Fulde

101 **High Magnetic Fields in Semiconductor Physics III**
Quantum Hall Effect, Transport and Optics By G. Landwehr

101 **High Magnetic Fields in Semiconductor Physics III**
Quantum Hall Effect, Transport and Optics By G. Landwehr

102 **Conjugated Conducting Polymers**
Editor: H. Kiess

103 **Molecular Dynamics Simulations**
Editor: F. Yonezawa

104 **Products of Random Matrices**
in Statistical Physics By. A. Crisanti, G. Paladin, and A. Vulpiani

105 **Self-Trapped Excitons**
2nd Edition By K.S. Song and R.T. Williams

106 **Physics of High-Temperature Superconductors**
Editors: S. Maekawa and M. Sato

107 **Electronic Properties of Polymers**
Orientation and Dimensionality of Conjugated Systems Editors: H. Kuzmany, M. Mehring, and S. Roth

108 **Site Symmetry in Crystals**
Theory and Applications
2nd Edition By R.A. Evarestov and V.P. Smirnov

109 **Transport Phenomena in Mesoscopic Systems**
Editors: H. Fukuyama and T. Ando

110 **Superlattices and Other Heterostructures**
Symmetry and Optical Phenomena 2nd Edition
By E.L. Ivchenko and G.E. Pikus

111 **Low-Dimensional Electronic Systems**
New Concepts
Editors: G. Bauer, F. Kuchar, and H. Heinrich

112 **Phonon Scattering in Condensed Matter VII**
Editors: M. Meissner and R.O. Pohl

Springer Series in

SOLID-STATE SCIENCES

Series Editors:
M. Cardona P. Fulde K. von Klitzing R. Merlin H.-J. Queisser H. Störmer

113 **Electronic Properties of High-T_c Superconductors**
Editors: H. Kuzmany, M. Mehring, and J. Fink

114 **Interatomic Potential and Structural Stability**
Editors: K. Terakura and H. Akai

115 **Ultrafast Spectroscopy of Semiconductors and Semiconductor Nanostructures**
By J. Shah

116 **Electron Spectrum of Gapless Semiconductors**
By J.M. Tsidilkovski

117 **Electronic Properties of Fullerenes**
Editors: H. Kuzmany, J. Fink, M. Mehring, and S. Roth

118 **Correlation Effects in Low-Dimensional Electron Systems**
Editors: A. Okiji and N. Kawakami

119 **Spectroscopy of Mott Insulators and Correlated Metals**
Editors: A. Fujimori and Y. Tokura

120 **Optical Properties of III–V Semiconductors**
The Influence of Multi-Valley Band Structures By H. Kalt

121 **Elementary Processes in Excitations and Reactions on Solid Surfaces**
Editors: A. Okiji, H. Kasai, and K. Makoshi

122 **Theory of Magnetism**
By K. Yosida

123 **Quantum Kinetics in Transport and Optics of Semiconductors**
By H. Haug and A.-P. Jauho

124 **Relaxations of Excited States and Photo-Induced Structural Phase Transitions**
Editor: K. Nasu

125 **Physics and Chemistry of Transition-Metal Oxides**
Editors: H. Fukuyama and N. Nagaosa

126 **Physical Properties of Quasicrystals**
Editor: Z.M. Stadnik

127 **Positron Annihilation in Semiconductors**
Defect Studies. By R. Krause-Rehberg and H.S. Leipner

128 **Magneto-Optics**
Editors: S. Sugano and N. Kojima

129 **Computational Materials Science**
From Ab Initio to Monte Carlo Methods. By K. Ohno, K. Esfarjani, and Y. Kawazoe

130 **Contact, Adhesion and Rupture of Elastic Solids**
By D. Maugis

131 **Field Theories for Low-Dimensional Condensed Matter Systems**
Spin Systems and Strongly Correlated Electrons. By G. Morandi, P. Sodano, A. Tagliacozzo, and V. Tognetti

132 **Vortices in Unconventional Superconductors and Superfluids**
Editors: R.P. Huebener, N. Schopohl, and G.E. Volovik

133 **The Quantum Hall Effect**
By D. Yoshioka

134 **Magnetism in the Solid State**
By P. Mohn

135 **Electrodynamics of Magnetoactive Media**
By I. Vagner, B.I. Lembrikov, and P. Wyder